NEUROINFLAMMATION AND THE VISUAL SYSTEM

EDITED BY: Gemma Caterina Maria Rossi, Ahmed Toosy and
Claudia Angela Michela Gandini Wheeler-Kingshott

PUBLISHED IN: Frontiers in Neurology

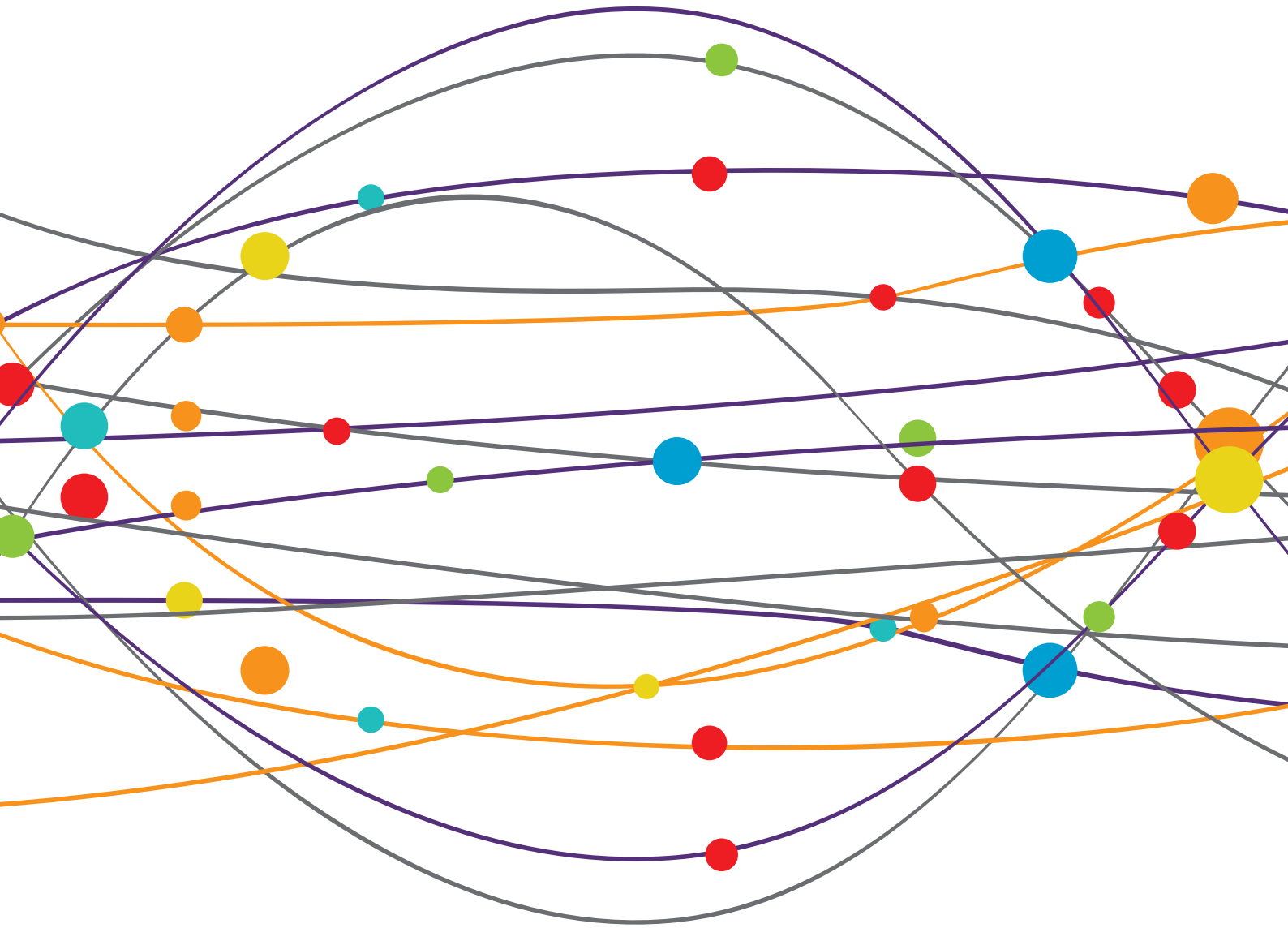

frontiers Research Topics

Frontiers eBook Copyright Statement

The copyright in the text of individual articles in this eBook is the property of their respective authors or their respective institutions or funders. The copyright in graphics and images within each article may be subject to copyright of other parties. In both cases this is subject to a license granted to Frontiers.

The compilation of articles constituting this eBook is the property of Frontiers.

Each article within this eBook, and the eBook itself, are published under the most recent version of the Creative Commons CC-BY licence. The version current at the date of publication of this eBook is CC-BY 4.0. If the CC-BY licence is updated, the licence granted by Frontiers is automatically updated to the new version.

When exercising any right under the CC-BY licence, Frontiers must be attributed as the original publisher of the article or eBook, as applicable.

Authors have the responsibility of ensuring that any graphics or other materials which are the property of others may be included in the CC-BY licence, but this should be checked before relying on the CC-BY licence to reproduce those materials. Any copyright notices relating to those materials must be complied with.

Copyright and source acknowledgement notices may not be removed and must be displayed in any copy, derivative work or partial copy which includes the elements in question.

All copyright, and all rights therein, are protected by national and international copyright laws. The above represents a summary only. For further information please read Frontiers' Conditions for Website Use and Copyright Statement, and the applicable CC-BY licence.

ISSN 1664-8714
ISBN 978-2-88971-651-7
DOI 10.3389/978-2-88971-651-7

About Frontiers

Frontiers is more than just an open-access publisher of scholarly articles: it is a pioneering approach to the world of academia, radically improving the way scholarly research is managed. The grand vision of Frontiers is a world where all people have an equal opportunity to seek, share and generate knowledge. Frontiers provides immediate and permanent online open access to all its publications, but this alone is not enough to realize our grand goals.

Frontiers Journal Series

The Frontiers Journal Series is a multi-tier and interdisciplinary set of open-access, online journals, promising a paradigm shift from the current review, selection and dissemination processes in academic publishing. All Frontiers journals are driven by researchers for researchers; therefore, they constitute a service to the scholarly community. At the same time, the Frontiers Journal Series operates on a revolutionary invention, the tiered publishing system, initially addressing specific communities of scholars, and gradually climbing up to broader public understanding, thus serving the interests of the lay society, too.

Dedication to Quality

Each Frontiers article is a landmark of the highest quality, thanks to genuinely collaborative interactions between authors and review editors, who include some of the world's best academicians. Research must be certified by peers before entering a stream of knowledge that may eventually reach the public - and shape society; therefore, Frontiers only applies the most rigorous and unbiased reviews.
Frontiers revolutionizes research publishing by freely delivering the most outstanding research, evaluated with no bias from both the academic and social point of view. By applying the most advanced information technologies, Frontiers is catapulting scholarly publishing into a new generation.

What are Frontiers Research Topics?

Frontiers Research Topics are very popular trademarks of the Frontiers Journals Series: they are collections of at least ten articles, all centered on a particular subject. With their unique mix of varied contributions from Original Research to Review Articles, Frontiers Research Topics unify the most influential researchers, the latest key findings and historical advances in a hot research area! Find out more on how to host your own Frontiers Research Topic or contribute to one as an author by contacting the Frontiers Editorial Office: frontiersin.org/about/contact

NEUROINFLAMMATION AND THE VISUAL SYSTEM

Topic Editors:
Gemma Caterina Maria Rossi, Fondazione Ospedale San Matteo (IRCCS), Italy
Ahmed Toosy, University College London, United Kingdom
Claudia Angela Michela Gandini Wheeler-Kingshott, University College London, United Kingdom

Citation: Rossi, G. C. M., Toosy, A., Gandini Wheeler-Kingshott, C. A. M., eds. (2021). Neuroinflammation and the Visual System. Lausanne: Frontiers Media SA. doi: 10.3389/978-2-88971-651-7

Table of Contents

frontiers in Neurology

EDITORIAL
published: 13 August 2021
doi: 10.3389/fneur.2021.724447

Editorial: Neuroinflammation and the Visual System

Gemma Caterina Maria Rossi[1,2*], *Claudia Angela Michela Gandini Wheeler-Kingshott*[3] *and Ahmed Toosy*[3]

[1] *Fondazione Ospedale San Matteo (Istituto di Ricovero e Cura a Carattere Scientifico), Pavia, Italy,* [2] *Department of Surgical Sciences, University Eye Clinic of Pavia, Pavia, Italy,* [3] *Faculty of Brain Sciences, Queen Square Institute of Neurology, University College London, London, United Kingdom*

Keywords: neuroinflammation, glaucoma, diabetic retinopathy, optic neuritis, multiple sclerosis, neuromyelitis optica spectrum disorders, microglia, OCT

Editorial on the Research Topic

Neuroinflammation and the Visual System

The eye is an extension of the central nervous system (CNS) and degenerative diseases of the retina and optic nerve can lead to progressive loss of vision. The causes of degeneration are different and can overlap between genetic predisposition, environmental factors, metabolic alterations, and inflammatory processes.

New diagnostic methods and biomarkers are needed to examine and identify the role of neuroinflammation in the degenerative diseases affecting the visual system, not only to aid early diagnosis but also to monitor neuroprotective treatments.

The purpose of the present Research Topic was to publish new research describing potential new advances in the diagnosis, treatment, and pathological understanding of conditions that possess inflammatory components affecting the eye and the visual central nervous system.

OPEN ACCESS

Edited and reviewed by:
Aki Kawasaki,
Hôpital ophtalmique Jules-Gonin, Switzerland

***Correspondence:**
Gemma Caterina Maria Rossi
gemma.rossi.md@gmail.com

Specialty section:
This article was submitted to Neuro-Ophthalmology, a section of the journal Frontiers in Neurology

Received: *13 June 2021*
Accepted: *21 July 2021*
Published: *13 August 2021*

Citation:
Rossi GCM, Gandini Wheeler-Kingshott CAM and Toosy A (2021) Editorial: Neuroinflammation and the Visual System. Front. Neurol. 12:724447. doi: 10.3389/fneur.2021.724447

NEUROINFLAMMATION AND THE EYE

Diabetic retinopathy and glaucoma are two of the most prominent causes of vision loss (1). The pathogenesis of these conditions is complex and not yet fully known but there is consensus on the crucial role of neuroinflammation together with the mechanical/ischemic determine the onset and progression of these two pathologies. Previous studies have shown that microglial cells play an active role in maintaining the normal structure and functioning of the retina and the CNS, but also that a chronic proinflammatory environment is a common and important denominator of retinal degenerative diseases and neurological disorders affecting the vision (2).

The mini-review on neuroprotection and glaucoma by Rolle et al. reminds us that inflammatory responses within the retina are regulated by microglia and astroglia Rolle et al. These cells include Müller cells and astrocytes and provide metabolic support to neurons, neurological regulation of ion concentrations, and neuroprotective activities. Microglial cells originate from primitive erythromyeloid progenitors; after maturation, they participate in the inflammatory process activated by DAMPs (damage-associated molecular patterns) released by neural cells and also by astroglia: heat shock proteins (HSPs) are produced by retinal ganglion cells (RGC) when intraocular pressure (IOP) is high. In response to the neuroinflammatory process, microglial cytokines and chemokines (complement factors and interleukin 6) amplify the response and promote the morphological change of microglia into macrophages. There are two phenotypes of activated macrophages, M1 and M2, which produce IL-1β, IL-12, TNF-α and IL-10, TGF-β, and neurotrophic factor insulin-like growth factors, respectively. The review points out

that animal model studies have improved our understanding of cellular mechanisms and pathways of neuroinflammation, paving the way for new therapeutic possibilities to modulate neuroinflammation such as antioxidants, ketogenic diet, hydrophilic saffron extract.

Another review by Tirendi et al. describes recent developments related to the new 3D trabecular meshwork (3d-TM) culture model that uses microengineering techniques to create systems that mimic cell-cell and cell-environment interactions found *in vivo*. The authors have recently studied, as markers of activation of the inflammatory response, the changes in pro-inflammatory cytokine transcriptions and NF-kB protein levels following oxidative stress stimulation, allowing to analyze the phases of cellular damage that underlie glaucoma and its adverse outcomes.

The relationship between diabetes and inflammation is studied by Filippelli et al. in patients with proliferative diabetic retinopathy. In this condition, oxidative stress is promoted by several mechanisms, including pathways involving polyols, vascular dysfunction, proinflammatory cytokine, and protein kinase C production, accumulation of advanced glycation products, activation of the renin-angiotensin-aldosterone system, increased growth factors, and leukostasis. Several papers have reported an increase in the intravitreal concentration of the main proinflammatory cytokines and chemokines and have highlighted a key role of these mediators in the onset and progression of diabetic retinopathy. The study by Filippelli et al. examines the vitreous composition in patients with diabetic retinopathy and reports an *in vivo* protective role *in vivo* of some components of the diet (curcumin, omotaurine, and vitamin D3) that could be used in addition to anti-neovascularization agents, to reduce cytokine levels, to regulate the inflammation network and reduce the rate of administration of intravitreally injected agents. An additional gene expression experiment demonstrated that the combination of curcumin, vitamin D3, and homotaurine down-regulate the expression of the cyclinD1 gene and the proinflammatory cytokine genes TNFα and IL6, supporting their anti-inflammatory action in combination.

Finally, Tong et al. present an interesting resting-state functional magnetic resonance imaging study in patients with iridocyclitis and demonstrate altered and disturbed synchronous neural activity within certain areas of the brain, suggesting some form of neuroplasticity in this condition.

NEUROINFLAMMATION AND CENTRAL NERVOUS VISUAL SYSTEM

Acute optic neuritis is a frequent manifestation of inflammatory CNS conditions, multiple sclerosis (MS), and neuromyelitis optic spectrum disorder (NMOSD), with the latter predisposing to significant and irreversible vision loss. Key research areas aim at understanding the disability and recovery mechanisms with acute neuroinflammation and neurodegeneration of the optic nerves in these conditions. This Research Topic presents a large selection of articles that enhance our understanding of these areas, but which can also be grouped into several important research themes.

The first theme concerns the use of animal models. Redler and Levy present a comprehensive review article on the application of rodent models of optic neuritis and how they contributed to our understanding of the pathological mechanisms of inflammation, demyelination, axonal loss, and therapies such as antioxidants, neuroprotective agents, and remyelinating agents. Another article by Dietrich et al. reports that dimethyl fumarate, a disease-modifying treatment commonly used in MS, has no protective effects on retinal degeneration after optic nerve crushing in mice, but appears to exhibit antioxidant and anti-inflammatory effects after light-induced photoreceptor loss.

The second main theme concerns biomarkers, both imaging and immunopathogenic. For imaging, articles related to optical coherence tomography (OCT) dominate this Research Topic. Kleerekooper et al. present an excellent review of the recently available imaging modality, OCT angiography, capable of visualizing retinal and choroidal vasculature in high detail with the promise of providing new insights into the pathobiology of MS and NMOSD. Ziccardi et al. report an application of OCT to MS patients with a history of optic neuritis (ON) and find that post-ON neurodegeneration affects both the outer and inner retinal layers in patients with poor visual recovery whereas it occurs only in the inner retinal layers with good visual recovery. Murphy et al. report significant correlations between OCT angiography derived superficial vascular plexus (SVP) density for inter-eye differences, as well as for ganglion cell-inner plexiform (GCIPL) thickness, and visual outcomes in MS ON patients, providing insights into the interactions between retinal tissue and vascular changes. For immunological markers, Schmetzer et al. controversially question the pathogenic nature of the aquaporin 4 IgG antibody (AQP4-IgG) in NMOSD with the finding that Ab-positive patients showed no correlation between titer levels and clinical disease activity. Finally, Kang et al. report elevated serum levels of T-helper cell-related cytokines in patients with positive myelin-oligodendrocyte glycoprotein antibodies (MG-IgG), suggesting that Th17 cells may play a role in its autoimmunity.

The third theme is more directly concerned with clinical outcomes. Park et al. report the potential clinical utility of low-contrast visual acuity (2.5%) in detecting patients with prior ON, being superior to more conventional high-contrast visual acuity measures. Zhao et al. performed an observational study of low-dose rituximab treatment in NMO-ON, demonstrating good tolerance, reductions in aquaporin-4 antibody titers ($p = 0.01$), and good reductions in CD19 + B cells. For acute ON relapses in AQP4-IgG NMOSD, Akaishi et al. provide further evidence of the benefit of early systemic corticosteroid treatment in preserving visual acuity. Finally, Klumbies et al. reveal secondary analyzes from the SUPREME study (Sunphenon in Progressive Forms of MS, NCT00799890), which evaluates the effect of epigallocatechin-gallate (EGCG), an anti-inflammatory and antioxidant ingredient in green tea, on OCT. Unfortunately, they found no differences between the treated and placebo groups after 2 years for the peripapillary retinal nerve fiber layer and ganglion cell/inner plexiform layer thicknesses. Although the study may have been underpowered, it is important to investigate potential

neuroprotective agents in progressive MS where there is a paucity of effective therapies.

In conclusion, this research topic contains articles that communicate the latest knowledge and developments from a wide range of conditions related to neuroinflammation affecting both the eye and the CNS visual system. Topics include understanding the pathophysiological mechanisms, studying imaging and immunological markers of the diseases, clinical outcomes, and exploring potential treatments. The experiments described range from animal models and cell-based tests to human *in vivo* studies. We hope that this collection of research work on this topic will help readers and researchers interested in seeing the eye and visual system as a model for dealing with inflammation from different angles. The breath of the works presented here enhance understanding across multiple disciplines and hopefully inspire innovative research that accelerates understanding of disease mechanisms and develops effective therapies.

AUTHOR CONTRIBUTIONS

GR wrote the draft of the editorial. CG and AT revised and corrected it. All authors contributed to the article and approved the submitted version.

REFERENCES

1. Bourne RRA, Jonas JB, Bron AM, Cicinelli MV, Das A, Flaxman SR, et al. Prevalence and causes of vision loss in high-income countries and in Eastern and Central Europe in 2015: magnitude, temporal trends and projections. *Br J Ophthalmol.* (2018) 102:575–85. doi: 10.1136/bjophthalmol-2017-311258
2. Rashid K, Akhtar-Schaefer I, Langmann T. Microglia in retinal degeneration. *Front Immunol.* (2019) 10:1975. doi: 10.3389/fimmu.2019.01975

Conflict of Interest: The authors declare that the research was conducted in the absence of any commercial or financial relationships that could be construed as a potential conflict of interest.

Publisher's Note: All claims expressed in this article are solely those of the authors and do not necessarily represent those of their affiliated organizations, or those of the publisher, the editors and the reviewers. Any product that may be evaluated in this article, or claim that may be made by its manufacturer, is not guaranteed or endorsed by the publisher.

Copyright © 2021 Rossi, Gandini Wheeler-Kingshott and Toosy. This is an open-access article distributed under the terms of the Creative Commons Attribution License (CC BY). The use, distribution or reproduction in other forums is permitted, provided the original author(s) and the copyright owner(s) are credited and that the original publication in this journal is cited, in accordance with accepted academic practice. No use, distribution or reproduction is permitted which does not comply with these terms.

frontiers in Neurology

ORIGINAL RESEARCH
published: 02 September 2020
doi: 10.3389/fneur.2020.00932

Rapid Administration of High-Dose Intravenous Methylprednisolone Improves Visual Outcomes After Optic Neuritis in Patients With AQP4-IgG-Positive NMOSD

Tetsuya Akaishi[1,2], Takayuki Takeshita[3], Noriko Himori[3], Toshiyuki Takahashi[1,4], Tatsuro Misu[1], Ryo Ogawa[1], Kimihiko Kaneko[1], Juichi Fujimori[5], Michiaki Abe[2], Tadashi Ishii[2], Kazuo Fujihara[6], Masashi Aoki[1], Toru Nakazawa[3] and Ichiro Nakashima[5]*

[1] Department of Neurology, Tohoku University Graduate School of Medicine, Sendai, Japan, [2] Department of Education and Support for Regional Medicine, Tohoku University Hospital, Sendai, Japan, [3] Department of Ophthalmology, Tohoku University Graduate School of Medicine, Sendai, Japan, [4] Department of Neurology, National Hospital Organization Yonezawa National Hospital, Sendai, Japan, [5] Department of Neurology, Tohoku Medical and Pharmaceutical University, Sendai, Japan, [6] Department of Multiple Sclerosis Therapeutics, Fukushima Medical University, Fukushima, Japan

OPEN ACCESS

Edited by:
Ahmed Toosy, University College London, United Kingdom

Reviewed by:
Olivier Outteryck, Université de Lille, France
Mark Paine, Royal Brisbane and Women's Hospital, Australia

***Correspondence:**
Tetsuya Akaishi
t-akaishi@med.tohoku.ac.jp

Specialty section:
This article was submitted to Neuro-Ophthalmology, a section of the journal Frontiers in Neurology

Received: *21 May 2020*
Accepted: *20 July 2020*
Published: *02 September 2020*

Citation:
Akaishi T, Takeshita T, Himori N, Takahashi T, Misu T, Ogawa R, Kaneko K, Fujimori J, Abe M, Ishii T, Fujihara K, Aoki M, Nakazawa T and Nakashima I (2020) Rapid Administration of High-Dose Intravenous Methylprednisolone Improves Visual Outcomes After Optic Neuritis in Patients With AQP4-IgG-Positive NMOSD. Front. Neurol. 11:932. doi: 10.3389/fneur.2020.00932

Objective: The purpose of this study was to elucidate the rapid impact of high-dose intravenous methylprednisolone pulse therapy (1,000 mg/day for 3 days) on the eventual visual prognosis in patients with serum anti-aquaporin-4 immunoglobulin G (AQP4-IgG)–positive neuromyelitis optica spectrum disorders (NMOSDs) who had an attack of optic neuritis (ON).

Methods: Data from 32 consecutive NMOSD patients (1 male and 31 female) with at least one ON attack, involving a total of 36 ON-involved eyes, were evaluated. The following variables at ON onset were evaluated: sex, age at the first ON episode, visual acuity at nadir, visual acuity after 1 year, duration from ON onset to treatment for an acute ON attack, cycles of high-dose intravenous methylprednisolone pulse therapy for the ON attack, and cycles of plasmapheresis for the ON attack. Among the 36 ON-involved eyes, 27 eyes were studied using orbital MRI with a short-T1 inversion recovery sequence and gadolinium-enhanced fat-suppressed T1 imaging before starting treatment in the acute phase.

Results: In univariate analyses, a shorter duration from ON onset to the initiation of high-dose intravenous methylprednisolone pulse therapy favorably affected the eventual visual prognosis 1 year later (Spearman's rho = 0.50, $p = 0.0018$). The lesion length on orbital MRI was also correlated with the eventual visual prognosis (rho = 0.68, $p < 0.0001$). Meanwhile, the days to steroid pulse therapy and lesion length on orbital MRI did not show a significant correlation. These findings suggest that the rapidness of steroid pulse therapy administration affects the eventual visual prognosis independent of the severity of ON. In multivariate analysis, a shorter time from ON onset to the start of acute treatment ($p = 0.0004$) and a younger age at onset ($p = 0.0071$) were significantly associated with better visual outcomes.

Conclusions: Rapid initiation of high-dose intravenous methylprednisolone pulse therapy is essential to preserve the eventual visual acuity in patients with serum AQP4-IgG-positive NMOSD. Once clinicians suspect acute ON with serum AQP4-IgG, swift administration of steroid pulse therapy before confirming the positivity of serum AQP4-IgG would be beneficial for preserving visual function.

Keywords: neuromyelitis optica spectrum disorders, optic neuritis, steroid pulse therapy, timing, visual prognosis

INTRODUCTION

Neuromyelitis optica spectrum disorder (NMOSD) is an autoimmune-related neurological disorder that primarily causes astrocytic damage throughout the central nervous system and is characterized by the presence of serum anti-aquaporin-4 immunoglobulin G (AQP4-IgG) (1, 2). Patients with NMOSD typically present with repeated attacks of optic neuritis (ON) and/or myelitis (3, 4), and are likely to relapse without proper relapse prevention treatments, acquiring neurological disabilities accumulated in a stepwise manner (5–7). In the acute phase of attacks in NMOSD, immune suppression with high-dose intravenous methylprednisolone (IVMP) pulse therapy with or without oral tapering is the gold standard treatment at present (8–12). In addition to IVMP, plasma exchange (PLEX) and intravenous immunoglobulin (IVIg) therapy are also known to be effective for treating acute NMO exacerbations and preventing relapse (13–15). To prevent relapses in the chronic phase, mycophenolate mofetil, rituximab, azathioprine, and IVIg are being used (12, 16). Although not a standard strategy, long-term oral low-dose corticosteroids are also used as relapse prevention therapy in some facilities (17, 18). Other monoclonal antibodies, such as eculizumab, tocilizumab, satralizumab, and inebilizumab, are also known to effectively suppress autoimmunity and relapses in NMOSD, although not all these listed drugs have been approved yet (19–22).

Compared with other demyelinating neurological disorders of the central nervous system, such as multiple sclerosis (MS) or anti-myelin oligodendrocyte glycoprotein antibody (MOG-IgG)-associated demyelination, neurological disability resulting from attacks of ON in NMOSD is known to be much more severe (9, 23, 24). If untreated, it is empirically believed that up to half of the patients will eventually become wheelchair bound and/or blind (25–27). Even if properly treated with timely acute therapies and adequate relapse prevention therapies, patients with NMOSD may eventually become wheelchair bound or blind. The disease is known to have a female predominance and is associated with an increased rate of complications with other autoimmune-related diseases (i.e., Sjögren's syndrome), but there have been no established patient background factors that significantly affect the subsequent neurological disability in the disease (28, 29).

As for the manifestation of ON, patients with MOG-IgG and those with AQP4-IgG often show similar appearance on orbital MRI, often with longitudinally extensive ON lesions and swollen optic nerves in the acute phase (30), but the eventual visual prognosis with appropriate acute therapies is thought to be generally worse in AQP4-IgG-positive cases than in MOG-IgG-positive cases (31). As a result, there is an urgent need to develop an effective therapeutic strategy to preserve long-term visual outcomes in patients with AQP4-IgG-positive ON. In this study, to clarify the impact of acute therapies on the eventual neurological prognosis in NMOSD, we assessed the impacts of rapidity and total amount of acute ON treatment on eventual visual acuity (VA) in the chronic phase.

METHODS

Study Design

A total of 32 consecutive patients with AQP4-IgG-positive NMOSD with at least one ON episode who became legally blind (i.e., corrected VA $\leq$ 20/200, 0.1 decimal) at nadir in the acute phase were retrospectively studied. All patients were diagnosed and followed at a single university hospital in Japan between 1995 and 2019. Three other NMOSD patients whose VA at nadir was >20/200 were excluded because they had mild visual impairment; their inclusion may have biased the results. Positivity of serum AQP4-IgG and MOG-IgG was examined in all enrolled patients, and brain MRI and contrast-enhanced orbital MRI were performed to make an accurate diagnosis. There were no cases of double-positive AQP4-IgG and MOG-IgG. Only the first ON attack in each eye was evaluated; thus, relapsing ON episodes in each eye were not taken into consideration. Because four patients had ON attacks in both eyes (3 simultaneous and 1 asynchronous), a total of 36 ON-involved eyes in 32 NMOSD patients were evaluated in this study. A flow diagram of the subgroup classification according to the acute therapies is shown in **Figure 1**.

Studied Variables

At each occasion of ON attack (i.e., the first ON attack in each eye), the following clinical information was comprehensively collected: sex, age, and medical history (i.e., complication of other autoimmune-related diseases), details of the acute treatment for ON, serum AQP4-IgG titer, longitudinal length of ON lesions on orbital MRI before the acute treatments, corrected VA at nadir in the acute phase, corrected VA 1 year later in the chronic phase, the required days from the ON onset to starting the acute treatments with IVMP pulse therapy, and the required days from the ON onset to starting PLEX as an adjunctive therapy.

Contrast-Enhanced Orbital MRI

Before starting the treatment, the longitudinal length of the ON lesion on orbital MRI was evaluated in 28 of the 36 ON episodes, which was semi-quantitatively represented by the

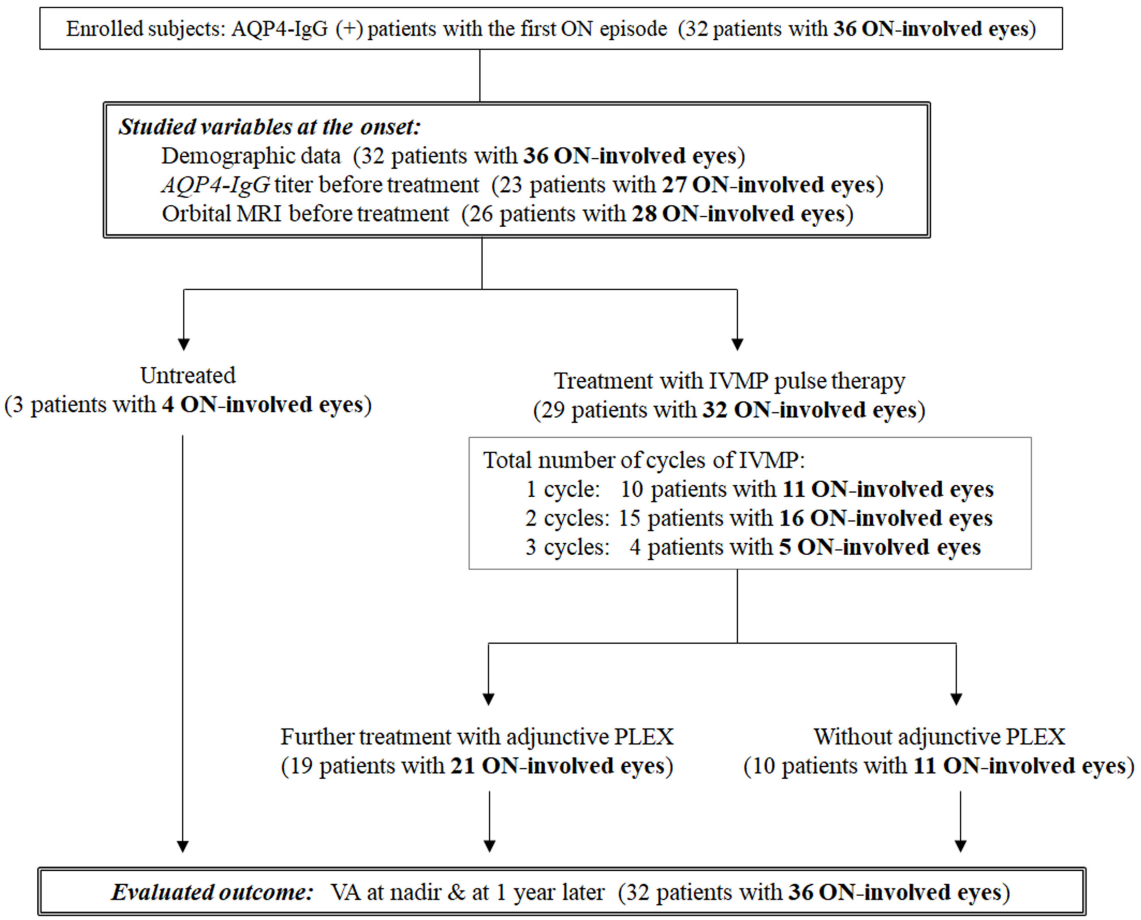

FIGURE 1 | Flow diagram of the subgroup classification according to the acute therapies. A total of 32 AQP4-IgG (+) patients with a first episode of optic neuritis (ON; 36 ON-involved eyes) were enrolled. Three patients were untreated, and the remaining 29 patients (32 ON-involved eyes) were initially treated with intravenous methylprednisolone pulse therapy. A total of 19 patients (21 ON-involved eyes) were further treated with adjunctive plasma exchange. AQP4-IgG, anti-aquaporin-4 autoantibodies; IVMP, intravenous methylprednisolone pulse therapy; ON, optic neuritis; PLEX, plasma exchange; VA, visual acuity.

number of involved segments in the following six areas of the optic nerves: anterior orbital, posterior orbital, canalicular, intracranial, chiasmal, and optic tract (32). Involvement of the optic nerves was judged based on imaging with short-T1 inversion recovery (STIR) sequence and gadolinium-enhanced fat-suppressed T1 imaging.

Subsequent Visual Prognosis

Corrected VA was initially measured by decimal acuities and later converted to the logarithmic minimum angle of resolution (logMAR) scale because of its statistical usability (33). The logMAR scores <0.0 were all regarded as 0.0, and logMAR scores >2.0 were all regarded as 2.0, resulting in the measured logMAR scores ranging between 0.0 (corrected decimal VA ≥ 1.0) and 2.0 (corrected decimal VA ≤ 0.01).

Serum AQP4-IgG Titration

Before the initiation of treatment, serum AQP4-IgG titer was evaluated in 27 of the 36 ON episodes with a microscopic live cell–based assay method, using human embryonic kidney 293 (HEK293) cells expressing the human M23-AQP4 protein and Alexa Fluor 488-conjugated secondary antibody (Life Technologies, Frederick, MD, USA) (34). The titration was performed semi-quantitatively with a serial two-fold end-point dilution method (35).

Data Analysis

Correlations between two continuous variables were evaluated with Spearman's rho, followed by a test of no correlation. When drawing the scatter plot for the days from ON onset to the initiation of acute treatment (i.e., IVMP pulse therapy, adjunctive PLEX), data from untreated patients were tentatively set to 1,000 for visual convenience after log transformation. Because the correlations were evaluated with a non-parametric statistical method, this tentative numerical conversion did not affect the results of the statistical analyses. After evaluating the correlation between each explanatory variable and the subsequent visual outcomes, multiple regression analysis was performed by employing variables of particular clinical interest and additional variables that had a significant impact ($p < 0.10$)

on the subsequent visual outcomes in the univariate analysis (36). Statistical analyses were performed using IBM SPSS Statistics 22.0 (IBM, Armonk, New York, USA) and MATLAB R2015a software.

RESULTS

Patient Backgrounds

Among the 32 enrolled NMOSD patients, 1 was male and 31 were female. The average ± SD of the age at ON onset (36 ON episodes) was 44.4 ± 15.8 years. The median (IQR; 25th−75th percentiles) of the serum AQP4-IgG titer was 1:8192 (1:1024–1:65,536); median (IQR) number of ON-involved optic nerve segments on orbital MRI was 3 segments (2–4 segments); median (IQR) days from ON onset to IVMP pulse therapy initiation was 9 days (4–33 days); median (IQR) number of cycles of IVMP pulse therapy in the acute phase was 2 cycles (1–2 cycles); and median (IQR) number of cycles of PLEX in the acute phase was 3 times (0–4 times). Six of the 32 patients had a clinical history of accompanying autoimmune-related diseases (rheumatoid arthritis, 2; Sjögren's syndrome, 2; systemic lupus erythematosus, 1; polymyositis, 1).

Among the 36 ON-involved eyes from 32 patients, 32 ON-involved eyes from 29 patients were treated in the acute phase with high-dose IVMP pulse therapy (1,000 mg/day) for 3 days, followed by low-dose oral prednisolone therapy for relapse prevention, whereas the remaining four ON episodes in three patients were not treated for unknown reasons. A single cycle of IVMP was administered to 11 ON-involved eyes from 10 patients, two cycles of IVMP were administered to six ON-involved eyes from 15 patients, and three cycles of IVMP were administered to five ON-involved eyes from four patients. Of the 32 ON-involved eyes from 29 patients who were treated with IVMP pulse therapy, 21 ON-involved eyes from 19 patients were later treated with adjunctive PLEX 3–6 times to achieve greater recovery in VA, and 1 of them was further treated with IVIg. Intravenous cyclophosphamide was not used in any of the enrolled subjects.

Factors That May Affect the Visual Prognosis

Correlation coefficients between the studied candidates of prognostic variables and the subsequent visual prognosis, represented by logMAR VA a year later, are listed in **Table 1**. The strongest prognostic variable at ON onset was the longitudinal length of the ON lesion (rho = 0.669, $p < 0.0001$). The days from ON onset to starting IVMP pulse therapy also showed a moderate to strong positive correlation with the visual prognosis (rho = 0.502, $p = 0.0018$). Moreover, the AQP4-IgG titer (rho = 0.24, $p = 0.23$), repeated cycles of IVMP pulse therapy (rho = −0.24, $p = 0.17$), days from ON onset to starting PLEX (rho = 0.13, $p = 0.44$), or cycles of PLEX (rho = −0.16, $p = 0.36$) showed no significant correlation with the subsequent visual prognosis. The cycles of IVMP pulse therapy (rho = −0.01, $p = 0.95$), days from ON onset to starting PLEX (rho = 0.21, $p = 0.37$), or cycles of PLEX (rho = −0.25, $p = 0.28$) showed no significant correlation with the subsequent visual outcomes even when being calculated within those who received these therapies.

TABLE 1 | Correlation coefficients between studied variables and visual outcome.

	Patients (eyes)	Spearman's rho with VA after 1 year	*p*-value
Age at ON onset	*n* = 32 (36)	0.404	0.0146
AQP4-IgG titer before starting IVMP	*n* = 23 (27)	0.237	0.23
ON-involved segments in orbital MRI (0–6)	*n* = 26 (28)	0.669	<0.0001
Treatments in the acute phase of ON			
Days from ON onset to starting IVMP	*n* = 32 (36)	0.502	0.0018
Cycles of IVMP	*n* = 32 (36)	−0.235	0.17
Cycles of IVMP among those treated	*n* = 29 (32)	−0.013	0.95
Days from ON onset to starting PLEX	*n* = 32 (36)	0.132	0.44
Cycles of PLEX	*n* = 32 (36)	−0.156	0.36
ON-involved eyes further treated by adjunctive PLEX after IVMP pulse therapy			
Days from ON onset to starting PLEX	*n* = 19 (21)	0.21	0.37
Cycles of PLEX	*n* = 19 (21)	−0.25	0.28

The p-values shown are the results of the test of no correlation.
AQP4-IgG, anti-aquaporin-4 autoantibody; IVMP, intravenous methylprednisolone; ON, optic neuritis; PLEX, plasma exchange; VA, visual acuity.

To visually confirm the observed correlation between rapidity of treatment in the acute phase and the subsequent visual prognosis, scatter plots with these two variables are shown in **Figure 2A**. Scatter plots with each of these variables and the ON-involved lesion length as a representative of ON severity are shown in **Figures 2B,C**. Because there was no significant correlation between rapidity of treatment and ON severity on MRI, the confounding effect of ON severity on the implied significance of rapidity of treatment in the acute phase for preserving subsequent VA was unlikely. When the partial correlation coefficient was calculated using ON-lesion length, days from ON onset to the start of IVMP, and visual outcomes at 1 year, the partial correlation coefficient between the rapidity of IVMP and visual outcomes was still statistically significant with a value of 0.437 ($p = 0.0248$, test of no correlation).

After univariate analyses, multiple regression analysis was additionally performed by employing demographic or therapeutic variables of particular clinical interest and further variables that showed $p < 0.10$ in the aforementioned univariate regression analyses. Consequently, the time from ON onset to the start of IVMP pulse therapy, cycles of IVMP pulse therapy, cycles of adjunctive PLEX, and age at ON onset were used as explanatory variables. The eventual VA after 1 year was used as the outcome variable. Shorter duration from ON onset to the start of IVMP pulse therapy [$F = 15.81$, $p = 0.0004$] and younger age at ON onset [$F = 8.31$, $p = 0.0071$] significantly contributed to better visual outcomes, whereas the number of cycles of IVMP [$F = 2.15$, $p = 0.15$] and adjunctive PLEX [$F = 0.29$, $p = 0.60$] did not. On removing the cycles of adjunctive PLEX from the

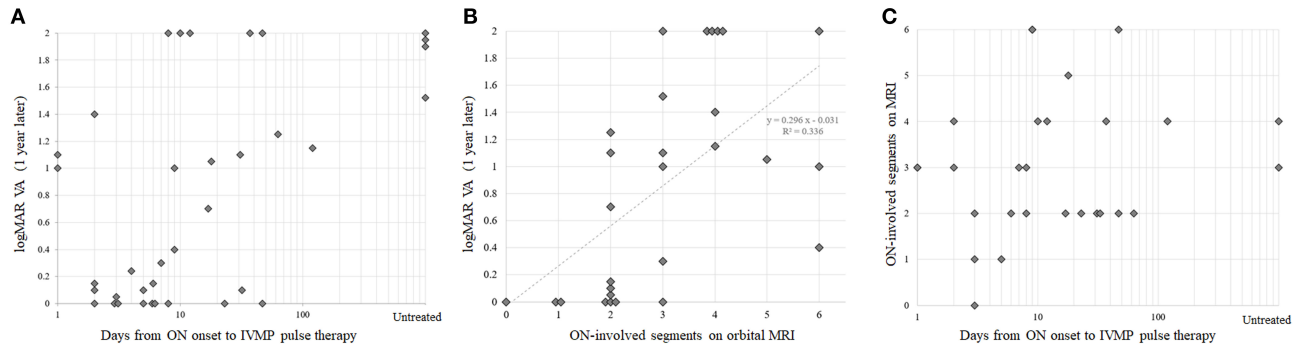

FIGURE 2 | Correlations between treatment rapidity, optic neuritis (ON) severity, and visual prognosis. Scatter plots with visual prognosis and therapeutic rapidity **(A)**, with visual prognosis and ON severity **(B)**, and with ON severity and therapeutic rapidity **(C)**. Note that the horizontal axes in panels **(A,C)** are log transformed. IVMP, intravenous methylprednisolone; logMAR, logarithmic minimum angle of resolution; ON, optic neuritis; VA, visual acuity.

explanatory variables, a shorter duration from ON onset to the start of IVMP pulse therapy [$F = 15.98$, $p = 0.0004$] and younger age at ON onset [$F = 9.04$, $p = 0.0051$] still significantly contributed to better visual outcomes, but the number of cycles of IVMP [$F = 1.78$, $p = 0.0840$] did not.

In addition to these clinical data at ON onset, the prognostic effect of other coexisting autoimmune-related diseases on eventual visual outcomes was also evaluated. The visual prognosis was suggested to be slightly worse in patients with other autoimmune-related diseases, but no statistically significant difference was observed (logMAR median 0.90 vs. 0.35; $p = 0.32$, Mann–Whitney U-test).

Adjunctive Effect of PLEX

Next, to exclude the possibility of confounding effect from PLEX to the prognostic impact of early IVMP pulse therapy, we calculated the partial correlation coefficient by using days from ON onset to start IVMP, times of performed PLEX, and visual outcomes at 1 year. As a result, the partial correlation coefficient between the rapidity of IVMP and visual outcomes was also statistically significant with the value of 0.567 ($p = 0.0004$, test of no correlation), suggesting that early administration of high-dose IVMP is important to preserve the long-term visual outcomes irrespective of the addition of PLEX as an adjunctive therapy. Meanwhile, the calculated partial correlation coefficient between times of PLEX and visual prognosis was 0.184 ($p = 0.29$). Based on these results, early IVMP pulse therapy was suggested to be more important than the timing or total times of adjunctive PLEX to preserve the subsequent visual outcomes.

DISCUSSION

In this study, we showed that rapid initiation of treatment (i.e., IVMP pulse therapy) in the acute phase of ON in patients with AQP4-IgG-positive NMOSD significantly improved the subsequent visual outcomes 1 year later. In line with our previous findings, the visual prognosis of ON in those with NMOSD was largely affected by the ON-lesion severity, which was represented by the number of ON-involved segments on orbital MRI in the acute phase (32). Moreover, the observed impact of rapid IVMP pulse therapy on the subsequent visual outcomes was independent of the severity of the ON lesion. A similar observation was reported in several previous reports. In a report from Germany (37), an early therapeutic intervention was suggested to result in a higher complete remission rate after NMOSD attacks. Same as the present study, this previous report also demonstrated the decreased therapeutic responses in the elderly patients. Another report suggested greater preservation of retinal nerve fiber layer thickness on optic coherence tomography in patients with NMOSD who were swiftly treated with IVMP pulse therapy in the acute phase of ON (38). A more recent study (39), in which a total of 27 patients with either AQP4-IgG-positive ON (AQP4-ON) or MOG-IgG-positive ON (MOG-ON) were retrospectively enrolled for treatment-related subgroup analyses, showed that those who were treated with IVMP pulse therapy within 7 days showed better visual outcomes 3 months later than those who started treatment more than 7 days after ON onset. Together with these previous studies, the present study supports the effectiveness of timely IVMP pulse therapy in preserving long-term VA in patients with NMOSD. This finding could be hypothetically explained by irreversible severe astrocytic damage and subsequent neuronal damage, accompanied with impairments in the blood–brain barrier and complement-mediated vascular permeability, which may steadily progress without swift administration of high-dose IVMP (40). Furthermore, although the rapidity of IVMP pulse therapy was confirmed to be effective in preserving long-term VA, the total number of cycles of IVMP pulse therapy failed to show a significant effect on the subsequent visual outcomes. This is consistent with the findings of a previous study that showed no effect of repeated IVMP pulse therapy after the second cycle on subsequent neurological disability (41).

In the early 1990s, more than 10 years before the serum AQP4-IgG and MOG-IgG were measured in patients with ON, a landmark clinical trial of the Optic Neuritis Treatment Trial (ONTT) was performed (42, 43). In the ONTT, a total of 457 ON patients were enrolled and randomly allocated to each oral prednisone group ($n = 156$): IVMP + oral prednisone group ($n = 151$) and oral placebo group ($n = 150$). The result of

ONTT was that patients in the IVMP + oral prednisone group showed significantly faster improvement of VA than those in the oral placebo group, but there was no significant difference in the subsequent visual outcomes between the groups both at 6 months and at 1 year. Based on these results, the general opinion among ophthalmologists and neurologists about the effectiveness of IVMP pulse therapy as an acute treatment for ON has long remained controversial. In 2004, a groundbreaking discovery came from a research group of Mayo Clinic that showed the presence of AQP4-IgG in the serum of patients who previously had "atypical" MS that exclusively presented recurrent ON and/or myelitis (1, 2). Later, reports of serum MOG-IgG came to be known to appear in many isolated ON cases (44–46). After these discoveries, serum positivity of these antibodies was retrospectively checked by using the stored serum samples from 177 of the enrolled patients in ONTT, revealing the presence of MOG-IgG only in three patients and AQP4-IgG in none of them (47). Based on this fact, ONTT can be regarded as a randomized controlled trial for the acute treatment of MS-ON and idiopathic ON (i.e., double-seronegative for MOG-IgG and AQP4-IgG). Consequently, we have to admit that the effectiveness of IVMP pulse therapy in MOG-ON and AQP4-ON to preserve the long-term (i.e., more than 6 months) visual outcomes has not been concluded to date.

Based on the results obtained, we propose a possible therapeutic strategy for patients with undiagnosed ON, as shown in **Figure 3**. Before deciding to administer high-dose IVMP pulse therapy to patients suspected of ON, clinicians should exclude the possibility of infectious ON (e.g., syphilitic ON with HIV infection, Lyme ON, and tuberculous ON) because IVMP monotherapy without antibiotics may aggravate disease activity in such conditions (8, 48–50). Although the incidence of infectious ON is much lower than that of ON of other noninfectious inflammatory causes, a comprehensive examination including medical history taking, fundoscopy, imaging, and blood testing is required to correctly differentiate infectious ON before deciding on the therapeutic strategy. Once a clinician determines that the patient is unlikely to have infectious ON, the next step is to decide whether to administer high-dose IVMP pulse therapy to the patient. Currently, as discussed earlier, IVMP pulse therapy is only recommended for patients with AQP4-IgG-positive NMOSD to achieve better long-term visual outcomes; these patients are mostly female (51, 52). For patients with other diseases (i.e., MS-ON, MOG-ON, idiopathic ON), there have been no randomized controlled trials of acute treatments, and evidence regarding the use of IVMP pulse therapy to achieve better long-term visual outcomes is yet to be established. Consequently, although IVMP pulse therapy would surely quicken visual recovery from nadir VA in any of these diseases, swift administration of IVMP pulse therapy may not be mandatory to preserve the long-term visual prognosis in patients with ON without serum AQP4-IgG. However, as patients with AQP4-ON are recommended to receive IVMP pulse therapy as soon as possible after clinical onset, clinicians are often required to proceed with IVMP pulse therapy administration before obtaining the results of serological tests for serum AQP4-IgG positivity. Although the majority of patients with AQP4-ON are female, the proportions of female patients in AQP4-ON cohorts of previous studies involving different ethnicities varied to some extent between 80 and 95% (53–55). Thus, regardless of the sex of patients with ON, clinicians may consider administering IVMP pulse therapy before confirming the positivity of serum AQP4-IgG once the rare differential diagnosis of infectious ON has been ruled out or considered unlikely.

Intravenous administration is usually selected as the route of high-dose steroid (i.e., 1,000 mg/day) in the acute phase of ON, but oral administration of bioequivalent doses to high-dose IVMP may also be used as an alternative to IVMP (56). Meanwhile, low-dose oral steroid (e.g., 1 mg/kg/day) monotherapy as an acute treatment should be avoided because such an approach to the acute ON episode may not only be an insufficient immunosuppressive treatment but also increase the risk of recurrent ON in MS-ON and idiopathic ON, as suggested in ONTT (43). The serum sample for the determination of serum AQP4-IgG and MOG-IgG should ideally be collected before the administration of IVMP pulse therapy. However, serum samples should be submitted for AQP4-IgG checkup even when IVMP pulse therapy has begun before the sample collection because a recent article reported that serum AQP4-IgG titer may not significantly decrease after IVMP pulse therapy or long-term oral steroid usage, although IVMP pulse therapy may decrease the AQP4-IgG titer to some extent with a narrowly significant level (57).

As a limitation of this study, all enrolled patients with NMOSD were Asian. Further clinical studies are needed to determine whether the observed effectiveness of IVMP pulse therapy in the acute phase of AQP4-ON to improve long-term visual outcomes can be generalized to other ethnicities. In addition, because this study was performed in a retrospective manner, a randomized controlled trial with a pure cohort of AQP4-ON is desired in the future to establish high-level evidence of the impact of swiftly initiating IVMP pulse therapy in the acute phase of AQP4-ON. Furthermore, we did not consider visual field impairments in this study. As is well known, AQP4-ON patients often present with sectional visual field impairment, such as bitemporal or altitudinal hemianopia and non-central scotoma (58), and these patients may present a relatively preserved VA at the nadir (i.e., >20/200 VA) despite the disability in daily living. However, the possible bias from these cases to this study was unlikely because the excluded NMOSD patients with relatively preserved VA in the acute phase of suspected ON episodes were only 3; the visual outcomes of these patients was much better than that of others regardless of the acute treatments, and it was scientifically reasonable to exclude these patients in advance from this study that evaluated the long-term visual outcomes. Another limitation was that 10 of the 32 enrolled patients had been already evaluated for the correlation between retinal nerve fiber layer thickness and the swiftness of IVMP pulse therapy in a previous article (38). However, the achieved results in the present study was reproduced when we analyzed by using only the new 22 patients, with the calculated Spearman's rho between the swiftness of IVMP pulse therapy

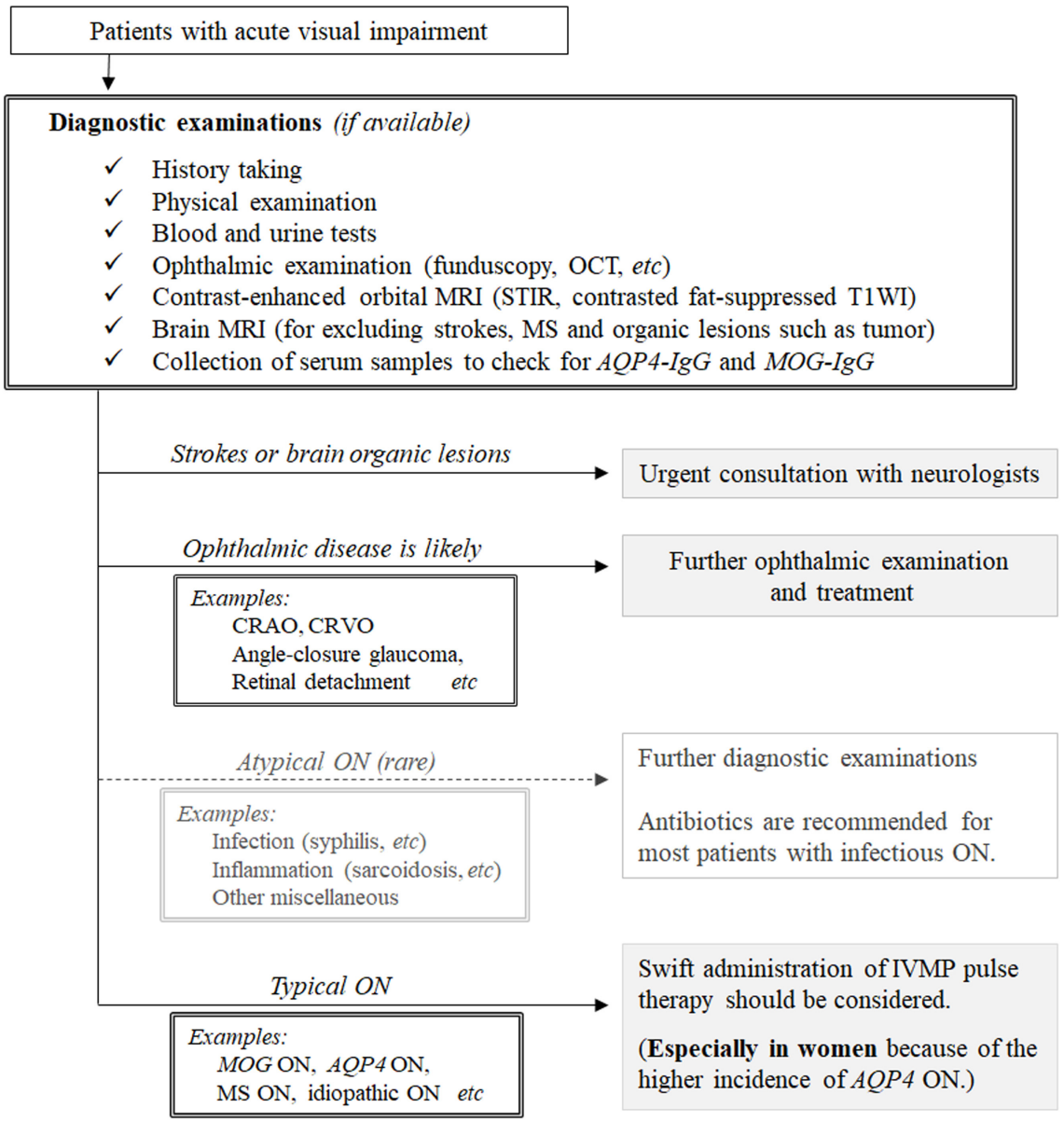

FIGURE 3 | A conceivable therapeutic strategy for patients suspected of having optic neuritis. AQP4-IgG, anti-aquaporin-4 autoantibodies; CRAO, central retinal artery occlusion; CRVO, central retinal vein occlusion; DDx, differential diagnosis; HIV, human immunodeficiency virus; IVMP, intravenous methylprednisolone; MS, multiple sclerosis; MOG-IgG, anti-myelin oligodendrocyte glycoprotein antibody; ON, optic neuritis; STIR, short T1 inversion recovery; T1WI, T1-weighted imaging.

and the visual outcomes of 0.433 ($p = 0.0348$). Thus, apart from the previous article, the present study further reinforced the rationale of swift IVMP pulse therapy in the acute phase of AQP4-ON to preserve long-term visual outcomes. Lastly, this study failed to show the effectiveness of the rapidity and cycles of adjunctive PLEX in preserving long-term visual outcomes, but this does not contradict the effectiveness of PLEX in patients with AQP4-ON. The relatively small number of patients treated with adjunctive PLEX and possible tendency of patients who were refractory to IVMP pulse therapy to be administered adjunctive PLEX may explain why the rapidity and cycles of adjunctive PLEX failed to yield significant results in this study. Overall, a randomized trial is needed to conclude the effectiveness of adjunctive PLEX after IVMP pulse therapy in patients with AQP4-ON.

CONCLUSIONS

In patients with AQP4-IgG-positive NMOSD, swift administration of high-dose IVMP pulse therapy is recommended to preserve the subsequent long-term visual

outcomes, even before obtaining the results of tests for serum AQP4-IgG positivity. Clinicians should consider immediate administration of IVMP pulse therapy in typical ON cases without waiting to confirm AQP4-IgG positivity, especially in female ON cases because of the female predominance in AQP4-ON.

DATA AVAILABILITY STATEMENT

The raw data supporting the conclusions of this article will be made available by the authors, without undue reservation.

ETHICS STATEMENT

The studies involving human participants were reviewed and approved by Tohoku University School of Medicine. The patients/participants provided their written informed consent to participate in this study.

AUTHOR CONTRIBUTIONS

TA drafted the article and created figures and tables. NH, TTake, and TN measured visual acuity at the nadir and 1 year later. TM, KF, and IN corrected MRI data. KF, MAo, TN, and IN supervised the study process. All authors contributed to the data review, interpretation of results, critical revision of article, and approval of final version of the article.

FUNDING

This study was supported by JSPS KAKENHI (grant number JP26293205).

REFERENCES

1. Lennon VA, Wingerchuk DM, Kryzer TJ, Pittock SJ, Lucchinetti CF, Fujihara K, et al. A serum autoantibody marker of neuromyelitis optica: distinction from multiple sclerosis. *Lancet.* (2004) 364:2106–12. doi: 10.1016/S0140-6736(04)17551-X
2. Lennon VA, Kryzer TJ, Pittock SJ, Verkman AS, Hinson SR. IgG marker of optic-spinal multiple sclerosis binds to the aquaporin-4 water channel. *J Exp Med.* (2005) 202:473–7. doi: 10.1084/jem.20050304
3. Wingerchuk DM, Banwell B, Bennett JL, Cabre P, Carroll W, Chitnis T, et al. International consensus diagnostic criteria for neuromyelitis optica spectrum disorders. *Neurology.* (2015) 85:177–89. doi: 10.1212/WNL.0000000000001729
4. Wingerchuk DM, Lennon VA, Pittock SJ, Lucchinetti CF, Weinshenker BG. Revised diagnostic criteria for neuromyelitis optica. *Neurology.* (2006) 66:1485–9. doi: 10.1212/01.wnl.0000216139.44259.74
5. Akaishi T, Takahashi T, Misu T, Abe M, Ishii T, Fujimori J, et al. Progressive patterns of neurological disability in multiple sclerosis and neuromyelitis optica spectrum disorders. *Sci Rep.* (2020) 10:13890. doi: 10.1038/s41598-020-70919-w
6. Akaishi T, Nakashima I, Takahashi T, Abe M, Ishii T, Aoki M. Neuromyelitis optica spectrum disorders with unevenly clustered attack occurrence. *Neurol Neuroimmunol Neuroinflamm.* (2020) 7:e640. doi: 10.1212/NXI.0000000000000640
7. Palace J, Lin DY, Zeng D, Majed M, Elsone L, Hamid S, et al. Outcome prediction models in AQP4-IgG positive neuromyelitis optica spectrum disorders. *Brain.* (2019) 142:1310–23. doi: 10.1093/brain/awz054
8. Horton L, Bennett JL. Acute management of optic neuritis: an evolving paradigm. *J Neuroophthalmol.* (2018) 38:358–67. doi: 10.1097/WNO.0000000000000700
9. Chen JJ, Pittock SJ, Flanagan EP, Lennon VA, Bhatti MT. Optic neuritis in the era of biomarkers. *Surv Ophthalmol.* (2020) 65:12–7. doi: 10.1016/j.survophthal.2019.08.001
10. Trebst C, Jarius S, Berthele A, Paul F, Schippling S, Wildemann B, et al. Update on the diagnosis and treatment of neuromyelitis optica: recommendations of the Neuromyelitis Optica Study Group (NEMOS). *J Neurol.* (2014) 261:1–16. doi: 10.1007/s00415-013-7169-7
11. Kimbrough DJ, Fujihara K, Jacob A, Lana-Peixoto MA, Leite MI, Levy M, et al. Treatment of neuromyelitis optica: review and recommendations. *Mult Scler Relat Disord.* (2012) 1:180–7. doi: 10.1016/j.msard.2012.06.002
12. Kleiter I, Gold R. Present and future therapies in neuromyelitis optica spectrum disorders. *Neurotherapeutics.* (2016) 13:70–83. doi: 10.1007/s13311-015-0400-8
13. Kleiter I, Gahlen A, Borisow N, Fischer K, Wernecke KD, Hellwig K, et al. Apheresis therapies for NMOSD attacks: a retrospective study of 207 therapeutic interventions. *Neurol Neuroimmunol Neuroinflamm.* (2018) 5:e504. doi: 10.1212/NXI.0000000000000504
14. Kowarik MC, Soltys J, Bennett JL. The treatment of neuromyelitis optica. *J Neuroophthalmol.* (2014) 34:70–82. doi: 10.1097/WNO.0000000000000102
15. Abboud H, Petrak A, Mealy M, Sasidharan S, Siddique L, Levy M. Treatment of acute relapses in neuromyelitis optica: Steroids alone versus steroids plus plasma exchange. *Mult Scler.* (2016) 22:185–92. doi: 10.1177/1352458515581438
16. Viswanathan S, Wong AH, Quek AM, Yuki N. Intravenous immunoglobulin may reduce relapse frequency in neuromyelitis optica. *J Neuroimmunol.* (2015) 282:92–6. doi: 10.1016/j.jneuroim.2015.03.021
17. Kessler RA, Mealy MA, Levy M. Treatment of neuromyelitis optica spectrum disorder: acute, preventive, and symptomatic. *Curr Treat Options Neurol.* (2016) 18:2. doi: 10.1007/s11940-015-0387-9
18. Watanabe S, Misu T, Miyazawa I, Nakashima I, Shiga Y, Fujihara K, et al. Low-dose corticosteroids reduce relapses in neuromyelitis optica: a retrospective analysis. *Mult Scler.* (2007) 13:968–74. doi: 10.1177/1352458507077189
19. Cree BAC, Bennett JL, Kim HJ, Weinshenker BG, Pittock SJ, Wingerchuk DM, et al. Inebilizumab for the treatment of neuromyelitis optica spectrum disorder (N-MOmentum): a double-blind, randomised placebo-controlled phase 2/3 trial. *Lancet.* (2019) 394:1352–63. doi: 10.1016/S0140-6736(19)31817-3
20. Pittock SJ, Berthele A, Fujihara K, Kim HJ, Levy M, Palace J, et al. Eculizumab in aquaporin-4-positive neuromyelitis optica spectrum disorder. *N Engl J Med.* (2019) 381:614–25. doi: 10.1056/NEJMoa1900866
21. Zhang C, Zhang M, Qiu W, Ma H, Zhang X, Zhu Z, et al. Safety and efficacy of tocilizumab versus azathioprine in highly relapsing neuromyelitis optica spectrum disorder (TANGO): an open-label, multicentre, randomised, phase 2 trial. *Lancet Neurol.* (2020) 19:391–401. doi: 10.1016/S1474-4422(20)30070-3
22. Yamamura T, Kleiter I, Fujihara K, Palace J, Greenberg B, Zakrzewska-Pniewska B, et al. Trial of satralizumab in neuromyelitis optica spectrum disorder. *N Engl J Med.* (2019) 381:2114–24. doi: 10.1056/NEJMoa1901747
23. Akaishi T, Sato DK, Nakashima I, Takeshita T, Takahashi T, Doi H, et al. MRI and retinal abnormalities in isolated optic neuritis with myelin oligodendrocyte glycoprotein and aquaporin-4 antibodies: a comparative study. *J Neurol Neurosurg Psychiatry.* (2016) 87:446–8. doi: 10.1136/jnnp-2014-310206
24. Mealy MA, Boscoe A, Caro J, Levy M. Assessment of patients with neuromyelitis optica spectrum disorder using the EQ-5D. *Int J MS Care.* (2019) 21:129–34. doi: 10.7224/1537-2073.2017-076
25. Huda S, Whittam D, Bhojak M, Chamberlain J, Noonan C, Jacob A. Neuromyelitis optica spectrum disorders. *Clin Med (Lond).* (2019) 19:169–76. doi: 10.7861/clinmedicine.19-2-169

26. Sherman E, Han MH. Acute and chronic management of neuromyelitis optica spectrum disorder. *Curr Treat Options Neurol.* (2015) 17:48. doi: 10.1007/s11940-015-0378-x
27. Wingerchuk DM, Hogancamp WF, O'Brien PC, Weinshenker BG. The clinical course of neuromyelitis optica (Devic's syndrome). *Neurology.* (1999) 53:1107–14. doi: 10.1212/WNL.53.5.1107
28. Akaishi T, Takahashi T, Fujihara K, Misu T, Abe M, Ishii T, et al. Risk factors of attacks in neuromyelitis optica spectrum disorders. *J Neuroimmunol.* (2020) 343:577236. doi: 10.1016/j.jneuroim.2020.577236
29. Shahmohammadi S, Doosti R, Shahmohammadi A, Mohammadianinejad SE, Sahraian MA, Azimi AR, et al. Autoimmune diseases associated with neuromyelitis optica spectrum disorders: a literature review. *Mult Scler Relat Disord.* (2019) 27:350–63. doi: 10.1016/j.msard.2018.11.008
30. Mealy MA, Whetstone A, Orman G, Izbudak I, Calabresi PA, Levy M. Longitudinally extensive optic neuritis as an MRI biomarker distinguishes neuromyelitis optica from multiple sclerosis. *J Neurol Sci.* (2015) 355:59–63. doi: 10.1016/j.jns.2015.05.013
31. Akaishi T, Nakashima I, Takeshita T, Kaneko K, Mugikura S, Sato DK, et al. Different etiologies and prognoses of optic neuritis in demyelinating diseases. *J Neuroimmunol.* (2016) 299:152–7. doi: 10.1016/j.jneuroim.2016.09.007
32. Akaishi T, Nakashima I, Takeshita T, Mugikura S, Sato DK, Takahashi T, et al. Lesion length of optic neuritis impacts visual prognosis in neuromyelitis optica. *J Neuroimmunol.* (2016) 293:28–33. doi: 10.1016/j.jneuroim.2016.02.004
33. Holladay JT. Proper method for calculating average visual acuity. *J Refract Surg.* (1997) 13:388–91.
34. Takahashi T, Fujihara K, Nakashima I, Misu T, Miyazawa I, Nakamura M, et al. Establishment of a new sensitive assay for anti-human aquaporin-4 antibody in neuromyelitis optica. *Tohoku J Exp Med.* (2006) 210:307–13. doi: 10.1620/tjem.210.307
35. Valentino P, Marnetto F, Granieri L, Capobianco M, Bertolotto A. Aquaporin-4 antibody titration in NMO patients treated with rituximab: a retrospective study. *Neurol Neuroimmunol Neuroinflamm.* (2017) 4:e317. doi: 10.1212/NXI.0000000000000317
36. Ranganathan P, Pramesh CS, Aggarwal R. Common pitfalls in statistical analysis: Logistic regression. *Perspect Clin Res.* (2017) 8:148–51. doi: 10.4103/picr.PICR_123_17
37. Kleiter I, Gahlen A, Borisow N, Fischer K, Wernecke KD, Wegner B, et al. Neuromyelitis optica: Evaluation of 871 attacks and 1,153 treatment courses. *Ann Neurol.* (2016) 79:206–16. doi: 10.1002/ana.24554
38. Nakamura M, Nakazawa T, Doi H, Hariya T, Omodaka K, Misu T, et al. Early high-dose intravenous methylprednisolone is effective in preserving retinal nerve fiber layer thickness in patients with neuromyelitis optica. *Graefes Arch Clin Exp Ophthalmol.* (2010) 248:1777–85. doi: 10.1007/s00417-010-1344-7
39. Stiebel-Kalish H, Hellmann MA, Mimouni M, Paul F, Bialer O, Bach M, et al. Does time equal vision in the acute treatment of a cohort of AQP4 and MOG optic neuritis? *Neurol Neuroimmunol Neuroinflamm.* (2019) 6:e572. doi: 10.1212/NXI.0000000000000572
40. Mitsdoerffer M, Kuchroo V, Korn T. Immunology of neuromyelitis optica: a T cell-B cell collaboration. *Ann N Y Acad Sci.* (2013) 1283:57–66. doi: 10.1111/nyas.12118
41. Yamasaki R, Matsushita T, Fukazawa T, Yokoyama K, Fujihara K, Ogino M, et al. Efficacy of intravenous methylprednisolone pulse therapy in patients with multiple sclerosis and neuromyelitis optica. *Mult Scler.* (2016) 22:1337–48. doi: 10.1177/1352458515617248
42. Beck RW, Cleary PA. Optic neuritis treatment trial. One-year follow-up results. *Arch Ophthalmol.* (1993) 111:773–5. doi: 10.1001/archopht.1993.01090060061023
43. Beck RW, Cleary PA, Anderson MM, Jr., Keltner JL, Shults WT, et al. A randomized, controlled trial of corticosteroids in the treatment of acute optic neuritis. The Optic Neuritis Study Group. *N Engl J Med.* (1992) 326:581–8.
44. Ramanathan S, Reddel SW, Henderson A, Parratt JD, Barnett M, Gatt PN, et al. Antibodies to myelin oligodendrocyte glycoprotein in bilateral and recurrent optic neuritis. *Neurol Neuroimmunol Neuroinflamm.* (2014) 1:e40. doi: 10.1212/NXI.0000000000000040
45. Rostásy K, Mader S, Hennes EM, Schanda K, Gredler V, Guenther A, et al. Persisting myelin oligodendrocyte glycoprotein antibodies in aquaporin-4 antibody negative pediatric neuromyelitis optica. *Mult Scler.* (2013) 19:1052–9. doi: 10.1177/1352458512470310
46. Rostasy K, Mader S, Schanda K, Huppke P, Gärtner J, Kraus V, et al. Anti-myelin oligodendrocyte glycoprotein antibodies in pediatric patients with optic neuritis. *Arch Neurol.* (2012) 69:752–6. doi: 10.1001/archneurol.2011.2956
47. Chen JJ, Tobin WO, Majed M, Jitprapaikulsan J, Fryer JP, Leavitt JA, et al. Prevalence of myelin oligodendrocyte glycoprotein and aquaporin-4-IgG in patients in the optic neuritis treatment trial. *JAMA Ophthalmol.* (2018) 136:419–22. doi: 10.1001/jamaophthalmol.2017.6757
48. Apinyawasisuk S, Poonyathalang A, Preechawat P, Vanikieti K. Syphilitic optic neuropathy: re-emerging cases over a 2-year period. *Neuroophthalmology.* (2016) 40:69–73. doi: 10.3109/01658107.2015.1134586
49. Smith GT, Goldmeier D, Migdal C. Neurosyphilis with optic neuritis: an update. *Postgrad Med J.* (2006) 82:36–9. doi: 10.1136/pgmj.2004.020875
50. Blanc F, Ballonzoli L, Marcel C, De Martino S, Jaulhac B, de Seze J. Lyme optic neuritis. *J Neurol Sci.* (2010) 295:117–9. doi: 10.1016/j.jns.2010.05.009
51. Yamagami A, Wakakura M, Inoue K, Ishikawa H, Takahashi T, Tanaka K. Clinical characteristics of anti-aquaporin 4 antibody positive optic neuritis in Japan. *Neuroophthalmology.* (2019) 43:71–80. doi: 10.1080/01658107.2018.1520905
52. Pandit L, Asgari N, Apiwattanakul M, Palace J, Paul F, Leite MI, et al. Demographic and clinical features of neuromyelitis optica: a review. *Mult Scler.* (2015) 21:845–53. doi: 10.1177/1352458515572406
53. Peng Y, Liu L, Zheng Y, Qiao Z, Feng K, Wang J. Diagnostic implications of MOG/AQP4 antibodies in recurrent optic neuritis. *Exp Ther Med.* (2018) 16:950–8. doi: 10.3892/etm.2018.6273
54. Ishikawa H, Kezuka T, Shikishima K, Yamagami A, Hiraoka M, Chuman H, et al. Epidemiologic and clinical characteristics of optic neuritis in Japan. *Ophthalmology.* (2019) 126:1385–98. doi: 10.1016/j.ophtha.2019.04.042
55. Srikajon J, Siritho S, Ngamsombat C, Prayoonwiwat N, Chirapapaisan N. Differences in clinical features between optic neuritis in neuromyelitis optica spectrum disorders and in multiple sclerosis. *Mult Scler J Exp Transl Clin.* (2018) 4:2055217318791196. doi: 10.1177/2055217318791196
56. Morrow SA, Fraser JA, Day C, Bowman D, Rosehart H, Kremenchutzky M, et al. Effect of treating acute optic neuritis with bioequivalent oral vs intravenous corticosteroids: a randomized clinical trial. *JAMA Neurol.* (2018) 75:690–6. doi: 10.1001/jamaneurol.2018.0024
57. Akaishi T, Takahashi T, Nakashima I, Abe M, Ishii T, Aoki M, et al. Repeated follow-up of AQP4-IgG titer by cell-based assay in neuromyelitis optica spectrum disorders (NMOSD). *J Neurol Sci.* (2020) 410:116671. doi: 10.1016/j.jns.2020.116671
58. Nakajima H, Hosokawa T, Sugino M, Kimura F, Sugasawa J, Hanafusa T, et al. Visual field defects of optic neuritis in neuromyelitis optica compared with multiple sclerosis. *BMC Neurol.* (2010) 10:45. doi: 10.1186/1471-2377-10-45

Conflict of Interest: The authors declare that the research was conducted in the absence of any commercial or financial relationships that could be construed as a potential conflict of interest.

Copyright © 2020 Akaishi, Takeshita, Himori, Takahashi, Misu, Ogawa, Kaneko, Fujimori, Abe, Ishii, Fujihara, Aoki, Nakazawa and Nakashima. This is an open-access article distributed under the terms of the Creative Commons Attribution License (CC BY). The use, distribution or reproduction in other forums is permitted, provided the original author(s) and the copyright owner(s) are credited and that the original publication in this journal is cited, in accordance with accepted academic practice. No use, distribution or reproduction is permitted which does not comply with these terms.

frontiers in Neurology

ORIGINAL RESEARCH
published: 15 September 2020
doi: 10.3389/fneur.2020.00858

Morphological Outer Retina Findings in Multiple Sclerosis Patients With or Without Optic Neuritis

Lucia Ziccardi[1], *Lucilla Barbano*[1]*, *Laura Boffa*[2], *Maria Albanese*[2], *Andrzej Grzybowski*[3,4], *Diego Centonze*[2,5] *and Vincenzo Parisi*[1]

[1] *Istituto di Ricovero e Cura a Carattere Scientifico - Fondazione Bietti, Rome, Italy,* [2] *Unit of Neurology, Department of Systems Medicine, Tor Vergata University, Rome, Italy,* [3] *Department of Ophthalmology, University of Warmia and Mazury, Olsztyn, Poland,* [4] *Institute for Research in Ophthalmology, Foundation for Ophthalmology Development, Poznan, Poland,* [5] *Istituto di Ricovero e Cura a Carattere Scientifico Neuromed - Unit of Neurology and Neurorehabilitation, Pozzilli, Italy*

Purpose: To investigate on the morphology of the macular inner (IR) and outer (OR) layers in multiple sclerosis (MS) patients with and without history of optic neuritis (ON), followed by good or poor recovery of best corrected visual acuity (BCVA).

Methods: Thirty-five normal control subjects and 93 relapsing remitting MS patients were enrolled. Of this, 40 MS patients without ON (MS-noON, 40 eyes), 27 with history of ON and good BCVA recovery (MS-ON-G, 27 eyes), and 26 with history of ON and poor BCVA recovery (MS-ON-P, 26 eyes) were studied. Controls and MS patients underwent an extensive ophthalmological examination including spectral-domain optical coherence tomography evaluating in 3 localized macular areas (0–1 mm, Area 1; 1–3 mm, Area 2; 3- 6 mm, Area 3), volumes (MV), and thicknesses (MT) of the whole retina (WR), further segmented in IR and OR. The differences of MV and MT between the groups were tested by ANOVA. In the MS-ON-P group, the correlations between MV and MT and BCVA were evaluated by Pearson's test.

Results: When compared to controls, the MS-noON group showed not significantly ($p > 0.01$) different MVs, whereas MTs were significantly ($p < 0.01$) reduced in the evaluation of WR and IR. In the MS-ON-G group, a significant ($p < 0.01$) reduction of WR and IR MVs and MTs was found in Areas 2 and 3; OR MVs and MTs were similar ($p > 0.01$) to controls. In the MS-ON-P group a significant ($p < 0.01$) reduction of WR, IR, and OR MVs and MTs was detected in all areas; the BCVA reduction was significantly ($p < 0.01$) correlated with WR and IR MVs and MTs.

Conclusions: In MS without history of ON or when ON is followed by a good BCVA recovery, the neurodegenerative process is limited to IR macular layers; in the presence of ON, with a poor BCVA recovery, a morphological impairment of both IR and OR macular layers occurs.

Keywords: multiple sclerosis, optic neuritis (ON), SD-OCT imaging, neurodegeneration, outer retina

OPEN ACCESS

Edited by:
Gemma Caterina Maria Rossi, Fondazione Ospedale San Matteo (IRCCS), Italy

Reviewed by:
Raed Behbehani, Al Bahar Eye Center, Kuwait
Piero Barboni, Studio Oculistico d'Azeglio, Italy

***Correspondence:**
Lucilla Barbano
lucilla.barbano@fondazionebietti.it

Specialty section:
This article was submitted to Neuro-Ophthalmology, a section of the journal Frontiers in Neurology

Received: *21 May 2020*
Accepted: *07 July 2020*
Published: *15 September 2020*

Citation:
Ziccardi L, Barbano L, Boffa L, Albanese M, Grzybowski A, Centonze D and Parisi V (2020) Morphological Outer Retina Findings in Multiple Sclerosis Patients With or Without Optic Neuritis. Front. Neurol. 11:858. doi: 10.3389/fneur.2020.00858

INTRODUCTION

In about 20–25% of multiple sclerosis (MS) patients, the pathology can onset with retrobulbar optic neuritis (ON) (1), that is followed by a secondary neurodegenerative process, reflecting retrograde degeneration that involves retinal ganglion cells (RGCs) and their axons (2).

The effects of this neurodegenerative process on the neuro-retinal structure can be objectively studied by Optical Coherence Tomography (OCT), that usually detects a reduction of retinal nerve fibers layer (RNFL) thickness (3–5).

An interesting and widely discussed topic in MS with or without ON has been to investigate whether the retinal elements of the macular region are morphologically impaired.

Currently, with the innovative Spectral domain-OCT (Sd-OCT) technique, it is possible to selectively segment the macular volume (MV) and thickness (MT) of the outer (OR) and inner retinal (IR) layers (6). IR abnormalities [thinning of RGCs/inner plexiform layer (GC/IPL) and thinning/thickening of the inner nuclear layer (INL) and reduced whole macular volume (4, 7–10)] are known to occur in MS (11–13) with and without previous optic neuritis, whereas data about morphological macular OR changes are controversial (7, 12, 14–19). All this suggests that the MS neurodegenerative process involves the macular layers and mainly the ganglionic elements located in the IR.

However, it is not yet entirely clarified whether the neurodegeneration could extend beyond the level of the INL (14) toward the macular pre-ganglionic elements, thus involving photoreceptors and bipolar cells forming the OR (20). Indeed, it is of great interest to identify whether there is a morphological involvement of specific IR and/or OR macular elements in the neurodegenerative process of MS, in the occurrence of ON or not, and whether the macular morphological condition is linked to the recovery of visual acuity after the ON event.

Therefore, our aim was to evaluate the morphology of IR and OR layers in localized macular areas in MS patients with and without history of ON, with good or poor recovery of high-contrast best corrected visual acuity (BCVA). Relative results obtained in MS patients might identify whether macular OR layers are morphologically involved in the MS neurodegenerative process, contributing to this widely debated topic. In addition, we aimed to assess whether the OR and IR morphology may be related to the good or poor recovery of BCVA or not.

MATERIALS AND METHODS

Participants

All research procedures described in this work adhered to the tenets of the Declaration of Helsinki. The study protocol was approved by the local Ethical Committee (Comitato Etico Centrale IRCCS Lazio, Sezione IFO/Fondazione Bietti, Rome, Italy) and upon recruitment, informed consent after a full explanation of the procedure was obtained from each subject enrolled in the study.

Ninety-three relapsing remitting (RR) MS patients were enrolled at the Visual Neurophysiology and Neuro-Ophthalmology Research Unit, IRCCS- Fondazione Bietti referred by the Neurology Department of Tor Vergata Policlinic of Rome, between January 2014 and September 2018.

In order to obtain homogeneous MS groups (with ON and without ON followed by poor or good recovery of VA, see below), the MS patients were selected form a large cohort ($n = 358$) based on the following demographic and clinical characteristics:

1) Age between 28 and 45 years;
2) Diagnosis of RR MS according to validated 2010 McDonald criteria (21);
3) MS disease duration (MS-DD), estimated as the number of years from onset to the most recent assessment of disability, ranging from 5 to 22 years;
4) Expanded Disability Status Scale (EDSS), as ten-point disease severity derived from nine ratings for individual neurological domains (22), ranging from 0 to 3; this score was assessed by two trained (Neurostatus: available at http://www.neurostatus.net/index.php?file=start) neurologists (LaB and MA)
5) Treatment with disease-modifying therapies (DMT) currently approved for preventing MS relapses. DMT considered in our study were Interferon-β-1a, Interferon-β-1b, Peginterferon beta-1a, Glatiramer acetate, Natalizumab, Dimethyl fumarate, and Teriflunomide (23).
6) Absence of ON or a single episode of ON without recurrence, that elapsed from the onset of the disease at least 12 months (range 13–20 months) before the inclusion in the study. For MS patients with ON, this criteria was chosen, since it is known that the retrograde degeneration following ON occurs over a period of 6 months (24). When a MS patient was affected by ON in both eyes, we studied the eye affected longer that met the inclusion criteria.
7) Based on the ophthalmological examination, other inclusion criteria were: absence of glaucoma or other diseases involving cornea, lens, uvea, and retina; absence of systemic diseases (i.e., diabetes); BCVA between 0 and 1 LogMAR of the Early Treatment of Diabetic Retinopathy (ETDRS) charts; absence of central visual field defects and ability to maintain a stable fixation that allowed a Sd-OCT scan to be performed (see below).

A group of selected 35 age-matched healthy subjects (mean age: 39.5 ± 5.4 years), providing 35 normal eyes, with BCVA of 0.0 LogMAR, served as controls.

The selected MS patients were divided into two groups on the basis of previous history of ON or not. In the assignment to the two groups, similar age, MS-DD, and EDSS values were considered.

A total of 40 MS patients (mean age 40.6 ± 3.9 years; 26 females and 14 males; mean MS-DD 8.6 ± 4.23 years, range 5–21 years; mean EDSS score 1.48 ± 1.10, range 0–3) without history of unilateral or bilateral clinical signs of ON (i.e., painless reduction of BCVA, contrast sensitivity, color vision, and any type of visual filed defects) and a high-contrast BCVA of 0.0 logMAR were included. When both eyes met the inclusion criteria, only one eye was randomly chosen for the study. Therefore, we considered 40 eyes from 40 MS patients without ON (MS-noON Group).

TABLE 1 | Demographic and clinical features in Multiple Sclerosis patients without Optic Neuritis (MS-noON), with Optic Neuritis and good recovery of best corrected visual acuity (MS-ON-G) and with Optic Neuritis and poor recovery of best corrected visual acuity (MS-ON-P).

	MS-noON (*N* = 40) mean ± 1SD	MS-ON-G (*N* = 27) mean ± 1SD	MS-ON-P (*N* = 26) mean ± 1SD
Age (years)	40.6 ± 3.9	38.2 ± 4.7[§]	39.4 ± 3.8[§,#]
MS-DD (years)	8.6 ± 4.23	9.2 ± 6.2[§]	9.4 ± 6.6[§,#]
EDSS score	1.5 ± 1.1	1.6 ± 1.0[§]	1.6 ± 1.1[§,#]
ON (N)	-	1.0 ± 0.0	1.0 ± 0.0[#]
Time elapsed from ON (months)	-	15.3 ± 2.4	14.9 ± 2.7[#]

N, number; SD, one Standard Deviation of the mean; MS-DD, Multiple Sclerosis Disease Duration; EDSS, Expanded Disability Status Scale; ON, optic neuritis. One-way analysis of variance between groups: [§]p > 0.01 vs. MS-noON group, [#]p > 0.01 vs. MS-ON-G group.

A total of 53 MS patients (mean age 38.9 ± 4.2 years; 32 females and 21 males) with previous history of unilateral or bilateral ON were included. They were further divided in to two groups on the basis of the recovery of BCVA after ON:

A total of 27 MS patients (mean age 38.2 ± 4.7 years; 17 females and 10 males; mean MS-DD 9.2 ± 6.2 years, range 5–22 years; mean EDSS score 1.59 ± 1.02, range 0–3) with previous history of single unilateral or bilateral ON and with "good" recovery of high-contrast BCVA (0.0 logMAR) after ON were included. Therefore, we considered 27 eyes from 27 MS patients with ON for the (MS-ON-G) group;

A total of 26 MS patients (mean age 39.4 ± 3.8 years; 15 females and 11 males; mean MS-DD 9.4 ± 6.6 years, range 5–22 years; mean EDSS score 1.62 ± 1.08, range 0–3) with previous history of single unilateral or bilateral ON with "poor" recovery of high-contrast BCVA (between 0.2 and 1 logMAR) after ON were chosen. Therefore, we considered 26 eyes from 26 MS patients with ON for the (MS-ON-P) group.

Based on the previous mentioned inclusion criteria, the MS groups with or without ON were homogeneous for age, MS-DD, and EDSS and the MS groups with ON were homogeneous for the number of ON and for the time elapsed from ON (see below section Demographic and Clinical Features and **Table 1**).

Sd-OCT Assessment

The retinal morphology can be explored *in vivo* by Sd-OCT, providing layer-by-layer objective measurements of anatomical structures related to the macular area (25). Sd-OCT scans were obtained in a dark room after pupil dilation with tropicamide 1% eye drops and each scan was carefully reviewed for the accurate identification and segmentation of the retinal layers by two expert graders (LZ, LuB) to exclude cases of failed segmentation. Quality control and APOSTEL recommendations according to the published criteria were followed (26, 27). The OCT image quality signal strength index of the acquired scan was at least 40. Scans that did not fulfill the above criteria were excluded from the analysis.

We used the RTVue-100 device version 6.3 (Optovue, Fremont, CA), which uses a low-coherence light source centered at 840 nm with 50 nm bandwidth, which gives an axial resolution of 5 micrometers.

By using the MM5 protocol, we collected MV and MT data from the ETDRS 9 regions map. The MM5 grid scanning protocol consists of 11 horizontal lines with 5 mm scan length, 6 horizontal lines with 3 mm scan length, 11 vertical lines with 5 mm scan length, and 6 vertical lines with 3 mm scan length each at 0.5 mm intervals, all centered at the fovea. The number of A-scans in long horizontal and vertical lines is 668 and the number of A-scans in short horizontal and vertical lines is 400. This scan configuration provided an acquisition rate of 26.000 A-scans /second.

The segmentation algorithm of the MM5 scanning protocol also enables the automatic segmentation of MV and MT, of whole retina (WR), IR, and OR from the square grid centered on fixation target. The software automatically divides the inner and outer neurosensory retinas at the boundary between the INL and the outer plexiform layer (OPL). The OR encloses the OPL, the outer nuclear layer, and the photoreceptor layer. The IR examines the RNFL, the GC/IPL, and the INL. The boundaries of the OR were the posterior of the OPL and the photoreceptor inner segment/outer segment junction. The following boundaries were identified for the IR segmentation: the inner limiting membrane and the posterior of the INL.

Retinal thickness was generated automatically as thickness is measured between the two interfaces (the vitreoretinal surface and the basement membrane of the RPE-Bruch membrane complex) at each measurement point along the scan's x-axis. We selected the MT map analysis protocol on the device to display the numeric averages of the measurements in each of the 9 ETDRS map sectors. A 3D model of the retina was computed and MV were assessed for each of the subfields (within 1, 3, and 6 mm, respectively) as defined by the ETDRS. Mean values of MV and MT from a circular 1 mm area and from annular ETDRS regions outside the 1 mm central one were calculated averaging the supero-infero-nasal-temporal values.

For OR, IR, and for the whole retina (WR=IR+OR), the software provides mean volumes and thicknesses (within 1, 3, and 6 mm, measured in mm3 and microns, respectively) that are displayed topographically in each of the 9 ETDRS map sectors.

We considered MVs of WR, IR, and OR measured within:

1) the 1 mm central area (named as Area 1, directly provided by the Sd-OCT machine)
2) the middle 1–3 mm ring (named as Area 2, obtained by subtracting from the displayed volume within 3 mm of the ones within the 1 mm area),
3) the external 3–6 mm ring (named as Area 3, obtained by subtracting from the displayed volume within 6 mm of the one within 3 mm directly provided by the Sd-OCT machine),
4) the whole 6 mm area (named as Area 1+Area 2+ Area 3, directly provided by the Sd-OCT machine).

We also analyzed MTs of WR, IR, and OR from Areas 1, 2, and 3 as provided directly from the device for the ETDRS map: foveal (0–1 mm), perifoveal (1–3 mm), and parafoveal (3–6 mm) areas, respectively.

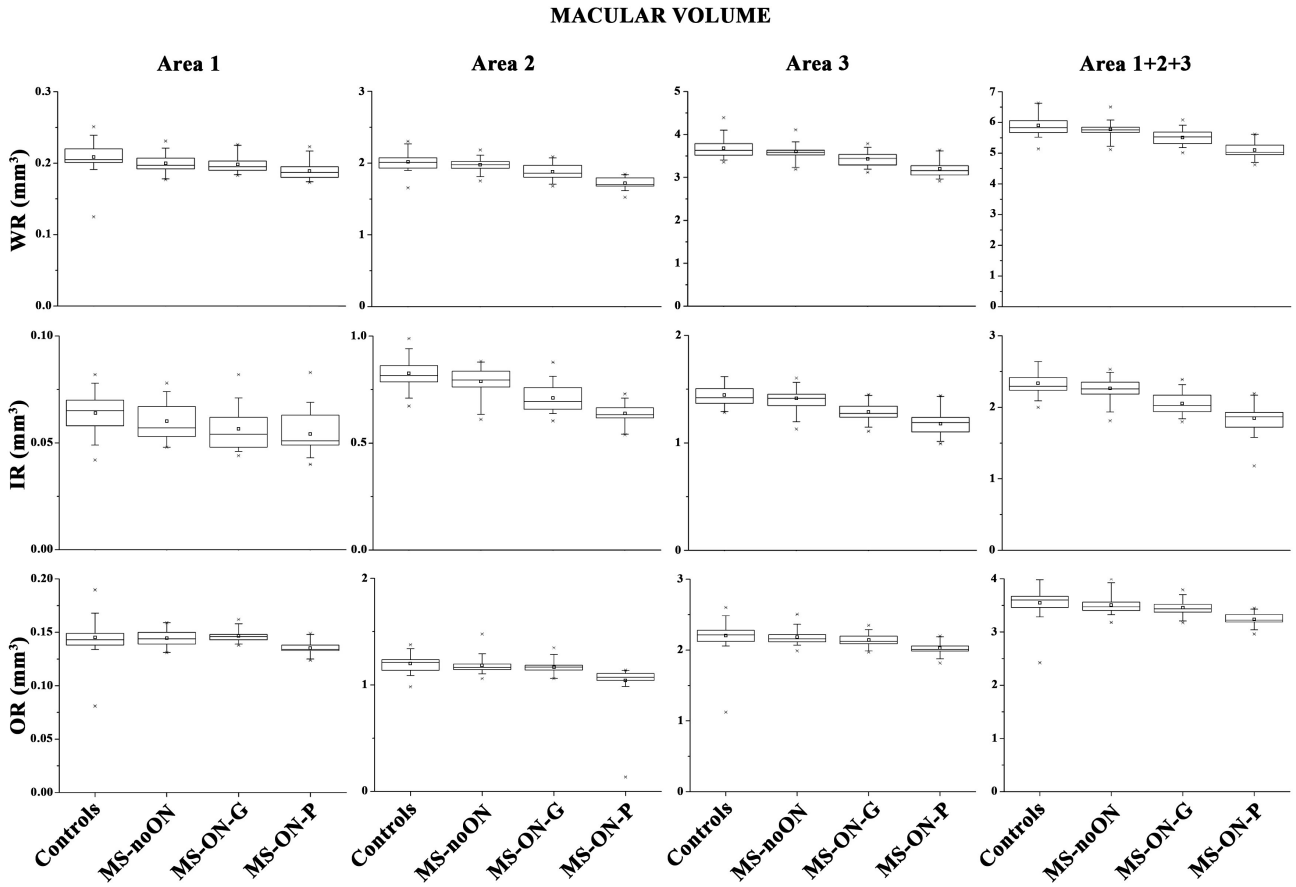

FIGURE 1 | Box plots of Spectral domain-Optical Coherence Tomography macular volumes in control (C) eyes, Multiple Sclerosis patients without Optic Neuritis (MS-noON), with Optic Neuritis and good recovery of best corrected visual acuity (MS-ON-G), and with Optic Neuritis and poor recovery of best corrected visual acuity (MS-ON-P). WR-MV= Whole Retinal Macular Volume; IR-MV= Inner Area Macular Volume; OR-MV = Outer Retina Macular Volume; Area 1= circular area 1 mm centered to the fovea; Area 2 = annular area 1–3 mm centered to the fovea; Area 3 = annular area 3–6 mm centered to the fovea; Area 1+2+3 = whole area within 6 mm.

Mean values of MV and MT from circular/annular ETDRS regions were calculated averaging the supero-infero-nasal-temporal values.

Statistical Analysis

The differences of age, MS-DD, and EDSS between the MS-noON, MS-ON-G, and MS-ON-P groups were evaluated by the one-way analysis of variance (ANOVA). The differences of the number of ON and the time elapsed from the ON between the MS-ON-G and MS-ON- P groups were evaluated by the ANOVA.

The difference of mean values of Sd-OCT parameters (MVs and MTs) detected in the controls, MS-noON, MS-ON-G, and MS-ON-P groups were also evaluated by ANOVA. A p-value of 0.01 was chosen as significant to compensate for multiple comparisons. Moreover, in the MS-ON-P group, multiple regression analysis was performed between BCVA and WR, IR, and OR MV and MT values, respectively. As usual, we chose a p-value of 0.05 as significant. Minitab 17 (version 1) software was used for statistical analysis.

RESULTS

Demographic and Clinical Features

On **Table 1** we reported the demographic and clinical features observed in the MS-noON, MS-ON-G, and MS-ON-P groups. The descriptive statistics of age, MS-DD, and EDSS values were not significantly different between the MS-noON, MS-ON-G, and MS-ON-P groups. The descriptive statistics of the number of ON and the time elapsed from ON were not significantly different between the MS-ON-G and MS-ON-P groups.

Sd-OCT Macular Volume Data

On **Figure 1** we presented the box plots of the values of the WR, IR, and OR MV measured from each localized area observed in the control, MS-noON, MS-ON-G, and MS-ON-P groups. On **Table 2**, the statistical analysis between groups is also reported.

On average, in the MS-noON group, the values of WR, IR, and OR MV detected in Areas 1, 2, and 3 and in the combined Area 1+2+3 were not significantly ($p > 0.01$) reduced with respect to controls.

TABLE 2 | Spectral domain-Optical Coherence Tomography macular volume (MV) segmentation analysis.

		WR-MV				IR-MV				OR-MV			
		AREA 1	**AREA 2**	**AREA 3**	**AREA 1+2+3**	**AREA 1**	**AREA 2**	**AREA 3**	**AREA 1+2+3**	**AREA 1**	**AREA 2**	**AREA 3**	**AREA 1+2+3**
MS-noON vs. C	*f* (1,74)	3.265	2.441	3.321	3.522	0.602	4.299	1.152	2.563	0.132	1.078	0.299	0.611
	P	0.075	0.123	0.073	0.048	0.439	0.042	0.228	0.114	0.729	0.302	0.558	0.436
MS-ON-G vs. C	*f* (1,61)	4.011	16.429	21.632	25.858	1.789	32.222	28.035	35.792	0.111	2.862	1.614	2.295
	P	0.050	**<0.01**	**<0.01**	**<0.01**	0.186	**<0.01**	**<0.01**	**<0.01**	0.756	0.096	0.210	0.135
MS-ON-G vs. MS-noON	*f* (1,66)	0.132	14.301	15.789	17.041	0.632	23.222	27.403	19.859	1.642	0.789	2.588	1.783
	P	0.716	**<0.01**	**<0.01**	**<0.01**	0.431	**<0.01**	**<0.01**	**<0.01**	0.205	0.337	0.112	0.186
MS-ON-P vs. C	*f* (1,60)	41.22	99.75	70.66	89.02	0.22	119.75	68.36	83.40	11.09	19.24	13.71	25.54
	P	**<0.01**	**<0.01**	**<0.01**	**<0.01**	0.639	**<0.01**	**<0.01**	**<0.01**	**<0.01**	**<0.01**	**<0.01**	**<0.01**
MS-ON-P vs. MS-noON	*f* (1,65)	19.25	154.88	78.47	106.01	4.47	97.52	76.88	85.02	35.88	18.23	41.86	52.96
	P	**<0.01**	**<0.01**	**<0.01**	**<0.01**	0.038	**<0.01**	**<0.01**	**<0.01**	**<0.01**	**<0.01**	**<0.01**	**<0.01**
MS-ON-P vs. MS-ON-G	*f* (1,52)	14.51	42.78	23.35	32.08	0.97	20.75	14.66	16.71	62.76	10.56	23.17	36.36
	P	**<0.01**	**<0.01**	**<0.01**	**<0.01**	0.328	**<0.01**	**<0.01**	**<0.01**	**<0.01**	**<0.01**	**<0.01**	**<0.01**

Results of statistical analysis (one-way analysis of variance) between groups: control (C) eyes, Multiple Sclerosis patients without Optic Neuritis (MS-noON), with Optic Neuritis and good recovery of best corrected visual acuity (MS-ON-G), and with Optic Neuritis and poor recovery of best corrected visual acuity (MS-ON-P). WR-MV, Whole Retinal Macular Volume; IR-MV, Inner Area Macular Volume; OR-MV, Outer Retina Macular Volume; Area 1 = circular area 1 mm centered to the fovea; Area 2 = annular area 1–3 mm centered to the fovea; Area 3 = annular area 3–6 mm centered to the fovea; Area 1+2+3 = whole area within 6 mm; p < 0.01 were considered as statistically significant for group comparisons and are in bold.

In both the MS-ON-G and MS-ON-P groups, mean values of WR and IR MV detected in localized Areas 2 and 3 as well as in the combined Area 1+ Area 2 + Area 3 were significantly ($p < 0.01$) reduced when compared to controls and to MS-noON group. In the same areas, the mean values of WR and IR MV observed in the MS-ON-P group were further significantly ($p < 0.01$) reduced with respect to those detected in the MS-ON-G group. The values of WR MV detected in Area 1 were significantly ($p < 0.01$) reduced in the MS-ON-P group with respect to those of the controls, MS-noON, and MS-ON-G groups, whereas, in the same Area 1, IR MV values were not significantly reduced ($p > 0.01$).

When considering the OR MVs, not significant ($p > 0.01$) differences between the values observed in the controls, MS-noON, and MS-ON-G groups in any Area (1, 2, 3, or 1+2+3) were found. On the contrary, the values of OR MVs detected in all Areas (1, 2, 3, or 1+2+3) in the MS-ON-P group were significantly ($p < 0.01$) reduced with respect to those of the controls, MS-noON, and MS-ON-G groups.

Sd-OCT Macular Thickness Data

On **Figure 2** we presented the box plots of the values of WR, IR, and OR MT measured from each localized area observed in the control, MS-noON, MS-ON-G, and MS-ON-P groups. On **Table 3**, we reported the statistical analysis between the groups.

On average, in the MS-noON, MS-ON-G, and MS-ON-P groups the values of WR and IR MT detected in the Areas 1, 2, and 3, were significantly ($p < 0.01$) reduced with respect to the controls. With respect to the MS-noON group, in the MS-ON-G group a significant ($p < 0.01$) reduction of WR MT values were detected in the Areas 2 and 3, whereas IR MT values were significantly reduced ($p < 0.01$) exclusively in Area 2. The values observed in the MS-ON-P group were further significantly ($p < 0.01$) reduced with respect to those of the MS-noON and MS-ON-G groups, but the IR MT in Area 1.

When considering the OR MT from all Areas (1, 2, and 3), not statistically significant ($p > 0.01$) differences between the values observed in the controls, MS-noON, and MS-ON-G groups were found. On the contrary, the values of OR MT detected in all Areas (1, 2, and 3) in the MS-ON-P group were significantly ($p < 0.01$) reduced with respect to those of the controls, MS-noON, and MS-ON-G groups.

Multiple Regressions Between Best Corrected Visual Acuity and Sd-OCT Macular Volume and Thickness Data

On **Table 4**, the results of multiple regressions between the individual values of WR, IR, and OR MV and MT and those of BCVA observed in the MS-ON-P group are shown. WR and IR volumes and thickness were significantly ($p < 0.05$) related with BCVA. Not significant ($p > 0.05$) relationships between OR volumes and thickness and BCVA were found.

DISCUSSION

The purpose of this study was to investigate the morphology of the macular IR and OR layers in MS patients with and without

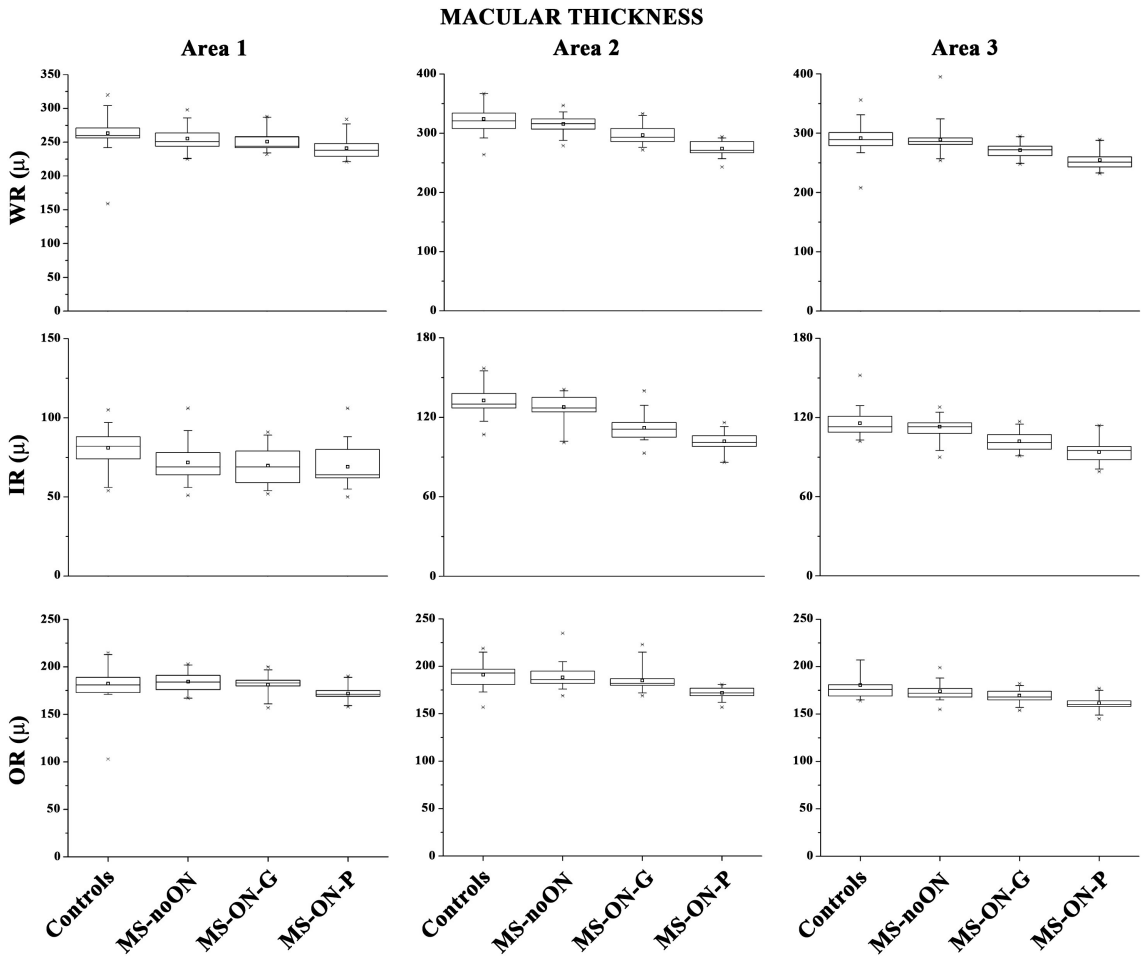

FIGURE 2 | Box plots of Spectral domain-Optical Coherence Tomography macular thicknesses in control (C) eyes, Multiple Sclerosis patients without Optic Neuritis (MS-noON), with Optic Neuritis and good recovery of best corrected visual acuity (MS-ON-G), and with Optic Neuritis and poor recovery of best corrected visual acuity (MS-ON-P). WR-MT= Whole Retinal Macular Thickness; IR-MT =Inner Retinal Macular Thickness; OR-MT = Outer Retinal Macular Thickness; μ = micron; Area 1= circular area 1 mm centered to the fovea; Area 2 = annular area 1–3 mm centered to the fovea; Area 3 = annular area 3–6 mm centered to the fovea.

a history of ON, followed by good or poor recovery of BCVA, to contribute to the controversial topic on the potential OR involvement in this neurodegenerative disorder.

The main results of the present study were that in MS patients without ON (the MS-noON group) and in MS patients with ON and a good recovery of BCVA (the MS-ON-G group) there was a morphological impairment of the IR layers, without changes of OR layers; in MS patients with ON and poor recovery of BCVA (the MS-ON-P group) there was a morphological impairment of both IR and OR layers.

All our results apply to a highly homogenous group of RR MS patients with not significant differences in age, MS-DD, and EDDS score.

In our work, the macular morphology was evaluated by the Sd-OCT assessment of segmented MV and MT. More commonly, automatic or manual segmentation of retinal layers' thicknesses, not volumes, is performed. This needs to be considered since different results obtained by using these morphological measurements could be a source of bias when comparing OCT studies.

Moreover, the literature has described reduced segmented OR (6, 15), and mainly IR layers (14, 17) MT, without the evaluation of MV, in MS eyes, mixing together eyes with and without ON in primary progressive and RR patients (6, 8, 12, 15).

For this reason and to add clarity on this matter, we present the discussion of MV and MT data separately in the three examined groups, as follows.

Sd-OCT Data in Multiple Sclerosis Patients Without History of Optic Neuritis (MS-noON Group)

When comparing data with controls, in the MS-noON group we found similar values of WR, IR, and OR MV, but significantly reduced WR and IR MT values in all examined areas. The different results obtained by measuring volumes or thickness may

TABLE 3 | Spectral domain-Optical Coherence Tomography macular thickness (MT) segmentation analysis.

		WR-MT			IR-MT			OR-MT		
		AREA 1	**AREA 2**	**AREA 3**	**AREA 1**	**AREA 2**	**AREA 3**	**AREA 1**	**AREA 2**	**AREA 3**
MS-noON vs. C	*f* (1,74)	8.019	6.803	7.389	9.499	21.388	35.579	0.262	0.753	2.331
	P	**<0.01**	**<0.01**	**<0.01**	**<0.01**	**<0.01**	**<0.01**	0.609	0.391	0.131
MS-ON-G vs. C	*f* (1,61)	22.861	52.802	61.022	11.441	425.062	59.471	0.453	0.159	0.019
	P	**<0.01**	**<0.01**	**<0.01**	**<0.01**	**<0.01**	**<0.01**	0.503	0.692	0.977
MS-ON-G vs. MS-noON	*f* (1,66)	1.362	27.756	15.932	0.509	239.188	3.387	1.392	1.402	2.352
	P	0.248	**<0.01**	**<0.01**	0.478	**<0.01**	0.070	0.243	0.241	0.130
MS-ON-P vs. C	*f* (1,60)	53.75	228.65	139.13	12.20	287.14	114.34	23.42	35.14	120.61
	P	**<0.01**	**<0.01**	**<0.01**	**<0.01**	**<0.01**	**<0.01**	**<0.01**	**<0.01**	**<0.01**
MS-ON-P vs. MS-noON	*f* (1,65)	32.53	167.69	50.85	0.85	127.97	30.93	30.50	45.23	132.32
	P	**<0.01**	**<0.01**	**<0.01**	0.350	**<0.01**	**<0.01**	**<0.01**	**<0.01**	**<0.01**
MS-ON-P vs. MS-ON-G	*f* (1,52)	7.62	34.39	19.45	0.04	18.45	13.47	15.25	25.57	15.26
	P	**<0.01**	**<0.01**	**<0.01**	0.853	**<0.01**	**<0.01**	**<0.01**	**<0.01**	**<0.01**

Results of statistical analysis (one-way analysis of variance) between groups: control (C) eyes, Multiple Sclerosis patients without Optic Neuritis (MS-noON), with Optic Neuritis and good recovery of best corrected visual acuity (MS-ON-G), and with Optic Neuritis and poor recovery of best corrected visual acuity (MS-ON-P). WR-MT, Whole Retinal Macular Thickness; IR-MT, Inner Retinal Macular Thickness; OR-MT, Outer Retinal Macular Thickness; Area 1 = circular area 1 mm centered to the fovea; Area 2 = annular area 1–3 mm centered to the fovea; Area 3 = annular area 3–6 mm centered to the fovea; $p < 0.01$ were considered as statistically significant for group comparisons and are expressed in bold.

TABLE 4 | Multiple regression analysis between best corrected visual acuity (BCVA) and Spectral domain-Optical Coherence Tomography macular volume (A) and macular thickness (B) values in Multiple Sclerosis patients with Optic Neuritis and poor recovery of BCVA (MS-ON-P group).

	Regression (F; p; R^2)	**AREA 1 (F; p)**	**AREA 2 (F; p)**	**AREA 3 (F; p)**	**Regression equation**
A					
WR-MV	5.55; 0.005; 43.06%	4.89; 0.038	13.21; 0.001	5.44; 0.029	BCVA = 1.69 + 8.52A1–3.381A2 + 0.902A3
IR-MV	7.43; 0.001; 50.31%	4.68; 0.042	15.86; 0.001	5.18; 0.033	BCVA = 1.792 + 10.00A1–5.47A2 + 1.30A3
OR-MV	0.29; 0.833; 3.79%	0.00; 0.966	0.73; 0.401	0.18; 0.672	BCVA = −0.47–0.5A1 + 0.281A2 + 0.304A3
B					
WR-MT	5.74; 0.005; 43.89%	4.85; 0.038	13.65; 0.001	5.69; 0.026	BCVA = 1.77 + 0.007A1–0.022A2 + 0.012A3
IR-MT	7.25; 0.001; 49.71%	4.40; 0.048	15.46; 0.001	4.95; 0.037	BCVA = 1.800 + 0.008A1–0.034t2 + 0.016A3
OR-MT	2.16; 0.122; 22.72%	1.24; 0.278	5.21; 0.032	5.44; 0.029	BCVA = 0.27 + 0.010A1–0.032A2 + 0.024A3

WR-MV, Whole Retinal Macular Volume; IR-MV, Inner Retina Macular Volume; OR-MV, Outer Retina Macular Volume; WR-MT, Whole Retinal Macular Thickness; IR-MT, Inner Retinal Macular Thickness; OR-MT, Outer Retinal Macular Thickness; Area 1= circular area 1 mm centered to the fovea; Area 2= annular area 1–3 mm centered to the fovea; Area 3 = annular area 3–6 mm centered to the fovea. The second column shows the regression model results and the third column shows F, p-values and coefficients' results.

be ascribed to the possibility that the retinal volume encloses not exclusively neuronal cellular elements, and specifically their soma, but also a large quantity of non-neuronal elements (such as astrocytes or Muller cells). Therefore, the finding that WR and IR MT were significantly reduced in this group, but not the MV, may be accounted to the specific impairment of all the neuro-retinal elements constituting the IR. Structural or non-neural elements are probably not involved in the neurodegenerative process of MS without ON.

The main result, however, relies on the finding that OR MV and MT were not significantly different with respect to controls, suggesting that the OR is spared from neurodegeneration even when no ON event occurs (12, 14, 16, 19). We are aware of different results in MS-noON patients that led Saidha et al. (15) to hypothesize the concept of "primary retinal pathology," based on the finding of IR and OR thinning mainly in patients with progressive MS-noON. However, we studied more selectively RR MS

patients and based on our results we cannot drive similar conclusive findings.

Sd-OCT Data in Multiple Sclerosis Patients With History of Optic Neuritis and Good Recovery of Visual Acuity (MS-ON-G Group)

Regarding our Sd-OCT volume findings, in the MS-ON-G group we detected a significant reduction of WR and IR MV in the parafoveal areas (Area 2 and Area 3), as well as in the wide 6 mm area, but in Area 1 which represents the fovea. This suggests that the morphological IR (and WR) impairment after ON, accordingly with previous observations (6, 8, 10, 12, 14–17, 24, 28, 29), occurs mainly in the parafovea with absence of morphological impairment of the fovea. This can be explained by considering macular anatomical characteristics. Indeed, a greater proportion of RGCs per unit volume is present in the parafovea, whereas in the fovea and in the periphery of the macula, RGCs and RNFL are less represented. Because the RGCs comprise about 35% of the total WR thickness of the macula (20, 28, 30), the main impact on IR and WR reduction may regard RGCs. Therefore, our results on volume analysis suggest that in MS, in the presence of ON and when a good recovery of BCVA was reached after ON, the neural elements of the fovea are likely morphologically spared from the retrograde degeneration.

Similarly to our findings, in previous OCT studies performed in MS-ON eyes, a significant reduction of IR volume was found in MS patients with poor (10) (as our MS-ON-P group) or good recovery (as our MS-ON-G group) of BCVA (18, 29) after ON, measuring the MV from the entire macular area (our Area 1+2+3). Therefore, no specific information about the foveal morphological integrity or abnormality were given, and it is conceivable that the observed reduction of the IR volume was influenced by a greater structural involvement of the parafoveal neural elements.

Also, when comparing data between the MS-ON-G and MS-noON groups, significant differences in WR and IR MV were found in all areas but in Area 1, thus confirming that in this neurodegenerative disorder the fovea (in terms of MV values) remains structurally spared, independently from the ON.

Similar results of WR and IR were obtained when segmenting MT, however the foveal measurements from Area 1 were significantly impaired compared to controls. This could be explained considering the above-mentioned possibility of MV to capture structural or non-neural elements which are not enclosed in the MT measurement.

By contrast, we found relative equivalent results in terms of MV and/or MT about OR values that were not significantly different from those of controls, suggesting that OR foveal and parafoveal elements are morphologically spared by the post-neuritis degenerative process; it is likely that this condition should induce the recovery of good high-contrast BCVA, as detected in our MS-ON-G cohort. This structural finding is in agreement with a previous report by Hanson et al. (29), who observed a not significant reduction of segmented OR volume in MS-ON patients with complete recovery of visual dysfunction who recovered a good high-contrast BCVA (< 0.2 logMAR), similarly to our enrolled MS-ON-G patients, and had no major visual field defects. Also other authors (16–18) identified the absence of thinning of the OR layers after ON in patients with recovery of high-contrast BCVA.

Sd-OCT Data in Multiple Sclerosis Patients With History of Optic Neuritis and Poor Recovery of Visual Acuity (MS-ON-P Group)

In our cohort of MS-ON with poor recovery of BCVA, we found reduced MV and MT values of WR in all areas, as well as MT of IR, compared to controls. Only MV values of IR from Area 1 were not significantly reduced when compared to the controls, MS-noON, and MS-ON-G groups. This means that also in MS after an event of ON, when BCVA is not fully recovered, as expected, WR and IR layers from the parafoveal areas are structurally impaired.

In the same group, however, differently from the MS-noON and MS-ON-G groups, we found significant abnormal OR MVs and MTs from all examined areas, thus assessing the pre-ganglionic elements morphological impairment. Our morphological results could indicate that the post-neuritis retrograde degeneration might also involve the elements located in the OR, impacting the neuronal chain of the fovea. Therefore, the wider morphological concomitant involvement of OR and IR layers could explain the absence of good recovery of BCVA in MS-ON-P patients with respect to MS-ON-G patients, in which an exclusive IR structural impairment was detected. These findings were also supported by adaptive optics data in optic neuropathies, including MS ON, by Choi et al. (31) who described photoreceptor structural abnormalities, when there is permanent damage to overlying IR layers.

The OR morphological changes were not related to BCVA decrease (see **Table 4**). It seems that in the reduction of BCVA, the main contribution is given by the morphological changes of the parafoveal IR layers, as also described in previous studies (18, 19, 28, 32) where it was found that GCL+IPL thinning is most significantly correlated with reduced high contrast BCVA in MS-ON patients, similarly to our cohort, at least 6 months after the ON occurrence (24).

Conclusive Remarks and Neurophysiological Hypotheses

We acknowledge that the Sd-OCT device used could not provide high definition segmentation data layer-by-layer of the OR and IR in both MS groups as a limitation of our study (33). However, by finding congruent results of OR integrity by using either volume and thickness segmentation analyses, we are confident that this limitation has been overcome.

In summary, our main findings led us to make some relevant conclusions and hypotheses: (1) in our selected cohort of RR MS patients, the well-known (6, 8, 10, 12, 14–17, 24, 28, 29) morphological involvement of the IR is confirmed with more exhaustive information provided by MT assessment rather than MV analysis, in specific localized areas; (2) no morphological

abnormalities can be found at the level of the OR in absence of ON; by contrast, in occurrence of ON with good recovery of BCVA, it is likely that the OR layers are preserved from the extent of the neurodegenerative process, and, in the absence of exhaustive data in literature, it can be hypothesized that in this case the retinal elements located outside the OR (i.e., middle retina) could play a role to counteract neurodegeneration; (3) by contrast, when there is an absence or an inadequate previously supposed protective role, then the morphological impairment extends also to OR structures and this, together with the IR damage, leads to poor recovery of BCVA.

Our hypotheses that retinal synaptic elements located between OR and IR layers are relevant for neuroinflammatory changes in MS and that the homeostasis of the middle retina is crucial to counteract MS-related neurodegeneration can be supported by preclinical (34, 35) and clinical (14, 15) evidences.

In fact, an early synaptic pathology occurs in well-validated MS mouse models of ON, altered synaptic vesicle cycling in ribbon synapses of the myelin-free retina was reported, which are likely targeted by an auto-reactive immune system process (34). The auto-immune response in these animal models is directed against two adhesion proteins (CASPR1/CNTN1) (36), that are present both in the paranodal region of myelinated nerves as well as at retinal ribbon synapses (34). Related to this topic, the retina has been considered a primary immune target in MS and in MS-related optic neuritis in many previous clinical studies (14, 15).

In order to better understand the role of middle retinal elements in this process, further studies on both experimental and clinical sides are needed.

DATA AVAILABILITY STATEMENT

The raw data supporting the conclusions of this article will be made available by the authors, without undue reservation.

ETHICS STATEMENT

The studies involving human participants were reviewed and approved by Comitato Etico Centrale IRCCS Lazio, Sezione IFO/Fondazione Bietti, Rome, Italy. The patients/participants provided their written informed consent to participate in this study.

AUTHOR CONTRIBUTIONS

LZ, VP, and DC: Concept and design. LBa, MA, and LBo: data collection. VP: statistical expertise. VP, LZ, and DC: analysis and interpretation. LZ, VP, and LBa: writing the article. VP, LZ, DC, and AG: critical revision of the article. VP, LZ, and DC: final approval of the article. All authors: reviewed the manuscript and agreed to be accountable for all aspects of the work.

ACKNOWLEDGMENTS

Research for this study was supported by the Ministry of Health and by Fondazione Roma. The authors would like to acknowledge Dr. Federica Petrocchi for executing BCVA measurements, Eng. Antonio Di Renzo for bio-statistical analysis, and Dr. Maria Luisa Alessi for technical assistance.

REFERENCES

1. Miller D, Barkhof F, Montalban X, Thompson A, Filippi M. Clinically isolated syndromes suggestive of multiple sclerosis, part 2: non-conventional MRI, recovery processes, and management. *Lancet Neurol.* (2005) 4:341–48. doi: 10.1016/S1474-4422(05)70095-8
2. Kupfer C. Retinal ganglion cell degeneration following chiasmal lesions in man. *Arch Ophthalmol.* (1963) 70:256–60. doi: 10.1001/archopht.1963.00960050258020
3. Tátrai E, Simó M, Iljicsov A, Németh J, Debuc DC, Somfai GM. *In vivo* evaluation of retinal neurodegeneration in patients with multiple sclerosis. *PLoS ONE.* (2012) 7:e30922. doi: 10.1371/journal.pone.0030922
4. Gupta S, Zivadinov R, Ramanathan M, Weinstock-Guttman B. Optical coherence tomography and neurodegeneration: are eyes the windows to the brain? *Expert Rev Neurother.* (2016) 16:765–75. doi: 10.1080/14737175.2016.1180978
5. Petzold A. Optical coherence tomography to assess neurodegeneration in multiple sclerosis. *Methods Mol Biol.* (2016) 1304:131–41. doi: 10.1007/7651_2014_153
6. Behbehani R, Abu Al-Hassan A, Al-Salahat A, Sriraman D, Oakley JD, Alroughani R. Optical coherence tomography segmentation analysis in relapsing remitting versus progressive multiple sclerosis. *PLoS ONE.* (2017) 12:e0172120. doi: 10.1371/journal.pone.0172120
7. Balcer LJ. Clinical trials to clinical use: using vision as a model for multiple sclerosis and beyond. *J Neuroophthalmol.* (2014) 34:S18–23. doi: 10.1097/WNO.0000000000000163
8. Hu SJ, You YA, Zhang Y. A study of retinal parameters measured by optical coherence tomography in patients with multiple sclerosis. *Int J Ophthalmol.* (2015) 8:1211–14. doi: 10.3980/j.issn.2222-3959.2015.06.24
9. Trip SA, Schlottmann PG, Jones SJ, Altmann DR, Garway-Heath DF, Thompson AJ, et al. Retinal nerve fiber layer axonal loss and visual dysfunction in optic neuritis. *Ann Neurol.* (2005) 58:383–91. doi: 10.1002/ana.20575
10. Cennamo G, Romano MR, Vecchio EC, Minervino C, Della Guardia C, Velotti N et al. Anatomical and functional retinal changes in multiple sclerosis. *Eye.* (2016) 30:456–62. doi: 10.1038/eye.2015.256
11. Lange AP, Zhu F, Sayao AL, Sadjadi R, Alkabie S, Traboulsee AL, et al. Retinal nerve fiber layer thickness in benign multiple sclerosis. *Mult Scler.* (2013) 19:1275–81. doi: 10.1177/1352458512474706
12. Garcia-Martin E, Polo V, Larrosa JM, Marques ML, Herrero R, Martin J et al. Retinal layer segmentation in patients with multiple sclerosis using spectral domain optical coherence tomography. *Ophthalmology.* (2014) 121:573–79. doi: 10.1016/j.ophtha.2013.09.035
13. Gundogan FC, Demirkaya S, Sobaci G. Is optical coherence tomography really a new biomarker candidate in multiple sclerosis?–A structural and functional evaluation. *Invest Ophthalmol Vis Sci.* (2007) 48:5773–81. doi: 10.1167/iovs.07-0834
14. Petzold A, Balcer LJ, Calabresi PA, Costello F, Frohman TC, Frohman EM, et al. Retinal layer segmentation in multiple sclerosis: a systematic review and meta-analysis. *Lancet Neurol.* (2017) 16:797–812. doi: 10.1016/S1474-4422(17)30278-8
15. Saidha S, Syc SB, Ibrahim MA, Eckstein C, Warner CV, Farrell SK, et al. Primary retinal pathology in multiple sclerosis as detected by optical coherence tomography. *Brain.* (2011) 134:518–33. doi: 10.1093/brain/awq346
16. Balk LJ, Tewarie P, Killestein J, Polman CH, Uitdehaag B, Petzold A. Disease course heterogeneity and OCT in multiple sclerosis. *Mult Scler.* (2014) 20:1198–206. doi: 10.1177/1352458513518626

17. Syc SB, Saidha S, Newsome SD, Ratchford JN, Levy M, Ford E, et al. Optical coherence tomography segmentation reveals ganglion cell layer pathology after optic neuritis. *Brain*. (2012) 135:521–33. doi: 10.1093/brain/awr264
18. Walter SD, Ishikawa H, Galetta KM, Sakai RE, Fller DJ, Henderson SB et al. Ganglion cell loss in relation to visual disability in multiple sclerosis. *Ophthalmology*. (2012) 119:1250–57. doi: 10.1016/j.ophtha.2011.11.032
19. Schneider E, Zimmermann H, Oberwahrenbrock T, Kaufhold F, Kadas EM, Petzold A, et al. Optical coherence tomography reveals distinct patterns of retinal damage in neuromyelitis optica and multiple sclerosis. *PLoS ONE*. (2013) 8:e66151. doi: 10.1371/journal.pone.0066151
20. Ishiwaka H, Stein DM, Wollstein G, Beaton S, Fujimoto JG, Schuman JS. Macular segmentation with optical coherence tomography. *Invest Ophthalmol Vis Sci*. (2005) 46:2002–17 doi: 10.1167/iovs.04-0335
21. Polman CH, Reingold SC, Banwell B, Clanet M, Cohen JA, Filippi M et al. Diagnostic criteria for multiple sclerosis: 2010 revisions to the McDonald criteria. *Ann Neurol*. (2011) 69:292–302. doi: 10.1002/ana.22366
22. Kurtzke JF. Rating neurologic impairment in multiple sclerosis: an expanded disability status scale (EDSS). *Neurology*. (1983) 33:1444–52. doi: 10.1212/WNL.33.11.1444
23. Williams UE, Oparah SK, Philip-Ephraim EE. Disease modifying therapy in multiple sclerosis. *Int Sch Res Notices*. (2014) 2014:307064. doi: 10.1155/2014/307064
24. Huang-Link YM, Fredrikson M, Link H. Benign multiple sclerosis is associated with reduced thinning of the retinal nerve fiber and ganglion cell layers in non-optic-neuritis eyes. *J Clin Neurol*. (2015) 11:241–47. doi: 10.3988/jcn.2015.11.3.241
25. Huang D, Swanson EA, Lin CP, Schuman JS, Stinson WG, Chang W, et al. Optical coherence tomography. *Science*. (1991) 254:1178–81. doi: 10.1126/science.1957169
26. Cruz-Herranz A, Balk LJ, Oberwahrenbrock T, Saidha S, Martinez-Lapiscina EH, Lagreze WA et al. IMSVISUAL consortium. The APOSTEL recommendations for reporting quantitative optical coherence tomography studies. *Neurology*. (2016) 86:2303–09. doi: 10.1212/WNL.0000000000002774
27. Tewarie P, Balk L, Costello F, Green A, Martin R, Schippling S, et al. The OSCAR-IB consensus criteria for retinal OCT quality assessment. *PLoS ONE*. (2012) 7:e34823. doi: 10.1371/journal.pone.0034823
28. Burkholder BM, Osborne B, Loguidice MJ, Bisker E, Frohman TC, Conger A, et al. Macular volume determined by optical coherence tomography as a measure of neuronal loss in multiple sclerosis. *Arch Neurol*. (2009) 66:1366–72. doi: 10.1001/archneurol.2009.230
29. Hanson JVM, Hediger M, Manogaran P, Landau K, Hagenbuch N, Schippling S, et al. Outer retinal dysfunction in the absence of structural abnormalities in multiple sclerosis. *Invest Ophthalmol Vis Sci*. (2018) 59:549–60. doi: 10.1167/iovs.17-22821
30. Wojtkowski M, Srinivasan V, Fujimoto JG, Ko T, Schuman JS, Kowalczyk A, et al. Three-dimensional retinal imaging with high-speed ultrahigh-resolution optical coherence tomography. *Ophthalmology*. (2005) 112:1734–46. doi: 10.1016/j.ophtha.2005.05.023
31. Choi SS, Zawadzki RJ, Keltner JL, Werner JS. Changes in cellular structures revealed by ultra-high resolution retinal imaging in optic neuropathies. *Invest Ophthalmol Vis Sci*. (2008) 49:2103–19. doi: 10.1167/iovs.07-0980
32. Al-Louzi OA, Bhargava P, Newsome SD, Balcer LJ, Frohman EM, Crainiceanu C et al. Outer retinal changes following acute optic neuritis. *Mult Scler*. (2016) 22:362–72. doi: 10.1177/1352458515590646
33. Oberwahrenbrock T, Weinhold M, Mikolajczak J, Zimmermann H, Paul F, Beckers I et al. Reliability of intra-retinal layer thickness estimates. *PLoS ONE*. (2015) 10:e0137316. doi: 10.1371/journal.pone.0137316
34. Dembla M, Kesharwani A, Natarajan S, Fecher-Trost C, Fairless R, Williams SK, et al. Early auto-immune targeting of photoreceptor ribbon synapses in mouse models of multiple sclerosis. *EMBO Mol Med*. (2018) 10:e8926. doi: 10.15252/emmm.201808926
35. Fairless R, Williams SK, Hoffmann DB, Stojic A, Hochmeister S, Schmitz F, et al. Preclinical retinal neurodegeneration in a model of multiple sclerosis. *J Neurosci*. (2012) 32:5585–97. doi: 10.1523/JNEUROSCI.5705-11.2012
36. Stathopoulos P, Alexopoulos H, Dalakas MC. Autoimmune antigenic targets at the node of Ranvier in demyelinating disorders. *Nat Rev Neurol*. (2015) 11:143–56. doi: 10.1038/nrneurol.2014.260

Conflict of Interest: The authors declare that the research was conducted in the absence of any commercial or financial relationships that could be construed as a potential conflict of interest.

Copyright © 2020 Ziccardi, Barbano, Boffa, Albanese, Grzybowski, Centonze and Parisi. This is an open-access article distributed under the terms of the Creative Commons Attribution License (CC BY). The use, distribution or reproduction in other forums is permitted, provided the original author(s) and the copyright owner(s) are credited and that the original publication in this journal is cited, in accordance with accepted academic practice. No use, distribution or reproduction is permitted which does not comply with these terms.

frontiers in Neurology

REVIEW
published: 03 November 2020
doi: 10.3389/fneur.2020.580951

Rodent Models of Optic Neuritis

Yael Redler[1]* *and Michael Levy*[2]

[1] Department of Neuro-Ophthalmology, Massachusetts Eye & Ear Infirmary/Harvard Medical School, Boston, MA, United States, [2] Department of Neurology, Massachusetts General Hospital/Harvard Medical School, Boston, MA, United States

Optic neuritis (ON) is an inflammatory attack of the optic nerve that leads to visual disability. It is the most common optic neuropathy affecting healthy young adults, most commonly women aged 20–45 years. It can be idiopathic and monophasic or as part of a neurologic disease such as multiple sclerosis with recurrence and cumulative damage. Currently, there is no therapy to repair the damage from optic neuritis. Animal models are an essential tool for the understanding of the pathogenesis of optic neuritis and for the development of potential treatment strategies. Experimental autoimmune encephalomyelitis (EAE) is the most commonly used experimental rodent model for human autoimmune inflammatory demyelinating diseases of the central nervous system (CNS). In this review, we discuss the latest rodent models regarding optic neuritis, focusing on EAE model, and on its recent achievements and developments.

Keywords: optic neuritis, rodent models, experimental autoimmune encephalomyelitis, multiple sclerosis, demyelination

OPEN ACCESS

Edited by:
Gemma Caterina Maria Rossi, Fondazione Ospedale San Matteo (IRCCS), Italy

Reviewed by:
Kenneth Shindler, University of Pennsylvania, United States
Prem Subramanian, University of Colorado, United States

***Correspondence:**
Yael Redler
yael_redler@hotmail.com

Specialty section:
This article was submitted to Neuro-Ophthalmology, a section of the journal Frontiers in Neurology

Received: *07 July 2020*
Accepted: *15 September 2020*
Published: *03 November 2020*

Citation:
Redler Y and Levy M (2020) Rodent Models of Optic Neuritis. Front. Neurol. 11:580951. doi: 10.3389/fneur.2020.580951

INTRODUCTION

Optic Neuritis

Optic neuritis is an inflammatory demyelinating disorder of the optic nerve. The typical form of optic neuritis is idiopathic or associated with multiple sclerosis (MS). Atypical forms of optic neuritis can occur in association with other inflammatory disorders or due to infections, immune-stimulating medications, and paraneoplastic disorders.

The prevalence of optic neuritis is estimated to be as high as 115/100,000 depending upon geography and ethnicity (1). The incidence is highest in populations located at higher latitudes such as northern USA, Europe, and Australia compared with geographic locations closer to the equator (2). There is a female preponderance with 3:1 ratio, with most patients 20–45 years old (3).

According to the involved site, optic neuritis can be classified as retrobulbar optic neuritis, affecting any part of the optic nerve behind its entry to the eyeball. This is the most common form of optic neuritis, and on examination, the disk often appears normal. Optic neuritis that includes inflammation of the optic disk is known as papillitis, which is visible on examination as hyperemia, swelling of the disk, blurring of disk margins, and distended veins (4). An afferent pupillary defect in the affected eye is usually detectable.

The common clinical presentation of a patient with optic neuritis is unilateral visual acuity loss, visual field loss, color vision deficits, decreased contrast, and brightness sense. There is also periocular pain precipitated by eye movements that may precede the visual loss by a few days. The extent of visual function damage may vary significantly according to the etiology of the optic neuritis. In typical optic neuritis and optic neuritis associated with MS, visual acuity loss is moderate, conversely, optic neuritis associated with neuromyelitis optica spectrum disorder (NMOSD) or myelin oligodendrocyte glycoprotein (MOG) often presents with severe vision loss (5, 6).

Diagnostic investigations include MRI, visual evoked potentials (VEP), and cerebrospinal fluid (CSF) examination. MRI is performed to characterize the location and extent of inflammation and to rule out other etiologies such as multiple sclerosis. VEPs measure optic nerve function and may be useful when anatomic studies by MRI are equivocal. Degeneration of retinal ganglion cells (RGC) and retinal thinning which correlate with measures of persistent visual dysfunction after optic neuritis is demonstrated by optical coherence tomography (OCT) (7, 8).

Treatment with high-dose corticosteroids shortens the period of acute visual dysfunction but does not affect the final visual outcome in typical optic neuritis (9). Atypical forms can necessitate prolonged immunosuppressive regimens. Recently, therapies to promote neuroprotection and remyelination have been investigated (10, 11) along with immunosuppressive therapies for autoimmune processes to prevent recurrence of immune-mediated damage (12).

RODENT MODELS OF OPTIC NEURITIS

Animal models are essential for the understanding of etiology and pathogenesis of immune-mediated processes and to develop therapeutic strategies which eventually will lead to effective treatments for human diseases. Many studies have been conducted in order to understand the pathophysiological mechanisms of optic neuritis using different models.

Experimental Autoimmune Encephalomyelitis Models

The EAE model is the most commonly used experimental rodent model for human autoimmune inflammatory demyelinating diseases of the CNS. EAE is a complex system of interaction between multiple immunological and neuropathological mechanisms leading to inflammation, demyelination, axonal loss, and gliosis. The regulatory mechanisms of resolution of inflammation and remyelination also occur in EAE.

In EAE, the optic nerve lesions are, in most cases, a part of the whole CNS disease process which includes the brain and the spinal cord. There are subtypes that are found to be more associated with optic nerve involvement. For example, in the dark agouti rat model, acute optic nerve inflammation manifests earlier than spinal cord inflammation (PMID: 31267597) whereas in C57BL6 mice, optic nerve inflammation occurs chronically along with inflammation in the rest of the CNS (PMID: 29903027).

Induction Phase

EAE is initiated by introducing a specific CNS antigen, such as MOG, myelin basic protein (MBP), or proteolipid protein (PLP), in the context of an inflammatory stimulus to induce encephalomyelitis. It is typically induced by either active immunization with myelin-derived proteins introduced into the CNS, emulsified in complete Freund's adjuvant (CFA), which contains heat-inactivated *Mycobacterium tuberculosis*. CFA enhances peripheral immune response by promoting Th1 response and increases blood-brain barrier (BBB) permeability (13). Pertussis toxin (PTX) which is administered in the process as well has been suggested to also modulate the blood-brain barrier and the immunological responsiveness.

Passive immunization, by adoptive transfer of activated myelin-specific CD4+ T lymphocytes (14–16), allows EAE to develop faster, without an adjuvant (17). Typically 10–14 days after initiation, the disease is manifested by a variety of clinical and pathological reactions. The extent and location of inflammation and demyelination is variable according to specific antigen introduced, rodent species, strain, age, and gender. As a consequence, an acute or chronic-relapsing inflammatory demyelinating autoimmune disease is acquired (18, 19).

Inflammatory Phase

The inflammatory process in the CNS is first indicated by activated microglia, local macrophages, and peripheral T lymphocytes. Activated T cells undergo maturation and clonal expansion; later, they differentiate into effector cells and migrate through the blood circulation to breach the BBB. Adhesion molecules are expressed on endothelial cells in CNS microvasculature, allowing activated T cells to bind to these molecules and penetrate the endothelium. To further penetrate the subendothelial basement membrane which is mainly composed of type IV collagen, T cells utilize matrix-degrading enzymes (20). Once they enter the CNS, T cells recognize antigen presented locally and become reactivated, enhance inflammation, and continuously recruit other cells (21). Secretion of cytokines and other proinflammatory mediators further exacerbate the inflammatory milieu which recruits additional immune cells into the CNS and culminates in demyelination (22, 23).

Demyelination and Axonal Loss

Myelin loss leads to a disruption of axonal function, and axons may eventually die back depending on the severity and persistence of the inflammatory response. Axons are vulnerable to damage by inflammatory cytokines, enzymes, and nitric oxide which are expressed by activated immune cells during the inflammatory process and cause direct cytotoxic effects. Axons that survive demyelination when the inflammation resolves may become remyelinated; however, in most EAE phenotypes, inflammatory damage leads to neuronal cell death, axonal loss, and gliosis (24–26). Irreversible axonal damage is seen by retinal nerve fiber layer (RNFL) thinning (27–29).

The clinical evaluation of the disease progression can be done in several ways. Due to the fact that active EAE is an ascending progressive disease that progresses into paresis, it initially affects rodent tail tone, followed by limb motor deficits. Daily scoring of these parameters provides information regarding spinal cord inflammation and demyelination (30). The optic neuritis progression can be assessed by examining the visual response to specific stimuli such as OKN response or by assessing the response to hand movements in front of the rodent, and in some studies, rodents who did not escape when a sharp-pointed object held in front of their eyes were thought to be blind (31). Optic neuritis was also assessed by RNFL thickness using an OCT and retinal ganglion cell count (32). Other ways to assess the optic

nerve inflammation and demyelination are through histology of the optic nerve (33).

Other Rodent Models of Optic Neuritis

Engineering a new MOG-specific TCR transgenic mouse, the 2D2 mouse made by Bettelli et al. in 2003 produces transgenic T cells with receptors capable of recognizing MOG presented by MHCII (34). Approximately 30% of these mice will develop spontaneous optic neuritis; when immunized with subclinical levels of MOG peptide, up to 56% developed histological evidence of EAE. When they were fully immunized, 80% developed optic neuritis. It was assumed that the specificity of inflammatory demyelination is related to the significantly higher levels of MOG in the optic nerve than the spinal cord.

Neuromyelitis optica (NMO) is an inflammatory demyelinating disease involving the optic nerves and spinal cord. The damage is caused due, in part, to autoantibodies against aquaporin-4, a water channel on astrocytic foot processes at the blood-brain barrier. There are several animal models of NMO that have been developed (35). By crossing 2D2 mice with MOG-specific Ig heavy-chain knock-in mice (IgHMOG mice), severe inflammatory demyelination involving the optic nerves and the spinal cord developed in about 60% of these mice. Immunoglobulin class switching was observed, indicating that B and T lymphocyte cooperation play a role in induction of autoimmune processes.

Several studies showed that passive transfer alone of the aquaporin-4 antibody from patients with neuromyelitis optica is insufficient to reproduce the disease in rodents unless extremely high levels are infused. In the context of EAE with myelin-targeted T cells or even after an injection of Freund's adjuvant, the antibody can reach its target in the CNS and contribute to inflammatory demyelination (36–39). Direct injection of the antibody into the brain along with human complement can also induce inflammatory demyelination (40). More recently, a mouse model of NMO could be recapitulated by adoptive transfer of T cells reactive to aquaporin-4 (41, 42).

OPTIC NEURITIS PATHOMECHANISM

In 1977, an experimental model for acute allergic optic neuritis was induced in guinea pigs. They exhibited two distinct clinical patterns: "retrobulbar optic neuritis" with normal fundus and "neuroretinitis" with hyperemia and swelling of the disk and retinal edema. Histopathology of the "retrobulbar neuritis" revealed that some of them had brain involvement without any involvement of the optic nerve, while others involved the retrobulbar portion of the optic nerve and chiasm with multiple foci of demyelination. In the neuroretinitic animals, the lesions were localized behind the lamina cribrosa and had an appearance characteristic of papilledema (43).

Due to a unique anatomic structure, where the anterior part of the optic nerve within the lamina cribrosa is unmyelinated and supported by modified astrocytes, a barrier between the optic nerve and the retina restricts the inflammation to the optic nerve during ON, and prevents retinal inflammation as well (44, 45). In New Zealand albino rabbits, the axons of the nerve fiber layer are myelinated over a long portion within the retina. Extensive inflammatory lesions were observed in the myelinated fibers within the retina following sensitization with bovine myelin and adjuvant (46).

Theories regarding specific proteins playing a critical role in the mechanism of EAE optic neuritis have been proposed. Lipocalin-2, a protein that regulates diverse cellular processes, is expressed and secreted by microglia and astrocytes due to inflammatory stimuli in the central nervous system (47). Lipocalin-2 is a pro-inflammatory activator of T cells during EAE development and progression (48). Mice deficient in lipocalin-2 showed a significant reduction of demyelination, inflammatory infiltration, and gliosis in the optic nerve in EAE (49). Another area of specific investigation was the site of vulnerability in the optic nerve head where an incomplete blood-brain barrier allows partial access to the immune-privileged CNS. Using the expression of αB-crystallin, which is a heat-shock protein expressed as an early stress response in oligodendrocytes, one of the earliest targets of EAE is the optic nerve head associated with IgG deposition suggesting that partial immune access at this area of the CNS may explain its specific vulnerability in EAE (50).

Astrocytes in the optic nerve are known to play a pivotal role in neuroinflammatory processes in the CNS. In the human disease NMOSD, the astrocytic water channel aquaporin-4 is the naïve target of an aberrant immune response, especially in the optic nerve (51). The role of astrocytes in typical optic neuritis was studied by characterizing the astrocyte-specific transcriptome in EAE optic neuritis. Their results showed a significant increase in the proinflammatory-complement cascade, especially complement component 3 (C3) and a decrease in factors of the cholesterol biosynthesis pathways involved in remyelination. Interestingly, these changes in astrocytes as well as increased axonal loss were greater in EAE females vs. males (32).

A study suggested that dietary supplementation with a balanced mixture of fatty acids (FAs) including omega 3 and omega 6, efficiently limit inflammation and prevent RGC degeneration, demonstrating a neuroprotective effect in EAE models (52). Further study investigating the mechanisms underlying the anti-inflammatory effects of fatty acids found that they shift macrophage polarization from the M1 inflammatory phenotype, which releases proinflammatory cytokines, leading to tissue damage in the CNS, toward the anti-inflammatory M2 phenotype associated with resolving inflammation and tissue repair (53).

MEDICATIONS

Antioxidants Therapies

Reactive oxygen species (ROS) are formed as byproducts in a variety of biochemical reactions. When generated in excess or not appropriately regulated, ROS may cause cellular damage and tissue injury. During an inflammatory process, activated immune cells release ROS, leading to oxidative stress and tissue damage and causing demyelination and axonal destruction (54). Reduction in oxidative damage is an important therapeutic strategy. In recent years, many studies are

focused on antioxidant-based treatment for neuro-inflammatory diseases (55).

Alpha lipoic acid (ALA) is a naturally occurring antioxidant which has recently been investigated for its neuroprotective capacities during inflammation (56). It has been demonstrated to reduce the rate of brain atrophy in progressive MS (57), and it is highly effective at suppressing and treating EAE. Mice that received ALA experienced a dose-dependent reduction in cumulative disease scores (58). In another study, it was demonstrated that mice with EAE that received ALA had a dramatic reduction in axonal injury compared with saline-treated mice (59). However, another study demonstrated that therapeutic treatment with ALA attenuates the clinical disability and improves the survival of RGCs in the EAE model while prophylactic ALA therapy is capable of preserving visual function and prevention of thinning of the inner retinal layer (60). A clinical trial that tried to determine whether lipoic acid is neuroprotective in acute optic neuritis in humans did not conclude that 6 weeks of oral LA supplementation treatment after acute optic neuritis was neuroprotective. It is safe though and well tolerated (61). The antioxidant idebenone is beneficial in two neurological disorders caused by mitochondrial alterations: Friedreich's ataxia and Leber's hereditary optic neuropathy. In a study using an EAE model, idebenone-treated mice showed no improvement in inflammation, demyelination, or axonal damage. It failed to affect disease when applied preventively or therapeutically (62). Bilirubin has previously been demonstrated to be a potent antioxidant *in vitro* (63). When administered to rats before the onset of EAE, it was shown to have a protective effect on BBB from increasing permeability due to ROS damage and by that, preventing invasion of inflammatory cells into CNS during inflammation. In rats that were treated after induction of EAE, bilirubin did not reduce the degree of inflammation or cytokine expression but did demonstrate clinical improvement (64). A study aimed to investigate the effect of melatonin demonstrated a neuroprotective effect against EAE, by suppressing the progression and lymphocytic infiltration. This effect was probably related to the decrease of the levels of oxidative stress (65). The amino acid acetyl-l-carnitine (ALCAR) was evaluated for its effects when used alone or together with corticosteroids for treatment of EAE. A combination of the two demonstrated an antioxidant, antiapoptotic, and immunosuppressive effect. It also improved the clinical outcome when compared with the untreated group or corticosteroid treatment alone (66).

Unfortunately, studies suggesting antioxidative-based treatment for optic neuritis that showed benefit in the EAE model, did not progress to clinical trial in humans, and if so, did not show any benefit for the treatment in these cases.

Neuroprotective Therapies

Optic neuritis may lead to permanent visual loss mediated by RGC damage. The goal of neuroprotection is to preserve axon structures and function; it is highly important given the poor regenerative capacity of neurons. The specific mechanism and timing of the RGC damage during the disease process are crucial for understanding the damage and how to prevent it. In a study aimed to determine whether axonal injury due to inflammation mediates apoptotic death of RGCs, EAE was induced followed by demyelination with significant axonal loss which was followed by loss of RGC. It was suggested that inflammatory cell infiltration mediates demyelination and leads to direct axonal injury. RGCs die by an apoptotic mechanism triggered by axonal injury (67). Another study demonstrated DNA degradation and activation of caspase-3 in RGCs of EAE-induced rats. This indicates that cell death of RGCs is apoptotic (68). Potential neuroprotective therapies to prevent permanent RGC loss from optic neuritis need to be initiated prior to axonal injury to preserve neuronal function. A study that examined potential neuroprotective effects in optic neuritis by SRT647 and SRT501, activators of SIRT1, an enzyme involved in cellular stress resistance and survival, demonstrated that SIRT1 activation prevents RGC loss in optic neuritis even in the presence of active inflammation, suggesting that their neuroprotective effects will be additive to other immunomodulatory treatments (69).

High-dose intravenous corticosteroids are the standard treatment for acute optic neuritis. The optic neuritis treatment trial (ONTT) demonstrated that intravenous methylprednisolone followed by oral prednisone helps recovery of visual acuity and results in slightly better vision at 6 months. Oral prednisone alone is not an effective treatment. It increases the risk of recurrent episodes of optic neuritis (9). However, a study demonstrated a proapoptotic effect of the RGCs induced by methylprednisolone treatment for acute optic neuritis, although inflammatory infiltration of the optic nerve was reduced (70).

Brimonidine (BMD) is a selective α2-adrenergic receptor agonist that is used clinically for the treatment of glaucoma. Topical administration of BMD at 0.2% was shown to result in vitreous concentration of 2 nM and above, which is known to activate alpha(2)-receptors (71). There have been several studies demonstrating a neuroprotective effect of BMD. One of them evaluated BMD effect on retinal degeneration during optic neuritis in EAE, showing a suppression of the significant reduction in the number of RGCs, indicating the functional significance of the neuroprotective effect of BMD (72).

Various mechanisms for neuroprotection by brimonidine have been suggested, including brain-derived neurotrophic factor (BDNF) activation in the retinal ganglion cells, glutamate inhibition, suppression of excitotoxicity in retinal ganglion cells, stimulating trophic factor release from Müller cells, and cell-survival signal upregulation, as well as apoptosis downregulation (73, 74).

Voltage-gated sodium channels (Nav) are suggested to have a key role in the etiology of EAE by causing axonal degeneration (75). Nav1.6 isoform is a promoter of neuronal degeneration and inflammation in EAE (76), suggesting that it plays a corresponding role in MS and possibly in other degenerative neurological diseases. It was shown that downregulating or blocking Nav1.6 on neuronal cells would be neuroprotective (77).

Phenytoin is a voltage-gated sodium channel blocker used as an antiseizure medication. A study evaluating the effect of phenytoin on axonal degeneration in the optic nerve in EAE, reported that whereas ∼50% of optic nerve axons are lost at 27–28 days in untreated EAE, only ∼12% of the axons are lost if mice with EAE are treated with phenytoin (78).

Remyelination-Based Therapies

Myelin is a lipid-rich protective covering that surrounds axons. It provides an electrical isolation that allows fast nerve transmission and metabolic support to neurons. In demyelinating diseases, myelin loss leads to disruption in electrical conduction (79). Following pathological loss of myelin, remyelination, the formation of new myelin sheaths around axons, occurs (80). Myelin is formed by newly differentiated oligodendrocytes (OLs) derived from oligodendrocyte progenitors (OPCs) at the lesion sites. Microglia activation plays a crucial role in promoting oligodendrocyte maturation and effective remyelination (81). Unfortunately, the remyelination process is often inefficient, leading to permanent deficits and dysfunction. Its failure results from the inability of OPCs to successfully generate new mature myelinating oligodendrocytes (82). Many processes have been identified as targets for therapies that enhance the remyelination process in neuro-inflammatory demyelinating diseases.

A major target is lipid metabolism in oligodendrocytes. Lipids account for about 70% of the myelin membrane. A decrease in cholesterol synthesis in astrocytes might affect demyelination of autoimmune disease (83). Cholesterols in the brain must be synthesized locally because peripheral cholesterol does not cross the BBB. It was shown that dietary cholesterol supplements promote the repair of demyelinated lesions. Concomitant with blood-brain barrier impairment, they directly supports oligodendrocyte precursor proliferation and differentiation (84). In the adult brain, cholesterols are synthesized in astrocytes, transported to neurons to make cell membranes and synapses, and to oligodendrocytes to make myelin (85–88). Thus, reduced cholesterol synthesis in astrocytes during an inflammatory process may lead to reduced cholesterol available for neurons and oligodendrocytes, hence limited reparative synaptic plasticity and remyelination.

Normally, there is a balance between the rate of demyelination and remyelination processes. Myelin debris are phagocytosed by microglia; when this balance is disrupted, such as in inflammatory demyelinating diseases, it causes an accumulation of myelin debris that impairs remyelination (89).

Another study hypothesized that the inability to repair the demyelination damage caused by the inflammation during EAE may result from decreased cholesterol synthesis by astrocytes. Upregulation of cholesterol-synthesis gene expression was observed in oligodendrocytes during remyelination (90).

Another study demonstrated an accelerated remyelination after EAE induction by direct lineage analysis and hypothesized that newly formed myelin remains stable during the inflammation process due to the absence of MOG expression in immature myelin. Furthermore, withholding oligodendrocyte differentiation and myelination results in acceleration of remyelination, thus preventing axonal loss and improving functional recovery (91).

CONCLUSIONS

Optic neuritis is an inflammatory demyelinating disorder of the optic nerve with up to 0.1% prevalence at certain regions and potentially devastating visual outcomes. Animal models using the EAE experimental rodent model are essential for the understanding of etiology, pathogenesis of immune-mediated processes and for the development of therapeutic strategies for optic neuritis.

In this review, we discussed the latest rodent models regarding optic neuritis, focusing on the widely used EAE model, on its recent achievements and developments. So far, none of the therapeutic strategies have shown a substantial achievement regarding optic neuritis in the field of neuroprotection and remyelination. Further investigation is required.

AUTHOR CONTRIBUTIONS

YR and ML contributed to the writing of the manuscript. Both authors contributed to the article and approved the submitted version.

REFERENCES

1. Rodriguez M, Siva A, Cross SA, O'Brien PC, Kurland LT. Optic neuritis: a population-based study in Olmsted County, Minnesota. *Neurology.* (1995) 45:244–50. doi: 10.1212/WNL.45.2.244
2. Shams PN, Plant GT. Optic neuritis: a review. *Int MS J.* (2009) 16:82–9.
3. Balcer LJ. Clinical practice. Optic neuritis. *N Engl J Med.* (2006) 354:1273–80. doi: 10.1056/NEJMcp053247
4. Pau D, Al Zubidi N, Yalamanchili S, Plant GT, Lee AG. Optic neuritis. *Eye.* (2011) 25:833–42. doi: 10.1038/eye.2011.81
5. Jarius S, Wildemann B, Paul F. Neuromyelitis optica: clinical features, immunopathogenesis and treatment. *Clin Exp Immunol.* (2014) 176:149–64. doi: 10.1111/cei.12271
6. Pache F, Zimmermann H, Mikolajczak J, Schumacher S, Lacheta A, Oertel F, et al. MOG-IgG in NMO and related disorders: a multicenter study of 50 patients. Part 4: Afferent visual system damage after optic neuritis in MOG-IgG-seropositive versus AQP4-IgG-seropositive patients. *J Neuroinflammation.* (2016) 13:282. doi: 10.1186/s12974-016-0720-6
7. Britze J, Frederiksen JL. Optical coherence tomography in multiple sclerosis. *Eye.* (2018) 32:884–8. doi: 10.1038/s41433-017-0010-2
8. Chaoying SX, Kardon RH, Leavitt JA, Flanagan EP, Pittock SJ, Chen JJ. Optical coherence tomography is highly sensitive in detecting prior optic neuritis. *Neurology.* (2019) 92:e527–35. doi: 10.1212/WNL.0000000000006873
9. Beck RW, Cleary PA, Anderson MM, Keltner JL, Shults WT, Kaufman DI, et al. A randomized, controlled trial of corticosteroids in the treatment of acute optic neuritis. The Optic Neuritis Study Group. *N Engl J Med.* (1992) 326:581–8. doi: 10.1056/NEJM199202273260901
10. Andorrà M, Alba-Arbalat S, Camos-Carreras A, Gabilondo I, Fraga-Pumar E, Torres-Torres R, et al. Using acute optic neuritis trials to assess neuroprotective and remyelinating therapies in multiple sclerosis. *JAMA Neurol.* (2019) 77:234–44. doi: 10.1001/jamaneurol.2019.3283
11. Aktas O, Albrecht P, Hartung HP. Optic neuritis as a phase 2 paradigm for neuroprotection therapies of multiple sclerosis: update on current trials and perspectives. *Curr Opin Neurol.* (2016) 29:199–204. doi: 10.1097/WCO.0000000000000327
12. Villoslada P, Steinman L. New targets and therapeutics for neuroprotection, remyelination and repair in multiple sclerosis. *Expert Opin Investig Drugs.* (2020) 29:443–59. doi: 10.1080/13543784.2020.1757647

13. Rabchevsky AG, Degos JD, Dreyfus PA. Peripheral injections of freund's adjuvant in mice provoke leakage of serum proteins through the blood-brain barrier without inducing reactive gliosis. *Brain Res.* (1999) 832:84–96. doi: 10.1016/S0006-8993(99)01479-1
14. Constantinescu CS, Farooqi N, O'Brien K, Gran B. Experimental autoimmune encephalomyelitis (EAE) as a model for multiple sclerosis (MS). *Br J Pharmacol.* (2011) 164:1079–6. doi: 10.1111/j.1476-5381.2011.01302.x
15. Libbey JE, Fujinami RS. Vaccine. Experimental autoimmune encephalomyelitis as a testing paradigm for adjuvants and vaccines. *J Vaccine.* (2011) 29:3356–62. doi: 10.1016/j.vaccine.2010.08.103
16. Robinson AP, Harp CT, Noronha A, Miller SD. Chapter 8 - The experimental autoimmune encephalomyelitis (EAE) model of MS: utility for understanding disease pathophysiology and treatment. *Handb Clin Neurol.* (2014) 122:173–89. doi: 10.1016/B978-0-444-52001-2.00008-X
17. Wekerle H, Kojima K, Lannes-Vieira J, Lassmann H, Linington C, et al. Animal models. *Ann Neurol.* (1994) 36 (Suppl):S47–53. doi: 10.1002/ana.410360714
18. Meeson AP, Piddlesden S, Morgan BP, Reynolds R. The distribution of inflammatory demyelinated lesions in the central nervous system of rats with antibody-augmented demyelinating experimental allergic encephalomyelitis. *Exp Neurol.* (1994) 129:299–310. doi: 10.1006/exnr.1994.1172
19. Bjelobaba I, Begovic-Kupresanin V, Pekovic S, Lavrnja I. Animal models of multiple sclerosis: focus on experimental autoimmune encephalomyelitis. *J Neurosci Res.* (2018) 96:1021–42. doi: 10.1002/jnr.24224
20. McQualter JL, Bernard CCA. Multiple sclerosis: a battle between destruction and repair. *J Neurochem.* (2007) 100:295–306. doi: 10.1111/j.1471-4159.2006.04232.x
21. Prat A, Biernacki K, Lavoie JF, Poirier J, Duquette P, Antel JP. Migration of multiple sclerosis lymphocytes through brain endothelium. *Arch Neurol.* (2002) 59:391–7. doi: 10.1001/archneur.59.3.391
22. Barnett MH, Henderson AP, Prineas JW. The macrophage in MS: just a scavenger after all? Pathology and pathogenesis of the acute MS lesion. *Mult Scler.* (2006) 12:121–32. doi: 10.1191/135248506ms1304rr
23. Duffy SS, Lees JG, Moalem-Taylor G. The contribution of immune and glial cell types in experimental autoimmune encephalomyelitis and multiple sclerosis. *Mult Scler Int.* (2014) 2014:285245. doi: 10.1155/2014/285245
24. Söderström M, Link H, Sun JB, Fredrikson S, Wang ZY, Huang WX. Autoimmune T cell repertoire in optic neuritis and multiple sclerosis: T cells recognising multiple myelin proteins are accumulated in cerebrospinal fluid. *J Neurol Neurosurg Psychiatry.* (1994) 57:544–51. doi: 10.1136/jnnp.57.5.544
25. Bjartmar C, Wujek JR, Trapp BD. Axonal loss in the pathology of MS: consequences for understanding the progressive phase of the disease. *J Neurol Sci.* (2003) 206:165–71. doi: 10.1016/S0022-510X(02)00069-2
26. Brück W, Stadelmann C. Inflammation and degeneration in multiple sclerosis. *Neurol Sci.* (2003) 24 (Suppl. 5):S265–7. doi: 10.1016/S0022-510X(02)00191-0
27. Costello F, Coupland S, Hodge W, Lorello GR, Koroluk J, Pan YI, et al. Quantifying axonal loss after optic neuritis with optical coherence tomography. *Ann Neurol.* (2006) 59:963–9. doi: 10.1002/ana.20851
28. Fisher JB, Jacobs DA, Markowitz CE, Galetta SL, Volpe NJ, Nano-Schiavit ML, et al. Relation of visual function to retinal nerve fiber layer thickness in multiple sclerosis. *Ophthalmology.* (2006) 113:324–32. doi: 10.1016/j.ophtha.2005.10.040
29. Cruz-Herranz A, Dietrich M, Hilla AM, Yiu HH, Levin MH, Hecker C, et al. Monitoring retinal changes with optical coherence tomography predicts neuronal loss in experimental autoimmune encephalomyelitis. *J Neuroinflammation.* (2019) 16:203. doi: 10.1186/s12974-019-1583-4
30. Muller DM, Pender MP, Greer JM. A neuropathological analysis of experimental autoimmune encephalomyelitis with predominant brain stem and cerebellar involvement and differences between active and passive induction. *Acta Neuropathol.* (2000) 100:174–82. doi: 10.1007/s004019900163
31. Sakuma H, Kohyama K, Park IK, Miyakoshi A, Tanuma N, Matsumoto Y. Clinicopathological study of a myelin oligodendrocyte glycoprotein-induced demyelinating disease in LEW.1AV1 rats. *Brain.* (2004) 127(Pt 10):2201–13. doi: 10.1093/brain/awh260
32. Tassoni A, Farkhondeh V, Itoh Y, Itoh N, Sofroniew MV, Voskuhl RR. The astrocyte transcriptome in EAE optic neuritis shows complement activation and reveals a sex difference in astrocytic C3 expression. *Sci Rep.* (2019) 9:10010. doi: 10.1038/s41598-019-46232-6
33. Wilmes AT, Reinehr S, Kühn S, Pedreiturria X, Petrikowski L, Faissner S, et al. Laquinimod protects the optic nerve and retina in an experimental autoimmune encephalomyelitis model. *J Neuroinflammation.* (2018) 15:183. doi: 10.1186/s12974-018-1208-3
34. Bettelli E, Pagany M, Weiner HL. Myelin oligodendrocyte glycoprotein–specific T cell receptor transgenic mice develop spontaneous autoimmune optic neuritis. *J Exp Med.* (2003) 197:1073–81. doi: 10.1084/jem.20021603
35. Jones MV, Collongues N, de Seze J. Review of animal models of neuromyelitis optica. *Mult Scler Relat Disord.* (2012) 1:174–9. doi: 10.1016/j.msard.2012.06.003
36. Saini H, Rifkin R, Gorelik M, Huang H, Ferguson Z, Jones MV, et al. Passively transferred human NMO-IgG exacerbates demyelination in mouse experimental autoimmune encephalomyelitis. *BMC Neurol.* (2013) 13:104. doi: 10.1186/1471-2377-13-104
37. Asavapanumas N, Ratelade J, Papadopoulos MC, Bennett JL, Levin MH, et al. Experimental mouse model of optic neuritis with inflammatory demyelination produced by passive transfer of neuromyelitis optica-immunoglobulin G. *J Neuroinflammation.* (2014) 11:16. doi: 10.1186/1742-2094-11-16
38. Kinoshita M, Nakatsuji Y, Kimura T, Moriya M, Takata K, Okuno T, et al. Anti-aquaporin-4 antibody induces astrocytic cytotoxicity in the absence of CNS antigen-specific T cells. *Biochem Biophys Res Commun.* (2010) 394:205–10. doi: 10.1016/j.bbrc.2010.02.157
39. Kinoshita M, Nakatsuji Y, Kimura T, Moriya M, Takata K, Okuno T, et al. Neuromyelitis optica: passive transfer to rats by human immunoglobulin. *Biochem Biophys Res Commun.* (2009) 386:623–7. doi: 10.1016/j.bbrc.2009.06.085
40. Asavapanumas N, Ratelade J, Verkman AS. Unique neuromyelitis optica pathology produced in naïve rats by intracerebral administration of NMO-IgG. *Acta Neuropathol.* (2014) 127:539–51. doi: 10.1007/s00401-013-1204-8
41. Jones MV, Huang H, Calabresi PA, Levy M. Pathogenic aquaporin-4 reactive T cells are sufficient to induce mouse model of neuromyelitis optica. *Acta Neuropathol Commun.* (2015) 3:28. doi: 10.1186/s40478-015-0207-1
42. Sagan SA, Winger RC, Cruz-Herranz A, Nelson PA, Hagberg S, Miller CN, et al. Tolerance checkpoint bypass permits emergence of pathogenic T cells to neuromyelitis optica autoantigen aquaporin-4. *Proc Natl Acad Sci USA.* (2016) 113:14781–6. doi: 10.1073/pnas.1617859114
43. Rao NA, Tso MO, Zimmerman EL. Experimental allergic optic neuritis in guinea pigs: preliminary report. *Invest Ophthalmol Vis Sci.* (1977) 16:338–42.
44. Anderson DR. Ultrastructure of human and monkey lamina cribrosa and optic nerve head. *Arch Ophthalmol.* (1969) 82:800–14. doi: 10.1001/archopht.1969.00990020792015
45. Lightman S, McDonald WI, Bird AC, Francis DA, Hoskins A, Batcholer JR, et al. Retinal venous sheathing in optic neuritis. Its significance for the pathogenesis of multiple sclerosis. *Brain.* (1987) 110 (Pt 2):405–14. doi: 10.1093/brain/110.2.405
46. Wiśniewski HM, Bloom BR. Experimental allergic optic neuritis (EAON) in the rabbit. A new model to study primary demyelinating diseases. *J Neurol Sci.* (1975) 24:257–63. doi: 10.1016/0022-510X(75)90237-3
47. Lee S, Park JY, Lee WH, Kim H, Park HC, Mori K, et al. Lipocalin-2 is an autocrine mediator of reactive astrocytosis. *J Neurosci.* (2009) 29:234–49. doi: 10.1523/JNEUROSCI.5273-08.2009
48. Nam Y, Kim JH, Seo M, Kim JH, Jin M, Jeon S, et al. Lipocalin-2 protein deficiency ameliorates experimental autoimmune encephalomyelitis: the pathogenic role of lipocalin-2 in the central nervous system and peripheral lymphoid tissues. *J Biol Chem.* (2014) 289:16773–89. doi: 10.1074/jbc.M113.542282
49. Chun BY, Kim JH, Nam Y, Huh MI, Han S, Suk K. Pathological involvement of astrocyte-derived lipocalin-2 in the demyelinating optic neuritis. *Invest Ophthalmol Vis Sci.* (2015) 56:3691–8. doi: 10.1167/iovs.15-16851
50. Stojic A, Bojcevski J, Williams SK, Bas-Orth C, Nessler S, Linington C, et al. Preclinical stress originates in the rat optic nerve head during development of autoimmune optic neuritis. *Glia.* (2019) 67:512–24. doi: 10.1002/glia.23560
51. Ratelade J, Verkman AS. Neuromyelitis optica: aquaporin-4 based pathogenesis mechanisms and new therapies. *Int J Biochem Cell Biol.* (2012) 44:1519–30. doi: 10.1016/j.biocel.2012.06.013
52. Dal Monte M, Cammalleri M, Locri F, Amato R, Marsili S, Rusciano D, et al. Fatty acids dietary supplements exert anti-inflammatory action and limit

ganglion cell degeneration in the retina of the EAE mouse model of multiple sclerosis. *Nutrients.* (2018) 10:325. doi: 10.3390/nu10030325
53. Locri F, Cammalleri M, Pini A, Dal Monte M, Rusciano D, Bagnoli P. Further evidence on efficacy of diet supplementation with fatty acids in ocular pathologies: insights from the EAE model of optic neuritis. *Nutrients.* (2018) 10:1447. doi: 10.3390/nu10101447
54. Horssen JV, Witte ME, Schreibelt G, de Vries HE. Radical changes in multiple sclerosis pathogenesis. *Biochim Biophys Acta.* (2011) 1812:141–50. doi: 10.1016/j.bbadis.2010.06.011
55. Witherick J, Wilkins A, Scolding N, Kemp K. Mechanisms of oxidative damage in multiple sclerosis and a cell therapy approach to treatment. *Autoimmune Dis.* (2010) 2011:164608. doi: 10.4061/2011/164608
56. Li B, Tan GJ, Lin HQ, Zhang JN, Guo L, Chen LP. Neuroprotective effects of α-lipoic acid on long-term experimental autoimmune encephalomyelitis. *Eur Rev Med Pharmacol Sci.* (2018) 22:6517–28. doi: 10.26355/eurrev_201810_16066
57. Spain R, Powers K, Murchison, Heriza E, Winges K, Yadav V. Lipoic acid in secondary progressive MS: a randomized controlled pilot trial. *Neurol Neuroimmunol Neuroinflamm.* (2017) 4:e374. doi: 10.1212/NXI.0000000000000374
58. Marracci GH, Jones RE, McKeon GP, Bourdette DN. Alpha lipoic acid inhibits T cell migration into the spinal cord and suppresses and treats experimental autoimmune encephalomyelitis. *J Neuroimmunol.* (2002) 131:104–14. doi: 10.1016/S0165-5728(02)00269-2
59. Chaudhary P, Marracci G, Yu X, Galipeau D, Morris B, Bourdette D. Lipoic acid decreases inflammation and confers neuroprotection in experimental autoimmune optic neuritis. *J Neuroimmunol.* (2011) 233:90–6. doi: 10.1016/j.jneuroim.2010.12.002
60. Dietrich M, Helling N, Hilla A, Heskamp A, Issberner A, Hildebrandt T. Early alpha-lipoic acid therapy protects from degeneration of the inner retinal layers and vision loss in an experimental autoimmune encephalomyelitis-optic neuritis model. *J Neuroinflammation.* (2018) 15:71. doi: 10.1186/s12974-018-1111-y
61. Falardeau J, Fryman A, Wanchu R, Marracci GH, Mass M, Wooliscroft L. Oral lipoic acid as a treatment for acute optic neuritis: a blinded, placebo controlled randomized trial. *Mult Scler J Exp Transl Clin.* (2019) 5:2055217319850193. doi: 10.1177/2055217319850193
62. Fiebiger SM, Bros H, Grobosch T, Janssen A, Chanvillard C, Paulet F, et al. The antioxidant idebenone fails to prevent or attenuate chronic experimental autoimmune encephalomyelitis in the mouse. *J Neuroimmunol.* (2013) 262:66–71. doi: 10.1016/j.jneuroim.2013.07.002
63. Stocker R, Yamamoto Y, McDonagh AF, Glazer AN, Ames BN. Bilirubin is an antioxidant of possible physiological importance. *Science.* (1987) 235:1043–6. doi: 10.1126/science.3029864
64. Liu Y, Zhu B, Wang X, Luo L, Li P, Paty DW, et al. Bilirubin as a potent antioxidant suppresses experimental autoimmune encephalomyelitis: implications for the role of oxidative stress in the development of multiple sclerosis. *J Neuroimmunol.* (2003) 139:27–35. doi: 10.1016/S0165-5728(03)00132-2
65. Long T, Yang Y, Peng L, Li Z. Neuroprotective effects of melatonin on experimental allergic encephalomyelitis mice via anti-oxidative stress activity. *J Mol Neurosci.* (2018) 64:233–41. doi: 10.1007/s12031-017-1022-x
66. Zidan A, Hedya SE, Elfeky DM, Abdin AA. The possible anti-apoptotic and antioxidant effects of acetyl l-carnitine as an add-on therapy on a relapsing-remitting model of experimental autoimmune encephalomyelitis in rats. *Biomed Pharmacother.* (2018) 103:1302–11. doi: 10.1016/j.biopha.2018.04.173
67. Shindler KS, Ventura E, Dutt M, Rostami A. Inflammatory demyelination induces axonal injury and retinal ganglion cell apoptosis in experimental optic neuritis. *Exp Eye Res.* (2008) 87:208–13. doi: 10.1016/j.exer.2008.05.017
68. Meyer R, Weissert R, Diem R, Storch MK, de Graaf KL, Kramer B, et al. Acute neuronal apoptosis in a rat model of multiple sclerosis. *J Neurosci.* (2001) 21:6214–20. doi: 10.1523/JNEUROSCI.21-16-06214.2001
69. Shindler KS, Ventura E, Rex TS. SIRT1 activation confers neuroprotection in experimental optic neuritis. *Invest Ophthalmol Vis Sci.* (2007) 48:3602–9. doi: 10.1167/iovs.07-0131
70. Diem R, Hobom M, Maier K, Weissert R, Storch MK, Meyer R, et al. Methylprednisolone increases neuronal apoptosis during autoimmune CNS inflammation by inhibition of an endogenous neuroprotective pathway. *J Neurosci.* (2003) 23:6993–7000. doi: 10.1523/JNEUROSCI.23-18-06993.2003
71. Kent AR, Nussdorf JD, David R, Tyson F, Small D, Fellows D. Vitreous concentration of topically applied brimonidine tartrate 0.2%. *Ophthalmology Z.* (2001) 108:784–7. doi: 10.1016/S0161-6420(00)00654-0
72. Guo X, Namekata K, Kimura A, Noro T, Azuchi Y, Semba K, et al. Brimonidine suppresses loss of retinal neurons and visual function in a murine model of optic neuritis. *Neurosci Lett.* (2015) 592:27–31. doi: 10.1016/j.neulet.2015.02.059
73. Gao H, QiaoX, Cantor LD, WuDunn D. Up-regulation of brain-derived neurotrophic factor expression by brimonidine in rat retinal ganglion cells. *Arch Ophthalmol.* (2002) 120:797–803. doi: 10.1001/archopht.120.6.797
74. Semba K, Namekata K, Kimura A, Harada C, Mitamura Y, Harada T. Brimonidine prevents neurodegeneration in a mouse model of normal tension glaucoma. *Cell Death Dis.* (2014) 5:1341. doi: 10.1038/cddis.2014.306
75. Craner MJ, Lo AC, Black JA, Waxman SG. Abnormal sodium channel distribution in optic nerve axons in a model of inflammatory demyelination. *Brain.* (2003) 126(Pt 7):1552–61. doi: 10.1093/brain/awg153
76. Craner MJ, Damarjian TG, Liu S, Hains BC, Lo AC, Black JA. Sodium channels contribute to microglia/macrophage activation and function in EAE and MS. *Glia.* (2005) 49:220–9. doi: 10.1002/glia.20112
77. Alrashdi B, Dawod B, Schampel A, Tacke S, Kuerten S, Marshall JS, et al. Nav1.6 promotes inflammation and neuronal degeneration in a mouse model of multiple sclerosis. *J Neuroinflammation.* (2019) 16:215. doi: 10.1186/s12974-019-1622-1
78. Lo AC, Black JA, Waxman SG. Neuroprotection of axons with phenytoin in experimental allergic encephalomyelitis. *Neuroreport.* (2002) 13:1909–12. doi: 10.1097/00001756-200210280-00015
79. Giuliodori MJ, DiCarlo SE. Myelinated vs. unmyelinated nerve conduction: a novel way of understanding the mechanisms. *Adv Physiol Educ.* (2004) 28:80–1. doi: 10.1152/advan.00045.2003
80. Verden D, Macklin WB. Neuroprotection by central nervous system remyelination: molecular, cellular, and functional considerations. *J Neurosci Res.* (2016) 94:1411–20. doi: 10.1002/jnr.23923
81. Liu Y, Given KS, Owens GP, Macklin WB, Bennett JL. Distinct patterns of glia repair and remyelination in antibody-mediated demyelination models of multiple sclerosis and neuromyelitis optica. *Glia.* (2018) 66:2575–88. doi: 10.1002/glia.23512
82. Kremer D, Göttle P, Hartung HP, Küry P. Pushing forward: remyelination as the new frontier in CNS diseases. *Trends Neurosci.* (2016) 39:246–63. doi: 10.1016/j.tins.2016.02.004
83. Marangon D, Boccazzi M, Lecca D, Fumagalli D. Regulation of oligodendrocyte functions: targeting lipid metabolism and extracellular matrix for myelin repair. *J Clin Med.* (2020) 9:470. doi: 10.3390/jcm9020470
84. Berghoff SA, Gerndt N, Winchenbach J, Stumpf SK, Hosang L, Odoardi F, et al. Dietary cholesterol promotes repair of demyelinated lesions in the adult brain. *Nat Commun.* (2017) 8:14241. doi: 10.1038/ncomms14241
85. Saher G, Stumpf SK. Cholesterol in myelin biogenesis and hypomyelinating disorders. *Biochim Biophys Acta.* (2015) 1851:1083–94. doi: 10.1016/j.bbalip.2015.02.010
86. Fester L, Zhou L, Bütow A, Huber C, Lossow RV, Prange-Kiel J, et al. Cholesterol-promoted synaptogenesis requires the conversion of cholesterol to estradiol in the hippocampus. *Hippocampus.* (2009) 19:692–705. doi: 10.1002/hipo.20548
87. Mauch DH, Nägler K, Schumacher S, Göritz C, Müller EC, Otto A, et al. CNS synaptogenesis promoted by glia-derived cholesterol. *Science.* (2001) 294:1354–7. doi: 10.1126/science.294.5545.1354
88. Saher G, Brügger B, Lappe-Siefke C, Möbius W, Tozawa RI, Wehr MC, et al. High cholesterol level is essential for myelin membrane growth. *Nat Neurosci.* (2005) 8:468–75. doi: 10.1038/nn1426
89. Lampron A, Larochelle A, Laflamme N, Préfontaine P, Plante MM, Sánchez MG, et al. Inefficient clearance of myelin debris by microglia impairs remyelinating processes. *J Exp Med.* (2015) 212:481–95. doi: 10.1084/jem.20141656
90. Voskuhl RR, Itoh N, Tassoni A, Matsukawa MA, Ren E, Tse V, et al. Gene expression in oligodendrocytes during remyelination reveals cholesterol homeostasis as a therapeutic target in multiple sclerosis. *Proc Natl Acad Sci USA.* (2019) 116:10130–9. doi: 10.1073/pnas.1821306116

91. Mei F, Lehmann-Horn K, Shen YA, Rankin KA, Stebbins KJ, Lorrain DS, et al. Accelerated remyelination during inflammatory demyelination prevents axonal loss and improves functional recovery. *Elife.* (2016) 5:e18246. doi: 10.7554/eLife.18246.013

Conflict of Interest: ML currently receives research support from the National Institutes of Health. He also received personal compensation for consultation with Alexion, Viela Bio, and Genentech and has served on the scientific advisory boards for Alexion, Genentech, and Viela Bio.

The remaining author declare that the research was conducted in the absence of any commercial or financial relationships that could be construed as a potential conflict of interest.

Copyright © 2020 Redler and Levy. This is an open-access article distributed under the terms of the Creative Commons Attribution License (CC BY). The use, distribution or reproduction in other forums is permitted, provided the original author(s) and the copyright owner(s) are credited and that the original publication in this journal is cited, in accordance with accepted academic practice. No use, distribution or reproduction is permitted which does not comply with these terms.

frontiers in Neurology

ORIGINAL RESEARCH
published: 13 November 2020
doi: 10.3389/fneur.2020.589288

Markedly Elevated Serum Level of T-Helper Cell 17-Related Cytokines/Chemokines in Acute Myelin Oligodendrocyte Glycoprotein Antibody-Associated Optic Neuritis

Hao Kang[1], Hongyang Li[2], Nanping Ai[3], Hongjuan Liu[3], Quangang Xu[3], Yong Tao[1] and Shihui Wei[3]**

[1] Department of Ophthalmology, Beijing Chaoyang Hospital, Capital Medical University, Beijing, China, [2] Department of Ophthalmology, Beijing Friendship Hospital, Capital Medical University, Beijing, China, [3] Department of Ophthalmology, The Chinese People's Liberation Army General Hospital, Beijing, China

OPEN ACCESS

Edited by:
Ahmed Toosy,
University College London,
United Kingdom

Reviewed by:
Mark Paine,
Royal Brisbane and Women's Hospital, Australia
Christopher Charles Glisson,
Michigan State University,
United States

***Correspondence:**
Shihui Wei
Shihuiwei706@163.com
Yong Tao
drtaoyong@sina.com

Specialty section:
This article was submitted to Neuro-Ophthalmology, a section of the journal Frontiers in Neurology

Received: 30 July 2020
Accepted: 05 October 2020
Published: 13 November 2020

Citation:
Kang H, Li H, Ai N, Liu H, Xu Q, Tao Y and Wei S (2020) Markedly Elevated Serum Level of T-Helper Cell 17-Related Cytokines/Chemokines in Acute Myelin Oligodendrocyte Glycoprotein Antibody-Associated Optic Neuritis. Front. Neurol. 11:589288. doi: 10.3389/fneur.2020.589288

Purpose: The purpose of this study was to examine the differences in immunopathogenesis based on the cytokine/chemokine profiles in myelin oligodendrocyte glycoprotein antibody (MOG-IgG)-positive and -negative groups.

Methods: We measured the levels of T-helper cell 17 (Th17) cell-related cytokines/chemokines in 74 serum samples, which were divided into four groups: healthy control (HC) group ($n = 15$), idiopathic demyelinating optic neuritis (IDON) group ($n = 20$), aquaporin 4 (AQP4)-IgG-positive optic neuritis (ON) group ($n = 18$), and MOG-IgG positive-ON group ($n = 21$). Serum IL17, IL21, IL28, IL31, CXCL1, CXCL2, CCL2, CCL11, CCL20, and LT-α were detected.

Results: The serum of the MOG-IgG-positive ON patients showed an obvious elevation of Th17 cell-related cytokines/chemokines compared with that of all the MOG-IgG-negative ON patients. Serum IL17 and IL21 were significantly higher in the ON patients with MOG-IgG positive than in all the other three groups. The serum levels of IL28, IL31, CXCL1, and CCL11 were higher in the ON patients with MOG-IgG positive than in the HC group and the IDON group. The serum concentration of CCL2, CXCL2, and CCL20 in the MOG-IgG-positive and AQP4-IgG-positive group is higher than that of the HC group. No difference in serum LT-α level was found among the four groups. Adjusted multiple regression analyses showed a positive association of IL17 and IL21 levels with the serum concentration of MOG-IgG in the ON patients.

Conclusion: The elevated serum level of Th17 cell-related cytokine/chemokines may play an important role in the pathogenesis of MOG-IgG-positive demyelinating ON.

Keywords: T helper cell 17 (Th17), cytokines, chemokines, optic neuritis, MOG-IgG, AQP4-IgG

INTRODUCTION

Optic neuritis (ON) is the most common optic neuropathy affecting young adults. ON can occur in isolation, or as the initial symptom of autoimmune-mediated demyelinating diseases, such as multiple sclerosis (MS) or neuromyelitis optica (NMO)/neuromyelitis optica spectrum disorders (NMOSD) (1). In most cases, NMO is caused by autoantibodies to aquaporin 4 (AQP4-IgG) (2, 3), but 10–20% of patients with NMO are negative for AQP4-IgG (4, 5). Recent studies have shown the presence of IgG antibodies to myelin oligodendrocyte glycoprotein antibody (MOG-IgG) in some NMO/NMOSD patients (6, 7). MOG-IgG is pathogenic in human demyelinating diseases, and it is a biomarker of autoimmune ON and longitudinally extensive transverse myelitis (LETM) (8, 9).

MOG-IgG-seropositive patients had some clinical features different from those with AQP4-IgG seropositive (7). In addition, the histopathology of brain and spinal cord lesions of MOG IgG+ patients has been demonstrated to be different from that of AQP4-IgG+ patients (10, 11). MOG-IgG-related disease is now considered as a disease entity in its own right, immunopathogenetically distinct from MS and from AQP4-IgG-related demyelinating diseases.

Cytokines/chemokines are biologically active intercellular messengers having pleiotropic effects on various cell types resulting in immune system activation (12) In the nervous system, cytokines, and chemokines are involved in the regulation of central nerve system (CNS)-immune system interactions that function as neuromodulators and control neurodevelopment, neuroinflammation, and synaptic transmission (13). CD4+ T helper cells can be divided into four major subsets, and Th17 lineage is a recently discovered subset of CD4+ T-helper cells, which can promote tissue inflammation by induction of inflammatory mediators and recruitment of inflammatory cells (14). Th17 cells coordinate local tissue inflammation through the regulation of inflammatory cytokines and chemokines such as IL-17, IL-21, IL-28, CXCL1, CCL2, CXCL2, CCL11, and CCL20 (15). In this study, we evaluated the levels of Th17-related cytokines and chemokines in serum samples from MOG-IgG-seropositive ON, AQP4-IgG-seropositive ON, and idiopathic demyelinating ON (IDON) patients in the acute phase, in order to investigate the differences in immunopathogenesis based on the cytokine/chemokine profiles.

MATERIALS AND METHODS

Patients

In this study, 59 patients with unilateral or bilateral isolated ON were recruited from the Ophthalmology Department of Beijing Chaoyang Hospital of Capital Medical University and the Chinese People's Liberation Army General Hospital (PLAGH). Recruitment was completed between April 2017 and July 2018. ON was the first symptom in all the patients who fulfilled the diagnosis criteria of ON. All the subjects were treated with methylprednisolone according to the suggestion with ONTT (16). If a minimal response to the corticosteroid therapy and the vision remained below 0.1 were clinically observed, the patient involved was given a total of three to five plasma exchanges.

All blood samples were collected during the acute phase of the disease or within a month of exacerbation. Seventy-four serum samples were drawn from the patients with acute demyelinating ON and from the controls, including 15 samples from the healthy control (HC) group, 20 samples from the IDON group, 18 samples from the AQP4-IgG-seropositive ON group, and 21 samples from the MOG-IgG-seropositive ON group.

Ophthalmic examinations including best-corrected visual acuity (BCVA), intraocular pressure, slit lamp examination, pupillary reactions in unilateral or bilateral asymmetric conditions, and ocular fundus examinations were conducted by professional ophthalmologists.

BCVA was tested by using a Snellen chart and was transformed into logarithm of the minimum angel of resolution (logMAR) values by using Petzold's et al. (17) VA conversion method. If a VA was below 0.01, finger-counting (FC), hand motion (HM), perception of light (LP), and no perception of light (NLP) were tested, and the results were documented accordingly. All patients underwent visual field, electrodiagnostic tests, and orbit and brain magnetic resonance imaging (MRI) examination.

Aquaporin 4 IgG and Myelin Oligodendrocyte Glycoprotein Antibody Testing

All serum samples were analyzed for the presence of AQP4-IgG by an extracellular live cell-staining immunofluorescence technique using transiently transfected AQP4-expressing cells as previously described (18). Samples were scored as positive or negative by at least two independent experiments. A dilution of 1:1,000 was employed as the maximum positive value and 1:10 as the cut-off for positive and negative cases. MOG-IgG detection was performed by CBA with full-length human MOG-transfected HEK293 cells. MOG-IgG titers of $\geq$1:10 were classified as positive.

Cytokine and Chemokine Assay

Th17-related cytokines (IL-17, IL-21, IL-28, and IL-31) and chemokines (CXCL1/GRO alpha, CXCL2/GRO beta, CCL2/MCP-1, CCL20/MIP-3, and CCL11/eotaxin) and LT-alpha/TNF-beta were measured by means of ELISA. The regression equation of the standard curve ($R^2 > 0.98$) was calculated on the basis of the standard concentration and the corresponding A-value. Similarly, the corresponding sample concentration was calculated with reference to the sample's A-value.

Ethics Statement

This study was approved by the Ethics Committee of Beijing Chaoyang Hospital and PLAGH, and was conducted following the Declaration of Helsinki in its currently applicable version. Written informed consents were obtained from each patient.

Statistical Analysis

Statistical analysis was performed by using SPSS for Windows, Version 21.0. Continuous variables were analyzed using a

TABLE 1 | Epidemiologic and disease characteristics of ON patients and healthy controls.

	IDON	AQP4 + ON	MOG + ON	HC	*P*-value
Number of patients	20	18	21	15	–
Age at onset (years)	34.50 ± 12.96	37.06 ± 12.95	35.81 ± 14.08	35.20 ± 12.39	0.945
Gender (male:female)	3:17	1:17	11:10	4:11	**0.005**
Ocular pain (*n*, %)	10 (50.0)	15 (83.3)	17 (81.0)	–	**0.036**
Disc swelling (*n*, %)	8 (40.0)	7 (38.9)	7 (33.3)	–	0.894
Bilateral, ever (%)	5 (25.0)	7 (38.9)	9 (42.9)	–	0.461
Recurrent ON onset (*n*, %)	8 (40.0)	18 (100.0)	21 (100.0)	–	**<0.001**
Median CSF white cell count (*no./*mm^3)	2.10 ± 4.12	6.89 ± 11.29	3.00 ± 3.67	–	0.095
CSF protein (mg/L)	288.82 ± 85.01	422.53 ± 132.88	304.42 ± 94.03	–	**<0.001**
CSF IgG level (mg/L)	2.48 ± 0.96	3.55 ± 3.02	2.14 ± 0.64	–	0.05
BCVA at first ON attacks in acute time (logMAR)	1.85 ± 0.89	2.17 ± 0.79	1.82 ± 0.81	–	0.369
BCVA recovery at last follow-up (logMAR)	0.64 ± 0.67	1.00 ± 0.78	0.37 ± 0.51	–	**0.015**

ON, optic neuritis; AQP4: aquaporin-4; MOG, myelin oligodendrocyte glycoprotein; IDON, idiopathic demyelinated optic neuritis; HC, healthy controls; CSF, cerebrospinal fluid; MRI: magnetic resonance imaging; BCVA, best-corrected visual acuity. The bold values are used to indicate values with P < 0.05.

nonparametric test (Mann–Whitney U test). The Chi-squared test, or Fisher's exact test if applicable, was used to analyze the categorical data. The differences among any three groups were identified by using the ANOVA or Kruskal–Wallis test. In order to reduce type I errors, Bonferroni correction had been applied on the *P*-values. Correlation ranks were evaluated by Spearman's rank correlation tests.

RESULTS

Demographic Data and Clinical Characteristics

The demographic data and clinical characteristics of all the 59 Chinese ON patients were compared (**Table 1**). The mean age at disease onset was similar in the three groups. Female predominance was apparent in the IDON patients (82.4%) and the AQP4-IgG seropositive-ON patient (94.1%), but the MOG-IgG-seropositive ON patients were mostly male, with a male-to-female ratio of 11:10. Compared to the IDON group (10/20, 50.0%), the AQP4-IgG-seropositive ON (15/18, 83.3%) and MOG-IgG-seropositive ON (17/21, 81.0%) patients were more likely to have accompanying ocular pain. The proportion of disc swelling and monocular/binocular involvement showed no difference between the three groups. Recurrent ON appeared frequently among all the AQP4-IgG-seropositive ON (18/18, 100.0%) and MOG-IgG-seropositive ON patients (21/21, 100.0%), and the IDON patients (8/20, 60%) had a more frequent monophasic course. In the routine CSF analysis, no significant difference in the median CSF white cell count (no/mm^3) and the CSF IgG level (mg/L) between the three groups was found. CSF total protein (mg/L) was significantly higher in the AQP4-IgG-seropositive ON group than that in the other two groups ($P < 0.001$; AQP4-IgG + ON vs. MOG-IgG + ON: $P = 0.003$, AQP4-IgG + ON vs. IDON: $P = 0.001$). There were no significant differences between the three groups in the proportion of optic lesion in MRI. None of the patients in the three groups had MRI results that met the radiological diagnostic criteria of MS or NMO. VA at first attacks in the acute phase and VA recovery at the last follow-up were compared in the AQP4-IgG-seropositive ON, MOG-IgG-seropositive ON, and IDON patients. No differences in visual loss during the acute stage were observed between the three groups. At the last follow-up, the AQP4-IgG-seropositive ON patients were significantly more likely to get poor VA recovery over time than the other patients ($P = 0.015$; AQP4-IgG + ON vs. MOG-IgG + ON: $P = 0.012$, AQP4-IgG + ON vs. IDON: $P = 0.272$).

Comparison of T-Helper Cell 17-Related Serum Cytokine/Chemokine Levels Between the Myelin Oligodendrocyte Glycoprotein Antibody-Seropositive Optic Neuritis, Aquaporin 4-IgG-Seropositive Optic Neuritis, Idiopathic Demyelinating Optic Neuritis Patients, and the Healthy Controls

The dot plots of individual serum cytokines/chemokines levels are shown in **Figure 1**, and the values are summarized in **Table 2**. IL-17, IL-21, IL-28, IL-31, CXCL1, CXCL2, CCL2, CCL20, and CCL11 were significantly elevated in the MOG-IgG-seropositive ON patients than in the MOG-IgG-patients. The mean concentration of IL-17 in the patients with MOG-IgG-seropositive ON was much higher than the other three groups of patients. Moreover, it was also higher in the patients with AQP4-IgG-seropositive ON than in the HC group (IL-17: AQP4-IgG + ON vs. HC: $P = 0.031$). The concentration of IL-21 in the patients with MOG-IgG-seropositive ON was also higher than in the AQP4-IgG-seropositive ON, IDON, and HC groups. The IL-23 concentration in the patients with MOG-IgG-seropositive ON was also higher than in the IDON and HC groups. The MOG-IgG-seropositive ON patients showed a significantly higher IL-31 level than the IDON and HC patients. The serum CXCL1 and CXCL2 concentration in the patients with MOG-IgG-seropositive ON and AQP4-IgG-seropositive ON was

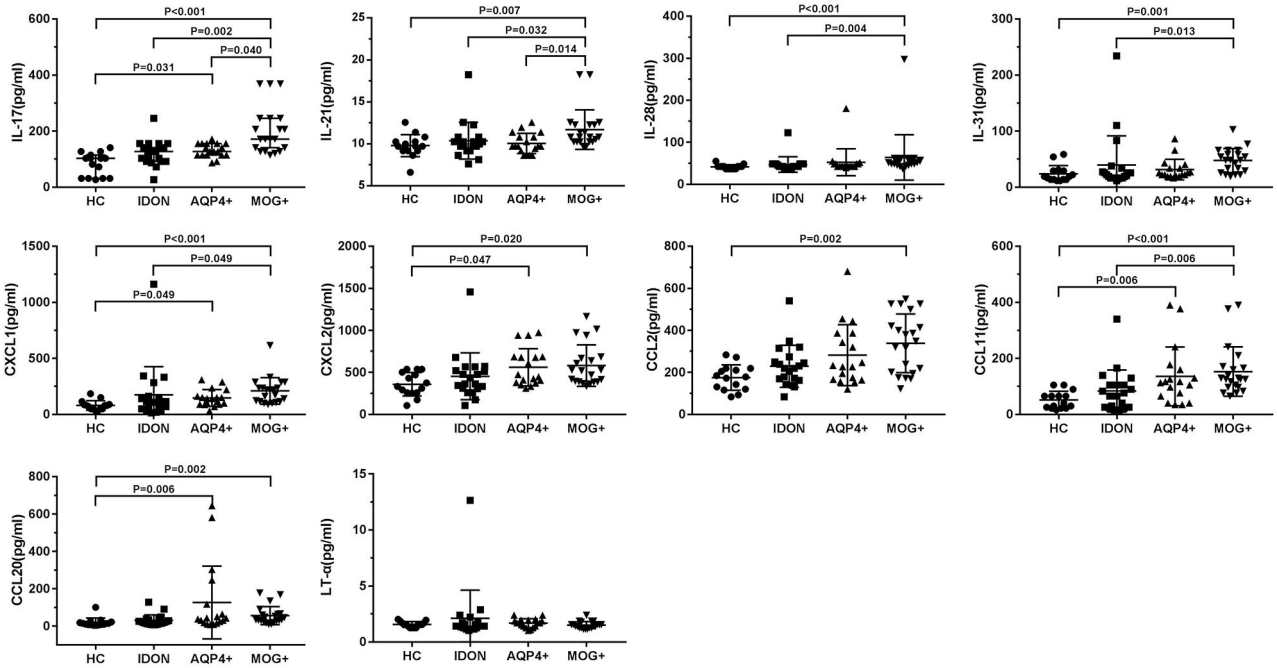

FIGURE 1 | Comparison of T-helper cell 17 (Th17)-related serum cytokine/chemokine levels between myelin oligodendrocyte glycoprotein antibody (MOG-IgG) + optic neuritis (ON), aquaporin 4 (AQP4-IgG) + ON, idiopathic demyelinating optic neuritis (IDON), and healthy controls.

TABLE 2 | Serum level of Th17-related cytokine/chemokines of optic neuritis patients.

	MOG-IgG + ON ($n = 21$)	AQP4-IgG + ON ($n = 18$)	IDON ($n = 20$)	HC ($n = 15$)	P[†]	P1[§]	P2[§]	P3[§]
IL-17 (pg/ml)	231.58 ± 156.74	131.33 ± 24.02	122.07 ± 44.56	81.73 ± 41.19	**<0.001**	**0.040**	**0.002**	**<0.001**
IL-21 (pg/ml)	11.70 ± 2.35	10.05 ± 1.20	10.38 ± 2.19	9.79 ± 1.32	**0.002**	**0.014**	**0.032**	**0.007**
IL-28 (pg/ml)	63.99 ± 54.00	52.49 ± 32.16	46.98 ± 18.46	41.34 ± 5.23	**<0.001**	0.081	**0.004**	**<0.001**
IL-31 (pg/ml)	47.51 ± 21.48	31.27 ± 18.28	39.61 ± 51.85	23.79 ± 14.67	**0.001**	0.167	**0.013**	**0.001**
CXCL1 (pg/ml)	209.71 ± 119.21	146.49 ± 74.65	175.12 ± 251.10	80.06 ± 42.96	**<0.001**	0.652	**0.049**	**<0.001**
CXCL2 (pg/ml)	581.23 ± 246.09	560.92 ± 221.33	453.84 ± 278.00	358.50 ± 139.63	**0.008**	>0.99	0.245	**0.020**
CCL2 (pg/ml)	56.44 ± 48.47	126.48 ± 194.93	30.52 ± 30.08	175.39 ± 60.81	**0.003**	>0.99	0.126	**0.002**
CCL20 (pg/ml)	2.31 ± 0.12	1.17 ± 0.21	1.66 ± 0.13	19.84 ± 23.87	**0.001**	>0.99	0.131	**0.002**
CCL11 (pg/ml)	152.83 ± 88.16	135.75 ± 104.86	83.41 ± 75.38	21.34 ± 31.11	**<0.001**	>0.99	**0.006**	**<0.001**
LT-α (pg/ml)	1.51 ± 0.31	1.68 ± 0.39	2.11 ± 2.52	1.57 ± 0.25	0.42	–	–	–

Th17, T-helper cell 17; ON, optic neuritis; AQP4, aquaporin 4; MOG, myelin oligodendrocyte glycoprotein; IDON, idiopathic demyelinated optic neuritis; HC, healthy controls; P1, MOG-IgG + ON and AQP4-IgG + ON; P2, MOG-IgG + ON and IDON; P3, MOG-IgG + ON and HC; [†] Kruskal–Wallis H-test; §Bonferroni method. The bold values are used to indicate values with $P < 0.05$.

also higher than that in the HC group (CXCL2: AQP4-IgG+ ON vs. HC: $P = 0.047$). The MOG-IgG-seropositive ON patients had a significantly higher CCL2 level than the HC patients. In the serum concentration of CCL20, the MOG-IgG-seropositive ON and AQP4-IgG-seropositive ON patients showed higher levels than the HC group (CCL20: AQP4-IgG + ON vs. HC: $P = 0.006$). CCL11 was significantly elevated in the two autoantibody-associated ON patients than in the HC group (CCL11: AQP4-IgG + ON vs. HC: $P = 0.006$). The CCL11 concentration in the MOG-IgG-seropositive ON patients was also higher than that in the IDON group. No significant difference was found in the serum concentration of LT-α between the four groups.

Relationship Between T-Helper Cell 17-Related Serum Cytokines/Chemokines and Serum Myelin Oligodendrocyte Glycoprotein Antibody Titer in the Myelin Oligodendrocyte Glycoprotein Antibody-Seropositive Optic Neuritic Patients

We then analyzed the potential correlations between the elevated Th17-related cytokines/chemokines levels and the titer of MOG-IgG in 21 MOG-IgG-seropositive ON patients (**Table 3**). Correlation analyses showed that serum IL-17 was positively

correlated with the titer of MOG-IgG in the patients' serum ($r = 0.534$, $P = 0.013$; **Figure 2**). The serum concentration of CCL11 was negatively correlated with the titer of MOG-IgG in the MOG-IgG-seropositive ON patients ($r = -0.481$, $P = 0.027$; **Figure 2**). However, no significant correlation between the other cytokines/chemokines and the serum titer of MOG-IgG was observed.

DISCUSSION

In the present study, we compared the Th17-related serum cytokines/chemokines in healthy adults and ON patients with different etiologies. In the MOG-IgG-seropositive ON patients, we noted a significant upregulation of Th17 cell-related serum cytokines/chemokines. These data are in agreement with previous studies of Th17 changes in other autoimmune diseases, as Th17 cells are a key stakeholder in the pathogenesis of many autoimmune disorders (15).

TABLE 3 | Spearman's correlation coefficient (r) of the association between serum cytokines/chemokines and MOG-IgG titer in 21 MOG-IgG-seropositive ON patients.

	MOG IgG ($n = 21$)	Correlation coefficient	*P*
IL-17 (pg/ml)		**0.534**	**0.013***
IL-21 (pg/ml)		0.163	0.479
IL-28 (pg/ml)		−0.104	0.653
IL-31 (pg/ml)		−0.195	0.397
CXCL1 (pg/ml)		−0.218	0.344
CXCL2 (pg/ml)		0.280	0.220
CCL2 (pg/ml)		−0.074	0.751
CCL20 (pg/ml)		0.176	0.445
CCL11 (pg/ml)		**−0.481**	**0.027***
LT-α (pg/ml)		−0.187	0.416

ON, optic neuritis; MOG, myelin oligodendrocyte glycoprotein. The bold values are used to indicate values with P < 0.05.
**P < 0.05.*

Th17 cells have been involved in several autoimmune disorders, and they seem to be relevant in CNS autoimmunity development. Th17-related molecules have also been shown to correlate with parameters of disease activity and severity in CNS inflammatory demyelinating diseases (19). IL-17 is a proinflammatory cytokine that upregulates the expression of inflammatory genes. More importantly, elevated IL-17 levels have been observed in autoimmune diseases like MS, inflammatory bowel disease, psoriasis, and rheumatoid arthritis (20). Although IL-17 is the signature cytokine of Th17 cells, many studies have shown that other cytokines related with Th17 cells are also significant in the pathogenesis of inflammatory responses. The release of IL-6 and IL-21 by polyclonally activated CD4+ T cells obtained from NMO patients was shown to have direct correlations with neurological disability (14). IL-31 is also produced mainly by CD4+ T cells. A recent report has shown that the serum concentration of IL-31 significantly increased in NMOSD patients and positively correlated with the serum level of IL-17 in those patients (21). Moreover, Th17 cells necessitate a large quantity of chemokines and chemokine receptors to cross the blood–brain barrier (BBB), which enables them to disrupt the BBB and access the CNS through some different pathways. IL-17 is a key factor in the disruption of the BBB by directly impairing its integrity (22). *In vitro* and *in vivo* studies have shown that through the action of IL-17, Th17 cells can efficiently break down BBB tight junctions, bring out high levels of the cytolytic enzyme granzyme B, and provide impetus to the recruitment of additional CD4+ lymphocytes from the systemic circulation into the CNS (23). In addition, Th17 cells are also capable of inducing CXCL1 and CXCL2, chemokines that are powerful attractants for polymorphonuclear cells, and of contributing much to the disruption of the BBB in experimental autoimmune encephalomyelitis (EAE) (24).

NMOSD is a severe CNS autoimmune inflammatory disorder, which has always been recognized as a B-cell-mediated humoral immune disease. However, B-cell depletion therapy was not efficacious in some NMOSD patients, including both antibody-seropositive or -seronegative patients (25). One possible reason is that B cell-mediated immunity may not be the sole contributor to NMOSD-like lesions, and other components like CD4+

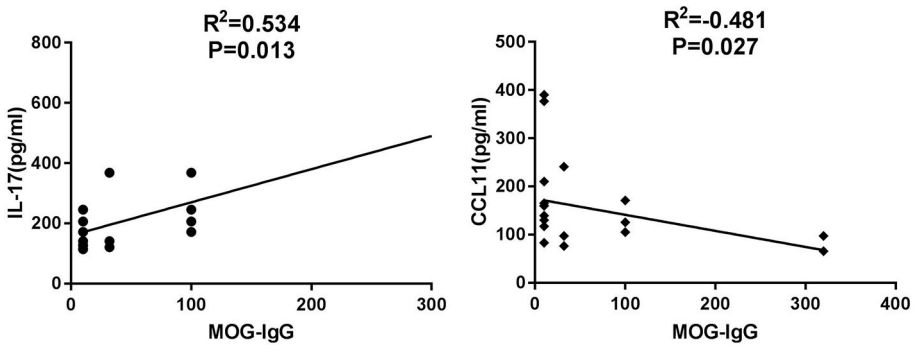

FIGURE 2 | Relationship between Th17-related serum cytokines/chemokines and serum MOG-IgG titer in MOG-IgG-seropositive ON patients.

T cells, especially Th17 cells, may also play potential roles. Studies have demonstrated that T-cell-mediated immunity may participate in the pathological process of NMOSD, especially in the Th17 phenotype (26–28). Another possible explanation is that MOG-IgG-related demyelination in the optic nerve and the spinal cord can partly explain AQP4-IgG-seronegative NMOSD patients. In this study, the results showed that both AQP4-IgG-seropositive ON and MOG-IgG-seropositive ON have increased the serum concentration of Th17-related cytokines and chemokines compared with that in the control subjects, while the change in MOG-IgG-seropositive ON is more significant. This result supported the hypothesis that Th17 cells are highly activated in MOG-IgG-seropositive ON patients during the disease's acute exacerbation and relapse stages. From a clinical point of view, the difference in cytokines and chemokines between different types of ON suggests its value in the differential diagnosis of disease, especially in the early stage of diseases.

MOG-IgG has been detected in a proportion of AQP4-IgG-seronegative NMOSD patients. MOG-IgG is a biomarker for patients with CNS demyelinating diseases that have distinct demographic, serologic, clinical, and radiologic features from classical MS and from AQP4-IgG-mediated NMOSD, suggesting that MOG-IgG might mediate a distinct disease (29). Moreover, the histopathology of the lesions of MOG-IgG-seropositive patients has been shown to differ from that of AQP4-IgG-mediated CNS lesions (10, 11). In a retrospective multicenter study of MOG-IgG-seropositive NMOSD patients, 88% of the patients developed acute ON at least once, 56% of the patients developed acute myelitis at least once, 44% of the patients only had a history of ON but not of myelitis, while only 12% of the patients had a history of myelitis but not of ON (29). This is consistent with another study that demonstrated that the optic nerve is more susceptible than the spinal cord in MOG-IgG-related CNS autoimmunity (30). A recent study has shown that autoimmune inflammatory infiltrates in the optic nerve are different from inflammation in other parts of the CNS, suggesting that the optic nerve might be an immunologic compartment different from the spinal cord. Compared with the spinal cord, Th17 cells prevailed in the optic nerve and the brain. Local tissue expression of IL-17 was the highest in the optic nerve, suggesting that Th17-related immunopathology was dominant in the optic nerve. The study concluded that the optic nerve compartment is particularly prone to supporting IL-17-mediated inflammatory immune responses during CNS autoimmunity, and neutralization of IL-17 is sufficient to prevent structural damage to the optic nerve (31). In the present study, the MOG-IgG-seropositive ON patients had a higher concentration of Th17-related cytokines and chemokines than the other types of ON patients. Furthermore, the serum level of IL 17 in the acute phase of the MOG-IgG-seropositive ON was positively correlated with serum MOG-IgG titer, indicating that a higher serum level of IL 17 during the acute phase was related to the MOG-IgG induced. The results of this study have further confirmed that MOG-IgG-related neuroinflammation is immunopathogenetically distinct from classical MS and AQP4-IgG-induced demyelinating disorders. More importantly, these results highlight the important role of the Th17 cells for neuronal demyelination in MOG-IgG-induced neuroinflammation.

There are some limitations in this study. First, the number of ON patients enrolled in the study was not sufficient, and no follow-up after treatment had been done. Second, we only detected the serum level of the cytokines and chemokines. It would have been much better if we had detected both the CSF and serum levels simultaneously, which could contribute to probing the underlying mechanisms of Th17 cells in MOG-IgG-related demyelinating diseases. Third, we did not compare the serum levels of the cytokines and chemokines of the same patient during the different stages of the disease. Long-term prospective multicenter studies are required to analyze the detailed immunopathologic mechanisms of Th17 cells in different types of demyelinating ON.

In conclusion, this study suggests that Th17 cells were highly activated in MOG-IgG-seropositive ON patients with significantly increased serum cytokines and chemokines. This cytokine/chemokine profiling provides new insights into ON pathogenesis and is useful in monitoring disease activity. Further research is required to clarify if interference in the Th17 pathway can reduce inflammation in the CNS during disease onset and relapses.

DATA AVAILABILITY STATEMENT

All datasets presented in this study are included in the article/supplementary material.

ETHICS STATEMENT

The studies involving human participants were reviewed and approved by Ethics Committee of the Chinese People's Liberation Army General Hospital and Beijing Chaoyang Hospital of Capital Medical University. The patients/participants provided their written informed consent to participate in this study.

AUTHOR CONTRIBUTIONS

HK, SW, and YT designed and conducted the study. HK, NA, HLiu, and QX collected, managed, analyzed, and interpreted the data. HK and HLi prepared the manuscript. All authors reviewed and made the final approval of the manuscript.

FUNDING

This work is supported by the National Natural Science Foundation of China (Grant No. 81900849).

REFERENCES

1. Toosy AT, Mason DF, Miller DH. Optic neuritis. *Lancet Neurol.* (2014) 13:83–99. doi: 10.1016/S1474-4422(13)70259-X
2. Jarius S, Wildemann B, Paul F. Neuromyelitis optica: clinical features, immunopathogenesis and treatment. *Clin Exp Immunol.* (2014) 176:149–64. doi: 10.1111/cei.12271
3. Jarius S, Wildemann B. AQP4 antibodies in neuromyelitis optica: diagnostic and pathogenetic relevance. *Nat Rev Neurol.* (2010) 6:383–92. doi: 10.1038/nrneurol.2010.72
4. Jarius S, Ruprecht K, Wildemann B, Kuempfel T, Ringelstein M, Geis C, et al. Contrasting disease patterns in seropositive and seronegative neuromyelitis optica: a multicentre study of 175 patients. *J Neuroinflamm.* (2012) 9:14. doi: 10.1186/1742-2094-9-14
5. Jarius S, Wildemann B. Aquaporin-4 antibodies (NMO-IgG) as a serological marker of neuromyelitis optica: a critical review of the literature. *Brain Pathol.* (2013) 23:661–83. doi: 10.1111/bpa.12084
6. Kitley J, Waters P, Woodhall M, Leite MI, Murchison A, George J, et al. Neuromyelitis optica spectrum disorders with aquaporin-4 and myelin-oligodendrocyte glycoprotein antibodies: a comparative study. *JAMA Neurol.* (2014) 71:276–83. doi: 10.1001/jamaneurol.2013.5857
7. Sato DK, Callegaro D, Lana-Peixoto MA, Waters PJ, de Haidar Jorge FM, Takahashi T, et al. Distinction between MOG antibody-positive and AQP4 antibody-positive NMO spectrum disorders. *Neurology.* (2014) 82:474–81. doi: 10.1212/WNL.0000000000000101
8. Reindl M, Di Pauli F, Rostasy K, Berger T. The spectrum of MOG autoantibody-associated demyelinating diseases. *Nat Rev Neurol.* (2013) 9:455–61. doi: 10.1038/nrneurol.2013.118
9. Probstel AK, Rudolf G, Dornmair K, Collongues N, Chanson JB, Sanderson NS, et al. Anti-MOG antibodies are present in a subgroup of patients with a neuromyelitis optica phenotype. *J Neuroinflamm.* (2015) 12:46. doi: 10.1186/s12974-015-0256-1
10. Spadaro M, Gerdes LA, Mayer MC, Ertl-Wagner B, Laurent S, Krumbholz M, et al. Histopathology and clinical course of MOG-antibody-associated encephalomyelitis. *Ann Clin Transl Neurol.* (2015) 2:295–301. doi: 10.1002/acn3.164
11. Jarius S, Metz I, Konig FB, Ruprecht K, Reindl M, Paul F, et al. Screening for MOG-IgG and 27 other anti-glial and anti-neuronal autoantibodies in 'pattern II multiple sclerosis' and brain biopsy findings in a MOG-IgG-positive case. *Mult Scler.* (2016) 22:1541–9. doi: 10.1177/1352458515622986
12. Kothur K, Wienholt L, Tantsis EM, Earl J, Bandodkar S, Prelog K, et al. B cell, Th17, and neutrophil related cerebrospinal fluid cytokine/chemokines are elevated in MOG antibody associated demyelination. *PLoS ONE.* (2016) 11:e0149411. doi: 10.1371/journal.pone.0149411
13. Ramesh G, MacLean AG, Philipp MT. Cytokines and chemokines at the crossroads of neuroinflammation, neurodegeneration, and neuropathic pain. *Mediators Inflamm.* (2013) 2013:480739. doi: 10.1155/2013/480739
14. Linhares UC, Schiavoni PB, Barros PO, Kasahara TM, Teixeira B, Ferreira TB, et al. The *ex vivo* production of IL-6 and IL-21 by CD4+ T cells is directly associated with neurological disability in neuromyelitis optica patients. *J Clin Immunol.* (2013) 33:179–89. doi: 10.1007/s10875-012-9780-2
15. Zepp J, Wu L, Li X. IL-17 receptor signaling and T helper 17-mediated autoimmune demyelinating disease. *Trends Immunol.* (2011) 32:232–9. doi: 10.1016/j.it.2011.02.007
16. The clinical profile of optic neuritis. Experience of the optic neuritis treatment trial. optic neuritis study group. *Arch. Ophthalmol.* (1991) 109:1673–8. doi: 10.1001/archopht.1991.01080120057025
17. Petzold A, Plant GT. Diagnosis and classification of autoimmune optic neuropathy. *Autoimmun Rev.* (2014) 13:539–45. doi: 10.1016/j.autrev.2014.01.009
18. Waters PJ, McKeon A, Leite MI, Rajasekharan S, Lennon VA, Villalobos A, et al. Serologic diagnosis of NMO: a multicenter comparison of aquaporin-4-IgG assays. *Neurology.* (2012) 78:665–71. doi: 10.1212/WNL.0b013e318248dec1
19. Dos Passos GR, Sato DK, Becker J, Fujihara K. Th17 cells pathways in multiple sclerosis and neuromyelitis optica spectrum disorders: pathophysiological and therapeutic implications. *Mediators Inflamm.* (2016) 2016:5314541. doi: 10.1155/2016/5314541
20. Binger KJ, Corte-Real BF, Kleinewietfeld M. Immunometabolic regulation of interleukin-17-producing T helper cells: uncoupling new targets for autoimmunity. *Front Immunol.* (2017) 8:311. doi: 10.3389/fimmu.2017.00311
21. Zhang Y, Yao XY, Gao MC, Ding J, Hong RH, Huang H, et al. Th2 axis-related cytokines in patients with neuromyelitis optica spectrum disorders. *CNS Neurosci Ther.* (2018) 24:64–9. doi: 10.1111/cns.12774
22. Huppert J, Closhen D, Croxford A, White R, Kulig P, Pietrowski E, et al. Cellular mechanisms of IL-17-induced blood-brain barrier disruption. *FASEB J.* (2010) 24:1023–34. doi: 10.1096/fj.09-141978
23. Kebir H, Kreymborg K, Ifergan I, Dodelet-Devillers A, Cayrol R, Bernard M, et al. Human TH17 lymphocytes promote blood-brain barrier disruption and central nervous system inflammation. *Nat Med.* (2007) 13:1173–5. doi: 10.1038/nm1651
24. Reboldi A, Coisne C, Baumjohann D, Benvenuto F, Bottinelli D, Lira S, et al. C-C chemokine receptor 6-regulated entry of TH-17 cells into the CNS through the choroid plexus is required for the initiation of EAE. *Nat Immunol.* (2009) 10:514–23. doi: 10.1038/ni.1716
25. Lindsey JW, Meulmester KM, Brod SA, Nelson F, Wolinsky JS. Variable results after rituximab in neuromyelitis optica. *J Neurol Sci.* (2012) 317:103–5. doi: 10.1016/j.jns.2012.02.017
26. Varrin-Doyer M, Spencer CM, Schulze-Topphoff U, Nelson PA, Stroud RM, Cree BA, et al. Aquaporin 4-specific T cells in neuromyelitis optica exhibit a Th17 bias and recognize clostridium ABC transporter. *Ann Neurol.* (2012) 72:53–64. doi: 10.1002/ana.23651
27. Mitsdoerffer M, Kuchroo V, Korn T. Immunology of neuromyelitis optica: a T cell-B cell collaboration. *Ann N Y Acad Sci.* (2013) 1283:57–66. doi: 10.1111/nyas.12118
28. Li Y, Wang H, Long Y, Lu Z, Hu X. Increased memory Th17 cells in patients with neuromyelitis optica and multiple sclerosis. *J Neuroimmunol.* (2011) 234:155–60. doi: 10.1016/j.jneuroim.2011.03.009
29. Jarius S, Ruprecht K, Kleiter I, Borisow N, Asgari N, Pitarokoili K, et al. MOG-IgG in NMO and related disorders: a multicenter study of 50 patients. Part 2: Epidemiology, clinical presentation, radiological and laboratory features, treatment responses, and long-term outcome. *J Neuroinflamm.* (2016) 13:280. doi: 10.1186/s12974-016-0718-0
30. Hoftberger R, Sepulveda M, Armangue T, Blanco Y, Rostasy K, Calvo AC, et al. Antibodies to MOG and AQP4 in adults with neuromyelitis optica and suspected limited forms of the disease. *Mult Scler.* (2015) 21:866–74. doi: 10.1177/1352458514555785
31. Knier B, Rothhammer V, Heink S, Puk O, Graw J, Hemmer B, et al. Neutralizing IL-17 protects the optic nerve from autoimmune pathology and prevents retinal nerve fiber layer atrophy during experimental autoimmune encephalomyelitis. *J. Autoimmun.* (2015) 56:34–44. doi: 10.1016/j.jaut.2014.09.003

Conflict of Interest: The authors declare that the research was conducted in the absence of any commercial or financial relationships that could be construed as a potential conflict of interest.

Copyright © 2020 Kang, Li, Ai, Liu, Xu, Tao and Wei. This is an open-access article distributed under the terms of the Creative Commons Attribution License (CC BY). The use, distribution or reproduction in other forums is permitted, provided the original author(s) and the copyright owner(s) are credited and that the original publication in this journal is cited, in accordance with accepted academic practice. No use, distribution or reproduction is permitted which does not comply with these terms.

frontiers in Neurology

REVIEW
published: 01 December 2020
doi: 10.3389/fneur.2020.591776

A 3D Model of Human Trabecular Meshwork for the Research Study of Glaucoma

Sara Tirendi[1,2*†], *Sergio Claudio Saccà*[3†], *Stefania Vernazza*[4†], *Carlo Traverso*[5†], *Anna Maria Bassi*[1,2†] *and Alberto Izzotti*[1,6,7†]

[1] *Department of Experimental Medicine (DIMES), University of Genoa, Genoa, Italy,* [2] *Inter-University Center for the Promotion of the 3Rs Principles in Teaching & Research (Centro 3R), Pisa, Italy,* [3] *Ophthalmology Unit, Istituto di Ricovero e Cura a Carattere Scientifico Ospedale Policlinico San Martino, Genoa, Italy,* [4] *Istituto di Ricovero e Cura a Carattere Scientifico, Fondazione Bietti, Rome, Italy,* [5] *Clinica Oculistica, Dipartimento di Neuroscienze, Riabilitazione, Oftalmologia, Genetica e Scienze Materno Infantili, University of Genoa and Istituto di Ricovero e Cura a Carattere Scientifico Ospedale Policlinico San Martino, Genoa, Italy,* [6] *Mutagenesis Unit, IST National Institute for Cancer Research, Istituto di Ricovero e Cura a Carattere Scientifico San Martino University Hospital, Genoa, Italy,* [7] *Department of Health Sciences, University of Genoa, Genoa, Italy*

OPEN ACCESS

Edited by:
Gemma Caterina Maria Rossi, Fondazione Ospedale San Matteo (IRCCS), Italy

Reviewed by:
Christian Cordano, University of California, San Francisco, United States
Zubair Ahmed, University of Birmingham, United Kingdom

****Correspondence:***
Sara Tirendi
tirendisara@gmail.com

† These authors have contributed equally to this work

Specialty section:
This article was submitted to Neuro-Ophthalmology, a section of the journal Frontiers in Neurology

Received: *05 August 2020*
Accepted: *22 October 2020*
Published: *01 December 2020*

Citation:
Tirendi S, Saccà SC, Vernazza S, Traverso C, Bassi AM and Izzotti A (2020) A 3D Model of Human Trabecular Meshwork for the Research Study of Glaucoma. Front. Neurol. 11:591776. doi: 10.3389/fneur.2020.591776

Glaucoma is a multifactorial syndrome in which the development of pro-apoptotic signals are the causes for retinal ganglion cell (RGC) loss. Most of the research progress in the glaucoma field have been based on experimentally inducible glaucoma animal models, which provided results about RGC loss after either the crash of the optic nerve or IOP elevation. In addition, there are genetically modified mouse models (DBA/2J), which make the study of hereditary forms of glaucoma possible. However, these approaches have not been able to identify all the molecular mechanisms characterizing glaucoma, possibly due to the disadvantages and limits related to the use of animals. In fact, the results obtained with small animals (i.e., rodents), which are the most commonly used, are often not aligned with human conditions due to their low degree of similarity with the human eye anatomy. Although the results obtained from non-human primates are in line with human conditions, they are little used for the study of glaucoma and its outcomes at cellular level due to their costs and their poor ease of handling. In this regard, according to at least two of the 3Rs principles, there is a need for reliable human-based *in vitro* models to better clarify the mechanisms involved in disease progression, and possibly to broaden the scope of the results so far obtained with animal models. The proper selection of an *in vitro* model with a "closer to *in vivo*" microenvironment and structure, for instance, allows for the identification of the biomarkers involved in the early stages of glaucoma and contributes to the development of new therapeutic approaches. This review summarizes the most recent findings in the glaucoma field through the use of human two- and three-dimensional cultures. In particular, it focuses on the role of the scaffold and the use of bioreactors in preserving the physiological relevance of *in vivo* conditions of the human trabecular meshwork cells in three-dimensional cultures. Moreover, data from these studies also highlight the pivotal role of oxidative stress in promoting the production of trabecular meshwork-derived pro-apoptotic signals, which are one of the first marks of trabecular meshwork damage. The resulting loss of barrier function, increase of intraocular pressure, as well the promotion of neuroinflammation

and neurodegeneration are listed as the main features of glaucoma. Therefore, a better understanding of the first molecular events, which trigger the glaucoma cascade, allows the identification of new targets for an early neuroprotective therapeutic approach.

Keywords: glaucoma pathogenesis, trabecular meshwork, endothelial dysfunction, extracellular matrix, aqueous humor proteome

INTRODUCTION

Primary open angle glaucoma (POAG) is a chronic disease that leads to retinal ganglion cell (RGC) loss and, consequently, the characteristic cupping of the papilla at the optic nerve level. In spite of the fact that it has been known since the time of Hippocrates, many aspects of this disease still remain obscure.

The only therapy recognized to be useful for glaucoma treatment is the lowering of intraocular pressure (IOP) although the exact relationships between IOP elevation and the optic nerve head (ONH) degeneration, which leads to visual field alteration, have not been understood yet. Indeed, IOP reduction alone is not always enough for slowing-down blindness progression (1, 2).

Many molecular mechanisms such as the ones involved in glaucoma etiology have been recognized, and in this regard, a wide range of substances with action either on a specific target or on multiple targets have been discovered (3).

Neuroprotection, neurodegeneration, and neuroenhancement have gained great importance over time because such approaches not only prevent RGCs from death but also repair or regenerate the cell damage, changing the course of the disease (4).

The primary molecular damage that occurs, which may be either of a degenerative/ischemic or a mechanical/metabolic nature, is able to induce changes in the extracellular matrix (ECM) of trabecular meshwork (TM) and in the TM itself that lead to retinal ganglion cell degeneration (5–8). The neuroprotective approach helps prevent these outcomes by improving neural recovery after pathologic insult, which results in a neural system optimization.

In glaucoma, the RGC degeneration induces trans-synaptic alterations capable of involving the entire visual chain up to the calcarine fissure (9). In these regard, any compounds able to interfere with the cascade of event that leads to visual field degeneration can be considered neuroprotective.

A wide variety of experimentally inducible animal glaucoma models ranging from large animals (i.e., non-human primates, cattle, dogs, and cats) to small animals (i.e., rats, mice, and zebrafish) are used in glaucoma research. Each of these animal models can help explain some molecular aspects of such a complex disease. Generally, however, the use of large animals offers better access to eye structures compared to the use of small ones due to larger eye size. In addition, non-human primates also show a resemblance to human ocular anatomy. However, for ethical and economic reasons, small animals such as rodents have gained ground in the research community. Among rodent models, the DBA/2J mouse is widely used because the mutations ($Tyrp1^{b}$ and $Gpnmb^{R150X}$) it presents cause a pigment dispersion syndrome similar to that found in humans and allows for the study of the effects of elevated IOP on the retina and optic nerve head (10–12).

There are several experimental manipulations to induce glaucoma in animal models that aim either to direct damage to ganglion cell axons (13–15) or indirect through IOP elevation (16, 17). In addition, mice can be genetically manipulated in order to express mutated human genes such as the MYOC Tyr437His mutation, which is responsible for an autosomal dominant form of human juvenile glaucoma (18).

Unfortunately, due to the heterogeneity of the disease and the addition of comorbidities, it is difficult to find an animal capable of reproducing the entire disease (19, 20). Moreover, the most common experimental techniques used for inducing IOP elevation [i.e., laser photocoagulation of entire trabecular meshwork (TM), intracameral injection either of latex microspheres or autologous fixed red blood cells to blockade TM, topical application of prednisolone, and so on] (21–24) cause an irreversible damage to the TM, which is the main tissue involved in the onset of the high-tension glaucoma cascade.

In humans, progressive TM degeneration is considered the "primum movens" for the decrease in outflow facility and, consequently, for the increase in IOP hypertension. Therefore, if in most animal models the TM is destroyed, these models may not provide complete information on glaucoma development (25, 26). Furthermore, the use of young animals as glaucoma models may represent an oversimplification of glaucoma issues because they do not show all those age-related factors that in human conditions promote and characterize glaucoma, i.e., genomic, biochemical, cellular, and system biology alterations (27–29). However, few studies on middle-aged or elderly animal models have not shown reliable results (30).

The proper measures to use animals of different ages as experimental models include a careful use of anesthetic agents as well as the attention for both physical decay and stress conditions (31).

However, differences in response to dexamethasone treatment were observed between young and elderly rabbits. Indeed, only the younger rabbits showed a hypertensive response probably due to their immature irido-corneal angle (32–34).

From a molecular point of view, glaucoma can be defined as a syndrome in which proapoptotic signals toward the head of the optic nerve (ONH) lead to glaucoma typical morpho-functional alterations such as both anterograde and retrograde RGC degeneration and trans-synaptic anterograde degeneration (35).

Given the fact that in high-tension glaucoma the TM plays a fundamental role in its pathogenesis, several previous studies (26, 36–38) have hypothesized that either the functional decay of TM

cells or the TM cellularity depletion lead to ocular hypertonus, which produces deleterious effects for both the outflow and the RGCs.

TM is essential for the passage of the aqueous humor through the conventional outflow pathway. Indeed, after damage, TM cells change their gene expression (25) encoding for proteins which, from the anterior to the posterior segment, become pro-apoptotic signals for the ganglion cells and the retina.

For the past 20 years, in addition to animal models, also animal- or human-derived *ex vivo* and *in vitro* models have been used for glaucoma study. In particular, these studies have the aim to fill the gap left by animal models. The main studies are focused on the role of oxidative stress in promoting cell/tissue defects found in glaucomatous patients (39). Over time, the continuous progress in the field of cell cultures has been able to improve the cell environment and to recreate a condition "closer to *in vivo*" (i.e., biocompatible scaffolds, bioreactors, lab-on-a chip) (40, 41). Moreover, *in vitro* models compared to *ex vivo* ones have the advantage of overcoming the problem of a limited incubation period, making longer experimental times possible (42).

The purpose of this review is to summarize our team's research progress using a 3D advanced human model of TM, arguing that the 2D model has limitations and hoping that our work may improve the performance in glaucoma studies.

3D CELL CULTURES AS A RESEARCH MODEL

Both animal and *in vitro* cell culture models are widely used in research to improve the knowledge about the mechanisms of disease onset and propagation and the development of preclinical drugs. However, the inconsistencies of animal researches and the oversimplification of conventional two-dimensional *in vitro* models have frequently delayed therapeutic advances, like in the case of glaucoma. Indeed, not all promising discoveries and treatments obtained from such models have given favorable outcomes with human evidence. Among the reasons behind animal model limitations, the poor standardization of experimental procedures and the variation of environmental conditions as well as interspecies variation (e.g., genetic differences) between animals are listed as the most relevant (43). In addition, in two-dimensional (2D) culture models, the loss of specific tissue function and physiology leads to a lack of predictability in terms of physiological significance and clinical response prediction (44).

One of the most important developments in this field has been the use of micro-engineering techniques for culturing cells in a three-dimensional (3D) system. Anyway, a more sophisticated *in vitro* model does not need to recapitulate every aspect of an animal model or human responses, but it needs to provide predictive data for a particular question (45).

Three-dimensional culture models aim to mimic the proper interactions of both cell–cell and cell–environment providing for the complex biochemical and physical signals as found in *in vivo* tissue structure (46, 47). Indeed, the maintenance both of cellular morphology and polarity enables gene expression, signaling, and metabolism similar to source tissue (48–50).

In order to accomplish this, the study of specific cell types (i.e., osteoblasts, hepatocytes, lymphocytes, trabecular meshwork cells, and so on) provides for an up-stream analysis both of structural architecture of tissue-derived cells and of the matrices/scaffold composition in which to embed the various cell types to obtain the proper 3D microenvironment (44, 47, 51).

In 3D cultures, matrices/scaffolds from several materials, within their structure, support cell growth, organization, and differentiation. Indeed, either biomaterials (e.g., natural or synthetic hydrogels) (52, 53) or the fabrication processes (e.g., electro-spinning, particulate-leaching, and solid free-form fabrication techniques) (54–56) used for these matrices/scaffolds confer mechanical and physical properties to them as well as other features including porosity and permeability, which provide the architecture for cellular supports.

Ideally, 3D cell culture matrices are able to recreate the extracellular cellular matrix (ECM) features to better mimic *in vivo* environments. As is known, the interaction between cells and ECM provide all those biophysical and biochemical functions including the transport of soluble signaling molecules, nutrients, and waste metabolites as well as mechanical integrity; to a certain extent, therefore, these matrices have to reflect the features of specific tissue ECM to each application (57–59). Mechanical properties of 3D matrix are important also because they can directly drive cell traction forces influencing both shape and responses of the cells. For example, the flattened shape of 2D cultures is due to the stiffness of the surfaces of the support to which they adhere (e.g., micro-well plates, tissue culture flasks, and Petri dishes) (60).

As mentioned above, among the biomaterials for cell embedding, polymers that form natural or synthetic hydrogels are mainly used. When mixed with cells, these polymers undergo fast and gentle polymerization, after which they can be degraded hydrolytically or enzymatically. However, natural hydrogels such as Matrigel^{TM}, fibrin gel, and alginate, compared to synthetic ones (e.g., PEG, peptide, and DNA gels) are more used both because of their better biocompatibility and mild gelification (47, 61).

3D *IN VITRO* GLAUCOMA MODELS

The advancement in *in vitro* model approaches for the study of glaucoma allowed the investigation of cellular behavior at molecular level in order to ameliorate the knowledge of disease onset and progression. Although *in vitro* models are not representative of the intricacy of glaucomatous disease, they have provided significant results when used for cell cultures, tissue cultures or *ex vivo* preparations. Additionally, according to the 3Rs principles, the use of the so-called alternative methods of which *in vitro* approaches are part promote the reduction in number of animals used in experimental tests and the replacement of animals when it is possible (62).

In this regard, several studies have mostly focused on setting up 3D models of TM, given its crucial role in conventional outflow pathway and in high-tension glaucoma onset.

Primary human trabecular meshwork (HTM) cells, for instance, were isolated from both juxtacanalicular and corneoscleral region, after which multiple HTM cell layers were included into a highly porous membrane, SU-8 scaffold, with predefined and well-controlled microstructure dimensions by standard photolithography techniques (63, 64). The bioengineered 3D HTM cell structures mimicked the TM structure found in *in vivo* conditions in terms of their spatial distribution, ECM synthesis/secretion, as well as their responsiveness after elevated hydrostatic pressure (EHP)-induced mechanical strain and drugs, i.e., latrunculin-B or steroids.

In a study on primary porcine TM cells, high viability and proliferation after seeding into a highly porous matrix of natural biopolymer construct, the collagen-chondroitin sulfate scaffold, was reported (65).

Moreover, *in vitro* models of 3D HTM cells (66) and 3D multipotent progenitors from HTM (67) were also obtained by embedment in a natural hydrogel scaffold such as Matrigel^{TM}. In this regard, the 3D HTM cells obtained in this way have shown, besides morphological and architectural changes after dexamethasone, TGFβ2 and benzalkonium chloride (BAK) stimulations, the upregulation of proinflammatory cytokines and MMPs after BAK treatment, and their migration through basement membranes. Therefore, the use of degradable scaffolds, compared to permanent ones, also offers an opportunity for further molecular investigations.

The second Matrigel^{TM}-based study revealed that the embedment of TM stem cell populations did not allow for cell expansion but provided the normal phenotype restoration able to express not only ESC and NC markers but also the TM ones (68).

However, all these 3D models of TM from natural or synthetic scaffolds have recapitulated important features of *in vivo* TM tissue morphology, highlighting the huge progress in tissue engineering in faithfully mimicking the native tissue.

In addition to innovative 3D TM cultures, a new *in vitro* approach based on lab-on-a-chip (LOC) technology has very recently been proposed, which consisted of a high-controlled EHP system and microculture system of purified primary rat RGCs (41). Such system has proved a useful tool to investigate the neuroprotective role of growth factors and mimic peptide in preserving the RGC death after EHP.

Over the years, in order to mimic the effects of oxidative stress in glaucoma *in vitro* models, repeated exposures of TM cells to different H_2O_2 concentrations (ranking from 100 μM to 1 mM) were evaluated (6, 69–72). H_2O_2 is the most widely used pro-oxidant because it easily crosses the cell membranes and, in presence of iron ions, produces reactive hydroxyl radicals, which are considered responsible for cytotoxicity (68, 73).

In previous studies, in which TM cells were exposed to 200 μM H_2O_2 for 30' (68), or 300 μM H_2O_2 for 1 h (74), or to 1 mM H_2O_2 for 24 h (71, 72), the typical changes of glaucomatous TM have been observed, including the promotion of cellular senescence (73), rearrangement of cytoskeleton structure (68), and the increase in proinflammatory mediators such as IL-6, IL-8, and endothelial–leukocyte adhesion molecule 1 (ELAM-1) (71).

In our model, on the other hand, TM cells of human origin (HTMC) were exposed to 500 μM H_2O_2 for 2 h every day followed by 22 h of recovery, in order to study the effects of oxidative stress administered in chronic/subtoxic manner. Several studies reported that, in the presence of cells, the H_2O_2 half-life is very short (∼1 h) (75, 76) because it passes rapidly through the cell membranes, and then, it is either detoxified by intracellular enzymes or converted to the above-mentioned reactive hydroxyl radical. Therefore, in our experimental model, 2 h a day of 500 μM H_2O_2 were sufficient to exert the cytotoxic/proinflammatory effect on TM cells (6).

ADVANCED HUMAN 3D TM MODEL

In the previous section, we have reported the most recent results of three-dimensional culture models of trabecular meshwork (TM) and the LOC technology. In both cases, it has been demonstrated that the cells cultured in a more similar way to their native-derived tissues provide physiological responses to different stimuli.

Moreover, also in our previous study, we showed the improved suitability of HTMCs (Cell Applications Inc., San Diego, CA, United States) (6, 25) cultured in a 3D model compared to the 2D one, both in basal conditions and after prolonged oxidative stress conditions. In our 3D culture model, we have chosen a degradable scaffold, namely, Corning® Matrigel® Matrix (Corning Life Sciences, Tewksbury, MA, United States) [dx.doi.org/10.17504/protocols.io.574g9qw], which consists of several proteins found in extracellular matrix (ECM) such as laminin, collagen IV, heparin sulfate proteoglycan, and entactin/nidogen (61).

However, the basic requirements for both viability and the functionality of cells, like *in vivo* conditions, are not only cell morphology maintenance but also the continuous supply of nutrients and oxygen, as well as the removal of metabolic waste products (77). Indeed, a more reliable cell and/or tissue micro-environment provides several complex biological responses such as cellular proliferation, migration, differentiation, matrix production, and apoptosis, similar to either the original organ or the tissue in which they arise (78).

Therefore, the development of 3D culture models, which are able to recapitulate some of the critical cell features including cell-to-cell and cell–ECM interactions, are not sufficient to study both the biochemical and biomechanical changes found in a complex disease such as glaucoma (79, 80).

Until today, there have been no standardized advanced *in vitro* models in ophthalmology consisting of both 3D culture models and milli-fluidic techniques for improving the physiological relevance of 3D cultures.

Here we describe the methodology combining a 3D human trabecular meshwork (TM) model and a bioreactor system, in order to overcome the issues related to cell responses under static culture conditions. In fact, the milli-fluidic technique offers

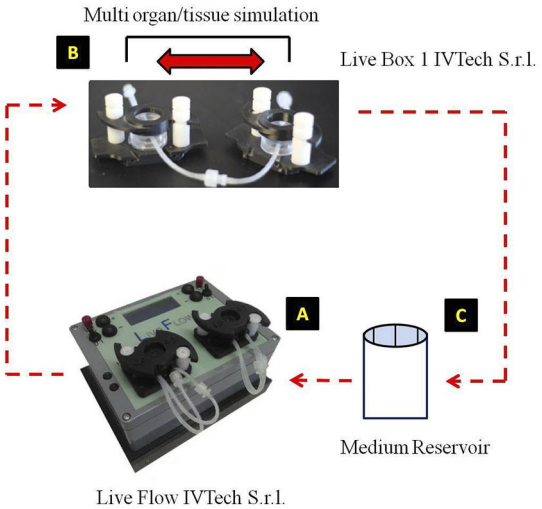

FIGURE 1 | Advanced human 3D model experimental design. From the medium reservoir **(C)**, the medium was pumped by the action of the live flow **(A)**, through the Live Box1 where 3D-trabecular meshwork (TM) cells of human origin (HTMC) were seeded **(B)**, then it returns to the medium reservoir, completing the circuit (Kind permission of IVTech S.r.l.).

precise control over gradients in a continuous manner under milli-metric-size channels (66, 81).

In our advanced *in vitro* model (82), the closed-circuit, the 3D-HTMCs received a constant medium supply, consisting of the single-flow bioreactor (Live Box1, IVTechs.r.l., Italy) culture chambers connected to a peristaltic pump (LiveFlow, IVTechs.r.l; Italy) (**Figure 1**). The medium flow was maintained at a constant rate of 70 μl/min to overcome both diffusional limitations and soft gel degradation on 3D-HTMC. The peristaltic pump takes the culture medium from a 10-ml final volume, so the percentage of turnover rate is 0.7%.

In order to study the effects of oxidative stress (OS) on TM, which is one of the main causes of TM damage, TM cells were treated with daily doses of 2 h of 500 μM H_2O_2, and in the remaining time (22 h), they were subjected to recovery under dynamic conditions (40, 76).

The milli-fluidic technology as well as the 3D culture model were capable of mimicking the cell responses found *in vivo* as a result of the increase in outflow resistance. In our model, therefore, it was possible to measure the expression of genes related to a specific cellular activity or function after OS conditions. Indeed, quantitative real-time PCR (qPCR) assays have proved to be a useful tool for assessing the expression of individual genes in order to measure the production of mRNA encoding for both profibrotic and metalloproteinase (MMPs) markers (40, 83–87). Moreover, both the changes in proinflammatory cytokine transcriptions and the NF-kB protein levels have been investigated as markers of activation of inflammatory response following OS stimulation. Finally, the apoptosis protein array was assessed to evaluate also the apoptosis pathway involvement during the experimental time. The increase in inflammatory and profibrotic markers as well as MMPs together with the absence of apoptosis led us to assume that a more efficient adaptive response to OS damage over time may be due to the constant medium supply to cell cultures (40, 71, 73).

In addition, the morphological comparison between 3D-HTMCs cultured under static conditions and those cultured under a dynamic one (**Figure 2**) showed, at the longest experimental time tested (168 h), a recovery of cytoskeleton integrity only in the advanced *in vitro* model, as confirmed also by the cell viability assay.

The perfusion of culture media through a 3D-culture structure using a pump system provide the proper nutrient circulation, metabolic waste expulsion, and homogeneity of the physical and chemical factors, which, in turn, allow for the study of early OS-derived molecular change without inducing the premature apoptosis as it happens under static culture condition. Therefore, bioreactor-based cell culture models are appropriate to study the stimuli-derived biomolecule cell productions to better understand the early alterations, which occur in glaucoma first steps (25).

Indeed, this 3D-TM milli-fluidic model represents a useful tool for providing a physiological cellular environment under controlled experimental conditions.

In addition, another way to think of this technology is either to combine the different modules/chambers in series for mimicking the tissue crosstalk between different tissues or equip it with a device to induce an increase in basal medium flow pressure. In these ways, this *in vitro* model would make it possible to analyze step-by-step the stages of cell damage, which underlie glaucoma and its adverse outcomes.

CONCLUSIONS AND FUTURE PROSPECTS

During the past three decades, a large number of studies have demonstrated that the increase in ROS rate, from endogenous and exogenous sources, can cause an unbalance in cell redox state, which leads to cellular damage (88, 89). Indeed, it is now known that the direct effects of the oxidative stress (OS) injury underlying the POAG onset seem to be linked in particular with TM damage, which is responsible for the increase in IOP in glaucomatous eyes (26–29). However, given the crucial role of TM in conventional outflow pathway regulation, it has also been hypothesized that glaucomatous TM could be involved in RGC death through the release of molecular signals harmful for RGC. Thus, molecular modifications borne by damaged TM tissue such as alterations in gene and protein products may affect the RGC viability (25).

In this review, we emphasize the importance of studying the first molecular changes in TM after oxidative stress by using an advanced human 3D-TM model. The novel therapeutic approaches are taking into account TM as a possible pharmacological target (90, 91). Therefore, the possibility of using an advanced *in vitro* model could represent an important tool for analyzing the cellular responses of a single-cell population, which in this case is represented by TM.

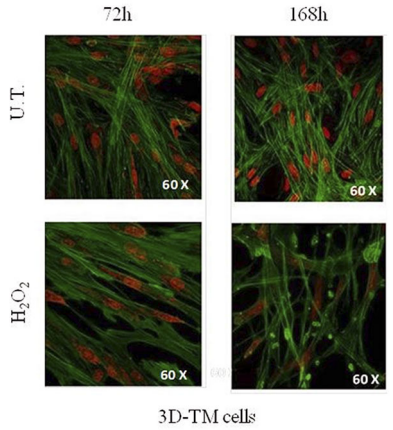

FIGURE 2 | Morphological changes in 3D-TM cells. Confocal analysis of nucleus and cytoskeletal markers were performed on untreated 3D-HTMC (top) and treated 3D-HTMC (bottom) after 72 and 168 h of experimental procedures. Representative images are related to immunoreactivity for To-PRO™ and Phalloidin, as nuclear and cytoskeleton markers, respectively. Merged images showed cytoskeleton plus nucleus (Image was published in Saccà et al. (40) "An Advanced *In Vitro* Model to Assess Glaucoma Onset").

Currently, the lack of experimental standardization for glaucoma study neither for *in vitro* nor for animal models (e.g., design, sample size, analytical techniques, statistics, reproducibility, lack of specific species, and so on) has partly compromised the proper identification of glaucoma biomarkers. Previous *in vitro* studies on TM have undoubtedly helped to understand the molecular changes in TM following OS treatment; however, most of the clinical trial results based on small animal models (i.e., rodents) revealed their translational failure mainly due to the different degree of similarity between human disease and the animal model used (21, 26, 92–94).

The TM is a porous tissue, and its structure is made up of connective tissue beams and sheets or lamellae covered by TM cells. Since the TM function is to filter AH, the 3D structure is a very important parameter to evaluate. In particular, in the 3D TM model *in vitro* proposed here, the TM cells embedded in a natural hydrogel seem to be more sensitive to OS, reflecting the OS-derived TM degeneration in a more realistic way (40). Furthermore, the cross-talk between cells, favored by 3D morphology, allows a more physiological cell-to-cell interaction (i.e., cytokines secretion) such as to promote both cell survival and cell proliferation even after harmful stimuli (e.g., oxidative stress) (40, 79). Moreover, our 3D TM *in vitro* model maintains power law metabolic scaling in cultures proving the physiological relevance for such a down-scaled *in vitro* system (95). In addition, the TM is an essential tissue, which together with a complex organ system, plays a pivotal role in modulating AH outflow (96, 97). In physiological conditions, the balance between aqueous humor inflow and outflow rate regulates the IOP in order to maintain the shape and related refractive properties of the eye. In relation to this, our innovative platform has been improved by adding an auxiliary device (Live Pa, IVTech S.r.l) to the millifluidic circuit in order to study the effects of increased flow pressure on TM cells (**Figure 1**) (98, 99).

Moreover, thanks to the features of this advanced *in vitro* model, which allows multiorgan approach through the communication between different tissues, it can be used to study the involvement of different cell types in glaucoma (e.g., neuron-like cells). In this way, it will be possible to evaluate how the TM damage, due to oxidative stress and/or increased pressure, influenced neuron homeostasis. In addition, such platform will allow to check the effectiveness of therapeutic compounds in counteracting the oxidative and/or pressure damage during the glaucoma evolution.

AUTHOR CONTRIBUTIONS

All authors listed have made a substantial, direct and intellectual contribution to the work, and approved it for publication.

FUNDING

ST was supported by Operative Program Por FSE, Liguria Region 2014–2020, Italy (RLOF18ASSRIC/62/1). SV was supported by the Italian Ministry of Health and by Fondazione Roma, Rome, Italy. This work was funded by Omikron Italia 2017-Marco Centofanti Neuroprotection and Glaucoma award, Omikron srl, Rome, Italy.

ACKNOWLEDGMENTS

We would like to express our gratitude to IVTech srl for their technical supporting information.

REFERENCES

1. Heijl A, Leske MC, Bengtsson B, Hyman L, Bengtsson B, Hussein M. Reduction of intraocular pressure and glaucoma progression: results from the early manifest glaucoma trial. *Arch Ophthalmol.* (2002) 120:1268–79. doi: 10.1001/archopht.120.10.1268
2. Group CNTGS. Comparison of glaucomatous progression between untreated patients with normal-tension glaucoma and patients with therapeutically reduced intraocular pressures. *Am J Ophthalmol.* (1998) 126:487–97. doi: 10.1016/S0002-9394(98)00223-2
3. Saccà SC, Corazza P, Gandolfi S, Ferrari D, Sukkar S, Iorio EL, et al. Substances of interest that support glaucoma therapy. *Nutrients.* (2019) 11:239. doi: 10.3390/nu11020239
4. Chang EE, Goldberg JL. Glaucoma 2.0: neuroprotection, neuroregeneration, neuroenhancement. *Ophthalmology.* (2012) 119:979–86. doi: 10.1016/j.ophtha.2011.11.003
5. Fuchshofer R, Tamm ER. The role of TGF-β in the pathogenesis of primary open-angle glaucoma. *Cell Tissue Res.* (2012) 347:279–90. doi: 10.1007/s00441-011-1274-7
6. Zhao J, Wang S, Zhong W, Yang B, Sun L, Zheng Y. Oxidative stress in the trabecular meshwork (review). *Int J Mol Med.* (2016) 38:995–1002. doi: 10.3892/ijmm.2016.2714

7. Izzotti A, Saccà SC, Cartiglia C, De Flora S. Oxidative deoxyribonucleic acid damage in the eyes of glaucoma patients. *Am J Med.* (2003) 114:638–46. doi: 10.1016/S0002-9343(03)00114-1
8. Tezel G. Oxidative stress in glaucomatous neurodegeneration: mechanisms and consequences. *Prog Retin Eye Res.* (2006) 25:490–513. doi: 10.1016/j.preteyeres.2006.07.003
9. Lawlor M, Danesh-Meyer H, Levin LA, Davagnanam I, De Vita E, Plant GT. Glaucoma and the brain: Trans-synaptic degeneration, structural change, and implications for neuroprotection. *Surv Ophthalmol.* (2018) 63:296–306. doi: 10.1016/j.survophthal.2017.09.010
10. Anderson MG, Smith RS, Hawes NL, Zabaleta A, Chang B, Wiggs JL, et al. Mutations in genes encoding melanosomal proteins cause pigmentary glaucoma in DBA/2J mice. *Nat Genet.* (2002) 30:81–85. doi: 10.1038/ng794
11. Dengler-Crish CM, Smith MA, Inman DM, Wilson GN, Young JW, Crish SD. Anterograde transport blockade precedes deficits in retrograde transport in the visual projection of the DBA/2J mouse model of glaucoma. *Front Neurosci.* (2014) 8:290. doi: 10.3389/fnins.2014.00290
12. Howell GR, Libby RT, Jakobs TC, Smith RS, Phalan FC, Barter JW, et al. Axons of retinal ganglion cells are insulted in the optic nerve early in DBA/2J glaucoma. *J Cell Biol.* (2007) 179:1523–37. doi: 10.1083/jcb.200706181
13. Dietz JA, Maes ME, Huang S, Yandell BS, Schlamp CL, Montgomery AD, et al. Spink2 modulates apoptotic susceptibility and is a candidate gene in the Rgcs1 QTL that affects retinal ganglion cell death after optic nerve damage. *PLoS ONE.* (2014) 9:e93564. doi: 10.1371/journal.pone.0093564
14. Li Y, Semaan SJ, Schlamp CL, Nickells RW. Dominant inheritance of retinal ganglion cell resistance to optic nerve crush in mice. *BMC Neuroscience.* (2007) 8:19. doi: 10.1186/1471-2202-8-19
15. Templeton JP, Freeman NE, Nickerson JM, Jablonski MM, Rex TS, Williams RW, et al. Innate immune network in the retina activated by optic nerve crush. *Invest Opthalmol Vis Sci.* (2013) 54:2599. doi: 10.1167/iovs.12-11175
16. Samsel PA, Kisiswa L, Erichsen JT, Cross SD, Morgan JE. A novel method for the induction of experimental glaucoma using magnetic microspheres. *Invest Opthalmol Vis Sci.* (2011) 52:1671–5. doi: 10.1167/iovs.09-3921
17. Sappington RM, Carlson BJ, Crish SD, Calkins DJ. The microbead occlusion model: a paradigm for induced ocular hypertension in rats and mice. *Invest Opthalmol Vis Sci.* (2010) 51:207–16. doi: 10.1167/iovs.09-3947
18. Fingert JH, Stone EM, Sheffield VC, Alward WLM. Myocilin Glaucoma. *Surv Ophthalmol.* (2002) 47:547–61. doi: 10.1016/S0039-6257(02)00353-3
19. Danesh-Meyer HV, Levin LA. Neuroprotection: extrapolating from neurologic diseases to the eye. *Am J Ophthalmol.* (2009) 148:186–91. doi: 10.1016/j.ajo.2009.03.029
20. Kimura A, Noro T, Harada T. Role of animal models in glaucoma research. *Neural Regen Res.* (2020) 15:1257–8. doi: 10.4103/1673-5374.272578
21. Bouhenni R, Dunmire J, Sewell A, Edward DP. Animal models of glaucoma. *J Biomed Biotechnol.* (2012) 2012:692609. doi: 10.1155/2012/692609
22. Epstein DL, Freddo TF, Anderson PJ, Patterson MM, Bassett-Chu S. Experimental obstruction to aqueous outflow by pigment particles in living monkeys. *Invest Ophthalmol Vis Sci.* (1986) 27:387–395.
23. Aihara M, Lindsey JD, Weinreb RN. Experimental mouse ocular hypertension: establishment of the model. *Invest Ophthalmol Vis Sci.* (2003) 44:4314–20. doi: 10.1167/iovs.03-0137
24. Levkovitch-Verbin H, Quigley HA, Martin KRG, Valenta D, Baumrind LA, Pease ME. Translimbal laser photocoagulation to the trabecular meshwork as a model of glaucoma in rats. *Invest Ophthalmol Vis Sci.* (2002) 43:402–410.
25. Saccà SC, Gandolfi S, Bagnis A, Manni G, Damonte G, Traverso CE, et al. The outflow pathway: a tissue with morphological and functional unity. *J Cell Physiol.* (2016) 231:1876–93. doi: 10.1002/jcp.25305
26. Saccà SC, Gandolfi S, Bagnis A, Manni G, Damonte G, Traverso CE, et al. From DNA damage to functional changes of the trabecular meshwork in aging and glaucoma. *Ageing Res Rev.* (2016) 29:26–41. doi: 10.1016/j.arr.2016.05.012
27. Caprioli J. Glaucoma: a disease of early cellular senescence. *Invest Opthalmol Vis Sci.* (2013) 54:ORSF60. doi: 10.1167/iovs.13-12716
28. Osborne NN, Álvarez CN, del Olmo Aguado S. Targeting mitochondrial dysfunction as in aging and glaucoma. *Drug Discov Today.* (2014) 19:1613–22. doi: 10.1016/j.drudis.2014.05.010
29. Liu B, McNally S, Kilpatrick JI, Jarvis SP, O'Brien CJ. Aging and ocular tissue stiffness in glaucoma. *Surv Ophthalmol.* (2018) 63:56–74. doi: 10.1016/j.survophthal.2017.06.007
30. Turner AJ, Vander Wall R, Gupta V, Klistorner A, Graham SL. DBA/2J mouse model for experimental glaucoma: pitfalls and problems. *Clin Exp Ophthalmol.* (2017) 45:911–22. doi: 10.1111/ceo.12992
31. Evangelho K, Mastronardi CA, de-la-Torre A. Experimental models of glaucoma: a powerful translational tool for the future development of new therapies for glaucoma in humans—a review of the literature. *Medicina.* (2019) 55:280. doi: 10.3390/medicina55060280
32. Knepper PA, Farbman AI, Telser AG. Aqueous outflow pathway glycosaminoglycans. *Exp Eye Res.* (1981) 32:265–77. doi: 10.1016/0014-4835(81)90032-4
33. Qin Y, Lam S, Yam GHF, Choy KW, Liu DTL, Chiu TYH, et al. A rabbit model of age-dependant ocular hypertensive response to topical corticosteroids. *Acta Ophthalmol.* (2012) 90:559–63. doi: 10.1111/j.1755-3768.2010.02016.x
34. Ke TL, Clark AF, Gracy RW. Age-related permeability changes in rabbit corneas. *J Ocul Pharmacol Ther.* (1999) 15:513–23. doi: 10.1089/jop.1999.15.513
35. Yu DY, Cringle SJ, Balaratnasingam C, Morgan WH, Yu PK, Su EN. Retinal ganglion cells: energetics, compartmentation, axonal transport, cytoskeletons and vulnerability. *Prog Retin Eye Res.* (2013) 36:217–46. doi: 10.1016/j.preteyeres.2013.07.001
36. Alvarado J, Murphy C, Juster R. Trabecular meshwork cellularity in primary open-angle glaucoma and nonglaucomatous normals. *Ophthalmology.* (1984) 91:564–79. doi: 10.1016/S0161-6420(84)34248-8
37. Alvarado J, Murphy C, Polansky J, Juster R. Age-related changes in trabecular meshwork cellularity. *Invest Ophthalmol Vis Sci.* (1981) 21:714–27.
38. Grierson I, Howes RC. Age-related depletion of the cell population in the human trabecular meshwork. *Eye.* (1987) 1:204–10. doi: 10.1038/eye.1987.38
39. Awai-Kasaoka N, Inoue T, Kameda T, Fujimoto T, Inoue-Mochita M, Tanihara H. Oxidative stress response signaling pathways in trabecular meshwork cells and their effects on cell viability. *Mol Vis.* (2013) 19:1332–40.
40. Saccà SC, Tirendi S, Scarfì S, Passalacqua M, Oddone F, Traverso CE, et al. An advanced *in vitro* model to assess glaucoma onset. *ALTEX.* (2020) 37:265–74. doi: 10.14573/altex.1909262
41. Nafian F, Azad BKD, Yazdani S, Rasaee MJ, Daftarian N. A lab-on-a-chip model of glaucoma. *Brain Behav.* (2019) 10:e01799. doi: 10.1101/704510
42. Ishikawa M, Yoshitomi T, Zorumski CF, Izumi Y. Effects of acutely elevated hydrostatic pressure in a rat *ex vivo* retinal preparation. *Invest Opthalmol Vis Sci.* (2010) 51:6414–23. doi: 10.1167/iovs.09-5127
43. Shrestha J, Razavi Bazaz S, Aboulkheyr Es H, Yaghobian Azari D, Thierry B, Ebrahimi Warkiani M, et al. Lung-on-a-chip: the future of respiratory disease models and pharmacological studies. *Crit Rev Biotechnol.* (2020) 40:213–30. doi: 10.1080/07388551.2019.1710458
44. Abbott A. Biology's new dimension. *Nature.* (2003) 424:870–2. doi: 10.1038/424870a
45. Alépée N. State-of-the-art of 3D cultures (organs-on-a-chip) in safety testing and pathophysiology. *ALTEX.* (2014) 441–77. doi: 10.14573/altex1406111
46. Cawkill D, Eaglestone SS. Evolution of cell-based reagent provision. *Drug Discov Today.* (2007) 12:820–5. doi: 10.1016/j.drudis.2007.08.014
47. Lee J, Cuddihy MJ, Kotov NA. Three-dimensional cell culture matrices: state of the art. *Tissue Eng Part B Rev.* (2008) 14:61–86. doi: 10.1089/teb.2007.0150
48. Ghosh S, Spagnoli GC, Martin I, Ploegert S, Demougin P, Heberer M, et al. Three-dimensional culture of melanoma cells profoundly affects gene expression profile: a high density oligonucleotide array study. *J Cell Physiol.* (2005) 204:522–31. doi: 10.1002/jcp.20320
49. Marushima H. Three-dimensional culture promotes reconstitution of the tumor-specific hypoxic microenvironment under TGFβ stimulation. *Int J Oncol.* (2011) 39:1327–36. doi: 10.3892/ijo.2011.1142
50. Petersen OW, Rønnov-Jessen L, Howlett AR, Bissell MJ. Interaction with basement membrane serves to rapidly distinguish growth and differentiation pattern of normal and malignant human breast epithelial cells. *Proc Natl Acad Sci USA.* (1992) 89:9064–8. doi: 10.1073/pnas.89.19.9064
51. Cukierman E. Taking cell-matrix adhesions to the third dimension. *Science.* (2001) 294:1708–12. doi: 10.1126/science.1064829
52. Shin H, Jo S, Mikos AG. Biomimetic materials for tissue engineering. *Biomaterials.* (2003) 24:4353–64. doi: 10.1016/S0142-9612(03)00339-9

53. Stupp SI, Donners JJJM, Li LS, Mata A. Expanding frontiers in biomaterials. *MRS Bull.* (2005) 30:864–73. doi: 10.1557/mrs2005.276
54. Pham QP, Sharma U, Mikos AG. Electrospinning of polymeric nanofibers for tissue engineering applications: a review. *Tissue Eng.* (2006) 12:1197–1211. doi: 10.1089/ten.2006.12.1197
55. Mikos AG, Thorsen AJ, Czerwonka LA, Bao Y, Langer R, Winslow DN, et al. Preparation and characterization of poly(l-lactic acid) foams. *Polymer.* (1994) 35:1068–77. doi: 10.1016/0032-3861(94)90953-9
56. Hollister SJ. Porous scaffold design for tissue engineering. *Nat Mater.* (2005) 4:518–24. doi: 10.1038/nmat1421
57. Bissell MJ, Rizki A, Mian IS. Tissue architecture: the ultimate regulator of breast epithelial function. *Curr Opin Cell Biol.* (2003) 15:753–62. doi: 10.1016/j.ceb.2003.10.016
58. Lukashev ME, Werb Z. ECM signalling: orchestrating cell behaviour and misbehaviour. *Trends Cell Biol.* (1998) 8:437–41. doi: 10.1016/S0962-8924(98)01362-2
59. Even-Ram S, Yamada KM. Cell migration in 3D matrix. *Curr Opin Cell Biol.* (2005) 17:524–32. doi: 10.1016/j.ceb.2005.08.015
60. Discher DE, Janmey P, Wang Y. Tissue cells feel and respond to the stiffness of their substrate. *Science.* (2005) 310:1139–43. doi: 10.1126/science.1116995
61. Kleinman HK, Martin GR. Matrigel: basement membrane matrix with biological activity. *Semi Cancer Biol.* 15:378–86. doi: 10.1016/j.semcancer.2005.05.004
62. Tannenbaum J, Bennett BT. Russell and burch's 3Rs then and now: the need for clarity in definition and purpose. *J Am Assoc Lab Anim Sci.* (2015) 54:120–32.
63. Torrejon KY, Pu D, Bergkvist M, Danias J, Sharfstein ST, Xie Y. Recreating a human trabecular meshwork outflow system on microfabricated porous structures: bioengineered human trabecular meshwork. *Biotechnol Bioeng.* (2013) 110:3205–18. doi: 10.1002/bit.24977
64. Torrejon KY, Papke EL, Halman JR, Stolwijk J, Dautriche CN, Bergkvist M, et al. Bioengineered glaucomatous 3D human trabecular meshwork as an in vitro disease model: steroid-induced glaucomatous 3D HTM model. *Biotechnol Bioeng.* (2016) 113:1357–68. doi: 10.1002/bit.25899
65. Osmond M, Bernier SM, Pantcheva MB, Krebs MD. Collagen and collagen-chondroitin sulfate scaffolds with uniaxially aligned pores for the biomimetic, three dimensional culture of trabecular meshwork cells: trabecular meshwork cell culture scaffolds. *Biotechnol Bioeng.* (2017) 114:915–23. doi: 10.1002/bit.26206
66. Bouchemi M, Roubeix C, Kessal K, Riancho L, Raveu AL, Soualmia H, et al. Effect of benzalkonium chloride on trabecular meshwork cells in a new *in vitro* 3D trabecular meshwork model for glaucoma. *Toxicol Vitro.* (2017) 41:21–9. doi: 10.1016/j.tiv.2017.02.006
67. Zhang Y, Cai S, Tseng SCG, Zhu YT. Isolation and expansion of multipotent progenitors from human trabecular meshwork. *Sci Rep.* (2018) 8:2814. doi: 10.1038/s41598-018-21098-2
68. Cheng K, Lai Y, Kisaalita WS. Three-dimensional polymer scaffolds for high throughput cell-based assay systems. *Biomaterials.* (2008) 29:2802–12. doi: 10.1016/j.biomaterials.2008.03.015
69. Vernazza S, Tirendi S, Scarfì S, Passalacqua M, Oddone F, Traverso CE, et al. 2D- and 3D-cultures of human trabecular meshwork cells: a preliminary assessment of an in vitro model for glaucoma study. *PLoS ONE.* (2019) 14:e0221942. doi: 10.1371/journal.pone.0221942
70. Li G, Luna C, Liton PB, Navarro I, Epstein DL, Gonzalez P. Sustained stress response after oxidative stress in trabecular meshwork cells. *Mol Vis.* (2007) 13:2282–8.
71. Famili A, Ammar DA, Kahook MY. Ethyl pyruvate treatment mitigates oxidative stress damage in cultured trabecular meshwork cells. *Mol Vis.* (2013) 19:1304–9.
72. Yu AL, Fuchshofer R, Kampik A, Welge-Lüssen U. Effects of oxidative stress in trabecular meshwork cells are reduced by prostaglandin analogues. *Invest Ophthalmol Vis Sci.* (2008) 49:4872–80. doi: 10.1167/iovs.07-0984
73. Bienert GP, Schjoerring JK, Jahn TP. Membrane transport of hydrogen peroxide. *Biochim Biophys Acta.* (2006) 1758:994–1003. doi: 10.1016/j.bbamem.2006.02.015
74. Tourtas T, Birke MT, Kruse FE, Welge-Lüssen UC, Birke K. Preventive effects of omega-3 and omega-6 Fatty acids on peroxide mediated oxidative stress responses in primary human trabecular meshwork cells. *PLoS ONE.* (2012) 7:e31340. doi: 10.1371/journal.pone.0031340
75. Kaczara P, Motterlini R, Rosen GM, Augustynek B, Bednarczyk P, Szewczyk A, et al. Carbon monoxide released by CORM-401 uncouples mitochondrial respiration and inhibits glycolysis in endothelial cells: a role for mitoBKCa channels. *Biochim Biophys Acta.* (2015) 1847:1297–309. doi: 10.1016/j.bbabio.2015.07.004
76. Poehlmann A, Reissig K, Schönfeld P, Walluscheck D, Schinlauer A, Hartig R, et al. Repeated H_2O_2 exposure drives cell cycle progression in an *in vitro* model of ulcerative colitis. *J Cell Mol Med.* (2013) 17:1619–31. doi: 10.1111/jcmm.12150
77. Hansmann J, Groeber F, Kahlig A, Kleinhans C, Walles H. Bioreactors in tissue engineering-principles, applications and commercial constraints. *Biotechnol J.* (2013) 8:298–307. doi: 10.1002/biot.201200162
78. Chaicharoenaudomrung N, Kunhorm P, Noisa P. Three-dimensional cell culture systems as an *in vitro* platform for cancer and stem cell modeling. *World J Stem Cells.* (2019) 11:1065–83. doi: 10.4252/wjsc.v11.i12.1065
79. Gu L, Mooney DJ. Biomaterials and emerging anticancer therapeutics: engineering the microenvironment. *Nat Rev Cancer.* (2016) 16:56–66. doi: 10.1038/nrc.2015.3
80. Huh D, Hamilton GA, Ingber DE. From 3D cell culture to organs-on-chips. *Trends Cell Biol.* (2011) 21:745–54. doi: 10.1016/j.tcb.2011.09.005
81. Berger E, Magliaro C, Paczia N, Monzel AS, Antony P, Linster CL, et al. Millifluidic culture improves human midbrain organoid vitality and differentiation. *Lab Chip.* (2018) 18:3172–83. doi: 10.1039/C8LC00206A
82. Giusti S, Sbrana T, La Marca M, Di Patria V, Martinucci V, Tirella A, et al. A novel dual-flow bioreactor simulates increased fluorescein permeability in epithelial tissue barriers. *Biotechnol J.* (2014) 9:1175–84. doi: 10.1002/biot.201400004
83. Kaczara P, Sarna T, Burke JM. Dynamics of H2O2 availability to ARPE-19 cultures in models of oxidative stress. *Free Rad Biol Med.* (2010) 48:1064–70. doi: 10.1016/j.freeradbiomed.2010.01.022
84. Keller KE, Aga M, Bradley JM, Kelley MJ, Acott TS. Extracellular matrix turnover and outflow resistance. *Exp Eye Res.* (2009) 88:676–82. doi: 10.1016/j.exer.2008.11.023
85. Inoue-Mochita M, Inoue T, Kojima S, Futakuchi A, Fujimoto T, Sato-Ohira S, et al. Interleukin-6–mediated trans-signaling inhibits transforming growth factor-β signaling in trabecular meshwork cells. *J Biol Chem.* (2018) 293:10975–984. doi: 10.1074/jbc.RA118.003298
86. De Groef L, Van Hove I, Dekeyster E, Stalmans I, Moons L. MMPs in the trabecular meshwork: promising targets for future glaucoma therapies? *Invest Ophthalmol Vis Sci.* (2013) 54:7756–63. doi: 10.1167/iovs.13-13088
87. Singh D, Srivastava SK, Chaudhuri TK, Upadhyay G. Multifaceted role of matrix metalloproteinases (MMPs). *Front Mol Biosci.* (2015) 2:19. doi: 10.3389/fmolb.2015.00019
88. Izzotti A, Bagnis A, Saccà SC. The role of oxidative stress in glaucoma. *Mutat Res.* (2006) 612:105–14. doi: 10.1016/j.mrrev.2005.11.001
89. Pinazo-Duran MD, Shoaie-Nia K, Zanon-Moreno V, Sanz-Gonzalez SM, del Castillo JB, Garcia-Medina JJ. Strategies to reduce oxidative stress in glaucoma patients. *Curr Neuropharmacol.* (2018) 16:903–18. doi: 10.2174/1570159X15666170705101910
90. Wang SK, Chang RT. An emerging treatment option for glaucoma: rho kinase inhibitors. *Clin Ophthalmol.* (2014) 8:883–90. doi: 10.2147/OPTH.S41000
91. Tanna AP, Johnson M. Rho kinase inhibitors as a novel treatment for glaucoma and ocular hypertension. *Ophthalmology.* (2018) 125:1741–56. doi: 10.1016/j.ophtha.2018.04.040
92. Quigley HA. Use of animal models techniques in glaucoma research: introduction. In: Jakobs TC, editor. *Glaucoma* New York, NY: Springer New York (2018). p. 1–10.
93. Quigley HA, Hohman RM. Laser energy levels for trabecular meshwork damage in the primate eye. *Invest Ophthalmol Vis Sci.* (1983) 24:1305–7.
94. Pederson JE, Gaasterland DE. Laser-induced primate glaucoma: I. Progression of cupping. *Arch Ophthalmol.* (1984) 102:1689–92. doi: 10.1001/archopht.1984.01040031373030
95. Duval K, Grover H, Han L-H, Mou Y, Pegoraro AF, Fredberg J, et al. Modeling physiological events in 2D vs. 3D cell culture. *Physiology.* (2017) 32:266–77. doi: 10.1152/physiol.00036.2016

96. Stamer WD, Clark AF. The many faces of the trabecular meshwork cell. *Exp Eye Res.* (2017) 158:112–23. doi: 10.1016/j.exer.2016.07.009
97. Acott TS, Kelley MJ, Keller KE, Vranka JA, Abu-Hassan DW, Li X, et al. Intraocular pressure homeostasis: maintaining balance in a high-pressure environment. *J Ocul Pharmacol Ther.* (2014) 30:94–101. doi: 10.1089/jop.2013.0185
98. Tirendi S, Vernazza S, Scarfì S, Saccà SC Bassi AM. Set-up of an *in vitro* physiological relevant 3D-model of human ocular trabecular meshwork to verify therapeutic strategies for glaucoma. *Altex Proc.* (2019) 8:207.
99. Vernazza S, Tirendi S, Scarfì S, Saccà SC Bassi AM. An innovative *in vitro* physiologically relevant model as a tool to test therapeutic strategies for glaucoma. *Altex Proc.* (2019) 8:211.

Conflict of Interest: The authors declare that the research was conducted in the absence of any commercial or financial relationships that could be construed as a potential conflict of interest.

Copyright © 2020 Tirendi, Saccà, Vernazza, Traverso, Bassi and Izzotti. This is an open-access article distributed under the terms of the Creative Commons Attribution License (CC BY). The use, distribution or reproduction in other forums is permitted, provided the original author(s) and the copyright owner(s) are credited and that the original publication in this journal is cited, in accordance with accepted academic practice. No use, distribution or reproduction is permitted which does not comply with these terms.

frontiers in Neurology

REVIEW
published: 10 December 2020
doi: 10.3389/fneur.2020.604049

Optical Coherence Tomography Angiography (OCTA) in Multiple Sclerosis and Neuromyelitis Optica Spectrum Disorder

Iris Kleerekooper[1,2*†], *Sarah Houston*[3†], *Adam M. Dubis*[4], *S. Anand Trip*[2] *and Axel Petzold*[1,2,5]

[1] *Department of Neuro-Ophthalmology, Moorfields Eye Hospital, London, United Kingdom,* [2] *Queen Square MS Centre, UCL Institute of Neurology and National Hospital for Neurology & Neurosurgery, London, United Kingdom,* [3] *Institute of Ophthalmology, University College London, London, United Kingdom,* [4] *National Institute for Health Research, Biomedical Resource Centre at University College London, Institute of Ophthalmology and Moorfields Eye Hospital National Health Service Trust, London, United Kingdom,* [5] *Dutch Expertise Centre of Neuro-Ophthalmology, Amsterdam UMC, Amsterdam, Netherlands*

Vascular changes are increasingly recognized as important factors in the pathophysiology of neuroinflammatory disease, especially in multiple sclerosis (MS). The relatively novel technology of optical coherence tomography angiography (OCTA) images the retinal and choroidal vasculature non-invasively and in a depth-resolved manner. OCTA provides an alternative quantitative measure of retinal damage, by measuring vascular density instead of structural atrophy. Preliminary results suggest OCTA is sensitive to retinal damage in early disease stages, while also having less of a "floor-effect" compared with commonly used OCT metrics, meaning it can pick up further damage in a severely atrophied retina in later stages of disease. Furthermore, it may serve as a surrogate marker for vascular pathology in the central nervous system. Data to date consistently reveal lower densities of the retinal microvasculature in both MS and neuromyelitis optica spectrum disorder (NMOSD) compared with healthy controls, even in the absence of prior optic neuritis. Exploring the timing of vascular changes relative to structural atrophy may help answer important questions about the role of hypoperfusion in the pathophysiology of neuroinflammatory disease. Finally, qualitative characteristics of retinal microvasculature may help discriminate between different neuroinflammatory disorders. There are however still issues regarding image quality and development of standardized analysis methods before OCTA can be fully incorporated into clinical practice.

Keywords: OCTA, OCT, multiple sclerosis, NMOSD, optic neuritis, microvascular

OPEN ACCESS

Edited by:
Gemma Caterina Maria Rossi, Fondazione Ospedale San Matteo (IRCCS), Italy

Reviewed by:
Donato Colantuono, Hospital Center Intercommunal de Créteil, France
Maurizio Versino, ASST Settelaghi, Italy

***Correspondence:**
Iris Kleerekooper
iris.kleerekooper.18@ucl.ac.uk

[†] These authors have contributed equally to this work

Specialty section:
This article was submitted to Neuro-Ophthalmology, a section of the journal Frontiers in Neurology

Received: *08 September 2020*
Accepted: *17 November 2020*
Published: *10 December 2020*

Citation:
Kleerekooper I, Houston S, Dubis AM, Trip SA and Petzold A (2020) Optical Coherence Tomography Angiography (OCTA) in Multiple Sclerosis and Neuromyelitis Optica Spectrum Disorder. Front. Neurol. 11:604049. doi: 10.3389/fneur.2020.604049

INTRODUCTION

In addition to well-established immune mediated processes, vascular and metabolic factors are increasingly recognized to play important parts in the pathophysiology of neuroinflammatory disease, especially in multiple sclerosis (MS) (1). Optical coherence tomography angiography (OCTA) is a relatively novel technology that images the retinal and choroidal vasculature in a non-invasive and depth-resolved manner (2). OCTA technology is derived from additional processing of optical coherence tomography (OCT), a structural retinal imaging modality first used in 1991 that has since secured its place as a staple of

neuro-ophthalmological clinical evaluation (3–5). Currently, some attention is diverted to the exciting potential that OCTA has in imaging the retinal vasculature using similar hardware and procedure.

Due to the design of the eye, the retina is one of the most easily accessible internal structures for imaging inside the human body. The retina is part of the central nervous system (CNS), as it contains the retinal nerve fiber layer (RNFL) and ganglion cell layer (GCL) which are formed of cells that relay visual information to the brain through the optic nerve (6, 7). Additionally, the anterior visual system is one of the most metabolically active structures in the human body and, accordingly, has a high perfusion rate which is rapidly adaptive to temporal changes in local demand (8–10).

The optic nerve is commonly injured in MS and neuromyelitis optica spectrum disorder (NMOSD) by optic neuritis (ON) (11–14). Demyelinating damage to the anterior visual system is virtually ubiquitous in postmortem studies of MS (15, 16). Thinning of the peripapillary RNFL (pRNFL) and GCL, as measured with OCT, have been shown to be markers of previous ON. However, retinal atrophy is also present in the absence of prior symptomatic ON and provides a valuable surrogate for more general, independent, CNS atrophy in neuroinflammatory disease (5, 11).

Even though immune mediated mechanisms are considered the most important drivers of neuroinflammatory disease, accumulating evidence indicates that CNS tissue energy failure, caused by hypoperfusion and hypoxia, is present in MS patients. This energy crisis may render neurons ineffective during an acute relapse and cause damage to oligodendrocytes which sets in action insidious processes of chronic demyelination and atrophy (1, 17). Neuropathologic studies of NMOSD affected tissue show that CNS lesions have a clear predilection for forming in perivascular locations (18). Furthermore, vessel walls in surrounding area are found to be fibrosed and hyalinised, a change in vessel morphology that can even be picked up on fundoscopy of NMOSD patients (19). In the acute clinical setting it can be difficult to differentiate between ON associated with MS and NMOSD, while the two diseases generally warrant different treatment decisions (13). Qualitative differences in vascular morphology picked up with OCTA may be diagnostically valuable in acute ON patients when differentiating between these conditions.

OCTA may be implemented in several interesting ways to advance the understanding of neuroinflammatory disease. Studies investigating OCTA in neuroinflammatory disease found that its findings are usually highly correlated to measurements of retinal layer thickness performed with the more consolidated technique of OCT (20–22). Therefore, OCTA can be an alternative quantitative measure of damage to the retina and optic nerve, as atrophied tissue requires less blood supply (20). Preliminary results in glaucoma research suggest that OCTA is sensitive to retinal damage in the earliest disease stages, while also being able to detect further damage in a severely atrophied retina, due to its low "floor-effect" (23, 24). In early-stage glaucoma, vascular density loss is faster compared with GCL thinning (25). Furthermore, another study concluded that the OCTA may be a promising tool to follow-up patients with late-stage glaucoma, as the measurement floor is lower compared with commonly used OCT metrics (26).

Additionally, OCTA may provide an avenue for investigations into vascular changes in the CNS. Preliminary OCTA research shows the retinal microvasculature is affected in both MS and NMOSD, even in eyes unaffected by ON and in some cases in the absence of structural retinal atrophy (20, 27). Investigating when vascular changes occur relative to thinning of retinal layers in neuroinflammatory disease may help answer important questions about the role of hypoperfusion in their pathophysiology (10). Finally, certain qualitative characteristics of the retinal microvasculature on OCTA may provide information for diagnostic discrimination between different causes of ON (28), similar to how the "central vein sign" on high-field MRI is a valuable diagnostic marker for MS (29). However, issues remain regarding image quality and the lack of standardization in image collection and analysis, which must be addressed before OCTA can be fully incorporated into clinical practice similar to what a network approach achieved for OCT (30).

In this review, we will discuss the potential value of OCTA in advancing research and clinical care in neuroinflammatory disease. First, we give an overview of the technical background of OCTA and the anatomy of retinal vasculature. Subsequently, we elaborate on the role of vascular alterations, particularly in the retina, in neuroinflammatory disease and we summarize research using OCTA in MS and NMOSD until now and finally, we discuss future prospects and the advantages as well as disadvantages of OCTA.

TECHNICAL BACKGROUND OCTA

OCT uses a technique that can be described as an optical analog to ultrasound-based imaging technology. OCT creates *in-vivo* structural images from biological tissue based on interferometry of low-coherence, near infrared light that is split into a reference arm, reflecting off a reference mirror, and a sample arm, reflecting from the investigated tissue. A strong interference occurs when both reflected beams recombine and a pattern of interference allows us to create a reflectivity profile, which is used to construct the OCT images (3). Currently, several generations of commercially available OCT devices are available and widely used.

OCTA expands on this technique by looking at temporal changes in the quality of backscattered light to distinguish locations of static tissues from blood flow. It detects blood vessels based on differences in amplitude, intensity, or phase variance between sequential OCT B-scans in the same position of the retina. Sequential B-scans are taken at the same transverse location and compared. The difference in signal between images reflects blood cells flowing through vessel lumen. Therefore, blood movement is used as an intrinsic contrast agent to create a vascular map (see **Figure 1**). Because of its reliance on picking up tiny temporal changes, a high sampling frequency is necessary to create sufficient quality OCTA images (31, 32). It is important

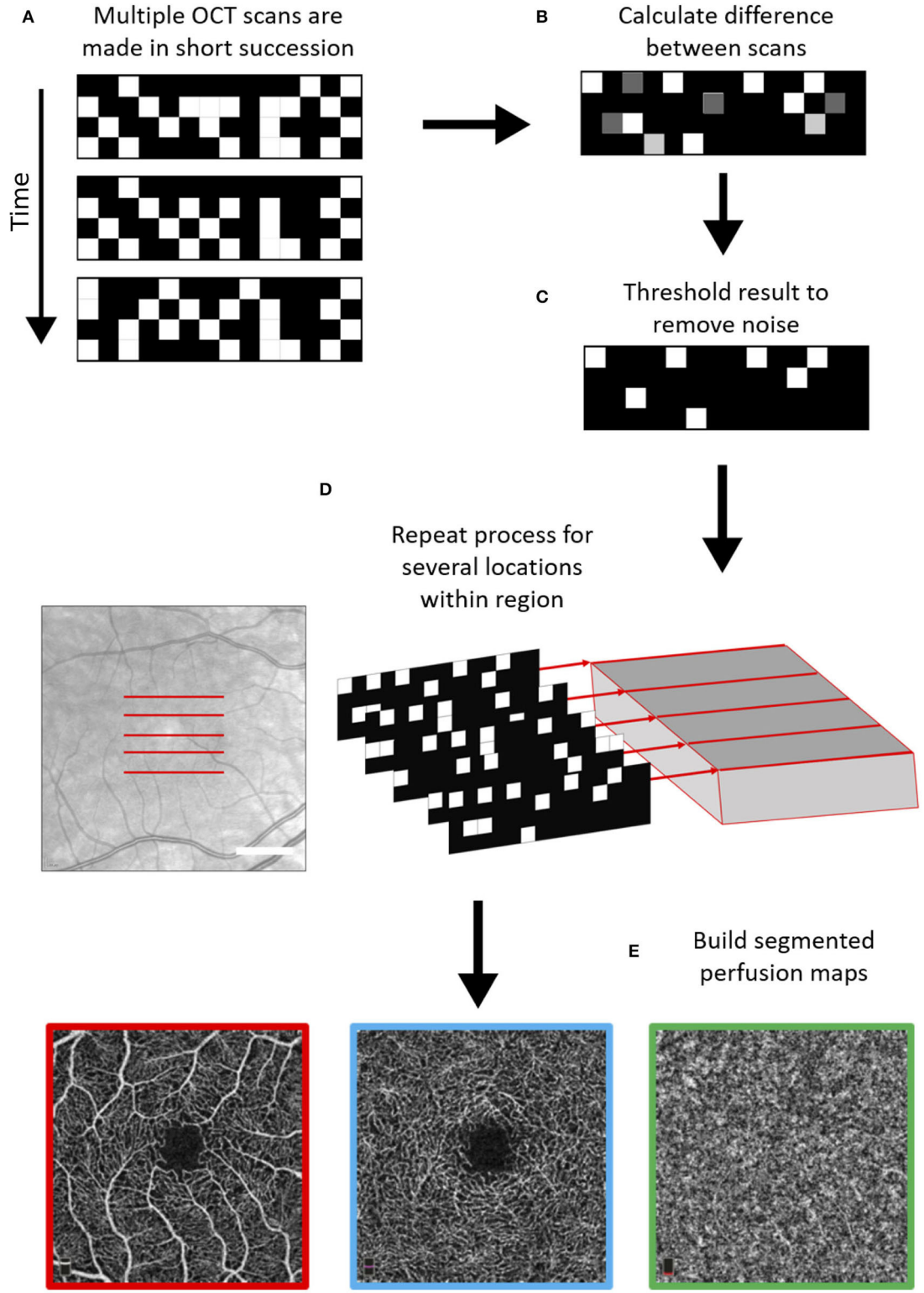

FIGURE 1 | Schematic of general optical coherence tomography angiography (OCTA) scanning technique. First, multiple OCT scans are repeated with a high frequency at the same location **(A)**, and based on differences between these scans in the phase, amplitude, and/or intensity of the backscattered light, areas with moving particles are differentiated from static tissue **(B,C)**. This process is repeated over several locations **(D)** and using a segmentation protocol perfusion maps are created for the different vascular plexi **(E)**. The example scans shown below are the superficial vascular plexus (red), the deep vascular plexus (blue), and the choroid (green) as obtained with the Heidelberg Engineering OCT2 system.

to remember that as a result of this technique, there is a floor to detectable OCTA signal that is slightly higher than slowest physiological flow, although the minimal detectable flow speed is not known.

Scans are visualized as en-face images of individual vascular layers, segmented from the volumetric map. The retinal vascular plexi are usually segmented in OCTA as a superficial layer, which consists of the superficial vascular plexus, and a deep layer, which takes the inner and deep vascular plexi together. But importantly, not all OCTA systems use the same segmentation algorithm for the superficial and deep vascular layers (33). Anatomical constraints and offsets from structural boundaries may vary between instruments (**Table 1**) (33).

OCTA images are generally analyzed by determining vessel density as the percentage of white pixels (representing vessels) in a segmented area. Although simple and easily implemented, this form of analysis is significantly influenced by the presence of artifacts, which are discussed later in this review. Most look at the vascular densities within a circular or square area around the fovea or optic disc. Densities of the macular SVP, DVP, and choroidal plexus are quantified separately in prespecified areas of investigation, generally a square of 3x3 or 6x6 mm. A separate outcome measure is the "foveal avascular zone" (FAZ), that estimates the size of the circular area in the center of the macula that has no SVP blood supply. The size and shape of the FAZ have both been used as an outcome, particularly in diabetes mellitus (DM) (34, 35). The FAZ has not yet been widely used as an outcome measure in neurological disorders.

A key feature of the healthy microvasculature is its fractal pattern, where shape of the vasculature is similar at every scale, fractal analysis has been gaining traction as an additional analysis tool (36, 37). This kind of analysis could be especially useful in cases of subtle microvascular change where there are no large regions of capillary dropout, but the highly specific pattern of the retina is altered due to the selective loss of small vessels.

TABLE 1 | OCTA platforms and segmentation of vascular plexi.

Platform	Instrument specifics	Vascular plexus	Slab boundary	Anatomic basis	Offset, μm
PLEX® Elite 9000 (Carl Zeiss Meditec)	Version 2018 v1.7 (Native seg); Version 2020 v2.1 (MLS)	Superficial (Native seg)	Top	ILM	0
			Bottom	IPL= ILM + 0.7·(OPL-ILM)	0
		Superficial (MLS)	Top	IML	0
			Bottom	IPL	−10
		Deep (Native seg)	Top	IPL	0
			Bottom	OPL (RPEFit – 110 μm)	0
		Deep (MLS)	Top	IPL	−10
			Bottom	OPL	0
CIRRUS™ HD-OCT 5000 with AngioPlex® (Carl Zeiss Meditec)	Version 9.5.0.8712; firmware 1.100.0.8; engine 6.5.0.8523	Superficial	Top	ILM	0
			Bottom	IPL= ILM + 0.7·(OPL-ILM)	0
		Deep	Top	IPL	0
			Bottom	OPL= RPEFit – 110 μm	0
RTVue XR Avanti (Optovue)	Version 2016.1.0.2	Superficial	Top	ILM	3
			Bottom	IPL	15
		Deep	Top	IPL	15
			Bottom	IPL	71
Triton DRI OCT (Topcon Medical Systems)	Version 10.07.003.03; IMAGEnet 6 version 1.14.8741	Superficial	Top	ILM	2.6
			Bottom	IPL/INL	15.6
		Deep	Top	IPL/INL	15.6
			Bottom	IPL/INL	70.2
Spectralis HRA OCTA (Heidelberg Engineering)	Version HEYEX V6.4a	Superficial	Top	ILM	0
			Bottom	IPL	0
		Deep	Top	IPL	0
			Bottom	IPL	0

ILM, inner limiting membrane; IPL, inner plexiform layer; OPL, outer plexiform layer; RPE, retinal pigmented epithelium; INL, inner nuclear layer.

ANATOMY RETINAL VASCULATURE

Retinal and optic nerve circulation has the challenging goal of supplying nourishment and removing waste without compromising vision. There are two discrete vascular systems in the retina; the retinal and choroidal vessels. Blood supply for both systems comes from the ophthalmic artery, a branch of the internal carotid artery. The ophthalmic artery in turn branches out in two main vessel types that supply the retina, the central retinal artery and the posterior ciliary arteries (**Figure 2**). The central retinal artery runs with the optic nerve inside the optic nerve sheath and enters the globe through the optic disc after which it branches out to supply the inner retina. The anatomy of the retinal microvasculature plexi is largely determined by constraints that are created by the anatomical organization of different regions in the retina. The three permeating retinal vascular plexi are organized based around the three cellular nuclear layers, the GCL, the inner nuclear layer (INL) and the outer nuclear layer (ONL) (**Figure 3**). The larger of the plexi, the superficial vascular plexus, mainly supplies the GCL, and roughly is located between the inner limiting membrane and the INL. The intermediate vascular plexus is located around the INL, while the deep vascular plexus is located primarily in the ONL (6, 7). The retinal venous system is interdigitated with the arterial vasculature and venous blood leaves the retina via the central retinal vein.

Retinal capillaries are formed of a layer of endothelial cells encapsulated by a basement membrane in which pericytes are embedded. Retinal capillaries are an important element of the blood-retinal barrier (BRB), the tightly controlled boundary between the intravascular and extravascular environment in the retina (38). Pericytes are essential for contractile function, endothelial barrier integrity and endothelial cell proliferation (38). Fluid and waste are drained from the eye through perivenous spaces, which are part of the ocular glymphatic drainage system (39). Beyond the lamina cribrosa there is no autonomic control of the retinal vasculature, therefore retinal capillaries are dependent on pericytes for local autoregulation of blood flow. Pericytes respond effectively to local tissue needs, and this relationship between local neural activity and changes in blood flow is known as neurovascular coupling. There is an approximate 1:1 ratio of pericytes to endothelial cells allowing for specific neurovascular coupling (40). The basement membrane between pericytes and endothelial cells is also very thin, allowing for increased communication between the two.

In the most common anatomical variant there are typically two posterior ciliary artery branches that run in parallel, but outside of the optic nerve sheath within the orbit. The posterior ciliary arteries supply the choroidal vascular plexus, which receives ∼65–85% of the total ocular blood flow. The choroid is responsible for the oxygen supply of the outermost retinal layers, particularly the photoreceptors and retinal pigment epithelium. The choroid is also the source of oxygen for the foveal avascular zone. Finally, the posterior ciliary arteries give rise to the capillary network supplying the exterior optic nerve head in the annulus of Zinn (6, 7).

OCTA IN NEUROINFLAMMATORY DISEASE

Multiple Sclerosis

Vascular Pathology and MS

MS is an immune mediated demyelinating disease of the CNS and is one of the most common neurological causes for permanent disability in young adults (41, 42). Although many advances have been made in the field of MS over the last years, its pathophysiology has not yet been fully elucidated. Recently, increasing evidence indicates that energy failure, due to hypoxia and hypoperfusion, may be an important causal factor in

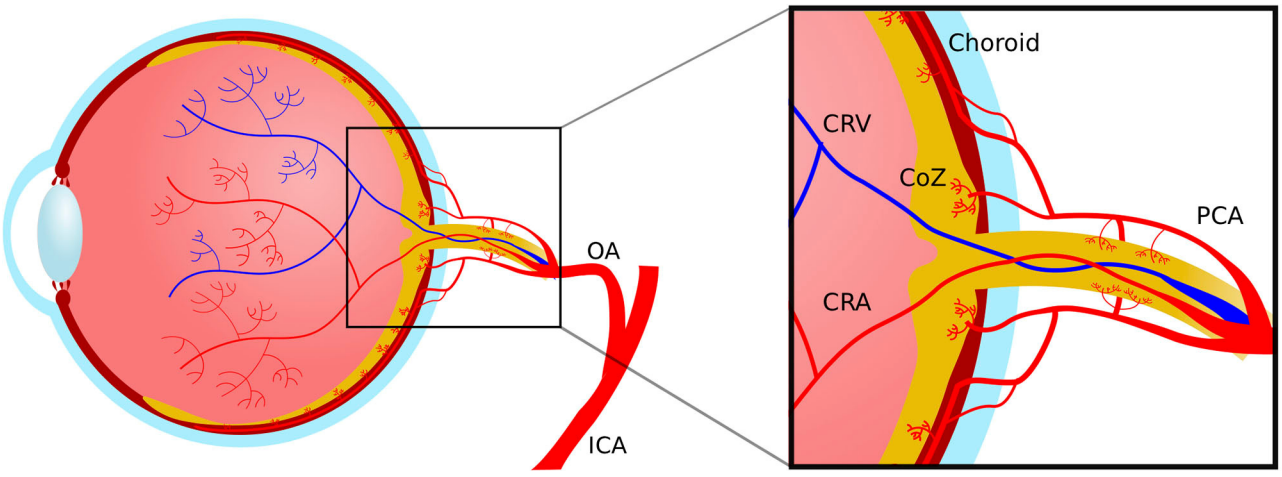

FIGURE 2 | Macrovascular anatomy of the blood supply to the eye. ICA, internal carotid artery; OA, ophthalmic artery; PCA, posterior choroidal artery; CRV, central retinal vein; CRA, central retinal artery; CoZ, circle of Zinn.

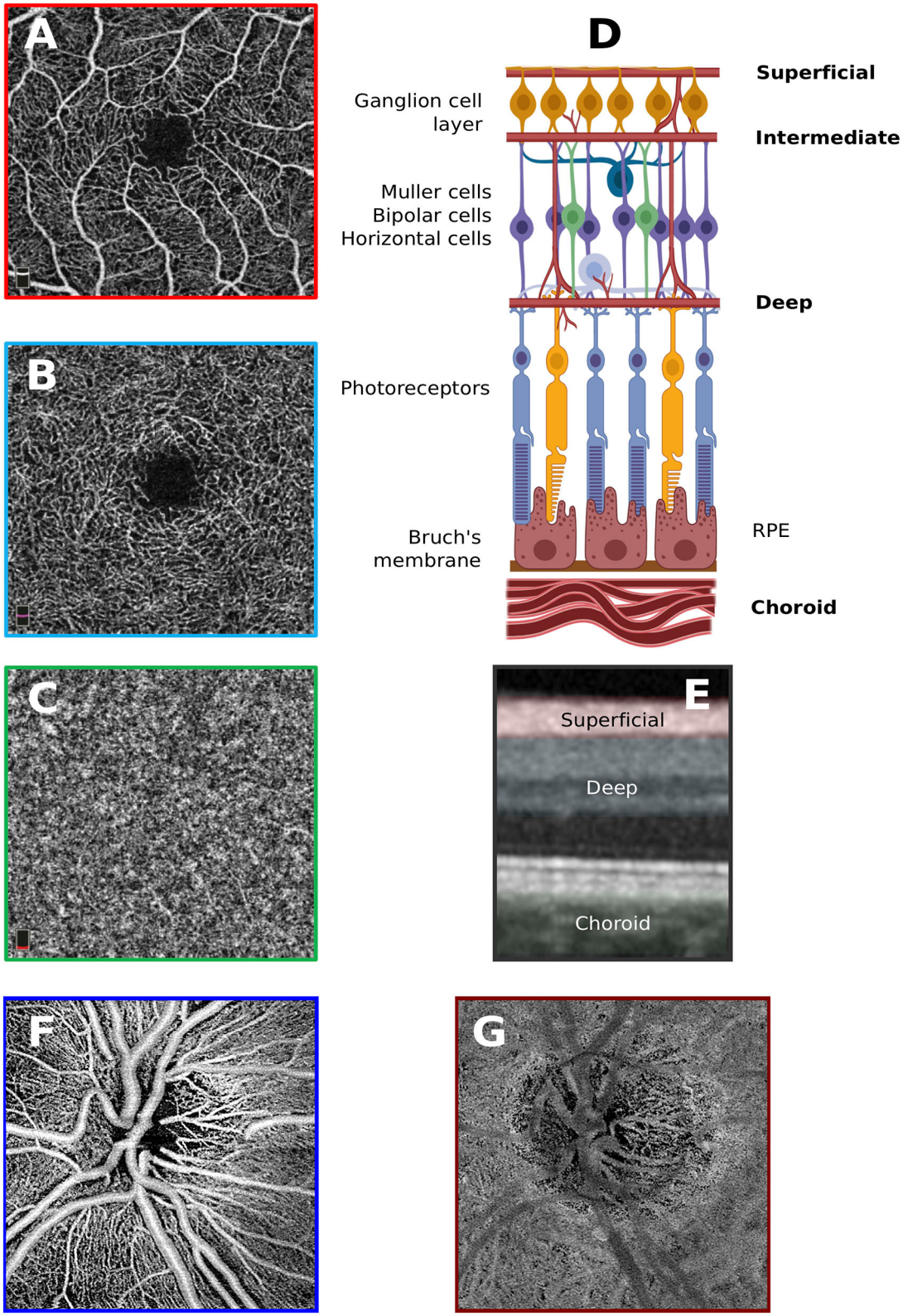

FIGURE 3 | Anatomy of the retinal vascular plexi. **(A)** Macular superficial vascular plexus centered around the fovea. **(B)** Macular deep vascular plexus. **(C)** Macular choroid. **(D)** Locations of the vascular plexi relative to the various cell types that construct the anatomy of the retina. Created with biorender.com. **(E)** Superficial and deep vascular plexi as well as choroid slabs overlain on OCT scan. **(F)** Superficial vascular plexus of the optic nerve head. **(G)** Choroid of the optic nerve head.

MS. Many studies have demonstrated the presence of hypoxia and hypoperfusion in the CNS of MS affected individuals clinically, radiologically, and histologically (1, 10). For example, cerebral type-III MS lesions histologically frequently resemble hypoxic insult and MS lesions tend to form in watershed areas of the areas of the brain, suggesting a role for hypoxia in its pathophysiology (18, 43). Several studies found a reduction in cerebral blood flow in MS affected individuals, even in the absence of structural damage (44, 45). Cerebral circulation times are increased from a mean of 2.8 s in controls to 4.9 s in all types of MS (46). Hypoperfusion in MS can be identified from very early in its disease course, as perfusion rates in patients with clinically isolated syndrome (CIS) have been found to be reduced (47). Additionally, a study which used near-infrared spectroscopy (NIRS) showed that almost half of MS patients had hemoglobin saturation values that were significantly reduced compared with healthy controls (48). Anemia more than doubles the risk of developing MS and also doubles the risk of experiencing a relapse in MS (49). Furthermore, patients with MS have an increased risk of ischaemic heart disease and stroke, suggesting further susceptibility to microvascular damage (50).

Interestingly, one exploratory case study found evidence for transient reduced blood flow focally in the optic nerve during acute MSON (51). Preliminary data suggests that blood flow in the retinal microcirculation is reduced in patients with relapsing-remitting MS compared with healthy controls (52, 53).

Animal work with experimental autoimmune encephalomyelitis (EAE) revealed that the inflamed spinal cord of affected animals was indeed severely hypoxic and hypoperfused (54–57). The level of hypoxia was temporally and spatially related to the clinical deficit, and predicted subsequent demyelinating damage. Investigations indicated that the hypoxia was caused by insufficient perfusion of the CNS, creating a shortage of oxygen delivery in the inflamed area (54). Accordingly, it was found that therapeutic approaches aimed at alleviating hypoxia, with inspired oxygen, or alleviating hypoperfusion, with vasodilating agents, were related to improved neurologic outcome and reduced later stage demyelination in the affected animals (17). These findings suggest that hypoxia and hypoperfusion may render nerve cells inexcitable through depolarization, causing disability in the acute stage, but also damage oligodendrocytes, causing subsequent demyelination.

Although hypoperfusion is increasingly recognized as a possible important component in the multifactorial etiology of MS, interpretation of its role is controversial. Ambiguity remains if it is a primary process, representing a causal factor in the disease mechanism, or a secondary process, representing the result of lower metabolic demand in atrophied tissue (1). As many existing methods for investigating CNS perfusion are invasive, time-consuming, or laborious, little follow-up data is available to discern the temporal patterns of vascular changes in neuroinflammatory disease. Combining OCT and OCTA may offer ways to explore temporal patterns in vascular changes and structural atrophy of the retinal layers, which might provide important insights into the pathophysiological processes that underlie MS.

OCTA in MS

With OCTA being a relatively novel technique, there is a high level of variability in choice of outcome metrics and OCTA system used in studies investigating the microvasculature in MS. Although the variability in test metrics and OCTA systems makes it difficult to make direct comparisons between studies, all currently published studies found a significant reduction in retinal vessel density, in the macular area, the peripapillary area, or both, in MS patients compared with controls. Most also identified clear correlations between structural retinal layer thickness OCT measurements and vessel density (20–22, 58, 59).

The largest study cohort to date consists of 111 RRMS or high-risk CIS patients, who were compared to 50 healthy controls using a Heidelberg Spectralis OCTA (20). This study focused on the macular microvasculature, and found a significant reduction in SVP vessel density from 29.1% in controls to 24.1% in MS eyes ($p < 0.001$), while the DVP was unaffected. Furthermore, MS eyes affected by ON (MSON) had a lower SVP vessel density at 21.7% compared with non-ON (MSNON) eyes at 26.0% ($p < 0.001$). Finally, the difference between vessel densities in MSNON eyes and control eyes just reached significance ($p = 0.03$). Reduced SVP density was related to combined GCL and inner plexiform layer (GCIPL) and pRNFL layer atrophy, while lower DVP densities were related to GCIPL and inner nuclear layer thickness. All analyses were adjusted for age, sex, ON history and within-subject inter-eye correlations. Interestingly, these changes were evident in a cohort of relatively early stage MS, with a mean EDSS scores of 1.5.

These results are corroborated by several smaller studies that recruited 20 to 50 MS patients and similar numbers of healthy controls, that identified reduced macular SVP vessel densities in eyes of MS patients compared with controls (21, 22, 58, 60), with a significant reduction in SVP vessel density in MSON compared with MSNON eyes being identified in the two larger cohort (21, 60). Two studies identified an additional significant reduction in DVP vessel density, one in MS compared with controls (21) and one only in MSON compared with MSNON (22) (**Figure 4**). However, not all studies have replicated the finding of reduced macular SVP vessel density in MS (61).

In two smaller cohorts of 35 and 45 patients with relatively more advanced MS, vessel density around the optic nerve head (ONH) was reduced in MS eyes compared to control eyes, as well as in MSON eyes compared with MSNON (61, 62). One study identified reduced vessel densities specifically in the inferior and nasal sections around the ONH in MS patients compared with controls (58), while another study found reductions only in the temporal zone (21). The finding of reduced vessel densities around the ONH has been classified as "capillary dropout" (61).

A recent study developed a novel metric, called volumetric vessel density (VVD), by dividing the macular vessel densities of the SVP and DVP by the tissue volume of the corresponding retinal layers (59). In a large cohort of 80 RRMS patients and

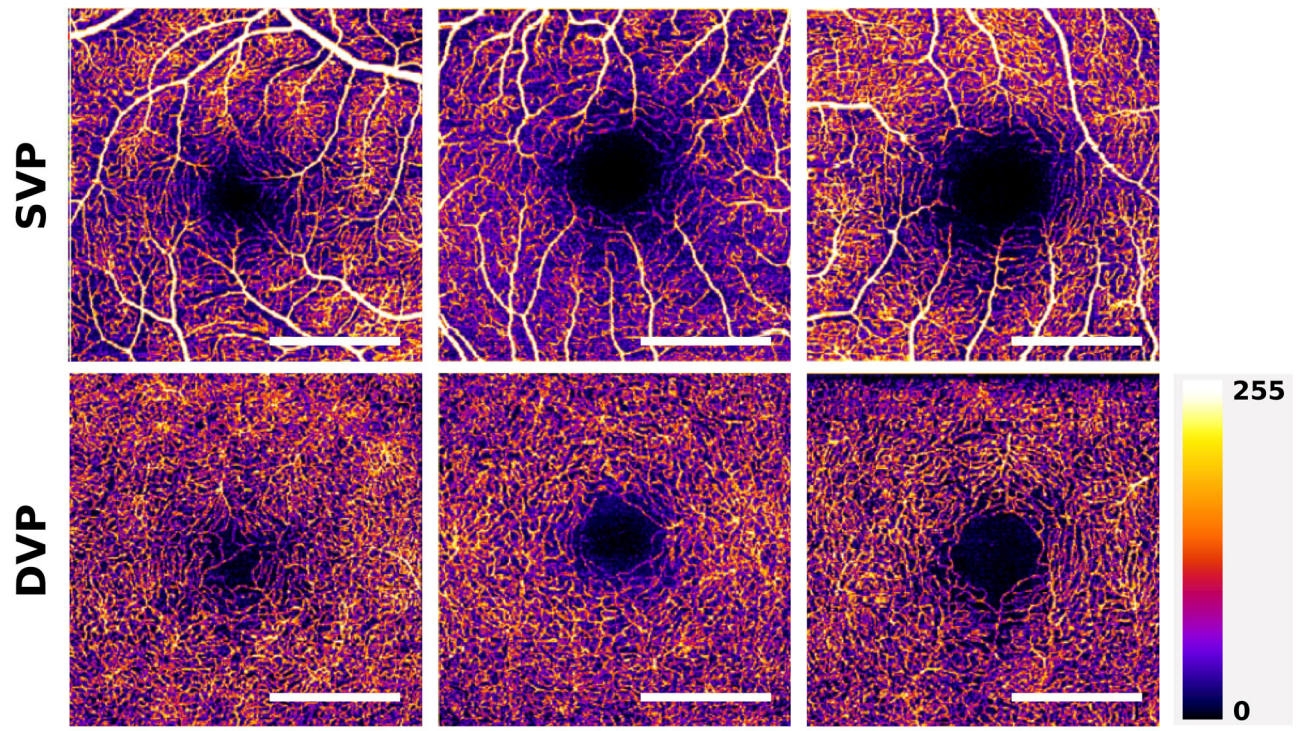

FIGURE 4 | Example of macular superficial vascular plexus (SVP) and deep vascular plexus (DVP) changes in MS and MOG-Ab seropositive NMOSD compared with a healthy control. The scans of MS and MOG-Ab seropositive NMOSD patients are made from eyes without prior optic neuritis. The foveal avascular zones (FAZ) of the MS and NMOSD eyes are greater than these in the healthy control. Scale bar: 1 mm. Scans are 3x3 mm and obtained with the Heidelberg Engineering OCT2 system.

99 matched controls, the VVD of the DVP was higher in MS patients compared with controls. Additionally, the VVD of the DVP and SVP of MSON eyes were significantly higher compared with MSNON eyes (59). This is an interesting new metric that combines structural and microvascular changes in the retina. However, one could argue that it might be clearer to estimate structural and microvascular measures independently, as the VVD is determined to a high degree by changes in retinal thickness. Therefore, the observed increase of the VVD might still reflect a strong decrease in vascular structure density that is obscured by a more pronounced decrease in retinal thickness. This seems not unlikely, as the volume of vascular structures is smaller compared with their corresponding retinal layers and structural retinal atrophy is severe after MSON. This appears to be affirmed by the fact that VVD measures were strongly and negatively correlated with analyzed tissue volumes. However, the VVD is an important step toward incorporating data as we look at the full integrated structural and functional system going forward.

The size and shape of the foveal avascular zone, readily visible using OCTA, has been used as an outcome metric in studies of diabetic retinopathy (63). The foveal avascular zone (FAZ) was used as the outcome metric in one study of MS, and found that neither the area nor perimeter of the FAZ differed between MS patients and healthy controls, even though the FAZ size was negatively related to the vessel density of the SVP and DVP (21).

OCTA data captured in the acute stages of ON is currently lacking, although one small case series of seven MSON patients with good clinical recovery did find significantly reduced SVP macular and ONH vessel densities in affected compared with unaffected eyes 2–8 months after the episode (64). These changes in vessel density were in all cases accompanied by structural thickness loss of the macular GCL layers. Prospective studies investigating the hyperacute stages of MSON might be able to delineate the temporal relationships between structural and vascular changes, which could further the understanding of the role of hypoperfusion in the pathophysiology of MS. The challenge here however will be disc swelling which limts OCTA signal strength.

Just one study has collected longitudinal OCTA data in MS patients to date. One-year follow-up OCTA scans were performed in a cohort of 50 MS patients (mean EDSS 3.5 and average disease duration of 11 years) who had stable disease and were on disease modifying treatment. Interestingly, parafoveal vessel densities increased slightly, a finding just

reaching significance ($p = 0.035$), while structural thickness of the pRNFL and GCL remained stable (65). This provides some evidence for possible vascular regeneration or increase of lumen thickness in chronic disease, but additional longitudinal data on the microvasculature in MS, including in its earlier stages, are needed to interpret these findings. Future longitudinal data are required to identify if OCTA can function as a biomarker to predict and monitor disease progression in MS and other neurodegenerative disease (66).

Finally, although glaucoma research suggests that vascular density loss is faster in early-stage disease and has a lower floor-effect in late-stage disease compared with common structural OCT measurements, this has not yet been demonstrated in studies of MS patients (23, 25, 26).

Correlation OCTA With Clinical Measures in MS

A lower vessel density of the macular SVP was found to be related to a higher EDSS score and lower low-contrast visual acuity in MS patients (20). Interestingly, in this study results of other clinical outcomes like the 9-hole peg test, the timed 25-foot walk test and the multiple sclerosis functional composite (MSFC) were related to macular SVP vessel density, while combined GCL and inner plexiform layer thickness was not. Another study describes an inverse correlation between visual evoked potential latency times and vessel density of the SVP and DVP (21). Additional, smaller, studies identify no relationship between vascular metrics and clinical or visual outcomes (62). Interestingly, increased vessel density of the macular choriocapillaris has been found to be associated with higher inflammatory disease activity prior to the OCTA examination, suggesting another possible OCTA biomarker in MS (22). Finally, VVD of the macular SVP was positively related to EDSS and disease duration, while being negatively related to low-contrast letter acuity (59).

Neuromyelitis Optica Spectrum Disorder (NMOSD)

Vascular Pathology and NMOSD

The autoimmune inflammatory conditions of NMOSD share cardinal features of ON, longitudinally extensive transverse myelitis and area postrema syndrome that are often relapsing (12, 67). Although attention for vascular changes in neuroinflammatory disease has been primarily focused on MS, there is also evidence that NMOSD pathophysiology is in part vascularly mediated (68, 69). In most cases NMOSD is caused by the pathogenic effects of auto-antibodies targeting the water channel protein aquaporin-4 (AQP4), for which the majority of patients test positive. As AQP4 is predominantly expressed on perivascular astrocytic foot processes in the spinal cord and by Müller cells in the retina, NMOSD has a predilection for the anterior visual system and the spinal cord (70). Approximately 40% of NMOSD patients that test negative for AQP4 antibodies, test positive for antibodies against myelin oligodendrocyte glycoprotein (MOG) (67).

Neuropathology of AQP4-antibody seropositive NMOSD lesions show a perivascular pattern (71, 72), with rim deposits of activated complement components and macrophages found around thickened, fibrosed, and hyalinised vessels (73). Active spinal cord lesions may have an increased density of vascular structures (71). Similar to MS lesions predominantly forming in watershed areas of the brain with poor perfusion, AQP4-Ab seropositive NMOSD lesions preferentially form in the hypo-perfused posterior and lateral spinal columns (74). Interestingly, the choroid plexus expresses AQP4 to a high degree, and immunoreactivity of choroidal plexus epithelial cells is profoundly affected or even lost in NMOSD, even though the choroidal plexus remained structurally intact in neuropathological investigation (75). AQP4 is expressed in a vasculocentric pattern in the optic nerve and spinal cord (72).

Importantly, the predominantly perivascular location of is one of the key neuropathological features that can distinguish AQP4-antibody associated NMOSD from MS lesions at autopsy (72). One study found that retinal vascular changes identified through fundoscopy, such as attenuation of the peripapillary vascular tree (present in 3/40 MS eyes and 22/32 NMOSD eyes; $p = 0.001$) and focal arteriolar narrowing (present in 0/40 MS eyes and 9/32 NMOSD eyes; $p < 0.001$) could successfully distinguish NMOSD from MS patients (19). OCTA may be diagnostically useful tool capable of picking up these vascular differences more easily and systematically. To become clinically useful the aim will be to get high diagnostic sensitivity and specificity levels.

Neuropathological studies of CNS lesions in MOG-antibody seropositive patients reveal distinctly different features compared with AQP4-antibody associated lesions. Although MOG associated lesions have a predilection for perivascular locations, this is less profound compared with AQP4-associated pathology. MOG lesions were found to share pathological characteristics with immunotype II and III MS lesions (76). Type III pattern of demyelination shows similar tissue changes as observed in early stage white matter ischemia, and is therefore hypothesized to potentially be caused in part by hypoxia (77).

OCTA in NMOSD

Although there is currently a very limited number of studies published on OCTA in NMOSD, all available data suggest profound decreases in microvascular densities in affected individuals exist (27, 78, 79). A recent study investigating differences in structural thickness and microvascular retinal density of 27 AQP4-antibody seropositive NMOSD patients and 31 healthy controls found a significant difference in vessel density of the peripapillary region and the macular SVP between patients with NMOSD and controls. Interestingly, there were also significant reductions in vessel density in the macular and ONH region when comparing NMOSD patient without previous ON to controls ($p = 0.023$ and $p = 0.029$), while retinal thickness measures of the macular GCL and pRNFL were similar in these groups (27). These findings were replicated by a second study, that also found that vascular densities in the macula and ONH were reduced in NMOSD patients without ON compared with healthy controls, while pRNFL and macular GCL were not (78). This suggests OCTA may be more sensitive to ON-independent damage to the anterior visual system in NMOSD compared with structural OCT (**Figure 4**).

Additionally, these findings of vascular dropout in the absence of structural thinning argue against the hypothesis that reductions in microvascular density are a result of reduced demand in atrophied tissue and, if replicated, may provide evidence for a role of microvascular dysfunction as an independent disease process in NMOSD.

Both the densities of the macular SVP and DVP have been found to be negatively correlated to visual acuity measures in NMOSD (79).

Given that neuropathological research suggests that vascular vessel walls seem to be affected by fibrosis and thickening in NMOSD, it is important to consider that OCTA depicts as a vessel is actually moving blood within a vascular lumen. Therefore, OCTA can depict vessel thinning and capillary dropout, but not the unmoving vessel wall itself. In order to visualize these changes *in-vivo*, devices capable of high-resolution imaging which are not dependent on motion contrast are required, such as adaptive optics coupled ophthalmoscopy. The potentially more profound vascular changes in the anterior visual system of NMOSD patients compared with MS might be the result of the reduced metabolic demand associated with more severe structural atrophy in NMOSD related ON, although the reduction in vascular density in the absence of atrophy argue against this. Furthermore, the vascular pathology might be a result of more mechanical constriction at the ONH due to more severe papilledema during ON. Although there is some evidence for more profound papilledema in ON associated with NMOSD compared with MS, the fact that vascular density reductions are also identifiable in patients without ON is incongruous.

Data on OCTA alterations observed in MOG associated disease and in MOG associated ON specifically is currently lacking. Finally, future research is needed to investigate if certain distinctive qualitative or quantitative differences in retinal microvascular changes exist between MS and NMOSD that might provide valuable additions to the diagnostic arsenal.

PRACTICAL SOURCES OF BIAS

There are several important practical factors that should be taken into account when designing an OCTA study, as these may influence outcome metrics and thereby confound findings (23). First, there are various demographic factors that are associated with differences in OCTA results. For example, older age is associated with reduced macular and peripapillary vessel density (80, 81). Furthermore, in glaucoma research, eyes of people from European descent have been identified to have lower vessel density measures compared with eyes of people from African descent (23). Both hypertension and diabetes mellitus are related with decreased macular vessel density, also in the absence of a retinopathy. Chronic use of topical beta-blockers may lead to some reduction in macular SVP density (81).

Myopia is another important factor that is related to significant reductions in vessel density measurements. Highly myopic individuals have been found to have significantly lower vessel densities in the peripapillary region compared with emmetropic eyes. Myopic glaucomatous eyes have more severely reduced vessel densities compared with emmetropic glaucomatous eyes (82, 83). Image magnification in myopic eyes may be in part responsible for these effects (23). On the other hand, a greater disc size was not related to changes in peripapillary vessel density in one cross-sectional study (84).

Besides these demographic factors, there are also some important considerations regarding the timing of OCTA measurements. One study reported that in a small cohort of 13 healthy subjects, vessel density decreased significantly after strenuous physical activity (85). Retinal vessel calibers vary slightly with the cardiac cycle (86). Preliminary data suggests that increases in heart rate and blood pressure are related to higher macular SVP density measurements (87). The same study showed no important diurnal changes in OCTA vessel density.

Interestingly, multiple studies have found that vessel densities were reduced in OCTA scans with lower signal strength (84, 85, 87, 88). This is important since low image quality and motion artifacts are common in OCTA, mainly due to the relatively long acquisition time. As the OCTA signal is based on a threshold of change (movement) detected across the volume, when signal is reduced, vessels are harder to detect leading to reduced vessel density in poor scan quality volumes. Small pupillary size can interfere with image acquisition and generally pupil dilation is necessary for high quality images (89). Finally, media opacities in the lens or especially in the vitreous, can significantly reduce image quality.

Glaucoma research has shown that intra- and intervisit variability of OCTA vessel density measures is between 2.5 and 6.6% in the peripapillary region and between 3.4 and 5.6% in the macular SVP (88, 90). This intra- and intervisit variability of vessel density measures is more than is reported for OCT structural measures of the pRNFL and GCL thicknesses, which is ∼1.5%. Importantly, glaucoma affected eyes had worse intervisit repeatability compared with healthy eyes, an effect that can be expected to occur in ON affected eyes as well due to problems with focusing (91). Future developments improving image acquisition speeds and eye-tracking of commercial OCTA systems are needed to bring intra- and intervisit repeatability into a range closer to OCT.

ADVANTAGES AND DISADVANTAGES OF OCTA

There are opportunities as well as obstacles when using OCTA in neuroinflammatory disease. Compared to other types of retinal vascular imaging, such as fluorescein angiography, OCTA is quick and non-invasive, with no intravenous dyes required. Most devices are user-friendly and require limited training to perform standard imaging. The speed at which OCTA can be obtained means it could be easily integrated into a clinical setting, especially where OCT is already performed and a multimodal retinal imaging setup is available.

The real strength of OCTA is in its multifunctional capacity. As it uses the change in the structural OCT images to map blood flow, both forms of imaging are collected simultaneously. Some studies have combined the information on tissue structure and vascular density to elucidate the vascular impact of multiple sclerosis, increasing diagnostic accuracy. Coupling structural information from retinal thicknesses with vascular density allows for a more complete picture of individual patients, which is highly useful especially in a disease with such variable presentation as MS.

OCTA also has certain disadvantages, namely imaging artifacts and inability to detect dynamic vessel related changes such as leakage or venous sheathing (92). There are yet no consensus quality control criteria similar to what has been achieved for OCT (30). Additionally, OCTA creates a binary 3D figure of moving components to static retinal tissue, but it cannot quantify retinal perfusion as it cannot measure blood velocity. It does not differentiate between areas of high and low flow. Multi-modal imaging approaches which combine Doppler OCT and OCTA are able to add this information, by adding velocimetry to the depth encoded OCTA image (93). In addition, novel high dynamic range OCTA systems are a promising extension to the technology that are sensitive to flow speeds, and are not compromised by angle issues present in Doppler OCT systems (94).

Imaging artifacts are a well-documented limitation to OCTA (95) which are further compounded by visual loss and nystagmus in neuroinflammatory disease (96). Small movements can have profound effects on an OCTA image. As the laser is scanned across the retina, small transverse motions of the eye in respect to that laser can lead to mass displacement of locations in the resulting image, causing a motion artifact. In order to choose the correct location for OCTA imaging, patients are required to fixate on a small target either internal or external to the imaging device. Patients with a history of ON may have poor fixation and are therefore more prone to these motion artifacts. These problems are enhanced in acute ON, where impact on the retinal vasculature may be most profound. Small eye movements can be compounded by larger movements caused by postural difficulties, especially in situations where the standard OCT set up is uncomfortable for the patient. Adjustments can be made but unfortunately there is not yet a handheld OCTA device commercially available to allow for complete accessibility for children and less mobile patients, especially in the later stages of disease. Fast and efficient scanning of the retina to avoid making patients sit or fixate for too long could rectify this issue of motion artifacts.

Segmentation of vascular layers, allowing the user to distinguish individual vessel networks, is a unique ability of OCTA. However, automated segmentation by the device is not always accurate, leading to segmentation artifacts in images which can appear as vessel dropout. Initial identification of the artifact is crucial, and segmentation can be manually adjusted by the user, but there is no consensus currently as to how these artifacts should be identified and remedied.

Ocular complications of MS can also lead to image artifacts. Media opacity, as found in uveitis, greatly diminishes the quality of imaging possible using OCTA. Changes in the optical pathway, such as that caused by microcystic macular oedema (MMO) that occur in MS and NMOSD, could also lead to distortions in the resulting signal.

Overall; motion artifacts, segmentation artifacts and opacity issues can have a profound impact in image quality in OCTA. The importance of quality control of OCT images has been widely accepted in recent times, as evidenced by the OSCAR-IB criteria being integrated into many clinical trials (97–99). Quality control of OCTA images is essential and should be stressed in both the design and interpretation of studies using OCTA in MS. The creation of a set of quality control criteria for OCTA may be very helpful for the standardization of methods between different studies.

The field of view available on OCTA devices is limited, with the largest scanning area available using commercial OCTA is 8x8 mm, a field of view of ∼30 degrees. Images may be collected separately and "stitched" together, but this extends the image collection time and this montaging capability is not available on all devices (**Figure 5**). Peripheral changes in the vasculature, such as those caused by vasculitis, are not likely to be detected using even the largest available field of view. Wide-field OCTA when available would be of great benefit to studying the retinal microvasculature in MS.

Each device has its own machine-specific algorithm to measure the difference between B-scans in order to build a picture of the retinal vessels with specific detection thresholds. Many instances where blood flow is altered, such as in leaking vessels, microaneurysms, and polypoidal lesions, will not be detected since they are below this threshold. Interesting vascular features that occur in neuroinflammatory disease, such as venous sheathing or vascular leakage, will not be picked up by OCTA.

FUTURE OUTLOOK

As discussed in this review, OCTA has only just started to be utilized in research into neuroinflammatory disease. Preliminary studies suggest that the microvascular network in the macula and the peripapillary area is less dense in MS patients, and while prior MSON insult exacerbates this finding it is also present in the absence of MSON. Similar findings are identified in the first studies reporting on AQP4-antibody seropositive NMOSD patients. Interestingly, reduced vascular densities are even identified prior to structural atrophy of retinal layers in NMOSD. Larger cohorts of ON patients in the acute stage are necessary to elucidate the timing of vascular relative to structural changes, to identify if OCTA is indeed more sensitive to early-stage damage and to find if disparities in timing of these two factors may be of diagnostic value in differentiating NMOSD and MS related ON. Furthermore, glaucoma research shows that OCTA has a lower "floor-effect" compared with OCT, being able to pick up further damage in a severely structurally atrophied retina (23–26). If research in neuroinflammatory disease could identify a similar effect, OCTA vascular densities may be more suitable outcome measures in clinical trials where participants

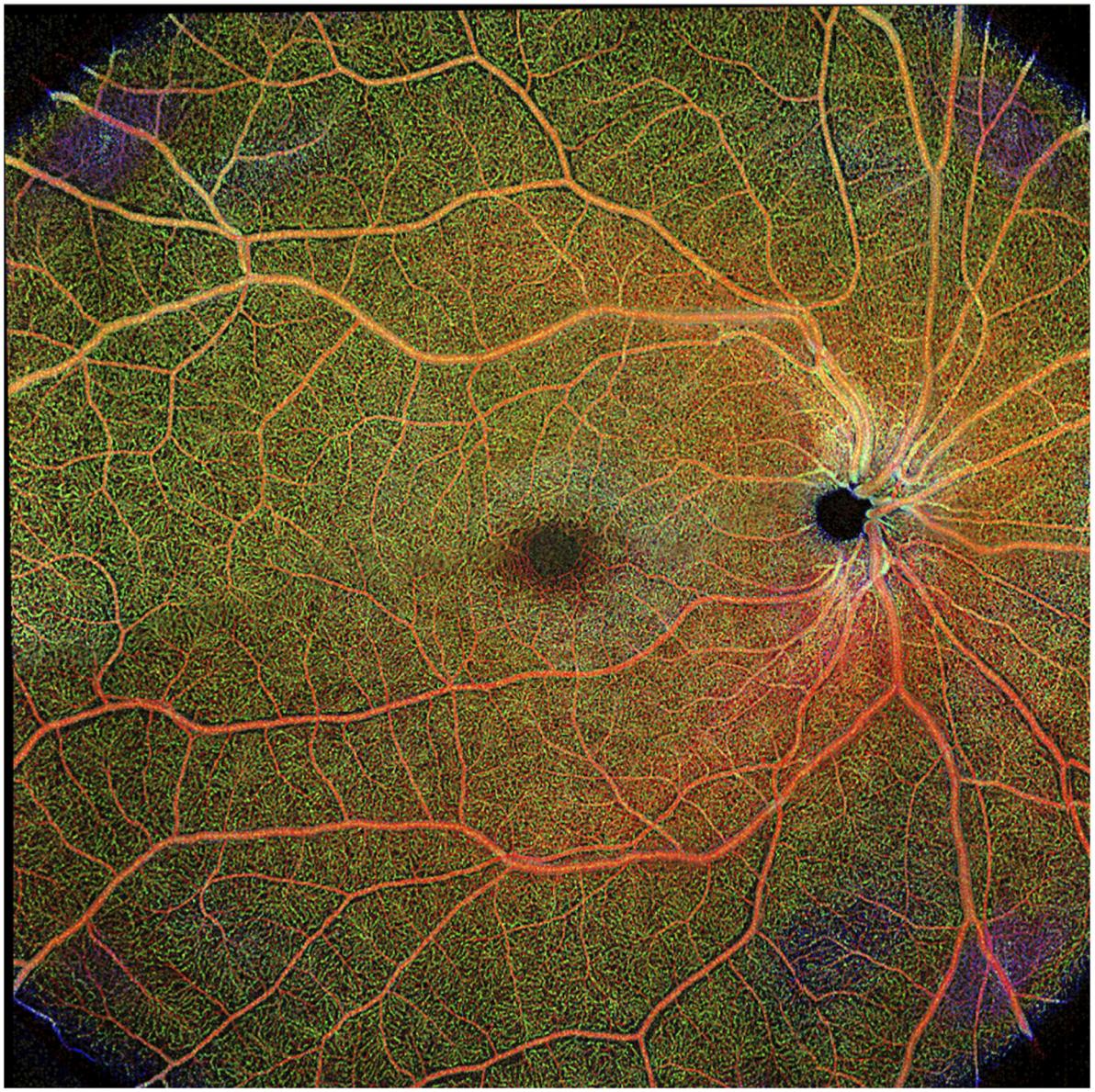

FIGURE 5 | Composite of wide-field optical coherence tomography angiography (OCTA) scan in healthy eye. Scan sample obtained with the Plex Elite 9000 (Carl Zeiss Meditec). Figure is a reprint from Kleerekooper et al. (10).

have advanced (progressive) disease or have suffered retinal insult due to prior ON compared with OCT. Additionally, choroidal density measures may be a valuable biomarker for disease activity.

The biggest cohort to date studying OCTA in MS (20) found that vascular density correlated with more clinical outcome measures compared with structural OCT metrics. This seems to suggest that the association between certain clinical parameters may be stronger with OCTA compared with OCT thickness measures, which is in line with results in glaucoma research (23). More data is necessary to see if OCTA may provide a more relevant outcome metric that is just as easily obtainable as OCT.

As mentioned before, the possibility to elucidate the timing of vascular relative to structural insult to the retina after acute ON may help to understand the role of hypoperfusion and energy failure in MS pathophysiology. If vascular damage occurs before structural atrophy can be identified, this would give argument to the important role of hypoperfusion in MS related damage. However, if vascular density loss occurs after thinning of retinal layers, this suggests that vascular supply may be reduced due to lower local

metabolic demand. This is an important question, given the potential therapeutic possibilities that may reduce MS disability accrual by alleviating hypoperfusion, that OCTA might help answer (17).

Most research has focused on the peripapillary vascular layers and the macular SVP and DVP. As alluded to shortly in this review, there may be benefit to looking into the other retinal vascular layers, such as the choroidal layer. One study identified that a more dense choroidal plexus was related to more severe disease activity in the time before, suggesting it may provide an interesting biomarker (22). However, caution needs to be taken when looking at layers situated more deeply, as it is difficult to accurately interpret the meaning of imaged data. As light travels deeper through retinal tissue, it is more distorted and affected by absorption at different levels, producing a less reliable image.

From personal experience, we know that MS patients may have abnormal phenotypes of the FAZ on OCTA (see **Figure 6** for unpublished observations). However, similar FAZ abnormalities are sometimes also observed in healthy controls, and additional study is required to see if these are more common in MS.

Finally, OCTA may be able to pick up temporal and spatial differences in the choroidal blood supply, that is highly

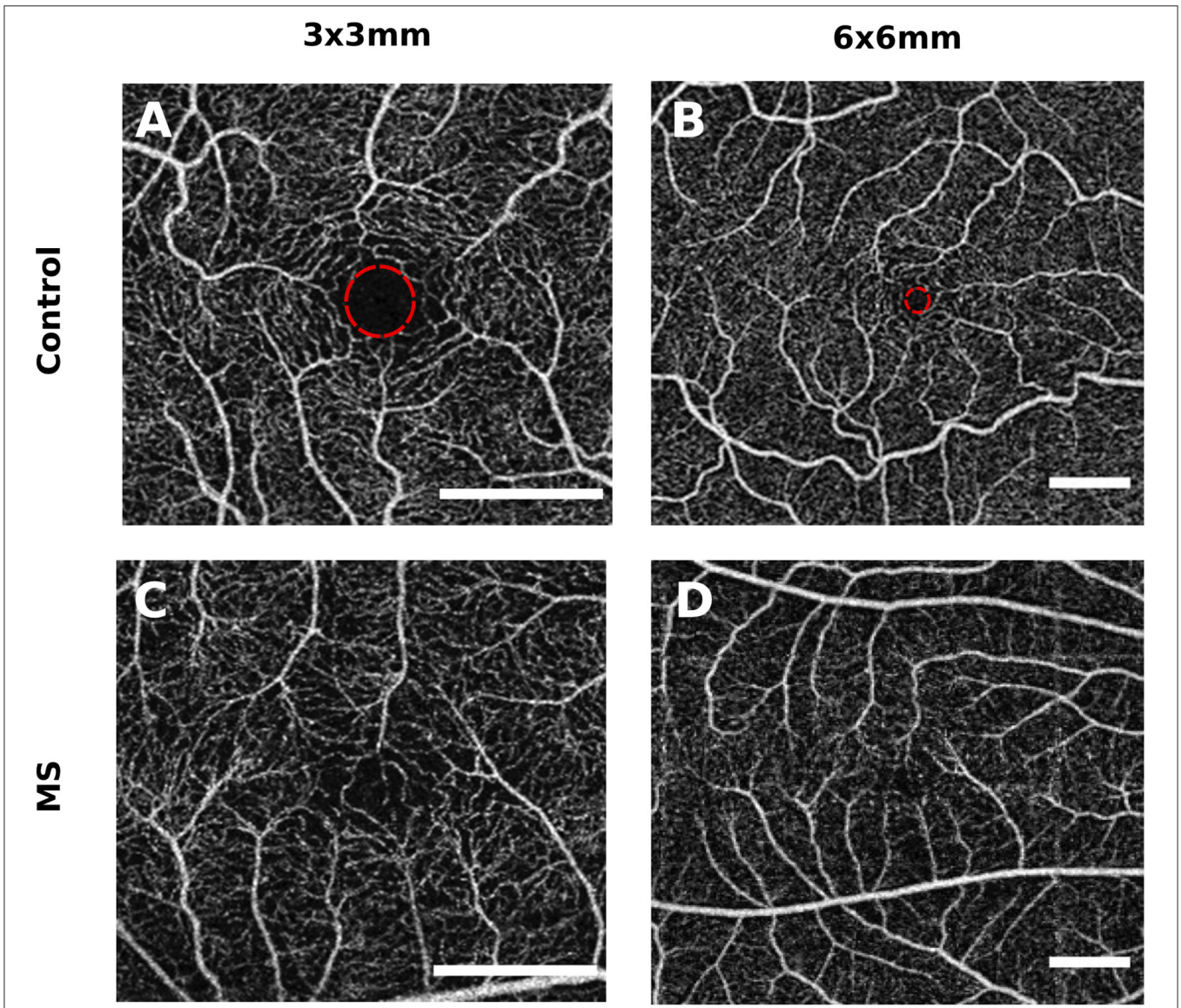

FIGURE 6 | Example of a foveal avascular zone (FAZ) abnormality in a patient with multiple sclerosis (MS). These figures represent an unpublished observation from the authors. However, abnormal FAZ phenotypes are also sometimes observed in healthy subjects, and additional research is necessary to investigate if these are more common in MS compared with healthy controls. **(A,B)** are from two different controls and show a symmetrical and round FAZ. **(C,D)** are from the same MS patient and show an asymmetric FAZ with vessels growing further into the center. Scale bar: 1 mm. The FAZ is delineated with a red circle in **(A,B)** (healthy control eyes).

adaptive to fluctuations in local demand. Preliminary animal studies have demonstrated spatial and temporal heterogeneity in retinal blood supply (8). OCTA may be used to investigate if neuroinflammatory disease decreases the adaptability of the ocular blood supply.

CONCLUSION

OCTA provides an alternative quantitative measure for retinal damage in MS and NMOSD. Early results suggest that in certain circumstances OCTA, compared with OCT, may be more sensitive to retinal changes both early in the disease process, making it useful for detection of disease, and late in the disease process, rendering it suitable for monitoring of disease. Furthermore, it may also serve as a surrogate measure for vascular pathology in the CNS. Preliminary data of patients both with and without optic neuritis consistently reveal lower densities of the retinal microvasculature in both MS and NMOSD compared with healthy controls. Exploring the temporality of vascular relative to structural changes may help answer important questions about the role of hypoperfusion in the pathophysiology of neuroinflammatory disease. Finally, qualitative characteristics of retinal microvasculature may help discriminate between different neuroinflammatory disorders. However, we have to be mindful of issues such as image quality and standardization before incorporating OCTA into clinical practice.

AUTHOR CONTRIBUTIONS

IK and SH: literature search, writing main text, and creating figures. AD, ST, and AP: manuscript writing and revision for intellectual content. All authors contributed to the article and approved the submitted version.

FUNDING

AP, AD, and SH receive support from the National Institute for Health Research (NIHR) Biomedical Research Centre based at Moorfields Eye Hospital NHS Foundation Trust and UCL Institute of Ophthalmology. ST receives support from the University College London Hospitals Biomedical Research Centre. SH receives additional support by the MS Society. The views expressed are those of the authors and not necessarily of the NHS, the NIHR or the Department of Health.

ACKNOWLEDGMENTS

We would like to thank the ECTRIMS for supporting IK through the ECTRIMS postdoctoral research fellowship.

REFERENCES

1. Martinez Sosa S, Smith KJ. Understanding a role for hypoxia in lesion formation and location in the deep and periventricular white matter in small vessel disease and multiple sclerosis. *Clin Sci.* (2017) 131:2503–24. doi: 10.1042/CS20170981
2. Koustenis A Jr, Harris A, Gross J, Januleviciene I, Shah A, Siesky B. Optical coherence tomography angiography : an overview of the technology and an assessment of applications for clinical research. *Br J Ophtalmol.* (2017) 101:16–20. doi: 10.1136/bjophthalmol-2016-309389
3. Huang D, Swanson EA, Lin CP, Schuman JS, Stinson WG, Chang W, et al. Optical coherence tomography. *Science.* (1991) 254:1178–81. doi: 10.1002/ccd.23385
4. Trip SA, Schlottmann PG, Jones SJ, Altmann DR, Garway-Heath DF, Thompson AJ, et al. Retinal nerve fiber layer axonal loss and visual dysfunction in optic neuritis. *Ann Neurol.* (2005) 58:383–91. doi: 10.1002/ana.20575
5. Petzold A, Balcer LJ, Calabresi PA, Costello F, Frohman TC, Frohman EM, et al. Retinal layer segmentation in multiple sclerosis: a systematic review and meta-analysis. *Lancet Neurol.* (2017) 16:797–812. doi: 10.1016/S1474-4422(17)30278-8
6. Joyal J, Gantner ML, Smith LEH. Retinal energy demands control vascular supply of the retina in development and disease: the role of neuronal lipid and glucose metabolism. *Prog Retin Eye Res.* (2018) 64:131–56. doi: 10.1016/j.preteyeres.2017.11.002
7. Campbell JP, Zhang M, Hwang TS, Bailey ST, Wilson DJ, Jia Y, et al. Detailed vascular anatomy of the human retina by projection-resolved optical coherence tomography angiography. *Sci Rep.* (2017) 7:1–11. doi: 10.1038/srep42201
8. Yu D, Cringle SJ, Yu PK, Balaratnasingam C, Mehnert A, Sarunic MV, et al. Retinal capillary perfusion: spatial and temporal heterogeneity. *Prog Retin Eye Res.* (2019). doi: 10.1016/j.preteyeres.2019.01.001
9. Wong-Riley M. Energy metabolism of the visual system. *Eye Brain.* (2010) 2:99–116. doi: 10.2147/EB.S9078
10. Kleerekooper I, Petzold A, Trip SA. Anterior visual system imaging to investigate energy failure in multiple sclerosis. *Brain.* (2020) 143:1999–2008. doi: 10.1093/brain/awaa049
11. Oertel FC, Zimmermann H, Paul F, Brandt AU. Optical coherence tomography in neuromyelitis optica spectrum disorders: potential advantages for individualized monitoring of progression and therapy. *EPMA J.* (2018) 9:21–33. doi: 10.1007/s13167-017-0123-5
12. Wingerchuk D, Banwell B, Bennett JL, Cabre P, Carroll W, Jacob A, et al. International consensus diagnostic criteria for neuromyelitis optica spectrum disorders. *Neurology.* (2015) 85:177–89. doi: 10.1212/WNL.0000000000001729
13. Toosy AT, Mason DF, Miller DH. Optic neuritis. *Lancet Neurol.* (2014) 13:83–99. doi: 10.1016/S1474-4422(13)70259-X
14. Petzold A, Woodhall M, Khaleeli Z, Tobin WO, Pittock SJ, Weinshenker BG, et al. Aquaporin-4 and myelin oligodendrocyte glycoprotein antibodies in immune-mediated optic neuritis at long-term follow-up. *J Neurol Neurosurg Psychiatry.* (2019) 90:1021–6. doi: 10.1136/jnnp-2019-320493
15. Toussaint D, Périer O, Verstappen A, Bervoets S. Clinicopathological study of the visual pathways, eyes, and cerebral hemispheres in 32 cases of disseminated sclerosis. *J Clin Neuroophthalmol.* (1983) 3:211–20.
16. Green AJ, McQuaid S, Hauser SL, Allen IV, Lyness R. Ocular pathology in multiple sclerosis: retinal atrophy and inflammation irrespective of disease duration. *Brain.* (2010) 133:1591–601. doi: 10.1093/brain/awq080
17. Desai RA, Davies AL, Del Rossi N, Tachrount M, Dyson A, Gustavson B, et al. Nimodipine reduces dysfunction and demyelination in models of multiple sclerosis. *Ann Neurol.* (2020) 88:123–36 doi: 10.1002/ana.25749
18. Haider L, Zrzavy T, Hametner S, Höftberger R, Bagnato F, Grabner G, et al. The topograpy of demyelination and neurodegeneration in the multiple sclerosis brain. *Brain.* (2016) 139:807–15. doi: 10.1093/brain/awv398
19. Green AJ, Cree BAC. Distinctive retinal nerve fibre layer and vascular changes in neuromyelitis optica following optic neuritis. *J Neurol Neurosurg Psychiatry.* (2009) 80:1002–5. doi: 10.1136/jnnp.2008.166207
20. Murphy OC, Kwakyi O, Iftikhar M, Zafar S, Lambe J, Pellegrini N, et al. Alterations in the retinal vasculature occur in multiple sclerosis and exhibit

novel correlations with disability and visual function measures. *Mult Scler J.* (2019) 26:815–28. doi: 10.1177/1352458519845116
21. Yilmaz H, Ersoy A, Icel E. Assessments of vessel density and foveal avascular zone metrics in multiple sclerosis: an optical coherence tomography angiography study. *Eye.* (2020) 34:771–8. doi: 10.1038/s41433-019-0746-y
22. Feucht N, Maier M, Lepennetier G, Pettenkofer M, Wetzlmair C, Daltrozzo T, et al. Optical coherence tomography angiography indicates associations of the retinal vascular network and disease activity in multiple sclerosis. *Mult Scler J.* (2018) 25:224–34. doi: 10.1177/1352458517750009
23. Rao HL, Pradhan ZS, Suh MH, Moghimi S, Mansouri K, Weinreb RN. Optical coherence tomography angiography in glaucoma. *J Glaucoma.* (2020) 29:355–7. doi: 10.1097/IJG.0000000000001463
24. Van Melkebeke L, Barbosa-Breda J, Huygens M, Stalmans I. Optical coherence tomography angiography in glaucoma: a review. *Ophthalmic Res.* (2018) 60:139–51. doi: 10.1159/000488495
25. Hou H, Moghimi S, Proudfoot JA, Ghahari E, Penteado RC, Bowd C, et al. Ganglion cell complex thickness and macular vessel density loss in primary open-angle glaucoma. *Ophthalmology.* (2020) 127:1043–52. doi: 10.1016/j.ophtha.2019.12.030
26. Moghimi S, Bowd C, Zangwill LM, Penteado RC, Hasenstab K, Hou H, et al. Measurement floors and dynamic ranges of OCT and OCT angiography in glaucoma. *Ophthalmology.* (2019) 126:980–8. doi: 10.1016/j.ophtha.2019.03.003
27. Chen Y, Shi C, Zhou L, Huang S, Shen M, He Z. The detection of retina microvascular density in subclinical aquaporin-4 antibody seropositive neuromyelitis optica spectrum disorders. *Front Neurol.* (2020) 11:35. doi: 10.3389/fneur.2020.00035
28. Petzold A, Wong S, Plant GT. Autoimmunity in visual loss. *Handb Clin Neurol.* (2016) 133:353–76. doi: 10.1016/B978-0-444-63432-0.00020-7
29. Sati P, Oh J, Todd Constable R, Evangelou N, Guttmann CRG, Henry RG, et al. The central vein sign and its clinical evaluation for the diagnosis of multiple sclerosis: a consensus statement from the North American Imaging in Multiple Sclerosis Cooperative. *Nat Rev Neurol.* (2016) 12:714–22. doi: 10.1038/nrneurol.2016.166
30. Tewarie P, Balk L, Costello F, Green A, Martin R, Schippling S. The OSCAR-IB consensus criteria for retinal OCT quality assessment. *PLoS ONE.* (2012) 7:e34823. doi: 10.1371/journal.pone.0034823
31. Kim DY, Fingler J, Werner JS, Schwartz DM, Fraser SE, Zawadzki RJ. *In vivo* volumetric imaging of human retinal circulation with phase-variance optical coherence tomography. *Biomed Opt Express.* (2011) 2:1504. doi: 10.1364/boe.2.001504
32. Schwartz DM, Fingler J, Kim DY, Zawadzki RJ, Morse LS, Park SS, et al. Phase-variance optical coherence tomography: a technique for noninvasive angiography. *Ophthalmology.* (2014) 121:180–7. doi: 10.1016/j.ophtha.2013.09.002
33. Spaide RF, Curcio CA. Evaluation of segmentation of the superficial and deep vascular layers of the retina by optical coherence tomography angiography instruments in normal eyes. *JAMA Ophthalmol.* (2017) 135:259–62. doi: 10.1001/jamaophthalmol.2016.5327
34. Falavarjani KG, Shenazandi H, Naseri D, Anvar P, Kazemi P, Aghamohammadi F, et al. Foveal avascular zone and vessel density in healthy subjects: an optical coherence tomography angiography study. *J Ophthalmic Vis Res.* (2018) 12:260–5. doi: 10.4103/jovr.jovr
35. Lu Y, Simonett JM, Wang J, Zhang M, Hwang T, Hagag AM, et al. Evaluation of automatically quantified foveal avascular zone metrics for diagnosis of diabetic retinopathy using optical coherence tomography angiography. *Investig Ophthalmol Vis Sci.* (2018) 59:2212–21. doi: 10.1167/iovs.17-23498
36. Zahid S, Dolz-Marco R, Freund KB, Balaratnasingam C, Dansingani K, Gilani F, et al. Fractal dimensional analysis of optical coherence tomography angiography in eyes with diabetic retinopathy. *Investig Ophthalmol Vis Sci.* (2016) 57:4940–7. doi: 10.1167/iovs.16-19656
37. Lu CD, Lee B, Schottenhamml J, Maier A, Pugh EN Jr, Fujimoto JG. Photoreceptor layer thickness changes during dark adaptation observed with ultrahigh-resolution optical coherence tomography. *Investig Ophthalmol Vis Sci.* (2017) 1:4632–43. doi: 10.1167/iovs.17-22171
38. Martin AR, Bailie JR, Robson T, McKeown SR, Al-Assar O, McFarland A, et al. Retinal pericytes control expression of nitric oxide synthase and endothelin-1 in microvascular endothelial cells. *Microvasc Res.* (2000) 59:131–9. doi: 10.1006/mvre.1999.2208
39. Wang X, Lou N, Eberhardt A, Yang Y, Kusk P, Xu Q, et al. An ocular glymphatic clearance system removes β-amyloid from the rodent eye. *Sci Transl Med.* (2020) 12:eaaw3210. doi: 10.1126/scitranslmed.aaw3210
40. Frank RN, Turczyn TJ, Das A. Pericyte coverage of retinal and cerebral capillaries. *Investig Ophthalmol Vis Sci.* (1990) 31:999–1007.
41. Reich DS, Lucchinetti CF, Calabresi PA. Multiple sclerosis. *N Engl J Med.* (2018) 378:169–80. doi: 10.1056/NEJMra1401483
42. Thompson AJ, Baranzini SE, Geurts J, Hemmer B, Ciccarelli O. Multiple sclerosis. *Lancet.* (2018) 391:1622–36. doi: 10.1016/S0140-6736(18)30481-1
43. Yang R, Dunn JF. Multiple sclerosis disease progression: contributions from a hypoxia–inflammation cycle. *Mult Scler J.* (2018) 25:1715–8. doi: 10.1177/1352458518791683
44. D'Haeseleer M, Hostenbach S, Peeters I, El Sankari S, Nagels G, De Keyser J, et al. Cerebral hypoperfusion: a new pathophysiologic concept in multiple sclerosis? *J Cereb Blood Flow Metab.* (2015) 35:1406–10. doi: 10.1038/jcbfm.2015.131
45. Juurlink BHJ. The evidence for hypoperfusion as a factor in multiple sclerosis lesion development. *Mult Scler Int.* (2013) 2013:1–6. doi: 10.1155/2013/598093
46. Monti L, Donati D, Menci E, Cioni S, Bellini M, Grazzini I, et al. Cerebral circulation time is prolonged and not correlated with EDSS in multiple sclerosis patients: a study using digital subtracted angiography. *PLoS ONE.* (2015) 10:e0116681. doi: 10.1371/journal.pone.0116681
47. Varga AW, Johnson G, Babb JS, Herbert J, Grossman RI, Inglese M. White matter hemodynamic abnormalities precede sub-cortical gray matter changes in multiple sclerosis. *J Neurol Sci.* (2009) 282:28–33. doi: 10.1016/j.jns.2008.12.036
48. Yang R, Dunn JF. Reduced cortical microvascular oxygenation in multiple sclerosis: a blinded, case-controlled study using a novel quantitative near-infrared spectroscopy method. *Sci Rep.* (2015) 5:16477. doi: 10.1038/srep16477
49. Tettey P, Siejka D, Simpson S, Taylor B, Blizzard L, Ponsonby AL, et al. Frequency of comorbidities and their association with clinical disability and relapse in multiple sclerosis. *Neuroepidemiology.* (2016) 46:106–13. doi: 10.1159/000442203
50. Jadidi E, Mohammadi M, Moradi T. High risk of cardiovascular diseases after diagnosis of multiple sclerosis. *Mult Scler J.* (2013) 19:1336–40. doi: 10.1177/1352458513475833
51. Haufschild T, Shaw SG, Kaiser HJ, Flammer J. Transient raise of endothelin-1 plasma level and reduction of ocular blood flow in a patient with optic neuritis. *Ophthalmologica.* (2003) 217:451–3. doi: 10.1159/000073079
52. Jiang H, Delgado S, Tan J, Liu C, Rammohan KW, DeBuc DC, et al. Impaired retinal microcirculation in multiple sclerosis. *Mult Scler.* (2016) 22:1812–20. doi: 10.1177/1352458516631035
53. Modrzejewska M, Karczewicz D, Wilk G. Assessment of blood flow velocity in eyeball arteries in multiple sclerosis patients with past retrobulbar optic neuritis in color doppler ultrasonography. *Klin Ocz.* (2007) 109:183–6.
54. Davies AL, Desai RA, Bloomfield PS, McIntosh PR, Chapple KJ, Linington C, et al. Neurological deficits caused by tissue hypoxia in neuroinflammatory disease. *Ann Neurol.* (2013) 74:815–25. doi: 10.1002/ana.24006
55. Nikić I, Merkler D, Sorbara C, Brinkoetter M, Kreutzfeldt M, Bareyre FM, et al. A reversible form of axon damage in experimental autoimmune encephalomyelitis and multiple sclerosis. *Nat Med.* (2011) 17:495–9. doi: 10.1038/nm.2324
56. Sadeghian M, Mastrolia V, Rezaei Haddad A, Mosley A, Mullali G, Schiza D, et al. Mitochondrial dysfunction is an important cause of neurological deficits in an inflammatory model of multiple sclerosis. *Sci Rep.* (2016) 6:33249. doi: 10.1038/srep33249
57. Nathoo N, Rogers JA, Yong VW, Dunn JF. Detecting deoxyhemoglobin in spinal cord vasculature of the experimental autoimmune encephalomyelitis mouse model of multiple sclerosis using susceptibility MRI and hyperoxygenation. *PLoS ONE.* (2015) 10:e0127033. doi: 10.1371/journal.pone.0127033

58. Ulusoy MO, Horasanli B, Işik-Ulusoy S. Optical coherence tomography angiography findings of multiple sclerosis with or without optic neuritis. *Neurol Res.* (2020) 42:319–26. doi: 10.1080/01616412.2020.1726585
59. Jiang H, Gameiro GR, Liu Y, Lin Y, Hernandez J, Deng Y, et al. Visual function and disability are associated with increased retinal volumetric vessel density in patients with multiple sclerosis. *Am J Ophthalmol.* (2020) 213:34–45. doi: 10.1016/j.ajo.2019.12.021
60. Lanzillo R, Cennamo G, Criscuolo C, Carotenuto A, Velotti N, Sparnelli F, et al. Optical coherence tomography angiography retinal vascular network assessment in multiple sclerosis. *Mult Scler J.* (2017) 24:1–9. doi: 10.1177/1352458517729463
61. Wang X, Jia Y, Spain R, Potsaid B, Liu JJ, Baumann B, et al. Optical coherence tomography angiography of optic nerve head and parafovea in multiple sclerosis. *Br J Ophtalmol.* (2014) 98:1368–73. doi: 10.1136/bjophthalmol-2013-304547
62. Spain RI, Liu L, Zhang X, Jia Y, Tan O, Bourdette D, et al. Optical coherence tomography angiography enhances the detection of optic nerve damage in multiple sclerosis. *Br J Ophthalmol.* (2018) 102:520–4. doi: 10.1136/bjophthalmol-2017-310477
63. Mastropasqua R, Toto L, Mastropasqua A, Aloia R, De Nicola C, Mattei PA, et al. Foveal avascular zone area and parafoveal vessel density measurements in different stages of diabetic retinopathy by optical coherence tomography angiography. *Int J Ophthalmol.* (2017) 10:1545–51. doi: 10.18240/ijo.2017.10.11
64. Higashiyama T, Nishida Y, Ohji M. Optical coherence tomography angiography in eyes with good visual acuity recovery after treatment for optic neuritis. *PLoS ONE.* (2017) 12:e0172168. doi: 10.1371/journal.pone.0172168
65. Lanzillo R, Moccia M, Criscuolo C, Cennamo G. Optical coherence tomography angiography detects retinal vascular alterations in different phases of multiple sclerosis. *Mult Scler J.* (2019) 25:300–1. doi: 10.1177/1352458518768060
66. Tsokolas G, Tsaousis KT, Diakonis VF, Matsou A, Tyradellis S. Optical coherence tomography angiography in neurodegenerative diseases: a review. *Eye Brain.* (2020) 12:73–87. doi: 10.2147/EB.S193026
67. Sato DK, Callegaro D, Aurelio Lana-Peixoto M, Waters PJ, De Haidar FM, Takahashi T, et al. Distinction between MOG antibody- positive and AQP4 antibody-positive NMO spectrum disorders. *Neurology.* (2014) 82:474–81. doi: 10.1212/WNL.0000000000000101
68. Marignier R, Nicolle A, Watrin C, Touret M, Confavreux C. Oligodendrocytes are damaged by neuromyelitis optica immunoglobulin G via astrocyte injury. *Brain.* Springer (2010) 133:2578–91. doi: 10.1093/brain/awq177
69. Kawachi I, Lassmann H. Neurodegeneration in multiple sclerosis and neuromyelitis optica. *J Neurol Neurosurg Psychiatry.* (2017) 88:137–45. doi: 10.1136/jnnp-2016-313300
70. Amann B, Kleinwort KJH, Hirmer S, Sekundo W, Kremmer E, Hauck SM, et al. Expression and distribution pattern of aquaporin 4, 5 and 11 in retinas of 15 different species. *Int J Mol Sci.* (2016) 17:1–12. doi: 10.3390/ijms17071145
71. Lucchinetti CF, Mandler RN, McGaver D, Bruck W, Gleich G, Ransohoff R, et al. A role for humoral mechanisms in the pathogenesis of Devic's neuromyelitis optica. *Brain.* (2002) 125:1450–61. doi: 10.1093/brain/awf151
72. Roemer SF, Parisi JE, Lennon VA, Benarroch EE, Lassmann H, Bruck W, et al. Pattern-specific loss of aquaporin-4 immunoreactivity distinguishes neuromyelitis optica from multiple sclerosis. *Brain.* (2007) 130:1194–205. doi: 10.1093/brain/awl371
73. Lefkowitz D, Angelo JN. Neuromyelitis optica with unusual vascular changes. *Arch Neurol.* (1984) 41:1103–5. doi: 10.1001/archneur.1984.04050210105027
74. Bradl M, Reindl M, Lassmann H. Mechanisms for lesion localization in neuromyelitis optica spectrum disorders. *Curr Opin Neurol.* (2018) 31:325–33. doi: 10.1097/WCO.0000000000000551
75. Guo Y, Weigand SD, Popescu BF, Lennon VA, Parisi JE, Pittock SJ, et al. Pathogenic implications of cerebrospinal fluid barrier pathology in neuromyelitis optica. *Acta Neuropathol.* (2017) 133:597–612. doi: 10.1007/s00401-017-1682-1
76. Höftberger R, Guo Y, Flanagan EP, Lopez-Chiriboga AS, Endmayr V, Hochmeister S, et al. The pathology of central nervous system inflammatory demyelinating disease accompanying myelin oligodendrocyte glycoprotein autoantibody. *Acta Neuropathol.* (2020) 139:875–92. doi: 10.1007/s00401-020-02132-y
77. Lassmann H. Pathology and disease mechanisms in different stages of multiple sclerosis. *J Neurol Sci.* (2013) 333:1–4. doi: 10.1016/j.jns.2013.05.010
78. Huang Y, Zhou L, ZhangBao J, Cai T, Wang B, Li X, et al. Peripapillary and parafoveal vascular network assessment by optical coherence tomography angiography in aquaporin-4 antibody-positive neuromyelitis optica spectrum disorders. *Br J Ophthalmol.* (2019) 103:789–96. doi: 10.1136/bjophthalmol-2018-312231
79. Kwapong WR, Peng C, He Z, Zhuang X, Shen M, Lu F. Altered macular microvasculature in neuromyelitis optica spectrum disorders. *Am J Ophthalmol.* (2018) 192:47–55. doi: 10.1016/j.ajo.2018.04.026
80. Chang R, Nelson AJ, LeTran V, Vu B, Burkemper B, Chu Z, et al. Systemic determinants of peripapillary vessel density in healthy African Americans: The African American eye disease study. *Am J Ophthalmol.* (2019) 207:240–7. doi: 10.1016/j.ajo.2019.06.014
81. Takusagawa HL, Liu L, Ma KN, Jia Y, Gao SS, Zhang M, et al. Projection-resolved optical coherence tomography angiography of macular retinal circulation in glaucoma. *Ophthalmology.* (2017) 124:1589–99. doi: 10.1016/j.ophtha.2017.06.002
82. Suwan Y, Aghsaei Fard M, Geyman LS, Tantraworasin A, Chui TY, Rosen RB, et al. Association of myopia with peripapillary perfused capillary density in patients with glaucoma an optical coherence tomography angiography study. *JAMA Ophthalmol.* (2018) 136:507–13. doi: 10.1001/jamaophthalmol.2018.0776
83. Wang X, Kong X, Jiang C, Li M, Yu J, Sun X. Is the peripapillary retinal perfusion related to myopia in healthy eyes? A prospective comparative study. *BMJ Open.* (2016) 6:1–7. doi: 10.1136/bmjopen-2015-010791
84. Rao HL, Pradhan ZS, Weinreb RN, Reddy HB, Riyazuddin M, Sachdeva S, et al. Determinants of peripapillary and macular vessel densities measured by optical coherence tomography angiography in normal eyes. *J Glaucoma.* (2017) 26:491–7. doi: 10.1097/IJG.0000000000000655
85. Alnawaiseh M, Lahme L, Treder M, Rosentreter A, Eter N. Short-Term effects of exercise on optic nerve and macular perfusion measured by optical coherence tomography angiography. *Retina.* (2017) 37:1642–6. doi: 10.1097/IAE.0000000000001419
86. Hao H, Sasongko MB, Wong TY, Che Azemin MZ, Aliahmad B, Hodgson L, et al. Does retinal vascular geometry vary with cardiac cycle? *Investig Ophthalmol Vis Sci.* (2012) 53:5799–805. doi: 10.1167/iovs.11-9326
87. Müller VC, Storp JJ, Kerschke L, Nelis P, Eter N, Alnawaiseh M. Diurnal variations in flow density measured using optical coherence tomography angiography and the impact of heart rate, mean arterial pressure and intraocular pressure on flow density in primary open-angle glaucoma patients. *Acta Ophthalmol.* (2019) 97:e844–9. doi: 10.1111/aos.14089
88. Venugopal JP, Rao HL, Weinreb RN, Pradhan ZS, Dasari S, Riyazuddin M, et al. Repeatability of vessel density measurements of optical coherence tomography angiography in normal and glaucoma eyes. *Br J Ophthalmol.* (2018) 102:352–7. doi: 10.1136/bjophthalmol-2017-310637
89. Frost S, Gregory C, Robinson L, Yu S, Xiao D, Mehdizadeh M, et al. Effect of pupil dilation with tropicamide on retinal vascular caliber. *Ophthalmic Epidemiol.* (2019) 26:400–7. doi: 10.1080/09286586.2019.1639198
90. Holló G. Intrasession and between-visit variability of sector peripapillary angioflow vessel density values measured with the angiovue optical coherence tomograph in different retinal layers in ocular hypertension and glaucoma. *PLoS ONE.* (2016) 11:e0161631. doi: 10.1371/journal.pone.0161631
91. Manalastas PIC, Zangwill LM, Saunders LJ, Mansouri K, Belghith A, Suh MH, et al. Reproducibility of optical coherence tomography angiography macular and optic nerve head vascular density in glaucoma and healthy eyes. *J Glaucoma.* (2017) 26:851–9. doi: 10.1097/IJG.0000000000000768
92. Littlewood R, Mollan SP, Pepper IM, Hickman SJ. The Utility of Fundus Fluorescein Angiography in Neuro-Ophthalmology. *Neuro Ophthalmol.* (2019) 43:217–34. doi: 10.1080/01658107.2019.1604764
93. Braaf B, Gräfe MGO, Uribe-Patarroyo N, Bouma BE, Vakoc BJ, de Boer JF, et al. High resolution imaging in microscopy and ophthalmology: new frontiers in biomedical optics. In: Bille JF, editor. *OCT-Based Velocimetry for Blood Flow Quantification*. Cham: Springer (2019). p. 161–79. doi: 10.1007/978-3-030-16638-0_7

94. Wei X, Hormel TT, Pi S, Guo Y, Jian Y, Jia Y. High dynamic range optical coherence tomography angiography (HDR-OCTA). *Biomed Opt Express.* (2019) 10:3560. doi: 10.1364/boe.10.003560
95. Spaide RF, Klancnik JM, Cooney MJ. Retinal vascular layers imaged by fluorescein angiography and optical coherence tomography angiography. *JAMA Ophthalmol.* (2015) 133:45–50. doi: 10.1001/jamaophthalmol.2014.3616
96. Iftikhar M, Zafar S, Gonzalez N, Murphy O, Ohemaa Kwakyi MS, Sydney Feldman BS, et al. Image artifacts in optical coherence tomography angiography among patients with multiple sclerosis. *Curr Eye Res.* (2019) 44:558–63. doi: 10.1080/02713683.2019.1565892
97. Sotirchos ES, Gonzalez Caldito N, Filippatou A, Fitzgerald KC, Murphy OC, Lambe J, et al. Progressive multiple sclerosis is associated with faster and specific retinal layer atrophy. *Ann Neurol.* (2020) 87:885–96. doi: 10.1002/ana.25738
98. Saidha S, Al-Louzi O, Ratchford J, Bhargava P, Oh J, Newsome S, et al. Optical coherence tomography reflects brain atrophy in multiple sclerosis: a four-year study. *Ann Neurol.* (2015) 75:801–13. doi: 10.1016/j.physbeh.2017.03.040
99. Pache F, Zimmermann H, Mikolajczak J, Schumacher S, Lacheta A, Oertel FC, et al. MOG-IgG in NMO and related disorders:a multicenter study of 50 patients. Part 4: afferent visual system damage after optic neuritis in MOG-IgG-seropositive versus AQP4-IgG-seropositive patients. *J Neuroinflammation.* (2016) 13:1–10. doi: 10.1186/s12974-016-0720-6

Conflict of Interest: AP reports that the Amsterdam UMC (location VUmc) MS Centre Amsteram and neuro-ophthalmology Expert Centre participated in the OCTIMS trial and the centre has received research support for OCT projects from the Dutch MS Society.

The remaining authors declare that the research was conducted in the absence of any commercial or financial relationships that could be construed as a potential conflict of interest.

Copyright © 2020 Kleerekooper, Houston, Dubis, Trip and Petzold. This is an open-access article distributed under the terms of the Creative Commons Attribution License (CC BY). The use, distribution or reproduction in other forums is permitted, provided the original author(s) and the copyright owner(s) are credited and that the original publication in this journal is cited, in accordance with accepted academic practice. No use, distribution or reproduction is permitted which does not comply with these terms.

frontiers in Neurology

ORIGINAL RESEARCH
published: 15 December 2020
doi: 10.3389/fneur.2020.618879

Optical Coherence Tomography and Optical Coherence Tomography Angiography Findings After Optic Neuritis in Multiple Sclerosis

*Olwen C. Murphy[1], Grigorios Kalaitzidis[1], Eleni Vasileiou[1], Angeliki G. Filippatou[1], Jeffrey Lambe[1], Henrik Ehrhardt[1], Nicole Pellegrini[1], Elias S. Sotirchos[1], Nicholas J. Luciano[1], Yihao Liu[2], Kathryn C. Fitzgerald[1], Jerry L. Prince[2], Peter A. Calabresi[1] and Shiv Saidha[1]**

[1] Division of Neuroimmunology and Neurological Infections, Department of Neurology, Johns Hopkins Hospital, Baltimore, MD, United States, [2] Department of Electrical and Computer Engineering, Johns Hopkins University, Baltimore, MD, United States

OPEN ACCESS

Edited by:
Gemma Caterina Maria Rossi, Fondazione Ospedale San Matteo (IRCCS), Italy

Reviewed by:
Young Joon Jo, Chungnam National University, South Korea
Prem Subramanian, University of Colorado, United States

***Correspondence:**
Shiv Saidha
ssaidha2@jhmi.edu

Specialty section:
This article was submitted to Neuro-Ophthalmology, a section of the journal Frontiers in Neurology

Received: *19 October 2020*
Accepted: *24 November 2020*
Published: *15 December 2020*

Citation:
Murphy OC, Kalaitzidis G, Vasileiou E, Filippatou AG, Lambe J, Ehrhardt H, Pellegrini N, Sotirchos ES, Luciano NJ, Liu Y, Fitzgerald KC, Prince JL, Calabresi PA and Saidha S (2020) Optical Coherence Tomography and Optical Coherence Tomography Angiography Findings After Optic Neuritis in Multiple Sclerosis. Front. Neurol. 11:618879. doi: 10.3389/fneur.2020.618879

Background: In people with multiple sclerosis (MS), optic neuritis (ON) results in inner retinal layer thinning, and reduced density of the retinal microvasculature.

Objective: To compare inter-eye differences (IEDs) in macular optical coherence tomography (OCT) and OCT angiography (OCTA) measures in MS patients with a history of unilateral ON (MS ON) vs. MS patients with no history of ON (MS non-ON), and to assess how these measures correlate with visual function outcomes after ON.

Methods: In this cross-sectional study, people with MS underwent OCT and OCTA. Superficial vascular plexus (SVP) density of each eye was quantified using a deep neural network. IEDs were calculated with respect to the ON eye in MS ON patients, and with respect to the right eye in MS non-ON patients. Statistical analyses used mixed-effect regression models accounting for intra-subject correlations.

Results: We included 43 MS ON patients (with 92 discrete OCT/OCTA visits) and 14 MS non-ON patients (with 24 OCT/OCTA visits). Across the cohorts, mean IED in SVP density was −2.69% (SD 3.23) in MS ON patients, as compared to 0.17% (SD 2.39) in MS non-ON patients ($p = 0.002$). When the MS ON patients were further stratified according to time from ON and compared to MS non-ON patients with multiple cross-sectional analyses, we identified that IED in SVP density was significantly increased in MS ON patients at 1–3 years ($p = <0.001$) and >3 years post-ON ($p < 0.001$), but not at <3 months ($p = 0.21$) or 3–12 months post-ON ($p = 0.07$), while IED in ganglion cell + inner plexiform layer (GCIPL) thickness was significantly increased in MS ON patients at all time points post-ON ($p \leqq 0.01$ for all). IED in SVP density and IED in GCIPL thickness demonstrated significant relationships with IEDs in 100% contrast, 2.5% contrast, and 1.25% contrast letter acuity in MS ON patients ($p < 0.001$ for all).

Conclusions: Our findings suggest that increased IED in SVP density can be detected after ON in MS using OCTA, and detectable changes in SVP density after ON may occur after changes in GCIPL thickness. IED in SVP density and IED in GCIPL thickness correlate well with visual function outcomes in MS ON patients.

Keywords: outcomes, inter-eye asymmetry, retinal vasculature, optical coherence tomography angiography, optical coherence tomography, optic neuritis, multiple sclerosis

INTRODUCTION

Retinal atrophy detected using optical coherence tomography (OCT) has emerged as a promising biomarker of neurodegeneration in multiple sclerosis (MS), demonstrating strong structure-function relationships, correlations with global measures of disease activity and disability progression, and differential modulation by disease-modifying therapies (1, 2). Retinal optical coherence tomography angiography (OCTA) represents a more recent evolution of OCT technology, offering a rapid, non-invasive, and inexpensive technique for examination of the retinal vasculature (3). The ability to image microvascular structure and therefore potentially metabolic demand of retinal tissue offers unique avenues for investigation in MS—a disease in which the anterior visual pathway is a key site of injury, and in which metabolic changes may play a crucial role in the pathway from inflammatory tissue injury to neurodegeneration (4, 5).

Studies employing OCTA have shown that retinal vascular plexus densities are reduced in MS—particularly within the superficial vascular plexus (SVP; which mainly supplies the ganglion cell layer), and the greatest reductions in SVP density are detectable in eyes with a history of optic neuritis (ON) (6–9). Relationships between OCTA measures and disability [both expanded disability status scale (EDSS) score and visual function] have been suggested in people with MS (6, 8). Furthermore, in one study, SVP density demonstrated significant relationships with multiple sclerosis functional composite (MSFC) score, while GCIPL thickness and MSFC scores were unrelated, suggesting that SVP density may provide additional information beyond retinal layer thicknesses as a biomarker of functional disability in MS (6). It is not yet known whether (1) increased IED in SVP density can be detected in individuals with MS after ON, (2) whether IEDs in SVP density may correlate with visual function outcomes after ON, and (3) how these relationships may compare to IEDs in retinal layer thickness measures after ON.

In this study, we aimed to establish whether IEDs in SVP density are greater in MS ON patients than in MS non-ON patients. Additionally, we set out to compare IEDs in OCT and OCTA measures after ON, and explore the relationships of these measures with visual function outcomes.

MATERIALS AND METHODS

Study Design and Participants

People with MS were recruited by convenience sampling from the Johns Hopkins MS Center for this cross-sectional study. Diagnoses were made according to the 2017 revised McDonald Criteria (10). We included patients with high-risk clinically isolated syndrome (CIS) or relapsing remitting MS (RRMS), and excluded patients with primary progressive MS (PPMS), secondary progressive MS (SPMS), seropositivity for myelin oligodendrocyte glycoprotein IgG (MOG-IgG), or seropositivity for aquaporin-4 IgG (AQP4-IgG). Patients were stratified into two groups according to ON history; (1) patients with a history of a single episode of unilateral ON [MS ON patients], and (2) patients with no history of ON in either eye [MS non-ON patients]. History of ON was established from the patients' medical records, with all diagnoses of ON made by attending neurologists with extensive clinical expertise in neuroimmunology. We excluded patients in whom (1) the diagnosis of ON was uncertain, (2) any elements of the history or ophthalmologic examination were suggestive of an alternative diagnosis (e.g., ischemic optic neuropathy, retinal artery, or vein occlusion), (3) the laterality (i.e., right vs. left) of an ON episode was unclear, (4) the history included multiple episodes of ON, or (5) the history included bilateral ON. Additional exclusion criteria included relevant known neurological or ophthalmological co-morbidities (e.g., glaucoma, macular degeneration, history of any other relevant retinal pathology such as retinal vascular occlusion or retinal detachment), prior eye trauma or ocular surgery, refractive errors of >6 or <-6 diopters, poorly-controlled hypertension, or poorly-controlled diabetes mellitus. All patients in the current study received routine, high-quality ophthalmological care. This is a standard of care for all patients with MS receiving care at our center, and therefore makes confounding from any other ophthalmological disorder highly unlikely.

OCT and OCTA Acquisition, Processing, and Quantification

OCT and OCTA scans were acquired under low-lighting conditions without pupillary dilation by experienced technicians, as described in detail elsewhere (6, 11, 12). OCT scans of the optic disc and macula were acquired using Cirrus HD-OCT (model 5000, software version 8.1, Carl Zeiss Meditec, California, United States), as our standard research protocol during the study period was to track retinal layer thicknesses in all patients using Cirrus HC-OCT, followed by Spectralis SD-OCTA imaging, and only to complete additional Spectralis SD-OCT imaging of retinal layer thicknesses where it was not burdensome on the patient. Acquired images underwent quality control in accordance with the OSCAR-IB criteria (13). Peripapillary retinal nerve fiber layer (pRNFL) thickness was quantified by the conventionally incorporated Cirrus HD-OCT algorithm.

Macular retinal layer thicknesses (ganglion cell + inner plexiform layer, GCIPL; inner nuclear layer, INL; outer nuclear layer, ONL; average macular thickness, AMT) were quantified using an algorithm developed at Johns Hopkins University that has been extensively validated and utilized in both cross-sectional and longitudinal studies across multiple OCT devices (12, 14–16)

Macular OCTA scans were acquired using Spectralis SD-OCTA (model Spec-CAM S2610 with OCT2 and OCTA modules, software version 6.9a-US-IRB, Heidelberg Engineering, Germany), with TruTrack active eye tracking and full-spectrum amplitude decorrelation algorithm (FS-ADA) for motion detection and image generation. The device acquires 85,000 A-scans per second at an axial resolution of 7 um, using a wavelength of 870 nm. We excluded images with a sustained signal strength of <25 dB. 3 × 3 mm images were automatically segmented by the device into the SVP and deep vascular plexus (DVP). Density of the SVP was quantified using a deep neural network which reduces imaging artifact, improves signal-to-noise ratio of OCTA images, and increases accuracy of derived SVP density measurements. This neural network algorithm was developed at Johns Hopkins University using a variational intensity cross channel encoder that finds vessel masks by examining the common vascular architecture shared by OCTA images of the same region acquired using different OCTA devices (**Figure 1**) (17). Rigorous quality control criteria were applied to the acquisition and processing of OCTA images consistent with prior publications by our group (6). OCTA imaging artifact was graded by a single rater (OCM), by viewing each raw OCTA image side-by-side with the segmented image which represents an artifact-reduced vessel mask. Segmented images which demonstrated impaired detection of >25% of the capillary micro-architecture were excluded from analyses (**Table 1**).

Visual Function Assessment

Visual function was measured monocularly and patients were instructed to use their habitual spectacles or contact lens where applicable. Retro-illuminated Early Treatment of Diabetic Retinopathy study charts were utilized at 4 m to assess 100% letter acuity (LA), while low-contrast Sloan letter charts were utilized at

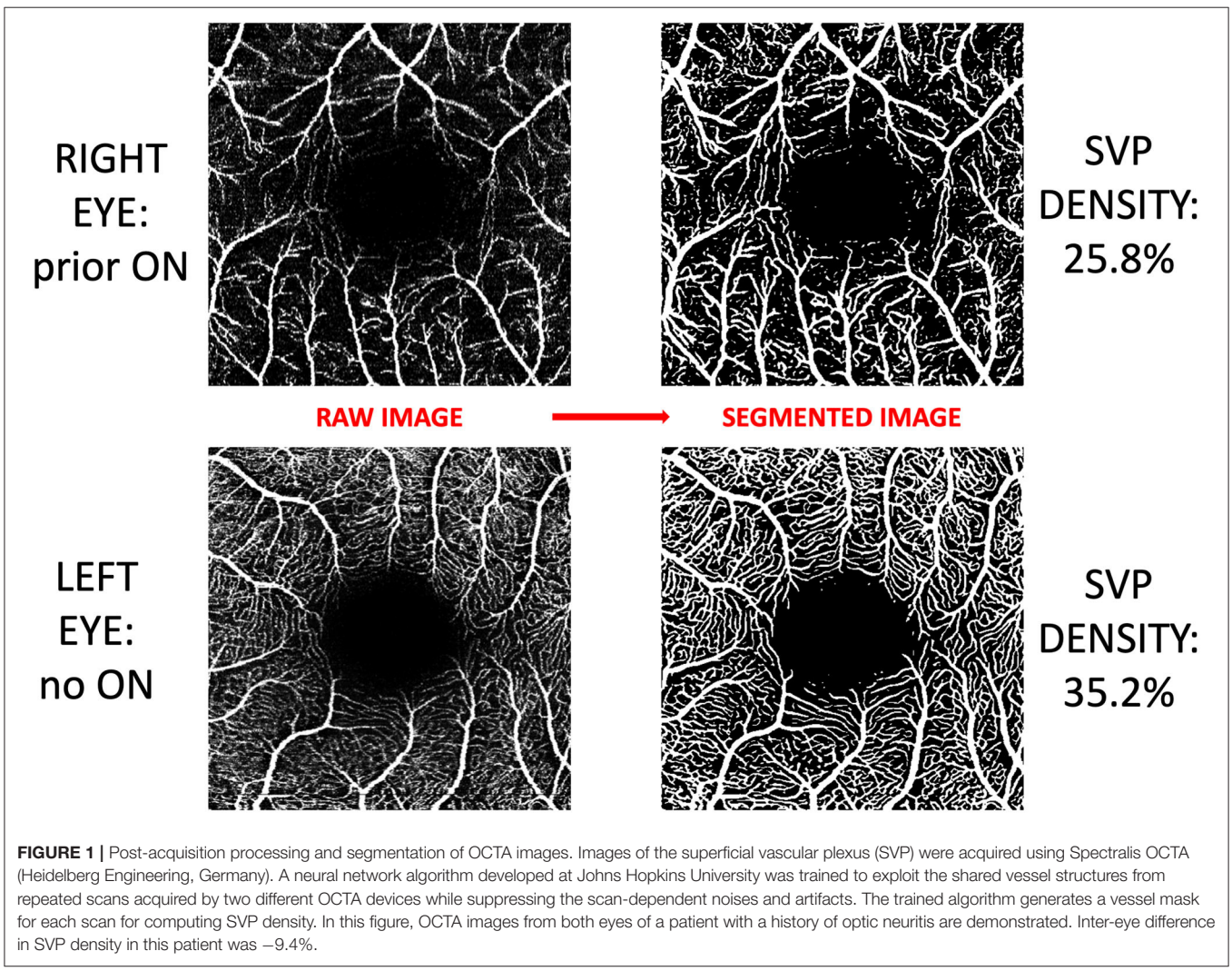

FIGURE 1 | Post-acquisition processing and segmentation of OCTA images. Images of the superficial vascular plexus (SVP) were acquired using Spectralis OCTA (Heidelberg Engineering, Germany). A neural network algorithm developed at Johns Hopkins University was trained to exploit the shared vessel structures from repeated scans acquired by two different OCTA devices while suppressing the scan-dependent noises and artifacts. The trained algorithm generates a vessel mask for each scan for computing SVP density. In this figure, OCTA images from both eyes of a patient with a history of optic neuritis are demonstrated. Inter-eye difference in SVP density in this patient was −9.4%.

TABLE 1 | OCTA image quality control.

	All patients ($n = 63$)	MS ON patients ($n = 45$)	MS Non-ON patients ($n = 18$)
Total OCTA images, *n* eyes	96	224	72
Minor image artifact (<25% of the capillary architecture), *n* eyes	260 (88%)	202 (90%)	58 (81%)
Major image artifact (>25% of the capillary architecture), *n* eyes	36 (12%)	22 (10%)	14 (19%)

Each raw OCTA image was viewed side-by-side with the post-processing artifact-reduced segmented image, and the proportion of the segmented image demonstrating impaired detection of the capillary micro-architecture was classified as <25 or >25%. Images with major artifact were excluded from all further analyses.

2 meters to assess 2.5% and 1.25% LA. LA scores were calculated based on the number of correct letters achieved in each chart.

Calculation of Inter-Eye Differences

IEDs in OCT, OCTA, and visual function measures were calculated with respect to the ON eye in MS ON patients, and with respect to the right eye in MS non-ON patients. For example, in a patient with a history of optic neuritis in the right eye, and a 100% contrast LA score of 65 in the right eye and 68 in the left eye, the IED for this measure would be −3.

Statistical Analyses

MS ON patients were compared to MS non-ON patients in initial analyses of baseline demographics and IEDs in OCT/OCTA measures and LA. MS ON patients were also grouped into 4 categories for further analyses, according to the time that had elapsed between the onset of ON, and the acquisition of OCT/OCTA images (<3 months, 3 to 12 months, 1–3 years, >3 years). Statistical analyses were completed using Stata version 16 (StataCorp, College Station, TX, United States). Wilcoxon rank sum test or the chi-squared test were used to compare demographic variables between the MS ON group and the MS non-ON group. For all other analyses, we used mixed-effects linear regression analyses accounting for intra-subject correlations. R^2-values were estimated using the Snijders and Bosker method (18). We used unadjusted models, since variables which may affect OCT/OCTA measurements in individual eyes (e.g., age, sex, race, disease duration) are not thought to have the same degree of confounding effect on IEDs. *P*-value for significance was defined as <0.05.

Ethical Approval

Johns Hopkins University institutional review board approval was obtained for study protocols, and all patients provided written informed consent.

RESULTS

Demographic and Clinical Characteristics

All SVP imaging sets underwent quality control protocols and image artifact rating (**Table 1**). After exclusion of imaging sets in which one or both eyes were affected by major artifact, our study population comprised 43 MS ON patients (with 92 study visits) and 14 MS non-ON patients (with 24 study visits). On average, MS ON patients were younger and had a shorter MS disease duration than MS non-ON patients ($p = 0.001$ for both, **Table 2**).

TABLE 2 | Demographic and clinical characteristics of participants.

	MS ON patients	MS Non-ON patients	*P*-value
N, participants	43	14	–
N, visits	92 (184 eyes)	24 (48 eyes)	–
Age, mean years (SD)	33.7 (9.3)	44.4 (7.7)	0.001[a]
Female, *n*	36 (84%)	11 (78%)	0.66[b]
Race			
Caucasian, *n*	29 (67%)	12 (86%)	0.18[b]
African/African-American, *n*	13 (33%)	1 (7%)	
Other, *n*	1 (2%)	1 (7%)	
Disease duration, mean years (SD)	4.5 (6.2)	14.9 (4.8)	<0.001[a]

Imaging sets in which one or both SVP images were affected by major artifact were excluded. ON, optic neuritis; SD, standard deviation. [a]Wilcoxon rank sum test, [b]Chi-squared test.

TABLE 3 | Inter-eye differences in OCT, OCTA, and visual function measures in MS ON vs. MS non-ON patients.

	MS ON patients	MS Non-ON patients	*P*-value
N, participants	43	14	–
N, visits	92 (184 eyes)	24 (48 eyes)	–
pRNFL IED, mean % (SD)	−9.49 (15.05)	2.29 (6.21)	0.001
GCIPL IED, mean % (SD)	−9.34 (8.48)	0.87 (3.63)	<0.001
INL IED, mean % (SD)	0.11 (1.76)	0.35 (0.97)	0.82
ONL IED, mean % (SD)	0.29 (1.52)	0.48 (1.30)	0.46
AMT IED mean % (SD)	−13.05 (12.0)	2.97 (6.63)	<0.001
SVP IED, mean % (SD)	−2.69 (3.23)	0.17 (2.39)	0.002
100% contrast LA IED, mean (SD)	−7.3 (15.8)	−0.06 (3.3)	0.06
2.5% contrast LA IED, mean (SD)	−11.5 (14.1)	−0.1 (8.2)	0.004
1.25% contrast LA IED, mean (SD)	−8.2 (12.0)	1.9 (6.6)	0.002

IED, inter-eye difference (using the ON eye as the reference eye in MS ON patients, and using the right eye as the reference eye in MS non-ON patients). ON, optic neuritis; SD, standard deviation; pRNFL, peripapillary retinal nerve fiber layer thickness; GCIPL, ganglion cell + inner plexiform layer thickness; INL, inner nuclear layer thickness; ONL, outer nuclear layer thickness; AMT, average macular thickness; LA, letter acuity. P-values were calculated using mixed effects linear regression accounting for intra-subject correlations.

Inter-Eye Differences in OCT, OCTA, and Visual Function Measures

IEDs in SVP density were larger in MS ON patients as compared to MS non-ON patients [mean −2.69% (SD 3.23) vs. mean 0.17% (SD 2.39) p=0.002]. Compared to MS non-ON patients, MS ON patients also demonstrated significantly larger IEDs in pRNFL thickness, GCIPL thickness, AMT, 2.5% contrast LA, and 1.25% contrast LA (**Table 3**). MS ON patients were then stratified into groups according to time from ON and compared

TABLE 4 | Inter-eye differences in OCT, OCTA, and visual function measures, with MS ON patients stratified by time from ON.

	MS ON: <3 months post-ON	MS ON: 3–12 months post-ON	MS ON: 1–3 years post-ON	MS ON: >3 years post-ON	MS Non-ON	*P*-value (<3 months vs. non-ON)	*P*-value (3-12 months vs. non-ON)	*P*-value (1-3 yrs vs. non-ON)	*P*-value (>3 yrs vs. non-ON)
N	13 visits in 9 patients	12 visits in 12 patients	37 visits in 18 patients	30 visits in 19 patients	24 visits in 14 patients	–	–	–	–
pRNFL IED, mean um (SD)	10.25 (18.63)	−6.17 (7.66)	−15.69 (11.68)	−14.02 (12.83)	2.29 (6.21)	0.15	**0.001**	**<0.001**	**<0.001**
GCIPL IED, mean um (SD)	−4.99 (6.34)	−5.74 (6.98)	−11.21 (8.59)	−11.22 (9.11)	0.87 (3.63)	**0.01**	**0.001**	**<0.001**	**<0.001**
INL IED, mean um (SD)	0.14 (0.67)	−0.32 (1.03)	−0.08 (1.35)	0.54 (2.53)	0.35 (0.97)	0.65	0.13	0.30	0.80
ONL IED, mean um (SD)	2.25 (2.19)	1.12 (1.31)	−0.09 (0.90)	−0.50 (1.12)	0.48 (1.30)	**0.04**	0.20	0.15	**0.02**
AMT IED, mean um (SD)	−3.54 (6.76)	−7.13 (7.66)	−16.85 (12.95)	−16.21 (12.11)	2.97 (6.64)	0.05	**<0.001**	**<0.001**	**<0.001**
SVP IED, mean % (SD)	−1.09 (2.14)	−1.45 (1.75)	−3.17 (3.20)	−3.79 (3.96)	0.17 (2.39)	0.21	0.07	**0.001**	**0.001**
100% contrast LA IED, mean (SD)	−12 (16)	−2 (8)	−4 (10)	−7 (17)	0 (3)	0.02	0.22	0.09	0.06
2.5% contrast LA IED, mean (SD)	−15 (15)	−8 (10)	−8 (12)	−9 (14)	0 (7)	**0.002**	**0.01**	**0.02**	**0.007**
1.25% contrast LA IED, mean (SD)	−11 (17)	−7 (11)	−8 (8)	−6 (10)	2 (6)	**0.04**	**0.004**	**0.001**	**0.004**

IED, inter-eye difference (using the ON eye as the reference eye in MS ON patients, and using the right eye as the reference eye in MS non-ON patients). ON, optic neuritis; pRNFL, peripapillary retinal nerve fiber layer thickness; GCIPL, ganglion cell + inner plexiform layer thickness; INL, inner nuclear layer thickness; ONL, outer nuclear layer thickness; AMT, average macular thickness; LA, letter acuity. Mean IEDs indicated were calculated using average values per subject within each timeframe. P-values were calculated using mixed effects linear regression accounting for intra-subject correlations. Bold indicates p value for significance of < 0.05.

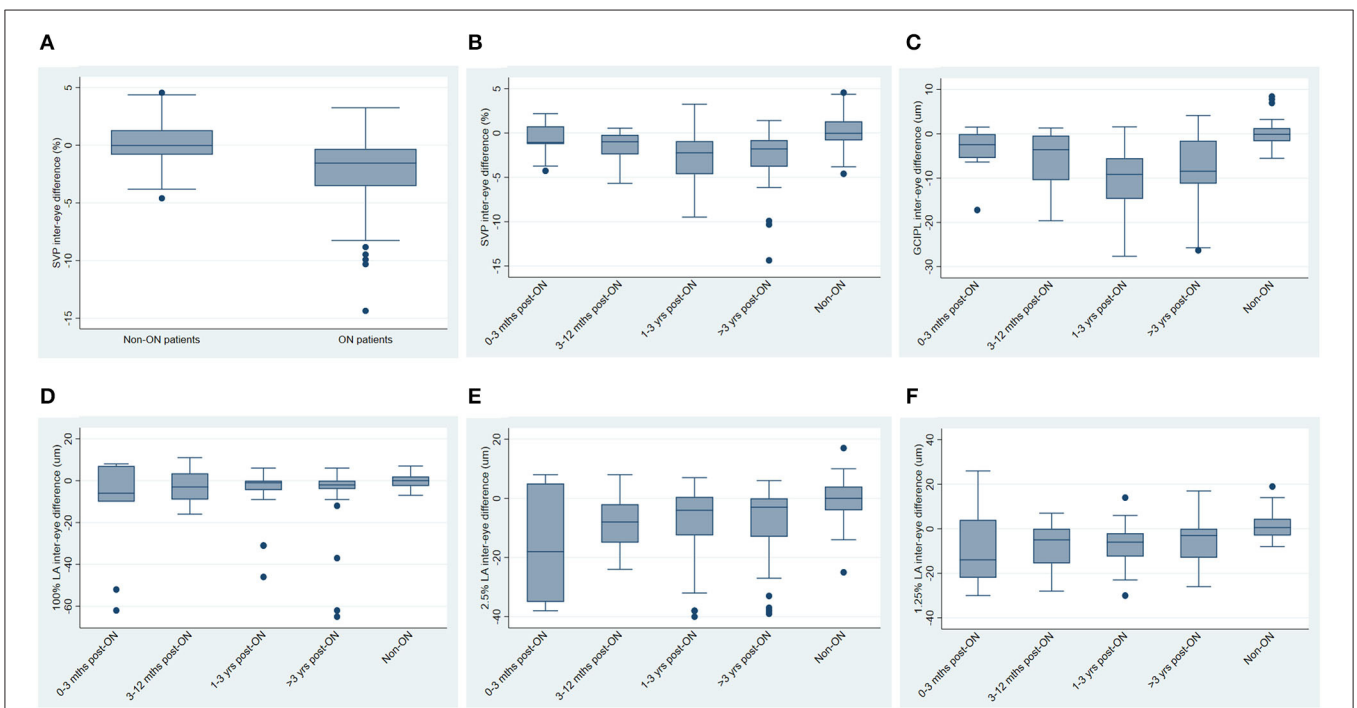

FIGURE 2 | Inter-eye differences in SVP density, GCIPL thickness and visual function, stratified by history of optic neuritis**. (A)** Inter-eye differences in SVP density in MS non-ON patients vs. MS ON patients. **(B)** Inter-eye differences in SVP density in MS ON patients stratified by time from ON, vs. MS non-ON patients. **(C)** Inter-eye differences in GCIPL thickness in MS ON patients stratified by time from ON, vs. MS non-ON patients. **(D–F)** Inter-eye differences in 100% contrast letter acuity **(D)**, 2.5% contrast letter acuity **(E)**, and 1.25% contrast letter acuity **(F)** in MS ON patients stratified by time from ON vs. MS non-ON patients.

to the reference group of MS non-ON patients in multiple cross-sectional analyses (**Table 4**, **Figure 2**). Compared to the MS non-ON group, IEDs in GCIPL thickness, pRNFL thickness, and AMT were significantly larger in MS ON patients at 3–12 months post-ON, 1–3 years post-ON, and >3 years post-ON. Additionally, relative to non-ON MS patients, larger IEDs in GCIPL thickness were even detectable in MS ON patients <3 months post-ON ($p = 0.01$). Regarding IEDs in SVP density, larger differences were identified in MS ON patients at 1–3 years and >3 years post-ON, as compared to MS non-ON patients, whereas differences in the earlier timeframes (<3 months and 3–12 months) were not significant. It is worth noting that the MS ON groups at 1–3 years and >3 years post-ON showed a greater variation in IEDs of GCIPL thickness, pRFNL thickness, AMT, and SVP density (**Figure 2**), which may impact the interpretation and comparison of the multiple cross-sectional analyses illustrated in **Table 4**.

Relationships Between OCT, OCTA, and Visual Function Measures

In analyses of MS ON patients excluding visits during the acute phase (i.e., excluding visits <3 months post-ON), a strong relationship was identified between larger IEDs in SVP density and larger IEDs in GCIPL thickness ($r^2 = 0.75$, $p < 0.001$, **Figure 3**), and between larger IEDs in SVP density and larger differences in 100% contrast LA ($r^2 = 0.31$, $p < 0.001$), 2.5% contrast LA ($r^2 = 0.62$, $p < 0.001$), and 1.25% contrast LA ($r^2 = 0.50$, $p < 0.001$, **Figure 4**). In the same patients, significant relationships were also identified between IEDs in GCIPL thickness and IEDs in 100% contrast LA ($r^2 = 0.36$, $p < 0.001$), 2.5% contrast LA ($r^2 = 0.62$, $p < 0.001$), and 1.25% contrast LA ($r^2 = 0.68$, $p < 0.001$, **Figure 4**). We also examined whether relationships between OCT/OCTA and visual function measures in individual MS ON eyes may differ to the relationships seen between inter-eye differences in the same measures. Results using measures from individual MS ON eyes were broadly similar to those identified using inter-eye differences (**Figure 5**).

DISCUSSION

Results of our study show that IEDs in SVP density are larger in MS ON patients than in MS non-ON patients. Additionally, we found significant relationships between IEDs in SVP density and visual function measures in MS ON patients (after the acute phase of ON), and similar relationships were also identified between IEDs in GCIPL thickness and visual function. ON eyes that exhibit greater reductions of SVP density or GCIPL thickness relative to the fellow eye are more likely to have greater reductions of high- and low-contrast LA scores. We also identified potential differences between the temporal dynamics of OCT and OCTA measures after ON, as increased IED in GCIPL thickness was detectable within 3 months after ON onset, while increased IED in SVP density was only detectable at least 1 year after ON. GCIPL thickness is already considered an excellent surrogate of neuroaxonal injury after ON due to its reliability, reproducibility, and strong structure-function relationships, and our data suggest that SVP density may offer additional insights into pathobiological processes and have value as a biomarker of visual outcomes following ON.

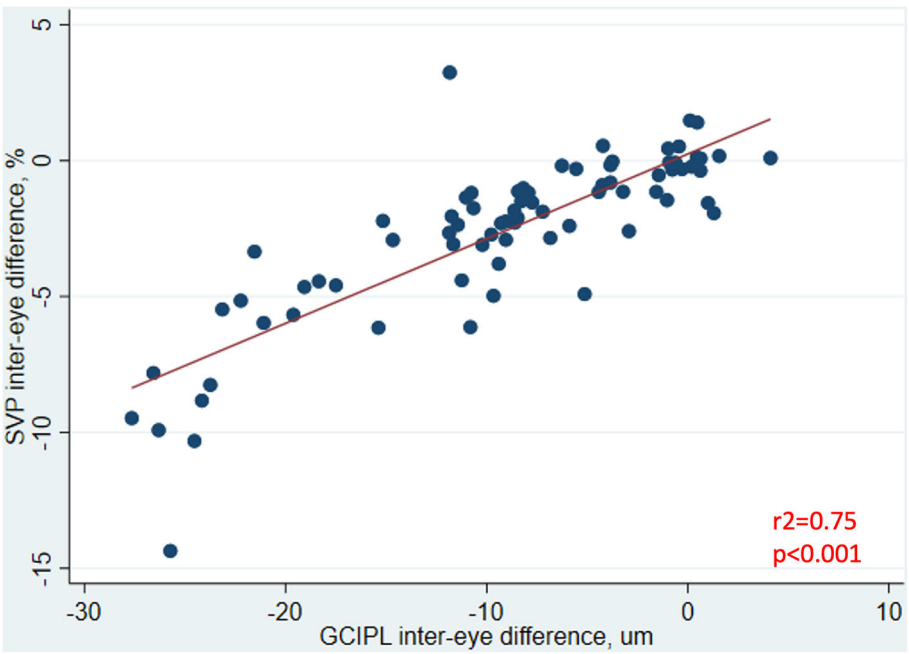

FIGURE 3 | Relationship between inter-eye differences in SVP density and GCIPL thickness in MS ON patients. In MS ON patients at least 3 months post-ON (after resolution of the acute phase of ON), the relationship between inter-eye differences in SVP density and GCIPL thickness is shown here. *P*-value was calculated using mixed-effects linear regression accounting for intra-subject correlations. R^2-value was estimated from the mixed-effects model using the Snijders and Bosker method.

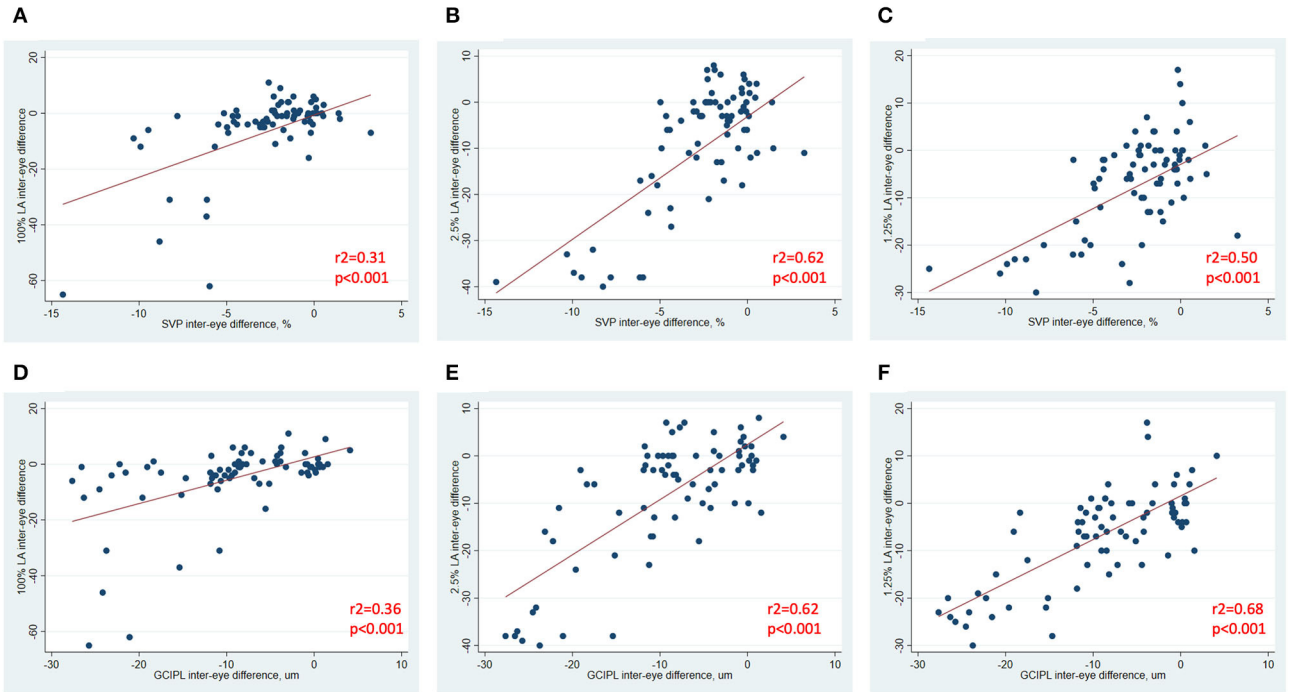

FIGURE 4 | Relationships between inter-eye differences in OCT/OCTA and visual function measures in MS ON patients. In MS ON patients at least 3 months post-ON (after resolution of the acute phase of ON), relationships between inter-eye differences in SVP density and 100% contrast LA, 2.5% contrast LA, and 1.25% contrast LA are demonstrated in **(A–C)**. In MS ON patients at least 3 months post-ON, relationships between inter-eye differences in GCIPL thickness and 100% contrast LA, 2.5% contrast LA, and 1.25% contrast LA are demonstrated in **(D–F)**. *P*-values were calculated using mixed-effects linear regression accounting for intra-subject correlations. R^2-values were estimated from the mixed-effects model using the Snijders and Bosker method.

Multiple studies have demonstrated reduced vascular plexus densities or flow indices in patients with MS, both at the optic nerve head and macula (6–9, 19–22). In the macula, SVP density has been consistently shown to be reduced in patients with MS compared to healthy controls, with reductions being greatest in eyes with a history of ON (6–9, 22). Furthermore, relationships between reduced SVP density and poorer visual function or higher global disability measures have been shown in a number of studies (6, 8). Some of the relationships between SVP density and disability measures have been stronger than those identified between GCIPL thickness and disability measures in the same patients (6). The reason for this is uncertain, but we have hypothesized that reductions SVP density may to some extent reflect not only reduced retinal tissue volume, but perhaps also provide insights into the metabolic function (or indeed dysfunction) of surviving tissue. Due to the relationships with disability measures, and good reliability and reproducibility (23, 24), OCTA has emerged in recent years as an attractive biomarker in MS. However, OCTA has a number of limitations in this population which may hamper interpretation of findings in individual patients, including quite a high frequency of imaging artifact (25) and lack of accepted normal ranges for vascular plexus densities that can be applied across devices in healthy individuals. Thus, the potential clinical utility of a single OCTA evaluation in patients with MS has not been well-demonstrated to date. To this end, examining IEDs can provide clinically-useful information at a single timepoint for individual patients, and we have demonstrated the important finding that IED in SVP density is increased after ON in MS.

The dynamics of changes in retinal layer thicknesses after ON have been well-described (26–28). The acute phase of ON is typically characterized by increased pRNFL thickness in ON eyes due to the effects of acute inflammation within the optic nerve (26, 27), and increased INL thickness may also be detectable during this phase (27). Edema and other components of the acute inflammatory process resolve over the subsequent 3–4 months, and the pRNFL and GCIPL layers undergo rapid thinning during this period reflecting neuroaxonal loss (27). By around 4–6 months after onset of ON, a new baseline in the ON eye appears to be established, and rates of retinal layer atrophy revert to being comparable to the fellow (non-ON) eye (27, 29). Over the long-term, the rate of change of GCIPL thickness may actually be lower in ON eyes than in non-ON eyes (since the proportion of tissue lost annually may be smaller when the baseline thickness is lower) (30). On the other hand, the temporal dynamics of OCTA changes following ON are not well-understood. Our data suggest that increased IED in SVP density is clearly established by 1 year after ON, but these differences may not be detectable within the initial 12 months after ON. While retinal tissue loss is likely to be a primary driver of reduced SVP density following ON, the reason for the potential temporal disconnect between these detectable changes is uncertain, and there are a number

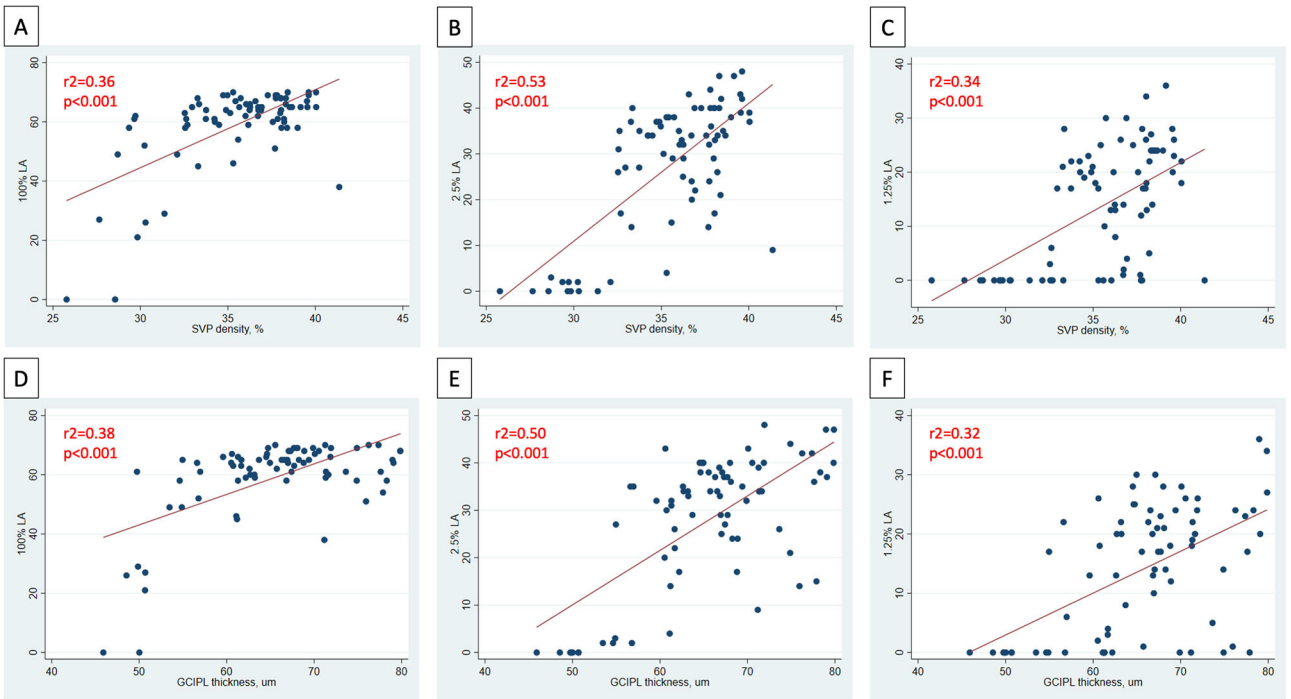

FIGURE 5 | Relationships between OCT/OCTA and visual function measures in individual MS ON eyes. In MS ON eyes at least 3 months post-ON (after resolution of the acute phase of ON), relationships between SVP density and 100% contrast LA, 2.5% contrast LA, and 1.25% contrast LA in the MS ON eye are demonstrated in **(A–C)**. In MS ON eyes at least 3 months post-ON, relationships between GCIPL thickness and 100% contrast LA, 2.5% contrast LA, and 1.25% contrast LA in the MS ON eye are demonstrated in **(D–F)**. *P*-values were calculated using mixed-effects linear regression accounting for intra-subject correlations. R^2-values were estimated from the mixed-effects model using the Snijders and Bosker method.

of potential explanations. First, post-ON changes in the retinal tissue structure and retinal vasculature may not be synchronous, and we hypothesize that reductions in SVP density may not only reflect initial tissue loss incited by inflammation-related axonal injury in the optic nerve, but may also be a marker of later reduced metabolic demand in injured but surviving tissue. Second, we noted that the severity of the retinal tissue loss appeared greater in our group of patients who were >1 year post-ON, and perhaps significant IEDs in SVP density are only detectable in cases where there is greater tissue injury. Third, the number of patients in our cohort who were <12 months post-ON was smaller than the number of patients who were >1 year post-ON, and so we may have been underpowered to detect differences within the earlier timeframes. Additionally, while SVP density and GCIPL thickness are known to be closely related cross-sectionally, it is not yet understood whether changes in these measures occur *proportionately* following ON–representing an important question for future longitudinal studies.

IEDs in retinal layer thicknesses are accepted as an informative and clinically-applicable way to measure retinal changes after optic neuritis. Since retinal layer thicknesses exhibit high inter-individual variability (even in healthy subjects), ON eyes may experience substantial tissue loss without the actual pRNFL or GCIPL thickness dropping into the "abnormal" range (considered <5th percentile in clinical practice) (31). This may partially explain why retinal layer thicknesses in individual eyes correlate well with history of ON and monocular visual function at a group level (32, 33), but monocular eye thresholds may have limited value for defining ON in individual patients (31, 34). IEDs in retinal layer thicknesses have been proposed as a more informative marker of ON in individuals, since the reliability and reproducibility of OCT-derived retinal layer thicknesses (particularly GCIPL thickness) is high, and the symmetry between right and left eyes in healthy individuals is also high (31, 34–36). IED in GCIPL thickness has emerged as a reasonably robust marker of prior ON, with a threshold of >4 um demonstrating reasonably good sensitivity and specificity for discriminating ON history (34, 35). Additionally, IED in GCIPL thickness has shown significant associations with visual function outcomes after ON (34). In our study, IED in SVP density showed similar correlations with low contrast LA (recognized as a more sensitive marker of visual dysfunction than high contrast VA in MS) (37, 38) as those identified with GCIPL thickness. This is in keeping with findings of prior work by our group, in which both SVP density and GCIPL thickness were found to correlate with EDSS and LA scores in MS patients, and SVP density was additionally found to correlate with MSFC scores (6). OCTA images are generated through the detection of motion within blood vessels according to a threshold effect, so reduced SVP density may reflect reduced tissue volume as well as reduced blood flow within surviving tissue due to tissue dysfunction or hypometabolism. For these reasons, SVP density may offer

additional insights into tissue function, that is perhaps reflected in the associations we identified with high- and low-contrast LA. Another potential advantage that OCTA may offer in post-ON eyes, is that the derived vascular measures might not be affected by the same "floor" phenomenon as OCT measures (whereby retinal tissue loss may be undetectable below a certain threshold) (39).

In considering the potential importance of changes in OCTA findings following ON, it is essential to remember that reductions in macular and peripapillary vascular measures have also been reported in other etiologies of optic neuropathy such as glaucoma and non-arteritic anterior ischemic optic neuropathy (NAION) (40–42). NAION eyes demonstrate similar although usually more marked reductions in SVP density to ON eyes (40), while glaucomatous optic neuropathy may be associated with changes in deep vascular plexus (DVP) density as well as SVP density (41). While all of these optic neuropathies are associated with loss of retinal ganglion cells, the different patterns of retinal vascular changes suggests that OCTA may provide clues regarding underlying pathophysiology, requiring further exploration in future studies.

Our study is novel in its approach to examine IEDs in both OCT and OCTA measures after ON in MS. We have employed careful quality control protocols and an effective neural network based-approach to systematically reduce the impact of artifact on OCTA analyses. However, our study has a number of limitations. Our study population was relatively small, and we may have been underpowered to detect differences in OCTA measures in all of the MS ON subgroups. The MS non-ON patients were on average older, had a longer MS disease duration, and were more frequently Caucasian than the MS ON patients, and it is uncertain whether age, disease duration, or race alone may have a substantial impact on the symmetry of OCTA measures between eyes in individuals. The differences in OCTA measures between African-American and Caucasian-American people with MS represents an important question for future research in larger cohorts, since it is known that African-American people with MS tend to have worse visual outcomes after ON and accelerated rates of retinal atrophy, compared to Caucasian-American people with MS (43–45). Our multiple cross-sectional comparisons included different patients at different timepoints after ON, and some patients may have experienced a greater severity of acute ON than others. Since OCTA is a relatively new technology and we have not been tracking patients for many years with this technique, we were unable to perform a longitudinal analysis to get a robust picture of the temporal dynamics of OCTA changes after ON. This represents a key area for future research. Another important area of further study would include longitudinal evaluation of not just SVP density, but also DVP density and whole vessel density in ON eyes.

CONCLUSIONS

Increased IED in SVP density in MS patients after ON can be detected using OCTA, and detectable changes in SVP density after ON may occur slightly later than those changes in GCIPL thickness. Additionally, IED in SVP density demonstrates robust correlations with visual function in MS ON patients. Our findings support the potential clinical utility of OCTA for detecting ON-related changes in patients with MS. Furthermore, our results provide important insights into the interplay between retinal tissue changes and retinal vascular changes following ON. OCTA represents a rapid reliable technique that may provide additional clinically-relevant information beyond standard OCT techniques in MS patients, and represents a potential biomarker of post-ON outcomes for future clinical trials.

DATA AVAILABILITY STATEMENT

The raw data supporting the conclusions of this article will be made available by the authors, subject to institutional review board approval and without undue reservation.

ETHICS STATEMENT

The studies involving human participants were reviewed and approved by Johns Hopkins University Institutional Review Board. The patients/participants provided their written informed consent to participate in this study.

AUTHOR CONTRIBUTIONS

OM was involved in study conceptualization and planning, data acquisition and analysis, data interpretation, drafting, and revising the manuscript. GK, EV, AF, JL, HE, NP, ES, NL, and YL were involved in data acquisition and analysis, data interpretation, and revising the manuscript. KF, JP, and PC were involved in data interpretation, and revising the manuscript. SS was involved in study conceptualization and planning, data acquisition and analysis, data interpretation, and revising the manuscript. All authors contributed to the article and approved the submitted version.

FUNDING

This study was funded by the National MS Society (RG-1606-08768 to SS), Race to Erase MS (to SS), and NIH/NINDS (R01NS082347 to PC).

REFERENCES

1. Lambe J, Saidha S, Bermel RA. Optical coherence tomography and multiple sclerosis: update on clinical application and role in clinical trials. *Mult Scler.* (2020) 26:624–39. doi: 10.1177/1352458519872751
2. Lambe J, Murphy O, Saidha S. Can optical coherence tomography be used to guide treatment decisions in adult or pediatric multiple sclerosis? *Curr Treat Options Neurol.* (2018) 20:9. doi: 10.1007/s11940-018-0493-6
3. Wang L, Murphy O, Caldito NG, Calabresi PA, Saidha S. Emerging applications of optical coherence tomography angiography (OCTA) in neurological research. *Eye Vis.* (2018) 5:11. doi: 10.1186/s40662-018-0104-3

4. Dutta R, Trapp BD. Mechanisms of neuronal dysfunction and degeneration in multiple sclerosis. *Prog Neurobiol.* (2011) 93:1–12. doi: 10.1016/j.pneurobio.2010.09.005
5. Salapa HE, Lee S, Shin Y, Levin MC. Contribution of the degeneration of the neuro-axonal unit to the pathogenesis of multiple sclerosis. *Brain Sci.* (2017) 7:69. doi: 10.3390/brainsci7060069
6. Murphy OC, Kwakyi O, Iftikhar M, Zafar S, Lambe J, Pellegrini N, et al. Alterations in the retinal vasculature occur in multiple sclerosis and exhibit novel correlations with disability and visual function measures. *Mult Scler.* (2019) 2019:815–28. doi: 10.1177/135245851984511
7. Feucht N, Maier M, Lepennetier G, Pettenkofer M, Wetzlmair C, Daltrozzo T, et al. Optical coherence tomography angiography indicates associations of the retinal vascular network and disease activity in multiple sclerosis. *Mult Scler.* (2018) 2018:224–34. doi: 10.1177/1352458517750009
8. Lanzillo R, Cennamo G, Criscuolo C, Carotenuto A, Velotti N, Sparnelli F, et al. Optical coherence tomography angiography retinal vascular network assessment in multiple sclerosis. *Mult Scler.* (2017) 2017:1352458517729463. doi: 10.1177/1352458517729463
9. Yilmaz H, Ersoy A, Icel E. Assessments of vessel density and foveal avascular zone metrics in multiple sclerosis: an optical coherence tomography angiography study. *Eye.* (2020) 34:771–8. doi: 10.1038/s41433-019-0746-y
10. Thompson AJ, Banwell BL, Barkhof F, Carroll WM, Coetzee T, Comi G, et al. Diagnosis of multiple sclerosis: 2017 revisions of the McDonald criteria. *Lancet Neurol.* (2018) 17:162–73. doi: 10.1016/S1474-4422(17)30470-2
11. Syc SB, Warner CV, Hiremath GS, Farrell SK, Ratchford JN, Conger A, et al. Reproducibility of high-resolution optical coherence tomography in multiple sclerosis. *Mult Scler.* (2010) 16:829–39. doi: 10.1177/1352458510371640
12. Caldito NG, Antony B, He Y, Lang A, Nguyen J, Rothman A, et al. Analysis of agreement of retinal-layer thickness measures derived from the segmentation of horizontal and vertical spectralis OCT macular scans. *Curr Eye Res.* (2018) 43:415–23. doi: 10.1080/02713683.2017.1406526
13. Tewarie P, Balk L, Costello F, Green A, Martin R, Schippling S, et al. The OSCAR-IB consensus criteria for retinal OCT quality assessment. *PLoS ONE.* (2012) 7:e34823. doi: 10.1371/journal.pone.0034823
14. Bhargava P, Lang A, Al-Louzi O, Carass A, Prince J, Calabresi PA, et al. Applying an open-source segmentation algorithm to different OCT devices in multiple sclerosis patients and healthy controls: Implications for clinical trials. *Mult Scler Int.* (2015) 2015:136295. doi: 10.1155/2015/136295
15. Lang A, Carass A, Al-Louzi O, Bhargava P, Solomon SD, Calabresi PA, et al. Combined registration and motion correction of longitudinal retinal OCT data. *Proc SPIE Int Soc Opt Eng.* (2016) 9784:97840X. doi: 10.1117/12.2217157
16. Sotirchos ES, Caldito NG, Filippatou A, Fitzgerald KC, Murphy OC, Lambe J, et al. Progressive multiple sclerosis is associated with faster and specific retinal layer atrophy. *Ann Neurol.* (2020) 87:885–96. doi: 10.1002/ana.25738
17. Liu Y, Zuo L, Carass A, et al. Variational intensity cross channel encoder for unsupervised vessel segmentation on OCT angiography. In: *Presented at the SPIE Medical Imaging*. Houston, TX (2020).
18. Snijders T, Bosker RJ. *Multilevel Analysis: An Introduction to Basic and Advanced Multilevel Modeling.* 2nd ed. London: Sage (2102).
19. Wang X, Jia Y, Spain R, Potsaid B, Liu JJ, Baumann B, et al. Optical coherence tomography angiography of optic nerve head and parafovea in multiple sclerosis. *Br J Ophthalmol.* (2014) 98:1368–73. doi: 10.1136/bjophthalmol-2013-304547
20. Spain RI, Liu L, Zhang X, Jia Y, Tan O, Bourdette D, et al. Optical coherence tomography angiography enhances the detection of optic nerve damage in multiple sclerosis. *Br J Ophthalmol.* (2018) 102:520–4. doi: 10.1136/bjophthalmol-2017-310477
21. Cennamo G, Carotenuto A, Montorio D, Petracca M, Moccia M, Melenzane A, et al. Peripapillary vessel density as early biomarker in multiple sclerosis. *Front Neurol.* (2020) 11:542. doi: 10.3389/fneur.2020.00542
22. Farci R, Carta A, Cocco E, Frau J, Fossarello M, Diaz G. Optical coherence tomography angiography in multiple sclerosis: A cross-sectional study. *PLoS ONE.* (2020) 15:e0236090. doi: 10.1371/journal.pone.0236090
23. Hosari S, Hohberger B, Theelke L, Sari H, Lucio M, Mardin C. OCT angiography: Measurement of retinal macular microvasculature with spectralis II OCT angiography – reliability and reproducibility. *Ophthalmologica.* (2020) 243:75–84. doi: 10.1159/000502458
24. Lei J, Durbin MK, Shi Y, Uji A, Balasubramanian S, Baghdasaryan E, et al. Repeatability and reproducibility of superficial macular retinal vessel density measurements using optical coherence tomography angiography en face images. *JAMA Ophthalmol.* (2017) 135:1092–8. doi: 10.1001/jamaophthalmol.2017.3431
25. Iftikhar M, Zafar S, Gonzalez N, Murphy O, Ohemaa Kwakyi MS, Sydney Feldman BS, et al. Image artifacts in optical coherence tomography angiography among patients with multiple sclerosis. *Curr Eye Res.* (2019) 44:558–63. doi: 10.1080/02713683.2019.1565892
26. Gabilondo I, Martínez-Lapiscina EH, Fraga-Pumar E, Ortiz-Perez S, Torres-Torres R, Andorra M, et al. Dynamics of retinal injury after acute optic neuritis. *Ann Neurol.* (2015) 77:517–28. doi: 10.1002/ana.24351
27. Al-Louzi OA, Bhargava P, Newsome SD, Balcer LJ, Frohman EM, Crainiceanu C, et al. Outer retinal changes following acute optic neuritis. *Mult Scler.* (2016) 22:362–72. doi: 10.1177/1352458515590646
28. Syc SB, Saidha S, Newsome SD, Ratchford JN, Levy M, Ford E, et al. Optical coherence tomography segmentation reveals ganglion cell layer pathology after optic neuritis. *Brain.* (2012) 135:521–33. doi: 10.1093/brain/awr264
29. Costello F, Hodge W, Pan Y, Eggenberger E, Coupland S, Kardon R. Tracking retinal nerve fiber layer loss after optic neuritis: A prospective study using optical coherence tomography. *Must Scler.* (2008) 14:893–905. doi: 10.1177/1352458508091367
30. Saidha S, Al-Louzi O, Ratchford JN, Bhargava P, Oh J, Newsome SD, et al. Optical coherence tomography reflects brain atrophy in multiple sclerosis: a four-year study. *Ann Neurol.* (2015) 78:801–13. doi: 10.1002/ana.24487
31. Behbehani R, Ali A, Al-Omairah H, Rousseff RT. Optimization of spectral domain optical coherence tomography and visual evoked potentials to identify unilateral optic neuritis. *Mult Scler Relat Disord.* (2020) 41:101988. doi: 10.1016/j.msard.2020.101988
32. Saidha S, Syc SB, Durbin MK, Eckstein C, Oakley JD, Meyer SA, et al. Visual dysfunction in multiple sclerosis correlates better with optical coherence tomography derived estimates of macular ganglion cell layer thickness than peripapillary retinal nerve fiber layer thickness. *Mult Scler.* (2011) 17:1449–63. doi: 10.1177/1352458511418630
33. Petzold A, Balcer LJ, Calabresi PA, Costello F, Frohman TC, Frohman EM, et al. Retinal layer segmentation in multiple sclerosis: a systematic review and meta-analysis. *Lancet Neurol.* (2017) 16:797–812. doi: 10.1016/S1474-4422(17)30278-8
34. Nolan-Kenney RC, Liu M, Akhand O, Calabresi PA, Paul F, Petzold A, et al. Optimal intereye difference thresholds by optical coherence tomography in multiple sclerosis: an international study. *Ann Neurol.* (2019) 85:618–29. doi: 10.1002/ana.25462
35. Bsteh G, Hegen H, Altmann P, Auer M, Berek K, Zinganell A, et al. Validation of inter-eye difference thresholds in optical coherence tomography for identification of optic neuritis in multiple sclerosis. *Mult Scler Relat Disord.* (2020) 45:102403. doi: 10.1016/j.msard.2020.102403
36. Coric D, Balk LJ, Uitdehaag BMJ, Petzold A. Diagnostic accuracy of optical coherence tomography inter-eye percentage difference for optic neuritis in multiple sclerosis. *Eur J Neurol.* (2017) 24:1479–84. doi: 10.1111/ene.13443
37. Mowry EM, Loguidice MJ, Daniels AB, Jacobs DA, Markowitz CE, Galetta SL, et al. Vision related quality of life in multiple sclerosis: Correlation with new measures of low and high contrast letter acuity. *J Neurol Neurosurg Psychiatr.* (2009) 80:767–72. doi: 10.1136/jnnp.2008.165449
38. Baier ML, Cutter GR, Rudick RA, Miller D, Cohen JA, Weinstock-Guttman B, et al. Low-contrast letter acuity testing captures visual dysfunction in patients with multiple sclerosis. *Neurology.* (2005) 64:992–5. doi: 10.1212/01.WNL.0000154521.40686.63
39. Moghimi S, Bowd C, Zangwill LM, Penteado RC, Hasenstab K, Hou H, et al. Measurement floors and dynamic ranges of OCT and OCT angiography in glaucoma. *Ophthalmology.* (2019) 126:980–8. doi: 10.1016/j.ophtha.2019.03.003
40. Fard MA, Yadegari S, Ghahvechian H, Moghimi S, Soltani-Moghaddam R, Subramanian PS. Optical coherence tomography angiography of a pale optic disc in demyelinating optic neuritis and ischemic optic neuropathy. *J Neuroophthalmol.* (2019) 39:339–44. doi: 10.1097/WNO.0000000000000775
41. Fard MA, Fakhraee G, Ghahvechian H, Sahraian A, Moghimi S, Ritch R. Macular vascularity in ischemic optic neuropathy compared to glaucoma

by projection-resolved optical coherence tomography angiography. *Am J Ophthalmol.* (2020) 209:27–34. doi: 10.1016/j.ajo.2019.09.015
42. Chen JJ, AbouChehade JE, Iezzi R, Leavitt JA, Kardon RH. Optical coherence angiographic demonstration of retinal changes from chronic optic neuropathies. *Neuro Ophthalmol.* (2017) 41:76–83. doi: 10.1080/01658107.2016.1275703
43. Caldito NG, Saidha S, Sotirchos ES, Dewey BE, Cowley NJ, Glaister J, et al. Brain and retinal atrophy in african-americans vs. caucasian-americans with multiple sclerosis: a longitudinal study. *Brain.* (2018) 141:3115–29. doi: 10.1093/brain/awy245
44. Kimbrough DJ, Sotirchos ES, Wilson JA, Al-Louzi O, Conger A, Conger D, et al. Retinal damage and vision loss in african american multiple sclerosis patients. *Ann Neurol.* (2015) 77:228–36. doi: 10.1002/ana.24308
45. Moss HE, Gao W, Balcer LJ, Joslin CE. Association of race/ethnicity with visual outcomes following acute optic neuritis: An analysis of the optic neuritis treatment trial. *JAMA Ophthalmol.* (2014) 132:421–7. doi: 10.1001/jamaophthalmol.2013.7995

Conflict of Interest: ES has served on a scientific advisory boards for Viela Bio and Genentech and is funded by a Sylvia Lawry physician fellowship award from NMSS. JP is a founder of Sonovex, Inc. and serves on its Board of Directors. He has received consulting fees from JuneBrain LLC and is PI on research grants to Johns Hopkins from 12Sigma Technologies and Biogen. PC has received consulting fees from Disarm and Biogen and is PI on grants to JHU from Biogen and Annexon. SS has received consulting fees from Medical Logix for the development of CME programs in neurology, and has served on scientific advisory boards for Biogen, Genzyme, Genentech Corporation, EMD Serono, and Celgene. He is the PI of investigator-initiated studies funded by Genentech and Biogen, was the site investigator of a trial sponsored by MedDay Pharmaceuticals, and received support from the Race to Erase MS foundation. He has received equity compensation for consulting from JuneBrain LLC, a retinal imaging device developer.

The remaining authors declare that the research was conducted in the absence of any commercial or financial relationships that could be construed as a potential conflict of interest.

Copyright © 2020 Murphy, Kalaitzidis, Vasileiou, Filippatou, Lambe, Ehrhardt, Pellegrini, Sotirchos, Luciano, Liu, Fitzgerald, Prince, Calabresi and Saidha. This is an open-access article distributed under the terms of the Creative Commons Attribution License (CC BY). The use, distribution or reproduction in other forums is permitted, provided the original author(s) and the copyright owner(s) are credited and that the original publication in this journal is cited, in accordance with accepted academic practice. No use, distribution or reproduction is permitted which does not comply with these terms.

frontiers in Neurology

ORIGINAL RESEARCH
published: 22 December 2020
doi: 10.3389/fneur.2020.602193

Low Contrast Visual Acuity Might Help to Detect Previous Optic Neuritis

*Soo-Hyun Park[1], Choul Yong Park[2], Young Joo Shin[3], Kyoung Sook Jeong[4] and Nam-Hee Kim[5]**

[1] Department of Neurology, Department of Critical Care Medicine, Department of Internal Hospital, Inha University, Incheon, South Korea, [2] Department of Ophthalmology, Dongguk University Ilsan Hospital and Dongguk University-Seoul Graduate School of Medicine, Goyang, South Korea, [3] Department of Ophthalmology, Hallym University Medical Center, Seoul, South Korea, [4] Department of Occupational and Environmental Medicine, Wonju Severance Hospital, Wonju, South Korea, [5] Department of Neurology, Dongguk University Ilsan Hospital and Dongguk University-Seoul Graduate School of Medicine, Goyang, South Korea

Optic neuritis (ON) has been considered to be an important factor in the diagnosis of multiple sclerosis (MS) and neuromyelitis optica spectrum disorder (NMOSD), making ON detection increasingly critical for early diagnosis. Furthermore, subclinical ONs presenting no distinct decrease in visual acuity can be missed. Low contrast visual acuity (LC-VA) is known to be able to capture visual loss not seen in conventional high-contrast visual acuity (HC-VA) in MS. Therefore, to increase the sensitivity of ON detection, we investigated the advantage of LC-VA over conventional HC-VA. One hundred and eight patients with demyelinating disease (35 MS, 73 NMOSD) with ON at least 3 months prior and 35 controls underwent neuro-ophthalmic evaluation, including best-corrected conventional high contrast visual acuity (HC-VA) and 2.5% and 1.25% low contrast visual acuity (LC-VA). Receiver operating characteristic (ROC) curve analysis and the area under the curve (AUC) of various visual functions were used to determine the most relevant visual function test for the detection of optic nerve involvement. Additionally, the optimal cutoff point was obtained from the Youden index (J-index) as the points with the best sensitivity-specificity balance. When distinguishing ON from non-ON, the area under the ROC curve (AUC) was highest for the 2.5% LC-VA (0.835, $P < 0.001$; sensitivity 71.5%, specificity 88.6%), while it was 0.710 ($P < 0.001$) for the HC-VA and 0.770 ($P < 0.001$) for the 1.25% LC-VA. In discriminating between controls and ON, the AUC was also highest for the 2.5% LC-VA 0.754 ($P < 0.001$; sensitivity 71.5%, specificity 78.5%), while it was 0.719 ($P < 0.001$) for HC-VA and 0.688 ($P < 0.001$) for 1.25% LC-VA. In eyes with a history of ON ($n = 137$), the HC-VA and 2.5% LC-VA were abnormal in 64.2 and 71.5%, respectively ($P < 0.001$), with their combination detecting abnormalities in approximately 85.4% ($P < 0.001$). The 2.5% LC-VA was superior to HC-VA in detecting ON when distinguishing ON from non-ON or control. The 2.5% LC-VA might be a useful, feasible, and rapid method to detect ON. Furthermore, combining 2.5% LC-VA with conventional HC-VA would be better for detecting optic nerve involvements.

Keywords: optic neuritis, visual acuity, low contrast visual acuity, neuromyelitis optica spectrum disorder, multiple sclerosis

OPEN ACCESS

Edited by:
Ahmed Toosy, University College London, United Kingdom

Reviewed by:
Mark Paine, Royal Brisbane and Women's Hospital, Australia
Christopher Charles Glisson, Michigan State University, United States

***Correspondence:**
Nam-Hee Kim
nheekim8@hanmail.net

Specialty section:
This article was submitted to Neuro-Ophthalmology, a section of the journal Frontiers in Neurology

Received: *02 September 2020*
Accepted: *09 November 2020*
Published: *22 December 2020*

Citation:
Park S-H, Park CY, Shin YJ, Jeong KS and Kim N-H (2020) Low Contrast Visual Acuity Might Help to Detect Previous Optic Neuritis. Front. Neurol. 11:602193. doi: 10.3389/fneur.2020.602193

INTRODUCTION

Optic neuritis (ON) has been reported to be accompanied by demyelinating diseases such as multiple sclerosis (MS) and neuromyelitis optica spectrum disorder (NMOSD). Although ON is often resolved after appropriate treatment (1), it can cause visual disturbance and reduce the quality of life (2). ON is related to retinal axon loss, and its morphological measurement is used as a parameter of disability (3). Demyelinating diseases sometimes may present subclinical changes in visual function, which impedes their early diagnosis (2, 4). The diagnosis of NMOSD and MS in the early phase is important for their treatments and prognoses. According to the recently revised criteria of MS and NMOSD (5, 6), ON has been regarded as a more important factor for their diagnoses (6). Additionally, asymptomatic or subclinical ONs are sometimes missed in the measurement of visual function with high contrast visual acuity (HC-VA), because of a normal result of HC-VA (3, 7). Therefore, it is challenging to diagnose MS or NMOSD with asymptomatic or subclinical ON. A lot of tests including optical coherence tomography (OCT), visual evoked potential (VEP), color vision, or visual field defect have been suggested to evaluate ON (8–12). Each test investigates a unique aspect of the visual system, and several variations of each test exist (8–12). The choice of the test depends on the purpose of the study, characteristics of the patient population, and types of diseases. Recent studies suggested that low-contrast visual acuity (LC-VA) could be a more sensitive measure of visual dysfunction in ON (8, 13, 14). LC-VA can be an easy, fast, and sensitive test to evaluate deficit in visual function caused by ON in a clinical setting. In our study, we aimed to investigate the usefulness of LC-VA as a diagnostic test for ON in a large cohort of demyelinating diseases.

MATERIALS AND METHODS

Patients

This observational and cross-sectional study was performed according to the tenets of the Declaration of Helsinki and was approved by the Institutional Review Board of Dongguk University Ilsan Hospital. All subjects provided informed written consent. Patients with NMOSD who were seropositive for aquaporin-4 antibody, as defined by the revised 2006 diagnostic criteria of Wingerchuk, and patients with MS who met the 2010 McDonald criteria were recruited. Patients who had an episode of ON within the last 3 months were excluded to evaluate the utility of LC-VA for assessing evidence of remote ON in eyes with stabilized visual function after optic nerve inflammation. Patients with diabetes, a history of ocular injury, glaucoma, or other ophthalmologic disorders were excluded. Ophthalmological evaluations were performed in all patients by an ophthalmologist. Finally, 143 subjects were enrolled that consisted of 35 control participants and 108 patients (35 MS and 73 NMOSD).

Visual Function

All visual tests were administered monocularly. Best-corrected conventional visual acuity (VA) with 100% contrast (high contrast visual acuity, HC-VA) was measured using the standard Snellen chart. Two-meter Sloan letter charts of 1.25 and 2.5% contrasts (Precision Vision, La Salle, IL) were used for LC-VA. LC-VA testing performed the discrimination of gradually smaller gray letters with 1.25 and 2.5% contrast level against a white background. Visual acuity (VA) was expressed using a decimal scale but was transformed to the logarithm of the minimum angle of resolution (logMAR) for statistical analyses.

Statistical Analysis

Data are presented mean (standard deviation), min, max, median (interquartile range), number (percentage), and percentile (25th, 50th, and 75th). Comparisons between groups were performed using the Student *t*-test or Mann–Whitney test considering normality and the properties of the variables. ANOVA test was used to compare the means of three or more groups. Detection capacity of the diagnosis for ON was tested by the receiver operating characteristic (ROC) curve analysis, and area under the curve (AUC) was calculated to determine the discriminative value of each VA test. Sensitivity and specificity analyses were performed for the diagnosis of ON. In addition, the optimal cutoff point was obtained from the Youden index (J-index) as the points with the best sensitivity-specificity balance. VA was analyzed using the logarithm of the minimum angle of resolution (9). $P < 0.05$ were considered to be significant. All *P*-values reported are two-sided. SPSS 26.0 for Windows (SPSS Inc., Chicago, IL, USA) was used for the statistical analysis. R 4.0.1 for Windows (Washington University, St. Louis, MO, USA) were used for graph data.

RESULTS

The clinical characteristics of each group are listed in **Table 1**. Total of 286 eyes (70 control eyes, 137 eyes with ON, and 79 eyes without ON) were assessed. Visual functions including HC-VA and 2.5 and 1.25% LC-VA in each group are shown in **Table 2** and **Figure 1**. HC-VA was not significantly different between the control and non-ON groups, whereas HC-VA was worse in ON compared with the non-ON or control. Although 2.5% LC-VA and 1.25% LC-VA were not different between control and Non-ON, 2.5 and 1.25% LC-VA were worse in the ON group compared with the control or non-ON.

The ROC curve analysis of the visual functions was used to determine the most appropriate test for discriminating between ON and non-ON (**Table 3** and **Figure 2A**). The area under the ROC curve (AUC) was highest in the 2.5% LC-VA (sensitivity 71.5%, specificity 88.6%). AUC was 0.710 for the HC-VA, 0.835 for the 2.5% LC-VA, and 0.770 for the 1.25% LC-VA.

The ROC curve analysis of visual functions was used to determine the most appropriate test to discriminate between the controls and ON (**Table 3** and **Figure 2B**). The AUC was also highest in the 2.5% LC-VA (sensitivity 71.5%, specificity 78.5%). The AUC was 0.719 for HC-VA, 0.754 for 2.5% LC-VA, and 0.688 for 1.25% LC-VA.

The findings of HC-VA and 2.5% LC-VA were abnormal in 64.2 and 71.5% with a history of ON, respectively (**Figure 3**). Of the 137 eyes with ON, 19 (13.9%) were abnormal only in HC-VA,

TABLE 1 | Baseline characteristics according to study groups.

	Control ($n = 70$)	Non-ON ($n = 79$)	ON ($n = 137$)	*P*-value		
				Control vs. non-ON	ON vs. non-ON	ON vs. control
Age, mean ± SD (years)	39.3 ± 11.1	39.1 ± 11.7	37.7 ± 11.5	0.996	0.673	0.634
Female, *n* (%)	20 (28.6%)	61 (77.2%)	111 (81.0%)			
Diagnosis						
MS, *n* (%)		33 (41.8%)	37 (27.0%)			
NMOSD, *n* (%)		46 (58.2%)	100 (73.0%)			
Number of ON attacks, mean (95% CI)			2.09 (1.71–2.47)			
Bilateral ON, *n* (%)			116 (84.7%)			
Disease duration, mean ± SD (months)		53.2 ± 49.8	79.6 ± 52.2		<0.001	
EDSS, mean ± SD		2.7 ± 2.0	3.7 ± 2.0		<0.001	

MS, multiple sclerosis; NMOSD, neuromyelitis optica spectrum disorder; ON, optic neuritis; Non-ON, non-optic neuritis; SD, standard deviation; EDSS, Expanded Disability Status Scale; CI, confidence interval.

TABLE 2 | Visual functions in LogMAR according to study groups.

	Mean	Min	Max	Percentile			*P*-value
				25th	50th	75th	
HC-VA							
Control	0.3	−0.1	1.6	0.0	0.1	0.7	0.95*
Non-ON	0.3	−0.1	1.3	0.0	0.1	0.6	<0.001**
ON	1.0	−0.1	3.0	0.1	0.8	1.6	<0.001***
2.5% LC-VA							
Control	0.5	0.2	1.8	0.3	0.4	0.6	0.092*
Non-ON	0.7	0.2	1.8	0.3	0.6	0.7	<0.001**
ON	1.3	0.2	1.8	0.6	1.8	1.8	<0.001***
1.25% LC-VA							
Control	1.0	0.3	1.8	0.6	0.8	1.8	0.114*
Non-ON	1.2	0.3	1.8	0.7	0.8	1.8	<0.001**
ON	1.6	0.4	1.8	1.8	1.8	1.8	<0.001***

*Control vs. non-ON; **Non-ON vs. ON; ***Control vs. ON. ANOVA in Scheffe.
HC-VA, high contrast visual acuity; LC-VA, low contrast visual acuity; ON, optic neuritis; Non-ON, non-optic neuritis.

29 (21.2%) were abnormal only in 2.5% LC-VA, and 69 (50.4%) were abnormal in both tests. The combination of HC-VA or 2.5% LC-VA detected abnormalities in 85.4% of ON and significantly improved the sensitivity relative to individual technique. Of the 79 eyes with non-ON, abnormalities were detected in 23 (29.1%) by HC-VA and 17 (21.5%) by 2.5% LC-VA. The combination of HC-VA or 2.5% LC-VA detected abnormalities in 33 (41.8%) of eyes and improved the sensitivity compared with those of each of the techniques individually.

DISCUSSION

This study showed that LC-VA was more sensitive compared with HC-VA for detecting ON. Our study supports the use of LC-VA in the detection of ON, given its high sensitivity and specificity, especially the use of 2.5% LC-VA. Moreover, the combination of HC-VA and 2.5% LC-VA was superior for the detection of ON than individually. This implies that 2.5% LC-VA may be a potential marker for ON.

Visual symptoms of ON may worsen as a result of various pathological processes, including inflammation, demyelination, and axonal degeneration of the visual pathway (15). Furthermore, discrimination of ON including subclinical ON is very important to assess the disease progression and recovery (16). Various diagnostic methods of ON have been studied for early detection of ON including VA, visual field, brain imaging, VEP, OCT, etc. (17). Although there are various tests for ON discrimination, the addition of the LC-VA test is easier and simpler to apply than the other tests (13, 18). Administering HC-VA and LC-VA tests requires a short testing time of approximately 5–10 min. Even though HC-VA has demonstrated normal results, patients with ON often complain of "discomfort" in their vision (13). HC-VA often did not differentiate slight changes in visual function by ON and cannot detect subtle visual disturbance or recovery over time (8, 19).

Previous studies investigated LC-VA and identified it to be a highly reliable visual assessment method in MS patients with and without ON (20). Additionally, the clinical relationship between ON or worsening LC-VA has been demonstrated (14, 19, 21), which suggests its role as an early indicator of ON associated with the visual disturbance (21). However, there have been limitations such as the lack of comparative studies in a large number of patients and being studied only in MS patients (19, 21). In our study, we applied the LC-VA test in a large number of patients with ON including more NMOSD patients than MS patients. We additionally analyzed the ROC in the subgroup of MS patients. As with the previous studies, 2.5% LC-VA was found to be most useful for detecting ON in the MS patient group (**Supplementary Table 1**). Thus, this study on a large number of demyelinating diseases added to evidence that LC-VA can be useful to detect significant visual dysfunction in both MS and NMOSD, especially in eyes with mild ON.

The very faint letters of 1.25% LC-VA are difficult to distinguish by healthy eyes. Our study also demonstrated that 2.5% LC-VA had high sensitivity and specificity for the detection

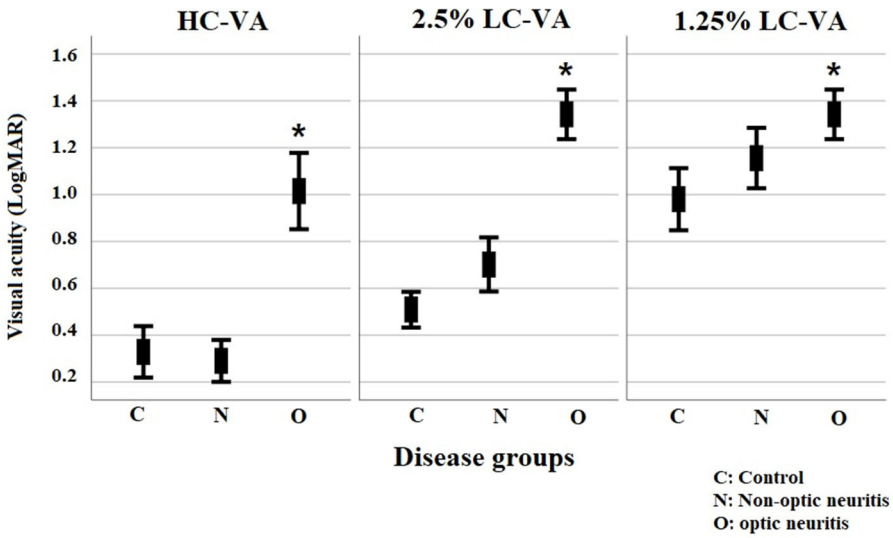

FIGURE 1 | Visual functions for high-contrast visual acuity and for Sloan charts at 2.5% and 1.25% contrast levels. VA, visual acuity; HC-VA, high contrast visual acuity; LC-VA, low contrast visual acuity. *$p < 0.05$, control vs ON.

TABLE 3 | Receiver operating characteristic curve analysis of visual functions to discriminate between ON and non-ON or control.

	AUC (95% CI)	*P*-value	Cutoff value	Specificity	Sensitivity	J-index
ON (*n* = 137) vs. non-ON (*n* = 79)						
HC-VA	0.710 (0.654–0.775)	<0.001	0.450	71.4%	64.2%	0.357
2.5% LC-VA	0.835 (0.780–0.891)	<0.001	0.715	88.6%	71.5%	0.601
1.25% LC-VA	0.770 (0.697–0.843)	<0.001	1.300	70.0%	78.8%	0.488
ON (*n* = 137) vs. control (*n* = 70)						
HC-VA	0.719 (0.652–0.785)	<0.001	0.450	83.5%	55.5%	0.390
2.5% LC-VA	0.754 (0.687–0.821)	<0.001	0.750	78.5%	71.5%	0.500
1.25% LC-VA	0.688 (0.611–0.764)	<0.001	1.300	57.0%	78.8%	0.358

HC-VA, high contrast visual acuity; LC-VA, low contrast visual acuity; ON, optic neuritis; Non-ON, non-optic neuritis; AUC, area under the receiver operating characteristic curve; CI, confidence interval.

of ON than did 1.25% LC-VA. Additionally, our study revealed that 2.5% LC-VA might detect subclinical ON that was missed by HC-VA in comparison with non-ON and control. Therefore, it is suggested that 2.5% LC-VA can be the most useful method to identify ON than HC-VA or 1.25% LC-VA.

A comparison of the sensitivity of these techniques (HC-VA and 2.5% LC-VA) has not been performed previously. As mentioned before, 1.25% LC-VA has a worse value of visual acuity even for the healthy eyes. Therefore, except 1.25% LC-VA, this study revealed a novel finding that the combination of HC-VA and 2.5% LC-VA significantly improved the sensitivity for the detection of ON than each of the techniques individually. These results are very important to make its use realizable in busy clinical settings or research for finding evidence to diagnose ON.

This study had several limitations. First, this was a single-center study. Additional multicenter studies should be conducted. Second, this study evaluated only Asians and more NMOSD patients than MS patients due to local epidemiological factors in South Korea. Therefore, in this study, a larger group of NMOSD could have a significant impact compared to the previous studies of other races. Third, our study was a retrospective study. Disease duration and number of events for individual patients varied significantly. We only analyzed the cases more than 3 months after ON. Therefore, our study helps to find remote ON attack evidence. Further study is needed for the utility of LC-VA in acute ON. Fourth, we could not calculate the cutoff value with the ROC curve of each visual test to discriminate between MS and NMOSD due to each group having eyes with very different visual severity. Retinal damage, including retinal nerve fiber layer and ganglion cell layer thinning, and VA is more severe with the number of ON attacks and relatively more severe in NMOSD than in MS (22). Therefore, very severe residual visual disturbance (<0.4 decimal in HC-VA) after the first episode of ON was suggested as an indicator of NMOSD compared with MS (23). If each group has large numbers of eyes with first ON presenting comparable visual severity, comparison of each visual test between MS and NMOSD can be possible. Further studies are warranted to investigate the cutoff values of LC-VA and its potential implications for the diagnosis in NMOSD or MS. Fifth, our study checked only the NMO-IgG in patients. Recently, myelin oligodendrocyte glycoprotein antibody (MOG-IgG) was found in a subset of

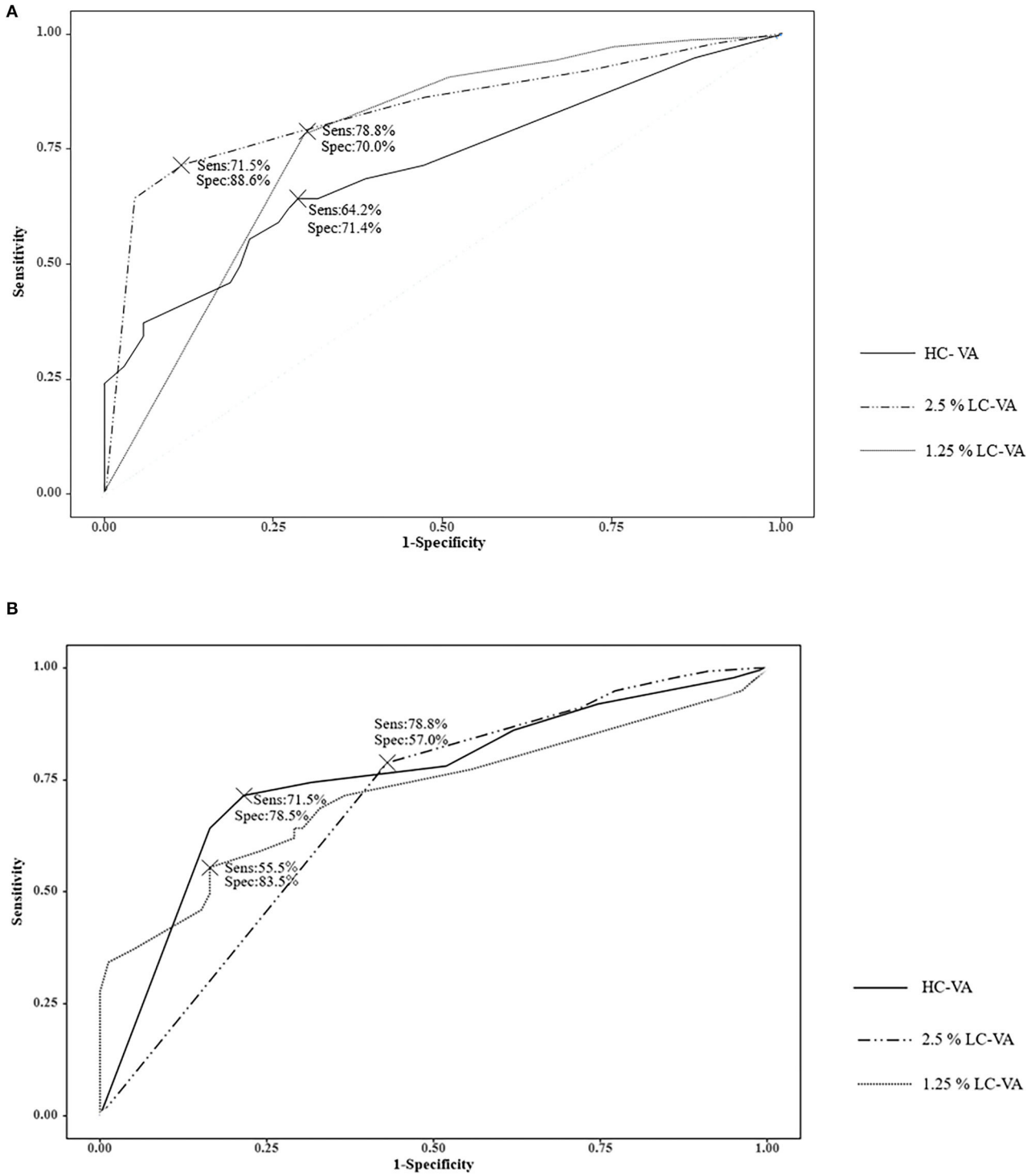

FIGURE 2 | Receiver operating characteristic (ROC) curve. **(A)** ROC curve analysis of the visual functions to discriminate between ON and Non-ON. **(B)** ROC curve analysis of the visual functions to discriminate between controls and ON. Sens, sensitivity; Spec, specificity; VA, visual acuity; HC-VA, high contrast visual acuity; LC-VA, low contrast visual acuity.

NMOSD-IgG negative NMOSD patients, extending the range of NMOSD (24–26). Therefore, patients with MOG-IgG positive require further investigation.

In conclusion, our study suggests that LC-VA can better detect the visual disturbance in ON than HC-VA in NMOSD as well as MS (8, 11, 14, 19–21, 27). Considering all of those, 2.5%

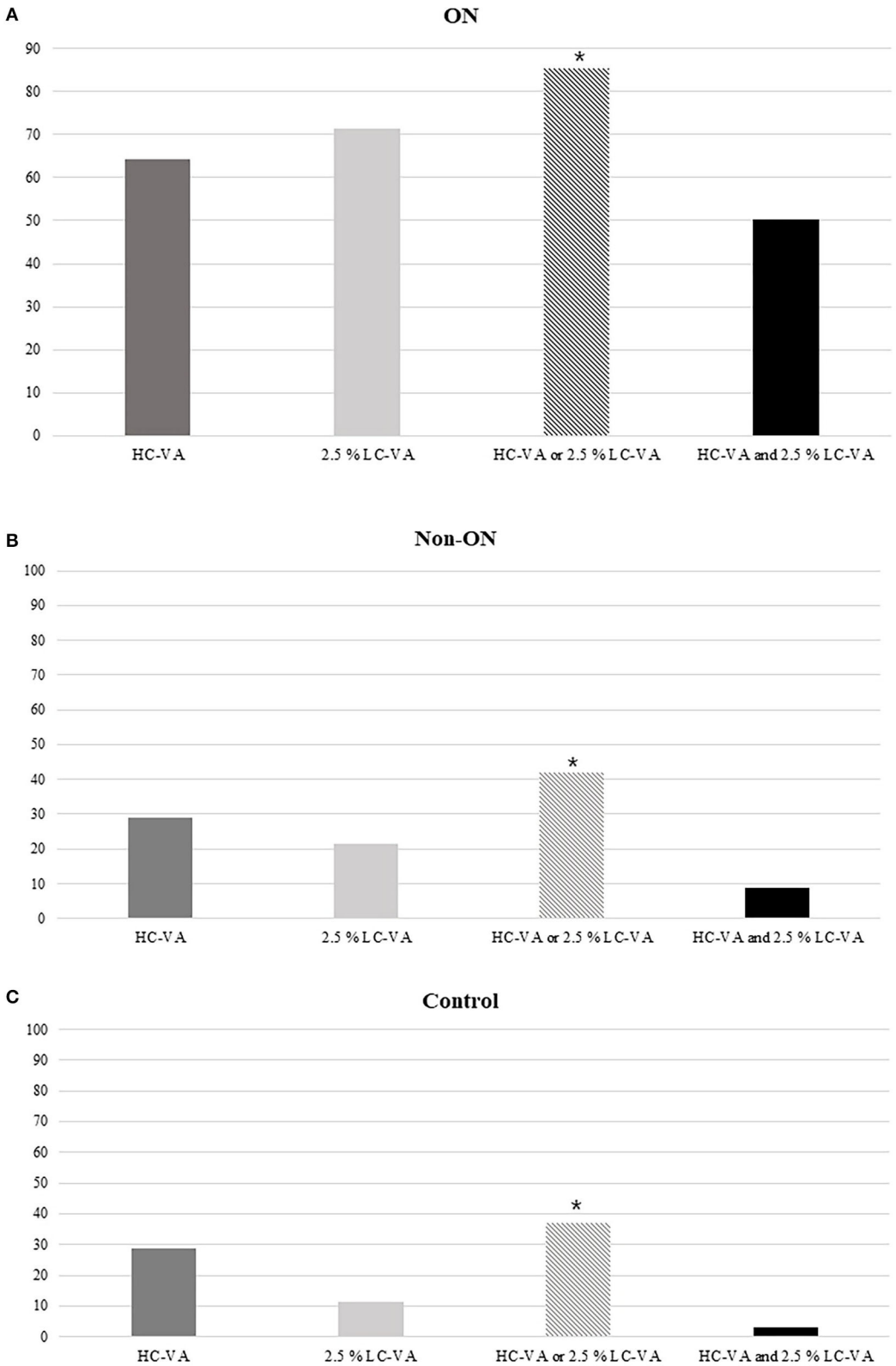

FIGURE 3 | Percentages of abnormal tests. **(A)** Percentages of the abnormal tests in ON. **(B)** Percentages of abnormal tests in Non-ON. **(C)** Percentages of abnormal tests in the control. HC-VA or 2.5% LC-VA, eyes with at least one abnormal HC-VA or 2.5% LC-VA finding; HC-VA and 2.5% LC-VA, eyes with abnormal HC-VA and abnormal 2.5% LC-VA findings. ON, optic neuritis; non-ON, non-optic neuritis; VA, visual acuity; HC-VA, high contrast visual acuity; LC-VA, low contrast visual acuity. *$p < 0.05$, control vs ON.

LC-VA might be the most useful, feasible, and rapid method to detect evidence of ON and could be used as a potential additive diagnostic tool of ON. HC-VA and 2.5% LC-VA test may yield more powerful result for ON detection in clinical practice.

DATA AVAILABILITY STATEMENT

The original contributions presented in the study are included in the article/**Supplementary Materials**, further inquiries can be directed to the corresponding author/s.

ETHICS STATEMENT

The studies involving human participants were reviewed and approved by the Institutional Review Board of Dongguk University Ilsan Hospital. The patients/participants provided their written informed consent to participate in this study. Written informed consent was obtained from the individual(s) for the publication of any potentially identifiable images or data included in this article.

AUTHOR CONTRIBUTIONS

S-HP, CYP, YJS, KSJ, and N-HK: conception and organization of the research project. S-HP, CYP, YJS, and N-HK: execution of the research project. S-HP, KSJ, and N-HK: analysis and interpretation, and review and critique of the manuscript. S-HP and N-HK: writing of the first draft of the manuscript. All authors contributed to the article and approved the submitted version.

FUNDING

This work was supported by the National Research Foundation (NRF) of Korea, funded by a Medical Research Center Grant (NRF-2014R1A5A2009392).

SUPPLEMENTARY MATERIAL

The Supplementary Material for this article can be found online at: https://www.frontiersin.org/articles/10.3389/fneur.2020.602193/full#supplementary-material

REFERENCES

1. Pau D, Al Zubidi N, Yalamanchili S, Plant G, Lee AG. Optic neuritis. *Eye.* (2011) 25:833–42. doi: 10.1038/eye.2011.81
2. Cole SR, Beck RW, Moke PS, Gal RL, Long DT, Optic Neuritis Study Group. The national eye institute visual function questionnaire: experience of the ONTT. *Invest Ophthalmol Vis Sci.* (2000) 4:1017–21. Available online at: https://iovs.arvojournals.org/article.aspx?articleid=2123148
3. Bock M, Brandt AU, Kuchenbecker J, Dörr J, Pfueller CF, Weinges-Evers N, et al. Impairment of contrast visual acuity as a functional correlate of retinal nerve fibre layer thinning and total macular volume reduction in multiple sclerosis. *Br J Ophthalmol.* (2012) 96:62–77. doi: 10.1136/bjo.2010.193581
4. Balcer L, Raynowska J, Nolan R, Galetta S, Kapoor R, Benedict R, et al. Multiple sclerosis outcome assessments consortium. Validity of low-contrast letter acuity as a visual performance outcome measure for multiple sclerosis. *Mult Scler.* (2017) 23:734–47. doi: 10.1177/1352458517690822
5. Wingerchuk DM, Banwell B, Bennett JL, Cabre P, Carroll W, Chitnis T, et al. International consensus diagnostic criteria for neuromyelitis optica spectrum disorders. *Neurology.* (2015) 85:177–89. doi: 10.1212/WNL.0000000000001729
6. Thompson AJ, Banwell BL, Barkhof F, Carroll WM, Coetzee T, Comi G, et al. Diagnosis of multiple sclerosis: 2017 revisions of the McDonald criteria. *Lancet Neurol.* (2018) 17:162–73. doi: 10.1016/S1474-4422(17)30470-2
7. Regan D, Raymond J, Ginsburg A, Murray TJB. Contrast sensitivity, visual acuity and the discrimination of Snellen letters in multiple sclerosis. *Brain.* (1981) 104:333–50. doi: 10.1093/brain/104.2.333
8. Balcer LJ, Frohman EMJN. Evaluating loss of visual function in multiple sclerosis as measured by low-contrast letter acuity. *Neurology.* (2010) 74:S16–S23. doi: 10.1212/WNL.0b013e3181dbb664
9. Lange C, Feltgen N, Junker B, Schulze-Bonsel K, Bach M. Resolving the clinical acuity categories "hand motion" and "counting fingers" using the freiburg visual acuity test (FrACT). *Graefes Arch Clin Exp Ophthalmol.* (2009) 247:137–42. doi: 10.1007/s00417-008-0926-0
10. Owidzka M, Wilczynski M. Evaluation of contrast sensitivity measurements after retrobulbar optic neuritis in multiple sclerosis. *Graefes Arch Clin Exp Ophthalmol.* (2014) 252:673–77. doi: 10.1007/s00417-014-2590-x
11. Schneck ME, Haegerstrom-Portnoy G. Color vision defect type and spatial vision in the optic neuritis treatment trial. *Invest Ophthalmol Vis Sci.* (1997) 38:2278–89.
12. Voss E, Raab P, Trebst C, Stangel M. Clinical approach to optic neuritis: pitfalls, red flags and differential diagnosis. *Ther Adv Neurol Disord.* (2011) 4:123–34. doi: 10.1177/1756285611398702
13. Balcer L, Baier M, Cohen J, Kooijmans M, Sandrock A, Nano–Schiavi M, et al. Contrast letter acuity as a visual component for the multiple sclerosis functional composite. *Neurology.* (2003) 61:1367–73. doi: 10.1212/01.WNL.0000094315.19931.90
14. Balcer LJ, Galetta SL, Polman CH, Eggenberger E, Calabresi PA, Zhang A, et al. Low-contrast acuity measures visual improvement in phase 3 trial of natalizumab in relapsing MS. *J Neurol Sci.* (2012) 318:119–24. doi: 10.1016/j.jns.2012.03.009
15. Sakai RE, Feller DJ, Galetta KM, Galetta SL, Balcer LJ. Vision in multiple sclerosis (ms): the story, structure-function correlations, and models for neuroprotection. *J Neuroophthalmol.* (2011) 31:362–73. doi: 10.1097/WNO.0b013e318238937f
16. Balcer LJ, Miller DH, Reingold SC, Cohen JA. Vision and vision-related outcome measures in multiple sclerosis. *Brain.* (2015) 138:11–27. doi: 10.1093/brain/awu335
17. Hoorbakht H, Bagherkashi F. Optic neuritis, its differential diagnosis and management. *Open Ophthalmol J.* (2012) 6:65–72. doi: 10.2174/1874364101206010065
18. Galetta SL, Villoslada P, Levin N, Shindler K, Ishikawa H, Parr E, et al. Acute optic neuritis: unmet clinical needs and model for new therapies. *Neurol Neuroimmunol Neuroinflamm.* (2015) 2:e135. doi: 10.1212/NXI.0000000000000135
19. Öcek Ö, Gedizlioglu M, Köşkderelioglu A, Ortan PK, Yüksel B, Türe M, et al. The value of tests evaluating visual functions in detecting overt or subclinical optic neuritis in multiple sclerosis. *Mult Scler Relat Disord.* (2018) 21:63–8. doi: 10.1016/j.msard.2018.01.030
20. Balcer LJ, Baier ML, Pelak VS, Fox RJ, Shuwairi S, Galetta SL, et al. New low-contrast vision charts: reliability and test characteristics in patients with multiple sclerosis. *Mult Scler.* (2000) 6:163–71. doi: 10.1177/135245850000600305
21. Longbrake EE, Lancia S, Tutlam N, Trinkaus K, Naismith RT. Quantitative visual tests after poorly recovered optic neuritis due to multiple sclerosis. *Mult Scler Relat Disord.* (2016) 10:198–203. doi: 10.1016/j.msard.2016.10.009
22. Thurtell MJ, Bala E, Yaniglos SS, Rucker JC, Peachey NS, Leigh RJ. Evaluation of optic neuropathy in multiple sclerosis using low-contrast visual evoked potentials. *Neurology.* (2009) 73:1849. doi: 10.1212/WNL.0b013e3181c3fd43

23. Kim NH, Kim HJ, Park CY, Jeong KS. Retinal degeneration after first-ever optic neuritis helps differentiate multiple sclerosis and neurymyelitis optica spectrum disorder. *Front Neurol.* (2019) 10:1076. doi: 10.3389/fneur.2019.01076
24. Pache F, Zimmermann H, Mikolajczak J, Schumacher S, Lacheta A, Oertel FC, et al. MOG-IgG in NMO and related disorders: a multicenter study of 50 patients. Part 4: afferent visual system damage after optic neuritis in MOG-IgG-seropositive versus AQP4-IgG-seropositive patients. *J Neuroinflammation.* (2016) 13:282. doi: 10.1186/s12974-016-0720-6
25. Schmidt F, Zimmermann H, Mikolajczak J, Oertel FC, Pache F, Weinhold M, et al. Severe structural and functional visual system damage leads to profound loss of vision-related quality of life in patients with neuromyelitis optica spectrum disorders. *Mult Scler Relat Disord.* (2017) 11:45–50. doi: 10.1016/j.msard.2016.11.008
26. Zamvil SS, Slavin AJ. Does MOG Ig-positive AQP4-seronegative opticospinal inflammatory disease justify a diagnosis of NMO spectrum disorder? *Neurol Neuroimmunol Neuroinflamm.* (2015) 2:e62. doi: 10.1212/NXI.0000000000000062
27. Balk LJ, Coric D, Nij Bijvank JA, Killestein J, Uitdehaag BM, Petzold A. Retinal atrophy in relation to visual functioning and vision-related quality of life in patients with multiple sclerosis. *Mult Scler.* (2018) 24:767–76. doi: 10.1177/1352458517708463

Conflict of Interest: The authors declare that the research was conducted in the absence of any commercial or financial relationships that could be construed as a potential conflict of interest.

Copyright © 2020 Park, Park, Shin, Jeong and Kim. This is an open-access article distributed under the terms of the Creative Commons Attribution License (CC BY). The use, distribution or reproduction in other forums is permitted, provided the original author(s) and the copyright owner(s) are credited and that the original publication in this journal is cited, in accordance with accepted academic practice. No use, distribution or reproduction is permitted which does not comply with these terms.

frontiers in Neurology

ORIGINAL RESEARCH
published: 13 January 2021
doi: 10.3389/fneur.2020.601628

Neuroprotective Properties of Dimethyl Fumarate Measured by Optical Coherence Tomography in Non-inflammatory Animal Models

*Michael Dietrich, Christina Hecker, Milad Nasiri, Sogol Samsam, Andrea Issberner, Zippora Kohne, Hans-Peter Hartung and Philipp Albrecht**

Department of Neurology, Medical Faculty, Heinrich-Heine University Düsseldorf, Düsseldorf, Germany

While great advances have been made in the immunomodulatory treatment of multiple sclerosis (MS), there is still an unmet need for drugs with neuroprotective potential. Dimethyl fumarate (DMF) has been suggested to exert both immunomodulatory and neuroprotective effects in MS. To investigate if DMF has neuroprotective effects independent of immunomodulation we evaluated its effects in the non-inflammatory animal models of light-induced photoreceptor loss and optic nerve crush. This might also reveal applications for DMF besides MS, such as age related macular degeneration. Retinal neurodegeneration was longitudinally assessed by *in vivo* retinal imaging using optical coherence tomography (OCT), and glutathione (GSH) measurements as well as histological investigations were performed to clarify the mode of action. For light-induced photoreceptor loss, one eye of C57BL/6J mice was irradiated with a LED cold light lamp while for optic nerve crush the optic nerve was clamped behind the eye bulb. The other eye served as control. GSH was measured in the optic nerve, choroid and retina and immunohistological staining of retinal microglia (Iba1) was performed. Mice were treated with 15 or 30 mg DMF/kg bodyweight or vehicle. While no protective effects were observed in optic nerve crush, in the light-induced retinal degeneration model DMF treatment significantly reduced retinal degeneration. In these mice, GSH levels in the retina and surrounding choroid were increased and histological investigations revealed less microglial activation in the outer retinal layers, suggesting both antioxidant and anti-inflammatory effects.

Keywords: dimethyl fumarate, neuroprotection, optical coherence tomography, optic nerve crush, light-induced photoreceptor loss

OPEN ACCESS

Edited by:
Claudia Angela Michela Gandini Wheeler-Kingshott, University College London, United Kingdom

Reviewed by:
Christian Cordano, University of California, San Francisco, United States
Pengfei Zhang, University of California, Davis, United States

****Correspondence:***
Philipp Albrecht
phil.albrecht@gmail.com

Specialty section:
This article was submitted to Neuro-Ophthalmology, a section of the journal Frontiers in Neurology

Received: *01 September 2020*
Accepted: *15 December 2020*
Published: *13 January 2021*

Citation:
Dietrich M, Hecker C, Nasiri M, Samsam S, Issberner A, Kohne Z, Hartung H-P and Albrecht P (2021) Neuroprotective Properties of Dimethyl Fumarate Measured by Optical Coherence Tomography in Non-inflammatory Animal Models. Front. Neurol. 11:601628. doi: 10.3389/fneur.2020.601628

INTRODUCTION

There is an urgent unmet need for new therapeutic approaches effectively preventing the chronic progression of disability and promoting repair in autoimmune diseases of the central nervous system like multiple sclerosis (MS) (1). Fumaric acid esters including dimethyl fumarate (DMF) have previously been used to treat autoimmune disorders like psoriasis and arthritis, where they exert anti-inflammatory effects (2). After two positive phase II trials (3, 4), DMF proved positive for most primary and secondary outcome parameters in the subsequent two large phase-III-trials

(5, 6) and has been approved as a disease-modifying therapy for the treatment of relapsing MS. The immunomodulatory effects of DMF have been studied *in vitro* and *in vivo*, revealing effects in several cell types, in particular T-cells. DMF and other fumaric esters have been reported to induce a shift from "Th1" cytokines (IL-2, TNF-α, IFN-γ) to "Th2" cytokines (IL-4, IL-5) as part of their treatment effect in human psoriasis. On the molecular level, these effects were reported to be due to inhibition of the NF-κB pathway (7).

In vitro, DMF and its primary metabolite monomethyl fumarate stabilized Nuclear factor erythroid 2-related factor 2 (Nrf2) and stimulated the Nrf2-dependent transcriptional activity of genes with antioxidant response elements (ARE) in their promoters, thereby increasing the expression of the ARE-driven genes NQO1, xCT, and GCL (8–10). *In vivo*, increased levels of Nrf2 and NQO1 activity were detected in the CNS of DMF-treated animals (9, 10). In MS patients, DMF treatment affected mainly memory T cells, resulting in a shift from Th1 toward Th2 responses (11). Although these anti-inflammatory and neuroprotective effects are attributed to DMF, its multifactorial mode of action is still not fully unraveled.

Optical coherence tomography (OCT) is a fast, non-invasive, interferometric technique allowing high resolution imaging of the eye's retina in patients and mice (12, 13). The *in vivo* assessments of retinal neurodegeneration hence allow preclinical studies that are directly transferable to clinical trials. Furthermore, the retinal degeneration of MS patients not only represents a morphological correlate of the functional visual deficits but also mirrors the overall disability assessed by clinical scores (14). Therefore, the anterior visual pathway is increasingly being used for clinical trials evaluating neuroprotective or remyelinating strategies (13). This makes OCT an ideal tool for visualizing the potential of DMF to prevent from neuroaxonal degeneration. In this study, we therefore investigated the effect of DMF in the non-inflammatory models optic nerve crush (ONC) and light-induced photoreceptor loss (Li-PRL). Axonal injury is a major pathological event during MS and therefore the ONC is suited to study protective effects of DMF independently of immunomodulation. The light-induced stress model might not be directly related to MS, however, the retinal degeneration is resulting from overstimulation of photoreceptors leading to accumulation of reactive oxygen species, which play a major role in MS. Additionally the model might reveal treatment options for other ocular pathologies, such as age related macular degeneration (AMD).

After the ONC and retinal irradiation an analysis of the visual pathway by OCT, histology and measurement of the important antioxidant glutathione was performed.

MATERIALS AND METHODS

Optic Nerve Crush

For the optic nerve crush, female, 6 weeks old C57BL6/J mice were used. The optic nerve was grasped approximately 3 mm from the globe with a bended forceps for 10 s. To assure a standardized clamping pressure only the self-clamping mechanism of the forceps was used to crush the nerve. The other eye served as control. DMF stock solution was prepared at 20 mg/mL in dimethyl sulfoxide (DMSO, Sigma-Aldrich) and stored at −80°C until use. Treatment started 1 week before the surgery by adding DMF for verum therapy or DMSO alone for vehicle control to the drinking water. Drinking water was replaced twice a week, uptake was measured daily, and the concentrations of the substances were adjusted to a daily treatment dose of 15 and 30 mg/kg body weight (BW) DMF per day.

Light-Induced Photoreceptor Loss

Mice (female, 6 weeks old C57BL6/J) were anesthetized (oxygen 20 mL/min with isoflurane (2 vol.%)) and the pupil of the eye was dilated with 0.5% Tropicamide/2.5% Phenylephrine before irradiation. An eye gel was applied to both eyes to prevent dehydration and the formation of cataracts. One eye was irradiated with an LED cold light lamp (KL 1500 LCD, Carl Zeiss AG, Germany) for 10 min at maximum light intensity and fully opened shutter (600 lumen, distance of optical fiber head and eye: 3 cm). The other eye was covered and served as control. During the irradiation procedure, the animals were kept warm by a heating mat. DMF treatment was started 1 week before the irradiation with 30 mg/kg BW or vehicle per os.

Optical Coherence Tomography Measurement

The measurements of retinal layers were performed using a Spectralis™ HRA+OCT device (Heidelberg Engineering, Germany) under ambient light conditions. The OCT device was equipped with several adaptions for rodents described elsewhere (15) and the scanning protocol was executed as previously described (16). Volume scans were used, which have recently reported to provide excellent inter-rater reliability (interclass correlation coefficient above 0.9) and high reproducibility (17). All measurements were performed using the TruTrack™ automated eye-tracking system incorporated in the Heidelberg Eye Explorer™ software, ensuring that the same area of the retina was assessed in all follow-up measurements. We report the methodology in line with the APOSTEL recommendations (18). Automated segmentation was carried out by the Heidelberg Eye Explorer™ software version 1.9.10.0 followed by manual correction of an investigator, blinded for the experimental groups. We calculated the total thickness of the retina (TRT), the inner retinal layers (IRL), consisting of the retinal nerve fiber layer, ganglion cell layer and inner plexiform layer as described elsewhere (19) as well as the outer retinal layers (ORL), consisting of the outer plexiform layer, outer nuclear layer and the photoreceptors. The different layers of the OCT scans are illustrated in **Figure 1A**. High-resolution mode was used; only scans with a quality of at least 20 decibels were included.

Iba1 Staining of the Optic Nerve

At the endpoint of the experiment (7 weeks for ONC and 10 weeks for Li-PRL), mice were sacrificed with an overdose of Isofluran (Piramal Critical Care). Ketamine (50 mg/kg, i.p.) was administered for analgesia before cardiac perfusion was performed with cold phosphate-buffered saline (PBS). Eyes were isolated and fixated in 4% PFA over night at 4°C and dehydrated

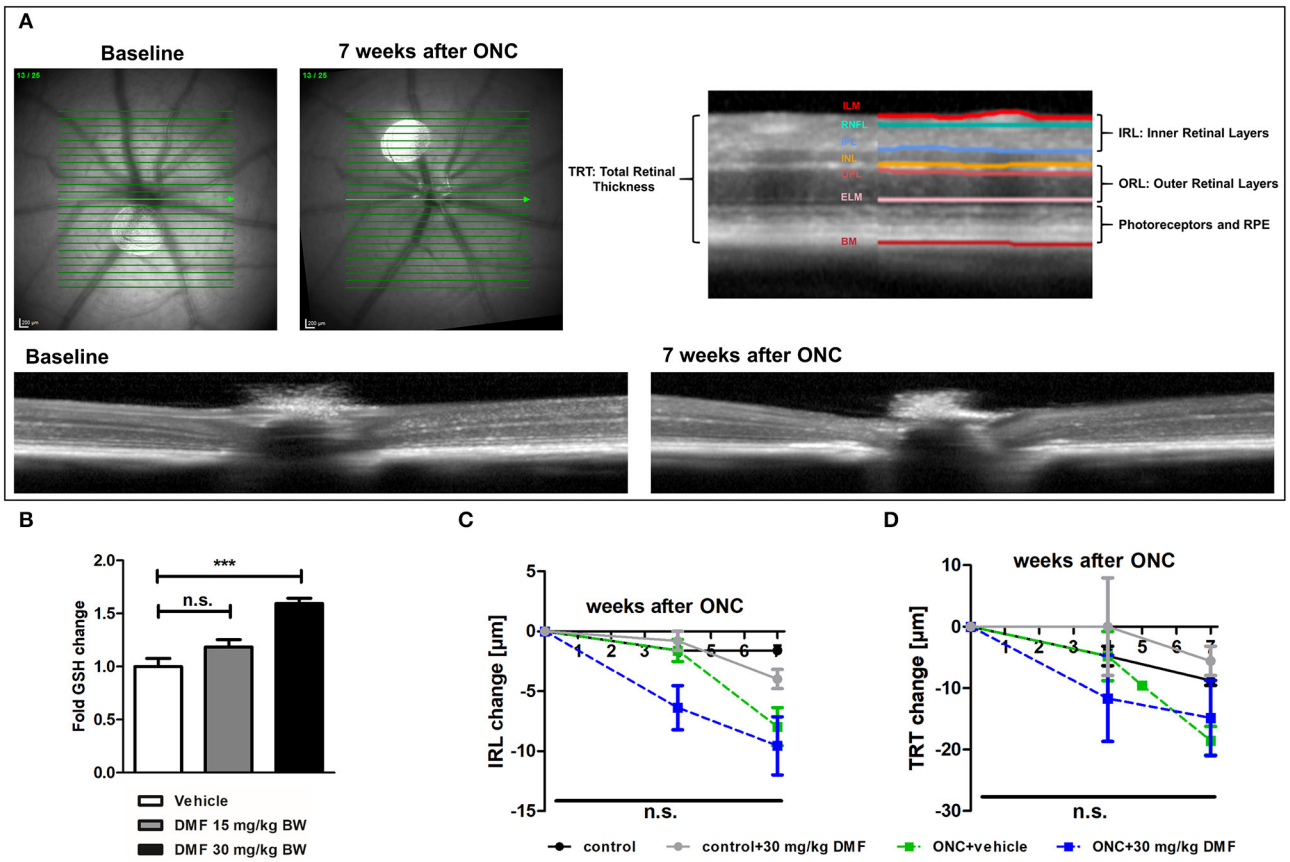

FIGURE 1 | OCT scan of C57Bl/6J mouse retina and ON-crush with GSH in optic nerve and retinal scans. **(A)** Retinal fundus and B-scans of mice before and 7 weeks after ON-crush with Heidelberg Engineering Spectralis^{TM} HRA+OCT device with semi-automated segmentation of the retinal layers. ILM, Inner Limiting Membrane; RNFL, Retinal Nerve Fiber Layer; IPL, Inner Plexiform Layer; INL, Inner Nuclear Layer; OPL, Outer Plexiform Layer; ELM, External Limiting Membrane; BM, Bruch's Membrane; RPE, Retinal Pigment Epithelium. **(B)** The GSH concentration in optic nerve tissue of mice treated with 15 or 30 mg/kg BW DMF at 7 weeks after ONC. Degeneration of the **(C)** total retinal thickness and **(D)** inner retinal layers and of mice over 7 weeks after ONC. All graphs represent the pooled mean ± SEM; $n = 3$ animals per group. $^{***}p < 0.001$ by ANOVA with Dunnett's *post hoc* test compared to vehicle for **(A)** and area under the curve compared by ANOVA with Dunnett's *post hoc* test for time courses compared to control for **(C)** and **(D)**.

in ethanol solutions with increasing concentrations. After embedding in paraffin (Paraplast, Leica, Germany), longitudinal sections of 5 µm were cut for immunohistological analysis. Slices of the retinae were incubated with an Iba1 antibody (1:500, Wako chemicals). Cy3 anti-rat (1:500, Millipore) was used as secondary antibody. Microglial infiltration and activation was quantified by fluorescence intensity measurement of the Iba1 staining. Fluorescence stained longitudinal optic nerve sections were acquired with a Leica HyD detector attached to a Leica DMi8 confocal microscope (63x objective lens magnification). At least four sections of the optic nerve from one eye of each mouse were analyzed per staining.

Glutathione Measurement

For glutathione (GSH) measurements, frozen tissue samples (optic nerve, choroid or retina) from the endpoint of the experiment were homogenized using a micro pestle in PBS/EDTA buffer, sonicated and transferred to lysis buffer. Tissue was further processed and measured enzymatically as previously described (8) using the whole protein amount assessed by the bicinchoninic acid assay for normalization.

Ethics

All animal procedures were performed in compliance with the experimental guidelines approved by the regional authorities (The Ministry for Environment, Agriculture, Conservation and Consumer Protection of the State of North Rhine-Westphalia; AZ 84-02.4.2014.A059 and AZ 84-02.04.2016.A137) and conform to the Association for Research in Vision and Ophthalmology (ARVO) Statement for the Use of Animals in Ophthalmic and Vision Research.

Statistics

Statistical analysis was performed using Prism 5 (version 5.00, Graphpad Software, Inc., USA) and IBM SPSS Statistics (version 20, IBM Corporation, USA). A one-way analysis of variance (ANOVA) with Dunnett's *post hoc* test was used to compare means of multiple groups to the control group and a Student's

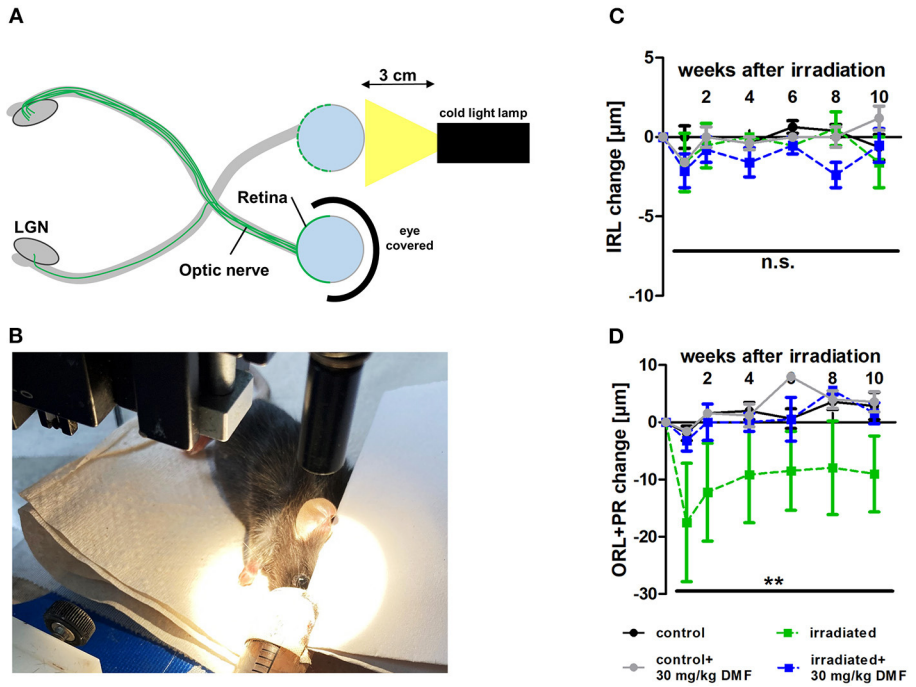

FIGURE 2 | Retinal degeneration after light-induced photoreceptor loss (Li-PRL). **(A)** Schematic image of Li-PRL and **(B)** image of irradiation of C57Bl/6J mouse. **(C)** Change of inner retinal layers (IRL) and **(D)** outer retinal layers (ORL) with photoreceptors (PR) of mice over 10 weeks after Li-PRL. All graphs represent the pooled mean ± SEM; $n = 3$ animals per group. $^{**}p < 0.01$ by area under the curve compared by ANOVA with Dunnett's *post hoc* test compared to irradiated control. LGN = lateral geniculate nucleus.

t-test was used to compare the means of two groups for histology and GSH measurements. For these analyses, one eye/optic nerve per animal was included in the analysis. For *in vivo* measurements, differences in retinal thickness were analyzed using area under the curve compared by ANOVA followed by Dunnett's *post hoc* test.

RESULTS

DMF Is Not Effective in Optic Nerve Crush

As first experimental approach, an optic nerve crush was performed in C57Bl/6J mice with and without prophylactic DMF (15 or 30 mg/kg BW, per os) treatment, starting 1 week before the surgery. Treatment with 30 mg/kg BW, but not 15 mg/kg BW DMF resulted in an increased GSH level in the optic nerve 7 weeks after the crush (**Figure 1B**). The retinal thickness was measured by OCT over 7 weeks with the follow-up function of the Heidelberg Engineering software. The measurement revealed that the optic nerve crush led to a strong degeneration of the inner retinal layer (IRL) (**Figures 1A,C**) and a decrease of the total retinal thickness. The loss of retinal tissue was a dynamic process, showing continuous degeneration over the 7 weeks (**Figure 1D**). We found an elevated level of the antioxidant GSH in the optic nerve of mice treated with 30 mg/kg BW DMF, while 15 mg/kg did not significantly increase GSH. The augmented GSH level was however not accompanied by a protective effect of DMF from tissue loss: Retinal degeneration after ONC progressed at the same level under DMF therapy as in vehicle treated mice (**Figures 1C,D**). Of note, the contralateral eye, which served as an internal control (no crush), also showed retinal degeneration at 7 weeks after the crush (TRT: −7.16 µm ± 2.4 µm; IRL: −2.78 ± 1.3 µm).

DMF Reveals Protective Capacities After Light-Induced Retinal Damage

As DMF led to an increase of total glutathione in optic nerve tissue in the ONC model, suggesting possible protective effects in a less severe model, light-induced photoreceptor loss was performed, treating animals using the same dosing protocol: DMF 30 mg/kg BW, per os, starting 7 days before the irradiation. One eye was irradiated at maximum power (600 lumen) for 10 min, while the other eye was covered and served as a control (**Figures 2A,B**). While the inner retinal layer thickness remained unchanged after irradiation over 10 weeks regardless of the treatment (**Figure 2C**), the outer retinal layers and photoreceptors showed a strong degeneration already after 1 week, regaining thickness until week 4 after Li-PRL. In contrast to the ONC, in mice treated prophylactically with 30 mg/kg BW DMF, the degeneration of the ORL and photoreceptors was completely prevented (**Figure 2D**) over 10 weeks.

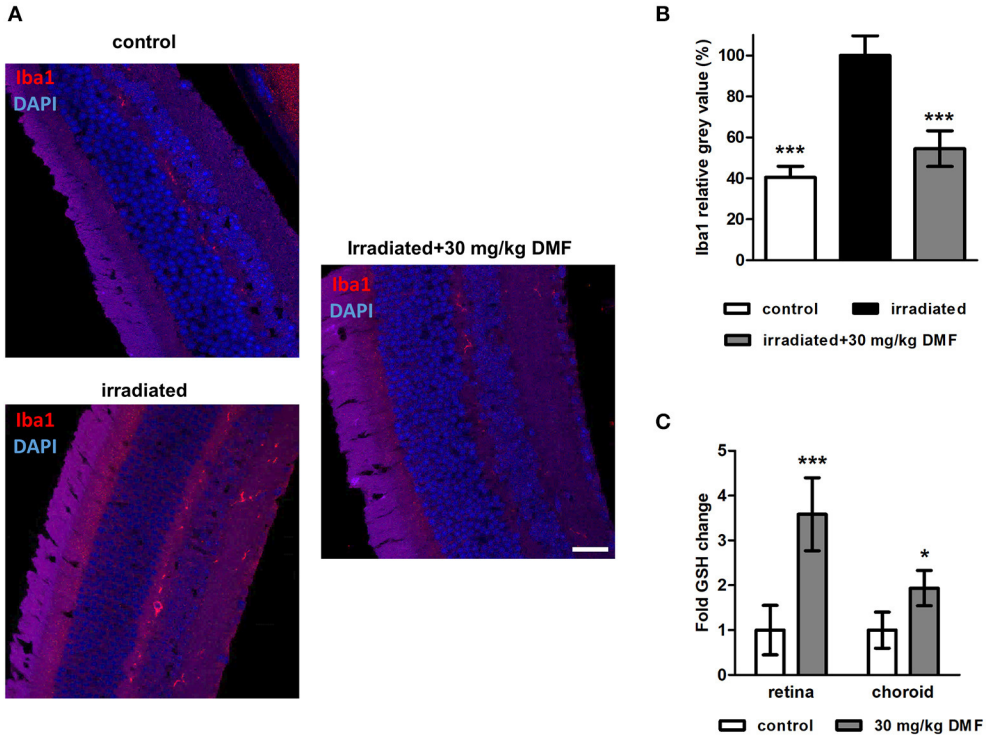

FIGURE 3 | Microglia staining and GSH measure in visual system after Li-PRL. **(A)** Longitudinal sections of retinae of mice 10 weeks after Li-PRL stained for Iba1. **(B)** Quantitative analyses of microglial activation by fluorescence intensity measurement; one eye per mouse was included. **(C)** GSH concentration in retina and choroid tissue of mice treated with 30 mg/kg BW DMF. All graphs represent the pooled mean ± SEM; $n = 3$ animals per group. $^{***}p < 0.001$, $^{*}p < 0.05$ by ANOVA with Dunnett's *post hoc* test.

Protection by DMF Is Mediated by Anti-inflammatory and Antioxidant Properties

Ten weeks after the Li-PRL, mice were sacrificed and longitudinal sections of the retina were stained for Iba1, a protein highly expressed in activated microglia and macrophages (**Figure 3A**). The irradiation led to an increased of Iba1^{+} cells, suggesting an enhanced microglial activation and/or macrophage infiltration, even 10 weeks after the overstimulation of the photoreceptors. These cells were mainly located in the outer retinal layers. In the non-irradiated control eye, almost no Iba1^{+} cells were detectable. DMF treatment diminished the increased activation of microglia and macrophages, leading to a baseline level of Iba1 in the retina (**Figure 3B**). Enzymatic measurement of the antioxidant GSH in the retina and surrounding choroid tissue of DMF treated mice showed an upregulation of total tissue glutathione by 3.5- and 2-fold, respectively (**Figure 3C**). The irradiation itself had no effect on the GSH level in the tissue (data not shown).

DISCUSSION

In the experimental autoimmune encephalomyelitis and optic neuritis (EAEON) model, an animal model for MS, DMF has already been extensively tested (9, 20, 21). This inflammatory model, inducing prominent retinal degeneration (17), is frequently used to study the protective effects of therapeutics (13). However, an increasing body of evidence suggested effects of DMF beyond the immunomodulatory characteristics (8, 9, 22). We therefore sought to characterize the effects of DMF independently of its immunomodulatory capacities using mouse models of non-inflammatory axonal damage and retinal degeneration. While the optic nerve crush induces axonal injury, which is also occurring in the progression of optic neuritis and MS, light-induced retinal stress might as well-model other ocular pathologies, such as AMD (23). In AMD, one of the most common vision-threatening diseases, the RPE is physiologically exposed to high levels of oxidative stress during its lifespan. For the well-functioning of its antioxidant systems, the Nrf2-pathway plays an important role (24). Both approaches led to a prominent degradation of retinal tissue. While the ONC damages the optic nerve mainly inducing a degeneration of the inner retinal layers, the light-induced damage affects the cells in the outer retinal layers including the photoreceptors. While the axonal damage of the optic nerve in the ONC model results in indirect Wallerian degeneration of the RNFL, the ganglion cells and their dendritic arbor, the light induced injury directly damages the retinal pigment epithelium (RPE), the photoreceptors and their cell bodies and synaptic processes in the outer nuclear and outer plexiform layer, respectively. Of note, we also observed retinal

degeneration after ON-crush in the contralateral, untreated eye. This might be due to sympathetic ophthalmia, which is a serious, bilateral uveitis that occurs after either eye surgery or penetrating or perforating eye trauma (25). The traumatic injury on the optic nerve and the surrounding tissue might therefore lead to impairment of the contralateral nerve and eye. Numerous other studies in rodents investigating retinal degeneration after ONC also found a decrease of the RNFL and TRT, as well as a loss of retinal ganglion cells (26–29). After a light-induced retinal damage, authors essentially found degeneration of the ORL and photoreceptors, in line with our results (30, 31).

Interestingly, DMF treatment only prevented retinal degeneration after Li-PRL, but not after ONC. The axonal damage in the ONC model is apparently too severe to be susceptible to the protective effects of DMF despite evidence of GSH increase in retinal tissue. Possibly, oxidative stress may not play an important role for the apoptosis of retinal ganglion cells (RGCs) in the context of the Wallerian degeneration resulting from ONC. On the other hand, the Li-PRL is resulting from overstimulation of photoreceptors leading to accumulation of reactive oxygen species, calcium overload and finally degeneration of the photoreceptors and their neurons in the outer nuclear layer. This degeneration is tightly linked to oxidative stress, which is more likely to be sensitive to the antioxidant mode of action of DMF and the resulting GSH increase. Other studies also found an enhancement of antioxidant pathways after DMF therapy. Treatment of mice with DMF or MMF resulted in increased nuclear levels of active Nrf2, with subsequent up-regulation of canonical antioxidant target genes with the effect being lost in mice lacking Nrf2 (10). In another study, DMF increased immunoreactivity for Nrf2 in neurons of the motor cortex and the brainstem as well as in oligodendrocytes and astrocyte in experimental autoimmune encephalomyelitis (EAE) mice (9). Contrastingly, Schulze-Topphoff and colleagues reported, that oral DMF therapy protected wildtype and Nrf2 deficient mice equally well from development of clinical and histologic EAE, suggesting, that the anti-inflammatory activity of DMF may occur through alternative pathways (21). *In vitro*, DMF and MMF significantly improved cell viability of astrocytes or neurons and increased glutathione levels after toxic oxidative challenge in a concentration-dependent manner (10). Additionally, DMF treatment stabilized Nrf2 and stimulated the Nrf2-dependent transcriptional activity of genes with ARE in their promoters (8, 9). In another *in vitro* study by our lab, DMF was demonstrated to increase GSH recycling through induction of glutathione reductase in the hippocampal neuronal cell line HT22 (22). Similar to our study, but in another mouse line, Jiang and colleagues treated albino BALB/c mice intraperitoneally with monomethyl fumarate (MMF), the primary metabolite of DMF, before light exposure for 1 h. 7 days later, mice were examined by OCT. MMF treatment prevented morphologic changes in the ORLs and photoreceptor layers in a dose-dependent manner (32). In an *in vitro* study, Nrf2 protected mouse photoreceptor cells from photo-oxidative stress induced by blue light (33). Interestingly, in the MS brain Nrf2 expression varies in different cell types and is associated with active demyelination in the lesions. Nuclear Nrf2 expression was particularly observed in oligodendrocytes, while only a minor number of Nrf2-positive neurons were detected, even in highly inflammatory cortical lesions. In degenerating cells, which showed signs of apoptotic or necrotic cell death, the most prominent Nrf2 expression was found (34).

To analyze the anti-inflammatory mode of action of DMF, we stained longitudinal retinal sections with the microglia marker Iba1. We found, that after light exposure, microglial activation was prominently increased in the ORL. In mice treated with DMF, this effect was diminished showing almost no Iba1 positive cells, similar to the non-irradiated condition. Similar findings were reported in the study of Jiang et al., where expression of the microglial marker Cd14 was upregulated after light exposure, but suppressed after MMF treatment (32). In an *in vivo* EAE study, treatment with DMF ameliorated clinical disability in C57Bl/6 mice and modulated activated microglia from a classically activated, pro-inflammatory phenotype to an alternatively activated, neuroprotective phenotype, presumably by activation of the hydroxycarboxylic acid receptor 2 (35).

Our own findings of neuroprotective capacities of DMF in the non-inflammatory model of light induced photoreceptor loss corroborate and extend previous reports and suggest that both antioxidant mechanisms leading to elevated GSH levels and immunomodulatory effects reducing microglial activation are involved. A limitation of the study is that the Li-PRL does not have a direct link to MS. We also do not show positive effects of DMF in an inflammatory model, which have however already been well-documented in numerous EAE and MS studies (5, 6, 8, 9, 20, 21). The main goal of our study was, to explore the effects of DMF beyond immunomodulation. After irradiation of the retina, the degeneration of the photoreceptors and outer retinal layers is mainly caused by the accumulation of reactive oxygen species, which is not only a pathological hallmark in MS, but also of other eye-related disorders. The fact that we observed no protective effects in the ONC model suggests that, despite upregulation of GSH, DMF may not be effective in traumatic axonal damage.

DATA AVAILABILITY STATEMENT

The original contributions generated for this study are included in the article/supplementary material, further inquiries can be directed to the corresponding author/s.

ETHICS STATEMENT

The animal study was reviewed and approved by The Ministry for Environment, Agriculture, Conservation and Consumer Protection of the State of North Rhine-Westphalia: AZ 84-02.4.2014.A059 and AZ 84-02.04.2016.A137.

AUTHOR CONTRIBUTIONS

MD, CH, MN, SS, AI, and ZK performed the experiments and analyzed the data. MD and PA wrote the manuscript. H-PH was involved in revising the manuscript critically for important intellectual content and made substantial contributions to interpretation of data. PA and MD conceived the study and supervised experiments. All authors read and approved the final manuscript.

FUNDING

This work was supported by grants from Biogen, the charitable Ilselore-Lückow Stiftung and the charitable Dr.-Robert-Pfleger Stiftung to PA.

ACKNOWLEDGMENTS

We acknowledge support by Heinrich Heine University Düsseldorf.

REFERENCES

1. Vargas DL, Tyor WR. Update on disease-modifying therapies for multiple sclerosis. *J Investig Med*. (2017) 65:883–91. doi: 10.1136/jim-2016-000339
2. Saidu NE, Kavian N, Leroy K, Jacob C, Nicco C, Batteux F, et al. Dimethyl fumarate, a two-edged drug: current status and future directions. *Med Res Rev*. (2019) 39:1923–52. doi: 10.1002/med.21567
3. Kappos L, Gold R, Miller DH, Macmanus DG, Havrdova E, Limmroth V, et al. Efficacy and safety of oral fumarate in patients with relapsing-remitting multiple sclerosis: a multicentre, randomised, double-blind, placebo-controlled phase IIb study. *Lancet*. (2008) 372:1463–72. doi: 10.1016/S0140-6736(08)61619-0
4. Schimrigk S, Brune N, Hellwig K, Lukas C, Bellenberg B, Rieks M, et al. Oral fumaric acid esters for the treatment of active multiple sclerosis: an open-label, baseline-controlled pilot study. *Eur J Neurol*. (2006) 13:604–10. doi: 10.1111/j.1468-1331.2006.01292.x
5. Gold R, Kappos L, Arnold DL, Bar-Or A, Giovannoni G, Selmaj K, et al. Placebo-controlled phase 3 study of oral BG-12 for relapsing multiple sclerosis. *N Engl J Med*. (2012) 367:1098–107. doi: 10.1056/NEJMoa1114287
6. Fox RJ, Miller DH, Phillips JT, Hutchinson M, Havrdova E, Kita M, et al. Placebo-controlled phase 3 study of oral BG-12 or glatiramer in multiple sclerosis. *N Engl J Med*. (2012) 367:1087–97. doi: 10.1056/NEJMoa1206328
7. Lee D-H, Linker RA, Gold R. Spotlight on fumarates. *Int MS J*. (2008) 15:12–8.
8. Albrecht P, Bouchachia I, Goebels N, Henke N, Hofstetter HH, Issberner A, et al. Effects of dimethyl fumarate on neuroprotection and immunomodulation. *J Neuroinflammation*. (2012) 9:163. doi: 10.1186/1742-2094-9-163
9. Linker RA, Lee D-H, Ryan S, van Dam AM, Conrad R, Bista P, et al. Fumaric acid esters exert neuroprotective effects in neuroinflammation via activation of the Nrf2 antioxidant pathway. *Brain*. (2011) 134:678–92. doi: 10.1093/brain/awq386
10. Scannevin RH, Chollate S, Jung M-y, Shackett M, Patel H, Bista P, et al. Fumarates promote cytoprotection of central nervous system cells against oxidative stress via the nuclear factor (erythroid-derived 2)-like 2 pathway. *J Pharmacol Exp Ther*. (2012) 341:274–84. doi: 10.1124/jpet.111.190132
11. Gross CC, Schulte-Mecklenbeck A, Klinsing S, Posevitz-Fejfár A, Wiendl H, Klotz L. Dimethyl fumarate treatment alters circulating T helper cell subsets in multiple sclerosis. *Neurol Neuroimmunol Neuroinflamm*. (2016) 3:e183. doi: 10.1212/NXI.0000000000000183
12. Dietrich M, Koska V, Hecker C, Göttle P, Hilla AM, Heskamp A, et al. Protective effects of 4-aminopyridine in experimental optic neuritis and multiple sclerosis. *Brain*. (2020) 143:1127–42. doi: 10.1093/brain/awaa062
13. Dietrich M, Aktas O, Hartung H-P, Albrecht P. Assessing the anterior visual pathway in optic neuritis: Recent experimental and clinical aspects. *Curr Opin Neurol*. (2019) 32:346–57. doi: 10.1097/WCO.0000000000000675
14. Albrecht P, Fröhlich R, Hartung H-P, Kieseier BC, Methner A. Optical coherence tomography measures axonal loss in multiple sclerosis independently of optic neuritis. *J Neurol*. (2007) 254:1595–6. doi: 10.1007/s00415-007-0538-3
15. Dietrich M, Cruz-Herranz A, Yiu H, Aktas O, Brandt AU, Hartung H-P, et al. Whole-body positional manipulators for ocular imaging of anaesthetised mice and rats: a do-it-yourself guide. *BMJ Open Ophthalmol*. (2017) 1:e000008. doi: 10.1136/bmjophth-2016-000008
16. Dietrich M, Helling N, Hilla A, Heskamp A, Issberner A, Hildebrandt T, et al. Early alpha-lipoic acid therapy protects from degeneration of the inner retinal layers and vision loss in an experimental autoimmune encephalomyelitis-optic neuritis model. *J Neuroinflammation*. (2018) 15:71. doi: 10.1186/s12974-018-1111-y
17. Cruz-Herranz A, Dietrich M, Hilla AM, Yiu HH, Levin MH, Hecker C, et al. Monitoring retinal changes with optical coherence tomography predicts neuronal loss in experimental autoimmune encephalomyelitis. *J Neuroinflammation*. (2019) 16:203. doi: 10.1186/s12974-019-1583-4
18. Cruz-Herranz A, Balk LJ, Oberwahrenbrock T, Saidha S, Martinez-Lapiscina EH, Lagreze WA, et al. The APOSTEL recommendations for reporting quantitative optical coherence tomography studies. *Neurology*. (2016) 86:2303–9. doi: 10.1212/WNL.0000000000002774
19. Dietrich M, Hecker C, Hilla A, Cruz-Herranz A, Hartung H-P, Fischer D, et al. Using optical coherence tomography and optokinetic response as structural and functional visual system readouts in mice and rats. *J Vis Exp*. (2019) 143:e58571. doi: 10.3791/58571
20. das Neves SP, Santos G, Barros C, Pereira DR, Ferreira R, Mota C, et al. Enhanced cognitive performance in experimental autoimmune encephalomyelitis mice treated with dimethyl fumarate after the appearance of disease symptoms. *J Neuroimmunol*. (2020) 340:577163. doi: 10.1016/j.jneuroim.2020.577163
21. Schulze-Topphoff U, Varrin-Doyer M, Pekarek K, Spencer CM, Shetty A, Sagan SA, et al. Dimethyl fumarate treatment induces adaptive and innate immune modulation independent of Nrf2. *Proc Natl Acad Sci U S A*. (2016) 113:4777–82. doi: 10.1073/pnas.1603907113
22. Hoffmann C, Dietrich M, Herrmann A-K, Schacht T, Albrecht P, Methner A. Dimethyl fumarate induces glutathione recycling by upregulation of glutathione reductase. *Oxid Med Cell Longev*. (2017) 2017:6093903. doi: 10.1155/2017/6093903
23. Ambati J, Fowler BJ. Mechanisms of age-related macular degeneration. *Neuron*. (2012) 75:26–39. doi: 10.1016/j.neuron.2012.06.018
24. Catanzaro M, Lanni C, Basagni F, Rosini M, Govoni S, Amadio M. Eye-light on age-related macular degeneration: targeting Nrf2-pathway as a novel therapeutic strategy for retinal pigment epithelium. *Front Pharmacol*. (2020) 11:844. doi: 10.3389/fphar.2020.00844
25. Cunningham ET, Jr., Kilmartin D, Agarwal M, Zierhut M. Sympathetic ophthalmia. *Ocul Immunol Inflamm*. (2017) 25:149–51. doi: 10.1080/09273948.2017.1305727
26. Gabriele ML, Ishikawa H, Schuman JS, Ling Y, Bilonick RA, Kim JS, et al. Optic nerve crush mice followed longitudinally with spectral domain optical coherence tomography. *Invest Ophthalmol Vis Sci*. (2011) 52:2250–4. doi: 10.1167/iovs.10-6311
27. Nagata A, Higashide T, Ohkubo S, Takeda H, Sugiyama K. *In vivo* quantitative evaluation of the rat retinal nerve fiber layer with optical coherence tomography. *Invest Ophthalmol Vis Sci*. (2009) 50:2809–15. doi: 10.1167/iovs.08-2764
28. Huang X-R, Kong W, Qiao J. Response of the retinal nerve fiber layer reflectance and thickness to optic nerve crush. *Invest Ophthalmol Vis Sci*. (2018) 59:2094–103. doi: 10.1167/iovs.17-23148
29. Chauhan BC, Stevens KT, Levesque JM, Nuschke AC, Sharpe GP, O'Leary N, et al. Longitudinal *in vivo* imaging of retinal ganglion cells and retinal

thickness changes following optic nerve injury in mice. *PLoS ONE*. (2012) 7:e40352. doi: 10.1371/journal.pone.0040352
30. Smith CA, Hooper ML, Chauhan BC. Optical coherence tomography angiography in mice: quantitative analysis after experimental models of retinal damage. *Invest Ophthalmol Vis Sci*. (2019) 60:1556–65. doi: 10.1167/iovs.18-26441
31. Leinonen H, Choi EH, Gardella A, Kefalov VJ, Palczewski K. A mixture of U.S. food and drug administration-approved monoaminergic drugs protects the retina from light damage in diverse models of night blindness. *Invest Ophthalmol Vis Sci*. (2019) 60:1442–53. doi: 10.1167/iovs.19-26560
32. Jiang D, Ryals RC, Huang SJ, Weller KK, Titus HE, Robb BM, et al. Monomethyl fumarate protects the retina from light-induced retinopathy. *Invest Ophthalmol Vis Sci*. (2019) 60:1275–85. doi: 10.1167/iovs.18-24398
33. Chen W-J, Wu C, Xu Z, Kuse Y, Hara H, Duh EJ. Nrf2 protects photoreceptor cells from photo-oxidative stress induced by blue light. *Exp Eye Res*. (2017) 154:151–8. doi: 10.1016/j.exer.2016.12.001
34. Licht-Mayer S, Wimmer I, Traffehn S, Metz I, Brück W, Bauer J, et al. Cell type-specific Nrf2 expression in multiple sclerosis lesions. *Acta Neuropathol*. (2015) 130:263–77. doi: 10.1007/s00401-015-1452-x
35. Parodi B, Rossi S, Morando S, Cordano C, Bragoni A, Motta C, et al. Fumarates modulate microglia activation through a novel HCAR2 signaling pathway and rescue synaptic dysregulation in inflamed CNS. *Acta Neuropathol*. (2015) 130:279–95. doi: 10.1007/s00401-015-1422-3

Conflict of Interest: The authors declare that they have no conflict of interest related to the work presented. The following financial disclosures are unrelated to the work MD received speaker honoraria from Novartis and Merck. H-PH has received fees for serving on steering and data monitoring committees from Bayer Healthcare, Biogen, Celgene BMS, CSL Behring, GeNeuro, MedImmune, Merck, Novartis, Octapharma, Roche, Sanofi Genzyme, TG Therapeutic sand Viela Bio; fees for serving on advisory boards from Biogen, Sanofi Genzyme, Merck, Novartis, Octapharma, and Roche; and lecture fees from Biogen, Celgene BMS, Merck, Novartis, Roche, Sanofi Genzyme. PA received compensation for serving on Scientific Advisory Boards for Ipsen, Novartis, Biogen; he received speaker honoraria and travel support from Novartis, Teva, Biogen, Merz Pharmaceuticals, Ipsen, Allergan, Bayer Healthcare, Esai, UCB and Glaxo Smith Kline; he received research support from Novartis, Biogen, Teva, Merz Pharmaceuticals, Ipsen, and Roche. The remaining author report no disclosures.

Copyright © 2021 Dietrich, Hecker, Nasiri, Samsam, Issberner, Kohne, Hartung and Albrecht. This is an open-access article distributed under the terms of the Creative Commons Attribution License (CC BY). The use, distribution or reproduction in other forums is permitted, provided the original author(s) and the copyright owner(s) are credited and that the original publication in this journal is cited, in accordance with accepted academic practice. No use, distribution or reproduction is permitted which does not comply with these terms.

frontiers in Neurology

MINI REVIEW
published: 04 February 2021
doi: 10.3389/fneur.2020.612422

The Role of Neuroinflammation in Glaucoma: An Update on Molecular Mechanisms and New Therapeutic Options

Teresa Rolle[1]*, *Antonio Ponzetto*[2] and *Lorenza Malinverni*[1]

[1] Eye Clinic, Department of Surgical Sciences, University of Torino, Torino, Italy, [2] Department of Medical Sciences, University of Torino, Torino, Italy

Glaucoma is a multifactorial optic neuropathy characterized by the continuous loss of retinal ganglion cells, leading to progressive and irreversible visual impairment. In this minireview, we report the results of the most recent experimental studies concerning cells, molecular mechanisms, genes, and microbiome involved in neuroinflammation processes correlated to glaucoma neurodegeneration. The identification of cellular mechanisms and molecular pathways related to retinal ganglion cell death is the first step toward the discovery of new therapeutic strategies. Recent experimental studies identified the following possible targets: adenosine A_{2A} receptor, sterile alpha and TIR motif containing 1 (neurofilament light chain), toll-like receptors (TLRs) 2 and 4, phosphodiesterase type 4 (PDE4), and FasL-Fas signaling (in particular ONL1204, a small peptide antagonist of Fas receptors), and therapies directed against them. The continuous progress in knowledge provides interesting data, although the total lack of human studies remains an important limitation. Further research is required to better define the role of neuroinflammation in the neurodegeneration processes that occur in glaucomatous disease and to discover neuroprotective treatments amenable to clinical trials. The hereinafter reviewed studies are reported and evaluated according to their translational relevance.

Keywords: glaucoma, neuroinflammation, microglia, astrocytes, target, therapy, microbiome

OPEN ACCESS

Edited by:
Ahmed Toosy,
University College London,
United Kingdom

Reviewed by:
Alessio Martucci,
University of Rome Tor Vergata, Italy
Rebecca M. Sappington,
Wake Forest School of Medicine,
United States

***Correspondence:**
Teresa Rolle
teresa.rolle@unito.it

Specialty section:
This article was submitted to Neuro-Ophthalmology, a section of the journal Frontiers in Neurology

Received: *30 September 2020*
Accepted: *21 December 2020*
Published: *04 February 2021*

Citation:
Rolle T, Ponzetto A and Malinverni L (2021) The Role of Neuroinflammation in Glaucoma: An Update on Molecular Mechanisms and New Therapeutic Options. Front. Neurol. 11:612422. doi: 10.3389/fneur.2020.612422

INTRODUCTION

Glaucoma is a chronic and progressive optic neuropathy characterized by death of retinal ganglion cells (RGCs) with consequent localized or diffuse thinning of the nerve fiber layer and increased cupping of the optic nerve head (ONH) (1). It is a social disease; its prevalence is believed to grow strongly, and about 80 million glaucomatous patients are expected in 2020 and 112 million in 2040 (2, 3). More than 7 million people worldwide are blind due to glaucoma, and the prevalence of bilateral blindness caused by this pathology varies from 6 to 16% in western countries (4).

The precise mechanisms leading to RGCs loss are not fully understood. Several studies have suggested that glaucoma has important analogies with other neurodegenerative pathologies correlated to inflammatory responses like amyotrophic lateral sclerosis, Alzheimer's disease, Parkinson's disease, Huntington's disease, and frontotemporal dementia (5–8).

The purpose of this minireview is to discuss the consolidated knowledge of neuroinflammation in glaucoma and to focus on new experimental evidences about possible therapeutic targets and latest treatment proposals.

MAIN ACTORS OF NEUROINFLAMMATION IN GLAUCOMA

Microglia and Astroglia

Microglia and astroglia are the cell types involved in inflammatory responses within the retina (9); they consist of Müller cells and astrocytes and provide metabolic support of neurons, neurological regulation of ionic concentrations, and neuroprotective activities (8, 10–12). Microglial cells originate from blood monocytes migrating to the central nervous system (CNS) and present cellular antigens like CD11b/c and chemokine fractalkine receptor (CX3CR1) (13). They start from primitive erythromyeloid progenitors and mature in microglia (14) differentiating through different pathways dependent on colony-stimulating factor 1 receptor (CSF-1R) (15), interleukin-34 (IL-34) (16), and transforming growth factor-β (TGF-β) (17). After becoming mature, they take part in the inflammation process, which is activated by damage-associated molecular patterns (DAMPs) released by neural cells and also by astroglia and microglia (18–20). Among DAMPs, heat shock proteins (HSPs) are produced by RGCs when intraocular pressure (IOP) is elevated (21), while Tenascin-C is upregulated in astrocytes and induces toll-like receptor (TLR) activation (22). In response to the neuroinflammatory process, microglia release cytokines and chemokines (22–24) such as complement factors, tumor necrosis factor-alpha (TNF-α), and interleukin-6 (IL-6) that amplify the response and contribute to promote morphological changes of microglia into macrophages (25). M1 and M2 are two phenotypes of activated macrophages. M1 is proinflammatory and produces IL-1β, IL-12, and TNF-α (26); on the other hand, M2 synthetizes anti-inflammatory intermediaries such as IL-10, TGF-β, and neurotrophic factor insulin-like growth factor (IGF-1) (27–32).

Recently, in a study in DBA/2J mice with experimental glaucoma, the triggering receptor expressed on myeloid cells/TYROsine kinase binding protein (TREM/TYROBP) signaling network has been identified as the principal regulator mechanism of microglial responses to elevated IOP; infiltrating monocyte-like cells are likely responsible for the early proinflammatory signals (33).

Microglial cells communicate with astroglia via signaling proteins. Depending on this interaction, astroglia are differentiated into two types of reactive astrocytes, A1 and A2 (34–36). A1 has a detrimental effect (37); on the other hand, A2 has a neuroprotective function (38). Indeed, microglia and astroglia collaborate to regulate the inflammation process.

Different genes are implicated in the inflammatory pathways and are upregulated in the retina and ONH (39, 40). The first to be upregulated are TLR signaling pathways: for example, HSPs increase the expression of major histocompatibility complex (MHC) II and cytokine production (21). The second pathway is represented by nuclear factor-kappa B (NF-κB), which causes an increased expression of IL-1 cytokine family that promotes the cascade of inflammatory cytokines (TNF-α and IL-6). TNF-α is found in the optic nerve in glaucoma patients (41–43) and also Fas ligand (FasL), a proapoptotic protein, both being implicated in glaucoma pathogenesis (44). Recently, Oikawa et al. (45) demonstrated in feline's early glaucoma the upregulation of genes related to cell proliferation and immune responses (linked with the TLR and NF-κB signaling pathway), and they observed that proliferating cell types are different in ONH sub-regions. Microglia–macrophages were found in the prelaminar region and in the lamina cribrosa, while oligodendrocytes were more numerous in the retrolaminar region.

MOLECULAR MECHANISMS

After reporting the fundamental concepts related to the neuroinflammation cells and the genes involved, we now refer to the latest studies on the main molecular mechanisms selected according to their presence in neurodegenerative diseases and their translational relevance.

The *exosomes* have a demonstrated role in neurodegenerative diseases. In an experimental glaucoma model (46), the exosomes, produced by naive microglia (BV-2 cells) in a condition of elevated hydrostatic pressure (BV-Exo-EHP, e.g., high IOP), induced the activation of retina microglia, production of cytokines, hypermotility, proliferation, and increase of phagocytosis. They promoted increase of reactive oxygen species and cell death, causing a reduction of retina ganglion cell number. The translation relevance of this study is that the exosomes own an autocrine function in the neuroinflammation pathway correlated to neurodegeneration.

Necroptosis, a recently discovered genetic form of cell death, has a fundamental role in neurodegenerative diseases (47). It is similar to necrosis with cell swelling, granular cytoplasm, chromatin fragmentation, and cellular lysis. Necroptosis differs from apoptosis because the cell content moves into the extracellular matrix in a passive way through the altered cell membrane. Necroptosis is induced by TNF-α and also by Fas and TNF-related apoptosis-inducing ligand (TRAIL), interferons (IFNs), TLR signaling, and viral infection via DAI (DNA sensor DNA-dependent activator of IFN regulatory factor). Ko et al. (47) in a neuroinflammation model of experimental glaucoma proved that the axon degeneration is sterile alpha and TIR motif1 (SARM1)-dependent and is induced by TNF-α with a consequent oligodendrocyte loss and RGC death. The necroptosis perpetrator is mixed lineage kinase domain-like pseudokinase (MLKL) through the reduction of the axon survival factors nicotinamide mononucleotide adenylyltransferase 2 (NMNAT2) and stathmin 2 (STMN2) that inhibit SARM1 NADase action. TNF-α also activates SARM1-dependent axon degeneration in sensory nerve cells through a different necroptotic signaling mechanism.

Several recent studies have dealt with the topic of *SARM1 axon degeneration pathway*. The axon health is preserved by the balance between the pro-survival NMNAT2 and STMN2 and

pro-degenerative molecules dual leucine zipper kinase (DLK) and SARM1 (48). Activated DLK reduces the concentration of protective factors (NMNAT2 and SCG10) and exposes axons to traumatic and metabolic damages; this event is also related to mitochondrial dysfunction that in an independent way reduces the NMNAT2 and SCG10 concentrations in the axons (49). The equilibrium between axon survival and self-destruction is strictly related to axonal NAD+ metabolism. Sasaki et al. (50) studied in cell cultures and *in vivo* the biomarker cADPR, which controls NAD+ levels via SARM1 and mobilizes calcium. SARM1 has a basal activity in normal conditions. After injury, the axon degeneration is preceded by SARM1-dependent rise in the amount of axonal cADPR, but the contribution of cADPR in degenerative mechanisms has not been proven. The mitochondrial dysfunction can produce an incomplete activation of SARM1 and could predispose the axons to neurodegeneration.

In the context of neuroinflammation, it is mandatory to report the interesting developments that have taken place in recent years regarding the relationship between *microbiome* and *glaucoma*. Chen et al. conducted a study in germ-free mice, demonstrating that the absence of gastrointestinal (GI) bacteria abolished the development of glaucoma (51). The immune mechanism involved in the pathogenesis of the neural damage is related to CD4+ T-lymphocytes that recognize HSPs. Bacterial HSPs cross-reacted with both mouse and human HSPs. High IOP values induced the passage of CD4+ T-cells in the retina, and these T-cells were to blame for the extended phase of neurodegeneration in glaucomatous disease. They recognized specifically both bacterial and human HSPs. The induction of neurodegeneration in glaucoma requires pre-exposure to microbial flora, either the GI and oral one (51). In the past century, the presence of elevated titers of antibodies directed against small HSPs and cross-reacting with human HSPs was demonstrated in glaucoma patients

TABLE 1 | New targets, their neuroinflammatory effects, impact of neurodegeneration and therapeutic options.

Targets	Authors	Neuroinflammatory effects	Progression of neurodegeneration	Therapeutic options
Adenosine A_{2A} receptor ($A_{2A}R$)	Madeira et al. (57); Aires et al. (58)	Microglia activation: increase in mRNA levels of MHC-II, up-regulation of mRNA expression of TSPO, CD11b, TREM2	Synaptotoxicity, excitotoxicity, impaired retrograde axonal transport, axon degenerative profiles, disorganized and abnormal myelin wrapping, loss of RGCs	Caffeine
Astroglial NF-κB	Yang et al. (59)	Cytokine signaling, toll-like receptor (TLR) signaling, inflammasome activation	Neurodegeneration at different neuronal compartments: dendrite degeneration and synapse dysfunction, death of oligodendrocytes, RGC soma injury	Transgenic deletion of astroglial $I_KKβ$ by pro-inflammatory cytokines
Endothelin-1 (ET-1)	Nor Arfuzir et al. (60)	Increase of IL-1β, IL-6 and TNF-α, NF-κB (activated by phosphorylation of $I_KKβ$), c-Jun (activated by JNK), STAT3 activation	Ischemia: retinal and optic nerve damage, NMDA induced excitotoxicity, induction of iNOS	Magnesium acetyltaurate (MgAT)
FasL-Fas signaling	Krishnan et al. (61)	Microglia activation: Induction of cytokines and chemokines (GFAP, Caspase-8, TNFα, IL-1β, IL-6, IL-18, MIP-1α, MIP-1β, MIP-2, MCPI, and IP10) complement factors (C3, C1Q) Toll-like receptor pathway (TLR4), inflammasome pathway (NLRP3), induction of apoptosis	Axon degeneration, RGCs death	ONL1204
Monocyte-like cells	Williams et al. (62)	Platelet adhesion, extravasation of the monocytes and enter the ONH (CD45hi/CD11b+/CD11c+)	Axon degeneration	DS-SILY, Itgam (CD11b, immune cell receptor)
ONH astrocytes (ONHAs)	Means et al. (63)	Activated caspases, Tau cleavage, NFTs formation, GFAP upregulation	ONHA dysfunction and degeneration, RGCs apoptosis	Polyphenolic phytostilbene and antioxidant *trans*-resveratrol (3,5,4′-trihydroxy-*trans*-stilbene)
PDE type 4 (PDE4) signaling	Cueva Vargas et al. (64)	Microglia activation: production of proinflammatory cytokines (TNFα, IL-1β, IL-6 and MIF), upregulation of TNFα/TNFR1 signaling, GFAP upregulation, increase of Iba1/CD68-positive cells	Axonal degeneration, low levels of cAMP-PKA	Ibudilast (inhibitor of cAMP phosphodiesterase type 4)
Sterile alpha and TIR motif containing 1 (SARM1)	Marion et al. (65); Krauss et al. (66)	TIR domain dimerization, NADase activation, reduction of NMNAT2, activation of calpains	Axonal degeneration	Biomarker Neurofilament light chain (NfL), therapeutic options not available yet
TLR2 and TLR4	Yang et al. (67); Ehlers et al. (68); Ji et al. (69)	Microglia activation: expression of GFAP and Iba-1, neuroinflammatory pathways TLR4-related	Production of inflammatory cytokines, leucocytes degranulation, modulation of neuroinflammatory response (local and systemic)	Alpha 1-antitrypsin (AAT) human umbilical cord mesenchymal stem cells (hUC-MSC) transplantation

(52). It was reported that these antibodies exert cytotoxicity when directly applied to human retina (53). It was proposed that immunomodulation should become the basis of glaucoma therapy. However, the immunosuppressive therapy could be dangerous and sometimes burdened by serious side effects. One solution could be the identification of antigens triggering or enhancing the autoimmune mechanism(s) and their elimination, aiming at reducing the active aggression by autoimmune T-cells. Since the development of glaucoma was shown to be linked to the microbiome, some of its components are potentially curable, such as *Helicobacter pylori*, a Gram-negative flagellar bacterium present worldwide, in 20–90% of individuals. Only active *H. pylori* infection induces cellular immune responses against the nervous system, due to molecular mimicry and cross-reactivity with components of host nerves. A large meta-analysis was recently published by Doulberis et al. (54). When the diagnosis of *H. pylori* infection was performed by gastric biopsy, the odds ratio (OR) for an association was very high (5.4), with confidence interval of 3.17–9.2 (highly significant); the strong association diminished to an OR of 2.08 when only serum antibodies were measured. Similarly, also in glaucoma, the antigens recognized by the immune system were reported in quite a large number. Geyer and Levo (55) suggested that the therapy should be directed not only against the IOP but also against autoreactive lymphocytes, on the basis of the lack of neurodegeneration in experimental mice models after depletion of either B-cells and in particular T-cells directed against HSP-derived peptides (55). However, this might not be sufficient. Beutgen et al. in a recent review reported elevated levels of a variety of autoantibodies (autoAbs) both in systemic circulation and in aqueous humor of glaucoma patients (56): not only anti-HSPs, but also against myelin basic protein and glial fibrillary acid protein. Such autoantibodies are typically involved in diseases of the nervous system.

NEW POSSIBLE TARGETS AND PROPOSALS ON PHARMACOLOGICAL THERAPIES

Hereinafter, the possible new therapeutic targets to reduce or block the neuroinflammation, which are more likely to be used in future clinical practice, are outlined. They are listed in alphabetical order. In **Table 1**, we provided more detail on new targets, their neuroinflammatory and neurodegenerative effects, and, where provided, the therapeutic options.

Adenosine A_{2A} Receptor ($A_{2A}R$)

Madeira et al. (57, 70) demonstrated in a Sprague Dawley rats model of ocular hypertension (OHT) that *caffeine* (antagonist of adenosine receptors) administration prevents OHT-induced microglial activation and causes the modulation of retinal neuroinflammation and prevention of the RGCs loss. A recent study outlined the protective effect of microglial adenosine A_{2A} receptor ($A_{2A}R$) blockade that can prevent, in human retina, microglial cell response to elevated IOP (58).

Astroglial Nuclear Factor-Kappa B

The astroglial NF-κB was evaluated as a possible treatment target for the modulation of immune response in an experimental transgenic glaucoma mouse with deletion of IkappaB kinase beta (IκKβ) in astroglial cells (59). The study showed a reduction of the increase in proinflammatory cytokines (in particular

TABLE 2 | New proposals of holistic treatments to contrast neuroinflammation in glaucoma.

New therapies	Authors	Upregulation	Downregulation
Antioxidants: Tempol	Yang et al. (72)	IL-13, IL-4, IL-6	Modulation of NF-κB signaling: decrease of TNF-α, IFN-γ, IL-1β, IL-2, IL-1α
Ketogenic diet	Harun-Or-Rashid et al. (73); Lu et al. (74); Shimazu et al. (75)	- Activation of Nrf2 - Increase of anti-inflammatory agents IL-4 and Arginase-1 - Increase of hydroxycarboxylic acid receptor 1 (HCAR1) - Increased levels of Arrestin β-2 protein, required for HCAR1 signaling - Increased GABAergic output and lowered presynaptic excitatory neurotransmitter release - Stimulation of HCAR2	Inhibition of - AMPK phosphorylation - Iba1 expression - NLRP3 inflammasome HCAR1-mediated - Oxidative stress by increased FOXO3A and MT2 activity - Class I histone deacetylases - NF-κB p65 nuclear translocation
Coriolus Versicolor and Hericium Erinaceus (Mushrooms)	Trovato Salinaro et al. (76)	IL-6, interferons immunoglobulin G, macrophages, T-lymphocytes, expression of Hsp70, TRX, HO-1	- Increase of Lipoxin A4 (endogenous eicosanoid) which blocks the production of pro-inflammatory mediators (ROS/RNS) - Stimulation NGF synthesis: modulation of cholineacetyltransferase + acetylcholinesterase
Hydrophilic Saffron extract (Crocus sativus)	Fernandez-Albarral et al. (77)	Inversion of OHT-induced down regulation of P2RY12	- Reduction of morphological signs of microglia activation - Reduction of various neurotoxic molecules (TNF-α, IL-β) - Suppression caspase-3 and caspase-9 activities: prevention of retinal ganglion cell death - Reduction of ROS: increase of blood flow in the retina and choroid

TNF-α) with consequent protection of axon from degeneration and RGCs from apoptosis, as demonstrated also by pattern electroretinogram (PERG) data.

Endothelin-1

Since 2012 (71), it was clarified that the increment of endothelin-1 (ET-1) in glaucomatous patients is linked to sub-clinical inflammation. Nor Arfuzir et al. (60), using Sprague Dawley rats that underwent intravitreal injection of ET-1, proved that the pre-treatment with magnesium acetyltaurate (MgAT) was protective against the increase induced by ET-1 in the retinal expression of IL-1β, IL-6, and TNF-α and against the activation of NF-κB and c-JUN induced by ET-1. MgAT promoted a higher RGC survival.

FasL-Fas Signaling

FasL, a type II transmembrane protein of the TNF group, promotes apoptosis after binding to the Fas receptor and is involved in the pathogenesis of glaucoma also through inflammatory pathways. Krishnan et al. (61) demonstrated in microbead-injected wild-type (WT) mice that the treatment with *ONL1204*, a small peptide antagonist of Fas receptors, significantly reduced RGC death and loss of axons. The authors proved that ONL1204 blocks microglial activation and inhibits the induction of multiple genes involved in glaucomatous disease, as cytokines and chemokines (GFAP, caspase-8, TNFα, IL-1β, IL-6, IL-18, MIP-1α, MIP-1β, MIP-2, MCPI, and IP10), elements of the complement (C3 and C1Q), inflammasome pathway (NLRP3), and TLR4.

Monocyte-Like Cells

Recently, in a mouse model of ocular hypertension (DBA/2J eyes), it was proved that monocyte-like cells enter the ONH and that monocyte–platelet interactions occur in glaucomatous tissue (62). Using these monocyte-like cells as therapeutic target, the authors demonstrated that the treatment with *DS-SILY*, a peptidoglycan that hinders the platelet adhesion to the vessel endothelium and to monocytes, and the treatment with genetic targeting of Itgam (CD11b), an immune cell receptor that blocks effusion of the monocytes from the vessels, can both be neuroprotective by reducing neuroinflammation.

Optic Nerve Head Astrocytes

Means et al. (63) demonstrated that pretreatment with polyphenolic phytostilbene and antioxidant *trans-resveratrol* (3,5,4′-trihydroxy-trans-stilbene) on ONHs underwent oxidative stress with *tert*-butyl hydroperoxide (tBHP) and induced a significant reduction in activated caspases, neurofibrillary tangle (NFT) formation, and cleaved Tau. These findings outlined that resveratrol can have protective properties to prevent ONH astrocyte (ONHA) dysfunction and degeneration.

Phosphodiesterase Type 4 Signaling

Cueva Vargas et al. (64) evaluated the anti-neuroinflammatory activity of ibudilast, a clinically approved cAMP phosphodiesterase (PDE) inhibitor with special affinity for PDE type 4 (PDE4). In an OHT rat model, the intraocular administration of ibudilast decreased the production of proinflammatory cytokines and reduced macroglia and microglial reactivity in the retina and optic nerve. Ibudilast had a positive effect on RGC soma survival, avoided axonal degeneration, and enhanced anterograde axonal transport in POAG eyes through activation of the cAMP/PKA pathway.

Sterile Alpha and TIR Motif Containing 1

Since SARM1 induces Wallerian degeneration, this pathway could be a therapeutic target (65). The SARM1 inhibition prevents axonal degeneration in traumatic injuries and neurodegenerative disorders. As reported before, SARM1 is involved in innate immune response, and it is possible that the relationship between immune regulation and neurodegenerative disorders will play an important role for new therapeutic possibilities. The discovery of a reliable biomarker of axonal damage, i.e., the neurofilament light chain (NfL) and the possibility of testing NfL in plasma or serum, could be an important step to develop SARM1 inhibitors that protect axons from degeneration (66).

Toll-Like Receptors 2 and 4

As reported, TLR signaling is involved in homeostasis and in pathology of CNS. TLR2 and TLR4 expressed by microglia take part in the glial response and in the neuroinflammation. Yang et al. (67) demonstrated that in C57BL/6J mice, the alpha 1-antitrypsin (AAT), a serine protease inhibitor, blocks microglial activation in chronic ocular hypertension model. It was shown that AAT inhibits leukocyte migration and has antithrombotic, antiapoptotic, and anti-inflammatory properties (68). In OHT rats, Ji et al. (69) demonstrated that the human umbilical cord mesenchymal stem cell (hUC-MSC) transplantation blocks TLR4-related microglial activation and neuroinflammatory pathways.

NEW PROPOSAL HOLISTIC APPROACHES

In this section, we reported studies proposing holistic medicinal treatments to modulate/reduce the neuroinflammation in an experimental model of glaucoma. **Table 2** illustrates new therapies with details on modulations of inflammatory mechanisms.

Antioxidants

Oxidative stress can alter the immune function of the glia and promotes the neuroinflammation in glaucoma. The effects of the antioxidant Tempol were tested on ocular hypertensive retina and optic nerve samples and on NF-κB, a redox-sensitive transcriptional regulator of neuroinflammation. The analysis of markers of oxidative stress (proinflammatory cytokines, including IL-1, IL-2, IFN-γ, and TNF-α) demonstrated that the treatment was able to decrease the neuroinflammation markers (72).

Ketogenic Diet

A recent research study (73) evidenced that the ketogenic diet reduces inflammation through inhibition of AMPK

activation and HCAR1-mediated inhibition of the NLRP3 inflammasome. The way by which ketogenic diet works in neuroprotection is not completely known up to now. Researches supposed that ketogenic diet reduces oxidative stress, inhibits class I histone deacetylases, promotes Nrf2 activation to upregulate antioxidants, and inhibits NF-κB to reduce inflammation (74, 75).

Coriolus and *Hericium* Nutritional Mushrooms

Trovato Salinaro et al. (76) reported the potential effect of *Coriolus* and *Hericium*, nutritional mushrooms, in the therapy of neurodegenerative diseases including Alzheimer's disease and glaucoma; they act as modulators of mechanisms of cellular protection (antioxidant properties) from mitochondrial dysfunction and neuroinflammation.

Hydrophilic Saffron Extract

Studies conducted (77) in a mouse model of laser-induced unilateral OHT on a hydrophilic saffron extract (crocin 3%) demonstrated the reduction of morphological features of microglial activation in OHT and in contralateral eyes. The treatment with saffron extract in part inverted the downregulation of P2RY12. The saffron extract administrated orally protected RGCs from death by reducing neuroinflammation correlated with increased IOP.

DISCUSSION

The co-participation of the innate immune response and the inflammation in the pathogenesis of optic nerve degeneration in glaucomatous disease is now an established and proven event (78–82). The purpose of this minireview was to outline potential targets for future therapies, some of which are already being studied, and to describe possible treatments related to alternative medicine. These recent studies performed on animal models have improved our knowledge on cellular mechanisms, partly already known, but mainly on the signaling pathways of neuroinflammation. The studies analyzed openly the way to new possibilities of modulation of neuroinflammation (such as

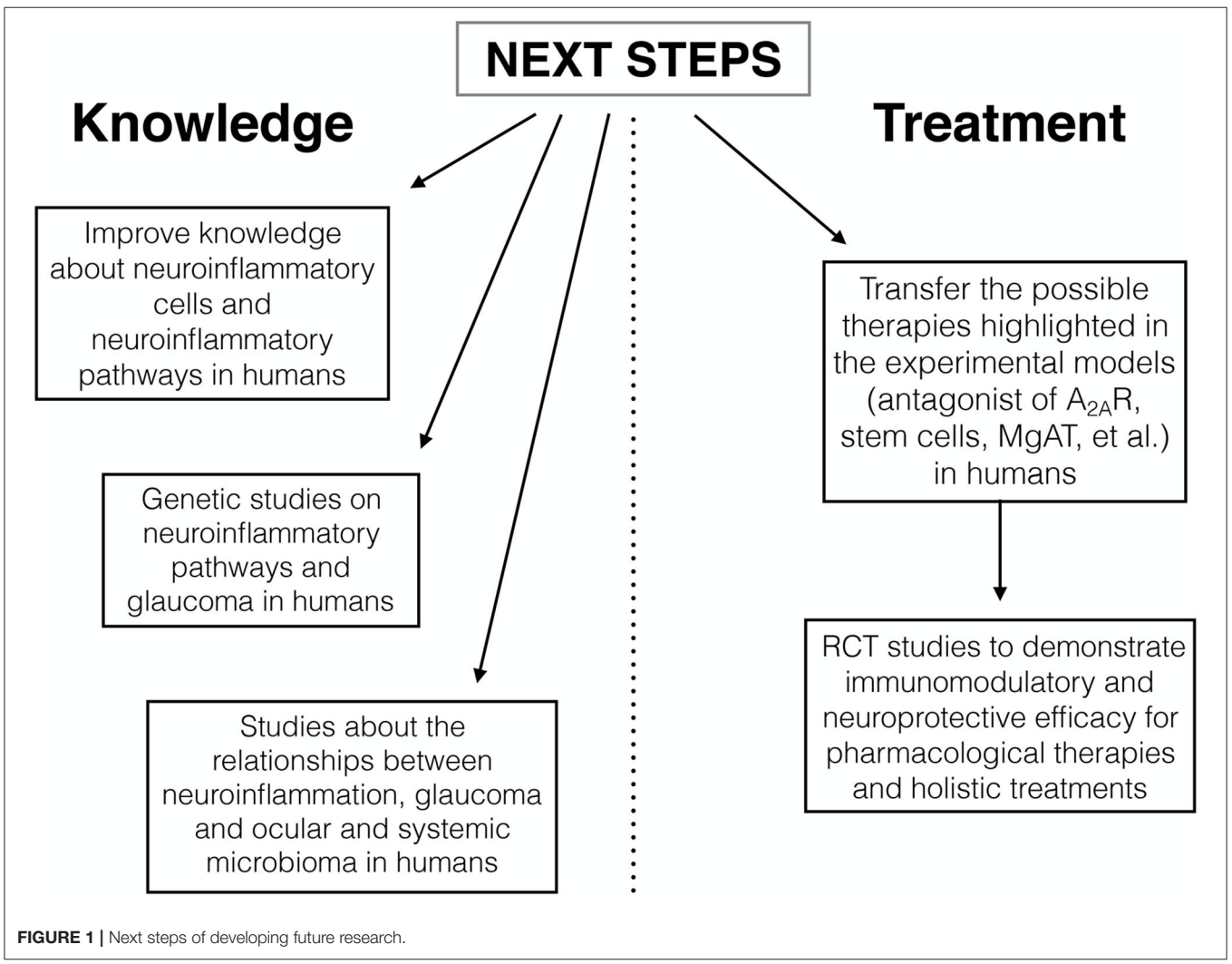

FIGURE 1 | Next steps of developing future research.

antagonist of $A_{2A}R$, stem cells, MgAT, resveratrol, and alpha 1-antitrypsin) with a view to achieve effective neuroprotective treatments for glaucomatous disease. An important limitation is the almost total lack of researches in human. On the basis of the data reported, the possible ways of developing future research are illustrated in **Figure 1**. Further studies are needed to transfer the current experimental evidence into clinical research in order to slow down or to prevent the progressive glaucoma neurodegeneration.

AUTHOR CONTRIBUTIONS

All authors listed have made a substantial, direct and intellectual contribution to the work, and approved it for publication.

ACKNOWLEDGMENTS

Carla Malinverni contributed to correcting the English version.

REFERENCES

1. European Glaucoma Society. *Terminology and Guidelines for Glaucoma*. 4th ed. Zug: European Glaucoma Society (2014).
2. Cook C, Foster P. Epidemiology of glaucoma: what's new? *Can J Ophthalmol.* (2012) 47:223–6. doi: 10.1016/j.jcjo.2012.02.003
3. Tham YC, Li X, Wong TY, Quigley HA, Aung T, Cheng CY. Global prevalence of glaucoma and projections of glaucoma burden through 2040: a systematic review and meta-analysis. *Ophthalmology.* (2014) 121:2081–90. doi: 10.1016/j.ophtha.2014.05.013
4. Rossetti L, Digiuni M, Montesano G, Centofanti M, Fea AM, Iester M, et al. Blindness and glaucoma: a multicenter data review from 7 academic eye clinics. *PLoS ONE.* (2015) 10:e0136632. doi: 10.1371/journal.pone.0136632
5. Toth RP, Atkin JD. Dysfunction of optineurin in amyotrophic lateral sclerosis and glaucoma. *Front Immunol.* (2018) 9:1017. doi: 10.3389/fimmu.2018.01017
6. Wiggs JL, Pasquale LR. Genetics of glaucoma. *Hum Mol Genet.* (2017) 26(R1):R21–7. doi: 10.1093/hmg/ddx184
7. Fingert JH, Robin AL, Scheetz TE, Kwon YH, Liebmann JM, Ritch R, et al. Tank-Binding kinase 1 (TBK1) gene and open-angle glaucomas (An American Ophthalmological Society Thesis). *Trans Am Ophthalmol Soc.* (2016) 114:T6
8. Ramirez AI, de Hoz R, Salobrar-Garcia E, Salazar JJ, Rojas B, Ajoy D, et al. The role of microglia in retinal neurodegeneration: Alzheimer's Disease, Parkinson, and Glaucoma. *Front Aging Neurosci.* (2017) 9:214. doi: 10.3389/fnagi.2017.00214
9. Soto I, Howell GR. The complex role of neuroinflammation in glaucoma. *Cold Spring Harb Perspect Med.* (2014) 4:a017269. doi: 10.1101/cshperspect.a017269
10. Iadecola C, Nedergaard M. Glial regulation of the cerebral microvasculature. *Nature neuroscience.* (2007) 10:1369–76. doi: 10.1038/nn2003
11. Rouach N, Koulakoff A, Abudara V, Willecke K, Giaume C. Astroglial metabolic networks sustain hippocampal synaptic transmission. *Science.* (2008) 322:1551–5. doi: 10.1126/science.1164022
12. Ullian EM, Sapperstein SK, Christopherson KS, Barres BA. Control of synapse number by glia. *Science.* (2001) 291:657–61. doi: 10.1126/science.291.5504.657
13. Dudvarski Stankovic N, Teodorczyk M, Ploen R, Zipp F, Schmidt MH. Microglia-blood vessel interactions: a double-edged sword in brain pathologies. *Acta Neuropathol.* (2016) 131:347–63. doi: 10.1007/s00401-015-1524-y
14. Ginhoux F, Greter M, Leboeuf M, Nandi S, See P, Gokhan S, et al. Fate mapping analysis reveals that adult microglia derive from primitive macrophages. *Science.* (2010) 330:841–5. doi: 10.1126/science.1194637
15. Erblich B, Zhu L, Etgen AM, Dobrenis K, Pollard JW. Absence of colony stimulation factor-1 receptor results in loss of microglia, disrupted brain development and olfactory deficits. *PLoS ONE.* (2011) 6:e26317. doi: 10.1371/journal.pone.0026317
16. Greter M, Lelios I, Pelczar P, Hoeffel G, Price J, Leboeuf M, et al. Stroma-derived interleukin-34 controls the development and maintenance of langerhans cells and the maintenance of microglia. *Immunity.* (2012) 37:1050–60. doi: 10.1016/j.immuni.2012.11.001
17. Butovsky O, Jedrychowski MP, Moore CS, Cialic R, Lanser AJ, Gabriely G, et al. Identification of a unique TGF-beta-dependent molecular and functional signature in microglia. *Nat Neurosci.* (2014) 17:131–43. doi: 10.1038/nn.3599
18. Rifkin IR, Leadbetter EA, Busconi L, Viglianti G, Marshak-Rothstein A. Toll-like receptors, endogenous ligands, and systemic autoimmune disease. *Immunol Rev.* (2005) 204:27–42. doi: 10.1111/j.0105-2896.2005.00239.x
19. Yu L, Wang L, Chen S. Endogenous toll-like receptor ligands and their biological significance. *J Cell Mol Med.* (2010) 14:2592–603. doi: 10.1111/j.1582-4934.2010.01127.x
20. Zhu H, Wang L, Ruan Y, Zhou L, Zhang D, Min Z, et al. An efficient delivery of DAMPs on the cell surface by the unconventional secretion pathway. *Biochem Bioph Res Co.* (2011) 404:790–5. doi: 10.1016/j.bbrc.2010.12.061
21. Luo C, Yang X, Kain AD, Powell DW, Kuehn MH, Tezel G. Glaucomatous tissue stress and the regulation of immune response through glial Toll-like receptor signaling. *Invest Ophthalmol Vis Sci.* (2010) 51:5697–707. doi: 10.1167/iovs.10-5407
22. Howell GR, Soto I, Zhu X, Ryan M, Macalinao DG, Sousa GL, et al. Radiation treatment inhibits monocyte entry into the optic nerve head and prevents neuronal damage in a mouse model of glaucoma. *J Clin Invest.* (2012) 122:1246–61. doi: 10.1172/JCI61135
23. Bosco A, Crish SD, Steele MR, Romero CO, Inman DM, Horner PJ, et al. Early reduction of microglia activation by irradiation in a model of chronic glaucoma. *PLoS ONE.* (2012) 7:e43602. doi: 10.1371/journal.pone.0043602
24. Ebneter A, Casson RJ, Wood JP, Chidlow G. Microglial activation in the visual pathway in experimental glaucoma: spatiotemporal characterization and correlation with axonal injury. *Invest Ophthalmol Vis Sci.* (2010) 51:6448–60. doi: 10.1167/iovs.10-5284
25. Callahan MK, Ransohoff RM. Analysis of leukocyte extravasation across the blood-brain barrier: conceptual and technical aspects. *Cur Allergy Asthma Rep.* (2004) 4:65–73. doi: 10.1007/s11882-004-0046-9
26. Varnum MM, Ikezu T. The classification of microglial activation phenotypes on neurodegeneration and regeneration in Alzheimer's disease brain. *Arch Immunol Ther Exp.* (2012) 60:251–66. doi: 10.1007/s00005-012-0181-2
27. Suh HS, Zhao ML, Derico L, Choi N, Lee SC. Insulin-like growth factor 1 and 2 (IGF1, IGF2) expression in human microglia: differential regulation by inflammatory mediators. *J Neuroinflamm.* (2013) 10:37. doi: 10.1186/1742-2094-10-37
28. Tang Y, Le W. Differential roles of M1 and M2 microglia in neurodegenerative diseases. *Mol Neurobiol.* (2016) 53:1181–94. doi: 10.1007/s12035-014-9070-5
29. Burguillos MA, Deierborg T, Kavanagh E, Persson A, Hajji N, Garcia-Quintanilla A, et al. Caspase signalling controls microglia activation and neurotoxicity. *Nature.* (2011) 472:319–24. doi: 10.1038/nature09788
30. Glezer I, Simard AR, Rivest S. Neuroprotective role of the innate immune system by microglia. *Neuroscience.* (2007) 147:867–83. doi: 10.1016/j.neuroscience.2007.02.055
31. Gonzalez H, Elgueta D, Montoya A, Pacheco R. Neuroimmune regulation of microglial activity involved in neuroinflammation and neurodegenerative diseases. *J Neuroimmunol.* (2014) 274:1–13. doi: 10.1016/j.jneuroim.2014.07.012
32. Gordon R, Anantharam V, Kanthasamy AG, Kanthasamy A. Proteolytic activation of proapoptotic kinase protein kinase Cdelta by tumor necrosis factor alpha death receptor signaling in dopaminergic neurons during neuroinflammation. *J Neuroinflamm.* (2012) 9:82. doi: 10.1186/1742-2094-9-82
33. Tribble JR, Jeffrey M, Harder JM, Williams PA, John SWM. Ocular hypertension suppresses homeostatic gene expression in

optic nerve head microglia of DBA/2J mice. *Mol Brain.* (2020) 13:81. doi: 10.1186/s13041-020-00603-7
34. Heppner FL, Ransohoff RM, Becher B. Immune attack: the role of inflammation in Alzheimer disease. *Nat Rev Neurosci.* (2015) 16:358–72. doi: 10.1038/nrn3880
35. Liddelow SA, Guttenplan KA, Clarke LE, Bennett FC, Bohlen CJ, Schirmer L, et al. Neurotoxic reactive astrocytes are induced by activated microglia. *Nature.* (2017) 541:481–87. doi: 10.1038/nature21029
36. Martinez FO, Gordon S. The M1 and M2 paradigm of macrophage activation: time for reassessment. *F1000prime Rep.* (2014) 6:13. doi: 10.12703/P6-13
37. Sofroniew MV, Vinters HV. Astrocytes: biology and pathology. *Acta Neuropathol.* (2010) 119:7–35. doi: 10.1007/s00401-009-0619-8
38. Zador Z, Stiver S, Wang V, Manley GT. Role of aquaporin-4 in cerebral edema and stroke. *Handb Exp Pharmacol.* (2009) 190:159–70. doi: 10.1007/978-3-540-79885-9_7
39. Ahmed F, Brown KM, Stephan DA, Morrison JC, Johnson EC, Tomarev SI. Microarray analysis of changes in mRNA levels in the rat retina after experimental elevation of intraocular pressure. *Invest Ophthalmol Vis Sci.* (2004) 45:1247–58. doi: 10.1167/iovs.03-1123
40. Yang Z, Quigley HA, Pease ME, Yang Y, Qian J, Valenta D, et al. Changes in gene expression in experimental glaucoma and optic nerve transection: the equilibrium between protective and detrimental mechanisms. *Invest Ophthalmol Vis Sci.* (2007) 48:5539–48. doi: 10.1167/iovs.07-0542
41. Yan X, Tezel G, Wax MB, Edward DP. Matrix metalloproteinases and tumor necrosis factor alpha in glaucomatous optic nerve head. *Arch Ophthalmol.* (2000) 118:666–73. doi: 10.1001/archopht.118.5.666
42. Sawada H, Fukuchi T, Tanaka T, Abe H. Tumor necrosis factor-alpha concentrations in the aqueous humor of patients with glaucoma. *Invest Ophthalmol Vis Sci.* (2010) 51:903–6. doi: 10.1167/iovs.09-4247
43. Tezel G, Li LY, Patil RV, Wax MB. TNF-alpha and TNF-alpha receptor-1 in the retina of normal and glaucomatous eyes. *Invest Ophthalmol Vis Sci.* (2001) 42:1787–94.
44. Gregory MS, Hackett CG, Abernathy EF, Lee KS, Saff RR, Hohlbaum AM, et al. Opposing roles for membrane bound and soluble Fas ligand in glaucoma-associated retinal ganglion cell death. *PLoS ONE.* (2011) 6:e17659. doi: 10.1371/journal.pone.0017659
45. Oikawa K, Ver Hoeve JN, Teixeira LBC, Snyder KC, Kiland JA, Ellinwood NM, et al. Sub-region-specific optic nerve head glial activation in glaucoma. *Mol Neurobiol.* (2020) 57:2620–38. doi: 10.1007/s12035-020-01910-9
46. Aires ID, Ribeiro-Rodrigues T, Boia R, Catarino S, Girão H, Ambrósio AF, et al. Exosomes derived from microglia exposed to elevated pressure amplify the neuroinflammatory response in retinal cells. *Glia.* (2020) 68:2705–24. doi: 10.1002/glia.23880
47. Ko KW, Milbrandt J, DiAntonio A. SARM1 acts downstream of neuroinflammatory and necroptotic signaling to induce axon degeneration. *J Cell Biol.* (2020) 219:e201912047. doi: 10.1083/jcb.201912047
48. Figley MD, DiAntonio A. The SARM1 axon degeneration pathway: control of the NAD+ metabolome regulates axon survival in health and disease. *Curr Opin Neurobiol.* (2020) 63:59–66. doi: 10.1016/j.conb.2020.02.012
49. Summers DW, Frey E, Walker LJ, Milbrandt J, DiAntonio A. DLK activation synergizes with mitochondrial dysfunction to downregulate axon survival factors and promote SARM1-dependent axon degeneration. *Mol Neurobiol.* (2020) 57:1146–58. doi: 10.1007/s12035-019-01796-2
50. Sasaki Y, Engber TM, Hughes RO, Figley MD, Wu T, Bosanac T, et al. cADPR is a gene dosage-sensitive biomarker of SARM1 activity in healthy, compromised, and degenerating axons. *Exp Neurol.* (2020) 329:113252. doi: 10.1016/j.expneurol.2020.113252
51. Chen H, Cho KS, Vu THK, Shen C-H, Kaur M, Chen G, et al. Commensal microflora-induced T cell responses mediate progressive neurodegeneration in glaucoma. *Nat Commun.* (2018) 9:3209. doi: 10.1038/s41467-018-05681-9
52. Tezel G, Seigel GM, Wax MB. Autoantibodies to small heat shock proteins in glaucoma. *Invest Ophthalmol Vis Sci.* (1998) 39:2277–87.
53. Tezel G, Yang J, Wax MB. Heat shock proteins, immunity and glaucoma. *Brain Res Bull.* (2004) 62:473–4. doi: 10.1016/S0361-9230(03)00074-1
54. Doulberis M, Papaefthymiou A, Polyzos SA, Bargiotas P, Liatsos C, Srivastava DS„ et al. Association between active *Helicobacter pylori* infection and glaucoma: a systematic review and meta-analysis. *Microorganisms.* (2020) 8:894. doi: 10.3390/microorganisms8060894
55. Geyer O, Levo Y. Glaucoma is an autoimmune disease. *Autoimmun Rev.* (2020) 19:102535. doi: 10.1016/j.autrev.2020.102535
56. Beutgen VM, Perumal N, Pfeiffer N, Grus FH. Autoantibody biomarker discovery in primary open angle glaucoma using serological proteome analysis (SERPA). *Front Immunol.* (2019) 10:381. doi: 10.3389/fimmu.2019.00381
57. Madeira MH, Ortin-Martinez A, Nadal-Nícolas F, Ambrósio AF, Vidal-Sanz M, Agudo-Barriuso M, et al. Caffeine administration prevents retinal neuroinflammation and loss of retinal ganglion cells in an animal model of glaucoma. *Sci Rep.* (2016) 6:27532; doi: 10.1038/srep27532
58. Aires ID, Boia R, Rodrigues-Neves AC, Madeira MH, Marques C, Ambrósio AF, et al. Blockade of microglial adenosine A2A receptor suppresses elevated pressure-induced inflammation, oxidative stress, and cell death in retinal cells. *Glia.* (2019) 67:896–914. doi: 10.1002/glia.23579
59. Yang X, Zeng O, Baris M Tezel G. Transgenic inhibition of astroglial NκB restrains the neuroinflammatory and neurodegenerative outcomes of experimental mouse glaucoma. *J Neuroinflamm.* (2020) 17:252. doi: 10.1186/s12974-020-01930-1
60. Nor Arfuzir NN, Agarwal R, Iezhitsa I, Agarwal P, Ismail NM. Magnesium acetyltaurate protects against endothelin-1 induced RGC loss by reducing neuroinflammation in *Sprague dawley* rats. *Exp Eye Res.* (2020) 194:107996. doi: 10.1016/j.exer.2020.107996
61. Krishnan A, Kocab AJ, Zacs DN, Marshak-Rothstein A, Gregory-Ksander M. A small peptide antagonist of the Fas receptor inhibits neuroinflammation and prevents axon degeneration and retinal ganglion cell death in an inducible mouse model of glaucoma. *J Neuroinflamm.* (2019) 16:184. doi: 10.1186/s12974-019-1576-3
62. Williams PA, Braine CE, Kizhatil K, Foxworth NE, Tolman NG, Harder JM, et al. Inhibition of monocyte-like cell extravasation protects from neurodegeneration in DBA/2J glaucoma. *Mol Neurodegener.* (2019) 14:6. doi: 10.1186/s13024-018-0303-3
63. Means JC, Lopez AA, Koulen P. Resveratrol protects optic nerve head astrocytes from oxidative stress-induced cell death by preventing caspase-3 activation, tau dephosphorylation at Ser422 and formation of misfolded protein aggregates. *Cell Mol Neurobiol.* (2020) 40:911–26. doi: 10.1007/s10571-019-00781-6
64. Cueva Vargas JL, Belforte N, Di Polo A. The glial cell modulator ibudilast attenuates neuroinflammation and enhances retinal ganglion cell viability in glaucoma through protein kinase A signaling. *Neurobiol Dis.* (2016) 93:156–71. doi: 10.1016/j.nbd.2016.05.002
65. Marion CM, McDaniel DP, Armstrong RC. Sarm1 deletion reduces axon damage, demyelination, and white matter atrophy after experimental traumatic brain injury. *Exp Neurol.* (2019) 321:113040 doi: 10.1016/j.expneurol.2019.113040
66. Krauss R, Bosanac T, Devraj R, Engber T, Hughes RO. Axons matter: the promise of treating neurodegenerative disorders by targeting SARM1-mediated axonal degeneration. *Trends Pharmacol Sci.* (2020) 41:281–93. doi: 10.1016/j.tips.2020.01.006
67. Yang S, Xian B, Li K, Luo Z, Liu Y, Hu D, et al. Alpha 1-antitrypsin inhibits microglia activation and facilitates the survival of iPSC grafts in hypertension mouse model. *Cell Immunol.* (2018) 328:49–57. doi: 10.1016/j.cellimm.2018.03.006
68. Ehlers MR. Immune-modulating effects of alpha-1 antitrypsin. *Biol Chem.* (2014) 395:1187–93. doi: 10.1515/hsz-2014-0161
69. Ji S, Xiao J, Liu J, Tang S. Human umbilical cord mesenchymal stem cells attenuate ocular hypertension-induced retinal neuroinflammation via toll-like receptor 4 pathway. *Stem Cells Int.* (2019) 2019:17. doi: 10.1155/2019/9274585
70. Madeira MH, Elvas F, Boia R, Gonçalves FQ, Cunha RA, Ambrósio AF, et al. Adenosine A2R blockade prevents neuroinflammation-induced death of retinal ganglion cells caused by elevated pressure. *J Neuroinflamm.* (2015) 12:115. doi: 10.1186/s12974-015-0333-5
71. Cellini M, Strobe E, Gizzi C, Balducci N, Toschi PG, Campos EC. Endothelin-1 plasma levels and vascular endothelial dysfunction in primary open angle glaucoma. *Life Sci.* (2012) 91:699–702. doi: 10.1016/j.lfs.2012.02.013
72. Yang X, Hondur G, Tezel G. Antioxidant treatment limits neuroinflammation in experimental glaucoma. *Invest Ophthalmol Vis Sci.* (2016) 57:2344–54. doi: 10.1167/iovs.16-19153

73. Harun-Or-Rashid M, Inman DM. Reduced AMPK activation and increased HCAR activation drive anti-inflammatory response and neuroprotection in glaucoma. *J Neuroinflamm*. (2018) 15:313. doi: 10.1186/s12974-018-1346-7
74. Lu Y, Yang YY, Zhou MW, Liu N, Xing HY, Liu XX, et al. Ketogenic diet attenuates oxidative stress and inflammation after spinal cord injury by activating Nrf2 and suppressing the NF-kappaB signaling pathways. *Neurosci Lett*. (2018) 683:13–8. doi: 10.1016/j.neulet.2018.06.016
75. Shimazu T, Hirschey MD, Newman J, He W, Shirakawa K, Le Moan N, et al. Suppression of oxidative stress by beta-hydroxybutyrate, an endogenous histone deacetylase inhibitor. *Science*. (2013) 339:211–4. doi: 10.1126/science.1227166
76. Trovato Salinaro A, Pennisi M, Di Paola R, Scuto M, Crupi R, Cambria MT, et al. Neuroinflammation and neurohormesis in the pathogenesis of Alzheimer's disease and Alzheimer-linked pathologies: modulation by nutritional mushrooms. *Immun Ageing*. (2018) 15:8. doi: 10.1186/s12979-017-0108-1
77. Fernández-Albarral JA, Ramírez AI, de Hoz R, López-Villarín N, Salobrar-García E, López-Cuenca I, et al. Neuroprotective and anti-inflammatory effects of a hydrophilic saffron extract in a model of glaucoma. *Int J Mol Sci*. (2019) 20:4110. doi: 10.3390/ijms20174110
78. Russo R, Varano GP, Adornetto AG, Nucci C, Corasaniti MT, Bagetta G, et al. Retinal ganglion cell death in glaucoma: exploring the role of neuroinflammation. *Eur J Pharmacol*. (2016) 787:134–42. doi: 10.1016/j.ejphar.2016.03.064
79. Williams P, Marsh-Armstrong N, Howell GR. Neuroinflammation in glaucoma: a new opportunity. *Exp Eye Res*. (2017) 157:20–7. doi: 10.1016/j.exer.2017.02.014
80. Adornetto AG, Russo R, Parisi V. Neuroinflammation as a target for glaucoma therapy. *Neural Regen Res*. (2019) 14:391–4. doi: 10.4103/1673-5374.245465
81. Wei X,Cho KS, Thee EF, Jager MJ, Chen DF. Neuroimmflammation and microglia in glaucoma – time for a paradigm shift. *J Neurosci Res*. (2019) 97:70–6. doi: 10.1002/jnr.24256
82. Parsadaniantz SM, A Réaux-le Goazigo A, Sapienza A, Habas C, Baudouin C. Glaucoma: a degenerative optic neuropathy related to neuroinflammation? *Cells*. (2020) 9:535. doi: 10.3390/cells9030535

Conflict of Interest: The authors declare that the research was conducted in the absence of any commercial or financial relationships that could be construed as a potential conflict of interest.

Copyright © 2021 Rolle, Ponzetto and Malinverni. This is an open-access article distributed under the terms of the Creative Commons Attribution License (CC BY). The use, distribution or reproduction in other forums is permitted, provided the original author(s) and the copyright owner(s) are credited and that the original publication in this journal is cited, in accordance with accepted academic practice. No use, distribution or reproduction is permitted which does not comply with these terms.

frontiers in Neurology

ORIGINAL RESEARCH
published: 05 February 2021
doi: 10.3389/fneur.2020.592274

Anti-inflammatory Effect of Curcumin, Homotaurine, and Vitamin D3 on Human Vitreous in Patients With Diabetic Retinopathy

Mariaelena Filippelli[1]*, *Giuseppe Campagna*[2], *Pasquale Vito*[3,4], *Tiziana Zotti*[3,4], *Luca Ventre*[5], *Michele Rinaldi*[6], *Silvia Bartollino*[1], *Roberto dell'Omo*[1] and *Ciro Costagliola*[1,3]

[1] Department of Medicine and Health Sciences "V. Tiberio", University of Molise, Campobasso, Italy, [2] Department of Medical-Surgical Sciences and Translational Medicine, University of Rome "La Sapienza", Rome, Italy, [3] Sannio Tech Consortium, Apollosa, Italy, [4] Department of Science and Technology, University of Sannio, Benevento, Italy, [5] Azienda Ospedaliero-Universitaria Città della Salute e della Scienza di Torino, University Eye Clinic, Turin, Italy, [6] Multidisciplinary Department of Medical, Surgical and Dental Sciences, Eye Clinic, University of Campania Luigi Vanvitelli, Naples, Italy

OPEN ACCESS

Edited by:
Ahmed Toosy,
University College London,
United Kingdom

Reviewed by:
Essam Mohamed Elmatbouly Saber,
Benha University, Egypt
Laura Giannì,
Azienda Socio-Sanitaria Territoriale di Pavia (ASST Pavia), Italy

***Correspondence:**
Mariaelena Filippelli
oftelena@gmail.com

Specialty section:
This article was submitted to Neuro-Ophthalmology, a section of the journal Frontiers in Neurology

Received: 06 August 2020
Accepted: 03 December 2020
Published: 05 February 2021

Citation:
Filippelli M, Campagna G, Vito P, Zotti T, Ventre L, Rinaldi M, Bartollino S, dell'Omo R and Costagliola C (2021) Anti-inflammatory Effect of Curcumin, Homotaurine, and Vitamin D3 on Human Vitreous in Patients With Diabetic Retinopathy. Front. Neurol. 11:592274. doi: 10.3389/fneur.2020.592274

Purpose: To determine the levels of pro-inflammatory cytokines and soluble mediators (TNF-α, IL6, IL2, and PDGF-AB) in 28 vitreous biopsies taken from patients with proliferative diabetic retinopathy (PDR) and treated with increasing doses of curcumin (0. 5 and 1 μM), with or without homotaurine (100 μM) and vitamin D3 (50 nM).

Materials and Methods: ELISA tests were performed on the supernatants from 28 vitreous biopsies that were incubated with bioactive molecules at 37°C for 20 h. The concentration of the soluble mediators was calculated from a calibration curve and expressed in pg/mL. Shapiro-Wilk test was used to verify the normality of distribution of the residuals. Continuous variables among groups were compared using the General Linear Model (GLM). Homoscedasticity was verified using Levene and Brown-Forsythe tests. *Post-hoc* analysis was also performed with the Tukey test. A $p \leq 0.05$ was considered statistically significant.

Results: The *post-hoc* analysis revealed statistically detectable changes in the concentrations of TNF-α, IL2, and PDGF-AB in response to the treatment with curcumin, homotaurine, and vitamin D3. Specifically, the *p*-values for between group comparisons are as follows: TNF-α: (untreated vs. curcumin 0.5 μM + homotaurine 100 μM + vitamin D3 50 nM) $p = 0.008$, (curcumin 0.5 μM vs. curcumin 0.5 μM + homotaurine 100 μM + vitamin D3 50 nM) $p = 0.0004$, (curcumin 0.5 μM vs. curcumin 1 μM + homotaurine 100 μM + vitamin D3 50 nM) $p = 0.02$, (curcumin 1 μM vs. curcumin 0.5 μM + homotaurine 100 μM + vitamin D3 50 nM) $p = 0.025$, and (homotaurine 100 μM + vitamin D3 50 nM vs. curcumin 0.5 μM + homotaurine 100 μM + vitamin D3 50 nM) $p = 0.009$; IL2: (untreated vs. curcumin 0.5 μM + homotaurine 100 μM + vitamin D3 50 nM) $p = 0.0023$, and (curcumin 0.5 μM vs. curcumin 0.5 μM+ homotaurine 100 μM + vitamin D3 50 nM) $p = 0.0028$; PDGF-AB: (untreated vs. curcumin 0.5 μM + homotaurine 100 μM + vitamin D3 50 nM) $p = 0.04$, (untreated vs. curcumin 1 μM + homotaurine 100 μM + vitamin D3 50 nM) $p = 0.0006$,

(curcumin 0.5 μM vs. curcumin 1 μM + homotaurine 100 μM + vitamin D3 50 nM) $p = 0.006$, and (homotaurine 100 μM + vitamin D3 50 nM vs. curcumin 1 μM + homotaurine 100 μM + vitamin D3 50 nM) $p = 0.022$. IL6 levels were not significantly affected by any treatment.

Conclusions: Pro-inflammatory cytokines are associated with inflammation and angiogenesis, although there is a discrete variability in the doses of the mediators investigated among the different vitreous samples. Curcumin, homotaurine, and vitamin D3 individually have a slightly appreciable anti-inflammatory effect. However, when used in combination, these substances are able to modify the average levels of the soluble mediators of inflammation and retinal damage. Multi-target treatment may provide a therapeutic strategy for diabetic retinopathy in the future.

Clinical Trial Registration: The trial was registered at clinical trials.gov as NCT04378972 on 06 May 2020 ("retrospectively registered") https://register.clinicaltrials.gov/prs/app/action/SelectProtocol?sid = S0009UI8&selectaction = Edit&uid = U0003RKC&ts = 2&cx = dstm4o.

Keywords: diabetic retinopathy, neuroprotection, vitreous, curcumin, homotaurine, vitamin D3, pro-inflammatory cytokines

INTRODUCTION

The number of people of all age groups who are visually impaired worldwide is estimated at 285 million; among these, 39 million are blind (1). Visual impairment is strongly associated with increasing age. In high-income regions of Central/Eastern Europe, diabetic retinopathy (DR) and glaucoma are the most important causes of vision loss (2). Glaucoma affects more than 70 million people worldwide (3) and it leads to progressive optic nerve degeneration, with a gradual loss of retinal ganglion cells (RGCs) (4, 5). The pathogenesis of glaucoma is not yet completely clarified (i.e., mechanical/ischemic insult, neuroinflammation, etc.) (6). Furthermore, although lowering intraocular pressure (IOP) has been clearly shown to decrease the progressive visual loss in most patients with glaucoma (7), there are some patients for whom IOP lowering is either insufficient, difficult to achieve, or associated with risks of adverse effects, especially when patients are treated with surgical procedures (8). Thus, other strategies are needed to reduce or reverse the progressive neurodegeneration, and this represents the rationale for therapies based on neuroprotection (9). By definition, neuroprotection is an effect that may result in rescue, recovery, or regeneration of the nervous system, its cells, structure, and function (10). In ophthalmology as well as for glaucoma, neuroprotection is also emerging as a therapeutic target for diabetic retinopathy (11).

Diabetic retinopathy (DR) is one of the most common complications of diabetes mellitus and is a leading cause of vision loss and blindness in the working-age population worldwide. Once considered solely as a microvascular disease, DR has been recognized as a neurodegenerative disease of the retina (12–13 effects of antioxidants). Progressive blindness is due to the long-term accumulation of pathological abnormalities in the retina of hyperglycemic patients. In the initial phase, non-proliferative diabetic retinopathy (NPDR) is almost asymptomatic, with the onset of microhemorrhagic and microischemic episodes and an increase in vascular permeability. Subsequently, the progression of the disease is accompanied by the onset of a chronic inflammatory state and neovascularization in a vicious circle that feeds and determines the accumulation of damage to the retina through hypoxia, oxidative stress, and widespread neurodegeneration. Among the metabolites, hyperglycemia is known to be the major factor activating several metabolic pathways that are harmful for the retina (12). Moreover, an increased level of glutamate has been reported in both the retina and vitreous of diabetic patients, suggesting a neurotoxic role of glutamate, which may damage retinal neurons, especially retinal ganglion cells, by excitotoxicity (12–15). Thus, glaucoma and diabetic retinopathy have in common the occurrence of a progressive neurodegeneration. In fact, several studies have shown that there is an overexpression of excitatory proteins, such as glutamate and NMDA, in the retina and vitreous in glaucoma, diabetic retinopathy, and multiple animal models of retinal ischemia (16, 17). In proliferative diabetic retinopathy (PDR), vitreous humor undergoes structural and molecular changes as well as changes in its composition, which play a pivotal role in supporting the disease progression (18). The vitreous is a transparent, gel-like structure of 4 mL in volume, which fills the space between the lens and the retina (19). It is composed of 98-99% of water, with traces of cations, ions, proteins (mainly collagen), and polysaccharides such as hyaluronic acid (20). In PDR patients undergoing pars plana vitrectomy, vitreous samples are characterized by altered levels of bioactive molecules, with pro-angiogenic, pro-inflammatory, and neuromodulatory activities (19). This clearly demonstrates that the vitreous acts as a reservoir of soluble signaling mediators

that may exacerbate retinal damage. On the other hand, the vitreous obtained from patients with PDR can be a powerful tool to evaluate the anti-angiogenic/anti-inflammatory activity of new biomolecules that could be potential candidates for the treatment of diabetic vitreoretinopathy. Currently, PDR is treated with laser photocoagulation, vitreoretinal surgery, or intravitreal injection of drugs targeting the vascular endothelial growth factor (VEGF) and steroid agents (21). However, although these protocols are effective in the short term, they cause side effects and are indicated only for the advanced stages of the disease.

Thus, non-invasive, non-destructive, and longer-duration treatment options are also needed (22). Recently, research efforts have been made to identify neuroprotective compounds that are able to prevent visual field loss and preserve visual function. A promising alternative for the treatment of early-stage NPDR comes from nutraceuticals. In fact, *in vitro* and *in vivo* studies have revealed that a variety of nutraceuticals offers important antioxidant and anti-inflammatory effects that can counteract the first diabetes-driven molecular events that cause vitreoretinopathy, acting as upstream regulators of the disease (23). Based on the results of several investigations, it is reasonable to assert that a single constituent that affects one target has limited efficacy in preventing the progression of multifactorial diseases. A large body of research revealed that the use of a combination of compounds with synergistic multitarget effects may offer a more powerful approach for the prevention of diseases, including retinal neurodegeneration (24–27). In experimental models, it has been shown that the co-treatment of citicoline and homotaurine has a direct neuroprotective effect on primary retinal cells exposed to glutamate toxicity and high glucose (HG) levels (28). Glutamate-induced excitotoxicity is implicated in the pathophysiology of several degenerative diseases of the retina, including glaucoma. Moreover, HG-induced neurotoxicity is a characteristic of diabetic retinopathy (29, 30). Curcumin, a yellowish non-flavonoid polyphenol that constitutes the main active compound of *Curcuma longa,* is widely known for its antioxidant and anti-inflammatory properties (31–33). Many studies have also described its marked protective effect on retinal cells against oxidative stress and inflammation (31–35). Lastly, vitamin D3 levels appear to be lower in diabetes mellitus type 2 patients, and this could have therapeutic implications (36). This study aimed to analyze the soluble mediators of inflammation and angiogenesis in the vitreous of patients with diabetic retinopathy treated with homotaurine, curcumin, and vitamin D3.

MATERIALS AND METHODS

The study was conducted at the Department of Medicine and Health Sciences "V. Tiberio" of Molise University, Campobasso (Italy), in accordance with the ethical principles of the Declaration of Helsinki. The CTS (technical scientific committee) of the Department approved the study protocol (registered at clinicaltrials.gov, identifier NCT0437897). All the study participants provided written informed consent. This was a prospective study including 28 eyes of 28 patients consecutively enrolled from September 16, 2019 to December 16, 2019. The patients were scheduled to undergo a 23-gauge, three-port pars plana vitrectomy for retinal detachment, and all the patients completed the study. Inclusion criteria were age $\geq$18 years, patients with diabetic retinopathy requiring vitrectomy, and willingness to participate in the study following the indications provided. The exclusion criteria were previous vitrectomy in the study eye, previous buckle surgery, previous intravitreal injection, concurrent retinovascular or other ocular inflammatory disease, history of ocular trauma and concomitant intake of any topical or systemic NSAID or corticosteroid therapy, and presence of systemic inflammations. All phakic patients were operated with phacoemulsification of the crystalline lens plus intraocular lens (IOL) implant at the time of vitrectomy to allow a careful cleaning of the vitreous base. Vitrectomy surgery was performed using a 23-gauge transconjunctival system; no triamcinolone was used during any step of the surgery.

After the removal of the posterior hyaloids, the vitreous base was thoroughly removed. All the visible proliferative vitreoretinopathy (PVR) membranes were dissected, and relaxing retinotomies were performed. The retinal periphery was inspected for retinal breaks that were marked with endodiathermy, after which the retina was reattached using perfluorocarbon liquid and air. Three rows of endolaser treatment were applied behind the posterior vitreous base in all the patients (200 spots, 200–250 mW according to retinal pigmentation). All the patients in both groups were prescribed topical dexamethasone (six times per day) and homatropine (two times per day).

At the beginning of the surgery, 0.5–1.0 mL of undiluted aqueous was removed, and samples were immediately frozen and stored at −80°C until analysis. This procedure was used to prevent the vitrectomy intervention itself from generating or altering the expression of cytokines and endothelial growth factors or the BSS (balanced salt solution) from diluting the vitreous.

TREATED GROUP: Twenty-eight portions of vitreous samples from 28 eyes of patients undergoing vitrectomy for diabetic retinopathy complications, incubated with curcumin, homotaurine, and vitamin D3. The substances were treated with increasing doses of curcumin (Cureit®) (0.5 μM and 1 μM), with or without homotaurine (100 μM) and vitamin D3 (50 nM), to evaluate a possible synergistic effect on the expression of inflammatory cytokines.

CONTROL GROUP: The same fractions of vitreous samples ($n = 28$) were evaluated for the expression of oxidative biomarkers, inflammatory cytokines, and metalloproteinases, without any treatment.

PRIMARY ENDPOINT: Evaluation of the anti-inflammatory effect of curcumin, homotaurine, and vitamin D3 on the expression of inflammatory cytokines in human vitreous samples of patients with PDR.

Reagents

Cholecalciferol (vitamin D3) and 3-Amino-1-propanesulfonic acid (homotaurine) were purchased from Sigma-Aldrich,

whereas Cureit® curcumin was provided by Fisher Chemicals Aurea Biolab. Curcumin and vitamin D3 were first dissolved in DMSO (dimethyl sulfoxide) to final concentrations of 250 and 25 mM, respectively. Homotaurine was resuspended in PBS to a final concentration of 500 mM.

ELISA Assays

Curcumin is a well-known bioactive molecule, largely employed in supplement formulation due to its anti-inflammatory properties. To evaluate its role in the regulation of the levels of pro-inflammatory soluble mediators in the vitreous fluid obtained from 28 patients with PDR, samples were exposed to curcumin at different concentrations for 24 h with or without homotaurine and vitamin D3. Subsequently, IL6, IL2, TNF-α, and PDGF-AB were measured by ELISA assays in 50 μl of diluted samples from different conditions.

Vitreous biopsies were thawed and centrifuged. Afterwards, 50 μL of vitreal fluid from each patient were aliquoted into 96-well plates and incubated for 24 h at 37°C in 100 μL HBSS (Hank's Balanced Salt Solution) with curcumin at different concentrations (0.5 and 1 μM) and with or without 100 μM homotaurine and 50 nM vitamin D3. Controls were exposed to HBSS containing DMSO. The day after, samples were diluted twice in sample diluent and cytokines were measured by ELISA assay.

Quantitative detection of soluble mediators in vitreal biopsies was performed using sandwich ELISA kits with High Sensitivity. IL2 and TNF-α were measured by Human Pre-coated ELISA Kit (BIOGEMS-PEPROTECH), whereas IL6 and PDGF-AB were detected using PicoKine ELISA Kits (Boster Biological Technology). All kit reagents, samples, and standards were prepared according to the manufacturer's instructions. The measured optical density was read at 450 nm and was directly proportional to the concentration of human recombinant proteins in the standards or samples. The concentration of soluble mediators was calculated from a calibration curve and expressed as pg/mL. Each experimental point was replicated three times, and absolute levels of IL6, IL2, TNF-α, and PDGF-AB were measured by ELISA. Subsequently, average levels of soluble mediators measured in treated vitreous were expressed as a percentage of the baseline level, considering the control aliquot from the same patient as baseline. According to manufacturer's instructions, optimal detection ranges were 15.6–1,000 pg/mL (sensitivity <0.1 pg/mL) for IL2; 15.6–1,000 pg/mL (sensitivity <1 pg/mL) for TNF-α; 4.69–300 pg/mL (sensitivity <0.3 pg/mL) for IL6; and 31.2–2,000 pg/mL (sensitivity <2 pg/mL) for PDGF-AB. Only the mean IL6 levels in vitreous biopsies were found to be close to the lower limit of detection, however, we could still measure significative optical densities in our experimental conditions.

Gene Expression

To verify whether curcumin in combination with vitamin D3 and homotaurine in the vitreal fluid could exert an anti-inflammatory and anti-angiogenic effect, we monitored the expression of pro-inflammatory genes and mitogen-activated genes in an immortalized cell line exposed for 24 h to vitreal biopsies from patients with diabetic retinopathy together with curcumin, vitamin D3, and homotaurine or not. A subset of four vitreous was used in this experiment.

Sample Size

The sample size was estimated with a suitable macro developed in the SAS language. We conducted a pilot study from which we derived the Mean Square Error (MSE). In order to make the data less variable, we applied the logarithmic transformation that made the residuals normal. The General Linear Model (GLM) provided the standard deviations (square root of MSE) necessary to perform the calculation of the Sample Size (±0.29, ±0.18, ±0.18, ±0.32, respectively, for PDGF-AB, IL2, IL6, and TNF-α).

Considering the following differences, on a logarithmic scale, $d = 0.32$, 0.13, 0.11, and 0.29, which correspond to a reduction of 52.1, 32.4, 22.4, and 48.7% relative to PDGF-AB, IL2, IL6, and TNF-α, we obtained with a power of 80% and $\alpha = 0.05$ the following sample sizes: $n = 19$, 26, 61, and 28 subjects, taking into account the correction for multiple comparisons. For clinical purposes, we considered $n = 28$ as the final sample size.

Statistical Analysis

Continuous variables (PDGF-AB, IL2, IL6, and TNF-α levels) were expressed as mean ± SD. Shapiro-Wilk test was used to verify the normality of distribution of the residuals.

To make the residuals normal, we applied suitable mathematical functions in order to respect the Gauss condition.

The continuous variables (PDGF-AB, IL2, IL6, and TNF–α levels) were compared among groups (untreated, curcumin 0.5 μM, curcumin 1 μM, homotaurine 100 μM + vitamin D3 50 nM, curcumin 0.5 μM + homotaurine 100 μM + vitamin D3 50 nM, and curcumin 1 μM + homotaurine 100 μM + vitamin D3 50 nM) using the GLM (General Liner Model) method. Homoscedasticity was verified by Levene and Brown-Forsythe tests. *Post-hoc* analysis was performed by the Tukey test.

A $p \leq 0.05$ was considered statistically significant. The statistical analysis was performed using SAS v. 9.4 and JMP v. 15 (SAS Institute Inc., Cary, NC, USA).

RESULTS

Twenty-eight vitreous biopsies from 28 patients with PDR were analyzed. The mean age (± standard deviation) was 68.9 ± 7.8 years. Of the 28 included patients, 16 (57.1%) were males and 12 (42.9%) were females. Mean time (± standard deviation) since diagnosis of diabetes mellitus in these patients was 31.4 ± 8.7 years. The mean age (± standard deviation) at the time of vitrectomy was 68.9 ± 7.9 years old. In vitreous samples, the pro-inflammatory cytokines IL6, TNF-α, and IL2 and the angiogenic factor PDGF-AB were all detectable in the conditions of the sample. Mean IL6, IL2, TNF-α, and PDGF-AB levels in the vitreous of the patients are reported in **Table 1**.

The *post-hoc* analysis revealed statistically detectable changes in the concentration of TNF-α, IL2, and PDGF-AB in response to treatment with curcumin, homotaurine, and vitamin D3. Specifically, the p-values for between group comparisons are as follows: TNF-α: (untreated vs. curcumin 0.5 μM + homotaurine

TABLE 1 | Levels of soluble mediators in vitreal biopsies from patients with diabetic retinopathy.

Parameter	Untreated	Curcumin 0.5 μM	Curcumin 1 μM	Homotaurine 100 μM + Vitamin D3 50 nM	Curcumin 0.5 μM+ Homotaurine 100 μM + Vitamin D3 50 nM	Curcumin 1 μM + Homotaurine 100 μM + Vitamin D3 50 nM	*p*
	Mean ± SD (95% CI)	Mean ± SD (95% CI)	Mean ± SD (95% CI)	Mean ± SD (95% CI)	Mean ± SD (95% CI)	Mean ± SD (95% CI)	
PDGF-AB[a] (pg/mL)	842.68 ± 459.61 (664.50–1020.86)	780.43 ± 466.58 (599.51–961.35)	657.58 ± 311.24 (536.89–778.26)	735.94 ± 466.40 (555.09–916.79)	538.32 ± 345.39 (404.40–672.25)	406.41 ± 213.85 (323.48–489.33)	**0.0003**
IL2[b] (pg/mL)	85.17 ± 47.33 (66.81–103.52)	81.95 ± 44.33 (64.76–99.14)	63.00 ± 30.51 (51.17–74.83)	71.81 ± 41.05 (55.89–87.73)	55.93 ± 26.73 (45.56–66.30)	60.21 ± 26.84 (49.80–70.62)	**0.0005**
IL6[c] (pg/mL)	16.71 ± 7.02 (13.99–19.43)	15.81 ± 6.11 (13.44–18.18)	15.28 ± 5.88 (13.00–17.56)	15.96 ± 7.63 (13.00–18.92)	13.78 ± 8.03 (10.67–16.90)	15.52 ± 8.39 (12.27–18.78)	0.32
TNF-α[c] (pg/mL)	112.56 ± 72.85 (84.32–140.81)	113.27 ± 50.20 (93.81–132.74)	110.68 ± 82.95 (78.52–142.85)	108.61 ± 74.37 (79.78–137.45)	59.31 ± 42.09 (42.99–75.63)	66.52 ± 43.59 (49.62–83.43)	**0.0001**

[a]*sqrt transformed.*
[b]*Inverse transformed.*
[c]*log_{10} transformed.*
Post-hoc Analysis: PDGF-AB - (untreated vs. curcumin 0.5 μM + homotaurine 100 μM + vitamin D3 50 nM) p = 0.04; (untreated vs. curcumin 1 μM + homotaurine 100 μM + vitamin D3 50 nM) p = 0.0006; (curcumin 0.5 μM vs. curcumin 1 μM + homotaurine 100 μM + vitamin D3 50 nM) p = 0.006; (homotaurine 100 μM + vitamin D3 50 nM vs. curcumin 1 μM + homotaurine 100 μM + vitamin D3 50 nM) p = 0.022. IL2 - (untreated vs. curcumin 0.5 μM + homotaurine 100 μM + vitamin D3 50 nM) p = 0.0023; (curcumin 0.5 μM vs. curcumin 0.5 μM + homotaurine 100 μM + vitamin D3 50 nM) p = 0.0028. TNF-α - (untreated vs. curcumin 0.5 μM + homotaurine 100 μM + vitamin D3 50 nM) p = 0.008; (curcumin 0.5 μM vs. curcumin 0.5 μM + homotaurine 100 μM + vitamin D3 50 nM) p = 0.0004; (curcumin 1 μM + homotaurine 100 μM + vitamin D3 50 nM) p = 0.02; (curcumin 1 μM vs. curcumin 0.5 μM + homotaurine 100 μM + vitamin D3 50 nM) p = 0.025; (homotaurine 100 μM + vitamin D3 50 nM vs. curcumin 0.5 μM + homotaurine 100 μM + vitamin D3 50 nM) p = 0.009. Bold values are those statistically significant.

100 μM + vitamin D3 50 nM) $p = 0.008$, (curcumin 0.5 μM vs. curcumin 0.5 μM + homotaurine 100 μM + vitamin D3 50 nM) $p = 0.0004$, (curcumin 0.5 μM vs. curcumin 1 μM + homotaurine 100 μM + vitamin D3 50 nM) $p = 0.02$, (curcumin 1 μM vs. curcumin 0.5 μM + homotaurine 100 μM + vitamin D3 50 nM) $p = 0.025$, and (homotaurine 100 μM + vitamin D3 50 nM vs. curcumin 0.5 μM + homotaurine 100 μM + vitamin D3 50 nM) $p = 0.009$ **(Figure 1)**; IL2: (untreated vs. curcumin 0.5 μM + homotaurine 100 μM + vitamin D3 50 nM) $p = 0.0023$ and (curcumin 0.5 μM vs. curcumin 0.5 μM + homotaurine 100 μM + vitamin D3 50 nM) $p = 0.0028$ **(Figure 2)**; PDGF-AB: (untreated vs. curcumin 0.5 μM + homotaurine 100 μM + vitamin D3 50 nM) $p = 0.04$, (untreated vs. curcumin 1 μM + homotaurine 100 μM + vitamin D3 50 nM) $p = 0.0006$, (curcumin 0.5 μM vs. curcumin 1 μM + homotaurine 100 μM + vitamin D3 50 nM) $p = 0.006$, and (homotaurine 100 μM + vitamin D3 50 nM vs. curcumin 1 μM + homotaurine 100 μM + vitamin D3 50 nM) $p = 0.022$ **(Figure 3)**. IL6 levels were not affected by any treatment **(Figure 4)**.

Gene expression performed on four vitreous biopsies demonstrated that vitreal fluids can induce the cyclinD1 gene and the pro-inflammatory cytokine genes TNFα and IL6 on human HEK293 cells; contrarily when vitreal fluids were used in combination with curcumin, vitamin D3, and homotaurine such levels were down-regulated **(Figure 5)**.

DISCUSSION

Intravitreal corticosteroids and anti-VEGF agents have become the first-line therapy for diabetic macular edema and PDR (37). However, in clinical practice, the use of anti-VEGF is not always applicable, due to the requirement of frequent injections and poor patient compliance. In fact, laser photocoagulation still plays an important role in the treatment of DR. However, in spite of a range of treatments such as those aforementioned, many patients with DR do not respond well to current approaches. Thus, there is still a need for more effective treatments, and biomarkers may help to gain knowledge of DR and contribute to the development of novel clinical strategies to prevent vision loss in people with diabetes (38). Optimization of current treatment therapies with regard to the number of intravitreal injections, dosage, and duration as well as of strategies for combination therapy is of great importance to improve the quality of life of patients with DR (37) and to enhance their chances of visual recovery.

The presence of a chronic systemic low-grade inflammation is characteristic of diabetes mellitus, contributing to the worsening of the inflammatory process that occurs in the eye (13, 22, 39–41). In DR, oxidative stress is promoted by several mechanisms, including the pathway of polyols (41–43), vascular dysfunction, production of pro-inflammatory cytokines (TNF-α, IL6, and interleukin-1 beta) and protein kinase C, accumulation of advanced glycation products, activation of the renin-angiotensin-aldosterone system, increment of growth factors, and leukostasis (44–53). Regarding cytokines, several studies have shown increased levels of pro-inflammatory cytokines in the vitreous

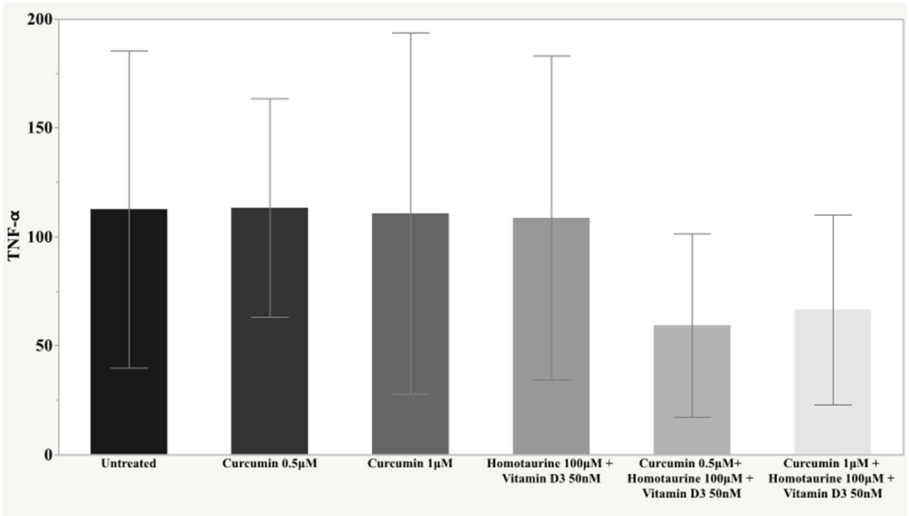

FIGURE 1 | Histogram of the mean and standard deviations of TNF-α (pg/ml) by experimental groups.

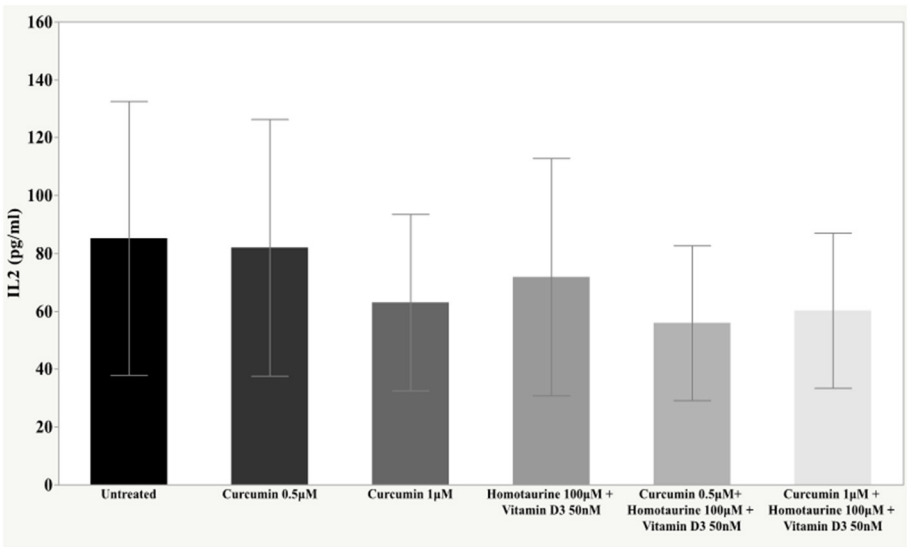

FIGURE 2 | Histogram of the mean and standard deviations of IL2 by experimental groups.

and retina of diabetic patients and animals (53, 54). Indeed, intravitreal concentrations of major pro-inflammatory cytokines and chemokines, including IL1β, TNF-α, IL6, and IL8, are markedly upregulated in the vitreous of patients with PDR (55–57). Furthermore, an increase of TNF-α, IL8, and soluble IL2 receptor was observed in the progression from DR to PDR (58). It is clear that inflammation plays a key role in DR and, for this reason, the inhibition of the inflammatory pathway could be an interesting treatment option for DR (44, 45, 58, 59).

It is well known that the changes occurring in the retina are closely linked to biochemical changes in the vitreous humor (57, 60, 61). In fact, the vitreous has metabolic activity, and although it is considered as an acellular structure, phagocytic mononuclear hyalocytes and other cellular components are found in its different regions (62). Moreover, due to its proximity to the retina, the vitreous can undergo structural and biochemical changes that reflect the pathophysiological processes occurring in the retinal tissue (19, 61).

Our study highlighted the ability of curcumin to reduce cytokine levels in the vitreous of diabetic patients. We also observed an additional anti-inflammatory effect when curcumin was combined with homotaurine and vitamin D3, suggesting that these molecules can regulate the inflammatory network between the vitreous and retina at different levels. This effect is confirmed by the gene expression experiment which demonstrated that the combination of curcumin, vitamin D3, and homotaurine

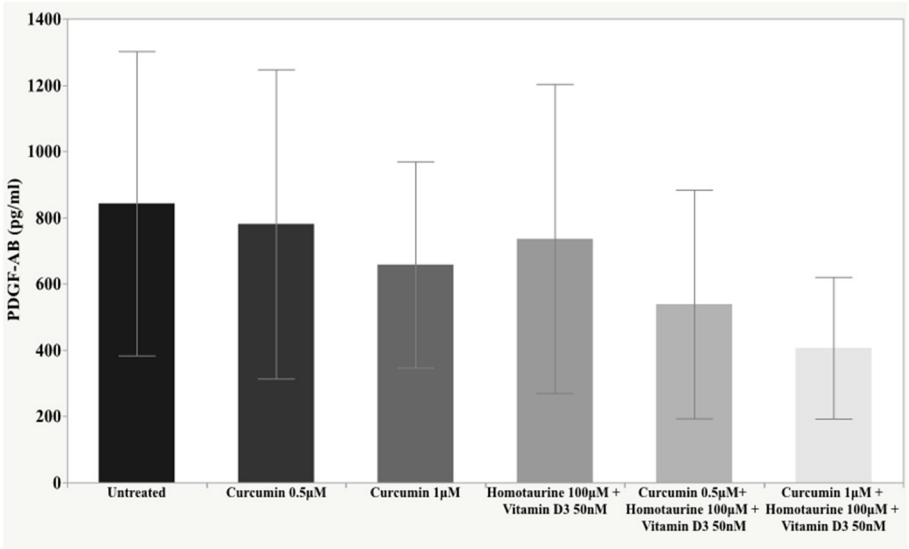

FIGURE 3 | Histogram of the mean and standard deviations of PDGF-AB by experimental groups.

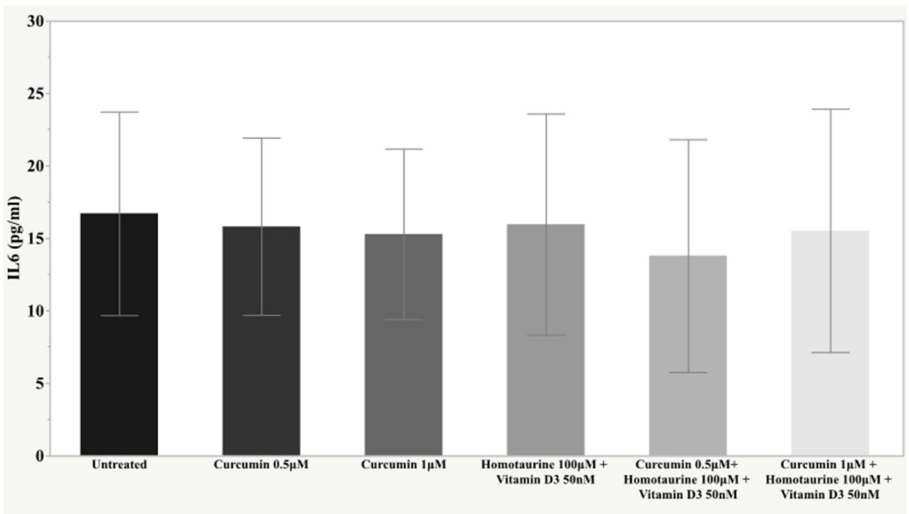

FIGURE 4 | Histogram of the mean and standard deviations of IL6 by experimental groups.

down-regulate the cyclinD1 gene and the pro-inflammatory cytokine genes TNFα and IL6 expression. It is well known that the synergism of curcumin with other bioactive molecules like those in turmeric makes a positive impact by generating high concentration of "free curcuminoids" in the blood plasma, as shown in previous studies (63). Moreover, homotaurine has been proven effective in reducing proinflammatory cytokines in synergy with other compounds. This result adds to the growing body of literature showing neuroprotective effects of homotaurine (30). Furthermore, the association of curcumin and homotaurine with vitamin D3 has also proved to be successful, confirming the results of numerous studies that have identified vitamin D as having a key role in diabetes. Vitamin D deficiency has been shown to impair insulin synthesis and secretion in animal models of diabetes (64, 65). Vitamin D3 decreases diabetes induced Reactive Oxygen Species (ROS) and exerts protective effects against retinal vascular damage and cell apoptosis in association with the inhibition of the ROS/TXNIP/NLRP3 inflammasome pathway (66, 67).

In our study, only IL6 levels showed no significant changes in response to treatment with the various compounds tested. This result could be due to the cross-talk between IL1β and IL6 signaling, more precisely due to the inhibitory action of IL1β on IL6 signaling, as has been reported by Shen et al. (68).

Finally, the identification of additional biomarkers in DR might lead to potential therapeutic targets and additive treatment

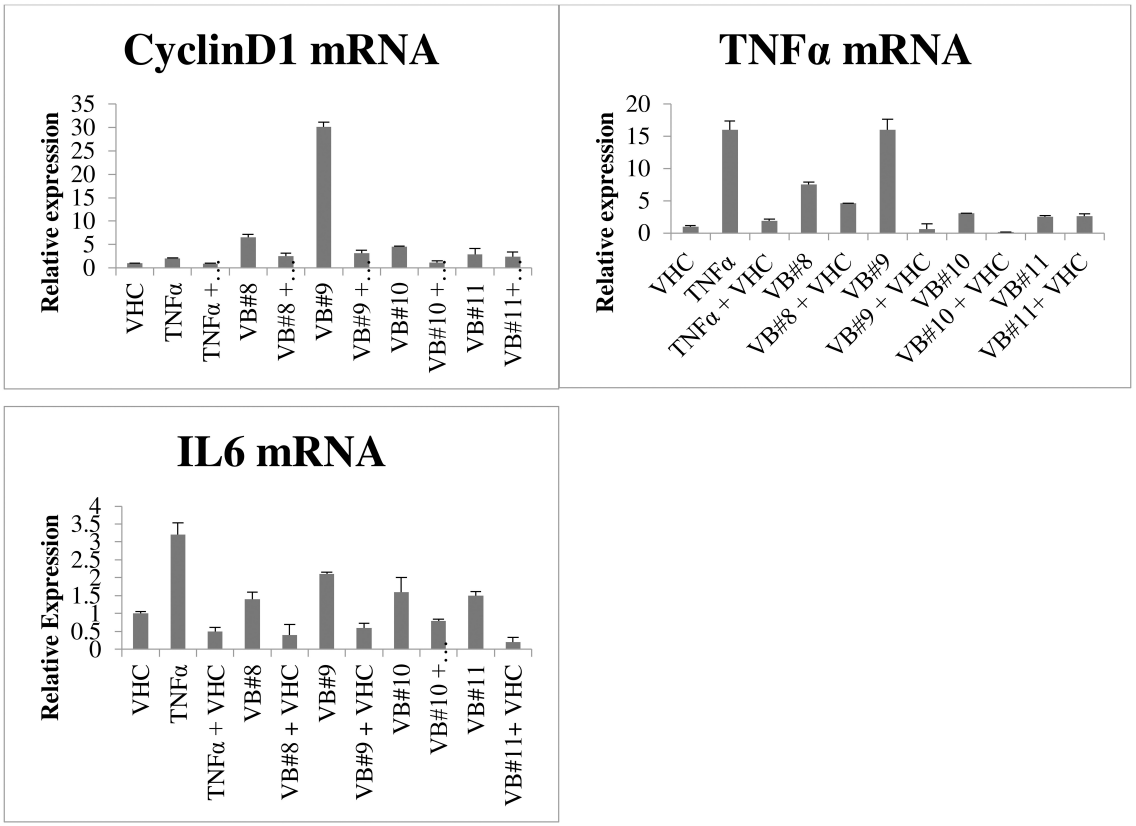

VHC = Vitamin D3 50nM + Homotaurine 100μM + Curcumin 1μM

TNFα = Tumor Necrosis Factor alpha 50ng/ml

VB# = Vitreal Biopsy #

FIGURE 5 | Gene expression in the vitreous of diabetic retinopathy patients.

options to improve metabolic control and neuroprotection in the context of individual customized therapy. This would maximize the patient's outcomes, with less collateral effects, leading to a reduction in the number of treatments, and enabling the control of lateral effects. In the DR treatment, anti-angiogenic therapy and anti-inflammatory agents could be used in combination, possibly simultaneously, to reduce the number of injections, risks, and costs (44).

CONCLUSION

These findings confirm that pro-inflammatory cytokines and angiogenetic factors are associated with inflammation and angiogenesis, which synergistically contribute to the pathogenesis of DR. Our results underline that a multi-target treatment may provide a therapeutic strategy for DR treatment in the future. Natural anti-inflammatory compounds play an important role through their ability to reduce cytokine levels and regulate the inflammatory network (40) and reduce the rate of administration of anti-neovascularization agents, leading to an improvement in the quality of life of these patients.

DATA AVAILABILITY STATEMENT

The original contributions presented in the study are included in the article/supplementary materials, further inquiries can be directed to the corresponding author/s.

ETHICS STATEMENT

The study was conducted at the Department of Medicine and Health Sciences V. Tiberio of Molise University, Campobasso (Italy), in accordance with the ethical principles of the Declaration of Helsinki. The CTS (technical scientific committee) of the Department approved the study protocol (registered

at clinicaltrials.gov, identifier NCT0437897). All the study participants provided written informed consent.

AUTHOR CONTRIBUTIONS

MF and CC contributed to study concept and design, data analyses, interpretation of data, drafting of the manuscript, critical review of the manuscript, and study supervision. PV, TZ, LV, MR, and Rd'O performed acquisition of data, data analyses, interpretation of data, drafting of the manuscript, critical review of the manuscript. SB and GC conducted the study per protocol, interpretation of data, drafting of the manuscript, critical review of the manuscript. GC contributed to interpretation of data and statistical analysis. All authors contributed to the article and approved the submitted version.

ACKNOWLEDGMENTS

We gratefully acknowledge the support of FB vision for providing curcumin, homotaurine, and vitamin D3 and Sanniotech for the technical assistance.

REFERENCES

1. Pascolini D, Mariotti SP. Global estimates of visual impairment: 2010. *Br J Ophthalmol*. (2012) 96:614–8. doi: 10.1136/bjophthalmol-2011-300539
2. Bourne RR, Jonas JB, Flaxman SR, Keeffe J, Leasher J, Naidoo K, et al. Prevalence and causes of vision loss in high-income countries and in Eastern and Central Europe: 1990-2010. *Br J Ophthalmol*. (2014) 98:629–38. doi: 10.1136/bjophthalmol-2013-304033
3. Nickells RW, Howell GR, Soto I, John SW. Under pressure: cellular and molecular responses during glaucoma, a common neurodegeneration with axonopathy. *Annu Rev Neurosci*. (2012) 35:153–79. doi: 10.1146/annurev.neuro.051508.135728
4. Weinreb RN, Aung T, Medeiros FA. The pathophysiology and treatment of glaucoma: a review. *JAMA*. (2014) 311:1901–11. doi: 10.1001/jama.2014.3192
5. Gauthier AC, Liu J. Neurodegeneration and Neuroprotection in Glaucoma. *Yale J Biol Med*. (2016) 89:73–9. Published 2016 Mar 24.
6. Morrone LA, Rombolà L, Corasaniti MT, Bagetta G, Nucci C, Russo R. Natural compounds and retinal ganglion cell neuroprotection. *Prog Brain Res*. (2015) 220:257–81. doi: 10.1016/bs.pbr.2015.05.004
7. Garway-Heath DF, Crabb DP, Bunce C, Lascaratos G, Amalfitano F, Anand N, et al. Latanoprost for open-angle glaucoma (UKGTS): a randomised, multicentre, placebo-controlled trial [published correction appears in Lancet. 2015 Jul 11;386(9989):136]. *Lancet*. (2015) 385:1295–304. doi: 10.1016/S0140-6736(14)62111-5
8. Levin LA, Crowe ME, Quigley HA; Lasker/IRRF initiative on astrocytes and glaucomatous neurodegeneration participants. Neuroprotection for glaucoma: requirements for clinical translation. *Exp Eye Res*. (2017) 157:34–7. doi: 10.1016/j.exer.2016.12.005
9. He S, Stankowska DL, Ellis DZ, Krishnamoorthy RR, Yorio T. Targets of neuroprotection in glaucoma. *J Ocul Pharmacol Ther*. (2018) 34:85–106. doi: 10.1089/jop.2017.0041
10. Vajda FJ. Neuroprotection and neurodegenerative disease. *J Clin Neurosci*. (2002) 9:4–8. doi: 10.1054/jocn.2001.1027
11. Hernández C, Dal Monte M, Simó R, Casini G. Neuroprotection as a therapeutic target for diabetic retinopathy. *J Diabetes Res*. (2016) 2016:9508541. doi: 10.1155/2016/9508541
12. Sasso FC, Zuchegna C, Tecce MF, Capasso A, Adinolfi LE, Romano A, et al. High glucose concentration produces a short-term increase in pERK1/2 and p85 proteins, having a direct angiogenetic effect by an action similar to VEGF [published online ahead of print, 2020 Mar 4]. *Acta Diabetol*. (2020) 57:947–58. doi: 10.1007/s00592-020-01501-z
13. Ola MS, Alhomida AS. Neurodegeneration in diabetic retina and its potential drug targets. *Curr Neuropharmacol*. (2014) 12:380–6. doi: 10.2174/1570159X12666140619205024
14. Semeraro F, Cancarini A, dell'Omo R, Rezzola S, Romano MR, Costagliola C. Diabetic retinopathy: vascular and Inflammatory disease. *J Diabetes Res*. (2015) 2015:582060. doi: 10.1155/2015/582060
15. Diederen RM, La Heij EC, Deutz NE, Kijlstra A, Kessels AGH, van Eijket HMH, et al. Increased glutamate levels in the vitreous of patients with retinal detachment. *Exp Eye Res*. (2006) 83:45–50. doi: 10.1016/j.exer.2005.10.031
16. Yu XH, Zhang H, Wang YH, Liu LJ, Teng Y, Liu P. Time-dependent reduction of glutamine synthetase in retina of diabetic rats. *Exp Eye Res*. (2009) 89:967–71. doi: 10.1016/j.exer.2009.08.006
17. Ng YK, Zeng XX, Ling EA. Expression of glutamate receptors and calcium-binding proteins in the retina of streptozotocin-induced diabetic rats. *Brain Res*. (2004) 1018:66–72. doi: 10.1016/j.brainres.2004.05.055
18. Pulido JE, Pulido JS, Erie JC, Arroyo J, Bertram K, Lu MJ, et al. A role for excitatory amino acids in diabetic eye disease. *Exp Diabetes Res*. (2007) 2007:36150. doi: 10.1155/2007/36150
19. Nawaz IM, Rezzola S, Cancarini A, Russo A, Costagliola C, Semeraro F, et al. Human vitreous in proliferative diabetic retinopathy: characterization and translational implications. *Prog Retin Eye Res*. (2019) 72:100756. doi: 10.1016/j.preteyeres.2019.03.002
20. Kishi S. Vitreous anatomy and the vitreomacular correlation. *Jpn J Ophthalmol. (*2016) 60:239–73 doi: 10.1007/s10384-016-0447-z
21. Schmidt-Erfurth U, Garcia-Arumi J, Bandello F, Berg K, Chakravarthy U, Gerendas BS, et al. Guidelines for the Management of Diabetic Macular Edema by the European Society of Retina Specialists (EURETINA). *Ophthalmologica*. (2017) 237:185–222. doi: 10.1159/000458539
22. Wang W, Lo ACY. Diabetic Retinopathy: pathophysiology and Treatments. *Int J Mol Sci. (*2018) 19:1816. doi: 10.3390/ijms19061816
23. Duh EJ, Sun JK, Stitt AW. Diabetic retinopathy: current understanding, mechanisms, and treatment strategies. *JCI Insight*. (2017) 2:e93751. doi: 10.1172/jci.insight.93751
24. Rossino MG, Casini G. Nutraceuticals for the treatment of diabetic retinopathy. *Nutrients*. (2019) 11:771. doi: 10.3390/nu11040771
25. Davinelli S, Sapere N, Visentin M, Zella D, Scapagnini G. Enhancement of mitochondrial biogenesis with polyphenols: combined effects of resveratrol and equol in human endothelial cells. *Immun Ageing*. (2013) 10:28. doi: 10.1186/1742-4933-10-28
26. Davinelli S, Calabrese V, Zella D, Scapagnini G. Epigenetic nutraceutical diets in Alzheimer's disease. *J Nutr Health Aging*. (2014) 8:800–5. doi: 10.1007/s12603-014-0552-y
27. Davinelli S, Maes M, Corbi G, Zarrelli A, Willcox DC, Scapagnini G. Dietary phytochemicals and neuro-inflammaging: from mechanistic insights to translational challenges. *Immun Ageing*. (2016) 13:16. doi: 10.1186/s12979-016-0070-3
28. Davinelli S, Scapagnini G, Marzatico F, Nobile V, Ferrara N, Corbi G. Influence of equol and resveratrol supplementation on health-related quality of life in menopausal women: a randomized, placebo-controlled study. *Maturitas*. (2017) 96:77–83. doi: 10.1016/j.maturitas.2016.11.016
29. Pescosolido N, Librando A. Oral administration of an association of forskolin, rutin and vitamins B1 and B2 potentiates the hypotonising effects of pharmacological treatments in POAG patients. *Clin Ter*. (2010) 161:e81–5.
30. Davinelli S, Chiosi F, Di Marco R, Costagliola C, Scapagnini G. Cytoprotective effects of citicoline and homotaurine against glutamate and high glucose neurotoxicity in primary cultured retinal cells. *Oxid Med Cell Longev*. (2017) 2017:2825703. doi: 10.1155/2017/2825703
31. Barber AJ. A new view of diabetic retinopathy: a neurodegenerative disease of the eye. *Prog Neuro-Psychoph*. (2003) 27:283–90. doi: 10.1016/S0278-5846(03)00023-X

32. Nucci C, Russo R, Martucci A, Giannini C, Garaci F, Floris R, et al. New strategies for neuroprotection in glaucoma, a disease that affects the central nervous system. *Eur J Pharmacol*. (2016) 787:119–26. doi: 10.1016/j.ejphar.2016.04.030
33. Kocaadam B, Sanlier, N. Curcumin, an active component of turmeric (Curcuma longa), and its effects on health. *Crit Rev Food Sci and Nutr*. (2015) 57:2889–95. doi: 10.1080/10408398.2015.1077195
34. Munia I, Gafray L, Bringer MA, Goldschmidt P, Proukhnitzky L, Jacquemot N, et al. Cytoprotective effects of natural highly bio-available vegetable derivatives on human-derived retinal cells. *Nutrients*. (2020) 12:879. doi: 10.3390/nu12030879
35. Tong F, Chai R, Jiang H, Dong B. *In vitro/vivo* drug release and anti-diabetic cardiomyopathy properties of curcumin/PBLG-PEG-PBLG nanoparticles. *Int J Nanomed*. (2018) 13:1945–62. doi: 10.2147/IJN.S153763
36. Kostoglou-Athanassiou I, Athanassiou P, Gkountouvas A, Kaldrymides P. Vitamin D and glycemic control in diabetes mellitus type 2. *Ther Adv Endocrinol Metab*. (2013) 4:22–128. doi: 10.1177/2042018813501189
37. Chawan-Saad J, Wu M, Wu A, Wu L. Corticosteroids for diabetic macular edema. *Taiwan J Ophthalmol*. (2019) 9:233–42. doi: 10.4103/tjo.tjo_68_19
38. Jenkins AJ, Joglekar MV, Hardikar AA, Keech AC, O'Neal DN, Januszewski AS. Biomarkers in diabetic retinopathy. *Rev Diabet Stud*. (2015) 12:159–95. doi: 10.1900/RDS.2015.12.159
39. Adamis AP. Is diabetic retinopathy an inflammatory disease? *Br J Ophthalmol*. (2002) 86:363–5. doi: 10.1136/bjo.86.4.363
40. Kern TS. Contributions of inflammatory processes to the development of the early stages of diabetic retinopathy. *Exp Diabetes Res*. (2007) 2007:95103. doi: 10.1155/2007/95103
41. Noda K, Nakao S, Ishida S, Ishibashi T. Leukocyte adhesion molecules in diabetic retinopathy. *J Ophthalmol*. (2012) 2012:279037. doi: 10.1155/2012/279037
42. Semeraro F, Morescalchi F, Cancarini A, Russo A, Rezzola S, Costagliola C. Diabetic retinopathy, a vascular and inflammatory disease: therapeutic implications. *Diabetes Metab*. (2019) 45:517–27. doi: 10.1016/j.diabet.2019.04.002
43. Kowluru RA, Chan PS. Oxidative stress and diabetic retinopathy. *Exp Diabetes Res*. (2007) 2007:43603. doi: 10.1155/2007/43603
44. Gürler B, Vural H, Yilmaz N, Oguz H, Satici A, Aksoy N. The role of oxidative stress in diabetic retinopathy. *Eye (Lond)*. (2000) 14(Pt 5):730–5. doi: 10.1038/eye.2000.193
45. Capitão M, Soares R. Angiogenesis and inflammation crosstalk in diabetic retinopathy. *J Cell Biochem*. (2016) 117:2443–53. doi: 10.1002/jcb.25575
46. Cai J, Boulton M. The pathogenesis of diabetic retinopathy: old concepts and new questions. *Eye (Lond)*. (2002) 16:242–60. doi: 10.1038/sj.eye.6700133
47. El-Asrar AM. Role of inflammation in the pathogenesis of diabetic retinopathy. *Middle East Afr J Ophthalmol*. (2012) 19:70–4. doi: 10.4103/0974-9233.92118
48. Wirostko B, Wong TY, Simó R. Vascular endothelial growth factor and diabetic complications. *Prog Retin Eye Res*. (2008) 27:608–21. doi: 10.1016/j.preteyeres.2008.09.002
49. Costagliola C. Oxidative state of glutathione in red blood cells and plasma of diabetic patients*: in vivo* and *in vitro* study. *Clin Physiol Biochem*. (1990) 8:204–10.
50. Costagliola C, Daniele A, dell'Omo R, Romano MR, Aceto F, Agnifili L, et al. Aqueous humor levels of vascular endothelial growth factor and adiponectin in patients with type 2 diabetes before and after intravitreal bevacizumab injection. *Exp Eye Res*. (2013) 110:50–4. doi: 10.1016/j.exer.2013.02.004
51. Simó-Servat O, Hernández C, Simó R. Genetics in diabetic retinopathy: current concepts and new insights. *Curr Genomics*. (2013) 14:289–99. doi: 10.2174/13892029113149990008
52. Goldin A, Beckman JA, Schmidt AM, Creager MA. Advanced glycation end products: sparking the development of diabetic vascular injury. *Circulation*. (2006) 114:597–605. doi: 10.1161/CIRCULATIONAHA.106.621854
53. Tarr JM, Kaul K, Chopra M, Kohner EM, Chibber R. Pathophysiology of diabetic retinopathy. *ISRN Ophthalmol*. (2013) 2013:343560. doi: 10.1155/2013/343560
54. Patel N. Targeting leukostasis for the treatment of early diabetic retinopathy. *Cardiovasc Hematol Disord Drug Targets*. (2009) 9:222–9. doi: 10.2174/187152909789007052
55. Brucklacher RM, Patel KM, VanGuilder HD, Bixler GV, Barber AJ, Antonetti DA, et al. Whole genome assessment of the retinal response to diabetes reveals a progressive neurovascular inflammatory response. *BMC Med Genomics*. (2008) 1:26. doi: 10.1186/1755-8794-1-26
56. Tang J, Kern TS. Inflammation in diabetic retinopathy. *Prog Retin Eye Res*. (2011) 30:343–58. doi: 10.1016/j.preteyeres.2011.05.002
57. dell'Omo R, Semeraro F, Bamonte G, Cifariello F, Romano MR, Costagliola C. Vitreous mediators in retinal hypoxic diseases. *Mediators Inflamm*. (2013) 2013:935301. doi: 10.1155/2013/935301
58. Doganay S, Evereklioglu C, Er H, Türköz Y, Sevinç A, Mehmet N, et al. Comparison of serum NO, TNF-alpha, IL-1beta, sIL-2R, IL-6 and IL-8 levels with grades of retinopathy in patients with diabetes mellitus. *Eye (Lond)*. (2002) 16:163–70. doi: 10.1038/sj.eye.6700095
59. Gologorsky D, Thanos A, Vavvas D. Therapeutic interventions against inflammatory and angiogenic mediators in proliferative diabetic retinopathy. *Mediators Inflamm*. (2012) 2012:629452. doi: 10.1155/2012/629452
60. Zorena K. Anti-inflammatory therapy in diabetic retinopathy. *Mediators Inflamm*. (2014) 2014:947896. doi: 10.1155/2014/947896
61. Murthy KR, Goel R, Subbannayya Y, Jacon HKC, Murthy PR, Manda SS, et al. Proteomic analysis of human vitreous humor. *Clin Proteomics*. (2014) 1:29. doi: 10.1186/1559-0275-11-29
62. Yoshimura T, Sonoda KH, Sugahara M, Mochizuki Y, Enaida H, Oshima Y, et al. Comprehensive analysis of inflammatory immune mediators in vitreoretinal diseases. *PLoS ONE*. (2009) 4:e8158. doi: 10.1371/journal.pone.0008158
63. Mitri J, Pittas AG. Vitamin D and diabetes. *Endocrinol Metab Clin North Am*. (2014) 43:205–32. doi: 10.1016/j.ecl.2013.09.010
64. Jude S, Amalraj A, Kunnumakkara AB, Divya C, Löffler BM, Gopi S. development of validated methods and quantification of curcuminoids and curcumin metabolites and their pharmacokinetic study of oral administration of complete natural turmeric formulation (Cureit^{TM}) in human plasma via UPLC/ESI-Q-TOF-MS spectrometry. *Molecules*. (2018) 23:2415. doi: 10.3390/molecules23102415
65. Snijder M, van Dam R, Visser M, Deeg D, Seidell J, Lips P. To: Mathieu C, Gysemans C, Giulietti A, Bouillon R. Vitamin D and diabetes. *Diabetologia*. (2005) 48:1247–57. *Diabetologia*. (2006) 49:217–8. doi: 10.1007/s00125-005-0047-9
66. Luo BA, Gao F, Qin LL. The association between vitamin D Deficiency and diabetic retinopathy in type 2 diabetes: a meta-analysis of observational studies. *Nutrients*. (2017) 9:307. doi: 10.3390/nu9030307
67. Lu L, Lu Q, Chen W, Li J, Li C, Zheng Z. Vitamin D_3 protects against diabetic retinopathy by inhibiting high-glucose-induced activation of the ROS/TXNIP/NLRP3 inflammasome pathway. *J Diabetes Res*. (2018) 2018:8193523. doi: 10.1155/2018/8193523
68. Shen X, Tian Z, Holtzman MJ, Gao B. Cross-talk between interleukin 1beta (IL-1beta) and IL-6 signalling pathways: IL-1beta selectively inhibits IL-6-activated signal transducer and activator of transcription factor 1 (STAT1) by a proteasome-dependent mechanism. *Biochem J*. (2000) 352:913–9.

Conflict of Interest: The authors declare that the research was conducted in the absence of any commercial or financial relationships that could be construed as a potential conflict of interest.

Copyright © 2021 Filippelli, Campagna, Vito, Zotti, Ventre, Rinaldi, Bartollino, dell'Omo and Costagliola. This is an open-access article distributed under the terms of the Creative Commons Attribution License (CC BY). The use, distribution or reproduction in other forums is permitted, provided the original author(s) and the copyright owner(s) are credited and that the original publication in this journal is cited, in accordance with accepted academic practice. No use, distribution or reproduction is permitted which does not comply with these terms.

frontiers in Neurology

ORIGINAL RESEARCH
published: 12 February 2021
doi: 10.3389/fneur.2021.609929

Disrupted Neural Activity in Individuals With Iridocyclitis Using Regional Homogeneity: A Resting-State Functional Magnetic Resonance Imaging Study

Yan Tong[1], *Xin Huang*[2], *Chen-Xing Qi*[1] *and Yin Shen*[1,3]*

[1] Eye Center, Renmin Hospital of Wuhan University, Wuhan, China, [2] Department of Ophthalmology, Jiangxi Provincial People's Hospital, Nanchang, China, [3] Frontier Science Center for Immunology and Metabolism, Medical Research Institute, Wuhan University, Wuhan, China

OPEN ACCESS

Edited by:
Ahmed Toosy, University College London, United Kingdom

Reviewed by:
Hai jun Li, Nanchang University, China
Gloria Castellazzi, University College London, United Kingdom

***Correspondence:**
Yin Shen
yinshen@whu.edu.cn

Specialty section:
This article was submitted to Neuro-Ophthalmology, a section of the journal Frontiers in Neurology

Received: *24 September 2020*
Accepted: *11 January 2021*
Published: *12 February 2021*

Citation:
Tong Y, Huang X, Qi C-X and Shen Y (2021) Disrupted Neural Activity in Individuals With Iridocyclitis Using Regional Homogeneity: A Resting-State Functional Magnetic Resonance Imaging Study. Front. Neurol. 12:609929. doi: 10.3389/fneur.2021.609929

Objective: This study used the regional homogeneity (ReHo) technique to explore whether spontaneous brain activity is altered in patients with iridocyclitis.

Methods: Twenty-six patients with iridocyclitis (14 men and 12 women) and 26 healthy volunteers (15 men and 11 women) matched for sex and age were enrolled in this study. The ReHo technique was used to comprehensively assess changes in whole-brain synchronous neuronal activity. The diagnostic ability of the ReHo method was evaluated by means of receive operating characteristic (ROC) curve analysis. Moreover, associations of average ReHo values in different brain areas and clinical characteristics were analyzed using correlation analysis.

Result: Compared with healthy volunteers, reduced ReHo values were observed in patients with iridocyclitis in the following brain regions: the right inferior occipital gyrus, bilateral calcarine, right middle temporal gyrus, right postcentral gyrus, left superior occipital gyrus, and left precuneus. In contrast, ReHo values were significantly enhanced in the right cerebellum, left putamen, left supplementary motor area, and left inferior frontal gyrus in patients with iridocyclitis, compared with healthy volunteers (false discovery rate correction, $P < 0.05$).

Conclusion: Patients with iridocyclitis exhibited disturbed synchronous neural activities in specific brain areas, including the visual, motor, and somatosensory regions, as well as the default mode network. These findings offer a novel image-guided research strategy that might aid in exploration of neuropathological or compensatory mechanisms in patients with iridocyclitis.

Keywords: iridocyclitis, regional homogeneity, resting-state fMRI, spontaneous brain activity, inflammation

INTRODUCTION

Uveitis is the most common type of inflammatory ophthalmological disease and has been estimated to cause up to 10% of legal blindness in the USA (1). Iridocyclitis is an acute inflammation of the iris and ciliary body; this is the most common pattern of uveitis, which is present in 85% of affected patients. Typical clinical features of iridocyclitis include eye redness, pain, blurred vision, photophobia, and miosis (2). HLA-B27 is a common risk factor for anterior uveitis, which has been found in ∼40–70% of patients with uveitis (3). A range of complications such as secondary glaucoma, high intraocular pressure, cystoid macular edema, and posterior synechiae often occur, especially in patients with HLA-B27 (4). Subsequently, visual acuity can decrease temporarily or permanently because of the underlying inflammatory process or ocular complications of iridocyclitis. Moreover, a variety of patients with non-infectious iridocyclitis exhibit immune-mediated diseases (5), such as ankylosing spondylitis (AS), interstitial nephritis, and sarcoidosis. Elucidation of the underlying etiology may be challenging, because there is considerable variability in these mechanisms (e.g., from infectious to autoimmune diseases); however, this elucidation remains important, especially for patients with recurrent iridocyclitis.

Over the past few years, extensive neuroimaging researches have been conducted to evaluate cortical structural abnormalities in patients with iridocyclitis. Multiple studies have recorded ocular morphologic alterations affected by uveitis, including alterations in peripapillary retinal nerve fiber layer thickness, macular volume, and retinal thickness (6–8). Both cellular and humoral responses to a series of retinal antigens and their epitopes are known to occur in patients with iridocyclitis (9). Thus, even mild ocular inflammation can affect the ocular posterior segment, potentially leading to retinal and brain neurodegeneration through the visual pathway (10). Moreover, the retinal vessels have the same physiological, anatomical, and embryological characteristics with cerebral vessels; various quantitative and qualitative alterations involving the retinal capillary plexuses or choriocapillaris have been observed in patients with uveitis by means of optical coherence tomography angiography (11, 12). In addition, patients with iridocyclitis were shown to have a greater risk of depression and tend to adopt negative coping strategies (13, 14). In a pilot clinical study, Maca et al. pointed out that patients with iridocyclitis showed symptoms of cognition impairment including cognitive avoidance, distraction, and self-revalorization deficit through standardized psychological questionnaires (15). However, the abovementioned studies were limited to analyses of neuronal morphological changes and structural abnormalities in patients with iridocyclitis. To our knowledge, there is a lack of direct evidence regarding altered brain function in patients with iridocyclitis. Here, we hypothesized that iridocyclitis would influence the functions of certain brain areas, which might facilitate identification of the underlying neural mechanism.

Resting-state functional magnetic resonance imaging (fMRI) permits visualization of functional changes in the whole brain *in vivo*; it has the advantage of non-invasiveness, accurate positioning, and no ionizing radiation (16). Synchronous neuronal activity has been shown to occur in the normal human brain, particularly during memory and learning, in previous fMRI and electroencephalographic studies (17, 18). Moreover, transmission of synchronous neuronal activity is known to be involved in neuronal information processing (19). Regional homogeneity (ReHo) is a highly reliable fMRI index for evaluation of local synchronous neural activity patterns at rest; it measures the coherence of the blood oxygen level-dependent signal between the time series of a given cluster and its nearest neighbors by using Kendall's coefficient of concordance (20). The principle of the blood oxygen level-dependent signal is based on the inconsistencies in the local hemodynamics of neurons following excitation, in order to reveal spontaneous neuronal activity by quantifying alterations in blood oxygen level signals (21). Areas with higher ReHo signals imply that those brain regions have similar activities, compared with their neighbors. In contrast to conventional seed-based functional connectivity technique, ReHo provides the possibility to search for abnormalities in the entire brain functional connectome without pre-definition the region of interests. Besides, it is more stable than amplitude of low-frequency fluctuation method and less affected by global nuisances in the retest analysis (22). Most previous researches have proven that the ReHo technique is a reliable technique for application in various neuro-ophthalmological assessments; it has been widely used to reveal the mechanisms of ophthalmologic diseases including diabetic retinopathy (23), optic neuritis (24), amblyopia (25), and retinal detachment (26).

Iridocyclitis can induce both structural and functional alterations to the retina and its vessels, thereby affecting visual function. fMRI can be used to visualize alterations in regional neuronal activity and serve as a valuable monitoring modality, thereby improving disease management. Thus far, the spontaneous brain activity patterns of patients with iridocyclitis has been unclear. This study applied the ReHo technique to investigate spontaneous neuronal activity in patients with iridocyclitis.

METHODS

Participants

The study followed the tenets of the Declaration of Helsinki and was approved by the institutional review board of the Eye Center, Renmin Hospital of Wuhan University. Each participant provided signed informed consent to participate in our study. This study enrolled 26 patients with iridocyclitis (mean age 45.15 ± 14.95) and 26 healthy volunteers (mean age 45.30 ± 13.87) who were matched on the basis of sex, age, and education. Patients with iridocyclitis enrolled in the study met the inclusion criteria as follows: [1] diagnosis of iridocyclitis, based on the Standardization of Uveitis Nomenclature Working Group classification (27); [2] ability to undergo magnetic resonance imaging scanning; [3] right-handed preference; and [4] no history of psychotropic drug use or psychiatric diseases. The exclusion criteria for patients with iridocyclitis were as

follows: [1] presence of other ocular diseases (e.g., age-related macular degeneration, high myopia, epiretinal membrane, and glaucoma); [2] history of refractive/vitreoretinal surgery or ocular trauma; and/or [3] systemic diseases.

Inclusion criteria for healthy volunteers were as follows: [1] no retinal diseases such as diabetic retinopathy, cataract, or macular edema; [2] no psychiatric or neurological disorders; [3] no contraindications for magnetic resonance imaging scanning; [4] right-handed preference; and [5] binocular visual acuity $\geq$ 1.0. All participants underwent a complete ophthalmic assessment (biomicroscopy, slit-lamp examination, best-corrected visual acuity measurement, fundus examination, indirect ophthalmoscopy, and fluorescein angiography).

MRI Parameters

Both whole-brain functional and T1-weighted MRI scans were carried out on a 3.0T GE MR750W scanner (GE Healthcare) with a standard head coil. Each participant was instructed to stay awake with eyes closed and relax their minds until the examination was over (28, 29). The whole-brain anatomical T1-weighted images were collected with a three-dimensional spoiled gradient-recalled echo sequence with following parameters: repetition time (TR)/echo time (TE), 8.5 ms/3.3 ms; gap, 0 mm; field of view (FOV), 240 × 240 mm^2; acquisition matrix, 256 × 256; thickness, 1.0 mm; and flip angle, 12°.

The whole-brain fMRI data was recorded by applying gradient-recalled echo-planar imaging sequence with parameters as follows: TR/TE, 2,000 ms/25 ms; gap, 1.2 mm, thickness, 3.0 mm; FOV, 240 × 240 mm^2; acquisition matrix, 64 × 64; 35 axial slices; and flip angle, 90°. The whole scanning time was ∼15 min, and a total of 240 volumes of functional images were acquired.

fMRI Data Preprocessing

Initially, functional images were checked by the MRIcro software (http://www.MRIcro.com) to exclude unqualified data. All preprocessing was performed using the Data Processing & Analysis of Brain Imaging (DPARSFA4.3, Institute of Psychology, Beijing) and the Statistical Parametric Mapping 12 (The MathWorks, Inc.) software running on Matlab 2014b (MathWorks, Natick, MA, USA) (30). [1] Original DICOM files were converted into NIFTI files. [2] The first 10 volumes of each functional time series were discarded to maintain magnetization equilibrium. [3] The remaining 230 volumes of functional images were modified for slice timing effects, motion corrected, and realigned. Data from subjects whose head motion with maximum displacement in any axis of >2.0 mm or head rotation of >1.5° were excluded. [3] Individual T1-weighted images were registered to the mean fMRI data, and then, the resulting aligned T1-weighted images were segmented using the Diffeomorphic Anatomical Registration Through Exponentiated Lie Algebra toolbox for improving spatial precision in the normalization of fMRI data (31). All the data were ultimately normalized to the standard Montreal Neurological Institute (MNI) space. [4] Detrend of the time course was performed. [5] Linear regression analysis was used to remove nuisance covariates (such as white matter signal, six head motion parameters, and cerebrospinal fluid signal); [5] After that, the fMRI images were band pass-filtered (0.01–0.08 Hz) to reduce the effects of low-frequency drift and high-frequency signals (32).

ReHo Calculation

Calculation of ReHo values for fMRI data was conducted using REST (http://www.restfmri.net) toolbox. ReHo reflects the local synchronization between the spontaneous activity of a given voxel and its nearest neighboring voxels (20). ReHo is calculated by Kendall's coefficient of concordance with the formula below, where W represents the Kendall's coefficient of concordance among given voxels; R_i represents the sum rank of the time point; n represents the number of ranks; $K = 27$; and $R = (n + 1)\ K\ /\ 2$ represents the mean of the R_is. To reduce the impact of individual variability, the ReHo index was divided by the global the mean ReHo value. Finally, the fMRI data were smoothed with a 4 × 4 × 4 mm^3 full-width at half-maximum Gaussian kernel.

$$W = \frac{\sum (R_i)^2 - n(\overline{R})^2}{\frac{1}{12}K^{2(n^3-n)}}$$

Statistical Analysis

Differences between participants' demographic and clinical variables were analyzed by independent sample t-tests or the chi-square test using SPSS software (SPSS version 20.0, IBM Corporation, Armonk, NY, USA). $P < 0.05$ was considered to imply statistical significance. Besides, values are displayed as the mean ± standard deviation. Multiple comparison correction was conducted using the false discovery rate (FDR) method, and the statistical threshold for significance was set at $P < 0.05$. All ReHo maps were z-transformed with Fisher' r-to-z transformation to reduce the impacts of individual variations for group statistical comparisons. One-sample t-tests were performed to evaluate patterns of z-value ReHo maps, and two-sample t-tests were performed to investigate differences in ReHo values between patients with iridocyclitis and the healthy volunteers using SPM 8 software. The specific anatomical locations of all statistically significant results were presented as an image by BrainNet Viewer software (https://www.nitrc.org/projects/bnv/).

Pearson's correlation coefficients were calculated to investigate possible relationships between the average z ReHo of different brain areas and clinical characteristics of patients with iridocyclitis using SPSS software. In addition, brain areas with a distinctly different mean ReHo values between patients with iridocyclitis and healthy volunteers were analyzed using the receiver operating characteristic (ROC) curve method (SPSS version 20.0).

RESULTS

Demographics and Clinical Data

The typical anterior segment photograph of iridocyclitis is displayed in **Figure 1**. There were no significant differences in age ($P = 0.97$), sex ($P = 0.780$), and educational status ($P = 0.871$) between the iridocyclitis group and healthy volunteer group. By contrast, the notable differences were observed in the

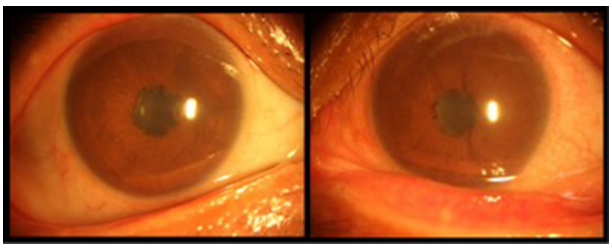

FIGURE 1 | Typical anterior segment photograph of iridocyclitis.

best-corrected visual acuity-left and best-corrected visual acuity-right ($P < 0.001$) between the two groups. More participants' demographic data are presented in **Table 1**.

ReHo Differences

Figure 2 shows the spatial distributions of ReHo values of the patients with iridocyclitis and healthy volunteers. Compared with healthy volunteers, significantly decreased ReHo value was observed in the patients of iridocyclitis in the following brain regions: the right inferior occipital gyrus, the right middle temporal gyrus, the bilateral calcarine, the right postcentral gyrus, the left superior occipital gyrus, and the left precuneus [FDR correction, $P < 0.05$; **Figure 3** (blue)]. In contrast, it was observed that the ReHo value was significantly enhanced in the right cerebellum, the left putamen, the left supplementary motor area, and the left inferior frontal gyrus in patients with iridocyclitis compared with healthy volunteers [FDR correction, $P < 0.05$; **Figure 3** (red)]. **Table 2** exhibited the altered brain areas and corresponding information between iridocyclitis group and healthy volunteer group (FDR correction, $P < 0.05$). The average values of alterations in ReHo between the two groups are displayed as a histogram (**Figure 4**). Nevertheless, no notable correlation was observed between average ReHo values in altered brain areas and patients' clinical features ($P > 0.05$).

ROC Curve

To explore whether the distinctive ReHo signal values obtained from the two groups could be a useful diagnostic marker to distinguish patients with iridocyclitis from healthy volunteers, ROC curve analysis was conducted. The areas under the ROC curve (AUCs) were as follows: right inferior occipital gyrus [0.815; $P < 0.001$; 95% confidence interval (CI), 0.693–0.937]; right middle temporal gyrus (0.815; $P < 0.001$; 95% CI, 0.695–0.936), right calcarine (0.834; $P < 0.001$; 95% CI, 0.726–0.942), left calcarine (0.806; $P < 0.001$; 95% CI, 0.683–0.930), right postcentral gyrus (0.926; $P < 0.001$; 95% CI, 0.854–0.998), left superior occipital gyrus (0.845; $P < 0.001$; 95% CI, 0.738–0.952), and left precuneus (0.843; $P < 0.001$; 95% CI, 0.733–0.954) (**Table 3** and **Figure 5A**, iridocyclitis < healthy volunteers); right cerebellum (0.833; $P < 0.001$; 95% CI, 0.719–0.947); left putamen (0.891; $P < 0.001$; 95% CI, 0.802–0.979); left inferior frontal gyrus (0.916; $P < 0.001$; 95% CI, 0.844–0.987); and left supplementary motor area (0.879; $P < 0.001$; 95% CI, 0.788–0.969) (**Table 3** and **Figure 5B**).

TABLE 1 | General clinical information of patients with iridocyclitis and healthy volunteers.

	Iridocyclitis group	HC group	*T*-values	*P*-values
Sex (male/ female)	14/12	15/11	N/A	0.780
Mean age (years)	45.15 ± 14.95	45.30 ± 13.87	−0.038	0.970
Education (years)	10.96 ± 3.73	11.12 ± 2.86	−0.164	0.871
BCVA-OD	0.44 ± 0.27	1.16 ± 0.16	−11.474	<0.001*
BCVA-OS	0.43 ± 0.37	1.19 ± 0.16	−9.352	<0.001*
Handedness	26 R	26 R	N/A	N/A
Diagnosis of iridocyclitis (right eye/left eye)	11/15	N/A	N/A	N/A

*Chi-square test for sex. Independent t-test was used for other normally distributed continuous data. Data are presented as mean ± standard deviation. Abbreviations: HC, healthy control; BCVA, best-corrected visual acuity; OD, oculus dexter; OS, oculus sinister; N/A, not applicable; R, right. *indicates statistically significant.*

DISCUSSION

ReHo values represent the local spontaneous coherence of neural activity and have been widely applied for analysis of multiple ophthalmologic diseases (23, 26, 33), such that this technique has considerable potential (**Table 4**). To our knowledge, it is the first study in which the ReHo technique has been applied to evaluate the effect of iridocyclitis on resting-state synchronous brain activity. The results of this study exhibited that, compared with healthy volunteers, patients with iridocyclitis had reduced ReHo in the right inferior occipital gyrus, bilateral calcarine, right middle temporal gyrus, left superior occipital gyrus, right postcentral gyrus, and left precuneus. They also had enhanced ReHo in the right cerebellum, left putamen, left inferior frontal gyrus, and left supplementary motor area (**Figure 6**).

We found that patients with iridocyclitis generally exhibited significant reduction of ReHo values in portions of vision-related regions. The occipital lobe is a crucial anatomical area for visual information processing. It also controls pupil accommodation reflex activities and eye movements related to vision (38). The calcarine sulcus is located in the medial surface of the occipital lobe, within the primary visual cortex (V1). Retinal photoreceptors take a core role in visual function. They convert light signals to nerve impulses and transmit these impulses to retinal ganglion cells. Numerous studies have shown that through the visual pathway, visual signals are projected to the visual cortex (39). Although iridocyclitis is defined as inflammation of the iris and ciliary body, recent studies have demonstrated retinal involvement (8, 40, 41). These findings imply that simultaneous fluid accumulation in the retina and choroid during acute inflammation, combined with deprivation of retinal input, might lead to functional alterations within the visual cortex. Thus, we presume that visual information processing in the brain might have deteriorated in patients with iridocyclitis because of this vision loss.

The main clusters with decreased ReHo values were observed in the right postcentral gyrus. Anatomically, the postcentral

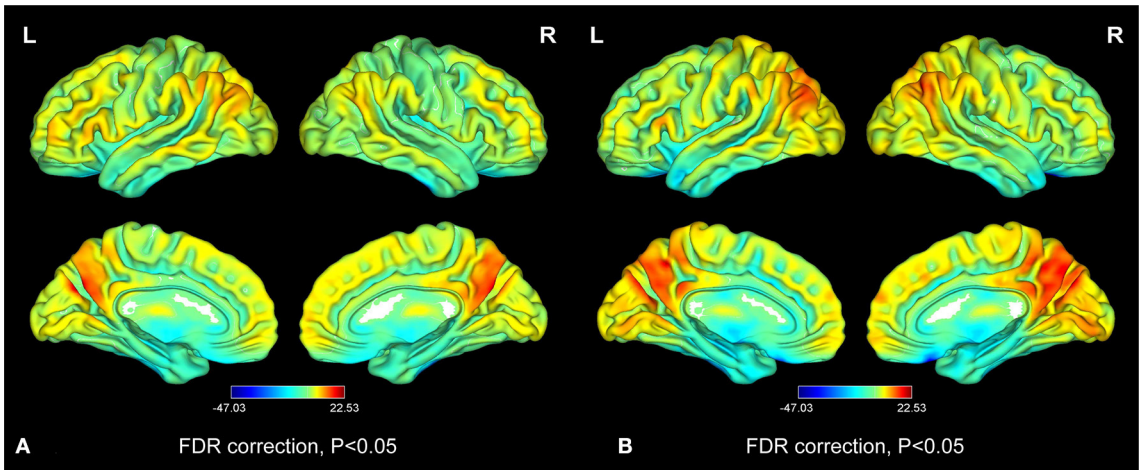

FIGURE 2 | Distribution patterns of the ReHo value at the group level in iridocyclitis patients and healthy volunteers. One-sample *t*-test result of ReHo maps within the iridocyclitis **(A)** and healthy volunteers **(B)**. The color bar represents the *t*-values (FDR correction, $P < 0.05$). Abbreviations: L, left; R, right; FDR, false discovery rate correction.

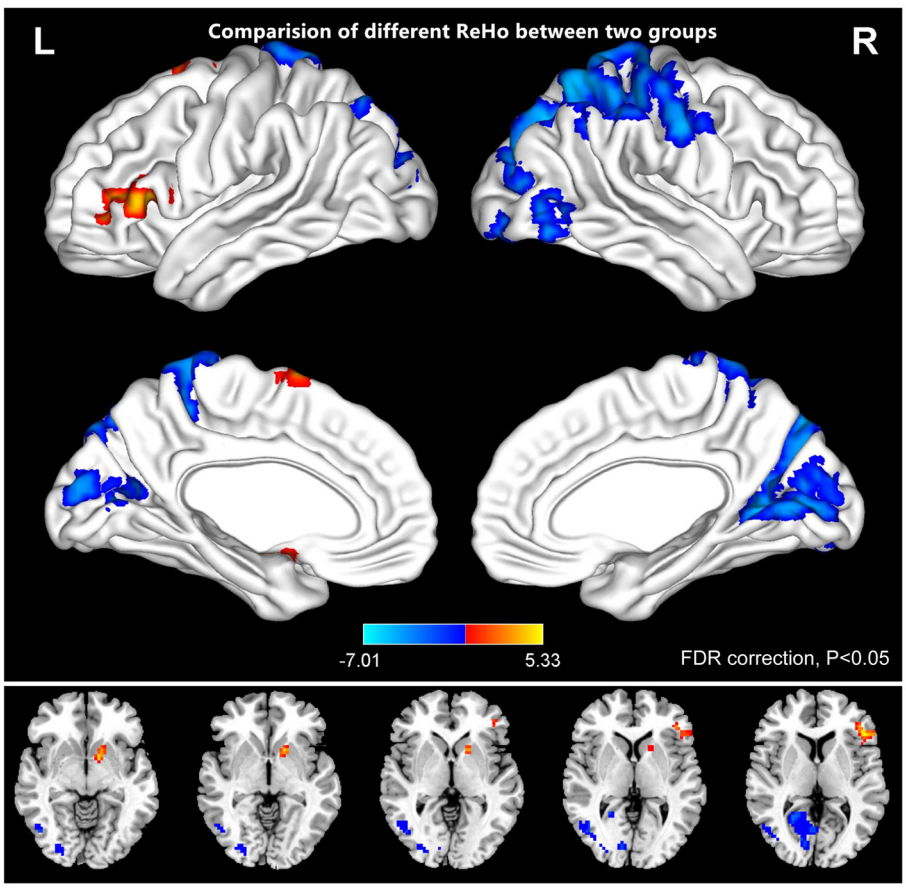

FIGURE 3 | The comparison of different ReHo between the patients of iridocyclitis and healthy volunteers. The iridocyclitis patients displayed significantly reduced ReHo values in the right inferior occipital gyrus, the right middle temporal gyrus, the bilateral calcarine, the right postcentral gyrus, the left superior occipital gyrus, and the left precuneus and displayed enhanced ReHo values in the right cerebellum, the left putamen, the left supplementary motor area, and the left inferior frontal gyrus compared with healthy volunteers (FDR correction, $P < 0.05$). Abbreviations: L, left; R, right; FDR, false discovery rate correction.

TABLE 2 | Brain regions with significantly different ReHo signal values between the iridocyclitis patients and healthy volunteers.

Conditions	Brain regions	Cluster size	MNI coordinates			*t*-score of peak voxel
			X	*Y*	*Z*	
IC < HCs	Right inferior occipital gyrus	37	27	−87	−3	−3.8763
IC < HCs	Right middle temporal gyrus	64	45	−69	−6	−4.0949
IC < HCs	Right calcarine	268	24	−57	9	−5.2475
IC < HCs	Left calcarine	30	−12	−63	18	−4.2266
IC < HCs	Right postcentral gyrus	1,234	30	−66	42	−7.0129
IC < HCs	Left superior occipital gyrus	88	−21	−87	18	−4.5975
IC < HCs	Left precuneus	118	−12	−42	57	−4.5016
IC > HCs	Right cerebellum	157	18	−42	−39	5.1730
IC > HCs	Left putamen	54	−12	3	−9	4.9854
IC > HCs	Left inferior frontal gyrus	96	−45	27	9	5.3275
IC > HCs	Left supplementary motor area	58	−9	6	63	4.2742

x, y, and z are the locations of the peak voxels in standard MNI coordinates. The statistical threshold was set at P < 0.05 after FDR correction. Abbreviations: IC, iridocyclitis; MNI, Montreal Neurological Institute.

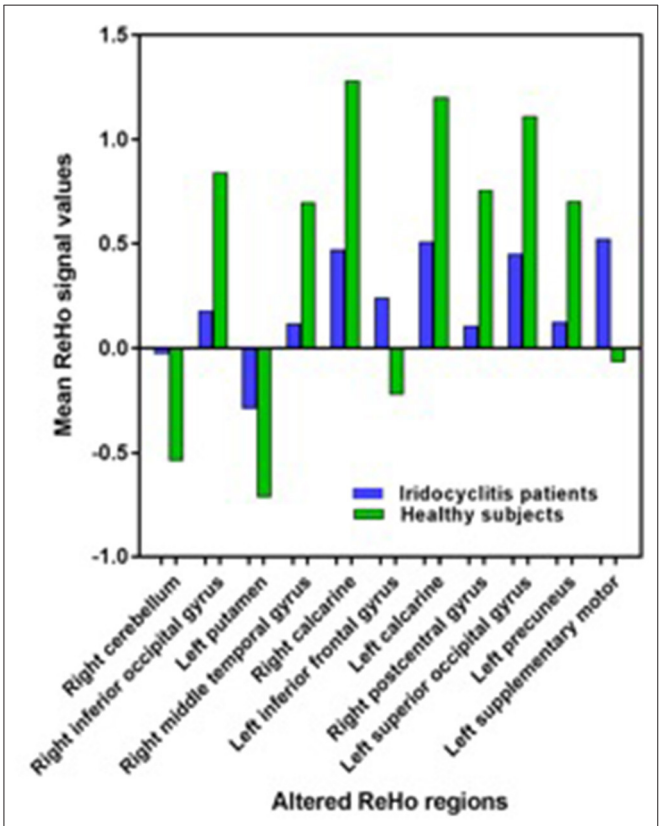

FIGURE 4 | The average values of changed ReHo signal values between the iridocyclitis patients and healthy volunteers.

TABLE 3 | ROC curves for the mean ReHo of changed brain areas.

Conditions	Brain regions	AUC	*P* values	95% CI
IC < Healthy volunteers	Right inferior occipital gyrus	0.815	<0.001	0.693–0.937
IC < Healthy volunteers	Right middle temporal gyrus	0.815	<0.001	0.695–0.936
IC < Healthy volunteers	Right calcarine	0.834	<0.001	0.726–0.942
IC < Healthy volunteers	Left calcarine	0.806	<0.001	0.683–0.930
IC < Healthy volunteers	Right postcentral gyrus	0.926	<0.001	0.854–0.998
IC < Healthy volunteers	Left superior occipital gyrus	0.845	<0.001	0.738–0.952
IC < Healthy volunteers	Left precuneus	0.843	<0.001	0.733–0.954
IC > Healthy volunteers	Right cerebellum	0.833	<0.001	0.719–0.947
IC > Healthy volunteers	Left putamen	0.891	<0.001	0.802–0.979
IC > Healthy volunteers	Left inferior frontal gyrus	0.916	<0.001	0.844–0.987
IC > Healthy volunteers	Left supplementary motor area	0.879	<0.001	0.788–0.969

Abbreviations: IC, iridocyclitis; AUC, area under the ROC curve; CI, confidence interval.

gyrus belongs to the primary somatosensory cortex (S1), which receives somatosensory input from the thalamocortical systems and sends these inputs to other parts of the somatosensory cortex (42). The postcentral gyrus participates in various sensory perceptions (such as the temperature and position perceptions) and is also involved in the central processing of the pain, tactile stimuli, and sense of touch (43, 44). Some neuroimaging researches have reported that multiple pain-related diseases are related to S1 dysfunction, including acute eye pain and low back pain (33, 45). Consistent with those findings, the reduced ReHo values observed in our study indicate that patients with iridocyclitis may exhibit abnormal local synchronization in the postcentral gyrus due to clinical symptoms of chronic recurrent eye pain. Furthermore, the postcentral gyrus is reportedly strongly associated with spontaneous activity in the primary

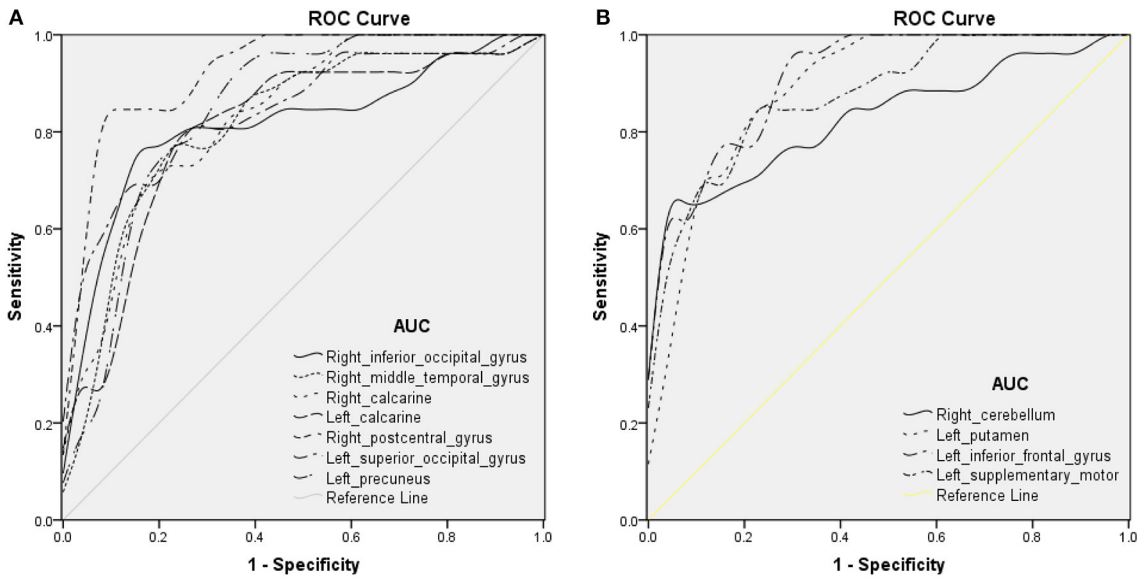

FIGURE 5 | ROC curve analysis of the average ReHo of altered brain areas. ROC curve in ReHo values: **(A)** iridocyclitis < healthy volunteers: right inferior occipital gyrus [0.815; $P < 0.001$; 95% confidence interval (CI), 0.693–0.937], right middle temporal gyrus (0.815; $P < 0.001$; 95% CI, 0.695–0.936), right calcarine (0.834; $P < 0.001$; 95% CI, 0.726–0.942), left calcarine (0.806; $P < 0.001$; 95% CI, 0.683–0.930), right postcentral gyrus (0.926; $P < 0.001$; 95% CI, 0.854–0.998), left superior occipital gyrus (0.845; $P < 0.001$; 95% CI, 0.738–0.952), and left precuneus (0.843; $P < 0.001$; 95% CI, 0.733–0.954); **(B)** iridocyclitis > healthy volunteers: right cerebellum (0.833; $P < 0.001$; 95% CI, 0.719–0.947), left putamen (0.891; $P < 0.001$; 95% CI, 0.802–0.979), left inferior frontal gyrus (0.916; $P < 0.001$; 95% CI, 0.844–0.987), and left supplementary motor area (0.879; $P < 0.001$; 95% CI, 0.788–0.969). Abbreviations: IC, iridocyclitis; AUC, area under the ROC curve.

TABLE 4 | Regional homogeneity method applied in ophthalmological diseases.

First author	Year	Disease	References
Chen et al.	2017	Glaucoma	(34)
Dan et al.	2019	Retinitis pigmentosa	(29)
Shao et al.	2015	Optic neuritis	(35)
Huang et al.	2017	Retinal detachment	(26)
Huang et al.	2016	Concomitant strabismus	(24)
Huang et al.	2017	Late monocular blindness	(36)
Yang et al.	2019	Amblyopia	(37)
Liao et al.	2018	Diabetic retinopathy	(23)
Tang et al.	2018	Eye pain	(33)

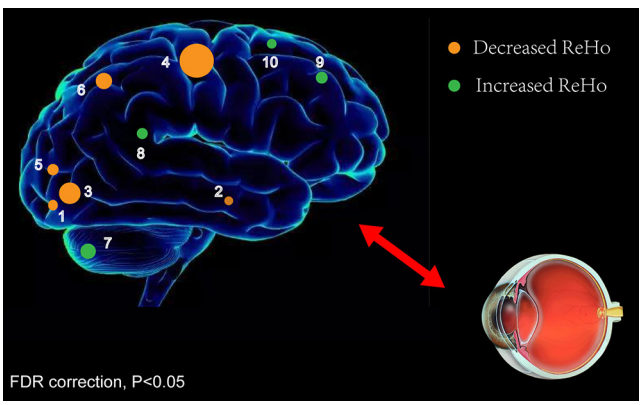

FIGURE 6 | ReHo results of spontaneous neuronal activity in the iridocyclitis group. Compared to the healthy volunteers, the ReHo value of iridocyclitis patients in regions 1–6 was decreased to various extents, while the value of regions 7–10 was increased: [1] right inferior occipital gyrus ($t = -3.8763$), [2] right middle temporal gyrus ($t = -4.0949$), [3] right calcarine ($t = -5.2475$), [3] left calcarine ($t = -4.2266$), [4] right postcentral gyrus ($t = -7.0129$), [5] left superior occipital gyrus ($t = -4.5975$), [6] left precuneus ($t = -4.5016$), [7] right cerebellum ($t = 5.1730$), [8] left putamen ($t = 4.9854$), [9] left inferior frontal gyrus ($t = 5.3275$), and [10] left supplementary motor area ($t = 4.2742$). Note: Spot sizes indicate degrees of quantitative changes. Abbreviations: ReHo, regional homogeneity; FDR, false discovery rate correction.

visual areas and is jointly activated with the occipital visual areas during visual imagery tasks (46). In support of these findings, we found patients with iridocyclitis showed lower ReHo area in the right postcentral gyrus compared to healthy volunteers, which may suggest a harmful effect on the postcentral gyrus.

The functions of the middle temporal gyrus are complex and diverse. It participates in the composition of the visual ventral processing stream and primary auditory projection, as well as in brain functional activities such as visual memory and semantic processing (47). The results of the present study showed that iridocyclitis may influence the visual memory functions of affected patients. In addition, the middle temporal gyrus is a critical component of the default mode network, which is primarily activated in the resting state and exhibits reduced activity in the task-based state. The default mode network is related to cognition, emotional processing, self-reflection, and memory; its dysfunction has been observed in many diseases,

such as depression and Alzheimer's disease (48, 49). Thus far, several studies have explored vision-related quality of life and mental health status in patients with uveitis (13, 14). Qian et al. found that depression is a major comorbidity in patients with ocular inflammatory disease, while Hoeksema et al. reported that patients with HLA-B27-anterior uveitis exhibited more depressive symptoms and negative coping strategies, compared with controls (15, 50). In this study, the results displayed reduced ReHo values in the middle temporal gyrus in patients with iridocyclitis, compared with healthy volunteers, suggesting that patients with iridocyclitis might exhibit dysfunction in terms of cognition and emotion regulation.

As a component of the superior parietal lobule and the core of the frontoparietal central-executive network, the precuneus connects with the adjacent visual cortical regions and with visual areas in the cuneus (51). Utevsky et al. demonstrated that the precuneus also serves as a critical component of the default mode network (52). Functionally, the precuneus has a key part in various highly integrated tasks, such as visuomotor coordination, episodic memory retrieval, visuospatial imagery, as well as working memory (53, 54). Thus, the reduction of ReHo signal values in the precuneus might reflect impaired precuneus function in the iridocyclitis group.

Notably, we observed that patients with iridocyclitis displayed enhanced ReHo values in regions of the right cerebellum. This brain area participates in multiple functions, especially motor control. Damage to the cerebellum may result in dysfunctions of movement, affective regulation, and visuomotor coordination (55, 56). Iridocyclitis is known to be the foremost clinical characteristic of ankylosing spondylitis in a subset of patients. Li et al. found that patients with ankylosing spondylitis exhibited enhanced activation in the cerebellum anterior lobe on fMRI (57). Consistent with those findings, we also observed patients with iridocyclitis exhibited increased ReHo values in the cerebellum. Therefore, we hypothesize iridocyclitis may contribute to compensatory motor function enhancement in the cerebellum.

The putamen is a large nucleus of the basal ganglia that participates in motor control and constitutes a core component of the basal ganglia network (58). Furthermore, the putamen is closely associated with learning (59). We observed that patients with iridocyclitis exhibited enhanced ReHo values in the left putamen. Therefore, we speculate iridocyclitis might contribute to functional alteration of the putamen. The finding of enhanced spontaneous neuronal activity in the left supplementary motor area further indicates the potential compensatory mechanism of the motor function in the patients of iridocyclitis.

The ROC curve indicates the reliability of the results. AUC values of 0.7–0.9 are presumed to indicate perfect accuracy, values of 0.5–0.7 are considered moderate accuracy, and values <0.5 are considered low accuracy. The ROC curve analysis in our study revealed that AUCs in each brain area exceeded 0.8, which suggested that those specific ReHo differences had high diagnostic accuracy in identification of iridocyclitis. In summary, our results indicate that the ReHo method might constitute a sensitive fMRI measurement for the future diagnosis of patients with iridocyclitis.

There were several limitations in this study. First, the impacts of physiological noise (e.g., respiratory fluctuations, head motion, and cardiac fluctuation) were not completely eliminated and might reduce the specificity of the results. To improve the reliability of ReHo, careful optimization and preprocessing of the data (such as linear regression analysis) can be performed. Second, relatively minimal data were included in the analysis, which may have restricted the generalizability of the results and the corresponding statistical power. In a future study, we will include additional data and conduct a multicenter investigation to verify the current findings. Further parameters, including comprehensive clinical assessments and the duration of iridocyclitis in affected patients, will also be included in the correlation analysis. Third, in addition to spontaneous neural activity in the brain measured by ReHo, multimodal MRI imaging technologies should be applied to further investigate the brain function alterations in individuals with iridocyclitis.

CONCLUSION

Our study demonstrated that patients with iridocyclitis exhibited disturbed synchronous neural activities in specific brain areas, including the visual, motor, and somatosensory regions, as well as the default mode network, compared with healthy volunteers. These results might offer valuable information for use in investigation of the neuropathological or compensatory mechanisms in patients with iridocyclitis and suggest a potential approach for further treatment development.

DATA AVAILABILITY STATEMENT

The original contributions presented in the study are included in the article/supplementary material, further inquiries can be directed to the corresponding author/s.

ETHICS STATEMENT

The studies involving human participants were reviewed and approved by Renmin Hospital of Wuhan University. The patients/participants provided their written informed consent to participate in this study.

AUTHOR CONTRIBUTIONS

YT contributed to study design, fMRI data analysis, and drafting the manuscript. XH contributed to design the protocol and data collection. C-XQ contributed to data collection and manuscript discussion. YS conceived the study, reviewed, and revised the manuscript. All authors read and approved the final manuscript.

FUNDING

This research was supported by the National Key R&D Program of China (Grant No. 2017YFE0103400) and the National Nature Science Foundation of China (Grant No. 81470628).

REFERENCES

1. Al-Ani HH, Sims JL, Tomkins-Netzer O, Lightman S, Niederer RL. Vision loss in anterior uveitis. *Brit J Ophthalmol.* (2020) 12:104. doi: 10.1136/bjophthalmol-2019-315551
2. Niccoli L, Nannini C, Cassarà E, Kaloudi O, Susini M, Lenzetti I, et al. Frequency of iridocyclitis in patients with early psoriatic arthritis: a prospective, follow up study. *Int J Rheum Dis.* (2012) 15:414–8. doi: 10.1111/j.1756-185X.2012.01736.x
3. Chang JH, McCluskey PJ, Wakefield D. Acute anterior uveitis and HLA-B27. *Surv Ophthalmol.* (2005) 50:364–88. doi: 10.1016/j.survophthal.2005.04.003
4. Menezo V, Lightman S. The development of complications in patients with chronic anterior uveitis. *Am J Ophthalmol.* (2005) 139:988–92. doi: 10.1016/j.ajo.2005.01.029
5. Forrester JV, Kuffova L, Dick AD. Autoimmunity, Autoinflammation, and infection in uveitis. *Am J Ophthalmol.* (2018) 189:77–85. doi: 10.1016/j.ajo.2018.02.019
6. Asrani S, Moore DB, Jaffe GJ. Paradoxical changes of retinal nerve fiber layer thickness in uveitic glaucoma. *JAMA Ophthalmol.* (2014) 132:877–80. doi: 10.1001/jamaophthalmol.2014.954
7. Din NM, Taylor SRJ, Isa H, Tomkins-Netzer O, Bar A, Talat L, et al. Evaluation of retinal nerve fiber layer thickness in eyes with hypertensive uveitis. *JAMA Ophthalmol.* (2014) 132:859–65. doi: 10.1001/jamaophthalmol.2014.404
8. Traill A, Stawell R, Hall A, Zamir E. Macular thickening in acute anterior uveitis. *Ophthalmology.* (2007) 114:2. doi: 10.1016/j.ophtha.2006.07.028
9. Tripathi P, Saxena S, Yadav VS, Naik S, Singh VK. Human S-antigen: peptide determinant recognition in uveitis patients. *Exp Mol Pathol.* (2004) 76:122–8. doi: 10.1016/j.yexmp.2003.10.007
10. Kim M, Choi SY, Park Y-H. Analysis of choroidal and central foveal thicknesses in acute anterior uveitis by enhanced-depth imaging optical coherence tomography. *BMC Ophthalmol.* (2017) 17:225. doi: 10.1186/s12886-017-0628-7
11. Pichi F, Sarraf D, Arepalli S, Lowder CY, Cunningham ET, Neri P, et al. The application of optical coherence tomography angiography in uveitis and inflammatory eye diseases. *Prog Retin Eye Res.* (2017) 59:178–201. doi: 10.1016/j.preteyeres.2017.04.005
12. Cerquaglia A, Iaccheri B, Fiore T, Fruttini D, Belli FB, Khairallah M, et al. New insights on ocular sarcoidosis: an optical coherence tomography angiography study. *Ocul Immunol Inflamm.* (2018) 27:1057–66. doi: 10.1080/09273948.2018.1497665
13. Franke GH, Schütte E, Heiligenhaus A. Psychosomatik der uveitis - eine pilotstudie. *Psychother Psychosom Med Psychol.* (2005) 55:65–71. doi: 10.1055/s-2004-828504
14. Scott IU. Visual functioning and general health status in patients with uveitis. *Evidence-Based Eye Care.* (2002) 3:92–3. doi: 10.1097/00132578-200204000-00015
15. Maca SM, Schiesser AW, Sobala A, Gruber K, Pakesch G, Prause C, et al. Distress, depression and coping in HLA-B27-associated anterior uveitis with focus on gender differences. *Brit J Ophthalmol.* (2010) 95:699–704. doi: 10.1136/bjo.2009.174839
16. Biswal BB. Resting state fMRI: a personal history. *NeuroImage.* (2012) 62:938–44. doi: 10.1016/j.neuroimage.2012.01.090
17. Sturm AK, König P. Mechanisms to synchronize neuronal activity. *Biol Cybern.* (2001) 84:153–72. doi: 10.1007/s004220000209
18. Jutras MJ, Buffalo EA. Synchronous neural activity and memory formation. *Curr Opin Neurobiol.* (2010) 20:150–5. doi: 10.1016/j.conb.2010.02.006
19. Bayati M, Valizadeh A, Abbassian A, Cheng S. Self-organization of synchronous activity propagation in neuronal networks driven by local excitation. *Front Comput Neurosci.* (2015) 9:69. doi: 10.3389/fncom.2015.00069
20. Zang Y, Jiang T, Lu Y, He Y, Tian L. Regional homogeneity approach to fMRI data analysis. *NeuroImage.* (2004) 22:394–400. doi: 10.1016/j.neuroimage.2003.12.030
21. Tononi G, McIntosh AR, Russell DP, Edelman GM. Functional clustering: identifying strongly interactive brain regions in neuroimaging data. *NeuroImage.* (1998) 7:133–49. doi: 10.1006/nimg.1997.0313
22. Li Z, Kadivar A, Pluta J, Dunlop J, Wang Z. Test-retest stability analysis of resting brain activity revealed by blood oxygen level-dependent functional MRI. *J Magn Reson Imaging.* (2012) 36:344–54. doi: 10.1002/jmri.23670
23. Liao X-L, Yuan Q, Shi W-Q, Li B, Su T, Lin Q, et al. Altered brain activity in patients with diabetic retinopathy using regional homogeneity: a resting-state fMRI study. *Endocr Pract.* (2019) 25:320–7. doi: 10.4158/ep-2018-0517
24. Shao Y, Huang X, Li S-H, Zhou F-Q, Zhang Y, Zhong Y-L, et al. Altered intrinsic regional brain spontaneous activity in patients with comitant strabismus: a resting-state functional MRI study. *Neuropsychiatr Dis Treat.* (2016) 12:1303–8. doi: 10.2147/ndt.S105478
25. Chen K, Lin X, Ding K, Liu Y, Yan X, Song S, et al. Altered spontaneous activity in anisometropic amblyopia subjects: revealed by resting-state fMRI. *PLoS ONE.* (2012) 7:e43373. doi: 10.1371/journal.pone.0043373
26. Huang X, Li D, Li H-J, Zhong Y-L, Freeberg S, Bao J, et al. Abnormal regional spontaneous neural activity in visual pathway in retinal detachment patients: a resting-state functional MRI study. *Neuropsychiatr Dis Treat.* (2017) 13:2849–54. doi: 10.2147/ndt.S147645
27. Standardization of Uveitis Nomenclature for Reporting Clinical Data. Results of the First International Workshop. *Am J Ophthalmol.* (2005) 140:509–16. doi: 10.1016/j.ajo.2005.03.057
28. Ni M-F, Zhang B-W, Chang Y, Huang X-F, Wang X-M. Altered resting-state network connectivity in panic disorder: an independent component analysis. *Brain Imaging Behav.* (2020) 14. doi: 10.1007/s11682-020-00329-z
29. Dan H-D, Zhou F-Q, Huang X, Xing Y-Q, Shen Y. Altered intra- and inter-regional functional connectivity of the visual cortex in individuals with peripheral vision loss due to retinitis pigmentosa. *Vision Res.* (2019) 159:68–75. doi: 10.1016/j.visres.2019.02.013
30. Yan C-G, Wang X-D, Zuo X-N, Zang Y-F. DPABI: data processing & analysis for (resting-state) brain imaging. *Neuroinformatics.* (2016) 14:339–51. doi: 10.1007/s12021-016-9299-4
31. Goto M, Abe O, Aoki S, Hayashi N, Miyati T, Takao H, et al. Diffeomorphic anatomical registration through exponentiated lie algebra provides reduced effect of scanner for cortex volumetry with atlas-based method in healthy subjects. *Neuroradoilogy.* (2013) 55:869–75. doi: 10.1007/s00234-013-1193-2
32. Lowe MJ, Mock BJ, Sorenson JA. Functional Connectivity in single and multislice echoplanar imaging using resting-state fluctuations. *NeuroImage.* (1998) 7:119–32. doi: 10.1006/nimg.1997.0315
33. Tang L-Y, Li H-J, Huang X, Bao J, Sethi Z, Ye L, et al. Assessment of synchronous neural activities revealed by regional homogeneity in individuals with acute eye pain: a resting-state functional magnetic resonance imaging study. *J Pain Res.* (2018) 11:843–50. doi: 10.2147/jpr.S156634
34. Chen W, Zhang L, Xu Y-g, Zhu K, Luo M. Primary angle-closure glaucomas disturb regional spontaneous brain activity in the visual pathway: an fMRI study. *Neuropsychiatr Dis Treat.* (2017) 13:1409–17. doi: 10.2147/ndt.S134258
35. Shao Y, Cai F, Zhong Y, Huang X, Zhang Y, Hu P-H, et al. Altered intrinsic regional spontaneous brain activity in patients with optic neuritis: a resting-state functional magnetic resonance imaging study. *Neuropsychiatr Dis Treat.* (2015) 11:3065–73. doi: 10.2147/ndt.S92968
36. Huang X, Ye C-L, Zhong Y-L, Ye L, Yang Q-C, Li H-J, et al. Altered regional homogeneity in patients with late monocular blindness. *Neuroreport.* (2017) 28:1085–91. doi: 10.1097/wnr.0000000000000855
37. Yang X, Lu L, Li Q, Huang X, Gong Q, Liu L. Altered spontaneous brain activity in patients with strabismic amblyopia: a resting-state fMRI study using regional homogeneity analysis. *Exp Ther Med.* (2019) 18:3877–84. doi: 10.3892/etm.2019.8038
38. Shao Y, Li QH, Li B, Lin Q, Su T, Shi WQ, et al. Altered brain activity in patients with strabismus and amblyopia detected by analysis of regional homogeneity: a resting-state functional magnetic resonance imaging study. *Mol Med Report.* (2019) 19:4832–40. doi: 10.3892/mmr.2019.10147
39. Hadjikhani N, Tootell RBH. Projection of rods and cones within human visual cortex. *Hum Brain Mapp.* (2000) 9:55-—63. doi: 10.1002/(sici)1097-0193(2000)9:1<55::Aid-hbm6>3.0.co;2-u
40. Castellano CG, Stinnett SS, Mettu PS, McCallum RM, Jaffe GJ. Retinal thickening in iridocyclitis. *Am J Ophthalmol.* (2009) 148:341–9.e1. doi: 10.1016/j.ajo.2009.03.034
41. Géhl Z, Kulcsár K, Kiss HJM, Németh J, Maneschg OA, Resch MD. Retinal and choroidal thickness measurements using spectral domain optical coherence

tomography in anterior and intermediate uveitis. *BMC Ophthalmol.* (2014) 14:103. doi: 10.1186/1471-2415-14-103
42. Wang Z, Chen Li M, Négyessy L, Friedman Robert M, Mishra A, Gore John C, et al. The relationship of anatomical and functional connectivity to resting-state connectivity in primate somatosensory cortex. *Neuron.* (2013) 78:1116–26. doi: 10.1016/j.neuron.2013.04.023
43. Mori K, Osada H, Yamamoto T, Nakao Y, Maeda M. Pterional keyhole approach to middle cerebral artery aneurysms through an outer canthal skin incision. *Minim Invasive Neurosurg.* (2007) 50:195–201. doi: 10.1055/s-2007-985837
44. Wrigley PJ, Press SR, Gustin SM, Macefield VG, Gandevia SC, Cousins MJ, et al. Neuropathic pain and primary somatosensory cortex reorganization following spinal cord injury. *Pain.* (2009) 141:52–9. doi: 10.1016/j.pain.2008.10.007
45. Frot M, Magnin M, Mauguière F, Garcia-Larrea L. Cortical representation of pain in primary sensory-motor areas (S1/M1)-a study using intracortical recordings in humans. *Hum Brain Mapp.* (2013) 34:2655–68. doi: 10.1002/hbm.22097
46. Wang K, Jiang T, Yu C, Tian L, Li J, Liu Y, et al. Spontaneous activity associated with primary visual cortex: a resting-state fMRI study. *Cereb Cortex.* (2007) 18:697–704. doi: 10.1093/cercor/bhm105
47. Visser M, Jefferies E, Embleton KV, Lambon Ralph MA. Both the middle temporal gyrus and the ventral anterior temporal area are crucial for multimodal semantic processing: distortion-corrected fMRI evidence for a double gradient of information convergence in the temporal lobes. *J Cog Neurosci.* (2012) 24:1766–78. doi: 10.1162/jocn_a_00244
48. Yu-Feng Z, Yong H, Chao-Zhe Z, Qing-Jiu C, Man-Qiu S, Meng L, et al. Altered baseline brain activity in children with ADHD revealed by resting-state functional MRI. *Brain Dev.* (2007) 29:83–91. doi: 10.1016/j.braindev.2006.07.002
49. Weissman-Fogel I, Moayedi M, Taylor KS, Pope G, Davis KD. Cognitive and default-mode resting state networks: do male and female brains "rest" differently? *Hum Brain Mapp.* (2010) 11:1713–26. doi: 10.1002/hbm.20968
50. Qian Y, Glaser T, Esterberg E, Acharya NR. Depression and visual functioning in patients with ocular inflammatory disease. *Am J Ophthalmol.* (2012) 153:370–8.e2. doi: 10.1016/j.ajo.2011.06.028
51. Cavanna AE, Trimble MR. The precuneus: a review of its functional anatomy and behavioural correlates. *Brain.* (2006) 129:564–83. doi: 10.1093/brain/awl004
52. Utevsky AV, Smith DV, Huettel SA. Precuneus is a functional core of the default-mode network. *J Neurosci.* (2014) 34:932–0. doi: 10.1523/jneurosci.4227-13.2014
53. Wallentin M, Weed E, Østergaard L, Mouridsen K, Roepstorff A. Accessing the mental space—spatial working memory processes for language and vision overlap in precuneus. *Hum Brain Mapp.* (2008) 29:524–32. doi: 10.1002/hbm.20413
54. Wenderoth N, Debaere F, Sunaert S, Swinnen SP. The role of anterior cingulate cortex and precuneus in the coordination of motor behaviour. *Eur J Neuroscie.* (2005) 22:235–46. doi: 10.1111/j.1460-9568.2005.04176.x
55. Noroozian M. The role of the cerebellum in cognition. *Neurol Clin.* (2014) 32:1081–104. doi: 10.1016/j.ncl.2014.07.005
56. Kralj-Hans I, Baizer JS, Swales C, Glickstein M. Independent roles for the dorsal paraflocculus and vermal lobule VII of the cerebellum in visuomotor coordination. *Exp Brain Res.* (2006) 177:209–22. doi: 10.1007/s00221-006-0661-x
57. Li C, Wei X, Zou Q, Zhang Y, Yin X, Zhao J, et al. Cerebral functional deficits in patients with ankylosing spondylitis- an fMRI study. *Brain Imaging Behav.* (2016) 11:936–42. doi: 10.1007/s11682-016-9565-y
58. Vicente AF, Bermudez MA, Romero MdC, Perez R, Gonzalez F. Putamen neurons process both sensory and motor information during a complex task. *Brain Res.* (2012) 1466:70–81. doi: 10.1016/j.brainres.2012.05.037
59. Grahn JA, Parkinson JA, Owen AM. The role of the basal ganglia in learning and memory: neuropsychological studies. *Behav Brain Res.* (2009) 199:53–60. doi: 10.1016/j.bbr.2008.11.020

Conflict of Interest: The authors declare that the research was conducted in the absence of any commercial or financial relationships that could be construed as a potential conflict of interest.

Copyright © 2021 Tong, Huang, Qi and Shen. This is an open-access article distributed under the terms of the Creative Commons Attribution License (CC BY). The use, distribution or reproduction in other forums is permitted, provided the original author(s) and the copyright owner(s) are credited and that the original publication in this journal is cited, in accordance with accepted academic practice. No use, distribution or reproduction is permitted which does not comply with these terms.

frontiers in Neurology

ORIGINAL RESEARCH
published: 12 March 2021
doi: 10.3389/fneur.2021.635419

Anti-aquaporin 4 IgG Is Not Associated With Any Clinical Disease Characteristics in Neuromyelitis Optica Spectrum Disorder

Oliver Schmetzer[1,2,3]*, *Elisa Lakin*[1,2,3], *Ben Roediger*[4], *Ankelien Duchow*[1,2,3], *Susanna Asseyer*[1,2,3], *Friedemann Paul*[1,2,3] and *Nadja Siebert*[1,2,3]

[1] Corporate Member of Freie Universität Berlin, Humboldt-Universität zu Berlin, Charité – Universitätsmedizin Berlin, Berlin, Germany, [2] Berlin Institute of Health, NeuroCure Clinical Research Center (NCRC) and Experimental and Clinical Research Center (ECRC), Max Delbrück Center for Molecular Medicine (MDC), Berlin, Germany, [3] Department of Neurology, Charité – Universitätsmedizin Berlin, Berlin, Germany, [4] Novartis Institutes for Biomedical Research - Autoimmunity, Transplantation and Inflammation, Basel, Switzerland

OPEN ACCESS

Edited by:
Claudia Angela Michela Gandini Wheeler-Kingshott,
University College London,
United Kingdom

Reviewed by:
Michael S. Vaphiades,
University of Alabama at Birmingham,
United States
Carmen Tur,
University College London,
United Kingdom

***Correspondence:**
Oliver Schmetzer
oliver.schmetzer@charite.de

Specialty section:
This article was submitted to Neuro-Ophthalmology, a section of the journal Frontiers in Neurology

Received: 30 November 2020
Accepted: 22 February 2021
Published: 12 March 2021

Citation:
Schmetzer O, Lakin E, Roediger B, Duchow A, Asseyer S, Paul F and Siebert N (2021) Anti-aquaporin 4 IgG Is Not Associated With Any Clinical Disease Characteristics in Neuromyelitis Optica Spectrum Disorder. Front. Neurol. 12:635419. doi: 10.3389/fneur.2021.635419

Background: Neuromyelitis optica spectrum disorder (NMOSD) is a clinically defined, inflammatory central nervous system (CNS) disease of unknown cause, associated with humoral autoimmune findings such as anti-aquaporin 4 (AQP4)-IgG. Recent clinical trials showed a benefit of anti-B cell and anti-complement-antibodies in NMOSD, suggesting relevance of anti-AQP4-IgG in disease pathogenesis.

Objective: AQP4-IgG in NMOSD is clearly defined, yet up to 40% of the patients are negative for AQP4-IgG. This may indicate that AQP4-IgG is not disease-driving in NMOSD or defines a distinct patient endotype.

Methods: We established a biobank of 63 clinically well-characterized NMOSD patients with an extensive annotation of 351 symptoms, patient characteristics, laboratory results and clinical scores. We used phylogenetic clustering, heatmaps, principal component and longitudinal causal interference analyses to test for the relevance of anti-AQP4-IgG.

Results: Anti-AQP4-IgG was undetectable in 29 (46%) of the 63 NMOSD patients. Within anti-AQP4-IgG-positive patients, anti-AQP4-IgG titers did not correlate with clinical disease activity. Comparing anti-AQP4-IgG-positive vs. -negative patients did not delineate any clinically defined subgroup. However, anti-AQP4-IgG positive patients had a significantly ($p = 0.022$) higher rate of additional autoimmune diagnoses.

Conclusion: Our results challenge the assumption that anti-AQP4-IgG alone plays a disease-driving role in NMOSD. Anti-AQP4-IgG might represent an epiphenomenon associated with NMOSD, may represent one of several immune mechanisms that collectively contribute to the pathogenesis of this disease or indeed, anti-AQP4-IgG might be the relevant factor in only a subgroup of patients.

Keywords: immunology, autoimmunity, neuromyelitis optica, aquaporin, channelopathies, neuromyelitis optica, AQP4, anti-AQP4-IgG

Key Messages:

- No clinical differences between anti-AQP4-IgG positive or negative patients
- No significant change of anti-AQP4-IgG levels during disease progression, but a non- significant increase in the mean anti-AQP4-IgG titer was visible only after multiple relapses
- anti-AQP4-IgG^{+} patients have a significantly ($p = 0.022$) higher rate of additional autoimmune diagnoses.

INTRODUCTION

Neuromyelitis optica spectrum disorder (NMOSD) is a rare [prevalence about 1:100,000; incidence 0.1-0.4 per 100,000 (1–4)], devastating chronic inflammatory CNS disease. There is no clear cause for the disease, and NMOSD in the past had a grim prognosis in many cases due to limited therapeutic options (1, 5–7). NMOSD is clinically characterized by attacks of uni- or bilateral optic neuritis (ON), acute myelitis and/or brain/brainstem encephalitis (8) and is associated with specific autoantibodies (aAbs) such as anti-aquaporin-4 (AQP4), targeting an astrocytic water channel (9), or anti-myelin oligodendrocyte glycoprotein (MOG)-IgG (5, 10). Approximately 60% of all NMOSD patients are positive for anti-AQP4-IgG (11–13). Anti-AQP4-IgG is therefore thought to play a key or even causal role in disease pathogenesis, characterizing the anti-AQP4-IgG positive subset of NMOSD as a channelopathy (11).

There are several other lines of evidence suggesting that NMOSD is a humoral autoimmune disease: (1) Detection of substantial local deposition of vasculocentric, activated complement in active lesions in patients (14); (2) Recapitulation of NMOSD-like clinical features in rodents following passive transfer of patient serum (15, 16); (3) Capacity of NMO-IgG to bind to the extracellular domain of AQP4 on astrocytes and activate complement *in vitro* (17, 18); and (4) Quantitative measures of complement-mediated injury to AQP4-expressing cells *in vitro* could be correlated with clinical disease progression in a limited number of patients (19). Indeed, a recent clinical trial with eculizumab, a complement factor 5 (C5) antibody, demonstrated clinical efficacy in anti-AQP4-IgG-positive patients, supporting the notion that NMOSD is a complement-dependent disorder of the CNS (20, 21). Furthermore, complement-independent AQP4-antibody-mediated astrocytopathies have been proposed from *in vitro* cell culture models (22) and B cell targeting therapies such as anti-CD20 and anti-CD19 have been shown to prevent relapses and are now used as first line therapeutic options for this disease (23–25).

Despite this evidence, more recent trials have failed to show a correlation of complement-mediated cell killing activity with relapse rates or relapse severity (26) and questioned the role of anti-AQP4-IgG (27). In addition, in most rodent *in vivo* models, neither induction of anti-AQP4-IgG by immunization, its presence by transgenic anti-AQP4 expression nor continuous infusion of anti-AQP4-IgG was sufficient to cause disease (16). In these preclinical models, NMOSD-like pathology could only be recapitulated if human (not murine) complement was co-administered intracerebrally.

The question of the role and relevance of anti-AQP4-IgG is of high therapeutic relevance, as only approximately between half and two-thirds of the patients are positive for these antibodies, and eculizumab has only been trialed in AQP4-positive patients. Although NMOSD patients are clinically well-defined and relatively homogeneous, and robust endotypes have not been identified to date, the question of whether there exist clinically relevant, AQP4-positive and AQP4-negative subtypes has not been formally addressed.

Here, we investigated 63 clinically well-characterized NMOSD patients to better understand the pathogenesis of this debilitating disease and assess the relevance of anti-AQP4-IgG positivity. Our results challenge the currently assumed, disease-driving role for anti-AQP4-IgG, which holds therapeutic relevance for NMOSD sufferers. Our findings also expand our present understanding of antibody driven autoimmunity, complement and neurodegeneration. However, we finally cannot prove nor rule out that anti-AQP4-IgG might indeed play a major disease-driving role in a subset of patients.

MATERIALS AND METHODS

NMOSD Patients

Demographic characteristics, diagnoses, medical history, age at disease onset, time to diagnosis, duration of clinical observation, clinical attacks, attack-related factors such as clinical presentation, attack treatment, attack outcome and remission rate, resulting disability, other therapies, short-term remission status, laboratory values from routine tests, AQP4- and MOG-aAb status as determined by cell-based assays [due to its high relevance in this disease group (28–30)], annualized relapse rate (ARR), optical coherence tomography (OCT) (24) as well as magnetic resonance imaging (MRI) results (31) and an array of other variables (**Supplementary Table 1**) have been recorded from over 100 adult NMOSD patients from an ongoing prospective longitudinal observational study conducted at the NeuroCure Clinical Research Center of Charité Universitaetsmedizin Berlin according to standardized Wingerchuk 2015 criteria (32). In addition, an extensive test battery including Expanded Disability Status Scale (EDSS), Multiple Sclerosis Functional Composite (MSFC), The Short

Abbreviations: ARR, annual relapse rate; AD, Alzheimer's disease; aAgs, autoantigens; AU, arbitrary unit; APC, antigen-presenting cell; AQP4, aquaporine-4; ARR, annualized relapse rate; aAbs, autoantibodies; NMOSD, Neuromyelitis optica spectrum disorder; BBB, blood-brain barrier; C5, complement factor 5; CNS, central nervous system; CXCL12, CXC motif ligand 12; dbGaP, database of Genotypes and Phenotypes; EDSS, Expanded Disability Status Scale; GI, gastrointestinal; GTEx, Genotype-Tissue Expression; HGNC, HUGO gene nomenclature committee; HUGO, Human Genome Organization; IgG, immunoglobulin G; MOG, myelin oligodendrocyte glycoprotein; MRI, Magnetic resonance imaging; MSFC, Multiple Sclerosis Functional Composite; Nabs, natural occurring antibodies; NGS, next generation sequencing; SF-36 score, 36-item containing short form health survey; SVD, Singular Value Decomposition; ON, optic neuritis; OCT, Optical coherence tomography; PCA, Principal component analysis; PC, Principal components; SC, spinal cord.

Form (36) Health Survey (SF-36), fatigue severity scale (FSS), Fatigue Scale for Motor and Cognitive Functions (FSMC), Beck Depression Inventory (BDI), McGill Pain Questionnaire (MPQ), painDETECT questionnaire (PDQ), Brief Pain Inventory (BPI), National Eye Institute Visual Function Questionnaire (NEI-VFQ), National Eye Institute Visual Function Questionnaire (NEI-VFQ), Neuro-Ophthalmic Supplement (NOS) and visual analog scales (VAS) for general well-being, cognition, pain and fatigue, were also included. A complete list of all 1,232 variables can be found in **Supplementary Table 1**. We could include 351 of these variables in our analyses, all of which resulted in a numeric, non-descriptive value or which could be turned into a numeric result, and for which we had a reasonable amount of tested subjects.

Inclusion criterion for patients was a diagnosis of NMOSD according to Wingerchuk et al.'s 2015 criteria (32). The data collection started in 2008 in order to merge and facilitate clinical and research activities around NMOSD. Sixty-three patients had full datasets and were included in further analyses, demographic data and aAb status can be found in **Supplementary Table 2**. These patients (79% female, mean age at diagnosis 45 years) had a mean duration of disease of 4.1 years (median 5.5 years) with a mean of 2.73 relapses (median two relapses) and a mean disability of 7.42 points in the EDSS (median nine points) after enrollment.

All data was stored, archived and disposed in a safe and secure manner during and after the conclusion of the research project in line with current data protection regulations (General Data Protection Regulation: DSGVO). We have established policies and procedures to manage data handled electronically as well as through non-electronic means in accordance with good laboratory practice.

Ethics Statement

All data collected from patients and investigated in this study was used after written informed consent as approved by the ethics committee of the Charité–Universitätsmedizin Berlin (proposal EA1/041/14) according to the Declaration of Helsinki (59th WMA General Assembly, Seoul, October 2008).

Statistical Analyses

Principal Component Analyses (PCA) and heatmap visualization were performed using 'ClustVis' (33) as we did it before (34). In brief, SVD (Singular Value Decomposition) with imputation (as the most common method) or Nipals PCA model was used to calculate the principal components (PC). PC 1 and 2 were presented on the X and Y axis while the percentages of represented total variances were shown in brackets. Different methods (Pareto, vector, or mostly Unit variance) were used as scaling method applied to the rows or no scaling was used. Imputation and SVD (or Nipals PCA) were iteratively performed until estimates of missing values converged. We drew ellipses for each dataset, datapoints fall with a probability of 0.95 inside these ellipses.

In an attempt not to miss a fitting model due to artificial fragmentation of patients' populations due to overanalyses, we used a stepwise approach based on our initially collected 1,232 variables. The most extensive set consisted of all 351 numeric variables (listed in **Supplementary Figure 1** on the Y-axis). We also tested a medium sized set of 47 variables which was left after the extensive clinical score details and deeply investigating single symptom areas had been removed, leaving only the score results in the dataset. Two further reduced sets of a limited number of 20 and 25 key variables were also analyzed, after variables dealing with the relapses had been removed. This was done because we had only data on relapses for a fraction of all patients. Finally, a core set of 18 variables was analyzed after additional other diagnoses (mainly further autoimmune diseases) of the patients were removed.

Cladograms and heatmaps were generated after phylogenetic cluster analyses were performed. Patients were clustered in columns (shown on the X-axis) and variables were clustered in rows (presented on the Y-axis) which were centered. Different (correlation, binary, Canberra, Manhattan, maximum, euclidean and most often correlation) distance and different (*Ward as unsquared distances, simple Ward, McQuitty, complete, single and* most often average) linkage methods were used as models, as stated in the legends. Unit variance scaling was in some analyses applied only to the variables in the rows. On top of the rows, anti-AQP4 status or as an example the SF-36 variable: "limitations due to pain" are shown in red and blue. Imputation was used for missing value estimation. The results were expressed as Z-scores.

Additional autoimmune diseases correlated with anti-AQP4-IgG-positivity and we used chord plotting with "Circos" (35) to demonstrate this.

Normal distribution was tested with the Anderson-Darling, the D'Agostino & Pearson, the Shapiro-Wilk and the Kolmogorov-Smirnov tests. An approximately Gaussian distribution served as basis to perform Student's t and ANOVA tests using GraphPad Prism version 8.4.3 for Windows, GraphPad Software, La Jolla California USA, www.graphpad.com. Most data were not normally distributed, we therefore used a non-parametric, unpaired and two-tailed Mann–Whitney test. The null hypothesis of random results was rejected if the P-value was very small <0.05.

Exon expression was used from GTEx (Genotype-Tissue Expression) Analysis Release V8 (dbGaP, database of Genotypes and Phenotypes, Accession phs000424.v8.p2) based on expression data of AQP4: ENSG00000171885.13 from HGNC (Human Genome Organization, HUGO Gene Nomenclature Committee; HGNC Accession: 637; https://www.gtexportal.org/home/gene/AQP4).

RESULTS

Anti-AQP4-IgG Status Does Not Define a Subgroup

In order to better understand the spectrum of clinical and pathological features of NMOSD, we established a biobank of 63 clinically well-characterized NMOSD patients regularly seen at our institution (**Supplementary Tables 1, 2**) as part of an ongoing observational study with an extensive annotation of 351

singular symptoms, patient characteristics (such as biographic, demographic, and social data), laboratory results, clinical scores, imaging (MRI and OCT) findings and physical examination results. Of these 63 patients, 34 were anti-AQP4-IgG$^+$ and 29 were anti-AQP4-IgG$^-$. anti-MOG-IgG could be identified in 18 patients, one patient was double positive for anti-AQP4-IgG and anti-MOG-IgG. From this, we wanted to find a mathematical model, which fits to the anti-AQP4-IgG-status and correlates with the clinical variables. Therefore, we used numerous mathematical models to test whether aAbs such as anti-AQP4-IgG could play a role in the pathophysiology and the clinical characteristics of NMOSD. We repeated those analyses for different collections of variables as well as for the full set. This was performed as it was not clear, how many and which variables would be congruent and related to the anti-AQP4-IgG-status. Specifically, we applied phylogenetic clustering, PCA and longitudinal causal interference analysis.

We found that anti-AQP4-IgG status does not associate with any subgroup of patients, characterized by patterns of symptoms, patient characteristics, laboratory results, clinical scores or findings (**Figures 1**, **2**; **Supplementary Figures 1–7**), as demonstrated by overlap of the 95% prediction ellipses in PCA. Here all variables were converted to two most principal components, to be able to plot it in 2D. There were no anti-AQP4-IgG-dependent subgroups of patients identifiable, irrespective of whether a PCA was performed with a basic set of symptoms and clinical markers in the database ($N = 20$; **Figure 1A**) or with the complete set (351 variables; **Figure 1B; Supplementary Figure 1**). The anti-AQP4-IgG positive and negative patients form again fully overlapping groups in all 57 cluster analyses performed for this study, independent of PCA method, model used, as well as type or amount of input data. Only two of the 57 models were exemplary, shown in **Figure 1**. There was also a near full matching of the 0.95 CI prediction ellipses of anti-AQP4-IgG positive and negative patients in the PCAs. To show a contrary example, two distinct groups of patients could be defined using the variables of the "36-item containing short form health survey" (SF-36 score). The best group-defining single value from those 36 variables was the second pain variable (question 22) of this score, assessing the level of interference of pain with normal work (including work outside the home and housework) during the past 4 weeks. **Figure 1C** shows a PCA based on the remaining 35 variables taken from this score, except the mentioned pain variable two, for which the patient cases have been colored. Patients having high (values 50, 75 and 100) vs. low levels (values 0 and 25) of this work disturbing pain therefore form two different subgroups in the PCA (based on the remaining 35 variables) with largely non-overlapping 0.95 CI prediction ellipses. This finding is independent of model and data used.

We used the same datasets in **Figure 2** for heatmap-based phylogenetic clustering analyses. Again, a low number of 20 variables (**Figure 2A**) as well as a complete set of our database (**Figure 2B**) leads to two major groups, which are independent of anti-AQP4-IgG status (shown in red and blue on top of the heatmaps). In **Figure 2A** the patient group in the left main cluster are characterized by a higher age at disease onset, a higher degree of unemployment and disability, lower levels of education, higher scores in pain and fatigue questionnaires as compared to the cluster on the right side. In contrast, the patients in the right main cluster were younger at disease onset, report lower pain levels, but score worse in functional scores such as EDSS and MSFC.

In contrast, phylogenetic cluster analysis e.g., based only on the variables from the SF-36 score as done for **Figure 1C** leads to separation of two groups (**Figure 2C**): One mainly with high levels of work disturbing pain (**Figure 2** left side) and a group of patients where all but one have low levels of the pain variable 2 (**Figure 2** right side).

The anti-AQP4-IgG positive and negative patients form almost always fully heterogeneous groups in all 57 cluster analyses performed for this study, independent of clustering method, model used, as well as type or amount of input data (**Figures 2A,B**; **Supplementary Figures 1–5**).

Some subgroups roughly related only to a negative anti-AQP4-IgG status could be found, but only with certain, uncommon clustering methods (marked with green boxes in **Supplementary Figure 6**) and if the number of variables were extraordinarily reduced to 18. Specifically, only removal of all information dealing with relapses, drugs, therapies and response to therapy, all variables from more extensive clinical score details (which investigated single symptom areas such as motor function, vision, psychological scores, detailed characteristics of pain etc.), all imaging data, as well as by removing all data about additional other diagnoses led to formation of these single subgroups with a negative anti-AQP4-IgG status. Those remaining 18 variables consisted mainly of a set of limited biographical data, while only the age at symptom onset and diagnosis, the disability level and selected EDSS score results were the remaining disease relevant markers. As the more severely ill patients still always formed subgroups with completely mixed anti-AQP4 status, this finding represents very likely a stochastic artifact due to a high number of clustering attempts.

Anti-AQP4-IgG-Titer Does Not Correlate With Disease Activity

Anti-AQP4-IgG titers were determined as described previously (36), but did not increase significantly with increased number of attacks (**Figures 3A,B**) nor with increased disease activity, measured as increased number of relapses per year (ARR; **Figure 3C**). There was also no significant increase of the titer with the number of affected symptom areas as a surrogate for disease severity (**Figure 3D**). As higher disease activity (defined as increased number of ARR) was not associated with an increase of anti-AQP4-IgG titers, a biological gradient was not apparent. Even if no significant change of anti-AQP4-IgG levels could be identified after two relapses, a non-significant increase in the mean anti-AQP4-IgG titer was visible with multiple relapses. The mean titers (from 0.075 to 0.128), but not of the median, increased after the third relapse as compared to the second one. In addition, a non-significant increase in the median could be noted between relapse one and two (from 0

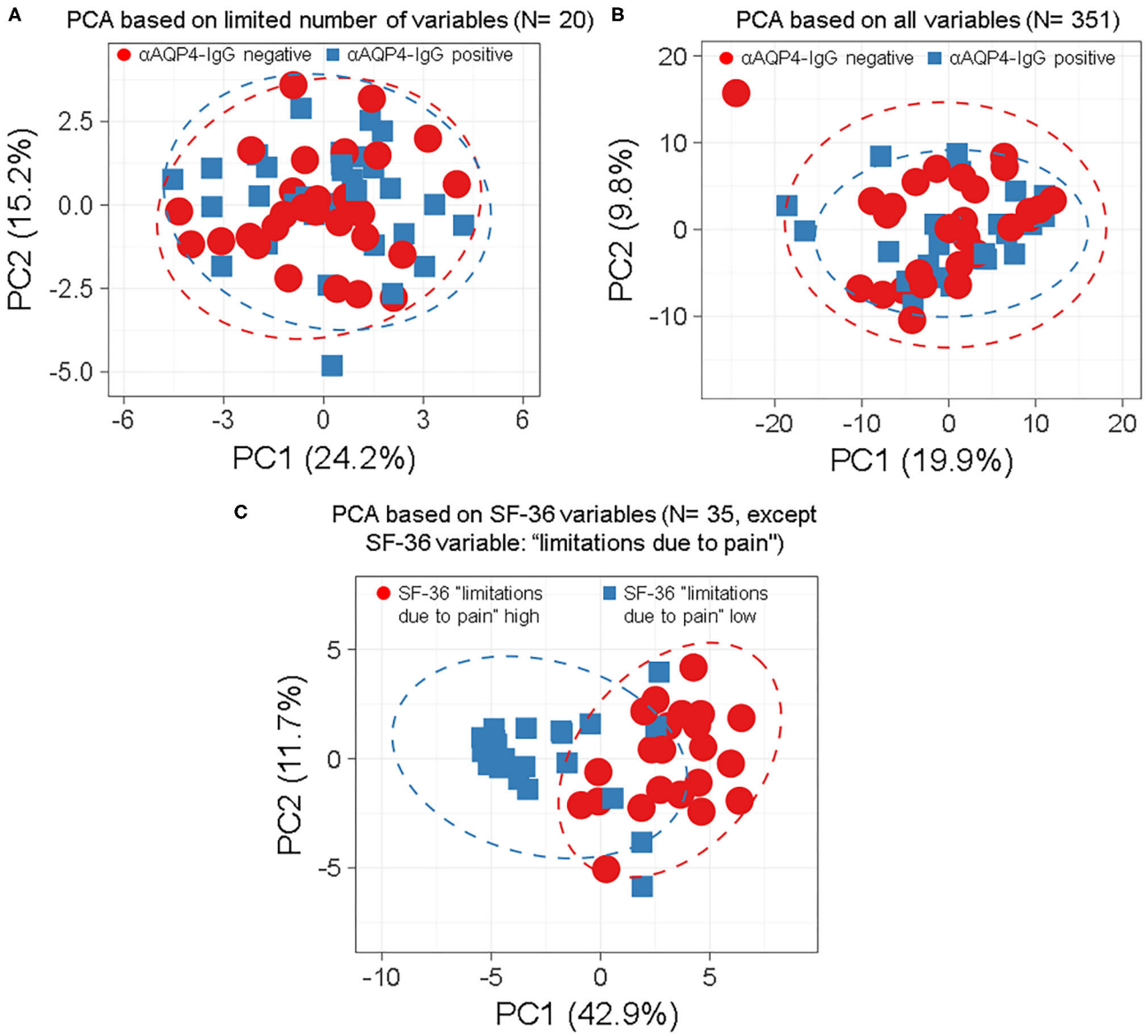

FIGURE 1 | Anti-aquaporin 4 (AQP4)-IgG status does not define distinct subgroups of patients by principle-component analyses (PCA) independent by model, number or type of markers used. Anti-AQP4-IgG status does not define a subgroup (such as anti-AQP4-IgG positive and -negative patients) as demonstrated by the full overlap of the 95% prediction ellipses in principle-component analyses (PCA). This is irrespective of how many and which markers are, or which model is used. Patients with Neuromyelitis optica spectrum disorder (NMOSD) were colored according to their anti-AQP4-IgG-status **(A,B)** or the second pain variable, describing levels of pain disturbing work during the last 4 weeks (question 22 from the "36-item containing short form health survey," SF-36 score; in **C**). Singular value decomposition (SVD) with imputation was used here in all PCAs to calculate principal components (PC). Prediction ellipses are such that with a probability of 0.95, a new observation from the same group will fall inside the ellipse. **(A)** A PCA was performed with all variables (but not anti-AQP4 statuses) and the patients were marked according to their anti-AQP4-IgG status. The PCA-plot shows PC1 and PC2, explaining 24 and 15% of the total variance, respectively, and was performed using only a limited number of key variables ($N = 20$) such as the Expanded Disability Status Scale (EDSS), disease activity and severity, sex and age. Prediction ellipses were drawn such that a new observation from the same group will fall inside the ellipse with a probability of 0.95. However, those prediction ellipses as well as the data points completely overlap. No difference based on anti-AQP4-IgG status is visible. **(B)** As in A, but all 351 variables (symptoms, disabilities, lab values, anamnestic, psychosomatic scores, and clinical markers) which have been recorded for the patients are included in the analysis, except for the anti-AQP4 statuses. Again, no difference based on anti-AQP4-IgG status is visible, in marked contrast to **(C)**: Same as in A but shown are patients having high vs. low levels of interference of pain with normal work (including work outside the home and housework) during the past 4 weeks. A PCA based on the remaining 35 variables from the SF-36 score (except the mentioned pain variable two, for which the patient cases have been colored) is shown. Here, the prediction ellipses for a probability of 0.95, as well as the dots *per se*, show a remarkable difference between the two groups. AQP4, aquaporin 4; EDSS, Expanded Disability Status Scale; NMOSD, neuromyelitis optica spectrum disorder; PC, principal components; PCA, principle-component analysis; SF-36, 36-item short form health survey; SVD, singular value decomposition.

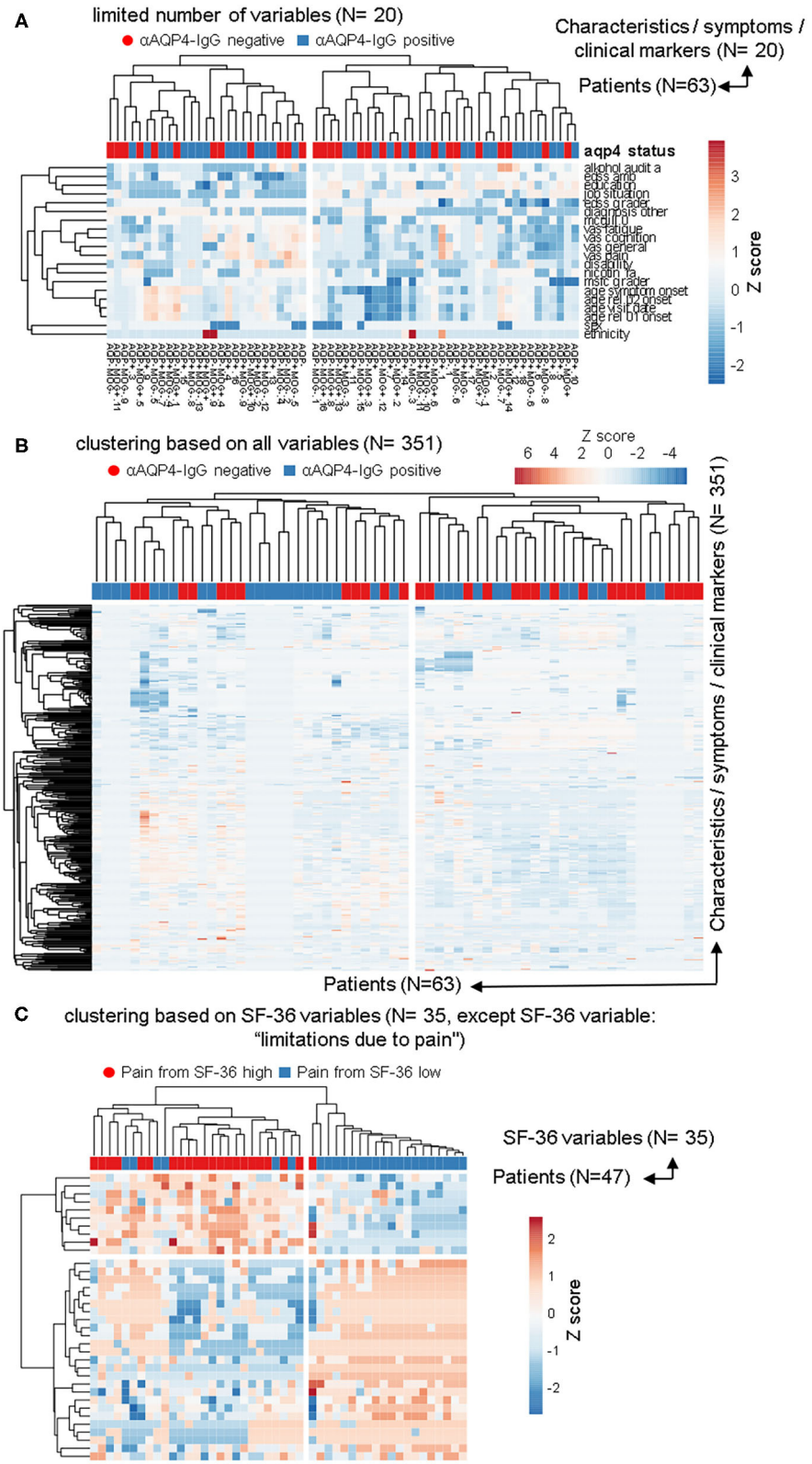

FIGURE 2 | The anti-aquaporin 4 (AQP4)-IgG status does not define a subgroup that would be detectable in heatmap-based clustering analyses. In addition to the PCAs, the same data sets as in **Figure 1** were used to perform calculations based on phylogenetic clustering analyses using heatmaps. As before, no difference based on anti-AQP4-IgG status were identifiable. This is in contrast to the two clearly visible different groups, which are based on the second pain variable taken from

(Continued)

FIGURE 2 | the 36-item short form health survey (SF-36). **(A,B)** Patients with Neuromyelitis optica spectrum disorder (NMOSD; $N = 63$) were clustered in columns using correlation distance and average linkage based either on only a limited number of key variables, such disease activity, severity, sex and age etc. (**A**; $N = 20$) or based on up to 351 symptoms and clinical markers (**B**; shown here in rows) were clustered. Unit variance scaling is applied to the symptoms and the clinical markers. On top of the rows, anti-AQP4 status is shown. No group based on anti-AQP4-IgG status is visible. **(C)** As in **(A,B)**, only the 35 variables of the SF-36 score were used and the same patients were clustered. In contrast to anti-AQP4-IgG, on the left side of the dendrogram, clearly visible a major group based on a high pain variable was formed. A difference to the anti-AQP4-IgG status can be seen due to the cluster on the left, formed by the residual variables of the SF-36 score. All patients are positive for a high second pain variable. On top of the rows, the second pain variable taken from the SF-36 score is color encoded shown.

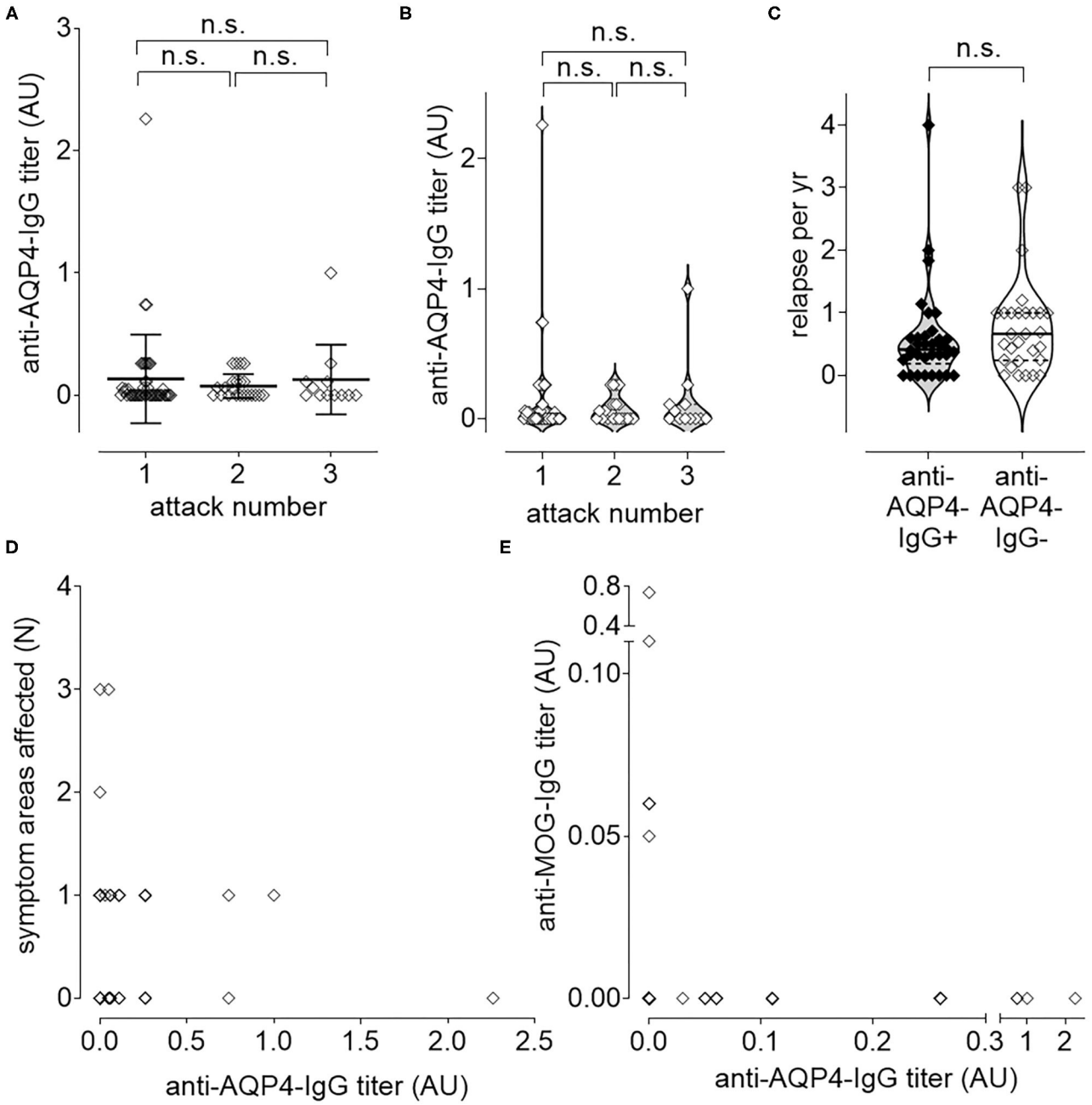

FIGURE 3 | Longitudinal causal interference analysis: anti-AQP4-IgG-Titer does not correlate with disease activity or progression. The level of anti-AQP4-IgG antibody titers remain unchanged after increased number of attacks **(A,B)**. Also, the number of relapses per year (ARR) do not correlate with the anti-AQP4-IgG status **(C)**. The level of anti-AQP4-IgG titers are not increased if more symptom areas are affected **(D)**. A dichotomy can be seen if the level of anti-AQP4-IgG is plotted vs. the anti-MOG-IgG titer **(E)**: NMOSD patients which are anti-MOG-IgG positive do not have anti-AQP4-IgG and vice versa. AU, arbitrary unit.

to 0.025), but no increase was found in the mean anti-AQP4-IgG levels.

Mean titer of anti-AQP4-IgG after attack 1 was 0.134 (median 0; range 0–2.26; SD 0.362; 95% CI 0.026–0.241; $N = 46$), after attack 2 it was 0.075 (median 0.025; range 0—.26; SD 0.099; 95% CI 0.031–0.119; $N = 22$) and after attack 3 0.128 (median 0; range 0–1.00; SD 0.2857; 95% CI −0.053–0.309; $N = 12$). There was no increase in titer, if the first attack was compared with the second ($P = 0.365$; 95% CI −0.239–0.575) or the second with the third attack ($P = 0.803$; 95% CI −0.517–0.626). Also, after two attacks there was no significant difference between the titer from attack 1 and 3 ($P = 0.606$; 95% CI −0.676–0.451; **Figures 3A,B**).

In addition, the ARR did not differ significantly ($P = 0.351$; 95% CI −0.206–0.571) between anti-AQP4-IgG positive (Mean 0.590; Median 0.414; range 0–4.000; SD 0.764; $N = 34$) and negative (Mean 0.773; Median 0.667; range 0–3.000; SD 0.774; $N = 29$) patients (**Figure 3C**).

The number of symptom areas affected (mean 0.563; median 0.500; range 0–3.000; SD 0.653; 95% CI 0.417–0.708; $N = 80$) did not correlate (Pearson $r = -0.050$; $P = 0.657$) with the titer of anti-AQP4-IgG (mean 0.117; median 0.000; range 0–2.260; SD 0.299; 95% CI 0.050–0.183; $N = 80$; **Figure 3D**). The number of attacks (mean 1.575; median 1.000; range 1–3; SD 0.743; 95% CI 1.410–1.740; $N = 80$) did also not correlate (Pearson $r = -0.036$; $P = 0.750$) with the titer of anti-AQP4-IgG (not shown).

NMOSD patients were either anti-MOG-IgG or anti-AQP4-IgG single positive, or double negative (**Figure 3E**).

The titer of anti-AQP4-IgG (mean 0.121; median 0.000; range 0–2.260; SD 0.204; 95% CI 0.052–0.190; $N = 77$) did not correlate (Pearson $r = -0.066$; 95% CI −0.286–0.160; $P = 0.568$) with the titer of anti-MOG-IgG (mean 0.014; median 0.000; range 0–0.740; SD 0.086; 95% CI −0.005–0.033; $N = 77$; **Figure 3E**).

In addition to the cluster analyses and PCAs, we could not identify any difference related to anti-AQP4-IgG in more classical analyses of various markers of disease history and severity, including age at relapses, treatment plans, pain, visual function, fatigue and psychometric scores (**Supplementary Figure 7**).

There was no significant difference in the temporal characteristics of the history of disease (disease onset, diagnosis, start and stop of therapies, ages at the first visit in our clinic as well as ages at the relapses) for Anti-AQP4-IgG positive and negative patients.

In full detail, in the "mean age at symptom onset (years)" with a P of 0.54 (mean age 41.82 vs. 39.37 years (yrs); median 42.50 vs. 39.00 a; range 14–65 vs. 7–70; SD 14.68 vs. 16.37; 95% CI 36.70–46.95 vs. 32.89–45.85; $N = 34$ vs. 27), in the "mean age at first diagnosis (years)" with a P of 0.84 (mean age 43.42 vs. 44.22 yrs; median 43.00 vs. 44.00 a; range 15–67 vs. 17–79; SD 14.26 vs. 15.51; 95% CI 38.37–48.48 vs. 38.09–50.36; $N = 3$3 vs. 27), in the "mean age at start of current therapy (years)" with a P of 0.72 (mean age 45.32 vs. 43.82 ysr; median 45.00 vs. 47.00 a; range 15–68 vs. 20–72; SD 14.23 vs. 15.05; 95% CI 39.80–50.84 vs. 37.15–50.49; $N = 28$ vs. 21), in the "mean age at start of first therapy (years)" with a P of 0.98 (mean age 44.15 vs. 44.00 yrs; median 41.50 vs. 45.00 a; range 20–67 vs. 19–70; SD 13.33 vs. 15.30; 95% CI 37.91–50.39 vs. 35.17–52.83; $N = 20$ vs. 14), in the "mean age at stop of current therapy (years)" with a P of 0.85 (mean age 46.10 vs. 45.21 yrs; median 44.00 vs. 46.00 a; range 28–68 vs. 20–71; SD 11.63 vs. 15.14; 95% CI 40.65–51.55 vs. 36.47–53.95; $N = 2$ 0 vs. 14), in the "mean age at first visit date (years)" with a P of 0.54 (mean age 49.04 vs. 46.50 yrs; median 50.00 vs. 48.50 a; range 21–73 vs. 21–79; SD 14.28 vs. 15.43; 95% CI 43.39–54.68 vs. 40.27–52.73; $N = 27$ vs. 26), in the "mean age at relapse 1 (years)" with a P of 0.79 (mean age 41.58 vs. 40.44 yrs; median 42.50 vs. 39.00 a; range 14–66 vs. 7–70; SD 14.31 vs. 15.98; 95% CI 35.80–47.36 vs. 33.85–47.03; $N = 26$ vs. 25), in the "mean age at relapse 2 (years)" with a P of 0.67 (mean age 44.38 vs. 42.25 yrs; median 46.00 vs. 44.00 a; range 14–66 vs. 9–70; SD 15.07 vs. 16.94; 95% CI 37.52–51.24 vs. 34.32–50.18; $N = 21$ vs. 20) or in the "mean age at relapse 3 (years)" with a P of 0.36 (mean age 43.25 vs. 37.33 yrs; median 43.50 vs. 40.50 a; range 15–66 vs. 10–67; SD 15.86 vs. 17.23; 95% CI 34.80–51.70 vs. 26.38–48.28; $N = 16$ vs. 12) as shown in **Supplementary Figure 7A**.

There was also no significant difference for Anti-AQP4-IgG positive and negative patients regarding different treatments. Anti-AQP4-IgG positive and negative patients did not differ significantly in receiving Rituximab (mean 0.56 vs. 0.38 cycles; median 1.00 vs. 0; range 0-1 for both; SD 0.50 vs. 0.49; 95% CI 0.38–0.73 vs. 0.19–0.57; $N = 34$ vs. 29) with a P of 0.16, Azathioprine (mean 0.15 vs. 0.14 cycles; median 0 for both; range 0-1 for both; SD 0.36 vs. 0.35; 95% CI 0.02–0.27 vs. 0.00–0.27; $N = 34$ vs. 29) with a P of 0.92 or Mycophenolate mofetil (mean 0.03 vs. 0.07 cycles; median 0 for both; range 0-1 for both; SD 0.17 vs. 0.26; 95% CI −0.03–0.09 vs. −0.03–0.17; $N = 34$ vs. 29) with a P of 0.47 (**Supplementary Figure 7B).**

We could also not identify any significant difference in pain as well as in visual function scores. Anti-AQP4-IgG positive and negative patients demonstrated no difference in the "McGill Pain Questionnaire (MPQ)" (mean 30.50 vs. 28.69; median 36 vs. 29; range 6–55 vs. 5–50; SD 14.38 vs. 15.61; 95% CI 22.84–38.16 vs. 19.26-38.12; $N = 16$ vs. 13) with a P of 0.75 (passed Test for normal distribution), in the "painDETECT questionnaire (PDQ)" (mean 28.10 vs. 26.15; median 28 vs. 20; range 2–49 vs. 9–63; SD 14.99 vs. 15.93; 95% CI 21.27–34.92 vs. 18.70–33.60; $N = 21$ vs. 20) with a P of 0.69 (passed Test for normal distribution), in the "Brief Pain Inventory (BPI)" (mean 34.50 vs. 35.64; median 35.5 vs. 28; range 10–54 vs. 2–78; SD 15.71 vs. 27.09; 95% CI 21.36–47.64 vs. 17.44–53.83; $N = 8$ vs. 11) with a P of 0.92 (passed Test for normal distribution), in the "visual analog scale (VAS) pain" (mean 35.43 vs. 31.88; median 34.0 vs. 26.5; range 0–100 vs. 0–98; SD 29.78 vs. 28.35; 95% CI 22.56–48.31 vs. 19.90–43.85; $N = 23$ vs. 24) with a P of 0.54 (not normal distributed), in the "National Eye Institute Visual Function Questionnaire (NEI-VFQ)" (mean 107.6 vs. 113.5; median 109.0 vs. 113.0; range 58–124 vs. 104–129; SD 12.88 vs. 7.20; 95% CI 102.0–113.1 vs. 110.5–116.5; $N = 23$ vs. 25) with a P of 0.10 (not normal distributed) or in the composite "National Eye Institute Visual Function Questionnaire (NEI-VFQ) and Neuro-Ophthalmic Supplement (NOS)" (mean 47.00 vs. 45.04; median 49 vs. 46; range 25–54 vs. 29–56; SD 6.82 vs. 6.03; 95% CI 44.05–49.95 vs. 42.55–47.53;

$N = 23$ vs. 25) with a P of 0.30 (normal distributed) as shown in **Supplementary Figure 7C**.

We also compared disability status Scales and could not identify a difference. Anti-AQP4-IgG positive and negative patients demonstrated no significant difference in the "Multiple Sclerosis Functional Composite (MSFC)" with a P of 0.68 (mean 7.96 vs. 8.21; median nine for both; range 4–9 for both; SD 2.07 vs. 1.87; 95% CI 7.08–8.83 vs. 7.31–9.11; $N = 24$ vs. 19) as shown in **Supplementary Figure 7D**.

There was no significant difference for Anti-AQP4-IgG positive and negative patients in the "The Short Form (36) Health Survey (SF-36)" with a P (passed Test for normal distribution) of 0.56 (mean 97.78 vs. 99.04; median 99 vs. 101; range 80–112 vs. 81–108; SD 7.99 vs. 7.01; 95% CI 94.33–101.2 vs. 96.15–101.9; $N = 23$ vs. 25), in the "visual analog scale (VAS). general" with a P (normal distributed) of 0.35 (mean 39.39 vs. 46.38; median 35 vs. 57.5; range 0–100 vs. 0–82; SD 27.06 vs. 23.91; 95% CI 27.69–51.09 vs. 36.28–56.47; $N = 23$ vs. 24), in the "visual analog scale (VAS) cognition" with a P (passed Test for normal distribution) of 0.65 (mean 31.61 vs. 31.70; median 25 vs. 26; range 0–98 vs. 0–69; SD 30.11 vs. 24.40; 95% CI 18.59–44.63 vs. 21.15–42.25; $N = 23$ for both), in the "fatigue severity scale (FSS)" with a P (data was normal distributed) of 0.89 (mean 34.65 vs. 35.36; median 30 vs. 33; range 9–63 vs. 10–63; SD 18.70 vs. 15.19; 95% CI 26.57–42.74 vs. 29.09–41.63; $N = 23$ vs. 25), in the "Fatigue Scale for Motor and Cognitive Functions (FSMC)" with a P (passed Test for normal distribution) of 0.96 (mean 36.90 vs. 36.58; median 29 vs. 38.5; range 4–76 vs. 1–69; SD 21.24 vs. 19.75; 95% CI 27.23–46.57 vs. 28.25–44.92; $N = 21$ vs. 24), in the "Beck Depression Inventory (BDI)" with a P (normal distributed data) of 0.30 (mean 9.32 vs. 11.82; median 7.5 vs. 10; range 1–27 for both; SD 7.42 vs. 8.36; 95% CI 6.03–12.61 vs. 8.11–15.52; $N = 22$ for both) or in the "visual analog scale (VAS) fatigue" with a P (results fitted to a normal distribution) of 0.22 (mean 36.61 vs. 46.67; median 23 vs. 54.5; range 0–100 vs. 0–76; SD 29.15 vs. 26.16; 95% CI 24.00–49.22 vs. 35.62–57.71; $N = 23$ vs. 24) as shown in **Supplementary Figure 7E**.

Even if a reduction of the Anti-AQP4-IgG titers was visible, there was no statistically significant difference ($P = 0.85$; no normal distribution) in the titer of Anti-AQP4-IgG between rituximab treated patients and untreated patients (mean 0.09 vs. 0.19; median 0 for both; range 0–0.74 vs. 0–2.26; SD 0.17 vs. 0.51; 95% CI 0.02–0.16 vs.−0.04–0.42; $N = 25$ vs. 21) as shown in **Supplementary Figure 7F**.

However, we identified a close to significant (P=0.09) increased rate of malignomas in the anti-AQP4-IgG negative as compared to the positive group (mean 0 vs. 0.10 malignomas; median was 0 in both cases; range 0 vs. 0–1; SD 0 vs. 0.31; 95% CI 0–0 vs.−0.014–0.221; $N = 34$ vs. 29; not shown). Further analysis showed that this increased rate in the anti-AQP4-IgG negative group was not present in anti-MOG-IgG positive patients, but only in anti-MOG-IgG negative patients (mean 0 vs. 0.20 tumors; median was 0 in both; range 0 vs. 0–1; SD 0 vs. 0.42; 95% CI 0-0 vs.−0.102–0.502; $N = 17$ vs. 10). However, this was even less significant ($P = 0.13$; not shown).

Positive Anti-aquaporin 4 (AQP4)-IgG Status Is Associated With Other Autoimmune Diseases in Addition to NMOSD

We identified a high number of additional diagnoses in addition to NMOSD in our patient collective (**Figure 4A**). While double aAb, anti-AQP4- and anti-MOG-IgG-negative patients had a higher rate of malignancies, anti-AQP4-IgG$^+$ patients had a significantly ($P = 0.022$; Mann–Whitney test as not normal distributed) higher rate of additional autoimmune diagnoses as compared to anti-AQP4-IgG-negative patients (mean 0.47 in AQP4-IgG$^+$ vs. 0.07 in AQP4-IgG$^-$; median was 0 in both; range 0–4 vs. 0–1; SD 0.90 vs. 0.26; 95% CI 0.16–0.78 vs.−0.03–0.17; $N = 34$ vs. 29; **Figure 4B**). Ten of the 34 anti-AQP4-IgG$^+$ patients (29%) had at least one additional autoimmune disorder as compared to only two of the 29 anti-AQP4-IgG$^-$ patients (7%). Of those ten anti-AQP4-IgG$^+$ patients, three had two and one had even four additional autoimmune diseases.

The two leading additional autoimmune disease were autoimmune thyroiditis in 4 and systemic lupus erythematosus (SLE) in five of the anti-AQP4-IgG$^+$ patients (**Supplementary Table 2**). In contrast, none of the anti-AQP4-IgG$^-$ patients had SLE and only one patient had autoimmune thyroiditis.

DISCUSSION

In this study, anti-AQP4-IgG positive or negative subgroups are not clearly associated with clinical parameters. The observation that patients without anti-AQP4-IgG are not clinically distinguishable from those patients with detected anti-AQP4-IgG argues challenges the hypothesis that anti-AQP4-IgG plays a major disease-driving role. However, we cannot exclude that the autoantibody assays were made at the wrong time point over the course of the disease. We used the data at baseline, the first visit of the patient as it might change after relapse therapy e.g., with rituximab.

This indiscernibility might be explained by either of the following: (1) with anti-AQP4-IgG we detect a polyreactive aAb and we know only one, maybe a minor, low affinity target of this aAb; (2) Anti-AQP4-IgG is a secondary, disease sustaining aAb (like in rheumatic fever), but not initiating it; patients can still benefit clinically from targeting it; (3) Anti-AQP4-IgG is an indicator for a yet unknown disease subgroup; or (4) Anti-AQP4-IgG is an epiphenomenon without salient clinical relevance for the course of NMOSD.

Emerging research suggests that autoimmune diseases, even when mediated by T cells, will frequently accompany the emergence of aAb to the same, often intracellular autoantigens (aAgs) (37, 38). aAbs, whose serum levels correlate with disease severity, have the potential to be used not only as biomarkers but also to identify relevant T cell targets (39–41). Nevertheless, the diversity and polyreactivity of aAbs in individuals with an autoimmune condition poses a significant barrier to determining which aAgs are pathogenic.

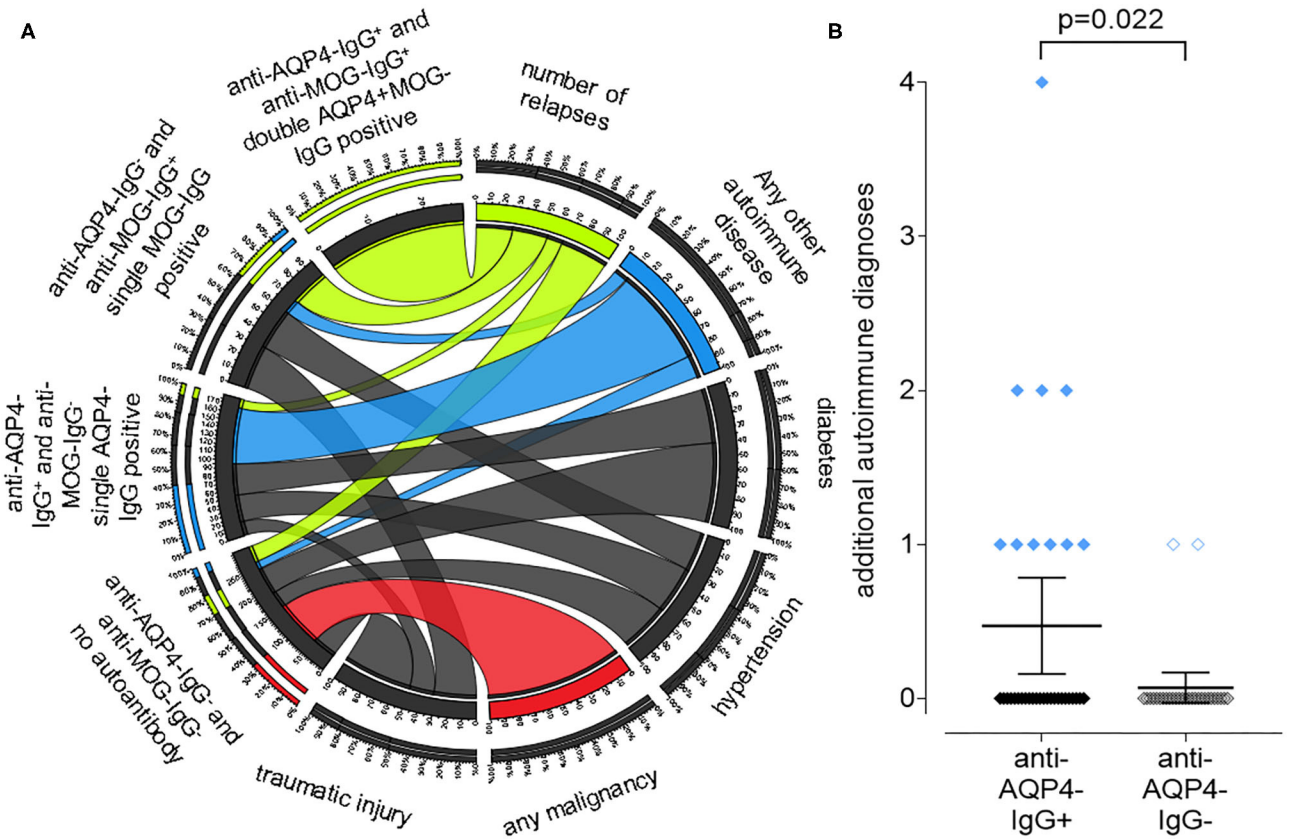

FIGURE 4 | A positive anti-aquaporin 4 (AQP4)-IgG status is associated with the presence of other autoimmune diseases in addition to NMOSD, while a negative status is associated with malignancies. A chord plot, based on the 59 patients for which we had both, anti-AQP4- and anti-MOG-IgG test results, is shown **(A)**. The patients were sorted according to these results into four groups, shown on the left side of the chord plot: anti-AQP4-IgG$^+$ and anti-MOG-IgG$^+$: double AQP4+MOG-IgG positive anti-AQP4-IgG$^-$ and anti-MOG-IgG$^+$: single MOG-IgG positive anti-AQP4-IgG$^+$ and anti-MOG-IgG$^-$: single AQP4-IgG positive anti-AQP4-IgG$^-$ and anti-MOG-IgG$^-$: no aAb. On the right side, key findings such as: number of relapses; any other autoimmune disease (thyroiditis; SLE; myasthenia; Sjogren's and other); diabetes; hypertension; any malignancy and traumatic injury are show. The thickness of the connecting chords between the four patient subgroups and the key findings represents the number of patients with each of those conditions. The chords connecting the patients with "any malignancy" have been colored red, however there is only one chord present, connecting "any malignancy" with the "anti-AQP4-IgG$^-$ and anti-MOG-IgG$^-$: no aAb" group. Therefore, all patients with malignancy do not have any of the aAbs. In contrast, the chords connecting patients with "any other autoimmune disease" have been colored blue. The thickest chord, representing about 80% of the autoimmune group, is connected to the "single AQP4-IgG positive" patients. Vice versa, in this "single AQP4-IgG positive" group, the connection to the autoimmune group represents about 40% of all its connections. Therefore, 80% of all patients with a second autoimmune condition were single AQP4-IgG positive and in this group, it was the largest contributing factor and showed a significant difference related to the AQP4-IgG status **(B)**.

According to the Bradford Hill criteria, a biological gradient should be present, to prove the causal role of a presumed cause and an observed effect (disease) (42). This missing biological gradient, the missing increase of the anti-AQP4-IgG with increasing disease activity, is hard to explain. In other autoimmune disease such as Lupus nephritis, there is a clear correlation of severity of the clinical disease with anti-dsDNA-autoantibodies (43, 44).

"Bystander" B cell responses have been observed in several autoimmune diseases, Hashimoto's thyroiditis being a good example. In Hashimoto's, high amounts of anti-thyroid aAb are produced and correlate well with the clinical course (45). These aAb can even fix complement and facilitate the destruction of thyroid cells (46, 47). However, they are a consequence of the disease process, not a cause (48, 49). Another example is polymyositis, where anti-myoglobin aAbs correlate well with clinical activity, but do not participate in the induction of tissue destruction (50). Whether aAbs play a pathogenic role in MS, a comparable CNS disease, remains unclear; but even when they lack a causative role in disease, aAbs nevertheless inform us about the identity of the aAgs that are available and recognized by the autoimmune T cell population. Many aAb are IgG type natural occurring antibodies (NAbs), which are present from birth and not induced later (51, 52). NAbs do not appear to depend on CD4 T cell help, noteworthy because anti-CD4 is ineffective in MS (53, 54). Identifying the

targets of NAbs is technically challenging. NAbs purified with immunoadsorbent columns with one aAg are often cross-reactive to other aAgs (51). Polyreactivity is a big problem, as we need to identify the set of best binding aAgs for each monoclonal Ab, select the disease-relevant targets and define possible pathogenic T cell epitopes of those aAgs (55). Nevertheless, we have extensive experience in aAb characterization and have developed protocols that overcome many of these challenges (56, 57).

The initiation of disease, how the blood-brain barrier (BBB) breaks down, is left unexplained. AQP4, the six transmembrane helix water channel, is not expressed on endothelial cells, therefore translocation of anti-AQP4-IgG through the BBB, due to a leaky BBB and/or local production of it is required (58). Those aAbs are thought to be of high pathophysiologic if not etiologic relevance even as a myriad of other aAgs have now been found in several major neurological diseases (37). As NMOSD is thought to be caused by an autoimmune reaction and as patients with NMOSD experience almost exclusively symptoms due to CNS involvement, an expression of the target of this autoimmune reaction limited selectively to the CNS would fortify the pathological hypothesis. Many new isoforms of AQP4 just have been identified (**Supplementary Figure 8**) with broad expression of the main transcript outside the CNS. Expression data of AQP4: ENSG00000171885.13 from HGNC (Acc: HGNC: 637) shows eight splice variants (**Supplementary Figure 8**), which represent different protein isoforms, the major one is also highly expressed in the lungs, thyroid, gastrointestinal (GI) system and other organs. Proteomics data reveals an AQP4 protein presence in lung and stomach which is comparable to its presence in astrocytes. However, in patients with anti-AQP4-IgG, pulmonary and gastric symptoms have not been described. Yet there are studies investigating binding of patients' anti-AQP4-IgG against two of the major AQP4 forms expressed on astrocytes (59), although others have proposed that anti-AQP4-IgG may not be the main direct cause of the astrocytopathy in NMOSD, but demonstrated that anti-AQP4-IgG down-regulates CXC motif ligand 12 (CXCL12) and impairs remyelination by oligodendrocyte progenitor cells (60). Indeed, the high degree of heterogeneity of the patients' IgGs to targeting different isoforms of AQP4 raises the question how well other isoforms are targeted, especially in non-CNS organs.

However, there are four CNS-specific transcripts, of which transcript six might be functional and exclusively use exon two, making it an ideal target for a CNS-selective aAb leading to a localized autoimmune reaction in NMOSD. In further studies, we should also test those isoforms, splice variants as well as other genotypes of AQP4 as target of the aAb. We cannot exclude that anti-AQP4-IgG plays a prominent role at an earlier or later stage, especially as the expression is heavily modified by inflammation (especially IFNγ) (61).

AQP4 represents only one of many so far described IgG aAgs in NMOSD such as anti-nuclear and anti-Ro aAbs (1, 62). Thus, it is possible that several autoreactive IgG against several targets collectively contribute to disease. The recent positive trial data demonstrating efficacy of anti-CD19 in NMOSD indirectly supports this notion (23, 63), although it should be noted that B cells serve additional functions beyond merely manufacturing IgG (64). Interestingly, we found no difference in anti-AQP4 status after treatment with rituximab, to which most patients responded with a clinical improvement. Similar as what has been described in other autoimmune diseases, a reduction in anti-AQP4 status would have been conceivable (65). This might be a further hint that the role of anti-AQP4-IgG as disease driving aAb has been overestimated.

The finding that a positive anti-AQP4-IgG status is significantly associated with the presence of other autoimmune diseases in addition to NMOSD might indicate that anti-AQP4 is indeed a "bystander" B cell response as explained above. Therefore, in some patients detectable anti-AQP4-IgG titers may signify the co-occurrence of NMOSD and additional autoimmune disease. In our patient cohort, five patients suffered from additional SLE, four from autoimmune thyroiditis and two from Sjogren's syndrome. This pattern fits in with the long-known association of NMOSD with these autoimmune syndromes, which first led to the discovery of NMO-IgG and turned out to be anti-AQP4-IgG (1). Interestingly, pathological changes in the IgG half-life have been described in all of these diseases, so that certain aAbs can be present at elevated titers (66–69). In addition, B cell survival and activation is enhanced in those autoimmune diseases (70). This might give a hint that anti-AQP4-IgG might be present in other NMOSD patients, but below the detection limits of the test as additional immune pathologies are needed to make it detectable with the current clinically used test procedures and available immunoassays. So far, our results challenge the assumption that anti-AQP4-IgG alone plays a disease-driving role in NMOSD as it is determined with the currently used immunoassays. We cannot finally rule out that Anti-AQP4-IgG might be the main pathologic factor in a subset of patients, but our analyses rather indicate that it is represent as an epiphenomenon or may be one of many immune mechanisms that collectively contribute to the pathogenesis of this disease.

In further studies, we would suggest evaluating the tissue specific expression of the target, it's splice variants, as well as a possible polyreactivity of Anti-AQP4-IgG. We would also suggest to use *ex vivo* translated AQP4 or more selective certain peptide epitopes to improve the capability of the immunoassay.

CAPSULE SUMMARY

We performed phylogenetic clustering, PCA and causal interference analyses to test for a role of anti-AQP4-IgG in 63 comparable patients suffering from NMOSD. Our results challenge the current concept that anti-AQP4-IgG plays a sole or predominant disease-driving role in many patients with this disease.

DATA AVAILABILITY STATEMENT

The original contributions presented in the study are included in the article/**Supplementary Material**,

further inquiries can be directed to the corresponding author/s.

ETHICS STATEMENT

All data collected from patients and investigated in this study was used after written informed consent as approved by the ethics committee of the Charité - Universitätsmedizin Berlin (proposal EA1/041/14) according to the Declaration of Helsinki (59th WMA General Assembly, Seoul, October 2008). The patients/participants provided their written informed consent to participate in this study.

AUTHOR CONTRIBUTIONS

OS did the main research and wrote the manuscript. EL and BR helped correcting the manuscript. AD, SA, FP, and NS helped collecting the patients' materials. FP and NS helped correcting the manuscript. All authors contributed to the article and approved the submitted version.

SUPPLEMENTARY MATERIAL

The Supplementary Material for this article can be found online at: https://www.frontiersin.org/articles/10.3389/fneur.2021.635419/full#supplementary-material

REFERENCES

1. Wingerchuk DM, Lennon VA, Lucchinetti CF, Pittock SJ, Weinshenker BG. The spectrum of neuromyelitis optica. *Lancet Neurol.* (2007) 6:805–15. doi: 10.1016/S1474-4422(07)70216-8
2. Asgari N, Lillevang ST, H.Skejoe PB, Kyvik KO. Epidemiology of neuromyelitis optica spectrum disorder in Denmark. (1998-2008, 2007-2014). *Brain Behav.* (2019) 9:e01338. doi: 10.1002/brb3.1338
3. Mori M, Kuwabara S, Paul F. Worldwide prevalence of neuromyelitis optica spectrum disorders. *J Neurol Neurosurg Psychiatry.* (2018) 89:555–6. doi: 10.1136/jnnp-2017-317566
4. Hor JY, Asgari N, Nakashima I, Broadley SA, Leite MI, Kissani N, et al. Epidemiology of neuromyelitis optica spectrum disorder and its prevalence and incidence worldwide. *Front Neurol.* (2020) 11:501. doi: 10.3389/fneur.2020.00501
5. Jarius S, Wildemann B. AQP4 antibodies in neuromyelitis optica: diagnostic and pathogenetic relevance. *Nat Rev Neurol.* (2010) 6:383–92. doi: 10.1038/nrneurol.2010.72
6. Stellmann JP, Krumbholz M, Friede T, Gahlen A, Borisow N, Fischer K, et al. Immunotherapies in neuromyelitis optica spectrum disorder: efficacy and predictors of response. *J Neurol Neurosurg Psychiatry.* (2017) 88:639–47. doi: 10.1136/jnnp-2017-315603
7. Jarius S, Paul F, Weinshenker BG, Levy M, Kim HJ, Wildemann B. Neuromyelitis optica. *Nat Rev Dis Primers.* (2020) 6:85. doi: 10.1038/s41572-020-0214-9
8. Ciccarelli O, Cohen JA, Reingold SC, Weinshenker BG, International Conference on Spinal Cord Involvement and Imaging in Multiple Sclerosis and Neuromyelitis Optica Spectrum Disorders. Spinal cord involvement in multiple sclerosis and neuromyelitis optica spectrum disorders. *Lancet Neurol.* (2019) 18:185–97. doi: 10.1016/S1474-4422(18)30460-5
9. Zekeridou A, Lennon VA, Aquaporin-4 autoimmunity. *Neurol Neuroimmunol Neuroinflamm.* (2015) 2:e110. doi: 10.1212/NXI.0000000000000110
10. Jarius S, Paul F, Aktas O, Asgari N, Dale RC, de Seze J, et al. MOG encephalomyelitis: international recommendations on diagnosis and antibody testing. *J Neuroinflammation.* (2018) 15:134. doi: 10.1186/s12974-018-1144-2
11. Pittock SJ, Lucchinetti CF. Neuromyelitis optica and the evolving spectrum of autoimmune aquaporin-4 channelopathies: a decade later. *Ann N Y Acad Sci.* (2016) 1366:20–39. doi: 10.1111/nyas.12794
12. O'Connell K, Hamilton-Shield A, Woodhall M, Messina S, Mariano R, Waters P, et al. Prevalence and incidence of neuromyelitis optica spectrum disorder, aquaporin-4 antibody-positive NMOSD and MOG antibody-positive disease in Oxfordshire, UK. *J Neurol Neurosurg Psychiatry.* (2020) 91:1126–8. doi: 10.1136/jnnp-2020-323158
13. Bukhari W, Prain KM, Waters P, Woodhall M, O'Gorman CM, Clarke L, et al. Incidence and prevalence of NMOSD in Australia and New Zealand. *J Neurol Neurosurg Psychiatry.* (2017) 88:632–8. doi: 10.1136/jnnp-2016-314839
14. Dalakas MC, Alexopoulos H, Spaeth PJ. Complement in neurological disorders and emerging complement-targeted therapeutics. *Nat Rev Neurol.* (2020) 16:601–17. doi: 10.1038/s41582-020-0400-0
15. Kinoshita M, Nakatsuji Y, Kimura T, Moriya M, Takata K, Okuno T, et al. Neuromyelitis optica: passive transfer to rats by human immunoglobulin. *Biochem Biophys Res Commun.* (2009) 386:623–7. doi: 10.1016/j.bbrc.2009.06.085
16. Wu Y, Zhong L, Geng J. Neuromyelitis optica spectrum disorder: pathogenesis, treatment, and experimental models. *Mult Scler Relat Disord.* (2019) 27:412–8. doi: 10.1016/j.msard.2018.12.002
17. Vincent T, Saikali P, Cayrol R, Roth AD, Bar-Or A, Prat A, et al. Functional consequences of neuromyelitis optica-IgG astrocyte interactions on blood-brain barrier permeability and granulocyte recruitment. *J Immunol.* (2008) 181:5730–7. doi: 10.4049/jimmunol.181.8.5730
18. Takeshita Y, Obermeier B, Cotleur AC, Spampinato SF, Shimizu F, Yamamoto E, et al. Effects of neuromyelitis optica-IgG at the blood-brain barrier *in vitro*. *Neurol Neuroimmunol Neuroinflamm.* (2017) 4:e311. doi: 10.1212/NXI.0000000000000311
19. Hinson SR, McKeon A, Fryer JP, Apiwattanakul M, Lennon VA, Pittock SJ. Prediction of neuromyelitis optica attack severity by quantitation of complement-mediated injury to aquaporin-4-expressing cells. *Arch Neurol.* (2009) 66:1164–7. doi: 10.1001/archneurol.2009.188
20. Pittock SJ, Berthele A, Fujihara K, Kim HJ, Levy M, Palace J, et al. Eculizumab in aquaporin-4-positive neuromyelitis optica spectrum disorder. *N Engl J Med.* (2019) 381: 614–25. doi: 10.1056/NEJMoa1900866
21. Pittock SJ, Lennon VA, McKeon A, Mandrekar J, Weinshenker BG, Lucchinetti CF, et al. Eculizumab in AQP4-IgG-positive relapsing neuromyelitis optica spectrum disorders: an open-label pilot study. *Lancet Neurol.* (2013) 12:554–62. doi: 10.1016/S1474-4422(13)70076-0
22. Nishiyama S, Misu T, Nuriya M, Takano R, Takahashi T, Nakashima I, et al. Complement-dependent and -independent aquaporin 4-antibody-mediated cytotoxicity in human astrocytes: Pathogenetic implications in neuromyelitis optica. *Biochem Biophys Rep.* (2016) 7:45–51. doi: 10.1016/j.bbrep.2016.05.012
23. Duchow A, Chien C, Paul F, Bellmann-Strobl J. Emerging drugs for the treatment of neuromyelitis optica. *Expert Opin Emerg Drugs.* (2020) 25:285–97. doi: 10.1080/14728214.2020.1803828
24. Graf J, Mares J, Barnett M, Aktas O, Albrecht P, Zamvil SS, et al. Targeting B cells to modify MS, NMOSD, and MOGAD: Part 2. *Neurol Neuroimmunol Neuroinflamm.* (2021) 8:e919. doi: 10.1212/NXI.0000000000000919
25. Graf J, Mares J, Barnett M, Aktas O, Albrecht P, Zamvil SS, et al. Targeting B cells to modify MS, NMOSD, and MOGAD: part 1. *Neurol Neuroimmunol Neuroinflamm.* (2021) 8. doi: 10.1212/NXI.0000000000000918
26. Jitprapaikulsan J, Fryer JP, Majed M, Smith CY, Jenkins SM, Cabre P, et al. Clinical utility of AQP4-IgG titers and measures of complement-mediated cell killing in NMOSD. *Neurol Neuroimmunol Neuroinflamm.* (2020) 7:e727. doi: 10.1212/NXI.0000000000000727
27. Reindl M, Are aquaporin antibody titers useful outcome measures for neuromyelitis optica spectrum disorders? *Neurol Neuroimmunol Neuroinflamm.* (2020) 7:e759. doi: 10.1212/NXI.0000000000000759

28. Borisow N, Mori M, Kuwabara S, Scheel M, Paul F. Diagnosis and treatment of NMO spectrum disorder and MOG-encephalomyelitis. *Front Neurol.* (2018) 9:888. doi: 10.3389/fneur.2018.00888
29. Narayan R, Simpson A, Fritsche K, Salama S, Pardo S, Mealy M, et al. MOG antibody disease: a review of MOG antibody seropositive neuromyelitis optica spectrum disorder. *Mult Scler Relat Disord.* (2018) 25:66–72. doi: 10.1016/j.msard.2018.07.025
30. Reindl M, Schanda K, Woodhall M, Tea F, Ramanathan S, Sagen J, et al. International multicenter examination of MOG antibody assays. *Neurol Neuroimmunol Neuroinflamm.* (2020) 7:e674. doi: 10.1212/NXI.0000000000000674
31. Schmidt FA, Chien C, Kuchling J, Bellmann-Strobl J, Ruprecht K, Siebert N, et al. Differences in advanced magnetic resonance imaging in MOG-IgG and AQP4-IgG seropositive neuromyelitis optica spectrum disorders: a comparative study. *Front Neurol.* (2020) 11:499910. doi: 10.3389/fneur.2020.499910
32. Wingerchuk DM, Banwell B, Bennett JL, Cabre P, Carroll W, Chitnis T, et al.M.O.D. International Panel for, International consensus diagnostic criteria for neuromyelitis optica spectrum disorders. *Neurology.* (2015) 85:177–89. doi: 10.1212/WNL.0000000000001729
33. Metsalu T, Vilo J. ClustVis: a web tool for visualizing clustering of multivariate data using principal component analysis and heatmap. *Nucleic Acids Res.* (2015) 43:W566–70. doi: 10.1093/nar/gkv468
34. Lakin E, Church MK, Maurer M, Schmetzer O. On the lipophilic nature of autoreactive ige in chronic spontaneous urticaria. *Theranostics.* (2019) 9:829–36. doi: 10.7150/thno.29902
35. Krzywinski M, Schein J, Birol I, Connors J, Gascoyne R, Horsman D, et al. Circos: an information aesthetic for comparative genomics. *Genome Res.* (2009) 19:1639–45. doi: 10.1101/gr.092759.109
36. Jarius S, Ruprecht K, Kleiter I, Borisow N, Asgari N, Pitarokoili K, et al. in cooperation with the Neuromyelitis Optica Study, MOG-IgG in NMO and related disorders: a multicenter study of 50 patients. Part 1: Frequency, syndrome specificity, influence of disease activity, long-term course, association with AQP4-IgG, and origin. *J Neuroinflammation.* (2016) 13:279. doi: 10.1186/s12974-016-0717-1
37. Lancaster E, Dalmau J. Neuronal autoantigens–pathogenesis, associated disorders and antibody testing. *Nat Rev Neurol.* (2012) 8:380–90. doi: 10.1038/nrneurol.2012.99
38. Boronat A, Sepulveda M, Llufriu S, Sabater L, Blanco Y, Gabilondo I, et al. Analysis of antibodies to surface epitopes of contactin-2 in multiple sclerosis. *J Neuroimmunol.* (2012) 244:103–6. doi: 10.1016/j.jneuroim.2011.12.023
39. Giovannoni G, Ebers G. Multiple sclerosis: the environment and causation. *Curr Opin Neurol.* (2007) 20:261–8. doi: 10.1097/WCO.0b013e32815610c2
40. Swaen G, van Amelsvoort L. A weight of evidence approach to causal inference. *J Clin Epidemiol.* (2009) 62:270–7. doi: 10.1016/j.jclinepi.2008.06.013
41. Schmetzer, O. (2007). *Identifikation und funktionelle Charakterisierung der neuen CD3 splice Variante CD3k in T-Helferzellen nach Stimulation mit heteroklitischen Peptiden*. [dissertation/master's thesis]. Humboldt-University Berlin.
42. Hill AB. The environment and disease: association or causation? *Proc R Soc Med.* (1965) 58:295–300. doi: 10.1177/003591576505800503
43. Rekvig OP. The anti-DNA antibody: origin and impact, dogmas and controversies. *Nat Rev Rheumatol.* (2015) 11:530–40. doi: 10.1038/nrrheum.2015.69
44. Rekvig OP. Systemic lupus erythematosus: definitions, contexts, conflicts, enigmas. *Front Immunol.* (2018) 9:387. doi: 10.3389/fimmu.2018.00387
45. McLachlan SM, Rapoport B. Autoimmune response to the thyroid in humans: thyroid peroxidase–the common autoantigenic denominator. *Int Rev Immunol.* (2000) 19:587–618. doi: 10.3109/08830180009088514
46. Trotter WR, Belyavin G, Waddams A. Precipitating and complement-fixing antibodies in Hashimoto's disease. *Proc R Soc Med.* (1957) 50:961–2.
47. Ludwig RJ, Vanhoorelbeke K, Leypoldt F, Kaya Z, Bieber K, McLachlan SM, et al. Mechanisms of autoantibody-induced pathology. *Front Immunol.* (2017) 8:603. doi: 10.3389/fimmu.2017.00603
48. Karanikas G, Schuetz M, Wahl K, Paul M, Kontur S, Pietschmann P, et al. Relation of anti-TPO autoantibody titre and T-lymphocyte cytokine production patterns in Hashimoto's thyroiditis. *Clin Endocrinol (Oxf).* (2005) 63:191–6. doi: 10.1111/j.1365-2265.2005.02324.x
49. Chistiakov DA. Immunogenetics of Hashimoto's thyroiditis. *J Autoimmune Dis.* (2005) 2:1. doi: 10.1186/1740-2557-2-1
50. Nishikai M, Homma M. Circulating autoantibody against human myoglobin in polymyositis. *JAMA.* (1977) 237:1842–4. doi: 10.1001/jama.237.17.1842
51. Guilbert B, Dighiero G, Avrameas S. Naturally occurring antibodies against nine common antigens in human sera. Detection I, isolation and characterization. *J Immunol.* (1982) 128:2779–87.
52. Madi A, Bransburg-Zabary S, Kenett DY, Ben-Jacob E, Cohen IR. The natural autoantibody repertoire in newborns and adults: a current overview. *Adv Exp Med Biol.* (2012) 750:198–212. doi: 10.1007/978-1-4614-3461-0_15
53. van Oosten BW, Lai M, Hodgkinson S, Barkhof F, Miller DH, Moseley IF, et al. Treatment of multiple sclerosis with the monoclonal anti-CD4 antibody cM-T412: results of a randomized, double-blind, placebo-controlled, MR-monitored phase II trial. *Neurology.* (1997) 49:351–7. doi: 10.1212/WNL.49.2.351
54. Jameson BA, McDonnell JM, Marini JC, Korngold R. A rationally designed CD4 analogue inhibits experimental allergic encephalomyelitis. *Nature.* (1994) 368:744–6. doi: 10.1038/368744a0
55. Sewell AK. Why must T cells be cross-reactive? *Nat Rev Immunol.* (2012) 12:669–77. doi: 10.1038/nri3279
56. Schmetzer O, Lakin E, Topal FA, Preusse P, Freier D, Church MK, et al. IL-24 is a common and specific autoantigen of IgE in patients with chronic spontaneous urticaria. *J Allergy Clin Immunol.* (2018) 142:876–82. doi: 10.1016/j.jaci.2017.10.035
57. Schmetzer O, Moldenhauer G, Riesenberg R, Pires JR, Schlag P, Pezzutto A. Quality of recombinant protein determines the amount of autoreactivity detected against the tumor-associated epithelial cell adhesion molecule antigen: low frequency of antibodies against the natural protein. *J Immunol.* (2005) 174:942–52. doi: 10.4049/jimmunol.174.2.942
58. Shimizu F, Schaller KL, Owens GP, Cotleur AC, Kellner D, Takeshita Y, et al. Glucose-regulated protein 78 autoantibody associates with blood-brain barrier disruption in neuromyelitis optica. *Sic Transl Med.* (2017) 9:eaai9111. doi: 10.1126/scitranslmed.aai9111
59. Crane JM, Lam C, Rossi A, Gupta T, Bennett JL, Verkman AS. Binding affinity and specificity of neuromyelitis optica autoantibodies to aquaporin-4 M1/M23 isoforms and orthogonal arrays. *J Biol Chem.* (2011) 286:16516–24. doi: 10.1074/jbc.M111.227298
60. Kang H, Cao S, Chen T, Jiang Z, Liu Z, Li Z, et al. The poor recovery of neuromyelitis optica spectrum disorder is associated with a lower level of CXCL12 in the human brain. *J Neuroimmunol.* (2015) 289:56–61. doi: 10.1016/j.jneuroim.2015.10.005
61. Satoh J, Tabunoki H, Yamamura T, Arima K, Konno H. Human astrocytes express aquaporin-1 and aquaporin-4 *in vitro* and *in vivo*. *Neuropathology.* (2007) 27:245–56. doi: 10.1111/j.1440-1789.2007.00774.x
62. Sinmaz N, Amatoury M, Merheb V, Ramanathan S, Dale RC, Brilot F. Autoantibodies in movement and psychiatric disorders: updated concepts in detection methods, pathogenicity, and CNS entry. *Ann N Y Acad Sci.* (2015) 1351:22–38. doi: 10.1111/nyas.12764
63. Cree BAC, Bennett JL, Kim HJ, Weinshenker BG, Pittock SJ, Wingerchuk DM, et al. investigators, Inebilizumab for the treatment of neuromyelitis optica spectrum disorder (N-MOmentum): a double-blind, randomised placebo-controlled phase 2/3 trial. *Lancet.* (2019) 394:1352–63. doi: 10.1016/S0140-6736(19)31817-3
64. Bennett JL, O'Connor KC, Bar-Or A, Zamvil SS, Hemmer B, Tedder TF, et al. B lymphocytes in neuromyelitis optica. *Neurol Neuroimmunol Neuroinflamm.* (2015) 2:e104. doi: 10.1212/NXI.0000000000000104
65. Ferraro AJ, Drayson MT, Savage CO, MacLennan IC. Levels of autoantibodies, unlike antibodies to all extrinsic antigen groups, fall following B cell depletion with Rituximab. *Eur J Immunol.* (2008) 38:292–8. doi: 10.1002/eji.200737557
66. Cuadrado MJ, Calatayud I, Urquizu-Padilla M, Wijetilleka S, Kiani-Alikhan S, Karim MY. Immunoglobulin abnormalities are frequent in patients with lupus nephritis. *BMC Rheumatol.* (2019) 3:30. doi: 10.1186/s41927-019-0079-2

67. Nocturne G, Mariette X. B cells in the pathogenesis of primary Sjogren syndrome. *Nat Rev Rheumatol.* (2018) 14:133–45. doi: 10.1038/nrrheum.2018.1
68. Skanse B, Nilsson SB. Hypergammaglobulinemia and thyroid antibodies. *Acta Med Scand.* (1962) 172:505–12. doi: 10.1111/j.0954-6820.1962.tb07185.x
69. Dayan CM, Daniels GH. Chronic autoimmune thyroiditis. *N Engl J Med.* (1996) 335:99–107. doi: 10.1056/NEJM199607113350206
70. Morais SA, Vilas-Boas A, Isenberg DA. B-cell survival factors in autoimmune rheumatic disorders. *Ther Adv Musculoskelet Dis.* (2015) 7:122–51. doi: 10.1177/1759720X15586782

Conflict of Interest: BR is presently an employee at Novartis Institutes for BioMedical Research. Novartis did not fund the study. AD received a speaker honorarium from Roche. FP served on the scientific advisory boards of Novartis and MedImmune; received speaker honoraria and travel funding from Bayer, Novartis, Biogen, Teva, Sanofi-Aventis/Genzyme, Merck Serono, Alexion, Chugai, MedImmune, and Shire; serves as academic editor of PLoS ONE and associate editor of Neurology: Neuroimmunology & Neuroinflammation; consulted for Sanofi-Genzyme, Biogen, MedImmune, Shire, and Alexion; and received research support from Bayer, Novartis, Biogen, Teva, Sanofi-Aventis/Genzyme, Alexion, Merck Serono, German Research Council, Werth Stiftung of the City of Cologne, German Ministry of Education and Research, Arthur Arnstein Stiftung Berlin, EU FP7 Framework Program, Guthy Jackson Charitable Foundation, and NMSS. NS received travel funding from Sanofi-Aventis/Genzyme and speaker honoraria from Bayer AG.

The remaining authors declare that the research was conducted in the absence of any commercial or financial relationships that could be construed as a potential conflict of interest.

Copyright © 2021 Schmetzer, Lakin, Roediger, Duchow, Asseyer, Paul and Siebert. This is an open-access article distributed under the terms of the Creative Commons Attribution License (CC BY). The use, distribution or reproduction in other forums is permitted, provided the original author(s) and the copyright owner(s) are credited and that the original publication in this journal is cited, in accordance with accepted academic practice. No use, distribution or reproduction is permitted which does not comply with these terms.

frontiers in Neurology

CLINICAL TRIAL
published: 28 April 2021
doi: 10.3389/fneur.2021.615790

Retinal Thickness Analysis in Progressive Multiple Sclerosis Patients Treated With Epigallocatechin Gallate: Optical Coherence Tomography Results From the SUPREMES Study

*Katharina Klumbies[1,2], Rebekka Rust[1,2], Jan Dörr[1,2,3], Frank Konietschke[4], Friedemann Paul[1,2,5], Judith Bellmann-Strobl[1,2], Alexander U. Brandt[1,2,6] and Hanna G. Zimmermann[1,2]**

[1] Experimental and Clinical Research Center, Max Delbrueck Center for Molecular Medicine and Charité—Universitätsmedizin Berlin, Corporate Member of Freie Universität Berlin and Humboldt-Universität zu Berlin, Berlin, Germany, [2] NeuroCure Clinical Research Center, Charité—Universitätsmedizin Berlin, Corporate Member of Freie Universität Berlin and Humboldt-Universität zu Berlin, Berlin, Germany, [3] Neurology Department, Oberhavel Clinic, Hennigsdorf, Germany, [4] Institute of Biometry and Clinical Epidemiology, Charité—Universitätsmedizin Berlin, Corporate Member of Freie Universität Berlin and Humboldt-Universität zu Berlin, Berlin, Germany, [5] Department of Neurology, Charité—Universitätsmedizin Berlin, Corporate Member of Freie Universität Berlin and Humboldt-Universität zu Berlin, Berlin, Germany, [6] Department of Neurology, University of California, Irvine, Irvine, CA, United States

OPEN ACCESS

Edited by:
Gemma Caterina Maria Rossi, Fondazione Ospedale San Matteo (IRCCS), Italy

Reviewed by:
Christian Cordano, University of California, San Francisco, United States
Simon Hickman, Royal Hallamshire Hospital, United Kingdom

***Correspondence:**
Hanna G. Zimmermann
hanna.zimmermann@charite.de

Specialty section:
This article was submitted to Neuro-Ophthalmology, a section of the journal Frontiers in Neurology

Received: 09 October 2020
Accepted: 25 March 2021
Published: 28 April 2021

Citation:
Klumbies K, Rust R, Dörr J, Konietschke F, Paul F, Bellmann-Strobl J, Brandt AU and Zimmermann HG (2021) Retinal Thickness Analysis in Progressive Multiple Sclerosis Patients Treated With Epigallocatechin Gallate: Optical Coherence Tomography Results From the SUPREMES Study. Front. Neurol. 12:615790. doi: 10.3389/fneur.2021.615790

Background: Epigallocatechin gallate (EGCG) is an anti-inflammatory agent and has proven neuroprotective properties in animal models of multiple sclerosis (MS). Optical coherence tomography (OCT) assessed retinal thickness analysis can reflect treatment responses in MS.

Objective: To analyze the influence of EGCG treatment on retinal thickness analysis as secondary and exploratory outcomes of the randomized controlled *Sunphenon in Progressive Forms of MS* trial (SUPREMES, NCT00799890).

Methods: SUPREMES patients underwent OCT with the Heidelberg Spectralis device at a subset of visits. We determined peripapillary retinal nerve fiber layer (pRNFL) thickness from a 12° ring scan around the optic nerve head and thickness of the ganglion cell/inner plexiform layer (GCIP) and inner nuclear layer (INL) within a 6 mm diameter grid centered on the fovea from a macular volume scan. Longitudinal OCT data were available for exploratory analysis from 31 SUPREMES participants (12/19 primary/secondary progressive MS (PPMS/SPMS); mean age 51 ± 7 years; 12 female; mean time since disease onset 16 ± 11 years). We tested the null hypothesis of no treatment*time interaction using nonparametric analysis of longitudinal data in factorial experiments.

Results: After 2 years, there were no significant differences in longitudinal retinal thickness changes between EGCG treated and placebo arms in any OCT parameter

(Mean change [confidence interval] ECGC vs. Placebo: pRNFL: −0.83 [1.29] μm vs. −0.64 [1.56] μm, $p = 0.156$; GCIP: −0.67 [0.67] μm vs. −0.14 [0.47] μm, $p = 0.476$; INL: −0.06 [0.58] μm vs. 0.22 [0.41] μm, $p = 0.455$).

Conclusion: Retinal thickness analysis did not reveal a neuroprotective effect of EGCG. While this is in line with the results of the main SUPREMES trial, our study was probably underpowered to detect an effect.

Clinical Trial Registration: www.ClinicalTrials.gov, identifier: NCT00799890.

Keywords: optical coherence tomography, retina, progressive multiple sclerosis, treatment response, epigallocatechin gallate

INTRODUCTION

Multiple sclerosis (MS) is the most common autoimmune inflammatory and degenerative central nervous system (CNS) disease, often resulting in sustained neurological deficits (1). The majority of patients manifest with a relapsing remitting (RRMS) disease course (2, 3), followed by a secondary progressive (SPMS) stage ∼20 years from onset (4). However, 15–20% show a primary progressive (PPMS) disease course from onset (3, 5, 6). Neurodegeneration may be present in any course from the onset of the disease (7–10).

The principle of disease modifying therapy (DMT) aims at decreasing relapse frequency and disability progression. Whereas various immunomodulatory drugs for the treatment of RRMS targeting the inflammatory aspect of the disease have been established in the last decades (11), treatment options for progressive MS are sparse (12, 13). Furthermore, due to the absence of clinical relapses, treatment response is difficult to measure in progressive MS and has to rely on measures not primarily associated with relapse activity (13).

Green tea anti-inflammatory, anti-oxidative, and anti-cancerogenic effects have been shown on various conditions such as energy metabolism, cell development, and neuroprotection (14–17). The most active agent is the polyphenol epigallocatechin-gallate (EGCG), comprising 50–80% of the total catechins in green tea (18). EGCG has shown immunomodulatory effects by inhibition of T cell proliferation and thus modulates the production of T cell-derived cytokines, e.g., Interferon-γ, Interleukin-2, and tumor necrosis factor (TFN) α (from T helper type 1 cell subset) (19–21). In an experimental animal model of MS (experimental autoimmune encephalomyelitis, EAE) the oral intake of EGCG suppressed inflammation via inhibition of TNFα and nuclear factor kappa-light-chain-enhancer of activated B cells in T cells, thus resulting in reduced clinical disease severity and fewer CNS lesions in mice (22–24). Furthermore, treatment with EGCG and glatiramer acetate in EAE mice delayed disease onset, reduced clinical disability and reduced inflammatory infiltrates (25). In clinical trials, oral intake of EGCG was associated with improved muscle metabolism during moderate exercise in RRMS (26) and improved cognitive rehabilitation in genetic disorders (27, 28).

Optical coherence tomography (OCT) allows quantification of anterior visual pathway damage in MS patients (29–33). While thinning of the peripapillary retinal nerve fiber layer (pRNFL), containing unmyelinated axons, and the ganglion cell layer, containing their cell bodies, reflect neuroaxonal atrophy as a consequence of retrograde neurodegeneration, the inner nuclear layer (INL) is associated with inflammation manifesting in thickening and edema (31, 34–40). The ganglion cell layer is usually—due to similar contrast on OCT images—analyzed in combination with the inner plexiform layer (GCIP). RNFL and GCIP changes are found even during early stages of MS and occur also in absence of a history of optic neuritis (ON) (8, 41–44). Response to DMT is reflected by decreased rates of GCIP thinning (45) and thinning of INL in RRMS patients (46). A recent study has shown faster retinal thinning—also compared to RRMS patients and no effect of DMT on thinning rates in progressive MS (47). The study has been discussed controversially (48).

The SUPREMES study (Sunphenon in progressive forms of multiple sclerosis) was a phase 2 monocentric, prospective, randomized double-blind placebo-controlled pilot study to evaluate the effect of EGCG/Sunphenon on brain atrophy in MRI over a period of 36 months in patients with primary and secondary progressive multiple sclerosis (NCT00799890). The primary results of the SUPREMES study have been published elsewhere (49). OCT parameters were assessed as secondary and exploratory outcomes. The aim of our study was to evaluate the impact of EGCG on longitudinal retinal component changes in patients with progressive MS.

MATERIALS AND METHODS

Patients and Study Design

In total, 61 patients were randomized to the SUPREMES trial (NCT00799890) at the NeuroCure Clinical Research Center (NCRC) at Charité—Universitätsmedizin Berlin, Germany. Inclusion and exclusion criteria, randomization, blinding process and primary and secondary endpoints are described in detail elsewhere (49). Primary outcome parameter of the main study was brain atrophy detected as the difference between brain parenchymal fraction after 36 months compared to baseline. Inclusion criteria were age between 18 and 65 years, diagnosis of primary progressive or secondary progressive multiple sclerosis according to the McDonald criteria version 2005 (50), expanded disability status scale (EDSS)

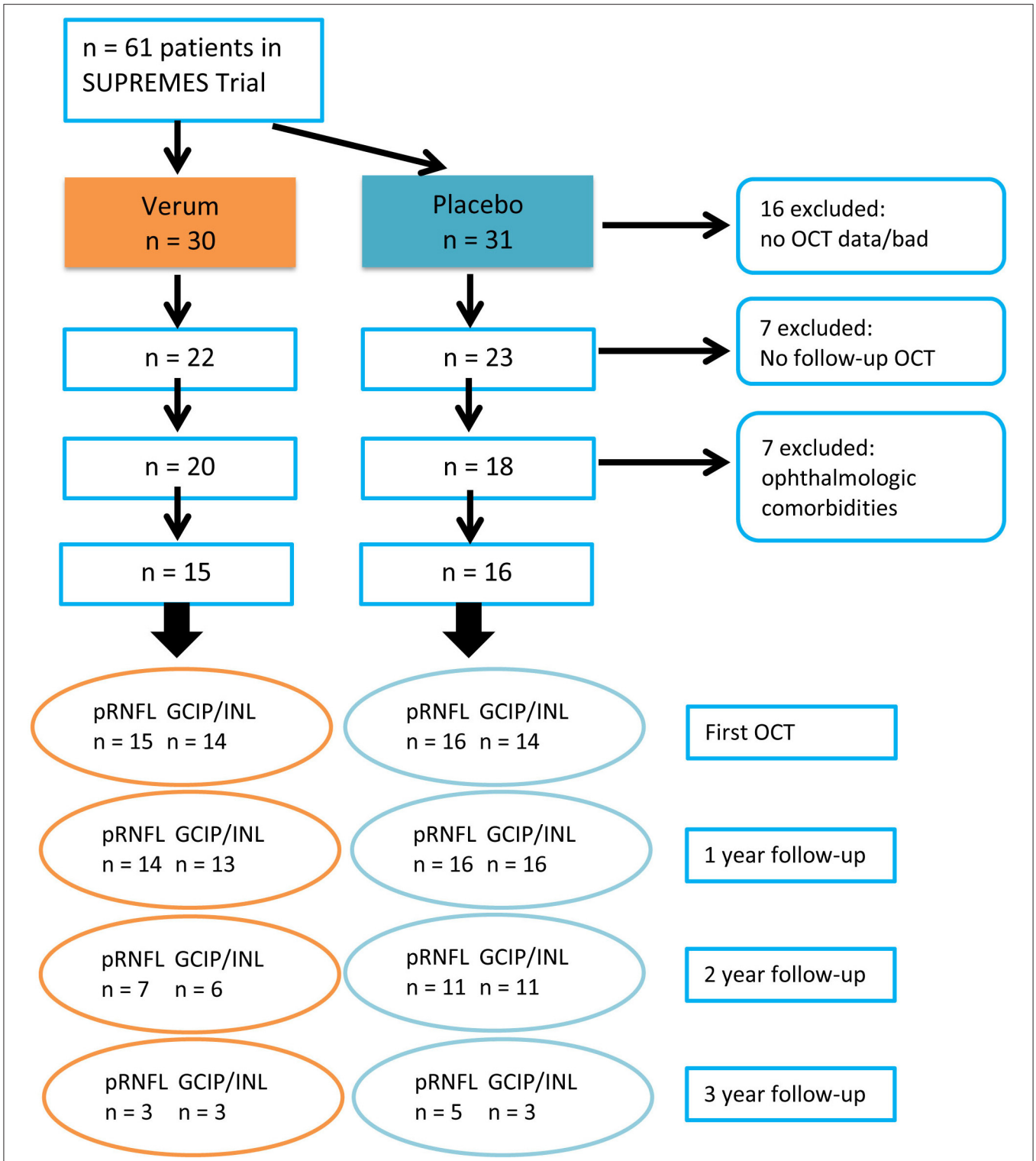

FIGURE 1 | CONSORT chart describing the enrolment process of OCT analysis and case numbers at each year of follow-up. PMS, progressive MS; OCT, Optical coherence tomography; pRNFL, peripapillary retinal nerve fiber layer; GCIP, ganglion cell and inner plexiform layer; INL, inner nuclear layer.

TABLE 1 | Baseline cohort description.

n		EGCG 15	Placebo 16	*p*
Age [years]		50.8 ± 8.4	50.7 ± 6.9	0.968
Sex female [*n* (%)]		5 (33.3)	7 (43.8)	0.821
Diagnosis	**PPMS [*n* (%)]**	6 (40.0)	6 (37.5)	>0.999
	SPMS [*n* (%)]	9 (60.0)	10 (62.5)	
Disease duration [years] (median, [IQR])		13.69 [8.90, 29.41]	12.12 [7.47, 20.17]	0.406
EDSS (median, IQR)		6.00 [4.00, 6.50]	5.75 [4.00, 6.00]	0.138
Time on trial at OCT baseline (median, IQR) [years]		1.06 [0.00, 1.50]	1.04 [0.00, 1.53]	0.919
Follow-up duration (median, IQR) [years]		1.47 [1.27, 2.01]	1.95 [1.47, 2.90]	0.213

Abbreviations: EGCG: epigallocatechin-gallate, SPMS: secondary progressive multiple sclerosis, PPMS: primary progressive multiple sclerosis, EDSS: Expanded disability status scale, IQR: interquartile range, OCT: optical coherence tomography.

TABLE 2 | First OCT measurements.

	EGCG		Placebo		EGCG vs. placebo
	Mean ± SD	**RTE**	**Mean ± SD**	**RTE**	***p***
pRNFL/μm	87.3 ± 11.1	0.554	82.9 ± 11.4	0.450	0.297
GCIP/μm	65.4 ± 7.4	0.609	59.9 ± 6.1	0.381	0.024
INL/μm	37.8 ± 2.2	0.599	36.1 ± 2.3	0.392	0.049

Test statistics from "nonparametric analysis of longitudinal data" of first examination OCT data. EGCG, epigallocatechin-gallate; CI, confidence interval; RTE, Relative treatment effect; pRNFL, peripapillary retinal nerve fiber layer; GCIP, ganglion cell and inner plexiform layer; INL, inner nuclear layer.

(51) between 3.0 and 8.0 and at least 30 days between the last exacerbation and study screening. Exclusion criteria were treatment with any immunomodulatory or immunosuppressive drugs, with exception of methylprednisolone up to 3 months before screening. Regarding OCT, pRNFL was a secondary outcome parameter; GCIP and INL were analyzed as exploratory endpoints. For inclusion in the analysis of OCT, ophthalmological diseases such as glaucoma, recurrent iritis, myopia <-5 dpt were considered as additional exclusion criteria. As for many patients OCT scanning was not available in the beginning, we only included patients to the OCT analysis who had at least one follow-up OCT at least 6 months from baseline OCT.

Study Medication

Patients in the treatment arm started treatment with one capsule containing Sunphenon 200 mg/day and placebo patients received identical capsules without active component. After 3 months, participants received two capsules per day of either EGCG or placebo medication. After 6 months, the medication increased to 600 mg/day, after 18 months to 800 mg/day and after 30 months they received the full amount of 1,200 mg/day.

Ethics

The SUPREMES trial was approved by the local ethics committee (LaGeSo ZS EK 10 407/08, new: 08/0407-EK 15) and by the German Federal Institute for Drugs and Medical Devices (BfArM). The trial is registered with EudraCT (2008-005213-22) and clinicaltrials.gov (NCT00799890) and was conducted in accordance with the current version of the Declaration of Helsinki and the applicable German law. All subjects provided written informed consent prior to enrolment.

Optical Coherence Tomography

Patients underwent spectral domain OCT (Spectralis SD-OCT; Heidelberg Engineering, Heidelberg, Germany) with the Eye Explorer 1.9.10.0 and automatic real-time (ART) image averaging. pRNFL was calculated from a standard ring scan around the optic nerve head (12°, 1536 A-scans, $16 \leq \text{ART} \leq 100$) using segmentation by the device's software with viewing module 6.0.14.0. A macular volume scan (25° × 30°, 61 B-scans, 768 A-scans per B-scan, $12 \leq \text{ART} \leq 15$) was acquired for intraretinal segmentation of GCIP and INL. Segmentation of macular scans was performed with SAMIRIX (52). All OCT scans were revised for retinal changes unrelated to MS, sufficient quality (53, 54), segmentation errors and were manually corrected by a blinded experienced grader if necessary. OCT methods are reported in line with the APOSTEL criteria (55).

Statistical Methods

Cohort baseline differences with subject reference in numerical variables were either given as mean ± standard deviation and analyzed with *t*-test, or as median and interquartile range (IQR) and analyzed with Wilcoxon rank-sum test, while Chi-Square test was applied for categorical variables. Due to overall low sample size and high number of missing data (**Figure 1**) we tested the OCT first examination and the longitudinal main hypothesis with "nonparametric analysis of longitudinal data in factorial experiments" as implemented in the R package nparLD (56). We modeled first OCT examination within an F1-LD-F1 design and used the ANOVA-Type test with treatment arm as whole-plot factor and eye as sub-plot factor for inference. We performed longitudinal analysis within the F1-LD-F2 experimental design with one whole-plot factor and two sub-plot factors, where the second sub-plot factor is the stratification of the first. Using this design, we used treatment group as whole-plot factor, time

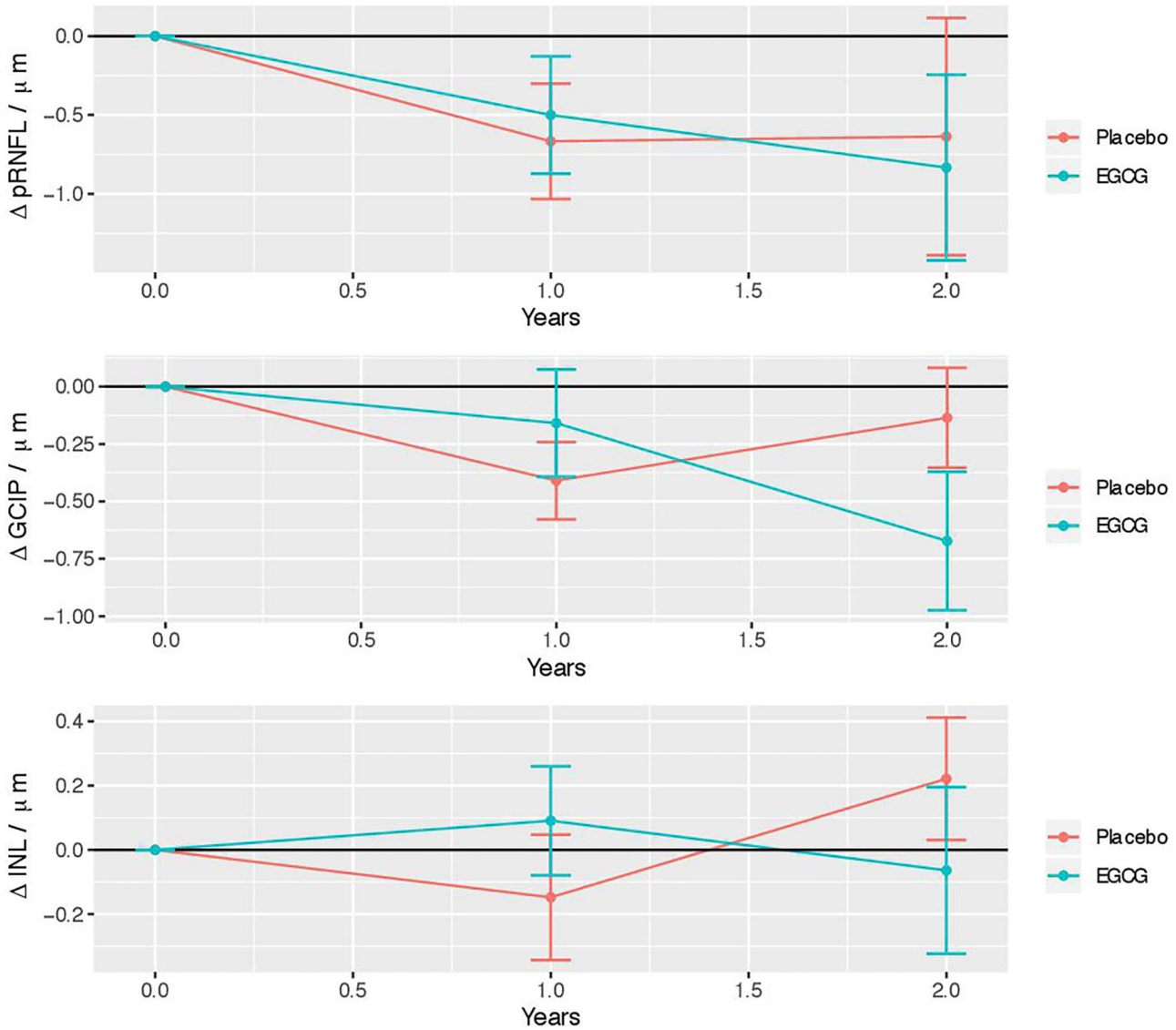

FIGURE 2 | Longitudinal retinal layer changes in the EGCG treated and placebo group. Error bars indicate the standard error to the mean. EGCG, epigallocatechin-gallate; pRNFL, peripapillary retinal nerve fiber layer; GCIP, ganglion cell and inner plexiform layer; INL, inner nuclear layer.

as the first subplot factor, and eye as the second to account for two eye measurements per patient at each time point. We excluded three-year follow up because of potential bias resulting from missing data. The main question was whether the time profiles of the two groups were parallel or diverging, i.e., if there exists a statistical interaction between treatment group and time after 2 year follow up, which would indicate an effect of EGCG on OCT changes over time. The effect size is represented by the relative marginal treatment effect (RTE), indicating whether data tend to be smaller/larger under respective factor level combinations. The analysis set included missing values as described in the flow chart (**Figure 1**). In this data set we rounded follow-up time to full years in order to use time as a categorical variable. To confirm our findings, changes in OCT parameters were estimated with linear mixed models (LMM) using the formula: OCT value ∼ group*time from baseline + (1 + time from baseline|patient/eye). In LMM, all sessions were considered including time since baseline as a continuous variable. No corrections for multiple comparisons were performed for this exploratory outcome analysis. Statistical analyses were performed with R (57) version 3.6.2 with packages nparLD (56), lme4, lmertest, tidyverse, tableone, ggplot2, beeswarm, ggplot, RMisc. Statistical significance was established at $p < 0.05$.

RESULTS

Cohort Description

Sixty-one patients with progressive MS were randomized in the SUPREMES trial to receive either EGCG treatment or placebo. From these patients, we had to exclude 16 patients because of

TABLE 3 | Longitudinal OCT changes in treatment arms—nonparametric analysis.

	EGCG		Placebo		EGCG vs. Placebo
	Mean change [CI]/μm	RTE treatment:time	Mean change [CI]/μm	RTE treatment:time	*p*
pRNFL/μm	−0.83 [1.29]	0.331	−0.64 [1.56]	0.492	0.156
GCIP/μm	−0.67 [0.67]	0.360	−0.14 [0.47]	0.429	0.476
INL/μm	−0.06 [0.58]	0.504	0.22 [0.41]	0.635	0.455

All results for the 2-year follow-up visit. Test statistics from "nonparametric analysis of longitudinal data." EGCG, epigallocatechin-gallate; RTE, Relative treatment effect; pRNFL, peripapillary retinal nerve fiber layer; GCIP, ganglion cell and inner plexiform layer; INL, inner nuclear layer.

TABLE 4 | Longitudinal OCT changes in treatment arms—linear mixed models.

		B	SE	*p*	Lower CI	Upper CI	R^2m	R^2c
pRNFL	Treatment EGCG	3.194	4.014	0.433	−4.673	11.062	0.032	0.982
	Time	−0.788	0.306	0.018	−1.387	−0.189		
	Treatment EGCG:Time	0.766	0.463	0.111	−0.140	1.673		
GCIP	Treatment EGCG	4.389	2.432	0.082	−0.379	9.156	0.092	0.994
	Time	−0.221	0.111	0.068	−0.439	0.003		
	Treatment EGCG:Time	0.0138	0.160	0.933	−0.300	0.327		
INL	Treatment EGCG	1.866	0.838	0.034	0.223	3.509	0.136	0.956
	Time	−0.075	0.084	0.374	−0.240	0.089		
	Treatment EGCG:Time	0.064	0.119	0.589	−0.168	0.297		

All result for the maximum available follow-up time (continuous) under treatment. Test statistics from linear mixed models. B, non-standardized correlation coefficient; SE, standard error; CI, 95% confidence interval; R^2m, Marginal R^2; R^2c, Conditional R^2; pRNFL, peripapillary retinal nerve fiber layer; GCIP, ganglion cell and inner plexiform layer; INL, inner nuclear layer.

missing OCT data. From the 45 patients with OCT data, seven patients had no follow-up OCT data, and 7 patients had to be excluded due to ophthalmological diseases such as glaucoma, recurrent iritis, and myopia <-5 dpt. Thus, 31 patients were included in analysis. The inclusion process is detailed in **Figure 1**. Moreover, from 2 patients (1 EGCG, 1 placebo), one eye was excluded from all analyses because of unilateral retinopathy. Two pRNFL scans from 2 patients (both EGCG) and 34 macular scans from 28 sessions of 20 patients (8 EGCG, 12 placebo) failed the OSCAR-IB quality criteria and had to be excluded (53, 54).

Baseline OCT Findings

Baseline cohort details are described in **Table 1**. Patients had their first OCT examination median 1.05 (interquartile range 0.00–1.52) years after randomization. The OCT cohort comprised 15 patients from the treatment and 16 patients from the placebo group. There were no significant differences in age, sex, time since disease onset, EDSS, time in the trial, and follow-up duration between treatment and placebo groups (**Table 1**). Patients in the EGCG treated arm had thicker GCIP, INL, and—though not significant—pRNFL (**Table 2**).

Longitudinal OCT Results

Figure 2 illustrates changes over time in the EGCG treated and Placebo group. **Table 3** depicts changes over time separately for the treatment and the placebo arms and their statistical comparison from non-parametric longitudinal data analysis. There was no significant interaction of treatment and time for any parameter. **Table 4** includes results from LMMs, as well not detecting any significant differences in change over time between ECGC and placebo group.

DISCUSSION

In this study, we performed an analysis of OCT data as secondary (pRNFL) and exploratory (GCIP, INL) outcomes in the SUPREMES trial. Specifically, we investigated differences in retinal thickness changes over time between patients treated with EGCG vs. placebo. We found no difference between the treatment groups.

These results support the findings in the analysis of the primary and secondary outcome parameters of the SUPREMES trial: no evidence for treatment was found on brain atrophy, lesion load, and clinical scores (49). The primary outcome parameter of the SUPREMES trial was brain atrophy, a commonly used outcome for neuroprotective trials in MS (58). While brain atrophy measurement is widely established, retinal thickness analysis has been included as an additional outcome as the use of brain atrophy is not without challenge: a reduction of acute swelling by a potent anti-inflammatory intervention may lead to the phenomenon of "pseudoatrophy," which is referred to as decreased brain volume due to the resolution of edema and inflammation after treatment (59, 60). Furthermore, as our cohort had an average age of 50 years, treatment effects on brain atrophy may be confounded by non-linear aging effects (61).

In contrast, retinal thickness measurements are less prone to aging (52). Furthermore, GCIP is not prone to swelling (62), whereas a subtle swelling of pRNFL outside of acute ON has not been reported so far. While they may be inferior to brain atrophy at face value, GCIP and pRNFL may be superior for detecting neuroprotective effects due to a lack of pseudoatrophy. Nevertheless, we did not find a significantly reduced atrophy of pRNFL and GCIP in the EGCG group.

While pRNFL and GCIP thinning reflect neuroaxonal damage, the INL is considered a marker of inflammation. Treatment response is considered to be associated with INL thinning (46). However, the INL is also subject to atrophy as indicated by thinning in a large progressive MS study (47). In our study, the INL showed no overall thickness changes. This suggests that either no time-dependent change occur, or that both atrophy and inflammation occur in our cohort, masking a treatment-associated thinning.

Other clinical trials also failed to show a treatment effect of EGCG: The SUNIMS trial (63) reported no treatment effect of EGCG on clinical or MRI measures in RRMS patients. Moreover, a recently published study demonstrated no impact of EGCG after 48 weeks of treatment on disease progression in multiple system atrophy (64). A potential reason for the failure of EGCG in clinical trials could be the lower bioavailability of oral EGCG than previously assumed (65, 66).

Several limitations may impact our results. First, the low sample size of our cohort. A previous study estimated that the sample size for a progressive MS trial on neuroprotective agents should be at least $n = 173$ for pRNFL and $n = 125$ for GCIP per trial arm for a 3-year study (power 80%, effect size 50%), numbers way larger than achieved in this exploratory outcome analysis (47).

Another weakness is that treatment and placebo groups were not well-matched regarding baseline OCT, with a significantly thicker GCIP and INL in the treatment group. In our non-parametric analysis, we used the change of retinal parameters as outcome and the linear mixed models we computed additionally consider the individual intercept at baseline. Thus, we assume that the differences at OCT baseline had no influence on the longitudinal analysis.

To date, there are few studies applying OCT as an outcome parameter in clinical trials of MS. To the best of our knowledge, there is no published prospective interventional study that applied OCT as outcome parameter in trials in the progressive forms of the disease. While OCT detected differences in retinal thickness change between different treatment groups in RRMS (45), it is possible that the retina of SPMS and PPMS patients are less responsive to treatment. Another aspect is the high frequency of primary eye disorders in a usually elder progressive MS population. In our study, almost 20% of patients needed to be excluded due to eye comorbidities. Furthermore, due to increased disability, progressive MS patients are often less compliant with the OCT examination, leading to a high number of noise or cut-off scans failing the quality control. While this does not preclude OCT as endpoint from clinical trials in progressive MS, it suggests that careful ophthalmological examination for comorbidities and rigorous quality control of OCT scans are of paramount importance. A recent retrospective study showed a decreased macular RNFL thinning associated with 4-aminopyridine treatment in a mixed cohort of RRMS and progressive MS patients (67). These and our results encourage the further evaluation of OCT measurements as outcome parameters in clinical trials of progressive MS.

To conclude, our study shows no effect over time of EGCG on pRNFL, GCIP, or INL. As such, our study does not provide sufficient evidence for a neuroprotective effect of EGCG on retinal thickness in patients with SPMS and PPMS. While this is in line with the outcomes of the main SUPREMES trial, our study was probably underpowered to detect a treatment effect.

DATA AVAILABILITY STATEMENT

The raw data supporting the conclusions of this article will be made available upon request to the corresponding author to any qualified researcher.

ETHICS STATEMENT

The studies involving human participants were reviewed and approved by The SUPREMES trial was approved by the local ethics committee (LaGeSo ZS EK 10 407/08, new: 08/0407-EK 15) and by the German Federal Institute for Drugs and Medical Devices (BfArM). The trial is registered with EudraCT (2008-005213-22) and clinicaltrials.gov (NCT00799890). The patients/participants provided their written informed consent to participate in this study. Written informed consent was obtained from the individual(s) for the publication of any potentially identifiable images or data included in this article.

AUTHOR CONTRIBUTIONS

KK drafting/revising the manuscript, analyzed and interpreted the data, and acquisition of data. RR acquisition of data, interpreted the data, and revised the manuscript for intellectual content. JD, FP, and JB-S study concept, acquisition of data, and revised the manuscript for intellectual content. FK analyzed and interpreted the data, statistical analysis, and revised the manuscript for intellectual content. AB study concept, analyzed and interpreted the data, statistical analysis, and drafting/revising the manuscript. HZ study concept, acquisition of data, analyzed and interpreted the data, statistical analysis, and drafting/revised the manuscript for intellectual content. All authors contributed to the article and approved the submitted version.

FUNDING

This study was partially funded by Taiyo International that supplied the study medication and German Research Council (DFG Exc 257 to FP). The sponsor of the study was Charité—Universitätsmedizin Berlin. Neither funding source nor sponsor was involved in the study design, data collection, analysis or interpretation, in writing or in the decision to submit the manuscript.

REFERENCES

1. Reich DS, Lucchinetti CF, Calabresi PA. Multiple sclerosis. *N Engl J Med.* (2018) 378:169–80. doi: 10.1056/NEJMra1401483
2. Ransohoff RM, Hafler DA, Lucchinetti CF. Multiple sclerosis-a quiet revolution. *Nat Rev Neurol.* (2016) 11:134–42. doi: 10.1038/nrneurol.2015.14
3. Weinshenker BG, Bass B, Rice GPA, Noseworthy J, Carriere W, Baskerville J, et al. The natural history of multiple sclerosis: a geographically based study: I. Clinical course and disability. *Brain.* (1989) 112:133–46. doi: 10.1093/brain/112.1.133
4. Krieger SC, Cook K, de Nino S, Fletcher M. The topographical model of multiple sclerosis: a dynamic visualization of disease course. *Neurol Neuroimmunol NeuroInflammation.* (2016) 3:e279. doi: 10.1212/NXI.0000000000000279
5. Faissner S, Plemel JR, Gold R, Yong VW. Progressive multiple sclerosis: from pathophysiology to therapeutic strategies. *Nat Rev Drug Discov.* (2019) 18:905–22. doi: 10.1038/s41573-019-0035-2
6. Miller DH, Leary SM. Primary-progressive multiple sclerosis. *Lancet Neurol.* (2007) 6:903–12. doi: 10.1016/S1474-4422(07)70243-0
7. Trapp BD, Nave K-A. Multiple sclerosis: an immune or neurodegenerative disorder? *Annu Rev Neurosci.* (2008) 31:247–69. doi: 10.1146/annurev.neuro.30.051606.094313
8. Oberwahrenbrock T, Ringelstein M, Jentschke S, Deuschle K, Klumbies K, Bellmann-Strobl J, et al. Retinal ganglion cell and inner plexiform layer thinning in clinically isolated syndrome. *Mult Scler J.* (2013) 19:1887–95. doi: 10.1177/1352458513489757
9. Azevedo CJ, Overton E, Khadka S, Buckley J, Liu S, Sampat M, et al. Early CNS neurodegeneration in radiologically isolated syndrome. *Neurol Neuroimmunol NeuroInflammation.* (2015) 2:e102. doi: 10.1212/NXI.0000000000000102
10. Kuchling J, Paul F. Visualizing the central nervous system: imaging tools for multiple sclerosis and neuromyelitis optica spectrum disorders. *Front Neurol.* (2020) 11:450. doi: 10.3389/fneur.2020.00450
11. Wingerchuk DM, Weinshenker BG. Disease modifying therapies for relapsing multiple sclerosis. *BMJ.* (2016) 354:i3518. doi: 10.1136/bmj.i3518
12. Montalban X, Hauser SL, Kappos L, Arnold DL, Bar-Or A, Comi G, et al. Ocrelizumab versus placebo in primary progressive multiple sclerosis. *N Engl J Med.* (2017) 376:209–20. doi: 10.1056/NEJMoa1606468
13. Ontaneda D, Fox RJ, Chataway J. Clinical trials in progressive multiple sclerosis: lessons learned and future perspectives. *Lancet Neurol.* (2015) 14:208–23. doi: 10.1016/S1474-4422(14)70264-9
14. Sato T, Miyata G. The nutraceutical benefit, part I: green tea. *Nutrition.* (2000) 16:315–7. doi: 10.1016/S0899-9007(99)00301-9
15. Bogdanski P, Suliburska J, Szulinska M, Stepien M, Pupek-Musialik D, Jablecka A. Green tea extract reduces blood pressure, inflammatory biomarkers, and oxidative stress and improves parameters associated with insulin resistance in obese, hypertensive patients. *Nutr Res.* (2012) 32:421–7. doi: 10.1016/j.nutres.2012.05.007
16. Syarifah-Noratiqah S-B, Naina-Mohamed I, Zulfarina MS, Qodriyah HM. Natural polyphenols in the treatment of Alzheimer's disease. *Curr Drug Targets.* (2017) 19:927–37. doi: 10.2174/1389450118666170328122527
17. Mähler A, Mandel S, Lorenz M, Ruegg U, Wanker EE, Boschmann M, et al. Epigallocatechin-3-gallate: a useful, effective and safe clinical approach for targeted prevention and individualised treatment of neurological diseases? *EPMA J.* (2013) 4:1–17. doi: 10.1186/1878-5085-4-5
18. Ashihara H, Deng WW, Mullen W, Crozier A. Distribution and biosynthesis of flavan-3-ols in *Camellia sinensis* seedlings and expression of genes encoding biosynthetic enzymes. *Phytochemistry.* (2010) 71:559–66. doi: 10.1016/j.phytochem.2010.01.010
19. Wu D, Wang J, Pae M, Meydani SN. Green tea EGCG, T cells, and T cell-mediated autoimmune diseases. *Mol Aspects Med.* (2012) 33:107–18. doi: 10.1016/j.mam.2011.10.001
20. Pae M, Wu D. Immunomodulating effects of epigallocatechin-3-gallate from green tea: Mechanisms and applications. *Food Funct.* (2013) 4:1287–303. doi: 10.1039/c3fo60076a
21. Wu D. Green tea EGCG, T-cell function, and T-cell-mediated autoimmune encephalomyelitis. *J Investig Med.* (2016) 64:1213–9. doi: 10.1136/jim-2016-000158
22. Aktas O, Prozorovski T, Smorodchenko A, Savaskan NE, Lauster R, Kloetzel P-M, et al. Green tea epigallocatechin-3-gallate mediates T cellular NF-κB inhibition and exerts neuroprotection in autoimmune encephalomyelitis. *J Immunol.* (2004) 173:5794–800. doi: 10.4049/jimmunol.173.9.5794
23. Wang J, Ren Z, Xu Y, Xiao S, Meydani SN, Wu D. Epigallocatechin-3-gallate ameliorates experimental autoimmune encephalomyelitis by altering balance among CD4 + T-cell subsets. *Am J Pathol.* (2012) 180:221–34. doi: 10.1016/j.ajpath.2011.09.007
24. Sun Q, Zheng Y, Zhang X. Novel immunoregulatory properties of EGCG on reducing inflammation in EAE. *Front Biosci.* (2013) 18:332–342. doi: 10.2741/4104
25. Herges K, Millward JM, Hentschel N, Infante-Duarte C, Aktas O, Zipp F. Neuroprotective effect of combination therapy of Glatiramer acetate and epigallocatechin-3-gallate in neuroinflammation. *PLoS One.* (2011) 6:e25456. doi: 10.1371/journal.pone.0025456
26. Mähler A, Steiniger J, Bock M, Klug L, Parreidt N, Lorenz M, et al. Metabolic response to epigallocatechin-3-gallate in relapsing-remitting multiple sclerosis: a randomized clinical trial. *Am J Clin Nutr.* (2015) 101:487–95. doi: 10.3945/ajcn.113.075309
27. de la Torre R, de Sola S, Hernandez G, Farré M, Pujol J, Rodriguez J, et al. Safety and efficacy of cognitive training plus epigallocatechin-3-gallate in young adults with Down's syndrome (TESDAD): a double-blind, randomised, placebo-controlled, phase 2 trial. *Lancet Neurol.* (2016) 15:801–10. doi: 10.1016/S1474-4422(16)30034-5
28. de la Torre R, de Sola S, Farré M, Xicota L, Cuenca-Royo A, Rodriguez J, et al. A phase 1, randomized double-blind, placebo controlled trial to evaluate safety and efficacy of epigallocatechin-3-gallate and cognitive training in adults with Fragile X syndrome. *Clin Nutr.* (2020) 39:378–87. doi: 10.1016/j.clnu.2019.02.028
29. Oberwahrenbrock T, Traber GL, Lukas S, Gabilondo I, Nolan R, Songster C, et al. Multicenter reliability of semiautomatic retinal layer segmentation using OCT. *Neurol Neuroimmunol Neuroinflammation.* (2018) 5:e449. doi: 10.1212/NXI.0000000000000449
30. Nolan-Kenney RC, Liu M, Akhand O, Calabresi PA, Paul F, Petzold A, et al. Optimal intereye difference thresholds by optical coherence tomography in multiple sclerosis: an international study. *Ann Neurol.* (2019) 85:618–29. doi: 10.1002/ana.25462
31. Petzold A, Balcer LJ, Calabresi PA, Costello F, Frohman TC, Frohman EM, et al. Retinal layer segmentation in multiple sclerosis: a systematic review and meta-analysis. *Lancet Neurol.* (2017) 16:797–812. doi: 10.1016/S1474-4422(17)30278-8
32. Oertel FC, Zimmermann HG, Brandt AU, Paul F. Novel uses of retinal imaging with optical coherence tomography in multiple sclerosis. *Expert Rev Neurother.* (2019) 19:31–43. doi: 10.1080/14737175.2019.1559051
33. Zimmermann HG, Knier B, Oberwahrenbrock T, Behrens J, Pfuhl C, Aly L, et al. Association of retinal ganglion cell layer thickness with future disease activity in patients with clinically isolated syndrome. *JAMA Neurol.* (2018) 75:1071–9. doi: 10.1001/jamaneurol.2018.1011
34. Costello F, Hodge W, Pan YI, Eggenberger E, Freedman MS. Using retinal architecture to help characterize multiple sclerosis patients. *Can J Ophthalmol J Can dophtalmologie.* (2010) 45:520–6. doi: 10.3129/i10-063
35. Wicki CA, Hanson JVM, Schippling S. Optical coherence tomography as a means to characterize visual pathway involvement in multiple sclerosis. *Curr Opin Neurol.* (2018) 31:662–8. doi: 10.1097/WCO.0000000000000604
36. Kaufhold F, Zimmermann H, Schneider E, Ruprecht K, Paul F, Oberwahrenbrock T, et al. Optic neuritis is associated with inner nuclear layer thickening and microcystic macular edema independently of multiple sclerosis. *PLoS One.* (2013) 8:e71145. doi: 10.1371/journal.pone.0071145
37. Gelfand JM, Nolan R, Schwartz DM, Graves J, Green AJ. Microcystic macular oedema in multiple sclerosis is associated with disease severity. *Brain.* (2012) 135:1786–93. doi: 10.1093/brain/aws098
38. Saidha S, Sotirchos ES, Ibrahim M a., Crainiceanu CM, Gelfand JM, Sepah YJ, et al., Newsome SD, et al. Microcystic macular oedema, thickness of the inner nuclear layer of the retina, and disease characteristics in multiple sclerosis: a retrospective study. *Lancet Neurol.* (2012) 11:963–72. doi: 10.1016/S1474-4422(12)70213-2
39. Balk LJ, Coric D, Knier B, Zimmermann HG, Behbehani R, Alroughani R, et al. Retinal inner nuclear layer volume reflects inflammatory disease activity in multiple sclerosis; a longitudinal OCT study. *Mult Scler.* (2019) 5:1–11. doi: 10.1177/2055217319871582
40. Brandt AU, Oberwahrenbrock T, Kadas EM, Lagrèze WA, Paul F. Dynamic formation of macular microcysts independent of vitreous

traction changes. *Neurology.* (2014) 83:73–7. doi: 10.1212/WNL.0000000000000545
41. Green AJ, McQuaid S, Hauser SL, Allen I V., Lyness R. Ocular pathology in multiple sclerosis: Retinal atrophy and inflammation irrespective of disease duration. *Brain.* (2010) 133:1591–601. doi: 10.1093/brain/awq080
42. Balk LJ, Cruz-Herranz A, Albrecht P, Arnow S, Gelfand JM, Tewarie P, et al. Timing of retinal neuronal and axonal loss in MS: a longitudinal OCT study. *J Neurol.* (2016) 263:1323–31. doi: 10.1007/s00415-016-8127-y
43. Oberwahrenbrock T, Schippling S, Ringelstein M, Kaufhold F, Zimmermann H, Keser N, et al. Retinal damage in multiple sclerosis disease subtypes measured by high-resolution optical coherence tomography. *Mult Scler Int.* (2012) 2012:530305. doi: 10.1155/2012/530305
44. Gelfand JM, Goodin DS, Boscardin WJ, Nolan R, Cuneo A, Green AJ. Retinal axonal loss begins early in the course of multiple sclerosis and is similar between progressive phenotypes. *PLoS One.* (2012) 7:e36847. doi: 10.1371/journal.pone.0036847
45. Button J, Al-Louzi O, Lang A, Bhargava P, Newsome SD, Frohman T, et al. Disease-modifying therapies modulate retinal atrophy in multiple sclerosis: a retrospective study. *Neurology.* (2017) 88:525–2. doi: 10.1212/WNL.0000000000003582
46. Knier B, Schmidt P, Aly L, Buck D, Berthele A, Mühlau M, et al. Retinal inner nuclear layer volume reflects response to immunotherapy in multiple sclerosis. *Brain.* (2016) 139:2855–63. doi: 10.1093/brain/aww219
47. Sotirchos ES, Gonzalez Caldito N, Filippatou A, Fitzgerald KC, Murphy OC, Lambe J, et al. Progressive multiple sclerosis is associated with faster and specific retinal layer atrophy. *Ann Neurol.* (2020) 87:885–96. doi: 10.1002/ana.25738
48. Cordano C, Yiu HH, Oertel FC, Gelfand JM, Hauser SL, Cree BAC, et al. Retinal INL Thickness in multiple sclerosis: a mere marker of neurodegeneration? *Ann Neurol.* (2021) 89:192–3. doi: 10.1002/ana.25933
49. Rust R, Chien C, Scheel M, Brandt AU, Dörr J, Wuerfel J, et al. Epigallocatechin gallate in progressive MS: a randomized, placebo-controlled trial. *Neurol Neuroimmunol NeuroInflammation*. (2020) 8:e964. doi: 10.1212/NXI.0000000000000964
50. Polman CH, Reingold SC, Edan G, Filippi M, Hartung H-P, Kappos L, et al. Diagnostic criteria for multiple sclerosis: 2005 revisions to the "McDonald Criteria." *Ann Neurol.* (2005) 58:840–6. doi: 10.1002/ana.20703
51. Kurtzke JF. Rating neurologic impairment in multiple sclerosis: an expanded disability status scale (EDSS). *Neurology.* (1983) 33:1444–52. doi: 10.1212/WNL.33.11.1444
52. Motamedi S, Gawlik K, Ayadi N, Zimmermann HG, Asseyer S, Bereuter C, et al. Normative data and minimally detectable change for inner retinal layer thicknesses using a semi-automated OCT image segmentation pipeline. *Front Neurol.* (2019) 10:1117. doi: 10.3389/fneur.2019.01117
53. Tewarie P, Balk L, Costello F, Green A, Martin R, Schippling S, et al. The OSCAR-IB consensus criteria for retinal OCT quality assessment. *PLoS One.* (2012) 7:e34823. doi: 10.1371/journal.pone.0034823
54. Schippling S, Balk LJ, Costello F, Albrecht P, Balcer L, Calabresi PA, et al. Quality control for retinal OCT in multiple sclerosis: validation of the OSCAR-IB criteria. *Mult Scler J.* (2015) 21:163–70. doi: 10.1177/1352458514538110
55. Cruz-Herranz A, Balk LJ, Oberwahrenbrock T, Saidha S, Martinez-Lapiscina EH, Lagreze WA, et al. The APOSTEL recommendations for reporting quantitative optical coherence tomography studies. *Neurology.* (2016) 86:2303–9. doi: 10.1212/WNL.0000000000002774
56. Noguchi K, Gel YR, Brunner E, Konietschke F. nparLD : an R Software Package for the nonparametric analysis of longitudinal data in factorial experiments. *J Stat Softw.* (2012) 50:1–23. doi: 10.18637/jss.v050.i12
57. R Core Team. *R: A Language and Environment for Statistical Computing* (2014).
58. Moccia M, de Stefano N, Barkhof F. Imaging outcome measures for progressive multiple sclerosis trials. *Mult Scler.* (2017) 23:1614–26. doi: 10.1177/1352458517729456
59. De Stefano N, Arnold DL. Towards a better understanding of pseudoatrophy in the brain of multiple sclerosis patients. *Mult Scler.* (2015) 21:675–6. doi: 10.1177/1352458514564494
60. Vidal-Jordana A, Sastre-Garriga J, Pérez-Miralles F, Tur C, Tintoré M, Horga A, et al. Early brain pseudoatrophy while on natalizumab therapy is due to white matter volume changes. *Mult Scler J.* (2013) 19:1175–81. doi: 10.1177/1352458512473190
61. Azevedo CJ, Cen SY, Jaberzadeh A, Zheng L, Hauser SL, Pelletier D. Contribution of normal aging to brain atrophy in MS. *Neurol Neuroimmunol neuroinflammation.* (2019) 6:e616. doi: 10.1212/NXI.0000000000000616
62. Syc SB, Saidha S, Newsome SD, Ratchford JN, Levy M, Ford E, et al. Optical coherence tomography segmentation reveals ganglion cell layer pathology after optic neuritis. *Brain.* (2012) 135:521–33. doi: 10.1093/brain/awr264
63. Bellmann-Strobl J, Paul F, Wuerfel J, Dörr J, Infante-Duarte C, Heidrich E, et al. Epigallocatechin gallate in relapsing-remitting multiple sclerosis: a randomized, placebo-controlled trial. *Neurol Neuroimmunol NeuroInflammation*. (2021) 8:e981. doi: 10.1212/NXI.0000000000000981
64. Levin J, Maaß S, Schuberth M, Giese A, Oertel WH, Poewe W, et al. Safety and efficacy of epigallocatechin gallate in multiple system atrophy (PROMESA): a randomised, double-blind, placebo-controlled trial. *Lancet Neurol.* (2019) 18:724–35. doi: 10.1016/S1474-4422(19)30141-3
65. Ullmann U, Haller J, Decourt JD, Girault J, Spitzer V, Weber P. Plasma-kinetic characteristics of purified and isolated green tea catechin epigallocatechin gallate (EGCG) after 10 days repeated dosing in healthy volunteers. *Int J Vitam Nutr Res.* (2004) 74:269–78. doi: 10.1024/0300-9831.74.4.269
66. Chakrawarti L, Agrawal R, Dang S, Gupta S, Gabrani R. Therapeutic effects of EGCG: a patent review. *Expert Opin Ther Pat.* (2016) 26:907–16. doi: 10.1080/13543776.2016.1203419
67. Dietrich M, Koska V, Hecker C, Göttle P, Hilla AM, Heskamp A, et al. Protective effects of 4-aminopyridine in experimental optic neuritis and multiple sclerosis. *Brain.* (2020) 143:1127–42. doi: 10.1093/brain/awaa062

Conflict of Interest: RR received speaking honoraria from Roche. JD reports research support by Bayer and Novartis, honoraria for lectures and advisory by Bayer, Novartis, Sanofi-Aventis, Merck-Serono, Biogen and Roche and travel support by Bayer, Novartis, Biogen, and Merck-Serono. FP reports non-financial support from Taiyo International, grants from TEVA GmbH, other from German Research Council (DFG), during the conduct of the study; He serves on scientific advisory boards of Novartis's OCTIMS study steering committee and MedImmune/Viela Bio steering committee. He received funding for travel or speaker honoraria from Bayer, Novartis, Biogen Idec, Teva, Sanofi-Aventis/Genzyme, and Merck Serono, Alexion, Chugai, MedImmune, Shire, Roche, Actelion, Celgene and serves on editorial Boards at PLos ONE (academic editor) and Neurology Neuroimmunology and Neuroinflammation (Associate Editor). He provided consultancies for SanofiGenzyme, BiogenIdec, MedImmune, Shire, Alexion; He received research support from Bayer, Novartis, Biogen Idec, Teva, Sanofi-Aventis/Genzyme, Alexion and Merck Serono, German Research Council (DFG Exc 257), Werth Stiftung of the City of Cologne, German Ministry of Education and Research (BMBF Competence Network Multiple Sclerosis), Arthur Arnstein Stiftung Berlin, EU FP7 Framework Program (combims.eu) Guthy Jackson Charitable Foundation, and National Multiple Sclerosis Society of the USA. JB-S has received travel grants and speaking honoraria from Bayer Healthcare, Biogen Idec, Merck Serono, Sanofi Genzyme, Teva Pharmaceuticals, Roche, and Novartis all unrelated to this work. AB is cofounder and shareholder of technology startups Motognosis GmbH and Nocturne GmbH. He is named as inventor on several patent applications describing serum biomarkers for multiple sclerosis, perceptive computing for motor symptoms and retinal image analysis using optical coherence tomography. HZ received research grants from Novartis and speaking fees from Bayer, unrelated to this study.

The remaining authors declare that the research was conducted in the absence of any commercial or financial relationships that could be construed as a potential conflict of interest.

Copyright © 2021 Klumbies, Rust, Dörr, Konietschke, Paul, Bellmann-Strobl, Brandt and Zimmermann. This is an open-access article distributed under the terms of the Creative Commons Attribution License (CC BY). The use, distribution or reproduction in other forums is permitted, provided the original author(s) and the copyright owner(s) are credited and that the original publication in this journal is cited, in accordance with accepted academic practice. No use, distribution or reproduction is permitted which does not comply with these terms.

frontiers in Neurology

ORIGINAL RESEARCH
published: 04 May 2021
doi: 10.3389/fneur.2021.637932

Efficacy of Low-Dose Rituximab on Neuromyelitis Optica-Associated Optic Neuritis

Shuo Zhao[1], Huanfen Zhou[2], Quangang Xu[2], Hong Dai[1] and Shihui Wei[2]*

[1] Department of Ophthalmology, Beijing Hospital, National Center of Gerontology, Institute of Geriatric Medicine, Chinese Academy of Medical Sciences, Beijing, China, [2] Department of Neuro-Ophthalmology, The Chinese People's Liberation Army General Hospital, Beijing, China

Purpose: To prospectively investigate the efficacy and tolerance of low-dose rituximab (RTX) for the treatment of neuromyelitis optica-associated optic neuritis (NMO-ON).

Methods: Optic Neuritis patients with seropositive aquaporin 4-antibody (AQP4-Ab) were diagnosed with NMO-ON and recruited for treatment with low-dose RTX (100 mg * 4 infusions) and were then followed monthly for a minimum of 3 months. Reinfusion of 100 mg RTX was given when the CD19+ B lymphocyte frequency was elevated to above 1%. The serum AQP4-Ab level was tested by an enzyme-linked immunosorbent assay (ELISA).

Results: A total of 43 NMO-ON patients (1 male/42 female, 75 involved eyes) were included in this study. CD19+ B cell clearance in the peripheral blood was induced in 97.7% of patients after induction treatment. A significant decrease in serum AQP4-Ab concentration was observed after induction treatment ($P = 0.0123$). The maintenance time of B cell clearance was 5.2 ± 2.25 months. The relapse-free rate was 92.3% in patients followed-up for over 12 months, and patients with non-organ-specific autoimmune antibodies tended to relapse within 6 months. A total of 96.2% of patients had stable or improved vision, and a decrease in the average expanded disability status scale (EDSS) score was found. Structural alterations revealed by optic coherence tomography were observed in both ON and unaffected eyes. The rates of infusion-related reactions and long-term adverse events (AEs) were 18.6 and 23.1%, respectively. No severe AEs was observed.

Conclusions: Low-dose rituximab is efficient and well-tolerated in treating NMO-ON.

Keywords: neuromyelitis optica, optic neuritis, rituximab, immunosuppression, aquaporin 4 antibody

OPEN ACCESS

Edited by:
Ahmed Toosy,
University College London,
United Kingdom

Reviewed by:
Mark Paine,
Royal Brisbane and Women's Hospital, Australia
Friedemann Paul,
Charité – Universitätsmedizin Berlin, Germany
Jacqueline Palace,
Oxford University Hospitals NHS Trust, United Kingdom

***Correspondence:**
Quangang Xu
dr_xuquangang@163.com

Specialty section:
This article was submitted to Neuro-Ophthalmology, a section of the journal Frontiers in Neurology

Received: *04 December 2020*
Accepted: *08 April 2021*
Published: *04 May 2021*

Citation:
Zhao S, Zhou H, Xu Q, Dai H and Wei S (2021) Efficacy of Low-Dose Rituximab on Neuromyelitis Optica-Associated Optic Neuritis. Front. Neurol. 12:637932. doi: 10.3389/fneur.2021.637932

INTRODUCTION

Neuromyelitis optica-associated optic neuritis (NMO-ON) is an inflammatory autoimmune optic neuropathy with severe visual loss. Relapse may occur in 90% of NMO-ON patients, which may lead to poor visual outcome and can be accompanied by progressing neurological disability (1, 2). Therefore, the most critical management strategy in the remission phase of NMO-ON is to control clinical relapses, thereby improving the prognosis.

Neuromyelitis optica-associated optic neuritis is diagnosed with a positive serum aquaporin-4 antibody (AQP4-Ab), which targets the astrocytic water channel in the central nervous system (CNS) (3). Aquaporin-4 antibody-mediated autoimmunity is considered to play the most critical role in the pathogenesis of NMO (4, 5). In the last decade, the monoclonal antibody rituximab (RTX) targeting B cells has been gradually applied for the management of relapses in Neuromyelitis optica spectrum disorders (NMOSDs) (5–7). Previous studies have suggested that RTX could significantly reduce the annual relapse rate (ARR) in approximately 90% of patients, improve the degree of disability, shorten the length of spinal cord lesions, and show good safety (6–10). Intravenous RTX, as an empirical immunotherapy in treating NMOSDs, has been listed as the first-line treatment in the remission phase (11, 12).

Regimens of RTX treatments in NMO were based on the use of RTX by patients with lymphoma (13) (375 mg/m^2 infused once per week for 4 weeks or 1,000 mg infused twice, with a 2-week interval), which were high-cost, off-label therapies, and might have a high risk of adverse reactions. In recent years, several studies have indicated that a reduced dose of RTX has therapeutic value for NMOSD, mostly based on the evaluation of expanded disability status scale (EDSS) scores and ARR (9, 14, 15). Expanded disability status scale scores, known as a classic disability assessment method in NMOSD, were insufficient for patients with ON as the main attack. The decrease in monocular vision might not even change the EDSS score. Furthermore, few studies have paid attention to the fluctuation of serum AQP4-Ab levels during the treatment procedure after low-dose RTX treatment. The relationship of AQP4-Ab levels with disease activity after low-dose RTX treatment remains unclear.

This study is the first to administer low-dose RTX to NMO-ON patients in a Chinese neuro-ophthalmologic center. In this study, comprehensive visual function evaluation was performed, risk factors associated with disease activity were evaluated. Neuromyelitis optica-associated optic neuritis was diagnosed with seropositive AQP4-Ab using cell-based assays (CBAs), and the fluctuation of antibody levels was tested using an enzyme-linked immunosorbent assay (ELISA) method throughout the follow-up period.

MATERIALS AND METHODS

Patients

Hospitalized patients diagnosed with relapsing NMO-ON in the remission phase were enrolled in the Chinese People's Liberation Army General Hospital (PLAGH) from February 2017 to August 2019 for this study. Neuromyelitis optica-associated optic neuritis was diagnosed with seropositive AQP4-Ab using both CBAs and ELISA methods (16). Patients with hepatic or retinal diseases, cardiac dysfunction, a history of cancer and chronic infection, abnormal blood cell count, pregnancy, and refractive error exceeding −6.0 D were excluded. The patients were followed for at least 3 months. Failure to follow up for 2 consecutive months was considered follow-up loss. All adverse events (AEs) during RTX treatment were recorded.

Treatment Protocol

In the induction phase, 100 mg of RTX was intravenously (IV) administered once a week 4 consecutive times. Peripheral blood B-cell counts (using CD19 expression) were obtained at baseline and every month. Further infusions were given at 100 mg IV when the B cell frequency was elevated to above 1%. All patients were pretreated with ibuprofen 0.3 g orally and promethazine hydrochloride 25 mg IV prior to each RTX infusion. High-dose methylprednisolone IV (IVMP) (1g/day for 3–5 days) was used for the management of acute disease attack.

Tests for Serum AQP4-Ab and Other Autoimmune Antibodies

For qualitative test of AQP4-Ab, we established a transfected cell line of EGFP-AQP4-m23-HEK293 using the published methods (16). The patient's serum was gradiently diluted and add to the fixed cells. Positive results were determined when fluorescent labeling of anti-human second antibody coincided with EGFP. For all NMO-ON patients, an ELISA method (RSR Co., US) was used to test AQP4-Ab at baseline and after RTX treatment at least once every 2 months. A flow cytometry method was used to detect the frequency of CD19+ B cells in peripheral blood before and after the first infusion, after the induction treatment (four infusions) and then per month. Blood was also drawn for total antinuclear antibody (ANA) titers and autoantibodies against double-stranded DNA, extractable nuclear antigens including Sjögren syndrome A (SSA)/B (SSB), ribosomal p protein, Scl-70, Jo-1, thyroglobulin (TG), thyroid peroxidase (TPO), and β2-glycoprotein I antigen in the rheumatologic research center in PLAGH.

Ophthalmological Examinations, OCT Procedures, and Evaluation of EDSS Score

Ophthalmologic examinations included slit lamp inspection, swinging-light tests for the search for RAPD, and direct or indirect ophthalmoscopy with dilated pupils for retinal examination. Best-corrected visual acuity (BCVA) was tested using a Snellen chart.

OCT was performed using Cirrus HD-OCT (software version 3.0, Model 4000; Carl Zeiss Meditec, Inc., Dublin, CA, USA). All OCT scanning was performed by an experienced operator in a darkroom. Patients with a pupil diameter <2 mm received mydriasis. We followed OSCAR-IB criteria in the retinal OCT quality assessment (17). Peripaillary retinal nerve fiber layer (pRNFL) thickness was calculated by averaging the following four quadrants: temporal, nasal, superior, and inferior. Macular data were evaluated by the cube average thickness (quadrant measurements of retinal thickness in a 6 × 6 mm volume cube between the inner limiting membrane and the retinal pigment epithelium: ILM-RPE) and the thickness map displaying measurements calculated from nine macular areas corresponding to the Early Treatment Diabetic Retinopathy Study (**Figure 5**).

Expanded disability status scale scores were evaluated in all NMO-ON patients using the Kurtzke Functional System Rating

Scale. Two doctors evaluated the same patient separately and calculated the average EDSS score at each evaluation.

Statistical Analysis

Statistical analyses were performed using the Statistical Program for Social Sciences statistical software (version 21.0; IBMSPSS, Inc., Chicago, IL). The numeric variable is represented as Mean ± SD. A paired *t*-test was used to compare measurement data in the follow-up period with those at baseline. The differences before and after treatment in the two groups were compared by analysis of variance (ANOVA) or rank-sum test. Categorical data were analyzed using the chi-squared test or Fisher's exact test. *P*-values < 0.05 were considered significant.

RESULTS

Demographic Manifestations

A total of 43 patients with NMO-ON (75 eyes) were included in this study. The average age at the time of enrollment was 33.5 ± 12.79 years, and females accounted for 97.7% (42/43). At the time of enrollment, 23 patients only experienced ON. The last attack was ON in 36 patients and or ON combined with acute myelitis in seven patients. The time from the last attack to enrollment was 2.4 ± 1.63 months. Ten patients were treated with immunotherapies before enrollment, including seven of azathioprine (oral 1.5–4.0 mg/Kg*days), one of mycophenolate mofetil (MMF, oral 1.5–3.0 g/days), and two of MMF combined low-dose prednisolone. A total of 12 patients had accompanying autoimmune diseases (ADs) at the time of enrollment (12/43, 27.9%), including seven organ-specific (OS) ADs (autoimmune thyroid disease, idiopathic thrombocytopenic purpura, myasthenia gravis) and five non-OS (NOS) ADs (systemic lupus erythematosus and Sjögren syndrome). Twenty-two patients (22/43, 48.8%) had other autoimmune antibodies. The frequency of combined OS autoantibodies (OS-Abs: TG-Ab, TPO-Ab) was 25.6% and that of combined NOS autoantibodies (NOS-Abs: ANA, SSA, etc.) was 37.2%. The demographic and clinical details of NMO-ON are summarized in **Table 1**.

TABLE 1 | Demographic and clinical manifestations of NMO-ON patients.

Numbers of patients, *n*	43
Age at enrollment, years, mean ± SD (range)	33.5 ± 12.79(13–55)
Age at onset, years, mean ± SD (range)	28.5 ± 11.81(10–55)
Sex ratio, M:F	1:42
Ethnicity	All Han Chinese
Involved eyes, *n*	75
Clinical characters of ON	
One episode, *n* (%)	6(14.0)
Multiple episodes, *n* (%)	37(86.0)
Unilateral involved, *n* (%)	11(25.6)
Bilateral involved, *n* (%)	32(74.4)
First episode	
ON, *n* (%)	37(86.0)
Myelitis, *n* (%)	4(9.3)
Other core clinical symptoms, *n* (%)	2(4.7)
Disease duration, months, mean ± SD (range)	58.2 ± 62.79(3–270)
Average EDSS score, mean ± SD	2.2 ± 1.12
Immunosuppression treatments before enrollment[a], *n* (%)	
None or oral low-dose prednisolone	33(76.7)
AZA	7(16.3)
MMF	1(2.3)
MMF combined prednisolone	2(4.7)
Accompanied autoimmune diseases, *n* (%)	12(27.9)
HT	6(14.0)
SS	4(9.3)
SLE	1(2.3)
ITP	1(2.3)
MG	1(2.3)
Accompanied autoimmune antibodies, *n* (%)	22(48.8)
ANA	13(30.2)
TG-Ab	9(20.9)
TPO-Ab	9(20.9)
SSA/SSB-Ab	12(27.9)
a-β2-GPI-Ab	3(7.0)
Anti-ribosomal p protein Ab	1(2.3)

[a] *Treatment for at least 3 months.*

NMO-ON, neuromyelitis optica associated optic neuritis; RTX, rituximab; AZA, azathioprine; MMF, mycophenolate Mofetil; HT, Hashimoto's thyroiditis; SS, Sjögren syndrome; SLE, systemic lupus erythematosus; ITP, idiopathic thrombocytopenic purpura; MG, myasthenia gravis; ANA, antinuclear antibody; TG-Ab, anti-thyroglobulin antibody; TPO-Ab, anti-thyroid peroxidase antibody; SSA/SSB-Ab, Sjögren syndrome A (SSA)/B (SSB) antibody; a-β2-GPI-Ab, anti-β2-glycoprotein I antibody.

Relapses and ARR

The patients were followed up for 3–19 months (median 8 months). A total of 11 relapses in eight patients, including two ON and nine acute myelitis, were observed during the follow-up period. The average time from induction to first recurrence was 3.3 ± 2.32 months (ranged 0.25–6 months). The relapses before and after low-dose RTX treatment are presented in **Figure 1**. Among 13 patients who were followed up for more than 1 year, the ARR decreased significantly from 1.19 ± 0.286 to 0.15 ± 0.154 ($p = 0.009$), and the relapse-free rate was 92.3% (12/13).

A total of 22 patients were followed up for more than 6 months. Of the 22 patients, six relapsed. The comparison of clinical characteristics between relapsed and non-relapsed patients indicated a higher frequency of NOS-Abs in relapsed patients ($p = 0.046$) (**Table 2**).

Dynamic Changes of B Cells and Serum AQP4-Ab

Complete B-cell clearance (CD19+ B cell ≤1%) was observed in 35 patients (81.4%) after the first RTX infusion and 42 patients (97.7%) after the induction treatment (**Figures 2A,B**). One patient experienced an increase in the frequency of B cells after the first infusion and relapsed within a short period of time after induction treatment (**Figure 4B**).

The maintenance time of B cell clearance ranged from 2 to 12 months (directly into the second cycle of treatment) within 1 year after induction (5.2 ± 2.25 months). Reinfusion was

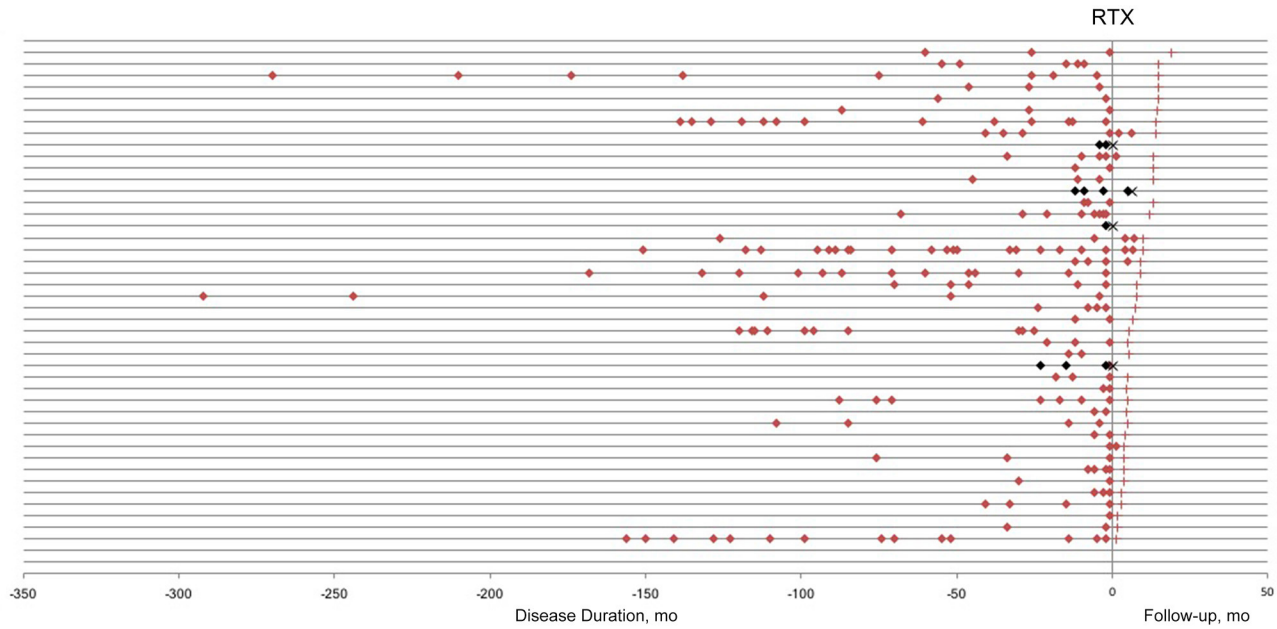

FIGURE 1 | Relapses in neuromyelitis optica-associated optic neuritis patients before and after low-dose rituximab (RTX) treatment. Each horizontal line represents a patient. Red/Black square, relapse; red cross, last follow-up; black cross, lost to follow-up.

TABLE 2 | Comparison of clinical characters between relapsed and non-relapsed patients within 6 months of RTX treatment.

	Relapsed (*N* = 6)	Non-relapsed (*N* = 16)	*p*
Serum AQP4-Ab concentration deduction percentage after RTX Induction, %	30.6	40.6	0.624
Age at Onset, years, mean ± SEM	27.0 ± 3.04	24.6 ± 2.52	0.598
ARR before enrollment[a], mean ± SEM	1.58 ± 0.428	0.96 ± 0.158	0.101
Combined with autoimmune diseases, *n* (%)	3(50.0)	3(18.8)	0.283
Combined with autoimmune antibodies, *n* (%)	5(83.3)	8(50.0)	0.333
NOS-Abs, *n* (%)	5(83.3)	4(25.0)	0.046*
OS-Abs, *n* (%)	0(0.0)	5(31.3)	–

[a]*Calculated based on data of 21 patients whose disease course was more than 1 year.*

**P < 0.05 (Fisher exact probability test).*

RTX, rituximab; AQP4-Ab, aquaporin-4 antibody; NOS-Abs, non-organ specific antibodies; OS-Abs, organ specific antibodies.

administered in 22 patients, of whom 20 were followed up for 6 months or more. The average treatment interval was 4.4 ± 2.26 months. Most of the reinfusion occurred in the eighth month after induction treatment (46.2%) (**Table 3**).

The overall serum AQP4-Ab levels decreased significantly after induction treatment ($P = 0.0123$), but AQP4-Ab level in four patients elevated (**Figure 2C**). The fluctuation of serum AQP4-Ab levels in 12 months is shown in **Figure 3**. Compared with baseline, the serum AQP4-Ab level decreased significantly after 1 month ($P = 0.009$) but increased significantly after 12 months of induction treatment ($P = 0.025$).

Among the 11 relapses, 6 (54.5%) were accompanied by B cell regeneration (ratio>1%), and 5 (45.4%) occurred within 14 days after RTX infusion. AQP4-Ab was tested in 10 relapses, of which 9 (90%) showed rapidly increased or continuous high levels of AQP4-Ab. The peripheral blood CD19+ B cell frequency and serum AQP4-Ab level in relapsed patients are shown in **Figure 4** (data from patient No. 24 are not shown because AQP4-Ab was not detected at relapse). The increase in AQP4-Ab could occur regardless of the regeneration of CD19+ B cells.

Ophthalmological Findings and EDSS Scores

A total of 13 patients (26 eyes) were followed up for at least 1 year, of whom BCVA, OCT parameters and EDSS scores after 1 year of treatment were compared with those at enrollment. The results showed that BCVA improved in six eyes (23.1%), remained stable in 19 eyes (73.1%), and was reduced in only one eye (3.8%). The average EDSS score of the 13 patients was 2.85 ± 0.291 after treatment for 1 year compared with 3.00 ± 0.291 at baseline ($p = 0.219$).

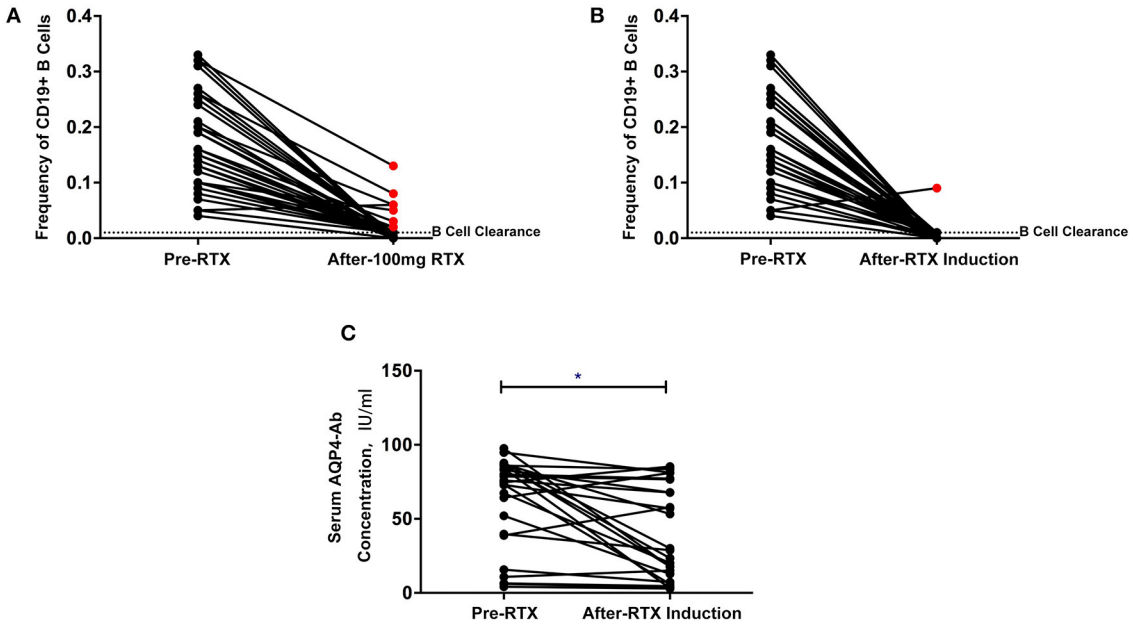

FIGURE 2 | (A,B) Changes in CD19+ B cell frequency before and after the first rituximab infusion **(A)** and induction treatment **(B)** (*red point*: patients without B cell clearance). **(C)** Changes in serum aquaporin-4 antibody (AQP4-Ab) before and after low-dose rituximab induction treatment. *$P < 0.05$.

TABLE 3 | Presentation of the re-infusion time after RTX induction treatment.

Time after RTX induction treatment, months	1	2	3	4	5	6	7	8	9	10	11	12
N[a]	29	23	25	15	13	12	11	13	7	11	4	13
Patients of Re-infusion, *n*	0	1	5	6	3	5	3	6	1	4	1	5
Re-infusion percentage, %	0.0	4.3	20.0	**40.0**	23.1	**41.7**	27.3	**46.2**	14.3	36.4	25.0	38.5

[a]*Patients undergone test for Serum AQP4-Ab concentration.*
The re-infusion percentage over 40% was presented in bold font.

OCT data was collected in 22 eyes (invalid data of four eyes with low vision was excluded). The peripapillary retinal nerve fiber layer (pRNFL) was significantly thinner in the superior, inferior, and nasal quadrants (**Figures 5B–D**); the macular neuroretinal thickness was significantly decreased in the inferior quadrant of both the inner and outer rings (**Figures 5H,L**). Moreover, structural alterations were observed in unaffected eyes (**Figure 5**, green points).

AEs and Severe AEs

There were a total of 8 (18.6%) mild infusion reactions reported in patients, including chills, nasal congestion, sore throat, fatigue, elevated body temperature, and dizziness. Seven cases occurred at the first infusion, and one case occurred at the fifth infusion. Spontaneous remission was noted in all of cases. Two cases of pulmonary infection and one case of urinary infection were observed in the 13 patients followed up for over 1 year, and all recovered after antibiotic treatment. There were no cases of SAEs observed throughout the observation period.

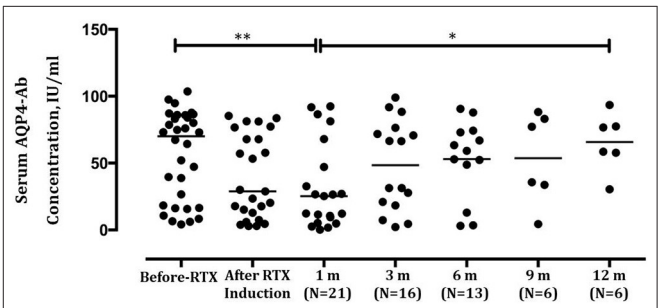

FIGURE 3 | Comparison of serum aquaporin-4 antibody (AQP4-Ab) levels in neuromyelitis optica-associated optic neuritis patients before and after low-dose rituximab induction within 12 months. **$P < 0.01$; *$P < 0.05$.

DISCUSSION

In this study, low-dose RTX was prospectively applied to NMO-ON patients for the first time. According to the 2015

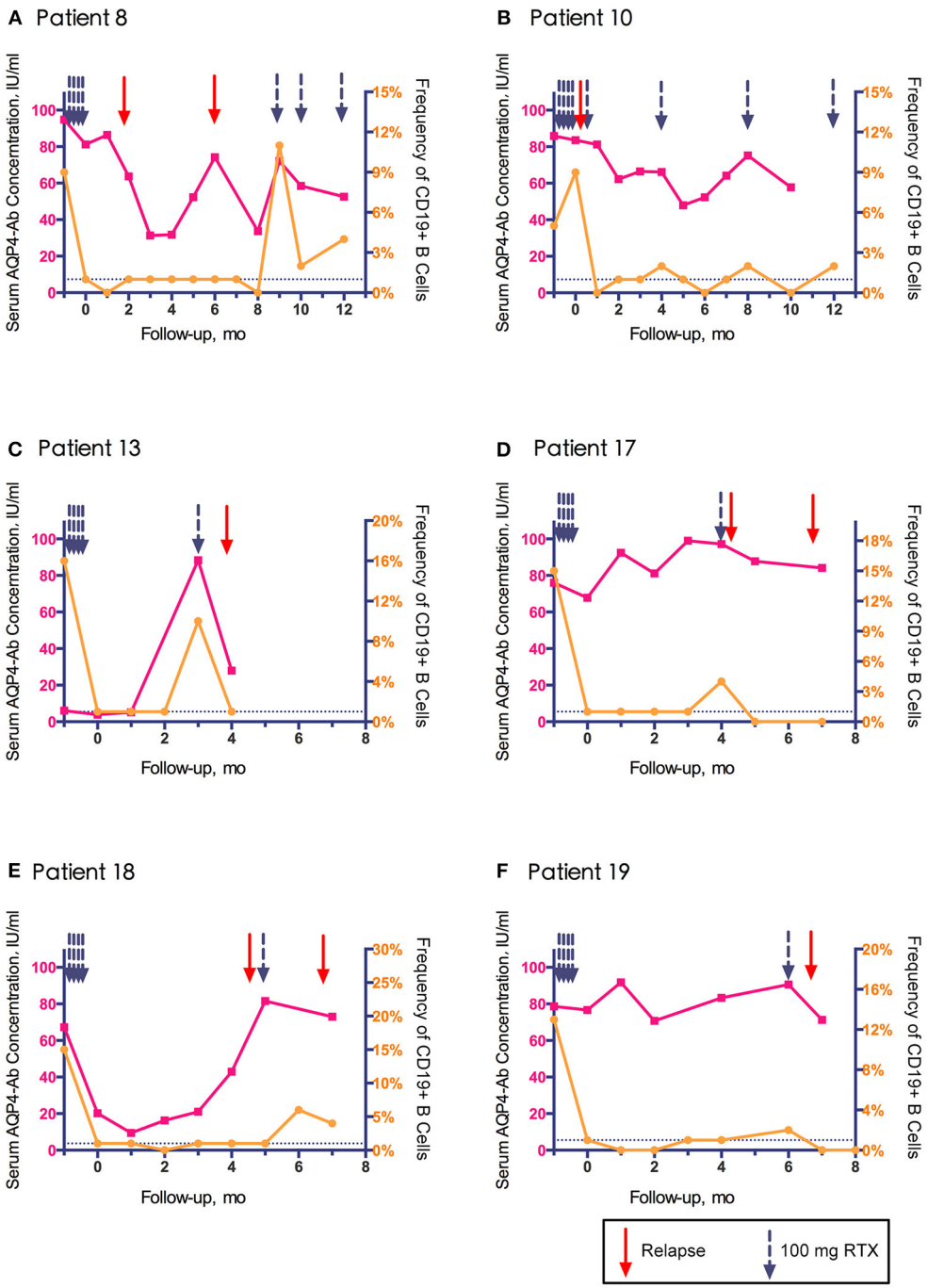

FIGURE 4 | Association of clinical relapse with CD19+ B cell frequency and aquaporin-4 antibody (AQP4-Ab) level in six relapsed patients with neuromyelitis optica-associated optic neuritis.

diagnostic criteria of NMOSDs (18), 43 AQP4-Ab seropositive NMO-ON patients were included in this study. At present, the detection methods of AQP4-Ab include CBA, tissue section immunofluorescence staining, flow cytometry, ELISA, and radioimmunoassay. Cell-based assay is considered to have higher sensitivity and specificity compared to ELISA and other method (16). So we used CBA for qualitative test of AQP4-Ab. In this study, all patients tested positive for AQP4-Ab by both CBA and ELISA methods, which ensured the accuracy of diagnosis and the consistency of our cohort. The average age of onset in this group was 28.5 years old, which was younger than that reported in other studies, and the majority (97.7%) were female. This might

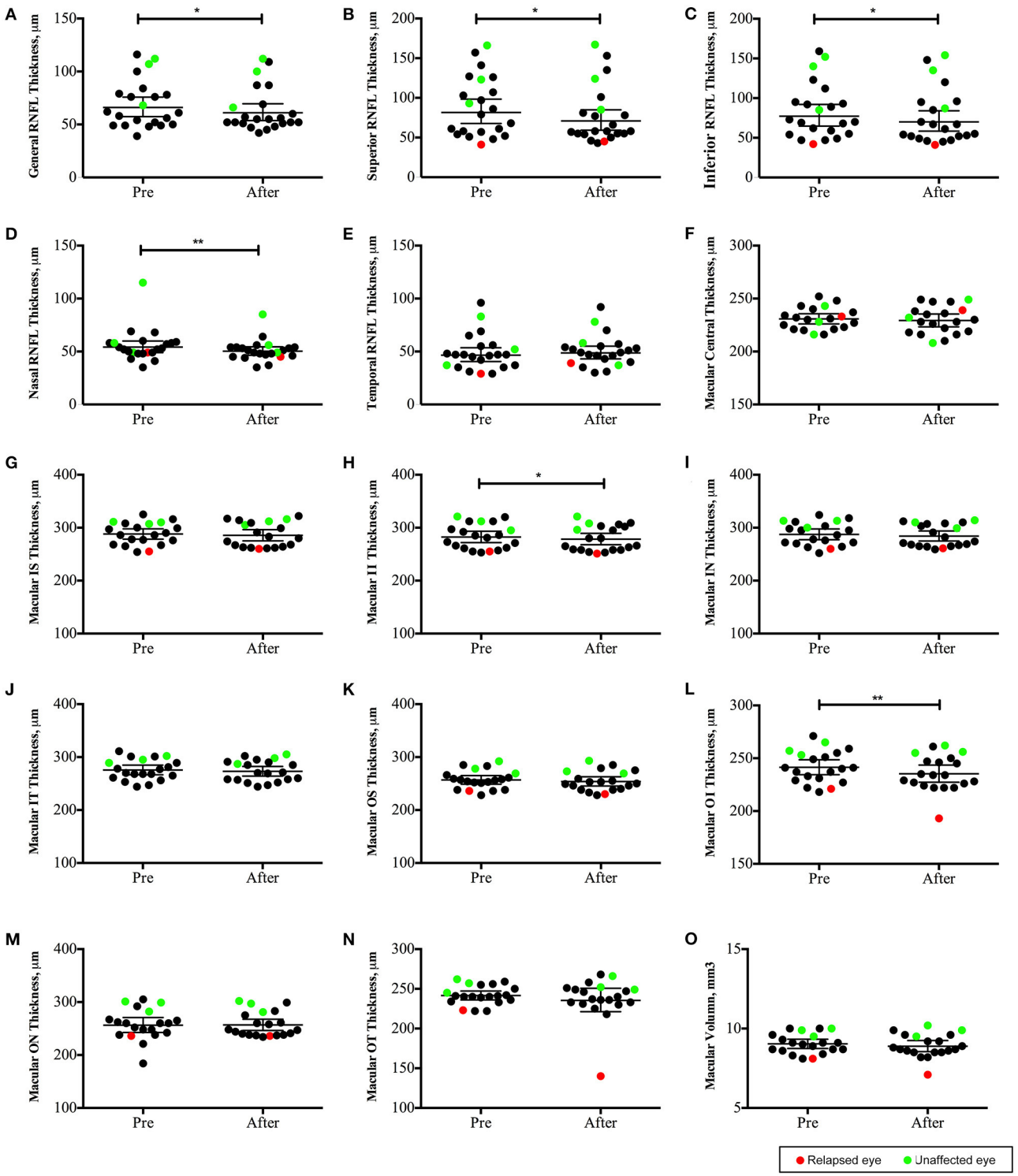

FIGURE 5 | Changes in optic coherence tomography (OCT) parameters in neuromyelitis optica-associated optic neuritis patients followed up for 12 months (22 eyes): The peripapillary retinal nerve fiber layer (pRNFL) was significantly thinner in the superior, inferior and nasal quadrants **(B–D)**; the macular neuroretinal thickness was significantly decreased in the inferior quadrant of both the inner and outer rings **(H,L)**. $^{**}P < 0.01$; $^{*}P < 0.05$. Red points: relapsed eyes; Green point: unaffected eye. IS, superior quadrant of the inner ring; II, inferior quadrant of the inner ring; IN, nasal quadrant of the inner ring; IT, temporal quadrant of the inner ring; OS, superior quadrant of the outer ring; OI, inferior quadrant of the outer ring; ON, nasal quadrant of the outer ring; OT, temporal quadrant of the outer ring).

be due to the bias caused by the younger patients, who were more likely to accept new treatment methods, which could not represent the demographic characteristics of NMOSD. However, high prevalence rates of multiple episodes and bilateral involved ON were observed in our cohort, which was in accordance with previous studies of NMO-ON (2).

Here, we found that after 1 year of low-dose RTX treatment (approximately 20% of the conventional dose), the ARR decreased significantly, and the relapse-free rate was 92.3%. Up to 96.2% of patients had stable or improved vision, and a decrease in the average EDSS score was found. The prognostic visual acuity in NMO-ON was found to be correlated with the time of acute treatment at ON onset, as well as ON relapses (19). So the decreased ARR could contribute to the favorable prognosis. In a study of conventional-dose RTX for NMOSD, the reduction rate of ARR ranged from 25% to 100% (6–8, 10, 20). We considered that the studies with relatively low effectiveness of RTX have the following commonalities: (1) patients included in most of the studies were diagnosed with NMO or long segment myelitis, which had higher EDSS scores than our ON patients; (2) positive serum AQP4-Ab was not included in the inclusion criteria in many studies, and patients with negative AQP4-Ab may have different pathological mechanisms, such as myelin oligodendrocyte glycoprotein antibody or glial fibrillary acidic protein antibody mediated autoimmunity (21–23); and (3) in some studies, RTX was used in refractory NMO treatment. Patients uncontrolled by other immunosuppression therapies might have higher disease activity. In our study, all patients were AQP4-Ab seropositive, and 76.7% of the patients had not used immunosuppressive therapy in the past. Therefore, this study might provide stronger clinical evidence of the usage of low-dose RTX for NMOSD treatment.

The dynamic changes in B cells and the fluctuation in serum AQP4-Ab were the focus of this study. We observed a high percentage of B cell clearance after either 100 mg RTX alone or induction treatment. The average time for B cell regeneration, which was not presented in small-sample studies of similar RTX dosages (9, 14), was 5.2 months. Greenberg et al. compared B cell regeneration time between different doses of RTX for B cell clearance (<2% of CD19+ B cells) and found that the maintenance time (average 6.1 months) after a single administration of 1,000 mg was significantly longer than 100 mg (average 3.3 months) (24). As the induction RTX dose was 400 mg in our study, the maintenance time of B cell clearance was between the two dosages. The proportion of reinfusion within 6 months after induction (90.9%) in our study is similar to that in other conventional dose studies. The results in our study indicated the similar efficacy of low-dose RTX to higher-dose RTX treatment on B cell clearance. In addition, low-dose RTX treatment was better than conventional dose treatment with respect to health care costs. In our cohort, the maximum dose of RTX applied for 12 months of follow-up was only 700 mg, which was less than half of the conventional dose.

However, while demonstrating the effectiveness of RTX, we found individual differences among patients with RTX treatment (**Figure 4**), which was consistent with conventional dose treatment (25, 26). Of the 11 episodes of relapse, five occurred within 2 weeks of the last RTX administration; the underlying baseline disease activity might contribute to the early relapses. Besides, application of RTX was considered to stimulate disease activity. Pellkofer et al. reported a synergistic increase in B cell-stimulating factor and AQP4-Ab in serum within a few days after RTX application (27), and another study speculated that monocytes were activated and proinflammatory cytokines were released after immature B cells were cleared (28). Therefore, there is a possibility that the application of RTX will cause short-term disease activation in some patients. In other studies, the heterogeneity of NMOSD patients' response to RTX treatment could also be observed, along with the worsening of the disease after RTX infusion (29–31). Kim et al. observed 100 NMO patients after RTX treatment and found that patients with different responses to treatment had FCGR3A gene polymorphisms. The FCGR3A-158F gene sequence may be related to incomplete clearance and short-term regeneration of memory B cells (32). Li et al. considered that the appearance of anti-RTX antibodies may lead to resistance to RTX treatment (15). However, the relationship between B cell regeneration and disease recurrence is still unclear. In our study, 45.4% of clinical recurrences in this study occurred with peripheral blood CD19+ B cell clearance. Previous studies have suggested that the activation of NMO pathogenic B cells occurs before CD19+ B cells, and it might be more accurate to monitor CD27+/CD20+ or class-switched memory B cells in subsequent studies (8, 33, 34).

Additionally, this study presented the fluctuation of serum AQP4-Ab concentration in NMO-ON and analyzed the correlation between relapse and AQP4-Ab. We found that 90% of clinical recurrences were accompanied by persistently high levels of serum AQP4-Ab or rapid elevation, which provided evidence of the relationship between AQP4-Ab and disease activity. Kim et al. presented the association of relapses with AQP4-Ab levels in nine NMO patients and concluded the temporal association of clinical relapses with increases in AQP4-Ab levels. However, 1/3 of the patients included in their studies were seronegative for AQP4-Ab, which might lead to bias in the analysis (26). This study also found that NMO-ON could be stable with high levels of AQP4-Ab, indicating that other related factors, such as the integrity of the blood-brain barrier, complement, and other cytokines, may also contribute to the pathological process.

The risk factors for patients with relapse within 6 months were analyzed in this study, and we found that the frequency of NOS-Abs in relapsed patients (83.3%) was higher than that in non-relapsed patients (25.0%; $P = 0.044$). The relationship between NOS-Abs and NMO recurrence is controversial. It was reported that NOS-Abs were unrelated to ARR and the severity of NMO (35), but it was also found that ANA-positive NMOSD patients have a reduced recurrence frequency and a better prognosis (36). However, this study is the first to report the relationship between NOS-Abs and NMO recurrence after RTX treatment, and a larger sample size study is needed to verify the results.

This study also dynamically observed the changes in OCT parameters in patients within 1 year. Significantly decreased thicknesses in the superior, inferior, and nasal quadrants of the

pRNFL and in the inferior quadrant of macular were observed. Although OCT has been used for the evaluation of ON in NMO or MS in many studies, longitudinal observation studies have been rare. It is reported that NMO-ON eyes have lower peripapillary retinal nerve fiber layer and macular ganglion cell + inner plexiform layer thicknesses, as well as a "flater" disc when compared with MS-ON eyes (21, 37). Moreover, while MS-ON mostly affected the small-diameter neurons in the temporal quadrant of the optic disc, NMO-ON more affected the nerve fibers above and below the optic disc (38, 39), consistent with the results in this study. In addition, we also observed that the patient's "unaffected eye" may also have gradual loss of retinal nerve fibers, indicating the subclinical involvement of the "unaffected" optic nerve in NMO-ON (40).

The proportion of AE in this study was lower than that in most conventional-dose studies (6, 8, 26, 27). In addition, no SAEs leading to discontinuation of treatment were observed in this study. Therefore, low-dose RTX treatment was generally well-tolerated in NMO-ON patients.

In summary, we reported the efficacy of low-dose RTX on the recurrence frequency of NMO-ON. The recurrence of NMO-ON was related to the ratio of CD19+ B cells in peripheral blood and the continuous high- or short-term increase in serum AQP4-Ab, and patients with NOS-Abs might tend to relapse early (within 6 months) after RTX induction. Low-dose RTX was well-tolerated in our cohort with a low proportion of AEs. Limitations existed in this study due to the uncontrolled design and relatively short follow-up time. Moreover, we were unable to draw a survival curve for possible risk factors for relapses due to the short follow-up time of 6 months. A multicenter randomized controlled trial comparing different RTX treatment strategies with other immunosuppression treatments for NMO-ON is needed in the future.

DATA AVAILABILITY STATEMENT

The raw data supporting the conclusions of this article will be made available by the authors, without undue reservation.

ETHICS STATEMENT

The studies involving human participants were reviewed and approved by The Chinese People's Liberation Army Hospital Ethics Committee. Written informed consent to participate in this study was provided by the participants' legal guardian/next of kin.

AUTHOR CONTRIBUTIONS

QX and SZ contributed to the study design. HZ and SZ contributed to the data collection. HD contributed to the data analysis and interpretation. SW contributed to the manuscript preparation. SZ provided fundings to this research. All authors contributed to the article and approved the submitted version.

FUNDING

This work was supported by The National Natural Science Foundation of China (grant number: 81701198) and the Nova Program of Beijing Hospital (grant number: BJ-2018-132).

REFERENCES

1. Jarius S, Paul F, Weinshenker BG, Levy M, Kim HJ, Wildemann B. Neuromyelitis optica. *Nat Rev Dis Primers*. (2020) 6:85. doi: 10.1038/s41572-020-0214-9
2. Zhou H, Zhao S, Yin D, Chen X, Xu Q, Chen T, et al. Optic neuritis: a 5-year follow-up study of Chinese patients based on aquaporin-4 antibody status and ages. *J Neurol*. (2016) 263:1382–9. doi: 10.1007/s00415-016-8155-7
3. Lennon VA, Wingerchuk DM, Kryzer TJ, Pittock SJ, Lucchinetti CF, Fujihara K, et al. A serum autoantibody marker of neuromyelitis optica: distinction from multiple sclerosis. *Lancet*. (2004) 364:2106–12. doi: 10.1016/S0140-6736(04)17551-X
4. Fujihara K, Bennett JL, de Seze J, Haramura M, Kleiter I, Weinshenker BG, et al. Interleukin-6 in neuromyelitis optica spectrum disorder pathophysiology. *Neurol Neuroimmunol Neuroinflamm*. (2020) 7:e841. doi: 10.1212/NXI.0000000000000841
5. Graf J, Mares J, Barnett M, Aktas O, Albrecht P, Zamvil SS, et al. Targeting B cells to modify MS, NMOSD, and MOGAD: part 1. *Neurol Neuroimmunol Neuroinflamm*. (2021) 8:e918. doi: 10.1212/NXI.0000000000000918
6. Jacob A, Weinshenker BG, Violich I, McLinskey N, Krupp L, Fox RJ, et al. Treatment of neuromyelitis optica with rituximab: retrospective analysis of 25 patients. *Arch Neurol*. (2008) 65:1443–48. doi: 10.1001/archneur.65.11.noc80069
7. Cree BA, Lamb S, Morgan K, Chen A, Waubant E, Genain C. An open label study of the effects of rituximab in neuromyelitis optica. *Neurology*. (2005) 64:1270–2. doi: 10.1212/01.WNL.0000159399.81861.D5
8. Kim SH, Huh SY, Lee SJ, Joung A, Kim HJ. A 5-year follow-up of rituximab treatment in patients with neuromyelitis optica spectrum disorder. *JAMA Neurol*. (2013) 70:1110–7. doi: 10.1001/jamaneurol.2013.3071
9. Yang CS, Yang L, Li T, Zhang DQ, Jin WN, Li MS, et al. Responsiveness to reduced dosage of rituximab in Chinese patients with neuromyelitis optica. *Neurology*. (2013) 81:710–3. doi: 10.1212/WNL.0b013e3182a1aac7
10. Cabre P, Mejdoubi M, Jeannin S, Merle H, Plumelle Y, Cavillon G, et al. Francophone society of multiple S, investigators O: treatment of neuromyelitis optica with rituximab: a 2-year prospective multicenter study. *J Neurol*. (2018) 265:917–25. doi: 10.1007/s00415-018-8771-5
11. Zephir H, Bernard-Valnet R, Lebrun C, Outteryck O, Audoin B, Bourre B, et al. Rituximab as first-line therapy in neuromyelitis optica: efficiency and tolerability. *J Neurol*. (2015) 262:2329–35. doi: 10.1007/s00415-015-7852-y
12. Trebst C, Jarius S, Berthele A, Paul F, Schippling S, Wildemann B, et al. Update on the diagnosis and treatment of neuromyelitis optica: recommendations of the Neuromyelitis Optica Study Group (NEMOS). *J Neurol*. (2014) 261:1–16. doi: 10.1007/s00415-013-7169-7
13. McLaughlin P, Grillo-Lopez AJ, Link BK, Levy R, Czuczman MS, Williams ME, et al. Rituximab chimeric anti-CD20 monoclonal antibody therapy for relapsed indolent lymphoma: half of patients respond to a four-dose treatment program. *J Clin Oncol*. (1998) 16:2825–33. doi: 10.1200/JCO.1998.16.8.2825
14. Yang Y, Wang CJ, Wang BJ, Zeng ZL, Guo SG. Comparison of efficacy and tolerability of azathioprine, mycophenolate mofetil, and lower dosages of rituximab among patients with neuromyelitis optica spectrum disorder. *J Neurol Sci*. (2018) 385:192–7. doi: 10.1016/j.jns.2017.12.034

15. Li T, Zhang LJ, Zhang QX, Yang CS, Zhang C, Li YJ, et al. Anti-rituximab antibody in patients with NMOSDs treated with low dose rituximab. *J Neuroimmunol.* (2018) 316:107–11. doi: 10.1016/j.jneuroim.2017.12.021
16. Waters PJ, McKeon A, Leite MI, Rajasekharan S, Lennon VA, Villalobos A, et al. Serologic diagnosis of NMO: a multicenter comparison of aquaporin-4-IgG assays. *Neurology*. (2012) 78:665–71; discussion 669. doi: 10.1212/WNL.0b013e318248dec1
17. Schippling S, Balk LJ, Costello F, Albrecht P, Balcer L, Calabresi PA, et al. Quality control for retinal OCT in multiple sclerosis: validation of the OSCAR-IB criteria. *Mult Scler*. (2015) 21:163–70. doi: 10.1177/1352458514538110
18. Wingerchuk DM, Banwell B, Bennett JL, Cabre P, Carroll W, Chitnis T, et al. International consensus diagnostic criteria for neuromyelitis optica spectrum disorders. *Neurology*. (2015) 85:177–89. doi: 10.1212/WNL.0000000000001729
19. Stiebel-Kalish H, Hellmann MA, Mimouni M, Paul F, Bialer O, Bach M, et al. Does time equal vision in the acute treatment of a cohort of AQP4 and MOG optic neuritis? *Neurol Neuroimmunol Neuroinflamm*. (2019) 6:e572. doi: 10.1212/NXI.0000000000000572
20. Evangelopoulos ME, Andreadou E, Koutsis G, Koutoulidis V, Anagnostouli M, Katsika P, et al. Treatment of neuromyelitis optica and neuromyelitis optica spectrum disorders with rituximab using a maintenance treatment regimen and close CD19 B cell monitoring. A six-year follow-up. *J Neurol Sci.* (2017) 372:92–6. doi: 10.1016/j.jns.2016.11.016
21. Filippatou AG, Mukharesh L, Saidha S, Calabresi PA, Sotirchos ES. AQP4-IgG and MOG-IgG related optic neuritis-prevalence, optical coherence tomography findings, and visual outcomes: a systematic review and meta-analysis. *Front Neurol. (*2020) 11:540156. doi: 10.3389/fneur.2020.540156
22. Reindl M, Schanda K, Woodhall M, Tea F, Ramanathan S, Sagen J, et al. International multicenter examination of MOG antibody assays. *Neurol Neuroimmunol Neuroinflamm.* (2020) 7:e674. doi: 10.1212/NXI.0000000000000674
23. Bruijstens AL, Wong YYM, van Pelt DE, van der Linden PJE, Haasnoot GW, Hintzen RQ, et al. HLA association in MOG-IgG- and AQP4-IgG-related disorders of the CNS in the Dutch population. *Neurol Neuroimmunol Neuroinflamm*. (2020) 7:e702. doi: 10.1212/NXI.0000000000000702
24. Greenberg BM, Graves D, Remington G, Hardeman P, Mann M, Karandikar N, et al. Rituximab dosing and monitoring strategies in neuromyelitis optica patients: creating strategies for therapeutic success. *Mult Scler.* (2012) 18:1022–6. doi: 10.1177/1352458511432896
25. Valentino P, Marnetto F, Granieri L, Capobianco M, Bertolotto A. Aquaporin-4 antibody titration in NMO patients treated with rituximab: a retrospective study. *Neurol Neuroimmunol Neuroinflamm. (*2017) 4:e317. doi: 10.1212/NXI.0000000000000317
26. Kim SH, Kim W, Li XF, Jung IJ, Kim HJ. Repeated treatment with rituximab based on the assessment of peripheral circulating memory B cells in patients with relapsing neuromyelitis optica over 2 years. *Arch Neurol*. (2011) 68:1412–20. doi: 10.1001/archneurol.2011.154
27. Pellkofer HL, Krumbholz M, Berthele A, Hemmer B, Gerdes LA, Havla J, et al. Long-term follow-up of patients with neuromyelitis optica after repeated therapy with rituximab. *Neurology.* (2011) 76:1310–5. doi: 10.1212/WNL.0b013e3182152881
28. Lehmann-Horn K, Schleich E, Hertzenberg D, Hapfelmeier A, Kumpfel T, von Bubnoff N, et al. Anti-CD20 B-cell depletion enhances monocyte reactivity in neuroimmunological disorders. *J Neuroinflamm. (*2011) 8:146. doi: 10.1186/1742-2094-8-146
29. Lindsey JW, Meulmester KM, Brod SA, Nelson F, Wolinsky JS. Variable results after rituximab in neuromyelitis optica. *J Neurol Sci.* (2012) 317:103–5. doi: 10.1016/j.jns.2012.02.017
30. Dai Y, Lu T, Wang Y, Fang L, Li R, Kermode AG, et al. Rapid exacerbation of neuromyelitis optica after rituximab treatment. *J Clin Neurosci. (*2016) 26:168–70. doi: 10.1016/j.jocn.2015.08.033
31. Perumal JS, Kister I, Howard J, Herbert J. Disease exacerbation after rituximab induction in neuromyelitis optica. *Neurol Neuroimmunol Neuroinflamm. (*2015) 2:e61. doi: 10.1212/NXI.0000000000000061
32. Kim SH, Jeong IH, Hyun JW, Joung A, Jo HJ, Hwang SH, et al. Treatment outcomes with rituximab in 100 patients with neuromyelitis optica: influence of FCGR3A polymorphisms on the therapeutic response to rituximab. *JAMA Neurol.* (2015) 72:989–95. doi: 10.1001/jamaneurol.2015.1276
33. Cohen M, Romero G, Bas J, Ticchioni M, Rosenthal M, Lacroix R, et al. Monitoring CD27+ memory B-cells in neuromyelitis optica spectrum disorders patients treated with rituximab: results from a bicentric study. *J Neurol Sci.* (2017) 373:335–8. doi: 10.1016/j.jns.2017.01.025
34. Trewin BP, Adelstein S, Spies JM, Beadnall HN, Barton J, Ho N, et al. Precision therapy for neuromyelitis optica spectrum disorder: a retrospective analysis of the use of class-switched memory B-cells for individualised rituximab dosing schedules. *Mult Scler Relat Disord. (*2020) 43:102175. doi: 10.1016/j.msard.2020.102175
35. Park JH, Hwang J, Min JH, Kim BJ, Kang ES, Lee KH. Presence of anti-Ro/SSA antibody may be associated with anti-aquaporin-4 antibody positivity in neuromyelitis optica spectrum disorder. *J Neurol Sci.* (2015) 348:132–5. doi: 10.1016/j.jns.2014.11.020
36. Masuda H, Mori M, Uzawa A, Muto M, Uchida T, Kuwabara S. Serum antinuclear antibody may be associated with less severe disease activity in neuromyelitis optica. *Eur J Neurol. (*2016) 23:276–81. doi: 10.1111/ene.12714
37. Motamedi S, Oertel FC, Yadav SK, Kadas EM, Weise M, Havla J, et al. Altered fovea in AQP4-IgG-seropositive neuromyelitis optica spectrum disorders. *Neurol Neuroimmunol Neuroinflamm.* (2020) 7:e805. doi: 10.1212/NXI.0000000000000805
38. Toosy AT, Mason DF, Miller DH. Optic neuritis. *Lancet Neurol. (*2014) 13:83–99. doi: 10.1016/S1474-4422(13)70259-X
39. Bertsch-Gout M, Loeb R, Finch AK, Javed A, Bernard J. High resolution retinal scanning reveals regional structural differences between MS and NMOSD optic neuritis regardless of antibody status. *J Neurol Sci. (*2018) 384:61–6. doi: 10.1016/j.jns.2017.11.017
40. Akaishi T, Kaneko K, Himori N, Takeshita T, Takahashi T, Nakazawa T, et al. Subclinical retinal atrophy in the unaffected fellow eyes of multiple sclerosis and neuromyelitis optica. *J Neuroimmunol. (*2017) 313:10–15. doi: 10.1016/j.jneuroim.2017.10.001

Conflict of Interest: The authors declare that the research was conducted in the absence of any commercial or financial relationships that could be construed as a potential conflict of interest.

Copyright © 2021 Zhao, Zhou, Xu, Dai and Wei. This is an open-access article distributed under the terms of the Creative Commons Attribution License (CC BY). The use, distribution or reproduction in other forums is permitted, provided the original author(s) and the copyright owner(s) are credited and that the original publication in this journal is cited, in accordance with accepted academic practice. No use, distribution or reproduction is permitted which does not comply with these terms.

Advantages of publishing in Frontiers

OPEN ACCESS
Articles are free to read for greatest visibility and readership

FAST PUBLICATION
Around 90 days from submission to decision

HIGH QUALITY PEER-REVIEW
Rigorous, collaborative, and constructive peer-review

TRANSPARENT PEER-REVIEW
Editors and reviewers acknowledged by name on published articles

Frontiers
Avenue du Tribunal-Fédéral 34
1005 Lausanne | Switzerland

Visit us: www.frontiersin.org
Contact us: frontiersin.org/about/contact

REPRODUCIBILITY OF RESEARCH
Support open data and methods to enhance research reproducibility

DIGITAL PUBLISHING
Articles designed for optimal readership across devices

FOLLOW US
@frontiersin

IMPACT METRICS
Advanced article metrics track visibility across digital media

EXTENSIVE PROMOTION
Marketing and promotion of impactful research

LOOP RESEARCH NETWORK
Our network increases your article's readership